UNIVERSITY OF LIVERPOOL

The Effect of Epac Activation on Human Coronary Artery Endothelial Cells

Thesis submitted in accordance with the requirements of the University of Liverpool for the Degree of Doctor in Philosophy by Rachael Ellen Quinn

September 2014

Acknowledgements

I would like to take this opportunity to thank my primary supervisor Dr John Quayle, and Dr Tomoko Kamishima, without whose expertise, support, and guidance this thesis would not have been possible. I would also like to thank my secondary supervisor Dr. Alec Simpson, for his help and support, particularly with the immunofluorescence sections of this thesis. In addition, the experimental expertise supplied by Dr Owain Roberts were also invaluable to this project, and as such my thanks also go out to him. I would also like to thank my colleagues and friends Paula Vickerton and Ailsa Dermody, and my parents, for their constant support, without which this process would not have been possible.

Contents

Abstract

The endothelial barrier is essential for vascular function, and its disruption may play a major role in the development of cardiovascular diseases. An increase in cAMP levels tightens the endothelial barrier by enhancing junction formation, and this is, in part, mediated by activation of exchange protein directly activated by cAMP (Epac). Vascular endothelial cells express vascular endothelial cadherin (VE-cadherin), and connexins 37, 40 and 43. Re-distribution of VE-cadherin in human coronary artery endothelial cells (HCAECs), induced by EGTA treatment or blocking VE-cadherin-VE-cadherin interactions through pre-treatment with anti-VE-cadherin primary antibody, triggered a subsequent re-distribution of Cx37 that was reversible. Epac activation with the Epac-selective agonist 8-pCPT induced a re-distribution of VE-cadherin and connexin 37 to sites of cell-cell contact in HCAECs, increasing the co-localisation of these two proteins, as detected by immunocytochemistry. This increased co-localisation was completely blocked by Epac1 siRNA. To test whether the re-distribution of Cx37 induced by Epac activation resulted in the formation of new functional gap junction channels, Lucifer yellow dye transfer was examined in HCAECs under varying conditions. Epac activation in HCAECs enhanced gap junction intercellular communication (GJIC), and this increase was completely blocked by the Epac inhibitor HJC0197. 8-pCPT addition was also shown to induce a transient increase in the intracellular calcium concentration in HCAECs, as detected with the calcium indicator Fluo-4. This calcium transient was independent of protein kinase A (PKA), and occurred in the absence of extracellular calcium, but was inhibited by the presence of the endoplasmic reticulum calcium ATPase inhibitor cyclopiazonic acid (CPA), indicating that Epac primarily mediated the increase, and that intracellular stores were the predominant source of calcium. Furthermore, the calcium transient induced by 8-pCPT was considerably reduced by the Epac inhibitor ESI-09 and completely inhibited by the Epac inhibitor HJC0197. Together, these data suggest that Epac strengthens the endothelial barrier through re-distribution of VE-cadherin and Cx37. In addition, GJIC is enhanced by Epac activation and there is a rise in intracellular calcium, a second messenger that can be transferred to adjacent cells through GJIC. It may be possible, therefore, that these effects of Epac promote endothelial cell-smooth muscle cell communication and therefore Epac could play a role in the regulation of vascular tone.

Abbreviations

8-pCPT	8-(4-Chlorophenylthio)-2'-O-methyladenosine-3', 5'-cyclic monophosphate, acetoxymethyl ester (Epac-selective agonist)
α-actin	α-smooth muscle actin
ABR	Actin-binding region
AC	Adenylate cyclase
AF488 / AF594	Alexa fluor 488 / 594
AJ	Adherens junction
AKAP	A-kinase anchoring protein
AM	Acetoxymethyl groups
Ang-1	Angiopoetin 1
ANOVA	Analysis of variance, statistical analysis
ANP	Atrial natriuretic peptide
AU	Arbitrary units
BBB/BRB	Blood brain barrier / blood retinal barrier
BCA	Bicinchonic acid (protein assay)
BFA	Brefeldin A
BSA	Bovine serum albumin
CaMKII	Calcium/calmodulin-dependent protein kinase II
cAMP	Cyclic adenosine monophosphate
CCE	Capacitative calcium entry
CCM-1	Cerebral cavernous malformation-1 protein (Krit1)

CD31	Cluster of differentiation 31 (endothelial cell marker)
CNB	Cyclic nucleotide binding
CNG channel	Cyclic nucleotide-gated cation channel
CPA	Cyclopiazonic acid (ER calcium ATPase inhibitor)
cPLA2α	Golgi-associated phospholipase A2α
CREB	cAMP response element-binding protein
Cx37/Cx40/Cx43	Connexin 37, 40, 43
DAPI	4’,6’-diamidino-2-phenylindole (nuclear stain)
DEP	Dishevelled Egl-10, Pleckstrin
DPBS	Dulbecco’s Phosphate Buffered Saline
E-cadherin	Epithelial cadherin
ECL	Enhanced chemiluminescence solutions
ECM	Extracellular matrix
EDHF	Endothelial-derived hyperpolarising factor
EDTA	Ethylenediaminetetraacetic acid
EGTA	Ethylene glycol tetraacetic acid
Epac	Exchange protein directly activated by cAMP
ER	Endoplasmic reticulum
ESAM	Endothelial cell-specific adhesion molecule
ESI-09	3- [5- (tert.- Butyl)isoxazol- 3- yl]- 2- [2- (3-chlorophenyl)hydrazono]- 3- oxopropanenitrile
FRAP	Fluorescence recovery after photobleaching
Fsk	Forskolin

GAP	GTPase-activating protein
GEF	Guanine nucleotide exchange factor
GFP	Green fluorescent protein
GJ	Gap junction
GJIC	Gap junctional intercellular communication
H	Heart, rat tissue section
HCAEC	Human coronary artery endothelial cell
HCASMC	Human coronary artery smooth muscle cell
HJC0197	Epac1 and Epac2 antagonist
HUVEC	Human umbilical vein endothelial cell
HRP	Horseradish peroxidise
IK_{ca}	Intermediate-conductance calcium-sensitive potassium channel
IP_3	Inositol-1,4,5-trisphosphate
IP_3R	IP_3 receptor
JAMs	Junctional adhesion molecules
kDa	Kilodalton (molecular weight unit)
KC	Kidney cortex, rat tissue section
KP	Kidney pyramid, rat tissue section
LPS	Lipopolysaccharide
MAGUK	Membrane-associated guanylate kinases
MLC	Myosin light chain
MLCK	Calcium/calmodulin-dependent myosin light chain kinase
MLCP	Myosin light chain phosphatase

MW	Molecular weight
N-cadherin	Neural cadherin
P1-P11	Passage number
P-cadherin	Placental cadherin
PAK	P21-associated Ser/Thr kinase
PDE	Phosphodiesterase
PDL	Poly D-lysine
PDZ	Postsynaptic density protein -95/discs large/ ZO-1
Pecam-1	Platelet/Endothelial Cell Adhesion Molecule 1
PFA	Paraformaldehyde
PGE2	Prostaglandin E2
PGI2	Prostaglandin I2 / prostacyclin
PKA	Cyclic AMP-dependent protein kinase
PKC	Protein kinase C
PKI	PKA-inhibitor
PLC	Phospholipase C
PMCA	Plasma membrane calcium ATPase
PTP	Protein tyrosine phosphatases
RA-domain	Ras-associating domain
RACK1	Receptor for activated PKC 1
RBD	Ras-binding domain
REM	Ras-exchange motif
RyR	Ryanodine receptor

S1P	Sphingosine-1-phosphate
SDS-PAGE	Sodium dodecyl sulphate polyacrylamide gel electrophoresis
SERCA pump	Sarco/endoplasmic reticulum calcium ATPase
SH3	Src homology 3
siRNA	Small interfering RNA
SK_{ca}	Small-conductance calcium-sensitive potassium channel
SOCE	Store-operated calcium entry
SSC	Sodium citrate buffer
STIM	Stromal interaction molecule
TBST	Tris-buffered saline and Tween 20
TEM	Transmission electron microscopy
TER	Transepithelial electrical resistance
TNF-α	Tumour necrosis factor α
TRPC	Transient receptor potential channel
UHQ	Ultra high quality
VASP	Vasodilator-stimulated phosphoprotein
VDCC	Voltage-dependent calcium channel
VE-cadherin	Vascular endothelial cadherin
VE-PTP	Vascular endothelial receptor-type PTP
VEGF	Vascular endothelial growth factor
vWF	Von Willebrand factor
WASP	Wiskott-Aldrich syndrome protein
ZO-1	Zonula occludins-1

Chapter 1:

General Introduction

1.1 - Introduction

The endothelium lines the lumen of the vasculature and acts as an important barrier. The endothelium is formed from a single layer of endothelial cells while multiple layers of smooth muscle cells form the tunica media. These two cell types are separated by the internal elastic lamina, however endothelial cells project through holes in this lamina to directly contact the vascular smooth muscle cells at the myoendothelial junction (MEJ)(Heberlein, Straub et al. 2009, Lilly 2014). The integrity of the endothelial barrier is essential for proper vascular function, and endothelial dysfunction is a hallmark for vascular diseases including atherosclerosis (Vanhoutte 2009). Homocellular junctions between endothelial cells include adherens junctions (AJ), formed by cadherins, and gap junctions (GJ), formed by connexins, and dynamic regulation of these junctions is fundamental to the role of the endothelium. Figure 1.1 represents the basic structure of an artery.

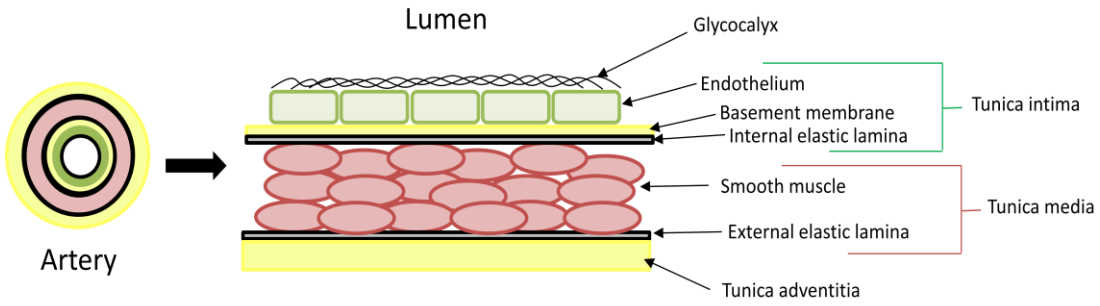

Figure 1.1: Structure of an artery

This schematic represents the major components of an artery. The lumen is lined by a single layer of endothelial cells (green), the surface of which is coated with a negatively-charged layer of glycosaminoglycans, proteoglycans and adsorbed plasma proteins, forming the glycocalyx (black lines). The basement membrane (thin yellow line) and the internal elastic lamina (grey) divide the endothelial cells from the multiple layers of smooth muscle cells (red) forming the tunica media. The smooth muscle cells are lined externally by the external elastic lamina which is encased within the tunica adventitia composed primarily of collagen.

1.2 - Development of the vasculature

The primitive vasculature develops from the mesodermal germ layer during embryogenesis (Coffin and Poole 1988, Heimark, Degner et al. 1990). Hemangioblasts develop in the yolk sac mesoderm and form clusters of cells termed blood islands (Nishikawa, Hirashima et al. 2001), and these bipotential stem cells form both angioblasts and hematopoietic cells (Asahara and Kawamoto 2004). Angioblasts form the endothelial cells which comprise the tunica intima lining the lumen of the vasculature (Coffin and Poole 1988, Heimark, Degner et al. 1990), while the hematopoietic cells are the progenitors to the blood cells. Vascular endothelial growth factor (VEGF), produced by perivascular cells, induces proliferation and migration of these angioblasts within the extracellular matrix (ECM), forming the primitive vascular plexus, a process termed vasculogenesis (Shalaby, Rossant et al. 1995). This primitive network of vessels is subsequently extended by the sprouting of capillaries in a process termed angiogenesis (Risau 1997, Risau, Esser et al. 1998). The basal lamina separates the endothelial layer from interstitial collagens of the extracellular matrix (Liu and Senger 2004). During resting conditions, endothelial cell contact with laminin I of the basal lamina induces a quiescent state in the endothelial cells. During angiogenesis, however, sprouting endothelial cells are exposed to collagen I, a component of the ECM, and this interaction promotes disruption of cell-cell contacts between endothelial cells and capillary morphogenesis, thereby allowing the vascular remodelling required for angiogenesis (Liu and Senger 2004).

1.3 - The glycocalyx and the endothelial barrier

The vascular endothelium is lined by a negatively-charged surface coat of glycosaminoglycans, proteoglycans and adsorbed plasma proteins termed the glycocalyx (Luft 1966, Pries, Secomb et al. 2000). The negative charge of the glycocalyx is important in the control of endothelial permeability, inhibiting the attachment of both red blood cells (Busch, Ljungman et al. 1979, Ryan and Ryan 1984, Damiano 1998, Secomb, Hsu et al. 2001) and leukocytes (Mehta and Malik 2006). Furthermore, this layer selectively regulates the passage of molecules based on their charge (Adamson, Huxley et al. 1988, Bansch, Nelson et al. 2011) and acts as a mechanosensor detecting changes in blood flow (Florian, Kosky et al. 2003, Curry and Adamson 2012). Digestion of the frog mesenteric artery glycocalyx with pronase results in a 2.5 fold increase in capillary hydraulic conductivity (Lp),

indicating the importance of this layer in the maintenance of the endothelial barrier (Adamson 1990).

1.4 - The extracellular matrix

The extracellular matrix (ECM) makes a major contribution to endothelial barrier function (Qiao, Wang et al. 1995, Moy, Winter et al. 2000), and disruption of the ECM directly disturbs the endothelial barrier, increasing endothelial permeability (Partridge, Jeffrey et al. 1993). The ECM in direct contact with the endothelium is termed the basement membrane and is comprised of two layers, the basal lamina and the reticular lamina (Paulsson 1992). The basement membrane consists primarily of collagen IV, laminin, fibronectin, entactin, chondroitin sulphate and heparin sulphates (perlecan and syndecan) (Kalluri 2003). The basal lamina is further subdivided into a layer in direct contact with the endothelium, the lamina rara which contains primarily laminin, and a layer closer to the connective tissue, termed the lamina densa which contains type IV collagen. The components of the basal lamina are derived from the endothelial cells which it underlies, while the structures of the reticular lamina are synthesised by cells of the underlying connective tissue. The first stage in the formation of the ECM requires secretion of laminin by the endothelial cells. These laminin polymers are then able to bind β1-integrins on the endothelial cells (Albelda, Daise et al. 1989, Languino, Gehlsen et al. 1989). In addition to laminin, endothelial cells also produce collagen IV polymers (Kalluri 2003) and these directly interact with laminin polymers in the extracellular space. The result is the formation of a scaffold to which other ECM proteins are then able to attach, ultimately forming a basement membrane of high elasticity and tensile strength (Kalluri 2003). The release of such ECM proteins from the endothelial cells is evident only during vasculogenesis and angiogenesis (Akhta, Carlso et al. 2001, Kalluri 2003) and interaction between the ECM and the endothelial cells (through integrins) inhibits endothelial proliferation and migration (Form, Pratt et al. 1986).

1.4.1 - Endothelial cell–ECM interactions: Integrins and focal adhesions

Focal adhesions were initially identified through electron microscopy as electron-dense plaques associated with actin filament bundles (Abercrombie, Heaysman et al. 1971). These junctions allow firm association between cells and the ECM, are formed by members of the integrin family of transmembrane proteins, and link directly to actin filaments of the

cytoskeleton. Integrins are type I transmembrane glycoproteins that form heterodimers on endothelial cells and act as receptors for proteins of the ECM (Ruoslahti 1991). These heterodimers are specifically expressed at focal adhesions on endothelial cells, primarily at the abluminal side of the endothelium, thereby allowing direct endothelium-ECM interaction (Burridge, Fath et al. 1988). Integrins are transmembrane proteins consisting of a large ectodomain and a normally small cytoplasmic domain (Ruoslahti 1991), and subtypes are defined by unique combinations of alpha and beta subunits (Albelda, Daise et al. 1989). Endothelial cells express numerous integrin subunit compositions, among which are the fibronectin receptor α5β1 (Tarone, Stefanuto et al. 1990), the laminin and collagen receptor α1β1 (Defilippi, van Hinsbergh et al. 1991) and a multifunctional receptor that binds fibronectin, collagen and laminin α3β1 (Albelda, Daise et al. 1989, Cheng and Kramer 1989, Tarone, Stefanuto et al. 1990). Integrins interact with the Arg-Gly-Asp (RGD) domain of ECM proteins (Cheng and Kramer 1989, Conforti, Zanetti et al. 1989, Lampugnani, Resnati et al. 1991) and integrins bind various ECM proteins including fibronectin, laminin and collagen. Addition of a synthetic peptide to competitively disrupt integrin-ECM interactions induces endothelial cell rounding and increased endothelial permeability (Stickel and Wang 1988, Wu, Ustinova et al. 2001). Furthermore, in intact vessels, peptides inhibiting integrin-fibronectin or integrin-vitronectin interactions induce increased permeability of the venular endothelial barrier (Wu, Ustinova et al. 2001). In addition to extracellular interactions, integrins also play a role in intracellular interactions with the actin cytoskeleton. The short cytoplasmic tail of integrins binds various actin-binding proteins including vinculin, α-actinin and filamin (Geiger, Bershadsky et al. 2001). These actin-binding proteins subsequently bind signalling molecules and therefore link integrins to downstream signalling events. Filamin can bind RhoA, Rac and Cdc42 (Ohta, Suzuki et al. 1999), members of the Rho family of GTPases which can modulate the actin cytoskeleton. Similarly, the hinge region of vinculin interacts with both the Arp2/3 complex, recruiting this complex to new sites of integrin aggregation (DeMali, Barlow et al. 2002), and phosphatidylinositol 4,5-bisphosphate (PIP_2), both of which are involved in the regulation of the actin cytoskeleton (further detail on these signalling events will be detailed under "Section 5.1.9 – Rap1 activates Rac through Tiam1 and Vav2"). Integrins also interact with kinases, and Focal adhesion kinase (FAK) is a non-receptor protein tyrosine kinase that indirectly interacts with the cytoplasmic domain of the β-subunit of integrins (Brakebusch and Fassler 2003, Geiger, Spatz et al. 2009). This kinase is activated by tyrosine phosphorylation in response to integrin activation induced by cell-cell interaction and

adhesion (Schlaepfer and Mitra 2004). Activated FAK is subsequently able to bind to, and phosphorylate, WASP (Wiskott-Aldrich syndrome protein) which induces actin polymerisation (Zigmond 2000), thereby stabilising endothelial cell-cell contacts and strengthening the barrier function. Global deletion of FAK in mice is embryonically lethal at E8.5 as the endothelial cells are unable to migrate to form the mature vasculature (Ilic, Kovacic et al. 2003). Similarly, endothelial cell-specific deletion of FAK produces mice with apparently normal vascular development during early embryonic stages, but after E12.5 angiogenic defects are evident in the embryo, yolk sac and placenta, and embryos die at E13.5 (Shen, Park et al. 2005). These results indicate the importance of integrin engagement with the ECM for proper function of the endothelial barrier as disruption of this interaction results in increased endothelial permeability, hemorrhage and edema (Partridge, Jeffrey et al. 1993, Shen, Park et al. 2005). Integrins have also been implicated in the progression of several diseases including cancer (Desgrosellier and Cheresh 2010) and Alzheimers (Grace and Busciglio 2003).

1.5 - Endothelial cell-cell contact

The region of contact between adjacent endothelial cells varies dependent upon tissue and vessel type. In microvascular endothelium, endothelial cell contact domains are typically 0.5-0.9 μm in length (Franke, Cowin et al. 1988), while in arteries cell-cell contact sites can be between 3-10 μm (Rhodin 1974, Franke, Cowin et al. 1988). The intercellular gap between adjacent endothelial cells is typically 10-20 nm outside the regions of direct cell-cell contact (Franke, Cowin et al. 1988), and this intercellular cleft allows the selective paracellular passage of small molecules and ions.

1.6 - Endothelial cell architecture

Endothelial cells contain three primary cytoskeletal components; actin microfilaments, intermediate filaments and microtubules, and all three components play a role in the regulation of the endothelial barrier.

1.6.1 - Intermediate filaments and complexus adhaerens

Intermediate filaments are designated as such due to their average diameter of 10 nm, which is between that of actin microfilaments (typically 7 nm) and microtubules (25 nm) (Ishikawa, Bischoff et al. 1968). In endothelial cells, intermediate filaments are composed of polymers of vimentin and cytokeratin (Patton, Yoon et al. 1990), and these filaments display no polarity and can extend their length from either end (Mehta and Malik 2006). In epithelial cells, intermediate filaments are involved in cell-cell junctions and cell-ECM junctions at desmosomes and hemidesmosomes, respectively. These interactions involve the transmembrane proteins desmoglein and desmocollin, which are members of the cadherin family (Mechanic, Raynor et al. 1991, Garrod and Chidgey 2008). Endothelial cells do not develop desmosomes (Franke, Cowin et al. 1988, Rubin 1992, Lampugnani and Dejana 1997). Vimentin can be linked to AJs in structures similar to desmosomes, however, and these are termed complexus adherens (Schmelz and Franke 1993, Schmelz, Moll et al. 1994, Valiron, Chevrier et al. 1996, Kowalczyk, Navarro et al. 1998). γ-catenin forms a complex with VE-cadherin (further details in "Section 4.1.2.2.2") and this catenin is able to link vimentin to VE-cadherin through the intermediate filament-binding protein desmoplakin, thereby linking the AJ to the intermediate filament network (Shasby, Ries et al. 2002). Similarly, the AJ armadillo protein p0071 also binds desmoplakin, thereby providing an alternative link between the AJ and the intermediate filament network (Valiron, Chevrier et al. 1996, Calkins, Hoepner et al. 2003). The interaction between AJ components and the intermediate filament network is disrupted by inflammatory mediators, and 60 seconds histamine treatment is sufficient to disturb the intermediate filament/γ-catenin/VE-cadherin interaction (Shasby, Ries et al. 2002). Interestingly, however, vimentin knock-out mice lack endothelial cell intermediate filaments but no abnormalities in phenotype or cell architecture were detected (Colucci-Guyon, Portier et al. 1994), indicating either a redundancy of intermediate filaments or a potential compensatory effect of other cytoskeletal components. In vivo inactivation of the desmoplakin gene, on the other hand, results in vascular defects including a reduced number of capillaries (Gallicano, Bauer et al. 2001). This defective vascular development was hypothesised to be due to a lack of correct organisation of the complexus adhaerens. Interestingly, the desmoplakin knock out phenotype was more severe than that detected in γ-catenin null embryos, thereby indicating the redundancy between armadillo proteins (Gallicano, Bauer et al. 2001).

1.6.2 - Microtubules

Microtubule networks provide pathways for the motor proteins dynein and kinesin, thereby allowing intracellular transport of proteins throughout the cell (Wade and Hyman 1997, Krylyshkina, Kaverina et al. 2002). Microtubules are formed from heterodimers organised by self-assembly of α and β tubulins, each with a molecular mass of 55 kDa (Chrétien and Wade 1991). These subunits interact in a head-to-tail fashion to form protofilaments aligned lengthwise along the microtubule (Chrétien and Wade 1991, Wade and Hyman 1997). These protofilaments then form lateral contacts with adjacent protofilaments to construct a hollow tube with a lumen diameter of approximately 12 nm (Kikkawa, Ishikawa et al. 1994). Typically, 13 or 14 protofilaments assemble to make a single microtubule, dependent upon the cell type (Chretien, Metoz et al. 1992). These rigid hollow rods span the cell from the nucleus to the periphery, resisting compression of the cell by opposing actin-myosin contractility (Mehta and Malik 2006). Unlike intermediate filaments, microtubules are polarised, with a faster-growing plus-end which is attached to the cortical actin layer on the inner face of the plasma membrane, and a slower-growing minus end. This plus-end is composed of β tubulin that binds to and hydrolyses GTP to GDP, thereby allowing 'dynamic treadmilling' where the microtubule switches between addition and removal of tubulin dimers to allow lengthening and shortening of the microtubule, respectively (Waterman-Storer and Salmon 1997, Grego, Cantillana et al. 2001). The minus end is composed of α tubulin and is able to bind to GTP but not hydrolyse it into GDP. These minus ends are typically joined at a common attachment site known as the microtubule-organising centre (MTOC). Although microtubules do not directly interact with cell junctions they mediate delivery of cell junction components to the cell surface and specifically to sites of cell-cell contact (Vincent, Xiao et al. 2004). p120 catenin, a component of the AJ complex, directly interacts with the heavy chain of the microtubule motor protein kinesin in non-endothelial cells (Chen, Kojima et al. 2003, Yanagisawa, Kaverina et al. 2004). As previously mentioned, these motor proteins regulate vesicular trafficking and therefore microtubule-delivery of AJ components may be targeted to the AJ by p120 catenin, thereby enhancing the endothelial barrier. In addition to components of the AJ, microtubules also mediate the delivery of connexin hemichannels to the plasma membrane to form functional gap junction channels (Jordan, Solan et al. 1999, Lauf, Giepmans et al. 2002, Shaw, Fay et al. 2007). These proteins can be selectively targeted to sites of cell-cell contact through preferential tethering of the microtubule plus-end at AJs. This involves microtubule plus-end tracking proteins called TIPS. EB1 is a dimeric TIP that

associates directly with this region of the microtubule. EB1 also has dual binding sites for a component of the dynein/dynactin complex, p150 (Glued), at its C-terminus (Berrueta, Tirnauer et al. 1999, Askham, Vaughan et al. 2002). β-catenin, a component of AJs, also binds dynein and therefore is suggested to link the microtubule plus-end to AJs (Chausovsky, Bershadsky et al. 2000, Ligon, Karki et al. 2001). In support of this preferential targeting of microtubule plus-ends to sites of cell-cell contact, Shaw *et al.* (2007) identified that the microtubule plus-end approached gap junction plaques more frequently than the remainder of the cortical membrane in HeLa cells transfected with the gap junction component Cx43. In addition, these experiments also identified that siRNA knock down of EB1, p150 (Glued) and β catenin disrupted gap junction formation in these transfected HeLa cells (Shaw, Fay et al. 2007). Similarly, inhibition of the motor protein activity of kinesin-1 (Krylyshkina, Kaverina et al. 2002) or addition of the depolymerising agent nocodazole (Verin, Birukova et al. 2001), resulted in decreased cell-substrate adhesion and increased endothelial permeability, respectively. The microtubule network is therefore essential for proper endothelial barrier function.

1.6.3 - The actin network

The actin network plays the greatest role in the control of endothelial permeability out of the three cytoskeletal components discussed here, and this is primarily due to its involvement in endothelial contraction. Endothelial F-actin exists in one of three subtypes within the cell cytoskeleton; the outer membrane skeleton, a cortical actin rim, and numerous cytosolic stress fibres. The outer membrane skeleton and the cortical actin rim are composed of short F-actin filaments, while stress fibres are formed from long F-actin bundles. The outer membrane skeleton is primarily composed of networks of spectrin fibres which are responsible for the interaction between cadherins, catenins and the cortical actin rim (further detail under “Section 4.1.2.2.2”). The cortical actin rim is responsible for the generation of outward centrifugal tension, ultimately ensuring the cell does not collapse in on itself due to the centripetal tension generated by the actin stress fibres (see below). The cytoplasmic actin stress fibres are closely associated with myosin motor proteins which track along the fibres to form actomyosin contractile bundles. As such, the endothelial contractile machinery consists of actin and non-muscle myosin, and requires ATP, calcium and calmodulin to generate contractile force (Surapisitchat and Beavo 2011). Bundles of polymerised actin and myosin filaments form the stress fibres which traverse the cell and form the primary elements of the endothelial cell contractile

machinery (Dudek and Garcia 2001). Actinomyosin-generated endothelial contraction requires phosphorylation of myosin light chain (MLC) on Ser19, termed mono-phosphorylation, or on both Ser19 and Thr18, termed di-phosphorylation, mediated by MLC kinase (MLCK) (Goeckeler and Wysolmerski 1995). MLCK is a calcium/calmodulin-dependent enzyme and therefore explains the requirement for calcium for actinomyosin-generated contraction (Mehta and Malik 2006). In human endothelial cells, MLCK is a 214 kDa protein encoded from a single gene on chromosome 3 (Dudek and Garcia 2001). Inflammatory mediators typically promote endothelial contraction to induce inter-endothelial cell gap formation to allow enhanced paracellular transport. Endothelial cell MLCK -/- mice are protected from increased lung vascular permeability induced by the injection of lipopolysaccharide (LPS) due to an inability to stimulate endothelial cell contraction (Wainwright, Rossi et al. 2003). Endothelial barrier stabilisers, on the other hand, typically inhibit endothelial cell contraction to prevent enhanced paracellular transport and tighten the endothelial barrier. Specific factors promoting or inhibiting endothelial contraction are detailed under "Section 1.12 - Barrier de-stabilisers" and "Section 1.13 - Barrier stabilisers".

In addition to the regulation of endothelial contraction, the actin cytoskeleton is also involved in the regulation of the endothelial barrier through interaction with components of anchoring, occluding and communicating junctions. In endothelial cells, the primary anchoring junctions are the adherens junctions (AJs). The occluding junctions of the vascular endothelium are the tight junctions (TJs) which were originally thought to form an impermeable barrier to paracellular transport but are now considered to act as selective inhibitors to such transport. Finally, the communicating junctions of the endothelium allow the direct exchange of chemical and electrical signals between adjacent cells, and are termed gap junctions (GJs). All three junction types are shown in Figure 1.2.

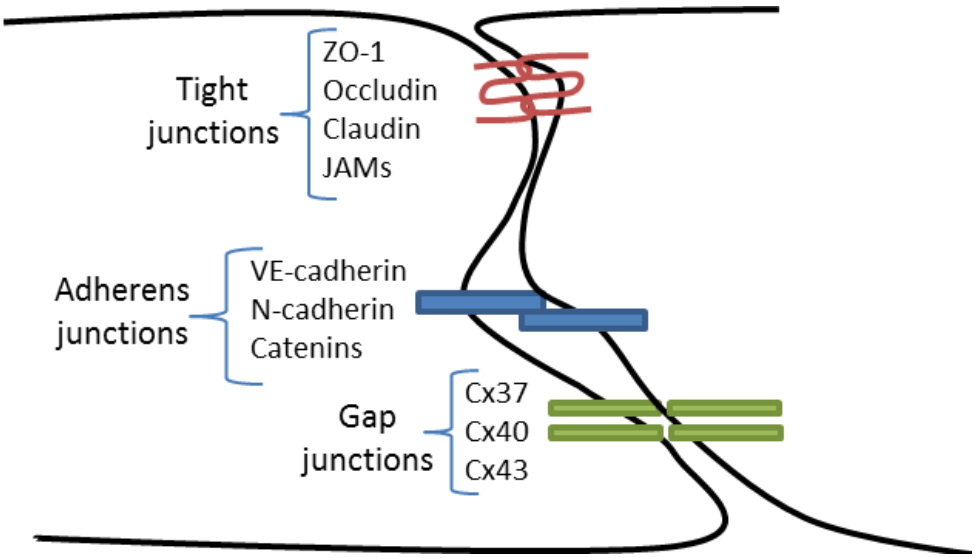

Figure 1.2: Cell junctions in endothelial cells

Three main types of cell junctions are found in vascular endothelial cells; tight junctions, adherens junctions and gap junctions. Tight junctions (red) are primarily formed from occludin and claudin with a contribution from ZO-1 and other junctional adhesion molecules (JAMs). In epithelia and other polarised cells, these are restricted to the apical region, however in endothelial cells tight junctions show a less restricted distribution. In endothelial cells, adherens junctions (AJs, blue) are formed primarily from VE-cadherin, although N-cadherin is also expressed in these cells. Cadherins interact with members of the Armadillo family of proteins to link to the actin cytoskeleton. Gap junctions (green) are formed from connexin proteins and connexin 37, 40 and 43 are expressed in the vascular endothelium. These junctions are channels that allow the direct exchange of ions and second messengers between adjacent cells.

1.7 - Adherens junctions

Endothelial cell adherens junctions consist primarily of vascular endothelial-cadherin (VE-cadherin) complexes, which include catenins, and nectins (Noda, Zhang et al. 2010), the latter of which are likely to mediate initial cell-cell contacts allowing cadherin interaction and the formation of mature adherens junctions (AJs) (Wallez and Huber 2008). Nectins are part of the immunoglobulin family with four subtypes (1-4), of which nectin 2 and nectin 3 are expressed in endothelial cells (Lopez, Aoubala et al. 1998). Nectin interaction is calcium-independent and can be either homotypic or heterotypic, binding to other nectin subtypes (Takai, Irie et al. 2003). The C-terminus of nectin interacts directly with the PDZ (postsynaptic density protein-95/ discs large/ ZO-1) domain of the actin-binding protein AF-6, and the nectin/AF-6 complex associates with both tight junctions and AJs (Takahashi, Nakanishi et al. 1999, Takai and Nakanishi 2003). Nectin is therefore able to recruit further AJ components to the AJ (Irie, Shimizu et al. 2004).

Cadherins are responsible for the calcium-dependent homotypic or hetertypic interaction of AJs (see Figure 1.3). These surface glycoproteins have a molecular mass of 120-140 kDa (Geiger and Ayalon 1992), and were initially identified within AJs through electron microscope analysis (Boller, Vestweber et al. 1985, Volk and Geiger 1986) and immunofluorescence (Volk, Geiger et al. 1984, Volk and Geiger 1986). Cadherins are comprised of a long extracellular domain, a transmembrane domain and a short cytoplasmic domain. The extracellular region consists of the N-terminus and 5 cadherin-like repeats (Liaw, Cannon et al. 1990, Lampugnani, Resnati et al. 1992). These 5 external domains are subdivided into two groups; EC1-3 are interhomologous ectodomains, each approximately 110 amino acids long, while EC4 and EC5 are less homologous repeats (Takeichi 1990). It is these extracellular domains that determine the specificity of cadherin-cadherin interactions and allow the formation of trans-oligomers between adjacent cells (Liaw, Cannon et al. 1990, Lampugnani, Resnati et al. 1992), while modification of the EC5 domain affects the reactivity and stability of the cadherin molecule (Ozawa, Hoschützky et al. 1990). Each extracellular region (EC1-5) expresses 2 putative calcium-binding sites (Ringwald, Schuh et al. 1987, Ozawa, Engel et al. 1990), and a single amino acid substitution in the calcium binding site of EC1 has the ability to abolish the adhesive potential of the molecule (Ozawa, Engel et al. 1990). Similarly, culture in low calcium medium induces splitting of AJs (Nilsson, Fagman et al. 1996). Taken together, this indicates the calcium-dependent nature of cadherin interactions. The presence of extracellular calcium also

protects cadherins from proteolytic degradation (Yoshida and Takeichi 1982, Vestweber and Kemler 1985), with cadherins displaying increased sensitivity to trypsinisation in the absence of calcium (Takeichi 1988). The cytoplasmic tail of cadherins is highly conserved between subtypes, although this region shows no similarity to the respective region in desmogleins or desmocollins, which are additional members of the cadherin family (Geiger and Ayalon 1992). This lack of similarity may allow these desmosome/hemi-desmosome components to bind to intermediate filaments instead of actin filaments like classical cadherins. The cadherin cytoplasmic tail is sub-divided into 2 functional domains; the juxtamembrane domain and the COOH-terminal domain. The juxtamembrane domain is responsible for cadherin-p120 catenin and cadherin-p0071 interactions, and the COOH-terminus binds to either β-catenin or γ-catenin in a mutually-exclusive manner (Zhurinsky, Shtutman et al. 2000, Bazzoni and Dejana 2004). With the exception of T-cadherin, a truncated form of cadherin with no cytoplasmic domain (Vestal and Ranscht 1992), cadherin-catenin interaction is essential for maturation of the AJ (Nagafuchi and Takeichi 1988, Ozawa, Ringwald et al. 1990). Classical cadherins are subdivided into Type I and Type II cadherins. Type I cadherins, such as neural-cadherin (N-cadherin) and epithelial-cadherin (E-cadherin), express a conserved histadine-alanine-valine (HAV) tripeptide motif in EC1, while type II cadherins, including VE-cadherin, lack this sequence (Blaschuk, Sullivan et al. 1990, Tanihara, Sano et al. 1994, Halbleib and Nelson 2006). Numerous cadherin subtypes exist but for the purpose of this study only those identified within vascular endothelial cells will be detailed. As previously mentioned, VE-cadherin forms the predominant cadherin of endothelial AJs. In addition to this cadherin, endothelial cells have also been shown to express N-cadherin (Navarro, Caveda et al. 1995, Liebner, Gerhardt et al. 2000, Williams, Williams et al. 2001), T-cadherin (Ivanov, Philippova et al. 2001), placental-cadherin (P-cadherin) (Rubin 1992) and VE-cadherin 2 (protocadherin 12) (Telo, Breviario et al. 1998, Rampon, Prandini et al. 2005). T-cadherin has been identified in the endothelial cells of human aorta tissue sections (Ivanov, Philippova et al. 2001), while P-cadherin expression has been identified in endothelial cells through PCR analysis but not through antibody staining (Rubin 1992). VE-cadherin 2 has been identified at inter-endothelial junctions, primarily in endothelium undergoing angiogenesis, and interestingly has a completely un-related cytoplasmic tail to other cadherins (Telo, Breviario et al. 1998). N-cadherin, although widely expressed in endothelial cells, is typically not involved in AJs as it is out-competed for membrane distribution by VE-cadherin (Salomon, Ayalon et al. 1992, Navarro, Ruco et al. 1998). Further detail on the competitive nature between VE-cadherin

and N-cadherin is detailed under “Section 4.4.11 - N -cadherin in HCAECs”. Although not significantly involved in inter-endothelial junctions, N-cadherin is thought to promote communication with mesenchymal cells also expressing N-cadherin *in vivo*, including pericytes, smooth muscle cells and astrocytes (Geiger and Ayalon 1992). Indeed, N-cadherin has been identified clustered at the basal surface of endothelial cells, directly in contact with pericytes and astrocytes in the brain (Liebner, Gerhardt et al. 2000). Further detail on VE-cadherin and its interaction with catenins can be found in Chapter 4: Connexins and Cadherins in HCAECs and HCASMCs.

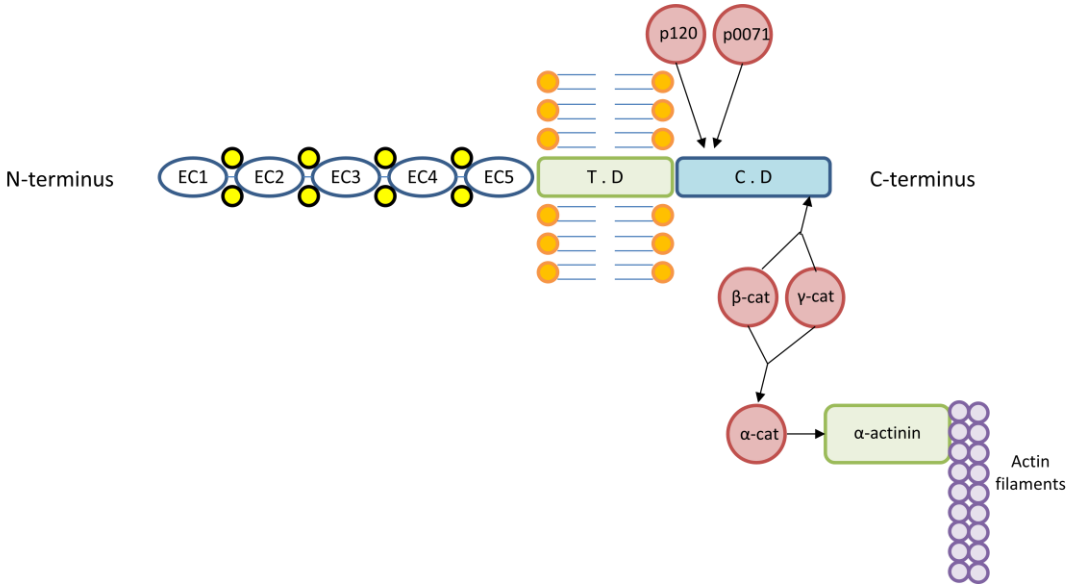

Figure 1.3: Classical cadherin structure

This schematic represents the structure of a classical cadherin such as VE-cadherin or N-cadherin. The extracellular region consists of the N-terminus and 5 extracellular domains (EC1-5), each of which expresses two calcium-binding sites (yellow). The transmembrane domain (T.D) is shown in green. The cytoplasmic domain (C.D, blue) is sub-divided into a juxtamembrane domain where the armadillo proteins p120 and p0071 bind (represented in red), and a COOH-terminal domain where either β-catenin or γ-catenin bind (represented in red). β-catenin and γ-catenin are able to bind α-catenin which binds α-actinin (green) and links the cadherin/catenin complex to the actin cytoskeleton (purple).

1.8 - Tight junctions

Tight junctions were originally identified by electron microscopy as distinct points where the outer layers of the lateral membranes of adjacent endothelial cells fused (Farquhar and Palade 1963). These junctions are considered to represent approximately 20% of the total junctional complexes in endothelial cells (Wojciak-Stothard, Potempa et al. 2001), and consist of claudins, occludins and junctional adhesion molecules (JAMs) (Noda, Zhang et al. 2010). These occluding junctions regulate paracellular permeability and maintain cell polarity, effectively dividing the endothelial cell membrane into an apical region that is directed towards the vessel lumen, and a basolateral region that faces the perivascular space (Bazzoni and Dejana 2004). Tight junctions vary markedly in their distribution patterns in different vascular beds, depending upon the requirement for endothelial permeability. Freeze fracture studies identified that arterial segments of the intrapulmonary vasculature display approximately twice as many tight junctions as venular segments from the same vascular bed (Schneeberger 1982). Similarly, large artery endothelial cells have been shown to display a well-developed tight junction system while tight junctions of capillaries are less complex (Wallez and Huber 2008). Furthermore, the blood-brain barrier (BBB) and blood-retinal barrier (BRB) which require an almost impermeable endothelial barrier are both rich in tight junctions (Wallez and Huber 2008). Post-capillary venules are the predominant site of increased endothelial permeability induced by inflammatory mediators, and these vessels have poorly organised tight junctions (Bazzoni and Dejana 2004).

1.8.1 – Tight junction components

1.8.1.1 - ZO-1

Zonula occludins-1 (ZO-1) was the first intracellular component of tight junctions to be discovered, and was named after the alternative name for the tight junction, the zonula occludins (Stevenson, Siliciano et al. 1986). Three subtypes of ZO proteins exist, and these belong to a family of membrane-associated guanylate kinases (MAGUK) (Bazzoni and Dejana 2004). These proteins consist of a PDZ domain , an SH3 (Src homology 3) domain and a guanylate kinase domain (Bazzoni and Dejana 2004). Calcium-dependent intercellular adhesion is required for localisation of ZO-1 to tight junctions (Siliciano and Goodenough 1988). Once at the tight junction, ZO-1 becomes insoluble in non-ionic detergents, indicating a strong association with the cortical actin rim (Anderson, Stevenson et al. 1988).

This cytoskeletal interaction is supported by co-precipitation of ZO-1 with F-actin (Itoh, Nagafuchi et al. 1997, Fanning, Jameson et al. 1998), an interaction that requires a 220 amino acid region in the C-terminal half of ZO-1, termed the actin-binding region (ABR) (Fanning, Ma et al. 2002). Indeed, it appears that this ABR is required for accumulation of ZO-1 at the free edge of cells prior to cell-cell contact formation, and once established, at the tight junction (Fanning, Ma et al. 2002). The N-terminal domain of ZO-1 interacts with the C-terminal domain of the gap junction component connexin 43 (Cx43) in cardiac myocytes, and therefore provides a link between tight junctions and gap junctions (Toyofuku, Yabuki et al. 1998). Indeed, over-expression of a dominant-negative mutant form of ZO-1 lacking the N-terminal domain required for Cx43 interaction led to re-distribution of Cx43 away from sites of cell-cell contact (Toyofuku, Yabuki et al. 1998).

1.8.1.2 - Occludin

In 1993 occludin was the first transmembrane protein to be identified in tight junctions through the use of monoclonal antibodies raised against the junctional fraction of chick liver cells (Furuse, Hirase et al. 1993). This 65 kDa protein consists of 4 putative membrane-spanning domains, 2 extracellular loops and cytoplasmic N- and C-termini (Furuse, Hirase et al. 1993). Occludin is exclusively localised to the tight junction in both epithelial and endothelial cells, and cell-cell adhesion is likely to be dependent upon the conserved first extracellular loop as synthetic peptides corresponding to this region inhibit adhesion (Van Itallie and Anderson 1997). Occludin is not required for tight junction formation and requires claudin expression to localise to tight junctions (Furuse, Sasaki et al. 1998), but this protein is associated with enhanced tight junction barrier function. This is reflected in the expression of 18-fold more occludin protein in human arterial endothelial cells than human venous endothelial cells, a region that is targeted for increased endothelial permeability during inflammation (Kevil, Okayama et al. 1998). Furthermore, occludin is highly expressed in the endothelial cells forming the BBB and BRB and its down-regulation is associated with stroke (Brown and Davis 2002) and diabetes (Antonetti, Barber et al. 1998), diseases that involve the regulation of permeability in the BBB and BRB, respectively. Occludin -/- mice, however, show no gross alterations in endothelial tight junction morphology (Saitou, Furuse et al. 2000), indicating that a loss of occludin may be compensated for by increased adherens junctions or additional tight junction components. These mice do, however, display chronic inflammation and hyperplasia of the gastric

epithelium, suggesting that occludin may play a role in other, unknown, downstream processes (Saitou, Furuse et al. 2000).

1.8.1.3 - Claudin

Claudin proteins are the primary component of endothelial tight junctions and are capable of both homophilic binding and heterophilic binding (between various claudin subtypes) (Furuse, Sasaki et al. 1999, Furuse and Tsukita 2006). Like occludins, claudins also consist of 4 membrane-spanning regions, 2 extracellular loops and 2 cytoplasmic termini (Bazzoni and Dejana 2004). These 22 kDa proteins, however, display no sequence similarity to occludin (Morita, Furuse et al. 1999). Endothelial cells specifically express claudin 5, claudin 3, claudin 11 and claudin 15 (Furuse, Sasaki et al. 1999, Kiuchi-Saishin, Gotoh et al. 2002, Wolburg, Wolburg-Buchholz et al. 2003, Enerson and Drewes 2006). Claudin 5 is the predominant form found in endothelial tight junctions, and claudin 5-deficient mice display a selective impairment in the BBB function for molecules smaller than 800 Da and die approximately 10 hours after birth (Nitta, Hata et al. 2003). Different claudin subtypes produce various tight junction profiles; claudin 1-based tight junctions are continuous and associated with the inner face of the inner lipid monolayer, while claudin 2-based tight junctions are fragmented and associated with the inner face of the outer lipid monolayer (Furuse, Sasaki et al. 1998). Claudin 5 is also located at the E-face of the plasma membrane, and such tight junctions are considered to be more 'leaky' than those associated with the P-face (Furuse, Sasaki et al. 1998, Morita, Sasaki et al. 1999). In addition to its extracellular interactions, the cytoplasmic domain of claudin also interacts with the first PDZ domain of ZO-1 (Itoh, Furuse et al. 1999).

1.8.1.4 - JAMs

Junctional adhesion molecules (JAMs) are additional components of endothelial tight junctions (Martin-Padura, Lostaglio et al. 1998). JAMs are a family of single-pass transmembrane adhesive proteins of the immunoglobulin superfamily (Aurrand-Lions, Duncan et al. 2000). These proteins have a long extracellular domain that allows homophilic adhesive activity, thereby reducing paracellular permeability (Martin-Padura, Lostaglio et al. 1998). JAMs also possess a cytoplasmic PDZ domain that may allow JAMs to recruit signalling molecules to the tight junction complex (Ebnet, Schulz et al. 2000). Three subtypes exist; JAM-A, JAM-B and JAM-C. JAM-A (also called hu-JAM) is a 32 kDa

glycoprotein expressed at both epithelial and endothelial intercellular junctions, in addition to the surface of platelets and leukocytes (Martin-Padura, Lostaglio et al. 1998, Williams, Martin-Padura et al. 1999). The extracellular domain of JAM-A contains 2 immunoglobulin-like domains, C-terminal folds and the N-terminal (Williams, Martin-Padura et al. 1999). JAM-A is also capable of binding both the tight junction component ZO-1 and the actin-binding protein AF-6 (Bazzoni, Martinez-Estrada et al. 2000, Ebnet, Schulz et al. 2000). Addition of a blocking antibody or recombinant fragment of JAM-A inhibits transepithelial electrical resistance (TER), a marker of a tight endothelial barrier (Liang, DeMarco et al. 2000). Unlike JAM-A, JAM-B is restricted to inter-endothelial junctions, particularly in post-capillary endothelial cells and lymphatic vessels (Cunningham, Arrate et al. 2000, Palmeri, van Zante et al. 2000). The final form, JAM-C, is expressed only in endothelial cells and is able to bind firmly to the Fc region of JAM-B (Arrate, Rodriguez et al. 2001).

Endothelial cell-specific adhesion molecule (ESAM) is a transmembrane immunoglobulin protein related to JAMs that is expressed in endothelial tight junctions and mediates homotypic binding (Hirata, Ishida et al. 2001). ESAM binds MAGI in the cytoplasm, recruiting it to cell-cell contacts (Wegmann, Ebnet et al. 2004). MAGI is an adaptor protein that interacts with adherens junctions, and ESAM therefore provides an additional link between tight junctions and adherens junctions. Coxsackievirus and adenovirus receptor (CAR) is an additional immunoglobulin-like protein with a similar extracellular profile to JAMs (Cohen, Shieh et al. 2001). CARs participate in tight junction assembly and regulate paracellular permeability (Cohen, Shieh et al. 2001).

Additional components of endothelial tight junctions include cingulin (Citi, Sabanay et al. 1988), 7H6 (Satoh, Zhong et al. 1996), Rab3b (Weber, Berta et al. 1994) and Rab13 (Zahraoui, Joberty et al. 1994). In contrast to the traditional view of tight junctions as an impermeable barrier to paracellular transport, these structures are now considered to act as paracellular channels, selectively allowing passage of specific molecules, and thereby contributing to the regulation of endothelial permeability (Bazzoni and Dejana 2004).

1.9 - Gap junctions

Gap junctions (GJs) form between adjacent cells to provide a low-resistance pathway for direct cell-cell communication via the exchange of chemical signals and electrical current (Carter and Ogden 1994). Gap junctions are essential for proper cell-cell communication and few terminally-differentiated cells do not communicate via these channels (skeletal muscle cells, erythrocytes and circulating lymphocytes) (Kumar and Gilula 1996). Within the vasculature, these channels are able to form both within, and between, cell layers and therefore mediate both endothelial cell-endothelial cell communication, and communication between the endothelium and additional vascular cells (including smooth muscle cells and pericytes) (Figueroa, Isakson et al. 2004). These channels are relatively non-selective, with a pore diameter of approximately 2 nm (De Mazière, Analbers et al. 1993, Goldberg, Valiunas et al. 2004), allowing the passive transfer of ions and second messenger molecules up to ~ 1,200 Da (Simpson, Rose et al. 1977, Elfgang, Eckert et al. 1995, Veenstra, Wang et al. 1995, Sáez, Berthoud et al. 2003). Gap junction channels are involved in a number of processes including the transmission of action potentials between excitable cells, such as in the heart (Simon, Goodenough et al. 1998), the passive diffusion of metabolites and nutrients (Goldberg, Lampe et al. 1999), and the exchange of second messengers such as calcium, inositol-1,4,5-trisphosphate (IP_3) and cyclic nucleotides (Saez, Connor et al. 1989). Interestingly, the exchange of calcium between GJ-coupled cells has been shown as a wave approaching the GJ and subsequently appearing in the neighbouring cell in transfected HeLa cells (Paemeleire, Martin et al. 2000, Evans and Martin 2002). Similarly, in rat aortic endothelial cells, changes in membrane potential were found to rapidly propagate between adjacent cells as detected by whole-cell patch clamp experiments (Carter and Ogden 1994). Rat pulmonary microvessel endothelium has also been shown to display longitudinal calcium waves in situ, presumably propagated by such GJ channels (Carter and Ogden 1994). Interestingly, Cx43 GJ aggregations in endothelial cells have been shown to measure approximately 8 times as large as aggregations in smooth muscle cells from the same vascular bed (Haas and Duling 1997), and as such endothelial cells have been proposed to represent a more permissive pathway for the longitudinal conduction of signals along the vessel wall. In the vasculature, such communication between adjacent cells is essential for the proper control of both endothelial barrier function and to mediate changes in vessel diameter in response to changes in blood flow (Dora 2001, Berman, Martin et al. 2002). Gap junction structure and formation, as well as details on connexin proteins and subtypes, is detailed in Chapter 4:

Connexins and Cadherins in HCAECs and HCASMCs. The effect of gap junction dysfunction in disease and knock out models is also detailed in this chapter. Gap junction turnover is detailed in Chapter 5: Control of Cadherin and Connexin Distribution, and gap junction selectivity and gating is detailed in Chapter 6: Functional Effect of Epac activation in HCAECs.

1.10 - cAMP

1.10.1 - Generation of cAMP – Adenylate cyclases

Cyclic adenosine monophosphate (cAMP) is a small water-soluble second messenger generated by adenylate cyclases (ACs) on ligand binding to a G-protein-coupled receptor (GPCR). Due to its ability to rapidly diffuse throughout the cytosol, cAMP is utilised to mediate a number of downstream signalling events. Binding of a specific extracellular signal to the GPCR induces a conformational change that allows the receptor to activate the associated trimeric GTP-binding protein (G-protein). This G-protein is coupled to a large multi-pass transmembrane protein, adenylyl cyclase (AC), which displays its catalytic domain on the cytosolic surface of the plasma membrane. Activation of this membrane protein induces the generation of cAMP from ATP. The resting concentration of cAMP within the cell is typically less than 10 nM but this concentration can increase up to 20 fold within seconds on binding of the appropriate ligand to the GPCR (Real-time monitoring of cAMP levels in living endothelial cells: thrombin transiently inhibits adenylyl cyclase 6, werthmann, 2009). Such ligands include epinephrine, norepinephrine and prostaglandin, among others. Several isoforms of ACs exist and AC_6 is the predominant isoform expressed in endothelial cells (Stevens, Nakahashi et al. 1995). AC_6 is a type IV calcium-inhibitable AC that is responsible for the majority of cAMP synthesised in endothelial cells (Stevens, Nakahashi et al. 1995, Cioffi, Moore et al. 2002). In contrast to AC_6, AC_8 is a calcium-stimulable AC, and over-expression of AC8 in endothelial cells using an adenoviral construct induces an elevation in cAMP (Cioffi, Moore et al. 2002). In addition to membrane-tethered ACs, soluble ACs also localise outside of membranous compartments (Sayner, Alexeyev et al. 2006). These ACs synthesize cAMP in a cytosolic pool and interestingly this alternative pool of cAMP produces different downstream effects to that generated in the membrane compartment, thereby highlighting the importance of cAMP compartmentalisation for specific downstream signalling events (Sayner, Alexeyev et al. 2006, Prasain, Alexeyev et al. 2009).

1.10.2 - Degradation of cAMP – Phosphodiesterases

The intracellular concentration of cAMP is also regulated by phosphodiesterases (PDEs). PDEs decrease the intracellular concentration of cAMP or cGMP by degrading the phosphodiester bond in these second messenger molecules. As a result, cAMP is hydrolysed to adenosine 5'-monophosphate (5'AMP). Various isoforms of PDEs exist and endothelial cells primarily express the cGMP-stimulated PDE2, the cGMP-inhibited PDE3, the cAMP-specific PDE4 and the cGMP-specific PDE5 (Netherton and Maurice 2005). Within endothelial cells, cAMP hydrolysis is primarily mediated by PDE3 and PDE4 (Lugnier and Schini 1990, Netherton and Maurice 2005). The relative contribution of these PDEs appears to vary between vascular beds and over the culture period. Early passage bovine aortic endothelial cells (BAECs, passages 4-6) typically express both PDE2 and PDE4, while BAECs at passage 10 and later predominantly express PDE4 (Ashikaga, Strada et al. 1997). PDEs also appear to be at least partly responsible for the compartmentalisation of cAMP. PDE4D4 is a splice variant of PDE4 expressed in pulmonary microvasulature endothelial cells and detected in plasma membrane fractions (Creighton, Zhu et al. 2008). PDE4D4 interacts with α-II spectrin, a component of the actin cytoskeleton that localises to the inner surface of the plasma membrane (Creighton, Zhu et al. 2008). The interaction between PDE4D4 and α-II spectrin therefore inhibits the spread of cAMP away from the membrane pool. Additional endothelial PDE isoforms include the calcium/calmodulin-regulated PDE1 and the cAMP-specific PDE7A (Keravis, Komas et al. 2000, Miro, Casacuberta et al. 2000).

1.11 - The cAMP pathway in endothelial cells

Three classes of proteins containing cyclic nucleotide-binding (CNB) domains have been shown to be regulated by cAMP; cAMP-dependent protein kinase (PKA), cyclic nucleotide-gated ion channels and exchange proteins directly activated by cAMP (Epacs)(Rehmann 2013).

1.11.1 - Protein Kinase A

The cAMP-dependent protein kinase (PKA) was first identified in rabbit skeletal muscle by Walsh *et al.* in 1968, and is, as its name suggests, entirely dependent upon cAMP for its activation (Walsh, Perkins et al. 1968). PKA holoenzymes consist of two regulatory subunits (R) each of which contain two cAMP-binding sites, and two catalytic (C) subunits that carry out the kinase activity of PKA. The binding of four cAMP molecules to a dormant PKA

holoenzyme results in a conformational change that releases the two C subunits from the regulatory subunit-cAMP complex, thereby activating PKA. Two R subunit classes are known to exist and it is these that distinguish between Type I and Type II holoenzymes (Corbin, Keely et al. 1975). Local cAMP levels must exceed threshold for PKA activation to occur, and four cAMP molecules are required for dissociation of the regulatory complex and activation of PKA. cAMP is rapidly metabolised to adenosine monophosphate (AMP) by phosphodiesterases leading to re-binding of the regulatory subunit. This may suggest that PKA must be co-localised with adenylate cyclase or contained within a cellular compartment that is able to concentrate cAMP levels in order to retain its kinase activity. In addition, PKA is a multifunctional enzyme, with over 30 hormones known to utilise its activation for downstream signalling (Coghlan, Bergeson et al. 1993). PKA compartmentalisation therefore provides a means to rapidly respond to local increases in cAMP concentrations and also regulate the downstream targets phosphorylated by PKA. The Type II R subunit previously mentioned is responsible for this compartmentalisation, and hormones preferentially activate each holoenzyme in a tissue-specific manner (Coghlan, Bergeson et al. 1993). In rat hepatocytes, for example, 0.1 µM -5 µM db-cAMP activates Type I PKA while elevation to 10 µM db-cAMP triggers activation of Type II PKA, with glucagon causing a similar response (Byus, Hayes et al. 1979). PKA holoenzymes are known to associate with the plasma membrane (Rubin, Erlichman et al. 1972), the golgi complex, the cytoskeleton and secretory granules (Joachim and Schwoch 1990). Joachim and Schwoch (1990) identified both the Type I and Type II PKA to be localised within the cisternae of the rough endoplasmic reticulum (rER) and in the golgi complex of rat pancreas and parotid cells, with the secretory granules of the parotid acinar cells also preferentially expressing Type II PKA (Joachim and Schwoch 1990). Interestingly, the proportion of Type II PKA within these secretory granules was found to increase on application of the cAMP agonist isoproterenol, indicating a role of Type II PKA in cAMP-mediated amylase secretion. Furthermore, Type II PKA was also localised to the Golgi complex in cells of the nervous system (De Camilli, Moretti et al. 1986), epithelial cells and fibroblasts (Nigg, Schafer et al. 1985). A-kinase anchoring proteins (AKAPs) have been found to tether Type II PKA to such specific subcellular locations through interaction with its RII subunit (Carr, Hausken et al. 1992). Indeed, all AKAPs have been shown to possess a conserved RII-binding site thought to be constructed of amphipathic helices (Carr, Hausken et al. 1992, Carr, Stofko-Hahn et al. 1992). In addition to the RII-binding domain, all AKAPs also contain a unique targeting domain which determines the specific subcellular localisation of the AKAP/PKA complex

(Coghlan, Bergeson et al. 1993). The AKAP MAP2, for example, links Type II PKA to microtubules (Obar, Dingus et al. 1989), and is the primary microtubule-associated protein in cells of the mammalian central nervous system (De Camilli, Moretti et al. 1986, Obar, Dingus et al. 1989). This AKAP binds the RII domain of PKA via an 83 amino acid stretch at its N-terminal end, and microtubules via its microtubule-binding domain at its carboxyl-terminus, and thus forms a Microtubule-AKAP-PKA complex, successfully localising this kinase to a specific subcellular location (Obar, Dingus et al. 1989). A further example is AKAP150, which directly associates with the calcium-binding protein calmodulin via its amino terminal domain (Carr, Stofko-Hahn et al. 1992). Similar to MAP2, the RII-binding domain of AKAP150 is also located at the opposite terminal to the subcellular structure-binding domain, and is located on the carboxyl-terminal domain. As a result, AKAP150 and Type II PKA co-localise in the dendrites of cultured hippocampal neurons (Coghlan, Bergeson et al. 1993). This close-association with the post-synaptic membrane positions PKA near to ionotrophic glutamate receptors which, when phosphorylated by PKA, are desensitised to the signal transduction across the synaptic membrane (Carr, Stofko-Hahn et al. 1992). In addition to phosphorylation of target proteins at the specific subcellular location, the AKAP/PKA complex is also likely to be responsible for phosphorlaytion of the AKAP itself as these proteins contain consensus PKA phosphorylation sites (Carr, Stofko-Hahn et al. 1992). As a result of such anchoring complexes, up to 75% of Type II PKA is attached to subcellular structures, and the remaining 25% of this subtype, and all of Type I PKA, is soluble and cytoplasmic (Coghlan, Bergeson et al. 1993). As a kinase, PKA is responsible for the phosphorylation of various proteins which either results in their activation or inactivation, depending on the target protein and the phosphorylation site. With regards to the endothelial barrier, the main function of PKA appears to be the inhibition of endothelial cell contraction. The requirement for phosphorylation of myosin light chain (MLC) by MLC kinase (MLCK) for endothelial cell contraction has already been detailed (see “Section 1.6.3 - The actin network”). PKA is capable of phosphorylating, and therefore inactivating, MLCK (Verin, Gilbert-McClain et al. 1998). PKA also phosphorylates RhoA on Ser188, thereby inactivating this GTPase (Lang, Gesbert et al. 1996, Ellerbroek, Wennerberg et al. 2003, Qiao, Huang et al. 2003). RhoA is a major regulator of actin-myosin-induced endothelial cell contraction (Carbajal and Schaeffer 1999) and microinjection of constitutively active Rho, V14Rho, induces endothelial cell contraction (Essler, Amano et al. 1998). ROCK (Rho kinase), is a downstream effector of RhoA which

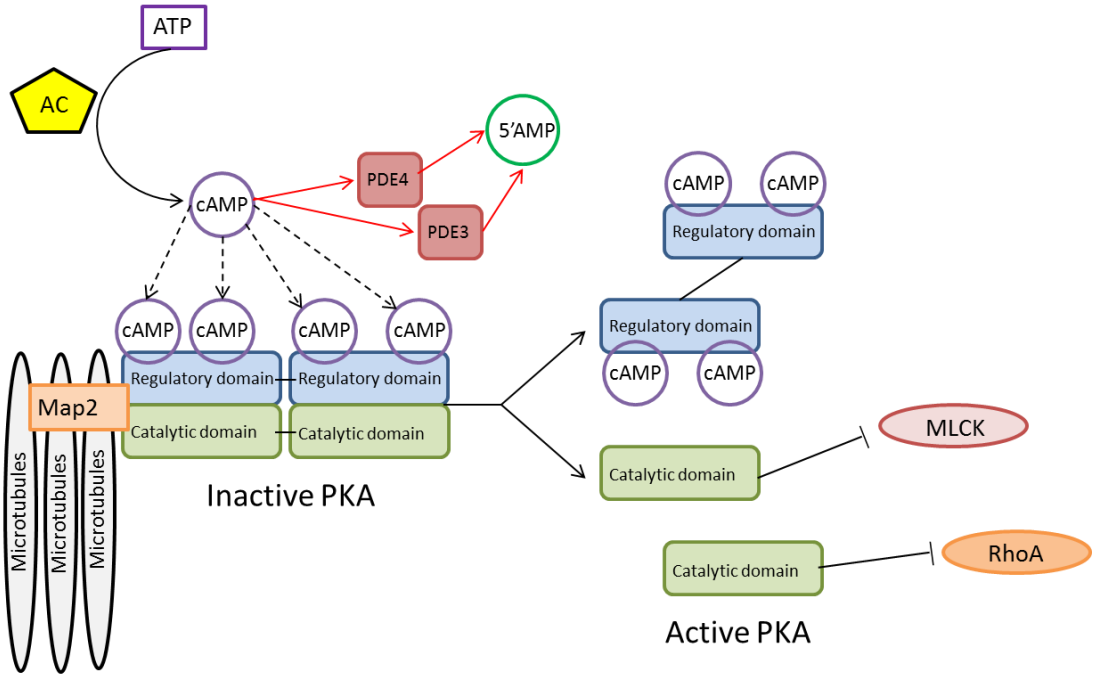

Figure 1.4: A brief overview of the PKA pathway

This schematic represents the basic PKA pathway in endothelial cells. Intracellular cAMP elevation induced by adenylate cyclase activity (AC, yellow) triggers binding of 4 cAMP molecules (purple) to the two regulatory domains (blue) of the PKA holoenzyme. This induces a conformational change that releases the two catalytic domains (green) from the regulatory subunit-cAMP complex, activating PKA and allowing it to act as a kinase. PKA is able to phosphorylate both MLCK and RhoA and therefore inhibits endothelial cell contraction and barrier disruption. cAMP may be dephosphorylated into 5'AMP by phosphodiesterases (PDEs), 2 common examples of which are shown in red (PDE3 and PDE4). PKA can also be anchored to specific subcellular locations via A Kinase anchoring proteins (AKAPs). Map2 is shown here as an example of an AKAP that tethers Type II PKA to microtubules.

stimulates phosphorylation of the regulatory subunit of myosin light chain phosphatase (PP1), decreasing its phosphatase activity and thereby inducing contraction (Essler, Amano et al. 1998, Birukova, Smurova et al. 2004). Increased Rho phosphorylation at Ser188 in pulmonary endothelial cells decreases the association between Rho and ROCK and attenuates Rho signalling (Lang, Gesbert et al. 1996). Similarly, PKA also phosphorylates the GTP-dissociation inhibitor, GDI, which promotes loss of GTP from RhoA thereby inactivating it and inhibiting contraction (Qiao, Holian et al. 2008). Interestingly, the PKA inhibitor H89 frequently used in the literature has been shown to also effect other kinases including ROCK, and as such may have un-desired downstream effects (Leemhuis, Boutillier et al. 2002, Murray 2008). In addition to this direct inactivation of endothelial contraction, PKA also mediates a similar inhibition through activation of Rac, a member of the Rho family of small GTPases. This activation is proposed to be via activation of the guanine nucleotide exchange factors (GEFs) specific for Rac1, Tiam1 and Trio which have consensus PKA phosphorylation sites (O'Connor and Mercurio 2001). Phosphorylation of these GEFs results in Rac1 activation that is dependent upon the involvement of the actin-binding protein vasodilator-stimulated phosphoprotein (VASP), β1-integrin binding and proper PKA compartmentalisation via AKAPs (Schlegel, Burger et al. 2008). The role of Rac in strengthening of the endothelial barrier is detailed further under “Section 5.1.9”.

1.11.2 - Cyclic nucleotide-gated ion channels

The second class of proteins capable of sensing cAMP concentration via their CNB domains are cyclic nucleotide-gated ion chanels. These ion channels are permeable to both monovalent and divalent cations and show varying selectivities for cAMP and cGMP depending on their physiological role (Zagotta and Siegelbaum 1996). The rod-type nucleotide-gated nonselective cation channel CNG1, for example, has been identified in vascular endothelial cells and vascular smooth muscle cells and is involved in calcium entry (Yao, Leung et al. 1999).

1.11.3 - Epac

The third class of proteins capable of sensing cAMP concentration via their CNB domains are exchange proteins directly activated by cAMP (Epac), which were independently identified by two groups in 1998 (De Rooij, Zwartkruis et al. 1998, Kawasaki, Springett et al. 1998). De Rooij and co-workers observed that the forskolin-induced activation of Rap1 to its GTP-bound form in Chinese hamster ovary cells was not inhibited by the cAMP-dependent protein kinase (PKA) inhibitor H-89 (De Rooij, Zwartkruis et al. 1998). Rap1 is a member of the Ras family of small G-proteins and plays a role in signal transduction cascade. It binds and hydrolyses GTP, the former state acting as an 'on' switch while the latter as an 'off' switch. Thus, activation of these G-proteins requires the exchange of GDP for GTP and this is catalysed by guanine nucleotide exchange factors (GEFs). As such a GEF was required for the cAMP-induced activation of Rap1 that was independent of PKA, De Rooij *et al.* (1998) searched for proteins with sequence homology to GEFs for Rap1 and to cAMP-binding sites. An 881-amino acid protein was identified with such a homology, and the cAMP-binding sites of this protein, termed Epac, showed significant sequence homology to those of PKA and cyclic nucleotide-gated ion channels (De Rooij, Zwartkruis et al. 1998). Furthermore, the N-terminal GEF domain of Epac was also found to share significant homology with the Rap1-specific GEF Crk SH3-domain-binding guanine-nucleotide releasing factor (C3G)(Gotoh, Hattori et al. 1995, De Rooij, Zwartkruis et al. 1998). Within the C-terminal catalytic region of Epac, a Ras-exchange motif (REM) was also identified (De Rooij, Zwartkruis et al. 1998). This REM domain is found in all Ras- and Rap1-specific GEFs and is important in stabilisation of the GEF structure (Boriack-Sjodin, Margarit et al. 1998, De Rooij, Rehmann et al. 2000). The cAMP-binding site of Epac was identified in the N-terminal region, and later this group identified the ability of the cAMP-binding site

of Epac1 (and the B site of Epac2, detailed later) to act as an auto-inhibitory domain, blocking interaction between the catalytic region of Epac and Rap1 in the absence of cAMP (De Rooij, Rehmann et al. 2000). Removal of these cAMP-binding sites produces constitutively active Epac1 and Epac2 (De Rooij, Zwartkruis et al. 1998). At the same time, work by Kawasaki *et al.* (1998) on a novel brain-enriched gene related to signalling in the striatum identified 2 genes with cAMP-binding motifs and motifs for Ras GEFs (Kawasaki, Springett et al. 1998). These proteins, termed cAMP-GEFI and cAMP-GEFII, were found to be responsible for forskolin-induced activation of Rap1 within 10 seconds of forskolin application. Both the Epac protein identified by De Rooij *et al.* (1998), and the cAMP-GEF proteins identified by Kawasaki *et al.* (1998), showed cAMP-induced, PKA-independent activation of Rap1 (and not R-Ras), and as such the terms Epac1/cAMP-GEFI and Epac2/cAMP-GEFII are interchangeable in the literature. Further work on Epac2 has identified its expression of a second N-terminal CNB domain (termed site A)(Rehmann, Das et al. 2006). This A site CNB domain shows much lower affinity for cAMP than the B site present in both Epac1 and Epac2 (De Rooij, Rehmann et al. 2000), and does not display the inhibitory effect of the B site (Rehmann, Das et al. 2006). The N-terminal region of Epac also contains a Dishevelled, Egl-10, Pleckstrin (DEP) domain which is responsible for membrane-localisation of this protein (De Rooij, Rehmann et al. 2000). In addition to Rap1, both Epac1 and Epac2 also activate Rap2A *in vitro* and *in vivo* (De Rooij, Rehmann et al. 2000). Repac (related to Epac, MR-GEF) is a constitutive activator of Rap1 and Rap2, consisting of only a catalytic domain and is therefore not regulated by cAMP (De Rooij, Rehmann et al. 2000, Bos, De Rooij et al. 2001). The Ras-binding domain of Repac does, however, show sequence homology with the corresponding regions in Epac1 and Epac2 (De Rooij, Rehmann et al. 2000). Further information on Epac's activity as a GEF and its role in stabilisation of the endothelial barrier is detailed in Chapter 5: Control of Cadherin and Connexin Distribution.

1.12 – Endothelial barrier de-stabilisers

Inflammatory mediators released on vascular injury typically induce increased endothelial permeability through inhibition of the cAMP pathway and stimulation of contraction. Examples of such factors are thrombin, bradykinin, histamine, vascular endothelial growth factor (VEGF), tumour necrosis factor α (TNF-α), lipopolysaccharides (LPS) and reactive

oxidant species (ROS). As such, several of these factors are used experimentally to disrupt the endothelial barrier and increase permeability, particularly thrombin, histamine and LPS.

1.12.1 - Thrombin

Thrombin is a pro-coagulant serine protease generated by proteolytic cleavage of the inactive proenzyme prothrombin by factor V (a protein of the coagulation system) and factor X (also termed prothrombinase due to its enzymatic activity) (Grand, Turnell et al. 1996). Prothrombin is produced in the liver and once converted to its active form has a short half-life in the circulation (approximately 5 minutes) and therefore thrombin itself can only produce a local response (Esmon 2004). Protease-activated receptor 1 (PAR-1) is the receptor on endothelial cells that responds to thrombin binding (Vu, Hung et al. 1991, Gerszten, Chen et al. 1994). This GPCR is a member of the 7 transmembrane domain receptor family that is activated through its own ligation. Thrombin binding to PAR-1 induces proteolysis of the extracellular extension of PAR-1 between Arg41 and Ser42 (Vu, Hung et al. 1991, Gerszten, Chen et al. 1994). This cleavage then allows the receptor to bind its own ligand domain and thus activate the associated G-proteins $G_{12,}$ G_{13}, $G_{\alpha q}$ and $G_{\alpha i}$ (Barr, Brass et al. 1997, Coughlin 2000, Macfarlane, Seatter et al. 2001). The alpha -subunits of G_{12} and G_{13} bind the Rho GEF p115 to initiate the activation of Rho GTPases (Hart, Jiang et al. 1998, Kozasa, Jiang et al. 1998). $G_{\alpha q}$ activates phospholipase Cβ (PLCβ) (Taylor, Chae et al. 1991) to generate diacylglycerol (DAG) and inositol-1,4,5-trisphosphate (IP_3) from PIP_2. $G_{\alpha i}$ inhibits adenylate cyclases (Taussig, Tang et al. 1994, Dessauer, Tesmer et al. 1998). The response to thrombin is therefore predominantly mediated by three pathways; activation of RhoA and the downstream signalling events that this induces, increased cytosolic calcium concentration due to IP_3-mediated release from the endoplasmic reticulum (ER), and inhibition of cAMP generation. The endothelial response to thrombin addition is rapid, with a decrease in intracellular cAMP levels evident within 30 seconds (Baumer, Spindler et al. 2009) and an almost 2 fold increase in endothelial cell monolayer contractile force (Kolodney and Wysolmerski 1992) peaking at 5 minutes (Goeckeler and Wysolmerski 1995). Similarly, 10 nM thrombin induces an increase in the concentration of activated RhoA within 1 minute (Qiao, Huang et al. 2003). The role of RhoA in inducing endothelial cell contraction has been previously discussed (see "Section 1.11.1 - Protein Kinase A"). Actin-myosin-mediated endothelial cell contraction requires intracellular calcium, and the increase in calcium stimulated through PLCβ-mediated IP_3 generation

therefore promotes endothelial contraction. In addition to calcium release, thrombin also stimulates store-operated calcium entry (SOCE) (Ahmmed, Mehta et al. 2004) to maintain the endothelial contraction for up to 2 hours (Goeckeler and Wysolmerski 1995). Thrombin induces phosphorylation of the SOCE channel transient receptor potential channel 1 (TRPC1) within 1 minute of application, and this modification promotes re-filling of the ER calcium store (Ahmmed, Mehta et al. 2004). Indeed, antisense depletion of TRPC1 in cultured endothelial cells, or inhibition of TRPC1 with the anti-TRPC1 primary antibody reduces calcium entry by 50% and decreased endothelial permeability in response to thrombin (Brough, Wu et al. 2001, Ahmmed, Mehta et al. 2004).

1.12.2 - Vascular endothelial growth factor

Vascular endothelial growth factor (VEGF) is produced by perivascular cells and is involved in the stimulation of proliferation and endothelial barrier destabilisation required for angiogenesis and vascular remodelling (Eriksson and Alitalo 1999, Mehta and Malik 2006). Endothelial cells express two phosphotyrosine-containing transmembrane receptors for VEGF; the Fms-like tyrosine kinase receptor (Flt-1, also called VEGFR1) and the kinase insert domain-containing receptor (KDR, also called VEGFR2)(Mehta and Malik 2006). The VEGFR2 receptor is responsible for the VEGF-induced increase in endothelial permeability (Esser, Lampugnani et al. 1998). Downstream signalling events induced by activation of VEGFR2 triggers phosphorylation of adherens junction components which promotes their dysfunction and increased paracellular permeability (Esser, Lampugnani et al. 1998). Specifically, VEGF induces the activation of the Rac-specific GEF Vav2 through Src activity (Chou, Wang et al. 2002). Rac subsequently activates p21-activated kinase (PAK) which phosphorylates VE-cadherin at Ser665. The phosphorylated form of Ser665 acts as a docking site for β-arrestin 2, and VE-cadherin is endocytosed (Gavard and Gutkind 2006). A further link between VEGFR2 and VE-cadherin also exists; VEGFR2 forms a complex with VE-cadherin, an interaction that is likely mediated by β-catenin (Carmeliet, Lampugnani et al. 1999). This cadherin-VEGFR2 complex is required for proper endothelial response to the VEGF signal and endothelial cell survival (Carmeliet, Lampugnani et al. 1999, Shay-Salit, Shushy et al. 2002). Indeed, VE-cadherin null mice suffer endothelial apoptosis and embryonic lethality at E9.5 due to a lack of transmission of the endothelial cell survival signal by VEGF (Carmeliet, Lampugnani et al. 1999).

1.13 – Endothelial barrier stabilisers

In response to inflammation several factors are released to inhibit excessive permeability and barrier disruption. These barrier stabilisers typically employ mechanisms involving cAMP elevation, thereby counteracting the de-stabilising pathways detailed above. Examples of such factors include sphingosine-1-phosphate (S1P), angiopoetin 1 (Ang1), epinephrine/ adrenaline, norepinephrine/noradrenaline, prostaglandin, prostacyclin, atrial natriuretic peptide (ANP) and hepatocyte growth factor (HGF). Much like barrier de-stabilisers, several of these factors are also used experimentally to stabilise the endothelial barrier and decrease permeability, particularly Ang-1 and prostaglandin E2 (PGE2).

1.13.1 - Angiopoetin 1

Ang1 is a vascular growth factor released from smooth muscle cells, pericytes and monocytes following barrier disruption (Moss 2013). Ang1 is then able to act as a ligand for the tyrosine kinase receptor, Tie-2, expressed specifically on endothelial cells. This kinase subsequently phosphorylates and thereby activates PI3 kinase (phosphatidylinositol-4,5-biphosphate 3-kinase, PI3K), which activates Rac1, a process that requires the scaffold protein IQ domain GTPase-activating protein (IQGAP1) (Kuroda, Fukata et al. 1998, Ho, Joyal et al. 1999, David, Ghosh et al. 2011, Moss 2013). Ang1 also triggers the phosphorylation of the RhoGAP P190, which inhibits RhoA activity and therefore actinomyosin contraction (Jho, Mehta et al. 2005, Mammoto, Parikh et al. 2007). Through the activation of Rac1, and the inhibition of RhoA, Ang1 maintains the barrier during resting conditions and also prevents the permeability-increasing effects of histamine and bradykinin (Thurston, Rudge et al. 2000, Pizurki, Zhou et al. 2003, David, Kumpers et al. 2013). Interestingly, angiopoetin 2 (Ang2) has opposing actions to Ang1, and is released from the Weibel-Palade bodies of endothelial cells where it is stored during periods of vascular growth and inflammation (Maisonpierre, Suri et al. 1997). Indeed, patients with severe systemic inflammation or sepsis express reduced levels of Ang1 and increased levels of Ang2 (David, Kumpers et al. 2013). This highlights the role of both forms of angiopoetin in angiogenesis; Ang2 for the initial barrier de-stabilisation to allow vessel growth, and Ang1 for maturation of the newly-formed vessels.

1.13.2 - Prostaglandin E2

PGE2 is a GPCR-agonist that protects the endothelial barrier through cAMP elevation and activation of both the PKA and Epac/ Rap pathways (Farmer, Bernier et al. 2001, Birukova, Zagranichnaya et al. 2007, Kobayashi, Tsubosaka et al. 2013). PGE2 is a product of the arachidonic acid metabolic pathway, is synthesised by vascular endothelial cells, and binds the prostonoid receptors EP1-4 on these cells (Alfranca, Iniguez et al. 2006). Binding of PGE2 to the G_s-coupled receptors EP_2 or EP_4 leads to activation of adenylate cyclase and elevation of intracellular cAMP concentration (Bos, Richel et al. 2004). Through activation of the PKA and Epac pathways, PGE2 is able to attenuate the hyperpermeability induced by the inflammatory mediator bradykinin (Farmer, Bernier et al. 2001). Similarly, prostacyclin (PGI2) is also a GPCR-agonist and its synthetic analog, beraprost, activates the PKA and Epac pathways to decrease endothelial permeability (Birukova, Zagranichnaya et al. 2007). As such, beraprost is used as treatment for pulmonary hypertension (Howard and Morrell 2005).

1.14 - Pathological conditions involving dysregulation of the endothelial barrier and therapeutic potential

Barrier disruption plays a key role in a number of pathological conditions ranging from systemic inflammation and oedema formation to atherosclerosis. Endothelial barrier disruption induced by LPS, TNF-α or thrombin are at least in part due to the loss of intracellular cAMP and Rac1 inactivation (Dellinger, Levy et al. 2013). Elevation of cAMP and Rac1 activation mediated through either the PKA or Epac/Rap pathways therefore offers a potential mechanism for stabilisation of the barrier. Systemic application of cAMP-elevating agents dobutamine and norepinephrine are effective for volume expansion in acute inflammation (De Backer, Creteur et al. 2006, Stephens, Uwaydah et al. 2011). Similarly, introduction of phosphodiesterase (PDE) inhibitors such as rolipram enhance the survival rates in animal models of systemic inflammation (Lin, Adamson et al. 2012, Schick, Wunder et al. 2012). Such PDE inhibitors, however, may not provide an efficient therapeutic target as the D4 splice variant of PDE4, PDE4D4, restricts cAMP to a membrane pool and inhibition of this PDE may increase the cytosolic pool of cAMP which can lead to increased permeability and barrier disruption (Creighton, Zhu et al. 2008). It is therefore necessary to identify a more appropriate therapeutic target for barrier stabilisation and activation of the Epac/rap pathway may provide such a mechanism

1.15 – Hypothesis

cAMP has long been recognised as an important stabiliser of the endothelial barrier. Since its discovery as a novel cAMP effector, Epac has been implicated in the cAMP-mediated decrease in endothelial permeability. The effect of Epac has previously been shown to be mediated by re-organisation of VE-cadherin. Cadherins and connexins are closely associated and as such a re-organisation of VE-cadherin is likely to affect the connexin distribution. We hypothesised that Epac activation in HCAECs enhances the endothelial barrier through re-distribution of cadherins and connexins, with a subsequent increase in gap junctional intercellular communication. In addition, Epac activation in HCAECs was hypothesised to trigger a rise in intracellular calcium concentration. This rise in intracellular calcium concentration, if stimulated in vivo, in combination with enhanced direct cell-cell communication via gap junctions, could trigger smooth muscle cell hyperpolarisation and therefore regulate vascular tone.

Chapter 2:

Materials and Methods

2.1 – Materials

2.1.1 – Cell culture

Cryopreserved human coronary artery endothelial cells (HCAECs, Cat no. C 12221, Lot no. 0113008.7) and human coronary artery smooth muscle cells (HCASMCs, Cat no. C 12511, Lot no. 9052004.5) were purchased from Promocell (Heidelberg, Germany) at passage 2 (P2). HCAECs were cultured in Promocell endothelial cell medium MV 2 (Cat no. C-22022) with the addition of Promocell endothelial cell growth medium MV 2 supplement mix (Cat no. C-39226), with a final supplement concentration of (per ml): 5% v/v fetal calf serum, 5 ng epidermal growth factor (recombinant human), 10 ng basic fibroblast growth factor (recombinant human), 20 ng insulin-like growth factor (Long R3 IGF-1), 0.5 ng vascular endothelial growth factor 165 (recombinant human), 1 µg ascorbic acid and 0.2 µg hydrocortisone. HCASMCs were cultured in Promocell smooth muscle cell growth medium 2 (Cat no. C-22062) supplemented with Promocell smooth muscle cell growth medium 2 supplement mix (Cat no. C-39267), giving a final supplement concentration of (per ml): 5% v/v fetal calf serum, 0.5 ng epidermal growth factor (recombinant human), 2 ng basic fibroblast growth factor (recombinant human) and 5 µg insulin (recombinant human).

2.1.2 – Animals

Male Wistar rats (200-300 g, Charles River Laboratories, Massachusetts, USA) were humanely killed via exposure to a rising concentration of CO_2 followed by cervical dislocation, in accordance with Schedule 1 of the Animals (Scientific Procedures) Act 1986.

2.1.3 – Primary antibodies

Polyclonal rabbit anti-human von Willebrand Factor (vWF) primary antibody (Cat no. A0082) and monoclonal mouse anti-human CD31 (cluster of differentiation 31) primary antibody (Cat no. M0823) were purchased from Dako (Denmark). Monoclonal mouse anti-α smooth muscle actin (α-actin) primary antibody was purchased from Sigma-Aldrich (Cat no. A 2547). Monoclonal mouse anti-calponin primary antibody was purchased from Sigma-Aldrich (Cat no. C2687). Polyclonal rabbit anti-mouse connexin primary antibodies were purchased from Source Bioscience (San Antonio, USA; anti-Cx37 Cat no. CX37A11-A, anti-Cx40 Cat no. CX40-A, anti-Cx43 Cat no. CX43A11-A). Monoclonal mouse anti-human

cadherin primary antibodies were purchased from BD Biosciences (Oxford, UK; N-cadherin Cat no. 610921, VE-cadherin Cat no. 610252). Anti-Epac1 monoclonal mouse primary antibody was purchased from Cell Signalling (USA; Cat no. 4155S) for Western blot. Anti-Epac1 monoclonal mouse primary antibody was purchased from Santa Cruz Biotechnology (USA; Cat no. Sc-28366) for immunocytochemistry. Monoclonal anti-actin mouse primary antibody was purchased from Sigma-Aldrich (Cat no. A 4700). Anti-IP_3R primary antibodies were kindly provided by Dr. Svetlana Voronina, University of Liverpool. Polyclonal rabbit anti-IP_3R1 primary antibody was originally sourced from Cell Signalling (USA; Cat no. 3763S), and both rabbit anti-IP_3R2 antibodies were provided by Dr. David Yule (University of Rochester, USA). Dilutions of all primary antibodies are detailed under individual experiments.

2.1.4 – Secondary antibodies

2.1.4.1 – Immunocytochemistry and Immunohistochemistry

Alexa fluor 488-conjugated goat anti-rabbit (Cat no. A-11034), Alexa fluor 488-conjugated goat anti-mouse (Cat no. A-11029) and Alexa fluor 594-conjugated goat anti-mouse IgG (Cat no. A-11032) secondary antibodies were purchased from Molecular Probes (USA). All secondary antibodies are highly cross-adsorbed.

2.1.4.2 – Western blot

Goat anti-rabbit horseradish peroxidase-conjugated (HRP-conjugated) secondary antibody was purchased from Sigma-Aldrich (Cat no. A0545) and goat anti-mouse HRP-conjugated secondary antibody was purchased from Fitzgerald Industries International (Cat no. 43C-CB1569-FIT, Stratech, Suffolk, England).

2.1.5 – Agonists

The Epac-specific agonist 8-(4-Chlorophenylthio)-2'-O-methyladenosine-3', 5'-cyclic monophosphate, acetoxymethyl ester (8-pCPT, Cat no. C 051) was purchased from Biolog, Life Science Institute, Germany. The cAMP-elevating agent forskolin (Fsk, Cat no. CN-100-0010) was purchased from Enzo Life Sciences, Inc., USA.

2.1.6 - Antagonists

Myristoylated PKI(14-22) amide (PKI), a protein Kinase A-inhibitor, was purchased from Enzo Life Sciences (Cat no. P-210, 5 μM), Cyclopiazonic acid (CPA), an inhibitor of endoplasmic reticulum calcium ATPase, was purchased from Sigma-Aldrich (Cat no. C1530, 10 μM), and Ryanodine was purchased from Merck Millipore (Germany, Cat no. 559276, 30 μM). The cell-permeant Epac1 and Epac2 inhibitors HJC0197 (Cat no. C 136) and ESI-09 (Cat no. B 133) were purchased from BioLog (Life Science Institute, Germany).

2.1.7 – Reagents

All reagents were purchased from Sigma-Aldrich (Gillingham, UK) BDH (Poole, UK) or Fisher Scientific (Loughborough, UK), unless otherwise stated, and at a grade suitable to experiments. Solutions were made using ultra high quality (UHQ) water (18 MΩ resistance).

2.2 - Methods

2.2.1 – Cell culture

HCAECs and HCASMCs were grown in T_{75} flasks containing 25 ml fully-supplemented media and passaged approximately every 72-96 hours. When 80-90% confluent, the media was aspirated and the cells washed with 25 ml warm Dulbecco's Phosphate Buffered Saline (DPBS, no Ca^{2+}/Mg^{2+}). The DPBS was then removed and replaced with 1.2 ml warm 0.25% w/v Trypsin-EDTA (Cat no. 25200-056, Gibco, Life Technologies, UK). Cells were incubated at 37˚C/ 5% CO_2 using a LEEC Precision 190D incubator for 20 seconds. Tapping of the flask facilitated dislodging cells, and this was confirmed under a light microscope. The trypsin was neutralised with 9 ml fully-supplemented media. Cells were then sub-cultured at the desired density (calculated using a haemocytometer [Neubauer double cell, rhodium-coated, Cat no. AC1000, Hawksley, Sussex, UK]). This typically equalled a dilution of 1:3.

2.2.2 - Western blot

2.2.2.1 – Preparation of rat tissue lysate

Rat heart and kidney were dissected into 5 mm^3 sections in solution containing (in mM): 137 NaCl, 0.44 $NaH_2PO_4H_2O$, 0.42 Na_2HPO_4, 4.17 $NaHCO_3$, 5.6 KCl, 1 $MgCl_2$, 10 HEPES, 2 CaCl, pH adjusted to 7.4 using NaOH. Chilled 1% v/v protease inhibitor cocktail (Sigma-Aldrich, Cat no. P8340) in lysis buffer (1 M Trizma HCl, 250 mM NaCl, 3 mM EDTA, 3 mM EGTA, 0.5% v/v Triton X-100, pH adjusted to 7.6) solution was added to a chilled 3 ml pestle/mortar homogenizer and the tissue lysed manually. The tissue lysate was then centrifuged at 18,200 g for 10 minutes at 4˚C. The supernatant was transferred to a 1.5 ml microcentrifuge tube (Eppendorf) kept on ice, and the pellet discarded. A portion of supernatent was kept without sample buffer for use in a Bicinchonic acid (BCA) protein assay and frozen at -20˚C. The remaining samples were mixed at a 1:1 ratio with x2 sample buffer (Sigma-Aldrich, Cat no. S3401) and heated in a dry heating block (Labnet Accublock digital dry bath) at 98˚C for 10 minutes to denature the proteins. Protein lysates were allowed to cool on ice and, if not required immediately, stored at -20˚C for up to 4 months.

2.2.2.2 – Preparation of cultured cell lysate

HCAECs and HCASMCs were seeded at a density of 100,000 cells/ml in a 10 cm cell culture Petri dish in 10 ml fully-supplemented media, and cultured until 80-90% confluent (approximately 48 hours). The dish was then transferred to a tray containing crushed ice, the media aspirated and immediately replaced with 5 ml ice-cold DPBS. With the dish still on ice, the DPBS was removed and replaced with 500 µl ice-cold 1% v/v protease inhibitor/lysis buffer solution for 5 minutes, tilting the dish gently to ensure even coverage. A 25 cm cell scraper (Sarstedt, Cat no. 83.1830) was used to dislodge cells by dragging across the culture surface. The cell suspension was then transferred to a chilled 1.5 ml microcentrifuge tube (Eppendorf) and centrifuged at 18,200 g for 10 minutes at 4˚C. Typically, 150 µl of the supernatant was kept for use in a BCA protein assay and frozen at -20˚C. The remaining supernatant was mixed with x5 sample buffer (Sigma-Aldrich) and heated at 98˚C for 10 minutes in a dry heating block. The cell lysate was then allowed to cool on ice and stored at -20˚C for up to 4 months if not required immediately.

2.2.2.3 – BCA protein assay

A Pierce Bicinchonic Acid (BCA) assay kit (Thermo Scientific, Cat no. 23227) was used to determine the total protein concentration of lysates. The protein standards were made using the bovine serum albumin (BSA) diluted in lysis buffer to produce 9 concentrations (in µg/ml): 2000, 1500, 1000, 750, 500, 250, 125, 25 and 0. Each unknown sample (cultured cell/rat tissue lysate) and standard dilutions were duplicated for measurements. Unknown samples were used neat or at a 5 fold dilution. Working Reagent was made according to manufacturer's instructions (50 parts reagent A: 1 part reagent B). 50 µl of each BSA standard and unknown sample was aliquoted into 1.5 ml microcentrifuge tubes. 1 ml of Working Reagent was added and vortexed. All samples were incubated in a water bath (Grant) at 37˚C for 30 minutes. The protein concentration was measured using a Jenway spectrophotometer (Genova, 1690) as absorbance at 562 nm.

2.2.2.4 – Casting of the SDS-PAGE gel

Sodium dodecyl sulphate polyacrylamide gel electrophoresis (SDS-PAGE) was used to separate proteins according to their size. A 10-well 10% resolving gel was made by combining 4.3 ml 30% w/v Acrylamide (Biorad, 16100158), 3.3 ml resolving buffer stock (2 M Trizma base, pH 8.8), 130 µl 10% w/v SDS, 930 µl 87% v/v glycerol, 4.4 ml UHQ water, 60 µl 10% w/v ammonium persulfate and 13 µl TEMED. 10% resolving gel was poured between the glass plates, topped up with isopropanol and allowed to set at room temperature for approximately 45 minutes. Once set, 4% stacking gel was made by combining 840 µl 30% w/v Acrylamide, 1.5 ml stacking buffer stock (0.5 M Trizma base, pH 6.8), 60 µl 10% w/v SDS, 3.8 ml UHQ water, 53 µl 10% w/v ammonium persulfate and 11 µl TEMED. The stacking gel was added between the plates and a comb inserted to form 10 wells for the addition of lysate. The stacking gel was allowed to set at room temperature for approximately 45 minutes.

2.2.2.5 – Running the Western blot

The cell culture and rat tissue lysates were heated in a dry heating block at 98˚C for 5 minutes to ensure denaturing of the proteins, then transferred to ice. 7 µl of rainbow protein mass marker (Amersham full-range rainbow MW marker, Cat no. RPN800E) and 25 µl of each lysate was added to the wells. The gels were run at 120 V for 1 hour in SDS

running buffer (25 mM Tris base, 192 mM Glycine and 3.5 mM SDS). Separated proteins were then transferred to nitrocellulose membrane (Amersham Hybond ECL, RPN303D) in transfer buffer containing 25 mM Trizma base, 192 mM Glycine and 20% v/v methanol, at 110 V for 1 hour. To keep the temperature low during transfer, the cell containing the gels and nitrocellulose membranes was encased in crushed ice. Membranes were washed twice in Tris buffered saline with TWEEN (TBST, 20 mM Trizma base, 137 mM NaCl, 0.1% v/v TWEEN 20, pH 7.6) and submerged in Ponceau S solution for 5 minutes to inspect protein transfer. After satisfactory protein banding was confirmed the membranes were washed in TBST on the rocker for 5 minutes, twice, to remove the dye. The membrane was then blocked with TBST containing 5% or 1% w/v non-fat powdered milk (Marvel) for 1 hour at room temperature on a rocker (Labnet Rocker 25). The membrane was placed in a continuous bag cut to size, 1 ml of the appropriate diluted primary antibody was added, and the bag was sealed and incubated at 4˚C overnight. Primary antibodies were typically used at 200-500 fold dilution in TBST with 5% or 1% w/v non-fat milk. The next day, the membranes were quickly rinsed in TBST twice. Membranes were then washed three times with TBST on the rocker for ten minutes each. Nitrocellulose membranes were then incubated with a horseradish peroxidase (HRP)-conjugated secondary antibody on the rocker at room temperature for 2 hours. HRP-conjugated secondary antibodies were used at a 10,000 fold dilution (mouse) or 5,000 fold dilution (rabbit) in TBST with 5% or 1% w/v milk solution. Following incubation with the secondary antibody membranes were again washed briefly with TBST twice and then washed with TBST on the rocker for ten minutes, repeated three times. Enhanced Chemiluminescence solutions 1 and 2 (ECL, Amersham, Cat no. RPN2109) were mixed in equal volume and 3 ml added to one membrane for 1 minute. The membranes were drained of excess ECL solution, slotted into a plastic wallet (Lyreco) and fixed into the hypercasette (Amersham Biosciences).

2.2.2.6 – Processing the photographic film

In a dark room, photographic film (Amersham Hyperfilm ECL high performance chemiluminescence film, Cat no. 28906836) was inserted into the hypercasette. Incubation period for the film typically ranged between 5–10 minutes, unless otherwise stated. The photographic film was processed using Kodak photographic solutions (Kodak GBX fixer and developer). Once films were dry, bands were sized using the rainbow ladder as reference. Developed films underwent densitometric analysis using Image J software.

2.2.2.7 – Re-blotting of Western blot membrane

Some experiments required the nitrocellulose membrane to be re-used. Membranes were re-hydrated with TBST for 30 minutes-1 hour then stripped of antibodies by incubating with a solution containing 100 mM β-mercaptoethanol, 2% w/v SDS, and 62.5 mM Tris base (pH 6.7) for 10 minutes, twice. Membranes were then washed twice with TBST and blocked as normal with TBST containing 1% or 5% w/v non-fat milk for up to 1 hour at room temperature. Membranes were then incubated with the primary antibody overnight at 4˚C and the normal Western blotting procedure resumed.

2.2.3 – Immunofluorescence

2.2.3.1 – Immunocytochemistry

2.2.3.1.1 – Plating of cultured cells

Size 1 coverslips (diameter, 13 mm) were flame-sterilised, coated with 1% v/v poly D-lysine (PDL, Millipore, Cat no. A-003-E) and incubated for 2 hours at 37°C/5% CO_2. Coverslips were then washed twice with UHQ water and allowed to dry under sterile conditions. Coverslips were placed in a 24-well cell culture plate and cells seeded at a density of 100,000 cells per well in 2 ml fully-supplemented medium (Promocell). UHQ water was added to empty wells to create a humidified environment. Cells were cultured at 37˚C/5% CO_2 typically for 48 hours.

2.2.3.1.2 – Fixation, quenching and permeabilisation of cultured cells

Once 90% confluent (approximately 48 hours post-seeding), cells were fixed. Culture media was aspirated and cells washed with 1 ml DPBS. DPBS was removed and cells were fixed with 1 ml 2% w/v Paraformaldehyde (PFA, w/v in PBS containing [in mM] 2.7 KCl, 1.5 KH_2PO_4, 137 NaCl, 8 Na_2HPO_4, pH 7.4) for 10 minutes at room temperature. The fixative was removed and quenched with 1 ml 100 mM Glycine buffer (pH 7.4) per well for 10 minutes at room temperature. Occasionally culture plates were stored prior to permeabilisation and in these plates Glycine buffer was replaced with DPBS containing 10 mM sodium azide, and stored at 4˚C. Using a fine-ended pasteur pipette (SLS select, PIP4101) 3 ml permeabilisation solution (0.1% v/v Triton X-100 in PBS, pH adjusted to 7.4 using 1 M NaOH) was added to each well and incubated at room temperature for 10

minutes to make intracellular epitopes accessible. Permeabilised cells were subsequently washed with 2 ml PBS for 5 minutes at room temperature, 3 times.

2.2.3.1.3 – Antibody labelling of cultured cells

Permeabilised cells were incubated with 200 µl antibody diluting solution for 30 minutes at room temperature to block non-specific binding sites. Antibody diluting solution contained 2% v/v goat serum, 0.05% v/v Triton X-100, 1% w/v bovine serum albumin in sodium citrate buffer (SSC, containing in mM; 150 NaCl and 15 Na_3 Citrate), pH 7.2. Antibody diluting solution was then removed and replaced with 200 µl diluted primary antibody per well and incubated at 4˚C overnight. The following day the cells were washed with 1 ml antibody wash solution (150 mM NaCl, 15 mM Na_3 Citrate and 0.05% v/v Triton X-100, pH 7.2) for 10 minutes at room temperature, 3 times. Primary antibodies were visualised using fluorescent Alexa fluor 488-conjugated goat anti-rabbit, Alexa fluor 488-conjugated goat anti-mouse or Alexa fluor 594-conjugated goat anti-mouse IgG secondary antibodies, all diluted 500 fold. 200 µl of the appropriate secondary antibody was added to each well and incubated in the dark for up to 2 hours at room temperature. The cells were then washed with antibody wash solution for 10 minutes at room temperature, 3 times. Exposure to light was avoided as much as practical and cells were covered with aluminium foil. Coverslips were post-fixed with 1 ml 2% w/v PFA in PBS for 10 minutes at room temperature then re-washed with antibody wash solution. Coverslips were then immersed into UHQ water, twice, and allowed to air dry in the dark for 2 hours. They were then mounted onto individual glass slides with 20 µl mounting medium (Dako, S3023) containing 5 nM 4',6'-diamidino-2-phenylindole (DAPI, Molecular probes, Cat no. D3571) for counter-staining of the nuclei. Slides were left to dry overnight at room temperature in the dark.

2.2.3.2 – Immunohistochemistry

2.2.3.2.1 – Dissection of rat tissue

Rat tissue was dissected in solution containing (in mM): 137 NaCl, 0.44 $NaH_2PO_4H_2O$, 0.42 Na_2HPO_4, 4.17 $NaHCO_3$, 5.6 KCl, 1 $MgCl_2$, 10 HEPES and 2 $CaCl_2$ (pH adjusted to 7.4). 5 mm sections of rat artery were isolated and embedded up-right in CRYO-M-BED embedding compound (Bright Instruments) on a cork disk and frozen in a bath of isopentane super-cooled in liquid nitrogen. The resulting tissue blocks were used immediately or stored at -

20˚C for up to 4 months. Tissue blocks were cut into 8-12 µm thick sections using a cryostat (Leica CM1950 or Bright Instruments 3050 microtome).

2.2.3.2.2 - Fixation, quenching and permeabilisation of tissue slices

Rat artery slices were transferred to gelatine-coated slides (0.2% w/v gelatine and 0.02% w/v chromic (III) potassium sulphate in UHQ water) and enclosed using a Dako wax pen (Dako, S200230-2) to create a hydrophobic barrier. Tissue sections were fixed using 2% w/v PFA in PBS, incubated for 5 minutes at room temperature. The fixative was aspirated and excess removed using laboratory tissue. Un-reacted aldehyde was quenched with 100 mM Glycine buffer (pH 7.4, see Immunocytochemistry solutions) for 10 minutes at room temperature. Glycine was removed and permeabilising solution (pH 7.4, see Immunocytochemistry solutions) was added to the sections for 10 minutes. Slides were then rinsed with PBS for 5 minutes at room temperature, 3 times.

2.2.3.2.3 – Antibody labelling of tissue sections

After permeabilisation, the slices were inspected using a light microscope (Nikon TMS) to ensure that they were still firmly attached to the slide glass. The tissue slices were incubated with 200 µl antibody diluting solution (pH 7.2, see Immunocytochemistry solutions) for 30 minutes at room temperature to block non-specific binding. Antibody diluting solution was removed and immediately replaced with diluted primary antibody at the appropriate dilution, and incubated at 4˚C overnight. Primary antibodies were typically used at 200-500 fold dilution using antibody diluting solution. The following day, tissue sections were washed with antibody wash solution (pH 7.2, see section "2.2.3.1.3 – Antibody labelling of cultured cells") for 10 minutes at room temperature, 3 times. After the final wash, the slices were incubated with 200 µl diluted Alexa fluor 488-conjugated goat anti-rabbit or Alexa fluor 594-conjugated goat anti-mouse IgG secondary antibodies in the dark at room temperature for up to 2 hours. Secondary antibodies were used at 500 fold dilution. Tissue sections were washed with antibody wash solution for 10 minutes at room temperature, 3 times. Slices subsequently underwent 2 washes with UHQ water and allowed to air dry for 2 hours at room temperature in the dark. Once dry, slices were mounted using 13 mm, size 1 coverslips, and Dako mounting medium containing 5 nM DAPI for nuclear visualisation.

2.2.3.3 – Visualisation of labelled cells and tissue slices

A Leica laser-scanning confocal microscope (Leica SP2 AOBS) was used to visualise the labelled cultured cells (x63 oil objective) and tissue sections (x10 dry objective). Samples labelled with Alexa fluor 488-conjugated secondary antibody were excited at 488 nm with an argon-ion laser, and the emission light captured at 510-560 nm. Samples labelled with Alexa fluor 594-conjugated secondary antibody were excited at 594 nm using a helium-neon laser and the emission light captured at 610-660 nm. For the detection of DAPI nuclear staining, a Mai Tai infra-red laser (Spectra-Physics) was used for two-photon excitation at a wavelength of 740 nm, providing the working excitation of 370 nm. Software analysis of the data was carried out using Leica confocal software Lite.

2.2.4 – Small interfering RNA (siRNA) knockdown of Epac1

Two siRNA duplexes for Epac1 (duplex 6 [Hs_RAPGEF3_6, 5 nM] and 7 [Hs_RAPGEF3_7, 5 nM]) were purchased from Qiagen at a stock concentration of 20 µM. Both Epac1 siRNA duplexes were used in combination at a total concentration of 10 nM, unless otherwise stated. AllStars Negative control siRNA (Qiagen, 20 nM, Cat no. 1027281) was used at a final concentration of 10 nM and provided a non-silencing control duplex. All steps were carried out under sterile conditions using Greiner Bio-one RNAse-free tips (100 µl: Cat no. 772288, 200 µl: Cat no. 739288, 1000 µl: Cat no. 740288) and Life Technologies PCR tubes (Cat no. AM12230) to ensure all plastics were nuclease- free.

2.2.4.1 – Plating of HCAECs

Cultured HCAECs were seeded at a density of 100,000 cells per well in a 6-well cell culture plate, and incubated at 37˚C/5% CO_2. After 24 hours cells were 70% confluent and ready for transfection.

2.2.4.2 - Epac1 siRNA transfection of HCAECs

Each siRNA duplex was aliquoted into individual sterile RNase-free 0.5 ml microfuge tubes (Ambion, Life Technologies, Cat no. AM12300) and diluted in 250 µl Opti-MEM (Opti-MEM I Reduced Serum Medium, GlutaMAX, Gibco, Life Technologies, Cat no. 51985-026) to the

appropriate concentration. RNAiMAX Lipofectamine transfection reagent (Invitrogen, Cat no. 13778-075) was diluted in Opti-MEM at a concentration of 1% to give a final concentration of 0.1% v/v in 2500 µl Opti-MEM. 250 µl 1% v/v Lipofectamine/Opti-MEM mix was added to each siRNA-containing microfuge tube, triturated 10 times and left at room temperature for 30 minutes to allow complex formation between the siRNA duplexes and the transfection reagent. The fully-supplemented endothelial cell media (Promocell) was removed from the 35 mm dishes and 2 ml Opti-MEM was added to each dish. 500 µl of the siRNA duplex/Lipofectamine mix was distributed evenly across the dish in a drop-wise manner, and the cells were incubated at 37˚C/5% CO_2 for 4 hours. Dishes were then washed twice with 2 ml DPBS (Gibco) and 2 ml fully-supplemented culture media replaced. Transfected cells were incubated at 37˚C/5% CO_2 for 48 hours.

2.2.4.3 – Quantification of Epac1 knockdown after Epac1 siRNA transfection

To monitor the time course of knock-down, cells were lysed at 24, 48 and 72 hours post-transfection and run through a SDS-page gel Western blot, targeting Epac1 (cell signalling, 4155S). Membranes were then re-blotted with mouse anti-actin primary antibody (Sigma-Aldrich, Cat no. A 4700) at a 500 fold dilution.

2.2.5 – Lucifer yellow scrape assay

2.2.5.1 – Plating of HCAECs

Cultured HCAECs were seeded at a density of 300,000 cells per dish in 35 mm glass-bottom tissue culture dishes (Greiner Bio-One) pre-coated with 1% v/v PDL. Cells were then incubated for 24-48 hours, and once 90% confluent were ready for use in a Lucifer yellow scrape assay.

2.2.5.2 – Lucifer yellow dye addition, scrape production and imaging of HCAECs

Lucifer yellow CH lithium salt (Molecular probes, Cat no. L-453) was used at a final concentration of 0.1% w/v in PBS (containing calcium chloride and magnesium), and stored in the dark until required. In control dishes the media was aspirated, 500 µl 0.1% w/v Lucifer yellow added to the glass centre of the dish and two scrapes made using a surgical blade (Feather size 15, World Precision Instruments Inc., USA, Cat no. 500242) intersecting

at the centre of the dish. The dish was then moved to a dark drawer for 2 minutes to allow the dye to penetrate the damaged cells with minimal photobleaching. After the incubation period the dye was aspirated and the dish washed twice with 2 ml PBS (containing calcium chloride and magnesium). The PBS wash was removed and 2 ml of the magnesium- and calcium chloride-containing PBS replaced. The dish was then immediately imaged using a Leica laser-scanning confocal microscope.

2.2.5.3 – Lucifer yellow scrape assay in the presence of 8-pCPT or forskolin

A subset of scrape dye transfer experiments were conducted in the presence of either the Epac-selective agonist 8-pCPT or the cAMP-elevating agent forskolin. Forskolin was used at a concentration of 10 µM in fully-supplemented HCAEC media and 8-pCPT was used at a concentration of 5 µM in fully-supplemented HCAEC media. The dishes were incubated with either agonist for 30 minutes at 37˚C/5% CO_2 prior to the dye addition. Following removal of the agonist the scrape proceeded as in the control condition (media removal, 500 µl 0.1% w/v Lucifer yellow dye addition, scrape, 2 minutes incubation, wash twice with PBS, replace PBS, imaging).

2.2.5.4 – Lucifer yellow scrape assay in the presence of Epac antagonists

Additional experiments required pre-incubation with the Epac antagonists HJC0197 (BioLog, Cat no. C 136) or ESI-09 (BioLog, Cat no. B 133) prior to incubation with 8-pCPT or Fsk. HJC0197 and ESI-09 are membrane-permeable inhibitors of both Epac1 and Epac2. These dishes were incubated with either HJC0197 or ESI-09 at a concentration of 5 nM in fully-supplemented HCAEC media at 37˚C/ 5% CO_2 for 10 minutes. This solution was then aspirated and replaced with media containing the Epac antagonist and either 8-pCPT (5 µM) or Fsk (10 µM) for 30 minutes at 37˚C/ 5% CO_2. Again, following the incubation with both the Epac antagonist and the subsequent incubation with the agonist the dish then underwent the scrape assay as previously described. All dishes were visualised using a Leica laser-scanning confocal microscope as previously mentioned, with a x10 dry objective. All dishes were excited at 488 nm with an argon-ion laser and the emitted light captured at 528 nm. Although 488 nm is the upper limit of Lucifer yellow excitation, sufficient light was emitted to allow comparison. All images were captured within 10 minutes of the dye removal.

2.2.6 – Fluo-4 live calcium imaging of HCAECs

Cultured HCAECs were seeded at a density of 150,000 cells per dish in 35 mm glass-bottom tissue culture dishes (Greiner Bio-One, Cat no. 627861), and incubated at 37˚C/ 5% CO_2 for 24 hours. Cell-permeant Fluo-4 AM (Molecular Probes, Cat no. F14201) was loaded at a concentration of 10 µM in PBS. Fluo-4 AM-containing PBS was pre-warmed, and the culture media was then aspirated from the 35 mm glass-bottom tissue culture dish and 100 µl of PBS containing 10 µM Fluo-4 AM added to the glass section at the centre of the dish. Fluo-4 is excited at 488 nm by an argon-ion laser and fluorescence intensity increases when calcium concentration rises. The dish was subsequently incubated for 20 minutes at 37˚C/ 5% CO_2. Following this incubation period, the Fluo-4 AM solution was aspirated and the culture surface washed twice with 2 ml PBS (containing calcium chloride and magnesium). The dish was then incubated with 2 ml PBS at 37˚C/ 5% CO_2 for 20 minutes. Following this 20 minute wash the PBS was replaced with fresh PBS (either with calcium chloride and magnesium or just with magnesium). A control image was taken using the x40 oil immersion lens. 2 µl of the required agonist (8-pCPT at 5 µM or forskolin at 10 µM) was then added to the centre of the dish and an image captured every 10 seconds.

Chapter 3:

Characterisation of Rat Tissues and Human Cells

Aims of this chapter:

- To examine the expression of endothelial markers vWF and CD31 in HCAECs through Western blot analysis and immunocytochemical technique
- To examine the expression of vascular smooth muscle markers α-actin and calponin in HCASMCs through Western blot analysis and immunocytochemical technique
- To ensure that these characteristic markers did not change throughout the culture period
- To compare the expression profiles of these endothelial and smooth muscle markers in the cultured cells to that observed in rat coronary and mesenteric arteries

Key findings of this chapter:

- HCAECs express the endothelial markers vWF and CD31 throughout passages 6-10
- HCAECs express both IP_3R1 and IP_3R2
- HCASMCs express the smooth muscle markers α-actin and calponin throughout passages 7-11
- Rat coronary and mesenteric artery endothelium expressed vWF
- Rat coronary and mesenteric artery smooth muscle cells expressed α-actin and calponin

3.1 - Introduction

The specific area of vasculature of interest for this research was that of the coronary arteries, and as such the cultured cells purchased from Promocell were extracted from human coronary artery endothelium and tunica media (HCAECs and HCASMCs, respectively) of right and left coronary arteries (including anterior descending and circumflex branches). In order to closely reflect the cultured cells the rat tissue used was sourced from rat right and left coronary arteries. In addition, to further verify the antibodies used throughout this study, rat mesenteric artery and rat heart lysate were used in immunohistochemical and Western blot analysis, respectively.

In addition to the specific antibodies mentioned below, staining of the nucleus was also achieved using 5 nM Dako 4'-6diamidino-2-phenylindole (DAPI). This fluorescent dye binds to double-stranded DNA and was applied to the pre-labelled coverslips, as outlined under "2.2.3.1.3 - Antibody labelling of cultured cells". Dilutions of both primary and secondary antibodies were optimised using varying concentrations. The dilutions ultimately selected provided the best conditions for selective binding of the antibodies. During Immunofluorescence protocols, antibody labelled cells and tissue slices were viewed under consistent conditions, with the same gain and offset.

3.1.1 - Characterisation of Human Coronary Artery Endothelial Cells (HCAECs)

HCAECs (Promocell, Cat no. C-12221, lot no. 0113008.7) were characterised using the endothelial-specific markers von Willebrand Factor (vWF) and CD31 ([Cluster of Differentiation 31] also referred to as Pecam-1 [Platelet/Endothelial Cell Adhesion Molecule 1] in the literature (Pusztaszeri, Seelentag et al. 2006)).

vWF is a frequently used endothelial marker (Zanetta, Marcus et al. 2000). vWF is a glycoprotein secreted by an endothelial cell-specific storage organelle, the Weibel-Palade body (for reference, vWF is also produced by megakaryocytes (Nachman, Levine et al. 1977, Tomer 2004)). vWF aids blood clotting by mediating the adhesion of platelets to subendothelial connective tissue, and a failure to synthesize this glycoprotein results in impaired coagulation after injury, a condition known as von Willebrand disease, a subtype of Haemophilia (Sadler 1998).

CD31 is a type 1 integral membrane glycoprotein that is responsible for a considerable proportion of endothelial cell intercellular junctions (Albelda, Muller et al. 1991, Cao, O'Brien et al. 2002). As such, this glycoprotein plays a key role in angiogenesis and the formation of new vessels (DeLisser, Christofidou-Solomidou et al. 1997, Sheibani, Newman et al. 1997).

3.1.2 - Characterisation of Human Coronary Artery Smooth Muscle Cells (HCASMCs)

HCASMCs (Promocell, Cat no. C-12511, lot no. 9052004.5) were characterised through the detection of both smooth muscle α-Actin (α-actin) and calponin. It was of particular importance that this cell type was thoroughly characterised as HCASMCs (and indeed all vascular smooth muscle cells) typically exist along a spectrum of phenotypes comprising two extremes; a quiescent, contractile phenotype and a synthetic phenotype characterised by increased production of extracellular matrix proteins (Beamish, He et al. 2010). Cultured cells typically exist in a contractile state; however HCASMCs are capable of shifting between these phenotypes (Worth, Rolfe et al. 2001). A change from the contractile phenotype of HCASMCs can be detected by a decrease in the expression of contractile marker proteins (i.e. α-actin), and this typically occurs in smooth muscle cells cultured for an extended period of time (Rensen, Doevendans et al. 2007). This was why cell cultures were continuously monitored for any change in phenotype, and why promocell (the company of purchase) recommended a maximum of 15 population doublings. To ensure the reliability of the data and to make results applicable to a consistent and reproducible population, HCASMC (and HCAEC) cultures were not maintained beyond passage 11.

Smooth Muscle α-actin is well established as a principle marker for smooth muscle cells across the vasculature (Gabbiani, Schmid et al. 1981, Vandekerckhove and Weber 1981, Fatigati and Murphy 1984). α-actin is one of six actin isoforms identified in mammalian cells, and is unique among these isoforms in that it is primarily restricted to vascular smooth muscle cells (McHugh, Crawford et al. 1991). It is this specificity that makes α-actin a common marker for smooth muscle cells of the vasculature. α-actin plays a fundamental role in maintaining the structure and integrity of the cell, and thus is involved in cell motility and migration, highlighting its role in distinguishing between synthetic (migratory) and contractile smooth muscle cells (Rensen, Doevendans et al. 2007).

More recently, calponin has become a major marker for the characterisation of smooth muscle cells due primarily to its high specificity for this cell type (Frid, Shekhonin et al. 1992, Duband, Gimona et al. 1993, Miano, Carlson et al. 2000). Calponin is a calcium-binding protein that is linked to the contractile machinery of smooth muscle cells through its interaction with α–actin (Gimona, Kaverina et al. 2003).

3.1.3 - Characterisation of rat tissue

In addition to the analysis of individual cell populations in culture, it was also necessary to examine the characteristics of the cell types *in situ*. In an ideal situation human tissue would be used as such a control but this was not possible for this project. Dissected rat coronary and mesenteric arteries provided the whole artery samples required for such immunohistochemical analysis.

3.2- Results

A combination of Western blot, immunocytochemistry and immunohistochemical techniques was used to characterise HCAECs, HCASMCs and rat tissues.

3.2.1 - Total protein concentration

Total protein concentrations of all cultured cell and rat tissue lysates were recorded using a BCA protein assay kit (full details under "2.2.2.3 BCA protein assay"). Initial recording of undiluted rat heart lysate total protein concentration indicated a consistently high level of protein within this lysate (data not shown). As such, subsequent experiments comparing the total protein concentrations of rat tissue and cultured human cells involved the use of rat heart lysate at a 5 fold dilution, unless otherwise stated. Preliminary data from the BCA protein assay can be seen in Figure 3.1. Rat heart lysate, even when used at this 5 fold dilution, recorded a total protein concentration of approximately 1.5 fold higher than that of the highest cell culture lysate recording (HCASMC P8). All primary human cells expressed relatively similar protein concentrations during these preliminary experiments (for full details refer to Supplementary Figure 1 in Appendix).

A further check on overall protein concentration was used in the form of the 'house-keeping' protein actin. This ubiquitously-expressed protein was examined in all human cell

culture lysates via Western blot. This allowed the verification that protein concentrations between the two cell types (HCAECs and HCASMCs) were comparable, and that the protein concentration did not decline over a number of passages (maximum 11). Data for actin expression in HCAECs and HCASMCs can be seen in Figure 3.2 below, with a single band at 42 kDa in both HCAEC and HCASMC lysates. In order to ensure efficient staining of both HCAECs and HCASMCs, actin was also used as an immunocytochemistry control antibody, and comparative actin staining using a Alexa fluor 488 (green) secondary antibody in HCAECs and HCASMCs can be seen in Figure 3.3 below. Actin was identified diffusely distributed throughout the cell in both HCAECs and HCASMCs, with areas of staining associated with the cytoskeletal framework (Figure 3.3B). Comparable maximum AF488 signal intensities were recorded in HCAECs and HCASMCs (169 arbitrary units (AU) and 203 AU, respectively).

The total protein concentration of all HCAEC and HCASMC lysates used in experiments were found to be comparable and consistent. Importantly, no decline in total protein concentration was reported over the culture period. Furthermore, when used at a 5 fold dilution, rat heart lysate provided a reliable control throughout experiments due to its high protein concentration.

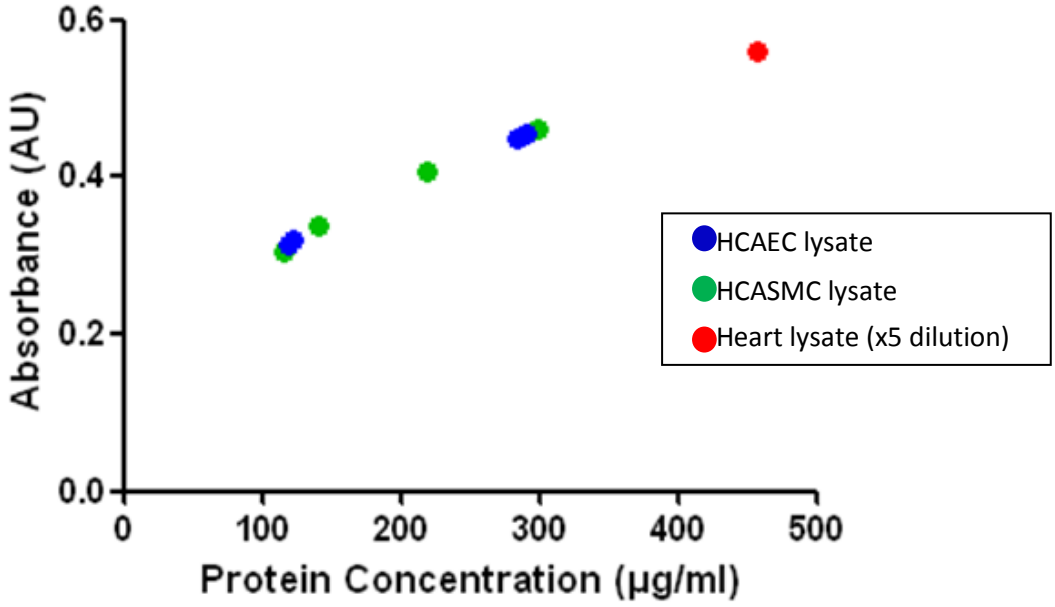

Figure 3.1: BCA Protein Assay of rat tissue and HCAEC and HCASMC lysates
Total protein concentration for HCAEC (blue) and HCASMC (green) lysates between passages 7-10, and rat heart lysate (red) at a 5 fold dilution. The protein concentration of HCAEC and HCASMC lysates are comparable while the high total protein concentration of rat heart lysate is evident, even at a 5 fold dilution. Absorbance recorded using spectrophotometer set at 562 nm. N=2.

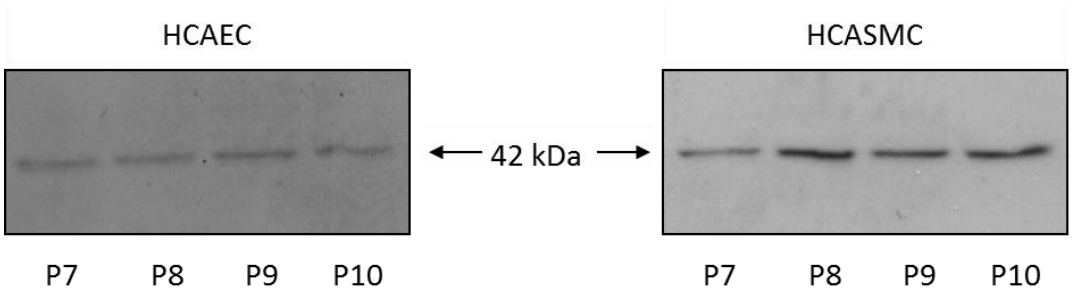

Figure 3.2: Western blot of actin in HCAECs and HCASMCs
Human cultured cell lysates (P7-P10) targeted with mouse anti-actin primary antibody (x500 dilution, 5% non-fat powdered milk), subsequently targeted with HRP-conjugated goat anti-mouse secondary antibody (x10,000 dilution, 5% non-fat powdered milk). Single band at 42 kDa. 10 minutes exposure. HCAEC, N=4. HCASMC, N=7.

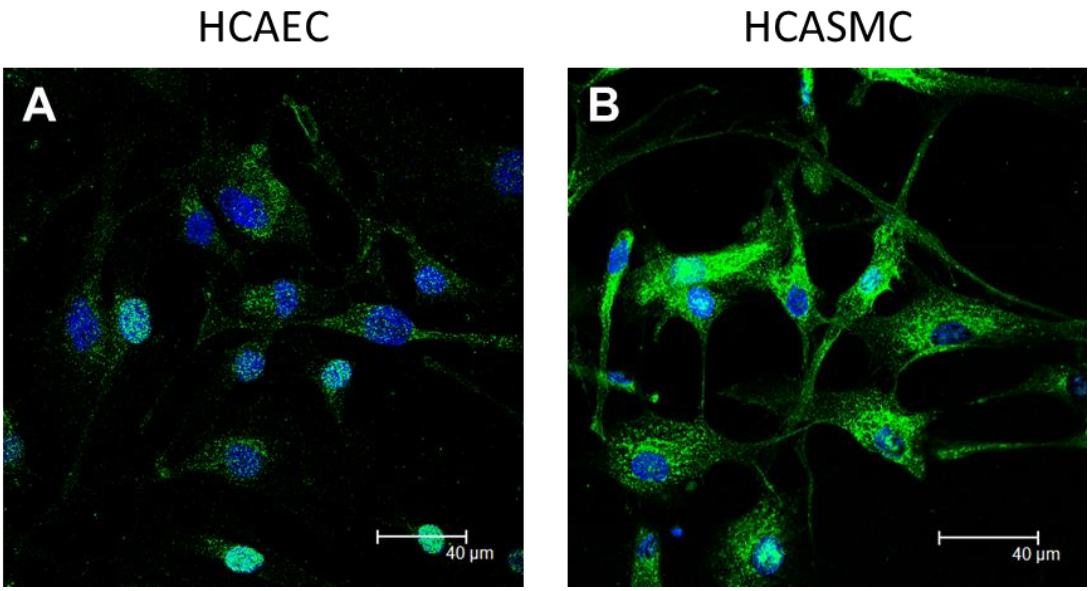

Figure 3.3: Immunocytochemistry of Actin expression in HCAECs and HCASMCs Immunofluorescent labelling of Actin (green) in HCAECs is shown in A and in HCASMCs in B. Actin was identified throughout the cell in both HCAECs and HCASMCs, with comparable fluorescence intensity (mean amplitudes of 22.24 AU and 39.82, respectively). DAPI nuclear staining is represented in blue. Mouse anti-actin primary antibody and AF488-tagged goat anti-mouse secondary antibody were used at x500 dilution. HCAECs, N=2. HCASMCs, N=3.

3.2.2 - Characterisation of HCAECs

3.2.2.1 - vWF

Preliminary experiments identified vWF in HCAECs as a smudge of banding in the region of 76- 225 kDa (Figure 3.4). Comparable banding between passages 6-10 (P6-P10) of HCAECs was detected, suggesting no decline in protein expression or change in characteristics of the cell population.

The distribution pattern of vWF in HCAECs was examined through immunocytochemistry techniques and is shown in Figure 3.5. Labelling of the anti-vWF primary antibody with an AF488-conjugated secondary antibody (green) identified vWF within the Weibel-Palade bodies of the endothelial cells (Figure 3.5).

3.2.2.2 - CD31

Preliminary experiments identified CD31 in P6-P10 HCAEC lysate as a single band at the MW of 135 kDa (Figure 3.6). Similar preliminary experiments also identified CD31 through immunocytochemistry, as shown in Figure 3.7. The involvement of CD31 in intercellular junctions is reflected in its identification along cell borders in HCAECs, as identified by the white arrows (Figure 3.7B). This membranous staining was supplemented by additional low-level staining (approximately 100 AU) throughout the cell (Figure 3.7A and 3.7B).

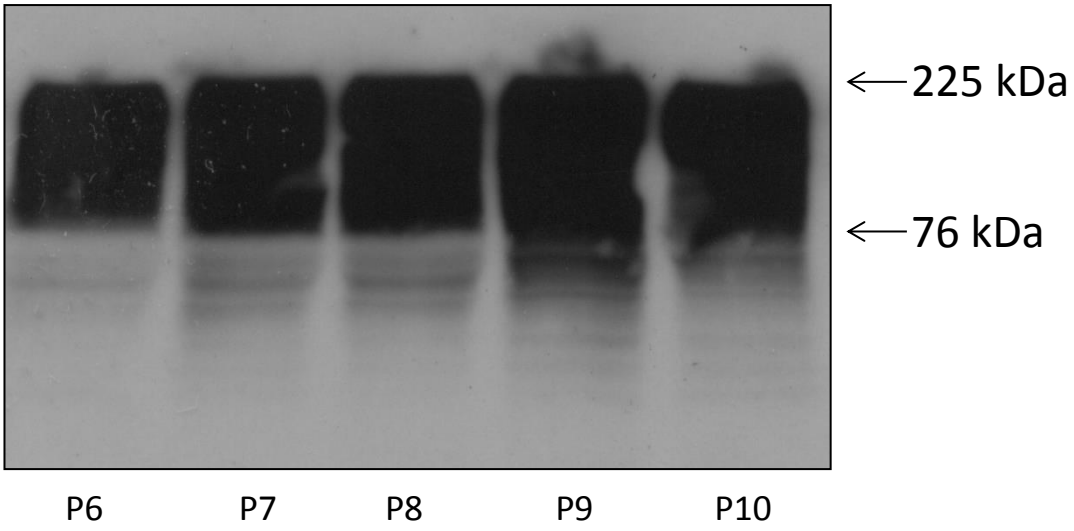

Figure 3.4: Western blot of vWF in HCAECs
HCAEC lysate (P6-P10) targeted with rabbit anti-human von Willebrand Factor (vWF) primary antibody (x500 dilution, 5% non-fat powdered milk), subsequently targeted with HRP-conjugated goat anti-rabbit secondary antibody(x5,000 dilution, 5% non-fat powdered milk). Continuous smear of banding in the high molecular weight regions, typical of vWF banding. 5 minutes exposure. N=1.

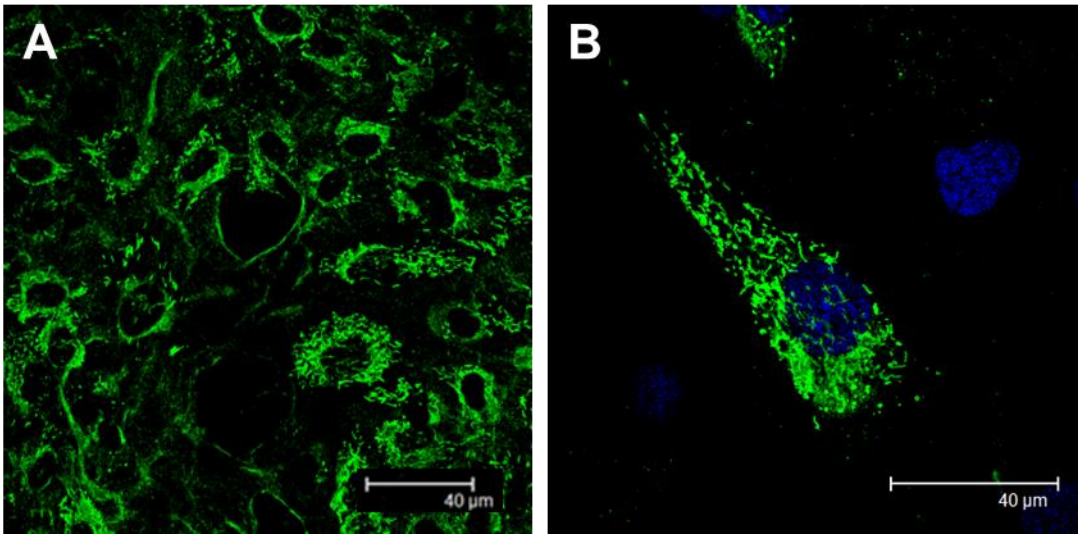

Figure 3.5: Immunocytochemistry of vWF expression in HCAECs
Immunofluorescent labelling of vWF (green) in HCAECs is shown in A and B. vWF is localised within the cigar-shaped Weibel-Palade bodies of these endothelial cells. DAPI nuclear staining is represented in blue. Rabbit anti-vWF primary antibody was used at a x300 dilution and the AF488-tagged goat anti-rabbit secondary antibody was used at x500 dilution. N=3.

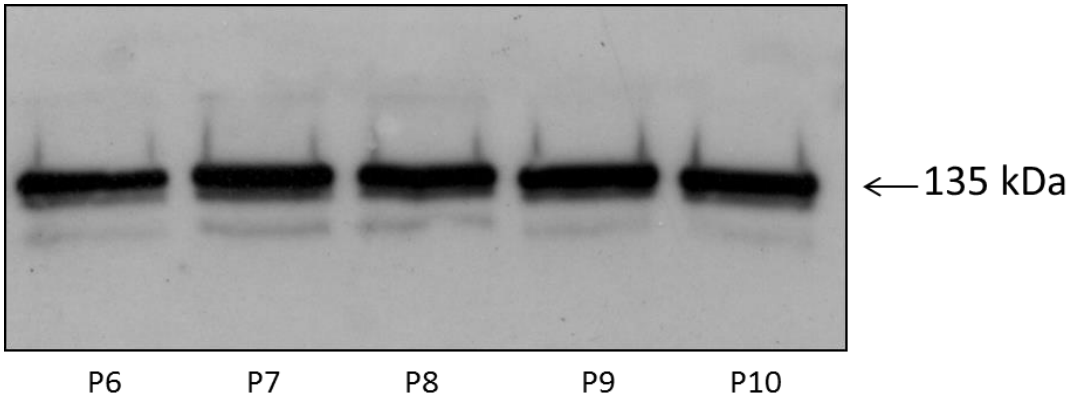

Figure 3.6: Western blot of CD31 in HCAECs
HCAEC lysate (P6-P10) targeted with mouse anti-human CD31 primary antibody (x500 dilution, 1% non-fat powdered milk), subsequently targeted with HRP-conjugated goat anti-mouse secondary antibody(x10,000 dilution, 1% non-fat powdered milk). Primary band at 135 kDa. 5 minutes exposure. N=2.

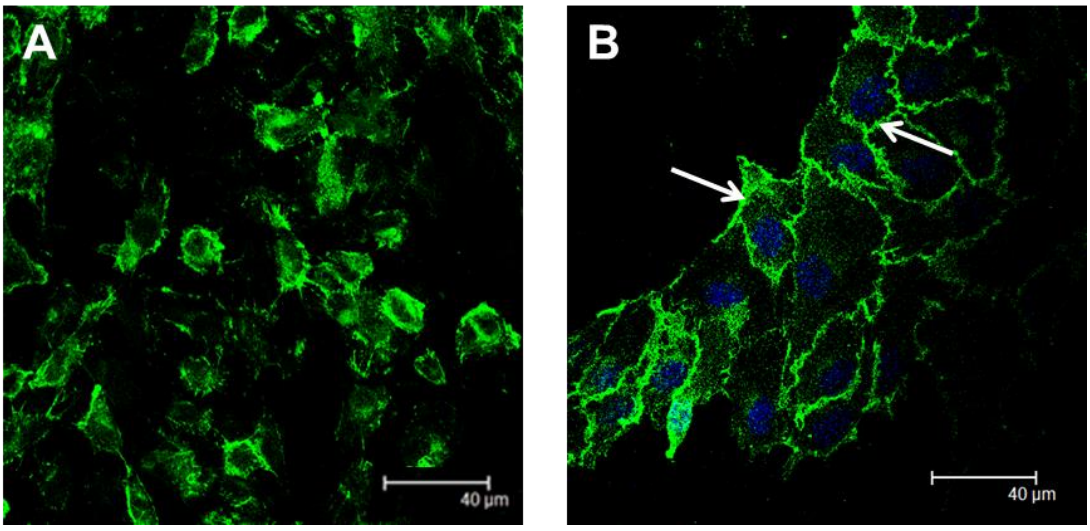

Figure 3.7: Immunocytochemistry of CD31 expression in HCAECs
Immunofluorescent labelling of CD31 (green) in HCAECs is shown in A and B. CD31 is localised at the cell membrane (white arrows) supplemented by low-level staining (approximately 100 AU) throughout the cell. DAPI nuclear staining is represented in blue. Mouse anti-CD31 primary antibody and AF488-tagged goat anti-mouse secondary antibody were used at x500 dilution. N=2.

3.2.2.3 – IP_3 receptor expression

Immunocytochemical labelling of two IP_3 receptor isoforms appeared to identify expresion of IP_3R1 and IP_3R2 in HCAECs (Figure 3.8). During these preliminary experiments, distinct areas of punctate staining were evident for both receptor subtypes, however IP_3R1 appeared to be more extensively expressed in HCAECs than IP_3R2. Two antibodies against either the C-terminus (Figure 3.8B) or the N-terminus (Figure 3.8C) of IP_3R2 were used.

3.2.2.4 - Characterisation of HCAECs - Summary

Primary human coronary artery endothelial cells were successfully characterised throughout their culture period through both Western blot analysis and immunocytochemistry. The endothelial marker CD31 was correctly identified at the appropriate molecular weight of 135 kDa and the HRP-conjugated secondary antibody targeted against the anti-vWF primary antbody displayed smeared banding. In support of this, confocal microscopy images identified expression of both vWF and CD31 in the Weibel-Pallade bodies and at cell membranes, respectively.

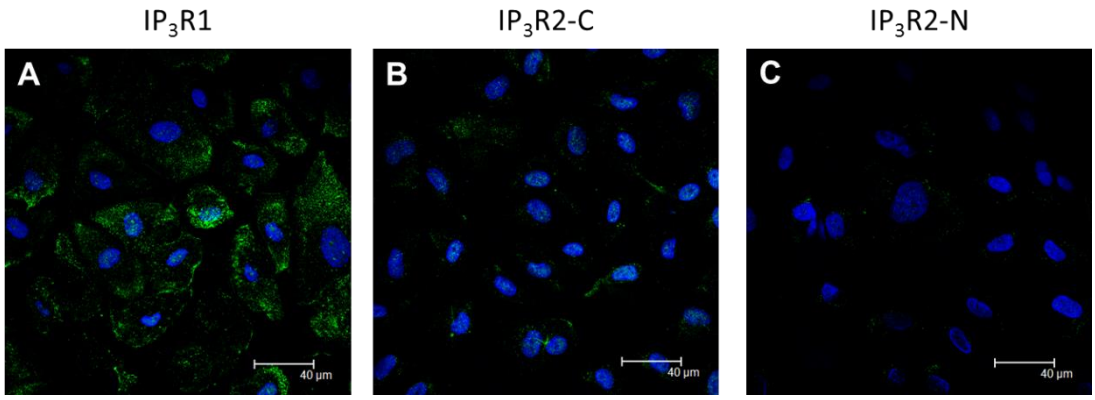

Figure 3.8: Immunocytochemical analysis of IP_3R expression in HCAECs

IP_3R1 distribution in HCAECs is shown in A. Preliminary experiments indicate that extensive staining for IP_3R1 is evident throughout the cells. The 2 antibodies against the C- (B) and N-terminus (C) of IP_3R2 show distinct areas of punctate staining for this IP_3R in HCAECs. DAPI nuclear staining is shown in blue. The anti-IP_3R primary antibodies were used at a 200 fold dilution, and the anti-rabbit secondary antibody at a 500 fold dilution. N=1.

3.2.3 - Characterisation of HCASMCs

3.2.3.1 - Detection of Endothelial Markers in HCASMCs – Negative Control

HCASMCs were labelled for both vWF and CD31 to ensure a pure smooth muscle cell culture. The preliminary results of this negative control experiment are shown in Figure 3.9. No staining for either endothelial cell marker was identified in the lysates of HCASMC populations. P10 endothelial cell lysate was used as a positive control. Although a single band was detected at approximately 225 kDa in P10 and p11 HCASMC lysates labelled for vWF, this is not the smear of banding reliably produced by vWF and was therefore disregarded.

3.2.3.2 - α-actin

α-actin has a molecular weight of 42 kDa and was identified as a single band in cultured HCASMCs throughout passages 7-11, as shown in Figure 3.10. Banding was consistent throughout the culture period, and no decline in protein expression, or change in characteristics, was observed. The distribution of α-actin in the HCASMCs was examined using immunocytochemistry techniques (Figure 3.11). An AF488-conjugated secondary antibody (green) directed against the anti- α-actin primary antibody was used to visualise α-actin. During these preliminary experiments, α-actin was found to be associated with the cytoskeleton in a uni-directional pattern (Figure 3.11) typical of contractile vascular smooth muscle cells.

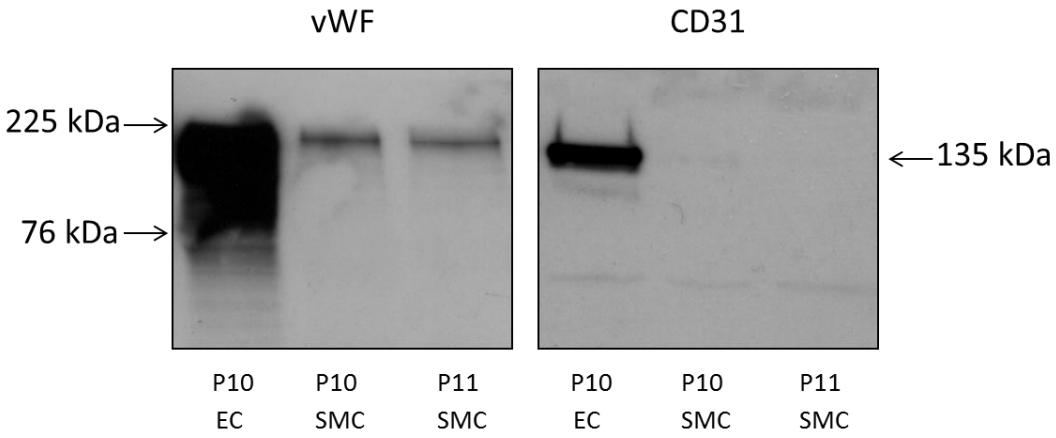

Figure 3.9: Western blot of endothelial markers in HCASMCs as negative control
HCASMC lysate (P10 and P11) targeted with two endothelial cell-specific markers; vWF and CD31. Primary and secondary antibodies used at dilutions previously detailed (vWF: 500/5,000 and CD31: 500/10,000) in 5% and 1% non-fat powdered milk, respectively. HCAEC lysate acted as positive control with smeared banding when probed for vWF, and single band at 135 kDa when targeted with CD31. No banding for either endothelial cell-specific marker in either P10 or P11 HCASMC lysates. 5 minutes exposure. For vWF, N=2. For CD31, N=1.

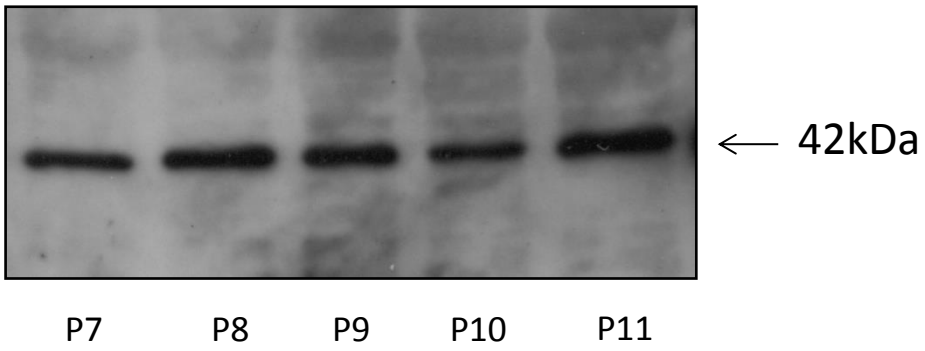

Figure 3.10: Western blot of α-actin in HCASMCs
HCASMC lysate (P7-P11) targeted with mouse anti-α smooth muscle actin primary antibody (x500 dilution, 5% non-fat powdered milk), subsequently targeted with HRP-conjugated goat anti-mouse secondary antibody (x10,000 dilution, 5% non-fat powdered milk). Single band at 42 kDa. 48 hours exposure. N=3.

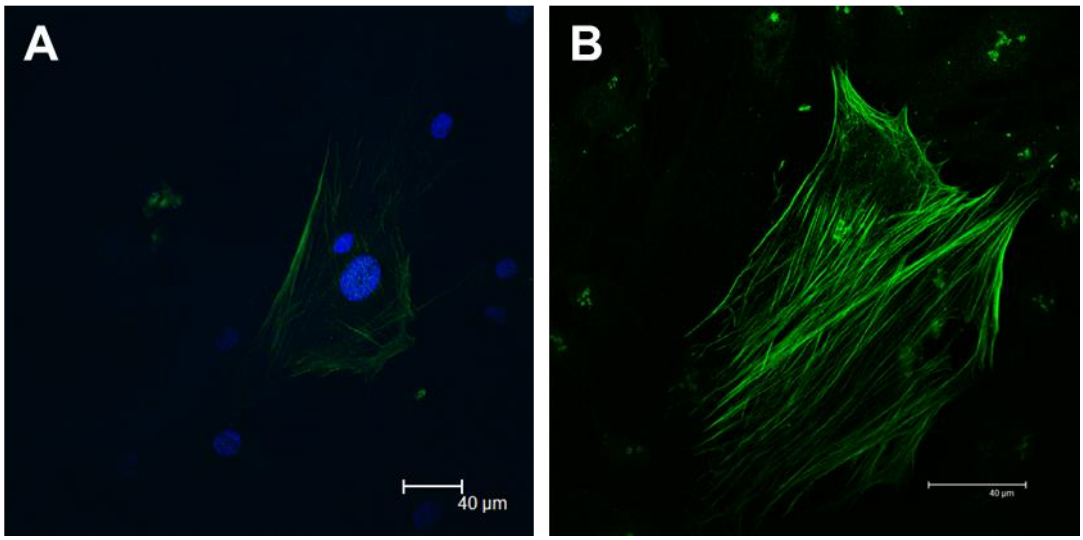

Figure 3.11: Immunocytochemistry of α-actin expression in HCASMCs
Immunofluorescent labelling of α-actin (green) in HCASMCs is shown in A and B. α -actin shows clear association with the cytoskeleton. DAPI nuclear staining is represented in blue. Mouse anti-α smooth muscle actin primary antibody was used at x300 dilution, and the AF488-tagged goat anti-mouse secondary antibody was used at x500 dilution. N=2.

3.2.3.3 - Calponin

Calponin was successfully identified in P7-P11 HCASMC lysates as a single band at the MW of 34 kDa (Figure 3.12). Calponin was also identified through immunocytochemistry, with an AF488-conjugated secondary antibody directed against the anti-calponin primary antibody (Figure 3.13). These preliminary experiments identified calponin distributed throughout the cell with areas of membranous and cytoskeletal association. Image A was also labelled with DAPI (blue) to determine the region of the nuclei (Figure 3.13A).

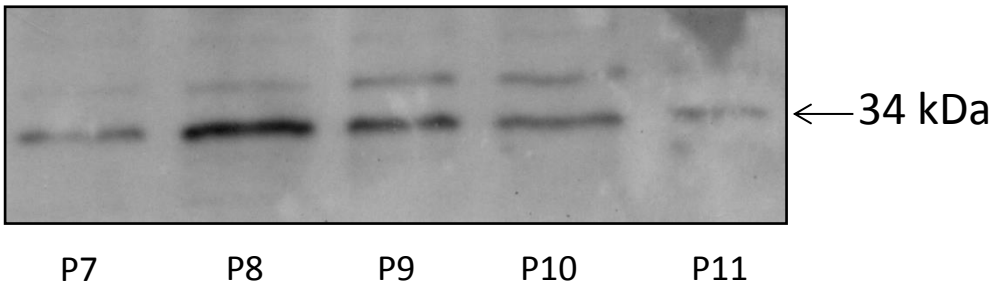

Figure 3.12: Western blot of calponin in HCASMCs
HCASMC lysate (P7-P11) targeted with mouse anti-calponin primary antibody (x500 dilution, 5% non-fat powdered milk), subsequently targeted with HRP-conjugated goat anti-mouse secondary antibody(x10,000 dilution, 5% non-fat powdered milk). Primary band at 34 kDa. 10 minutes exposure. N=5.

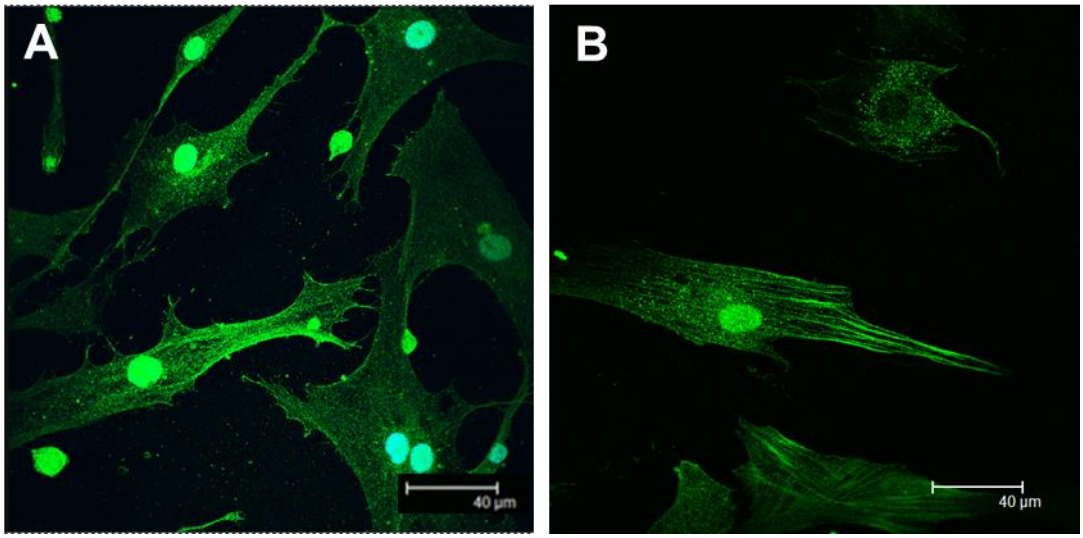

Figure 3.13: Immunocytochemistry of calponin expression in HCASMCs
Immunofluorescent labelling of calponin (green) in HCASMCs is shown in A and B. Calponin is distributed diffusely throughout the cell with moderate association with the cytoskeleton. DAPI nuclear staining is represented in blue. Mouse anti-calponin primary antibody was used at x200 dilution, and the AF488-tagged goat anti-mouse secondary antibody was used at x500 dilution. N=2.

3.2.3.4 - Characterisation of HCASMC - Summary

Through Western blot and immocytochemical analysis HCASMCs were shown to maintain a consistent phenotype throughout the culture period. This phenotype was skewed towards the contractile end of the continuous spectrum of smooth muscle cell phenotypes, highlighted by consistent α-actin staining during preliminary experiments (Figure 3.9). Identification of relatively consistent calponin staining throughout passages 7-11 further highlighted the maintenance of a single phenotype throughout culture.

3.2.4 - HCAEC and HCASMC Cell Culture Images

Photographs of cell cultures were taken throughout the culture period using a light microscope at x10 magnification (Figure 3.14). HCAECs (Figure 3.14A) displayed a cobblestone appearance while the HCASMCs (Figure 3.14B) had a more stellate or spindle-shaped morphology during these preliminary experiments. In order to ensure reliability throughout experiments, if any cell cultures varied from these phenotypes, or changes to proliferation rate or general cell behaviour were observed, the cultures were abandoned.

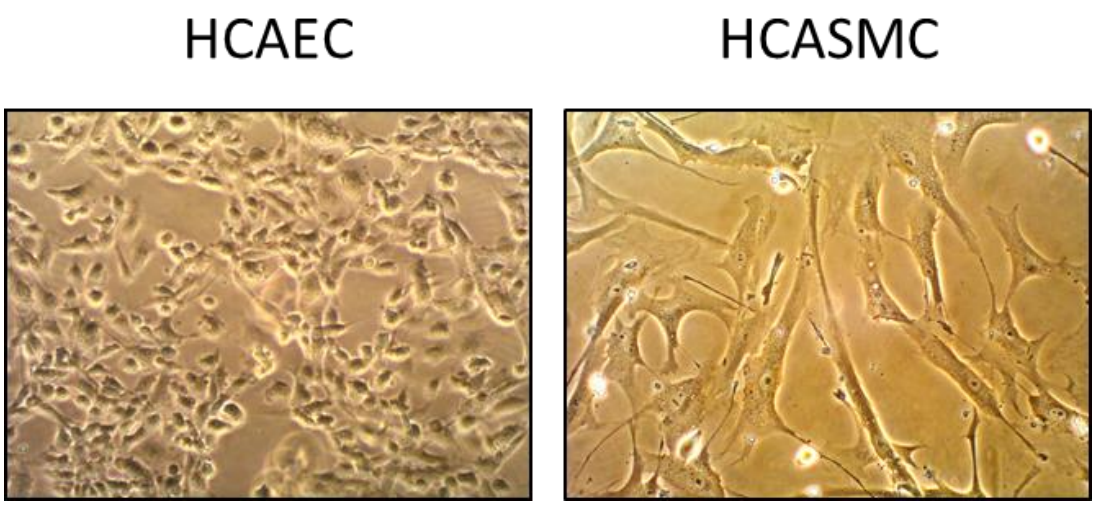

Figure 3.14: Typical HCAEC and HCASMC phenotype
Cell culture photographs of HCAECs (A) and HCASMCs (B). The HCAECs display the cobblestone appearance typical of cultured endothelial cells (A). HCASMCs of the contractile phenotype present a stellate form with numerous processes (B). Images recorded at x10 magnification. N=2.

3.2.5 - Characterisation of Rat Tissue

3.2.5.1 - Immunocytochemistry

vWF was identified in the single layer of endothelial cells of the rat coronary artery during preliminary experiments (Figure 3.15A & 3.15B). In addition, vWF was also identified in the endothelium lining the lumen of the rat mesenteric artery in these experiments (Figure 3.15C & 3.15D, and 3.15E & 3.15F). In Figure 3.15B DAPI nuclear staining is shown in blue.

Figure 3.16 shows preliminary α-actin staining within the multiple layers of smooth muscle cells of the tunica media in rat coronary (Figure 3.16A & 3.16B) and mesenteric (Figure 3.16C & 3.16D) arteries. Initial experiments identified calponin in rat coronary arteries (Figure 3.17A & 3.17B) and mesenteric arteries (Figure 3.17C & 3.17D). This smooth muscle marker was also identified distributed throughout the multiple smooth muscle layers during these experiments.

3.2.5.2 - Western blot

The smooth muscle markers α-actin and calponin were identified in rat heart lysate used at a 5 fold dilution (Figure 3.18). α-actin was identified as a strong band at 42 kDa (Figure 3.18A), and calponin as a single band at 34 kDa (Figure 3.18B). This lysate provided a consistently reliable source of smooth muscle marker protein staining, and provided a control for future experiments.

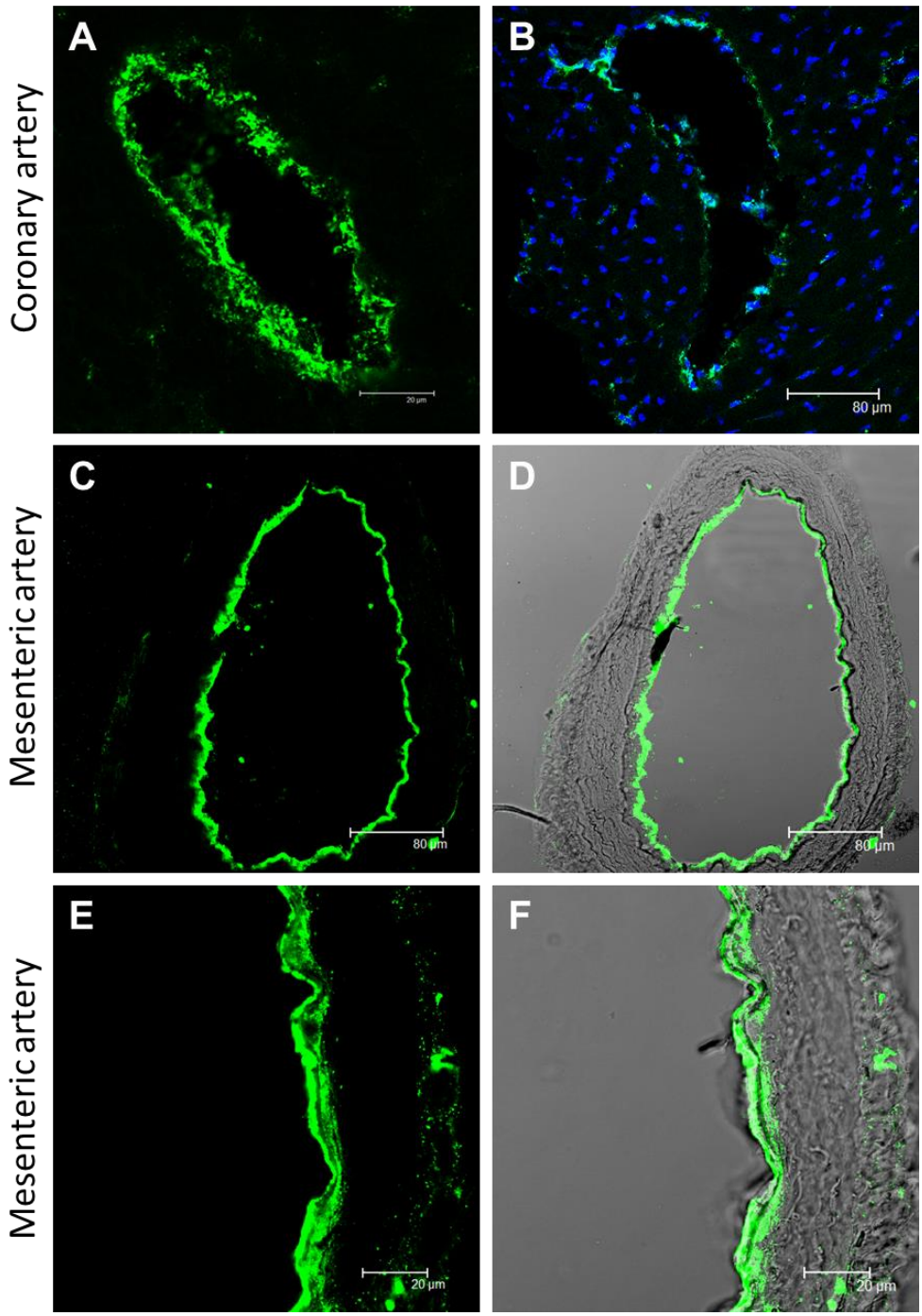

Figure 3.15: Immunohistochemistry of vWF expression in rat coronary and mesenteric arteries

Immunofluorescent labelling of vWF (green) is shown in rat coronary artery (A & B) and mesenteric artery (C & D and E & F). vWF is restricted to the single endothelial cell layer lining the lumen of these vessels. DAPI nuclear staining is represented in blue (B). Image D is the same as C with a brightfield image overlay. Images E and F are the same section as C and D at a higher magnification. Rabbit anti-vWF primary antibody was used at x300 dilution and the AF488-tagged goat anti-rabbit secondary antibody was used at x500 dilution. N=2.

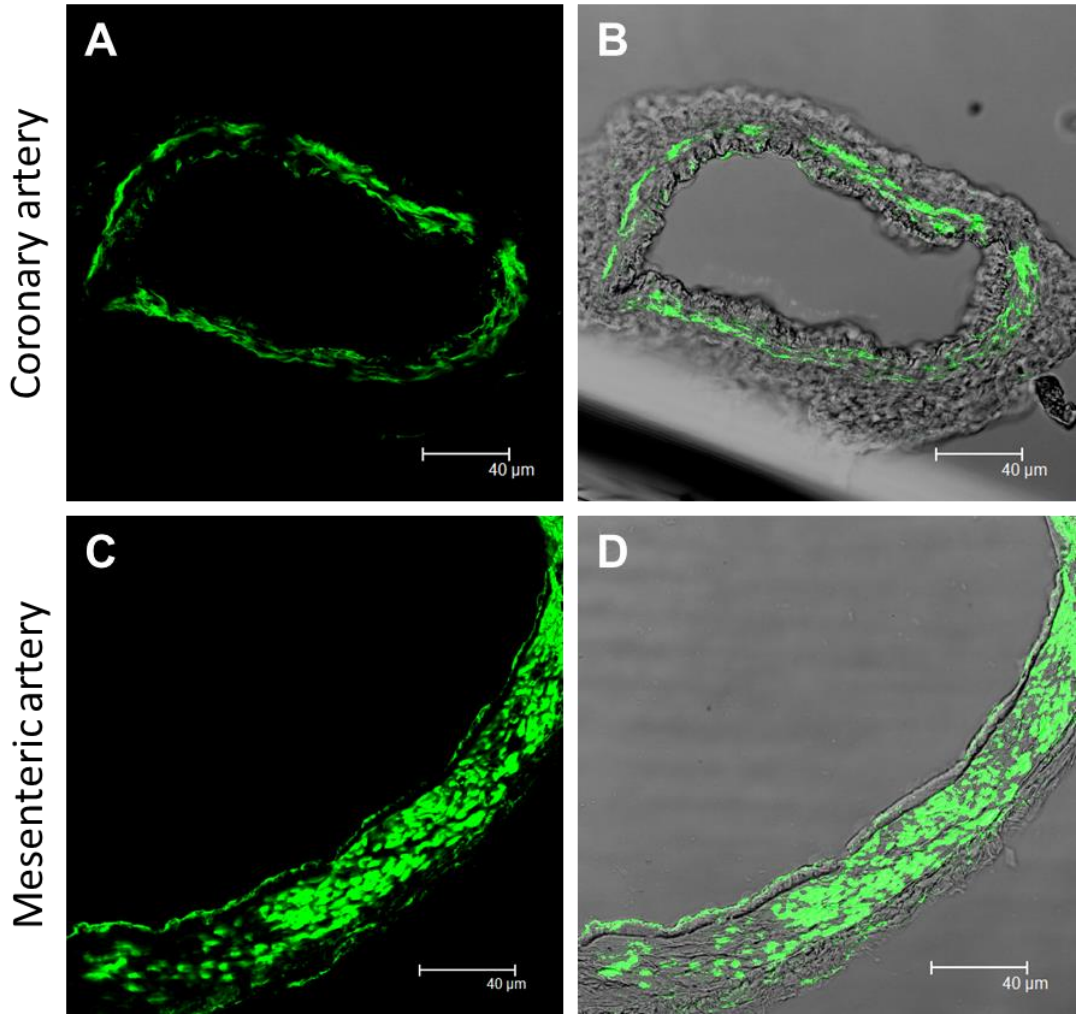

Figure 3.16: Immunohistochemistry of α-Actin expression in rat coronary and mesenteric arteries

Immunofluorescent labelling of α-Actin (green) is shown in rat coronary artery (A & B) and mesenteric artery (C & D). α-Actin was identified within the multiple layers of smooth muscle cells forming the Tunica Media of the vessel wall. Images B and D display the brightfield image overlay of the corresponding section shown in A and C, respectively. Mouse anti-α smooth muscle Actin primary antibody was used at x300 dilution, and the AF488-tagged goat anti-mouse secondary antibody was used at x500 dilution. N=1.

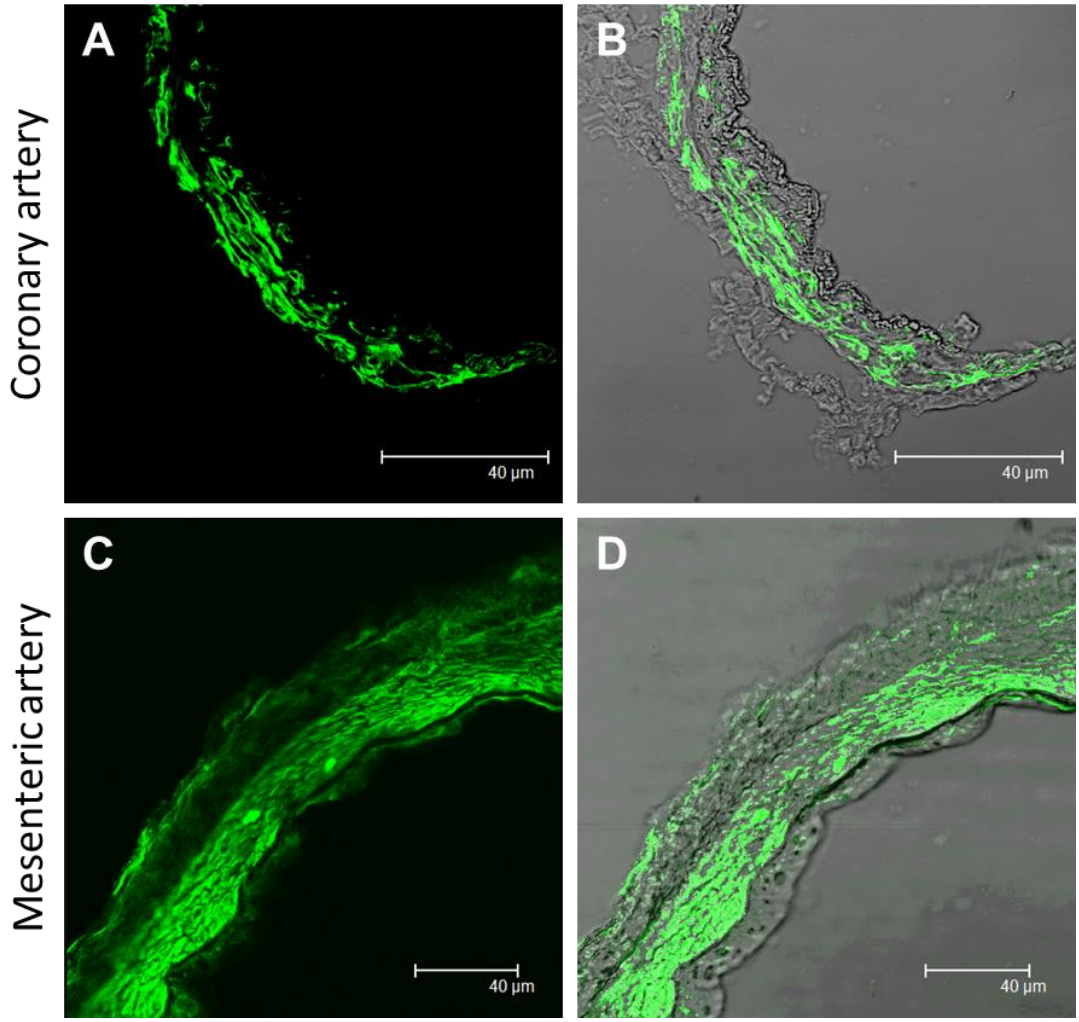

Figure 3.17: Immunohistochemistry of Calponin expression in rat coronary and mesenteric arteries

Immunofluorescent labelling of calponin (green) is shown in rat coronary artery (A & B) and mesenteric artery (C & D). Calponin was identified within the smooth muscle layers of both vessels. Images B and D display the brighfield image overlay of the corresponding section shown in A and C, respectively. Mouse anti-calponin primary antibody was used at x200 dilution, and AF488-conjugated goat anti-mouse secondary antibody used at x500 dilution. N=1.

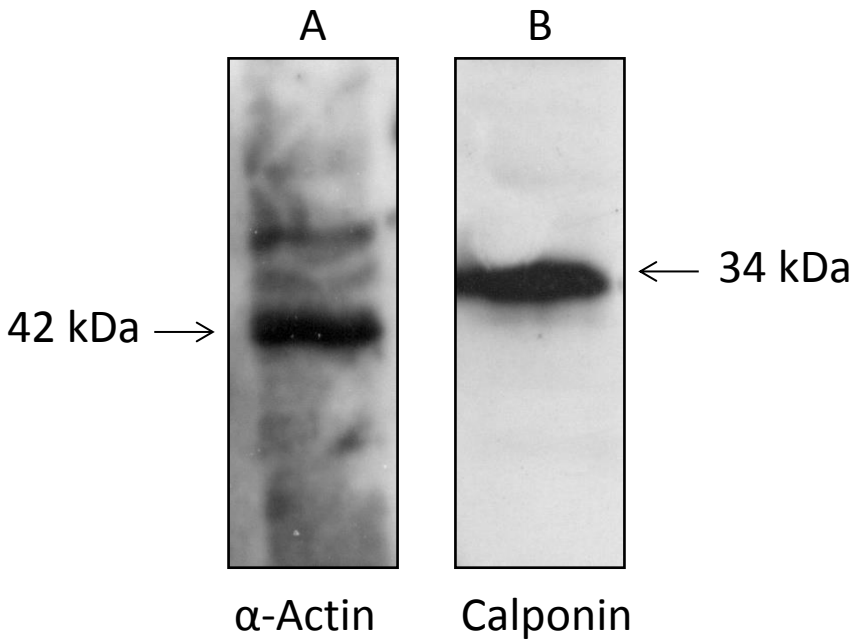

Figure 3.18: Western blot of SMC markers in rat heart lysate

Western blot analysis identified α-smooth muscle Actin (A) and calponin (B) within rat heart lysate. Mouse anti-α smooth muscle Actin and anti-Calponin primary antibodies were both used at x500 dilution in 5% non-fat powdered milk. The HRP-conjugated goat anti-mouse secondary antibody was used at x10,000 dilution in 5% non-fat powdered milk. Films shown represent 48 hours exposure (α-Actin) and 5 minutes exposure (Calponin). For α-actin, N=2. For calponin, N=3.

3.2.6 - Immunocytochemistry Negative Controls

Two negative control conditions were routinely carried out during immunocytochemistry experiments. The first was to label the cultured cells directly with the AF488-conjugated secondary antibody without prior incubation with a primary antibody. Two examples of the results obtained for this condition in HCAECs and HCASMCs are displayed in Figure 3.19A & 3.19B. Neither HCAECs nor HCASMCs showed any AF488 signal above 42 AU, and as such this level was taken to be background auto-fluorescence and set as the threshold for all immunocytochemistry experiments. The second negative control condition was to label the cultured cells with the incorrect AF488-conjugated secondary antibody. The example shown in Figure 3.19C shows HCAECs labelled with the mouse anti-actin primary antibody and the AF488-conjugated goat anti-rabbit secondary antibody. No AF488 signal was detected above 8 AU.

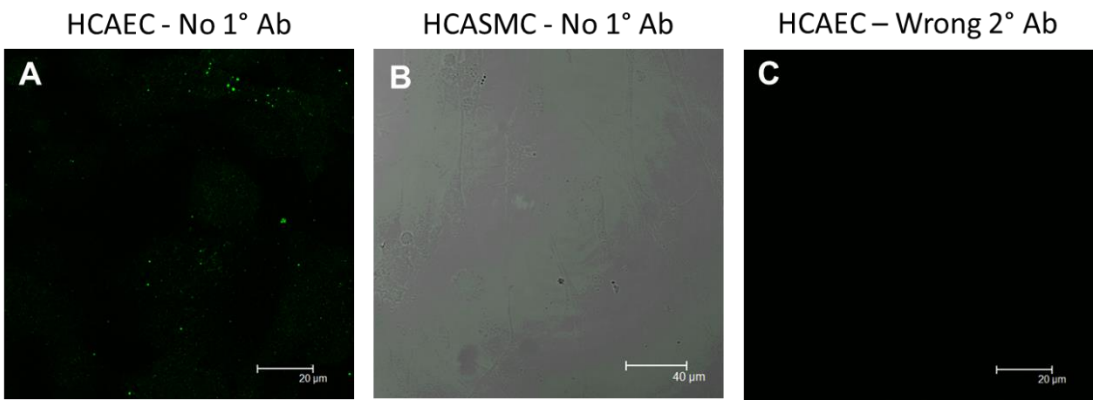

Figure 3.19: Immunohistochemistry negative controls

Labelling of HCAECs (A) and HCASMCs (B) with an AF488-conjugated secondary antibody without the application of a primary antibody. No staining was detected above 42 AU for either experiment so this was set as the level for background staining. B is displayed with a brightfield image overlay. C shows labelling of HCAECs with the goat anti-rabbit AF488-conjugated secondary antibody after labelling of the cells with the mouse anti-actin primary antibody. Mouse anti-actin primary antibody and AF488-tagged goat anti-rabbit secondary antibody were used at x500 dilution. N=2.

3.3 –Discussion

3.3.1 – Characterisation of HCAECs

Preliminary Western blot and immunocytochemistry experiments indicated that HCAECs expressed the endothelial markers vWF and CD31 throughout the culture period. vWF was identified as a smudge of banding in the high molecular weight region (Figure 3.4), staining that is typical of vWF banding due to its multimeric structure (Ruggeri and Ware 1993). Labelling of vWF with an AF488-conjugated secondary antibody identified its distribution within the Weibel-Palade bodies of the endothelial cells, and the elongated shape of these specialised lysosomal structures is typical of vWF staining in vascular endothelial cells (Weibel and Palade 1964, Wagner, Olmsted et al. 1982). HCAECs were further characterised using an additional endothelial marker, CD31. CD31 has a molecular weight of 135 kDa and is detected as a single band via Western blot (Stockinger, Gadd et al. 1990), as shown in Figure 3.6. The role played by CD31 in the regulation of endothelial cell intercellular junctions (Albelda, Muller et al. 1991, Cao, O'Brien et al. 2002) is highlighted by its identification at the membrane of HCAECs, as in Figure 3.7. HCAECs were also shown to express the IP_3 receptors IP_3R1 (Figure 3.8A) and IP_3R2 during preliminary experiments (Figure 3.8B and Figure 3.8C), with IP_3R1 appearing to be the predominant receptor subtype.

3.3.2 - Characterisation of HCASMCs

HCASMCs are well known to exist in numerous states along a spectrum of phenotypes from the extremes of quiescent and contractile cells, to those of a synthetic phenotype (Gabbiani, Schmid et al. 1981, Absher, Woodcock-Mitchell et al. 1989, Frid, Shekhonin et al. 1992, Worth, Rolfe et al. 2001, Rensen, Doevendans et al. 2007). As such, both Western blot analysis and immunocytochemical labelling of the smooth muscle markers α-actin and calponin was utilised to monitor the HCASMC phenotype throughout culture. Preliminary Western blot experiments identified α-actin as a single band at 42 kDa throughout passages 7-11 (Figure 3.10). Preliminary immunocytochemical staining for α-actin also identified this protein clearly associated with the cytoskeleton (Figure 3.11), and this uni-directional pattern is typical of smooth muscle cells of the contractile phenotype (Worth, Rolfe et al. 2001), and specifically HCASMCs, as demonstrated in work by (Grenier, Sandig et al. 2009) and (Beamish, He et al. 2010). Furthermore, additional preliminary experiments using the smooth muscle marker calponin re-enforced our hypothesis that these cells were of the contractile phenotype, as this calcium-binding protein is linked to the contractile

machinery of smooth muscle cells through its interaction with α–actin (Gimona, Kaverina et al. 2003) and can be seen arranged in a longitudinal orientation (Figure 3.13B). The lack of banding for either endothelial marker (vWF or CD31) in preliminary negative control experiments again implied that the HCASMC culture was purely smooth muscle cells (Figure 3.9).

The cultured HCASMCs were shown to display the elongated, spindle-shaped morphology typical of the contractile smooth muscle cell phenotype, and not the cobblestone morphology typically seen with those of the synthetic phenotype, as indicated by the preliminary experiments shown in Figure 3.14B (Absher, Woodcock-Mitchell et al. 1989, Rensen, Doevendans et al. 2007). Similarly, preliminary data indicated the HCAECs to have the cobblestone appearance typical of endothelial cells throughout the vasculature (3.14A) (Malek and Izumo 1996, Borg-Capra, Fournet-Bourguignon et al. 1997).

3.3.3 - Characterisation of rat tissues

Rat coronary and mesenteric arteries provided a suitable *in vivo* tissue for comparison with the cultured human cells. Both rat coronary and mesenteric arteries showed staining for vWF on the border of the vessel lumen in preliminary experiments, clearly identifying the endothelial cell layer (Figure 3.15), and this staining is typical of the endothelial marker in the rat vasculature (Roberts, Kamishima et al. 2013). Preliminary data also indicated the expression of α-actin within the multiple layers of smooth muscle cells forming the bulk of the tunica media of rat coronary and mesenteric arteries (Figure 3.16). This staining is typical of α-actin expression in a variety of vascular beds (Skalli, Ropraz et al. 1986, Frid, Shekhonin et al. 1992), including coronary arteries (Cai, Koltai et al. 2003). Similarly, calponin was also identified within this layer of the vasculature during these experiments (Figure 3.17), again reflecting its identification in the literature (Su, Xie et al. 2013).

3.3.4 – Concluding remarks

Preliminary Western blot and immunofluorescence data indicated that the primary HCAECs and HCASMCs expressed the characteristic markers of endothelial cells and smooth muscle cells, respectively. As such, these cultured cells were considered suitable representatives of their respective tissue and deemed appropriate for further experimental use.

Chapter 4:

Connexins and Cadherins in HCAECs and HCASMCs

Aims of this chapter:

- To use Western Blot analysis to determine whether HCAECs and HCASMCs express connexins (connexins 37, 40 and 43) and cadherins (VE-cadherin and N-cadherin)
- To use immunocytochemical technique to examine the distribution of these connexins and cadherins in HCAECs and HCASMCs
- To use immunocytochemical technique to determine whether these junctional proteins co-localise in HCAECs

Key findings of this chapter:

- HCAECs and HCASMCs express Cx37, Cx40 and Cx43, as determined by Western blot analysis and immunocytochemistry
- Cx37 and Cx43 appeared to be the predominant connexins expressed in HCAECs
- Cx43 appeared to be the primary connexin expressed in HCASMCs
- HCAECs express both VE-cadherin and N-cadherin, as determined by Western blot analysis and immunocytochemistry
- HCASMCs express N-cadherin, as determined by Western blot analysis and immunocytochemistry
- Co-localisation between VE-cadherin and Cx37, Cx40 and Cx43 was identified at the membrane in HCAECs. VE-cadherin and Cx37 appeared to show the most extensive co-localisation
- No co-localisation between N-cadherin and Cx37 or Cx40 was detected in HCAECs. Isolated areas of co-localisation between N-cadherin and Cx43 was observed in a subset of HCAECs

4.1 - Introduction

Cadherins and connexins form adherens junctions (AJs) and gap junctions (GJs), respectively, and are two of the major contributors to endothelial cell-cell communication and maintenance of the endothelial barrier (Van Rijen, van Kempen et al. 1997, Yeh, Rothery et al. 1998, Evans and Martin 2002, Noda, Zhang et al. 2010). The vascular endothelium primarily expresses VE-cadherin and N-cadherin, while only the former is thought to be responsible for AJs (Salomon, Ayalon et al. 1992, Navarro, Ruco et al. 1998). Vascular endothelial cells also express Cx37, Cx40 and Cx43 (Van Rijen, van Kempen et al. 1997, Yeh, Rothery et al. 1998, Evans and Martin 2002). The formation of AJs is considered to be a precursor for the formation of functional GJs (Wallez and Huber 2008), and as such the overlap of the expression profiles of these junctional components was examined in HCAECs.

4.1.1 – Gap Junctions

4.1.1.1 - Gap junction structure and formation

Connexins are the hydrophilic proteins in vertebrates that, upon interaction, form the intercellular gap junction channel (see Figure 4.1) (Goodenough 1974, Dejana, Corada et al. 1995, Yeh, Rothery et al. 1998, Evans and Martin 2002). Connexins were first identified by Goodenough in 1974 as bands identified at 10,000 Da in SDS-PAGE analysis. Innexins represent the proteins forming GJ channels in invertebrates, however these display little sequence homology to their vertebrate counterparts (Evans and Martin 2002). The assembly of connexins into functional GJ channels involves a number of tightly regulated steps. The connexin proteins are initially synthesised by membrane-bound ribosomes like most plasma membrane proteins (Rahman, Carlile et al. 1993, Falk, Kumar et al. 1994). These newly-formed proteins are then inserted into the endoplasmic reticulum (ER) membrane, and time-lapse imaging of green fluorescent protein-tagged connexins has shown that these proteins are routed through the golgi apparatus prior to transport to the plasma membrane (Thomas, Jordan et al. 2005). For the formation of active GJ channels, the connexin proteins must oligomerize to form a hexameric structure, formed from 6 connexin proteins, termed a connexon (Musil and Goodenough 1993, Diez, Ahmad et al. 1999, Das Sarma, Meyer et al. 2001). This oligomerisation is thought to be a sequential process that is initiated in the ER, specifically within the endoplasmic-golgi-intermediate compartment (ERGIC), and to be completed upon arrival at the golgi complex (Diez, Ahmad et al. 1999, Das Sarma, Meyer et al. 2001). In support of this, assembled oligomers were

identified at the ER membrane of cells transfected with Cx32 (Kumar, Friend et al. 1995), and the identification of connexin oligomers within subcellular fractions of rat hepatocytes (Rahman, Carlile et al. 1993, Falk, Kumar et al. 1994). Post-golgi carriers originating at the distal side of the golgi apparatus, and the trans-golgi network, then mediate the delivery of the connexon hemichannels to the plasma membrane (Segretain and Falk 2004, Thomas, Jordan et al. 2005). Microtubules have also been implicated in the regulation of the delivery of connexons to the cell surface. Experiments involving connexins labelled with fluorescent proteins have shown the preferential tethering of the microtubule growing end (the plus end) at adherens junctions, thereby indicating that microtubules can directly target these hemichannels to sites of cell-cell contact (Jordan, Solan et al. 1999, Lauf, Giepmans et al. 2002, Shaw, Fay et al. 2007). The formation of a diffuse cell-surface rim of fluorescently-tagged connexins prior to the appearance of punctate gap junctions, however, indicates that the post-golgi carriers randomly fuse with the plasma membrane and that subsequent lateral diffusion of connexins, within the plane of the plasma membrane, to sites of cell-cell contact allows the formation of function GJ channels (Thomas, Jordan et al. 2005). This is supported by the observation that connexon hemichannels can float freely within the cortical membrane, as detected by fluorescence recovery after photobleaching (FRAP) studies (Lauf, Giepmans et al. 2002). It appears that different connexin subtypes may undergo differential delivery to the plasma membrane as Cx43 delivery to the cell surface was inhibited by both brefeldin A (BFA) and nocodazole, while Cx26 was inhibited by BFA alone (Thomas, Jordan et al. 2005), indicating that Cx26 delivery to the plasma membrane does not involve microtubules or that microtubule-disrupted delivery can be compensated for. Once at the plasma membrane, the connexon of one cell joins that of an adjacent cell to form an intercellular channel, separated by a gap of approximately 2-3 nm, as identified by transmission electron microscopy (Revel and Karnovsky 1967). Open extra-junctional connexon hemichannels have also been identified, as shown by the induction of permeability to the dye Lucifer yellow on a reduction in extracellular calcium concentration in Xenopus oocytes transfected with Cx46 (Paul, Ebihara et al. 1991). This has since also been shown in Novikoff hepatoma cells (Li, Liu et al. 1996, Stout, Goodenough et al. 2004). Once a functional channel is established, connexons aggregate into GJ plaques through clustering of the channels at sites of cell-cell contact (Fujimoto, Nagafuchi et al. 1997, Gaietta, Deerinck et al. 2002, Lauf, Giepmans et al. 2002). New hemichannels initially associate with the periphery of the GJ plaque, and as GJs at the centre of the plaque are internalised for degradation the newer GJs migrate towards the

centre of the plaque (Gaietta, Deerinck et al. 2002, Lauf, Giepmans et al. 2002, Segretain and Falk 2004, Laird 2005).

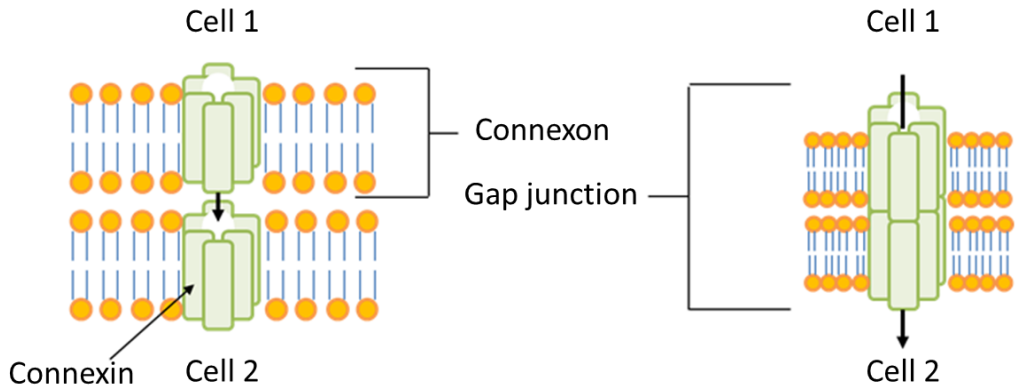

Figure 4.1: Structure of a gap junction channel
This schematic represents a gap junction (GJ) channel formed from connexin (Cx) subunits. Six connexin subunits combine to form a connexon hemichannel (left image). Two connexon hemichannels, one from each cell, unite to form a GJ channel with a pore diameter of approximately 2 nm (right image). These channels directly link the cytoplasm of two adjacent cells and are relatively non-selective allowing the passive transfer of ions and second messenger molecules up to ~ 1,200 Da.

4.1.1.2 – Connexins

Connexin proteins consist of 4 transmembrane domains (M1-M4), cytoplasmic N-terminal and C-terminal tails, 2 extracellular loops (E1 and E2), and a single intracellular loop (see Figure 4.2). The two disulphide-linked extracellular loops are arranged as anti-parallel β-sheets that project into the intercellular gap, and have been shown to be crucial for the docking of two hemichannels on adjacent cells to form a functional GJ channel (Krutovskikh and Yamasaki 2000) and for determining the compatibility of two hemichannels (White, Bruzzone et al. 1994, White, Paul et al. 1995). In addition, a set of three cysteine residues expressed in each extracellular loop (E1 and E2) may help to retain the rigid structure of the extracellular region that allows docking between two hemichannels (Kumar and Gilula 1996). As such, connexin mimetic peptides created from short amino acid sequences found in the extracellular loops of various connexins act as reversible inhibitors of gap junctional intercellular communication (GJIC) (Evans and Boitano 2001). The extracellular loops are highly conserved; however the single intracellular loop linking transmembrane domains M2 and M3 is variable among connexin subtypes and species (Evans and Martin 2002). The amino-terminal tail has been shown to be necessary for insertion of connexon hemichannels into the plasma membrane (Martin, Steggles et al. 2000), and this may be a result of the interaction of this region of the protein with other proteins. The carboxyl tail of Cx43, for example, interacts with the tight junction proteins ZO-1 (Giepmans and Moolenaar 1998) and occludin (Kojima, Sawada et al. 1999), the microtubule component tubulin (Giepmans, Verlaan et al. 2001) and the adherens junction-associated protein β-catenin (Ai, Fischer et al. 2000), among others. As such, similar interactions between the connexin tail and intracellular components may regulate the insertion of the protein into the cell membrane, particularly as connexin protein tails express presumptive Src homology 2 (SH2), SH3 and PDZ domain –binding regions (Brosnan, Scemes et al. 2001).

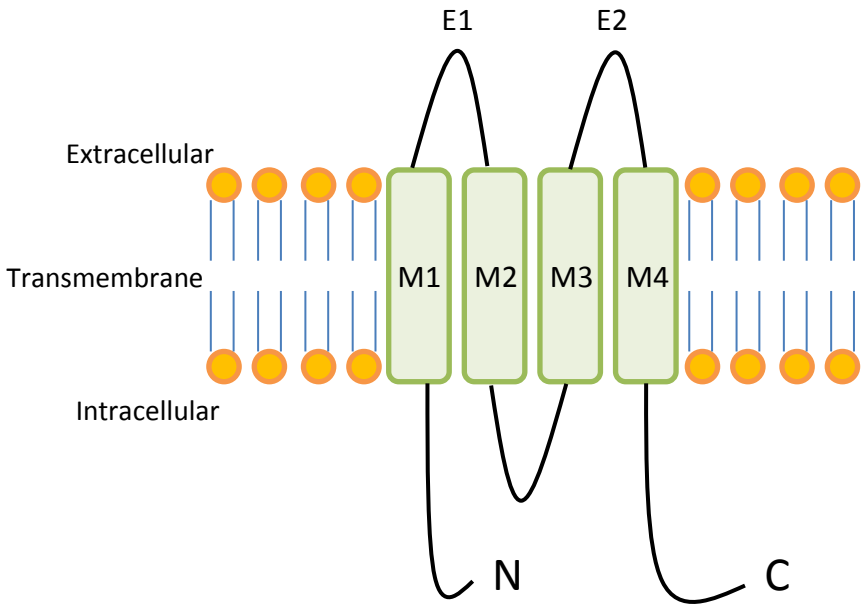

Figure 4.2: Typical connexin structure
Connexins typically consist of 4 transmembrane domains (M1-M4, green), cytoplasmic N-terminal and C-terminal tails, 2 extracellular loops (E1 and E2), and a single intracellular loop. The extracellular loops are generally accepted to be essential for the docking of two hemichannels to form a functional GJ channel. The N-terminal tail is necessary for insertion of connexon hemichannels into the cell membrane. The major differences between different connexin subtypes are determined by the sequence of motifs contained within the C-terminal region. This figure is adapted from Figure 1 of "The Gap Junction Communication Channel" (Kumar and Gilula 1996).

4.1.1.3 – Connexin subtypes

As has already been hinted at, different subtypes of connexins exist. Connexins are primarily divided between 2 classes; α- and β-connexins (a minor γ class also exists but this won't be detailed further here) (Evans and Martin 2002). Cx37, Cx40 and Cx43 are classified as α-connexins, hence their alternative names α4, α5 and α1, respectively (Kumar and Gilula 1996). The major differences between all connexins is determined by the sequence of motifs contained within the intracellular carboxy tail as the amino terminal tail is conserved among connexins (Evans and Martin 2002). GJs can form three types of functional channels; homotypic gap junctions where all 12 connexin subunits are identical, heterotypic gap junctions where each of the two hemichannels contains 6 identical connexins but the connexin type in each hemichannel is different to that displayed on the adjacent cell (White, Bruzzone et al. 1994, Brink 1998), or heteromeric gap junctions where each hemichannel contains more than one type of connexin, although normally restricted to the same class of connexin (α/β) (Jiang and Goodenough 1996, Evans and Martin 2002) (see Figure 4.3). Cx43, an α-type connexin, cannot form functional channels with Cx32, a β-type connexin (White, Paul et al. 1995). Some connexin subtypes, however, cannot form functional gap junctional channels with other subtypes, even when both are from the same class. Cx40 and Cx43, for example, fail to form functional GJs with each other (Elfgang, Eckert et al. 1995, White, Paul et al. 1995, Haubrich, Schwarz et al. 1996). Purkinje fibres of the conducting system of the heart express Cx40 while the ventricular myocardium predominantly expresses Cx43. The failure of Cx40 to form functional channels with Cx43 may prevent inappropriate activation of the ventricular myocardium by the purkinje fibres and thus contribute to the specialised electrical characteristics of this region (Bruzzone, Haefliger et al. 1993). GJ plaques can also be subdivided into various forms; a random mixture of homomeric or heteromeric connexins (or a combination of both), as detected in hepatic cells (Nicholson, Dermietzel et al. 1987, Traub, Look et al. 1989), segregated homomeric connexons in distinct areas within a single GJ plaque, as detected within the epidermis (Risek, Klier et al. 1994), or homomeric connexons that arrange into separate plaques and possibly even localise to distinct areas of the membrane, as identified in the epithelial cells of the thyroid gland (Guerrier, Fonlupt et al. 1995). Vascular endothelial cells express Cx37, Cx40 and Cx43 (Van Rijen, van Kempen et al. 1997, Yeh, Rothery et al. 1998, Evans and Martin 2002). Triple immuno-gold labelling at the EM-level has also revealed that GJs within aortic endothelial cells commonly contain all 3 connexin types (Yeh, Rothery et al. 1998). Some variation in connexin expression does exist between different vascular

beds, with large artery smooth muscle cells relying almost exclusively on Cx43, while in smaller muscular arteries and arterioles Cx43 expression is lower and GJIC is compensated for by increased Cx40 expression (Little, Beyer et al. 1995). As previously mentioned, heterocellular GJs occur between smooth muscle and endothelial cells at the myoendothelial junction (MEJ), thereby allowing direct endothelial cell- smooth muscle cell communication (Little, Beyer et al. 1995).

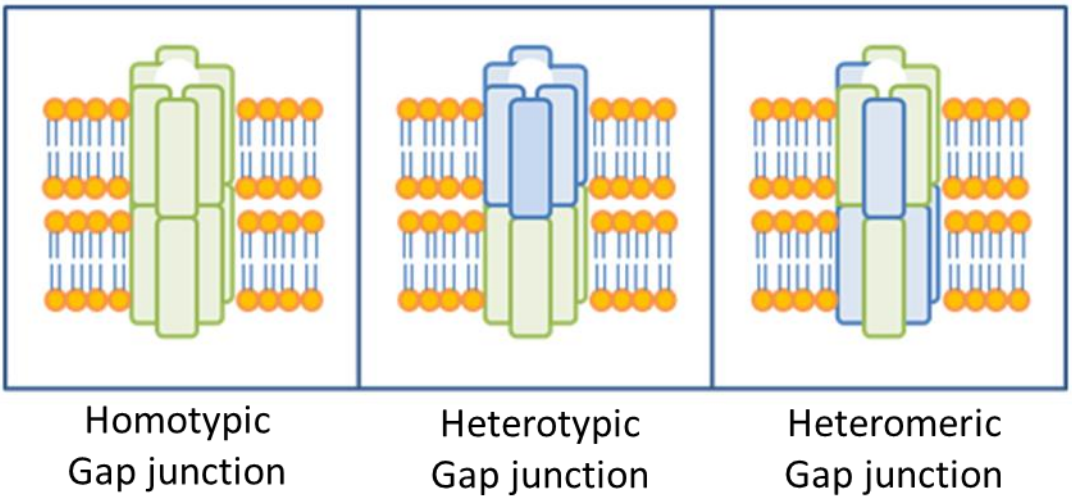

Figure 4.3: Potential arrangements of connexin subtypes to form a gap junction
This diagram shows the 3 types of GJ channel that can be formed from the various connexin subtypes. Homotypic GJs consist of 12 identical connexins (all green in left image). Heterotypic GJs consist of 2 connexin subtypes; the connexin subtype within each hemichannel is identicial, but different to the connexin subtype forming the adjacent hemichannel (centre image, green and blue represent two connexin subtypes). Heteromeric GJs can be formed from 2 or more connexin subtypes and each hemichannel contains more than one connexin subtype (right image, green and blue represent two connexin subtypes).

4.1.1.4 – Gap Junction channels in disease and knock out models

Direct cell-cell communication through gap junction channels is essential for survival. Different connexin proteins do, however, possess the ability to compensate for the loss of a single connexin subtype. Deletion of either Cx37 or Cx40 in mouse models results in no apparent vascular effects and the resulting mice are viable (Simon and McWhorter 2002). Double knock-out models (Cx37 -/- x Cx40 -/-), however, are embryonic lethal with embryos displaying gross vascular defects (Simon and McWhorter 2002). With regards to the dysregulation of GJ formation and the onset of disease, amino-terminal mutations in Cx43 are associated with non-syndromic deafness (Liu, Xia et al. 2001) and viscera-atrial heterotaxia, a severe heart malformation (Dasgupta, Martinez et al. 2001).

4.1.2 - Cadherins

4.1.2.1 - VE-cadherin

VE-cadherin mRNA is detected at the onset of vasculogenesis in the mouse embryo and expression is primarily restricted to vascular endothelial cells (Breier, Breviario et al. 1996). In addition, extra-endothelial expression of VE-cadherin has been noted in kidney podocytes (Cohen, Klingenhoff et al. 2006) and circulating endothelial progenitor cells (Peichev, Naiyer et al. 2000). VE-cadherin is distributed primarily to the border of endothelial cells and staining is reminiscent of silver nitrate staining of cell junctions (Heimark, Degner et al. 1990). The VE-cadherin promoter contains 3 domains important for the restriction of VE-cadherin expression to primarily within endothelial cells. The proximal domain promotes transcription in a cell-type dependent manner while the additional 2 regions act to negatively control inappropriate VE-cadherin transcription in non-endothelial cells (Gory, Vernet et al. 1999). Proteases, such as neutrophil elastase or cathepsin G, which are either released by, or displayed upon the surface of, stimulated neutrophils, cleave VE-cadherin to disrupt endothelial AJs and allow neutrophil transmigration (Carden, Xiao et al. 1998, Hermant, Bibert et al. 2003). VE-cadherin can also be degraded by matrix metalloproteinases (MMPs) (Herren, Levkau et al. 1998, Wu and Huang 2003) and through clathrin-dependent endocytosis and lysosomal targeting (Xiao, Garner et al. 2005). VE-cadherin expression is essential for survival and null mutations are embryonic lethal due to incomplete vascular development (Vittet, Buchou et al. 1997, Carmeliet, Lampugnani et al. 1999, Gory-Faure, Prandini et al. 1999).

As previously mentioned, cadherin-catenin interaction is essential for maturation of the AJ, and truncation of the β-catenin-binding domain of VE-cadherin is lethal in mice (Carmeliet, Lampugnani et al. 1999). The cytoplasmic domain of VE-cadherin contains binding sites for a number of armadillo proteins, including p120 catenin, p0071, β-catenin and γ-catenin (see below)(Knudsen, Soler et al. 1995, Ohkubo and Ozawa 1999, Calkins, Hoepner et al. 2003). The structure of VE-cadherin is represented in Figure 1.3 in Chapter 1.

4.1.2.2– Armadillo proteins as the accessory proteins of AJs

4.1.2.2.1 - p120 catenin and p0071

p120 catenin is an armadillo protein that is bound to the juxtamembrane domain of VE-cadherin and enhances AJ stability (Yap, Niessen et al. 1998, Ohkubo and Ozawa 1999, Thoreson, Anastasiadis et al. 2000). Association between VE-cadherin and p120 catenin in this membrane-proximal region inhibits interaction between VE-cadherin and the ubiquitin ligase Hakai, and p120 catenin association with VE-cadherin therefore prevents cadherin degradation (Vincent, Xiao et al. 2004). Furthermore, p120 catenin negatively regulates RhoA activity and promotes Rac activation through interaction with Vav2, which stabilises the AJ (Anastasiadis, Moon et al. 2000, Noren, Liu et al. 2000, Anastasiadis and Reynolds 2001, Iyer, Ferreri et al. 2004) (further details on this pathway are detailed under “Section 5.1.9”). p120 catenin, unlike β-catenin and γ-catenin which also bind VE-cadherin, does not interact with the actin cytoskeleton or actin-binding proteins (Thoreson, Anastasiadis et al. 2000, Reynolds and Roczniak-Ferguson 2004). p0071 is an additional armadillo protein that binds to the juxtamembrane domain of VE-cadherin through its armadillo repeat domain (Calkins, Hoepner et al. 2003). This protein also binds to the intermediate filament-binding protein desmoplakin, as previously mentioned, and therefore provides a link between the AJ complex and the intermediate filament network (Valiron, Chevrier et al. 1996, Calkins, Hoepner et al. 2003).

4.1.2.2.2 - β-catenin and γ-catenin

β-catenin and γ-catenin are homologous, containing between 10-13 armadillo repeats (Nieset, Redfield et al. 1997). β-catenin bound to cadherin is stabilised at the plasma membrane, while un-associated β-catenin in the cytosol is rapidly degraded (Bazzoni and Dejana 2004). When free in the cytosol, β-catenin is phosphorylated by casein kinase Iα and glycogen synthase kinase-3 (GSK-3), and phosphorylated β-catenin is then ubiquitinated and degraded in proteasomes (Liu, Li et al. 2002). Such an extra-junctional β-catenin pool

is able to regulate gene expression through translocation to the nucleus and interaction with the transcription factors t-cell factor (TCF), adenomatous polyposis coli (APC) and lymphoid enhancer factor-1 (LEF1) (Fan, Frey et al. 2003). Interaction between β-catenin and these transcription factors results in the transcription of intercellular adhesion molecule 1 (ICAM-1) which is required for neutrophil transmigration (Eastman and Grosschedl 1999, Fan, Frey et al. 2003). These interactions are part of the Wnt signalling cascade required for transcriptional regulation (Eastman and Grosschedl 1999, Fan, Frey et al. 2003). When β-catenin is bound to VE-cadherin at the AJ complex it is not free to initiate such transcription and therefore neutrophils cannot transmigrate through the endothelium and an effective barrier is maintained. Indeed, in conditions of pathological angiogenesis, β-catenin is identified primarily within the nucleus or cytoplasm and not at the plasma membrane (Blankesteijn, van Gijn et al. 2000). Un-associated γ-catenin also binds to these transcription factors and therefore plays a similar role to β-catenin in the regulation of the endothelial barrier (Miravet, Piedra et al. 2002). As previously mentioned, γ-catenin also allows association between VE-cadherin and the vimentin intermediate filament-binding protein desmoplakin, thereby providing a further link between the AJ and the intermediate filament network (Shasby, Ries et al. 2002).

VE-cadherin is able to bind to either β-catenin or γ-catenin in a mutually-exclusive manner, and these catenins subsequently link the AJ complex to α-catenin which is capable of binding the actin-binding protein α-actinin (Knudsen, Soler et al. 1995). α-catenin does not, however, simultaneously associate with both the cadherin/catenin complex and actin fibres (Yamada, Pokutta et al. 2005). Epithelial protein lost in neoplasm (EPLIN) has been identified as a potential stable link between the cadherin/catenin complex and the actin cytoskeleton as this protein binds to α-catenin and actin filaments simultaneously (Abe and Takeichi 2008).

4.2 – Methods

4.2.1 - Co-staining of cadherins and connexins in HCAECs

Cadherins were visualised using a AF594-tagged secondary (red) antibody directed against the mouse anti-cadherin primary antibodies. Connexins were labelled with a AF488-tagged secondary (green) antibody directed against the rabbit anti-connexin primary antibodies. Overlap of AF594 and AF488 staining, and thus co-expression of cadherins and connexins, represented as yellow staining in the resulting immunofluorescent Leica images.

4.3 - Results

4.3 .1 – Connexin 37 in HCAECs and HCASMCs

4.3.1.1 - Western Blot

Protein lysate made using rat kidney cortex, kidney pyramid and heart was used as a positive control in Western blot identification of Cx37. Kidney cortex constitutes the external portion of the kidney and contains the renal corpuscles and part of the renal tubules for filtration of liquid waste. The kidney pyramids comprise a section of the renal medulla, the region of the kidney containing, among other structures, the Loop of Henle. Both kidney pyramid and kidney cortex lysates were used in 'neat' forms while heart lysate was used at a 3 fold dilution due to high reading of total protein concentration using a BCA assay, as detailed under "Section 3.2 Total Protein Concentration" (Figure 3.1). Figure 4.4A shows preliminary banding for Cx37 at the appropriate molecular weight (MW) of 37 kDa in rat kidney cortex, kidney pyramid and heart lysates. The heart lysate provided a cleaner positive result for connexin targeting, even after just 10 minutes exposure.

Cx37 was then identified in HCAEC and HCASMC lysates. Figures 4.4B and 4.4C show Cx37 banding in passage 7 HCAEC lysate, and passage 8 HCASMC lysate, from preliminary experiments. Lysates from the cultured cells required an extended exposure period of 24 hours. This reflects the lower total protein concentration level present within the cultured cell lysates when compared to the rat tissue lysates, as detailed under "Section 3.2 Total Protein Concentration" (Figure 3.1). None the less, the Cx37 antibody appears to detect a protein of the expected molecular weight.

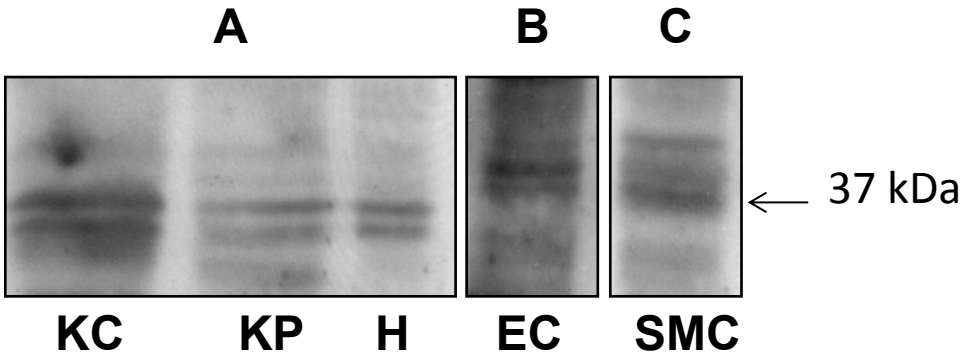

Figure 4.4: Western blot of Cx37 in rat tissues, HCAECs and HCASMCs

Expression of Cx37 within rat kidney cortex (KC), kidney pyramid (KP) and heart (H, 3 fold dilution) was identified through Western blot analysis (A), showing banding at 37 kDa. Banding at this MW was also identified in HCAEC P7 and HCASMC P8 lysates (B and C). The polyclonal rabbit anti-connexin 37 primary antibody was used at a x200 dilution and the goat anti-rabbit secondary antibody at a x5,000 dilution, both in 1% non-fat powdered milk. The membranes were exposed to the photographic film for 10 minutes (rat tissues) and 24 hours (cultured cells). N=1.

4.3.1.2 - Immunohistochemistry and Immunocytochemistry

Next, immunofluorescent technique was used to examine the distribution pattern of Cx37 in the rat renal vasculature, HCAECs and HCASMCs. Cx37 was identified primarily in the endothelial lining of the rat kidney vessel during preliminary experiments (Figure 4.5A). Figure 4.5B reflects the localisation of Cx37 within HCAECs to both the perinuclear region and the cell membrane. Cx37 expression in HCASMCs in contrast, was minimal (Figure 4.5C), with only isolated areas displaying fluorescence intensity above background levels. In addition, Cx37 appeared to display no real nuclear association in HCASMCs.

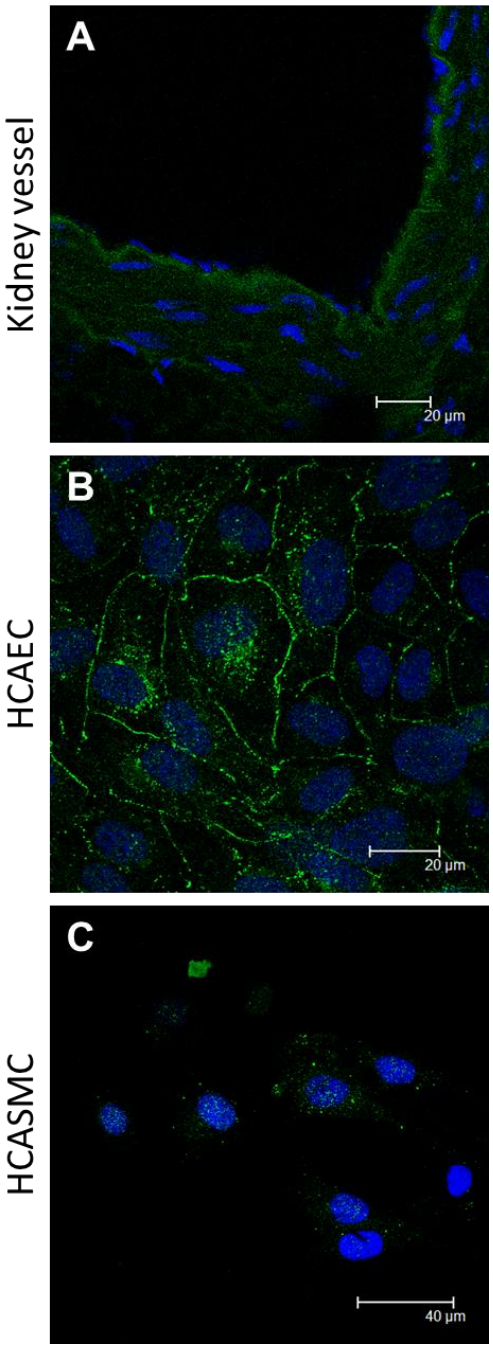

Figure 4.5: Immunofluorescent analysis of Cx37 expression in rat kidney, HCAECs and HCASMCs

Distribution pattern of Cx37 within rat tissue and cultured human cells using an AF488-tagged secondary antibody (green) is shown in A (kidney vessel), B (HCAECs) and C (HCASMCs). Cx37 is evident primarily in the endothelium of the kidney vessel (A). Cx37 is localised to both the perinuclear region (DAPI nuclear staining in blue), and the cell membrane of the endothelial cells (B). Cx37 staining in HCASMCs was minimal with only small areas of punctate staining (C). The anti-Cx37 primary antibody was used at a 200 fold dilution, and the anti-rabbit secondary antibody at a 500 fold dilution. Image C is at a lower magnification. Kidney vessel, N=2. HCAEC, N=7. HCASMC, N=3.

4.3.2 - Connexin 40 in HCAECs and HCASMCs

4.3.2.1 - Western Blot

Cx40 was successfully identified in rat kidney cortex, kidney pyramid and heart lysates at the MW of 40 kDa during preliminary experiments (Figure 4.6A). Cx40 banding was also observed at 40 kDa in both HCAEC and HCASMC lysates during preliminary experiments, as shown in Figures 4.6B and 4.6C. Identification of the band in cultured cell lysates required an extended exposure time (24 hours vs. 10 minutes), reflecting the lower total protein concentration of the cultured cells when compared to rat tissue.

4.3.2.2 - Immunohistochemistry and Immunocytochemistry

The distribution of Cx40 was then examined in rat kidney and cultured human cells. Isolated areas of punctate Cx40 staining were identified in the rat kidney during preliminary experiments (Figures 4.7A & 4.7B). Similarly, Figures 4.7C & 4.7D represent Cx40 staining in HCAECs. This protein was identified surrounding the nucleus, supplemented by moderate expression at the membranes of the cobblestone-like endothelial cells. Figures 4.7E & 4.7F show the distribution of Cx40 throughout the elongated HCASMCs as identified during preliminary experiments. Cx40 was also identified arranged into longitudinal networks within these smooth muscle cells, possibly showing association with the actin cytoskeleton (Figure 4.7F).

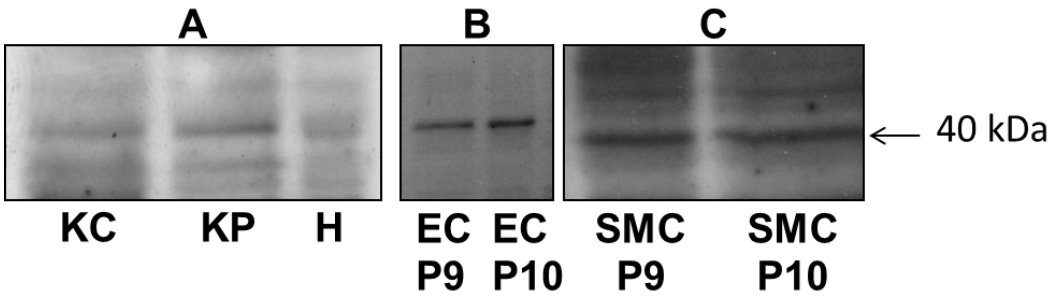

Figure 4.6: Western blot of Cx40 in rat tissues, HCAECs and HCASMCs

Cx40 expression within rat kidney cortex (KC), kidney pyramid (KP) and heart (H, 3 fold dilution) was identified through Western blot analysis (A), with banding at 40 kDa. A single distinct band at this MW was also identified in P9 and P10 lysates of HCAECs (B) and a strong band was identified in P9 and P10 lysates of HCASMCs (C). The rabbit anti-Cx40 primary antibody was used at a x200 dilution and the goat anti-rabbit secondary antibody at a x5,000 dilution, both in 1% non-fat powdered milk. The membranes were exposed to the photographic film for 10 minutes (rat lysate) and 24 hours (human cultured cell lysate), respectively. For kidney, HCAECs and HCASMCs, N=1. Heart, N=2.

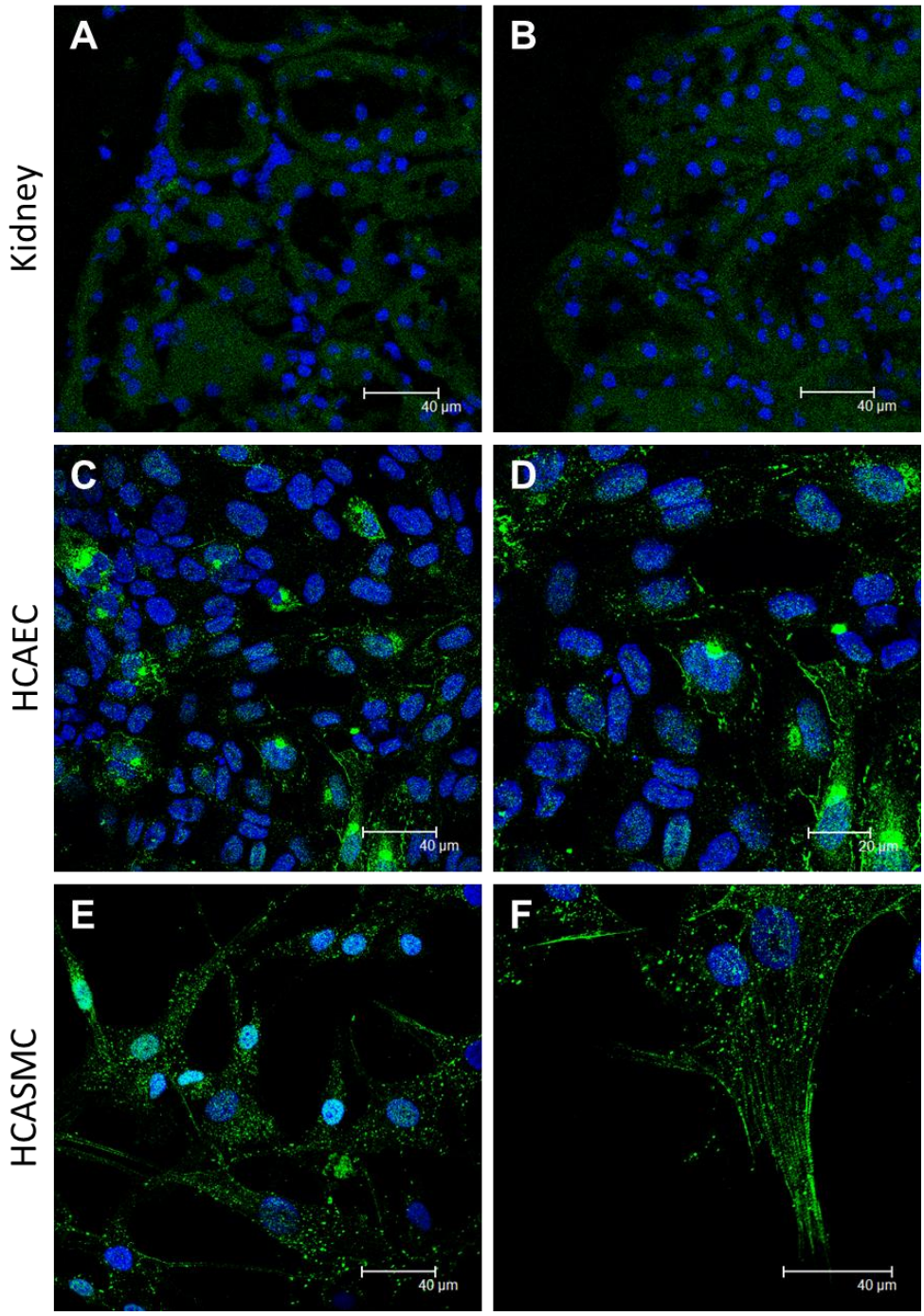

Figure 4.7: Immunofluorescent analysis of Cx40 expression in rat kidney, HCAECs and HCASMCs

Distribution pattern of Cx40 within rat tissue and cultured human cells using an AF488-tagged secondary antibody (green) is shown in A&B (rat kidney), C&D (HCAECs) and E&F (HCASMCs). Cx40 staining in rat kidney was minimal with only small areas of punctate staining (A&B). Within HCAECs, Cx40 was identified in close association with the nucleus and as patchy areas of membrane staining (C&D). Cx40 can be seen as diffuse staining throughout the HCASMCs with marginal association with the cytoskeleton (F). DAPI nuclear stain is shown in blue. The anti-Cx40 primary antibody was used at a 200 fold dilution, and the anti-rabbit secondary antibody at a 500 fold dilution. Image D is at a higher magnification. Kidney, N=2. HCAEC, N=5. HCASMC, N=4

4.3.3 - Connexin 43 in HCAECs and HCASMCs

4.3.3.1 - Western Blot

Preliminary Western blot experiments were carried out using rat kidney cortex, kidney pyramid and heart lysates. A single band was present at the appropriate MW of 43 kDa in both kidney lysates (Figure 4.8A). Although Cx43 is well established in the literature as the primary connexin expressed within heart tissue (Evans and Martin 2002), the heart lysate showed a smudge of banding, most likely due to excess protein (Figure 4.8A). During these experiments, Cx43 was identified as a single band throughout passages 6-10 of both HCAECs and HCASMCs (Figures 4.8B and 4.8C). Relatively high concentration of this protein within both HCAECs and HCASMCs was expected in the short exposure time of 10 minutes required to expose the band (compared to the 24 hours required to record Cx37 protein expression in the same cell lysates, Figures 4.8B and 4.8C), although this could be due to higher efficiency of the Cx43 primary antibody.

4.3.3.2 - Immunohistochemistry

The distribution of Cx43 within both rat tissue and cultured human cells was then examined using immunofluorescent technique. Figures 4.9A and 4.9B show preliminary results for Cx43 expression in rat kidney and renal vasculature. Although the majority of the AF488 staining evident was background, distinct areas of true AF488 expression were identified, primarily within the vasculature supplying this tissue. Figures 4.9C and 4.9D represent Cx43 distribution in the same section of rat coronary artery with (Figure 4.9D) and without (Figure 4.9C) a brightfield overlay image. Figures 4.9E and 4.9F are the same images at a higher magnification. The patency of the lumen of the rat coronary artery section allows clear identification of the distribution of Cx43. This junctional protein is clearly evident throughout both the single endothelial cell layer and a large proportion of the multiple smooth muscle cell layers forming the tunica media. Figures 4.9G & 4.9H represent Cx43 distribution in rat mesenteric artery during preliminary experiments, showing staining in both the endothelial layer and the smooth muscle layers.

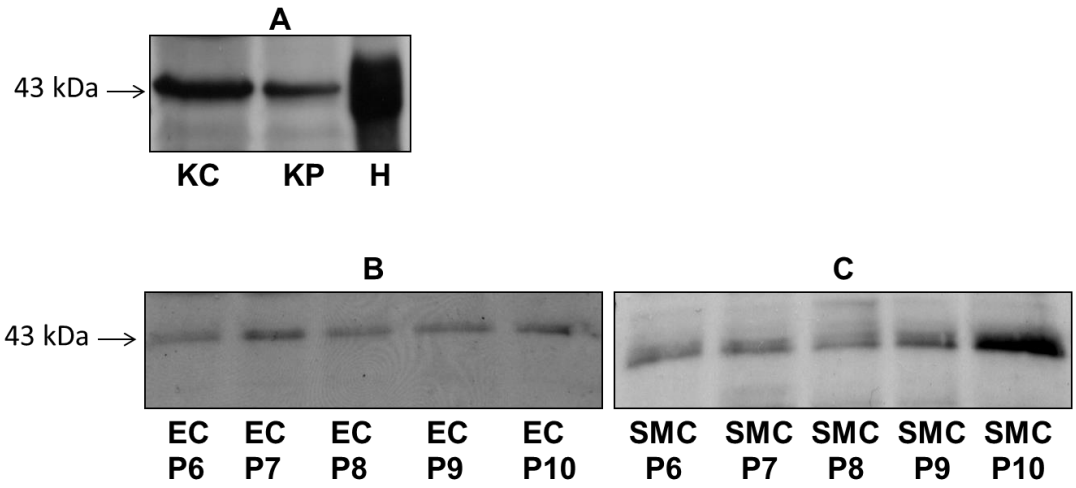

Figure 4.8: Western blot of Cx43 in rat tissue, HCAECs and HCASMCs

Expression of Cx43 within rat kidney cortex (KC), kidney pyramid (KP) and heart (H, 3 fold dilution) was detected through Western blot analysis (A). A single clear band was evident in the rat kidney tissue at the appropriate MW of 43 kDa. The rat heart lysate displayed a smudge of banding across multiple MW's. A single band at 43 kDa was identified in passages 6-10 of HCAEC and HCASMC lysates, respectively (B and C). The rabbit anti-connexin 43 primary antibody was used at a x200 dilution and the goat anti-rabbit secondary antibody at a x5,000 dilution, both in 1% non-fat powdered milk. The membranes were exposed to the photographic film for 5 minutes (rat tissue) and 10 minutes (human cultured cell lysate), respectively. For kidney, HCAECs and HCASMCs, N=1. Heart, N=3.

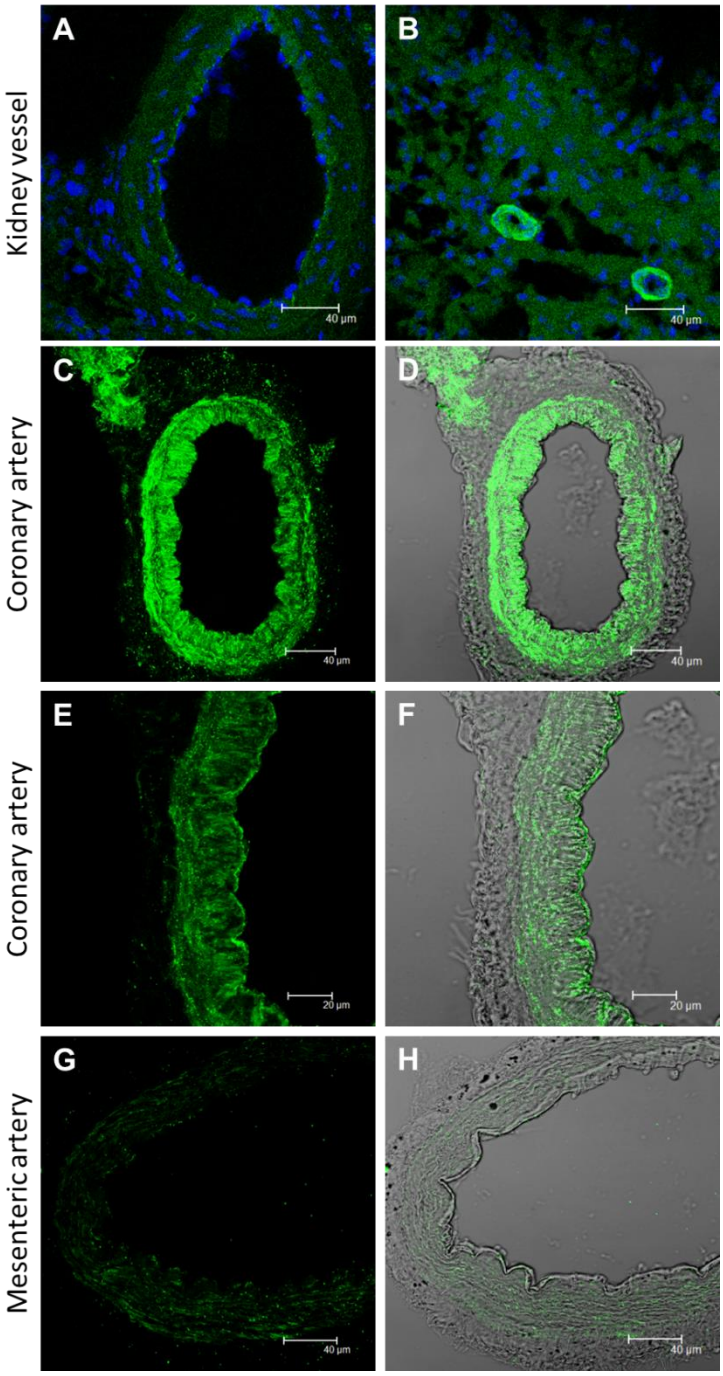

Figure 4.9: Immunohistochemical analysis of Cx43 expression in rat tissue
Distribution pattern of Cx43 within rat tissues using an AF488-tagged secondary antibody (green) is shown in A&B (kidney), C&D/E&F (coronary artery) and G&H (mesenteric artery). Cx43 expression in rat kidney was restricted primarily to the vasculature (A & B). C&D represent Cx43 distribution throughout the endothelial and smooth muscle layers of the rat coronary artery, with (D) and without (C) a brightfield image overlay. E&F are the same images at a higher magnification. G&H show low-level Cx43 expression in the endothelial and smooth muscle layers of the rat mesenteric artery. The anti-Cx43 primary antibody was used at a 200 fold dilution, and the anti-rabbit secondary antibody at a 500 fold dilution. DAPI nuclear staining is shown in blue in images A and B. N=2.

4.3.3.3 - Immunocytochemistry

Figures 4.10A shows Cx43 distribution in HCAECs, and 4.10B shows Cx43 distribution in HCASMCs. In HCAECs, Cx43 showed punctate near-membrane staining, with weaker staining throughout the cell interior. In HCASMCs, Cx43 was found to form aggregations across the cell, but appeared to be absent from the nucleus (Figure 4.10B). No distinct sections of membrane-associated Cx43 expression were identified in the HCASMCs (Figure 4.10B).

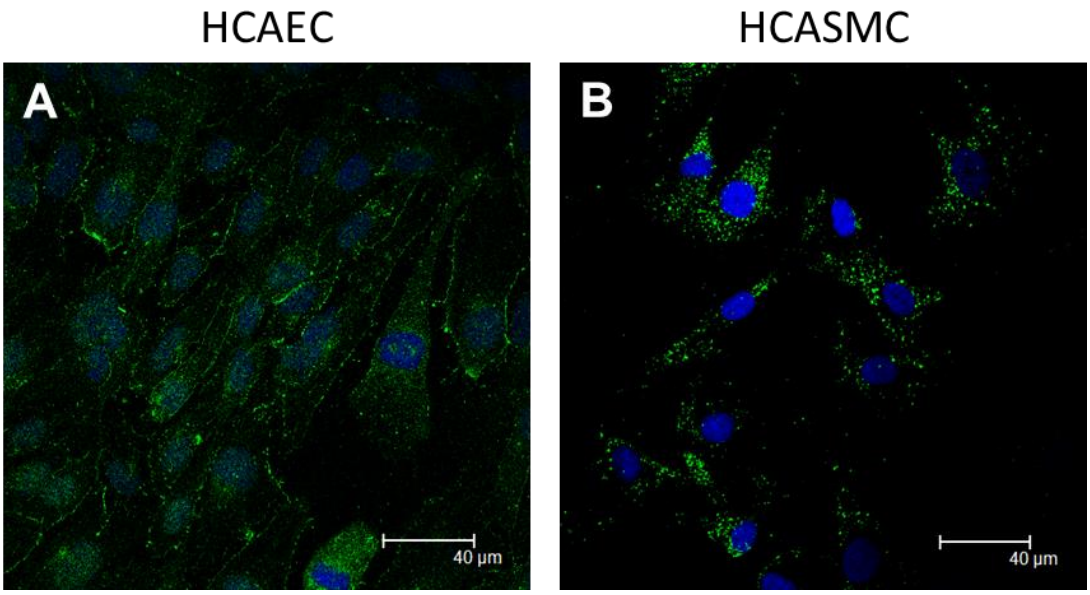

Figure 4.10: Immunocytochemical analysis of Cx43 expression in HCAECs and HCASMCs

Cx43 distribution in HCAECs is shown in A. Cx43 was identified diffusely throughout the cell and as discontinuous patches at the cell membrane. DAPI (blue) highlights nuclear Cx43 staining in HCAECs (A). Cx43 distribution in HCASMCs is shown in B. Cx43 was identified in aggregations throughout smooth muscle cells. No distinct sections of near-membrane or nuclear Cx43 were identified in HCASMCs (B). Antibody dilutions as previously detailed. HCAECs, N=6. HCASMCs, N=5.

4.3.4 – VE-cadherin in HCAECs and HCASMCs

4.3.4.1 - Western Blot

During preliminary experiments, VE-cadherin was identified as the darkest band in HCAEC lysate (P6 and P10) at the MW of 130 kDa (Figure 4.11). Other bands were also observed and this may be because the membranes had to be exposed to photographic film for 50 hours (typical exposure periods ranged from 5-10 minutes for most other experiments). Indeed, HCASMC (P6) lysate shows these fainter bands, but the 130 kDa band is absent (Figure 4.11). The specificity of VE-cadherin was therefore further examined using immunocytochemistry.

4.3.4.2 - Immunocytochemistry

Immunofluorescent technique was used to examine the distribution pattern of VE-cadherin in HCAECs (Figure 4.12). Figure 4.12A shows the distribution of VE-cadherin as detected with the AF488-conjugated secondary antibody. Figures 4.12B and 4.12C show the distribution of VE-cadherin as detected with the AF594-conjugated secondary antibody. Figure 4.12C is at a higher magnification. The staining of VE-cadherin appears discontinuous (Figure 4.12C), and it appears as though numerous short processes extend into the cell (Figure 4.12B). A notable proportion of the imaged cells also displayed perinuclear and general intracellular localisation of VE-cadherin, against the DAPI nuclear staining represented in blue (Figure 4.12A).

4.3.4.3 - VE-cadherin Summary

VE-cadherin is expressed by HCAECs as discontinuous membranous patches, with a proportion of cells also displaying perinuclear and general intracellular localisation of this junctional protein. A lack of VE-cadherin expression by HCASMCs was confirmed through Western blot targeting of the protein.

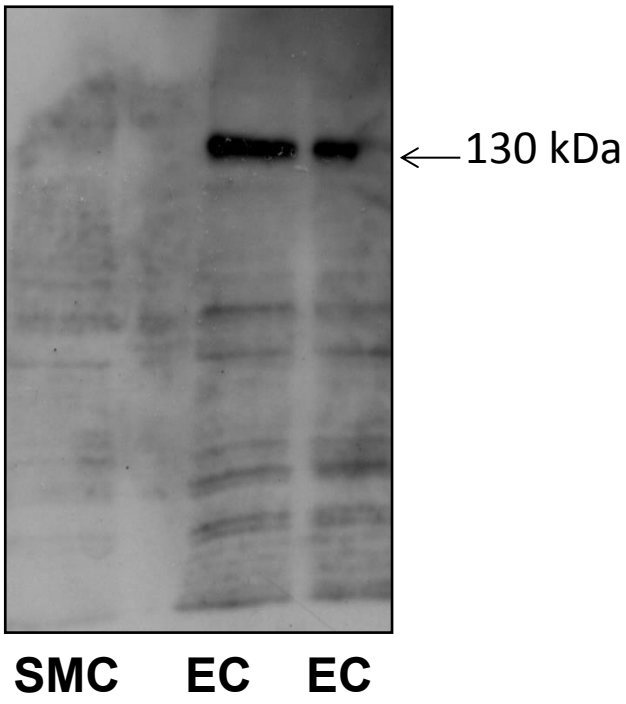

Figure 4.11: Western blot of VE-cadherin in HCAECs and HCASMCs
Expression of VE-cadherin by HCAECs (P6 and P10 lysate) was identified through Western blot analysis, showing a dense band at 130 kDa. HCASMC lysate (P6) acted as a negative control for this endothelial-specific protein. The mouse anti-VE-cadherin primary antibody was used at x200 dilution and the goat anti-mouse secondary antibody at x10,000 dilution, both in 1% non-fat powdered milk. The membrane was exposed to the photographic film for 50 hours. N=1.

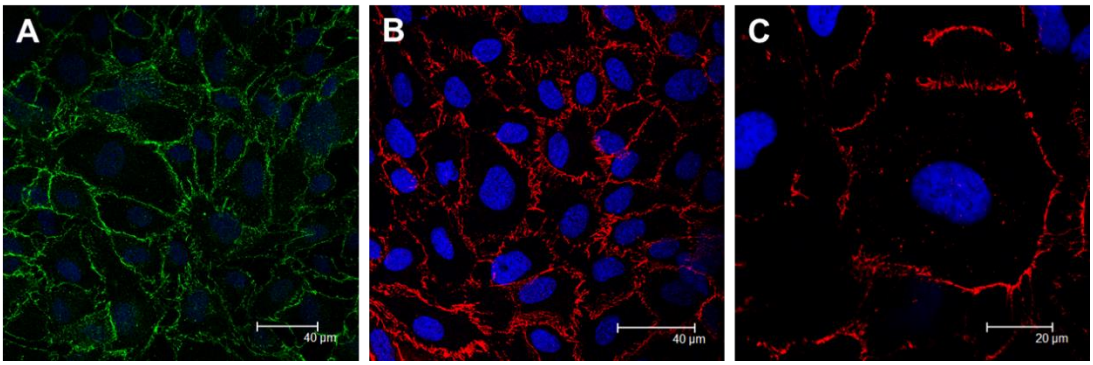

Figure 4.12: Immunocytochemical analysis of VE-cadherin expression in HCAECs
The distribution pattern of VE-cadherin within HCAECs was identified using both an AF488-tagged secondary antibody (A, green), and an AF595-tagged secondary antibody (B & C, red). VE-cadherin was identified primarily at the membrane as discontinuous segments of staining. Moderate perinuclear staining was identified in some cells (A). DAPI nuclear staining is shown in blue. The anti-VE-cadherin primary antibody was used at a 200 fold dilution, and the secondary antibody at a 500 fold dilution. Image C is at a higher magnification. N=6.

4.3.5 - N- Cadherin in HCAECs and HCASMCs

4.3.5.1 - Western Blot and Immunocytochemistry

N-cadherin was identified at the MW of 130 kDa in HCAEC (P6 and P10) and HCASMC (P6) lysates during preliminary experiments (Figure 4.13). The distribution of N-cadherin was then examined in HCAECs and HCASMCs through the use of immunocytochemical techniques. N-cadherin was identified at both the cell membrane and diffusely throughout HCAECs (Figure 4.14). Areas of peak signal were detected at the membrane, accompanied by relatively high fluorescence throughout the cell (Figure 4.14A). The membrane-bound N-cadherin appears to localise primarily at the leading edge of the cell, as highlighted by the white arrows in Figure 4.14A. Unlike VE-cadherin expression in HCAECs, N-cadherin expression in these cells does not display inward projections from the cell membrane, and the distribution is more continuous and less zipper-like (Figure 4.14A). Accumulations of N-cadherin staining into small aggregations were observed in HCAECs (white arrow, Figure 4.14B).

Preliminary immunocytochemistry experiments showed that N-cadherin distribution in HCASMCs was very similar to the expression pattern of this protein within HCAECs (Figure 4.15). As with HCAEC cultures, HCASMCs showed N-cadherin localisation to the cell membrane, once again represented as small sections of staining with a preference for the leading edge of the cell, as highlighted by the white arrow in Figure 4.15A. Aggregations of N-cadherin signal can also be seen in HCASMCs (Figure 4.15B), again similar to the expression profile of this protein in HCAECs.

The distribution pattern of N-cadherin in cultured HCAECs and HCASMCs was similar. Both cell populations display N-cadherin staining at the cell membrane and accumulations throughout the cell. In addition, both HCAECs and HCASMCs express N-cadherin as large segments of membrane staining, contrasting the zipper-like, discontinuous appearance of VE-cadherin in HCAECs. N-cadherin displayed no inward projections from the membrane, unlike those seen with VE-cadherin in HCAECs. Membranous N-cadherin appeared to localise primarily to specific sites in both HCAECs and HCASMCs.

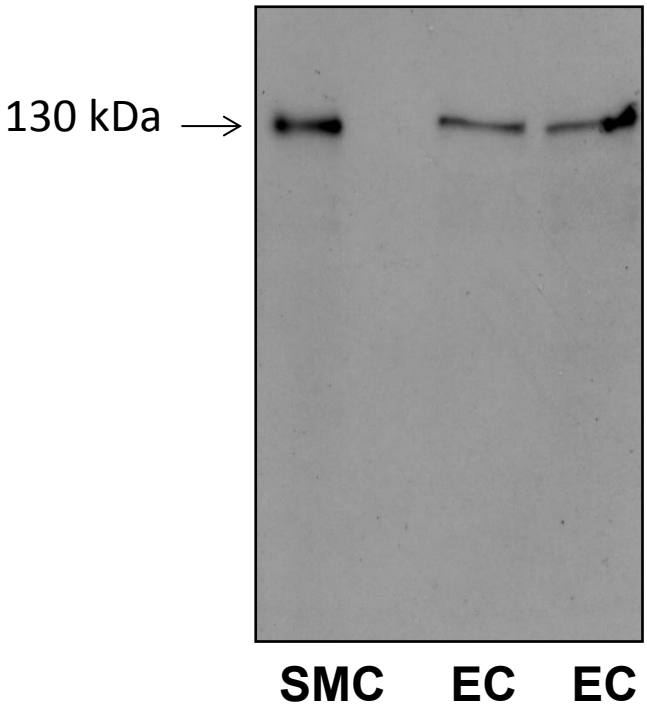

Figure 4.13: Western blot of N-cadherin in HCAECs and HCASMCs
Expression of N-cadherin by HCAEC (P6 and P10) and HCASMC (P6) lysates was identified through Western blot analysis, showing a single band at 130 kDa. The mouse anti-N-cadherin primary antibody was used at x300 dilution and the goat anti-mouse secondary antibody at x10,000 dilution, both in 1% non-fat powdered milk. The membrane was exposed to the photographic film for 10 minutes. N=1.

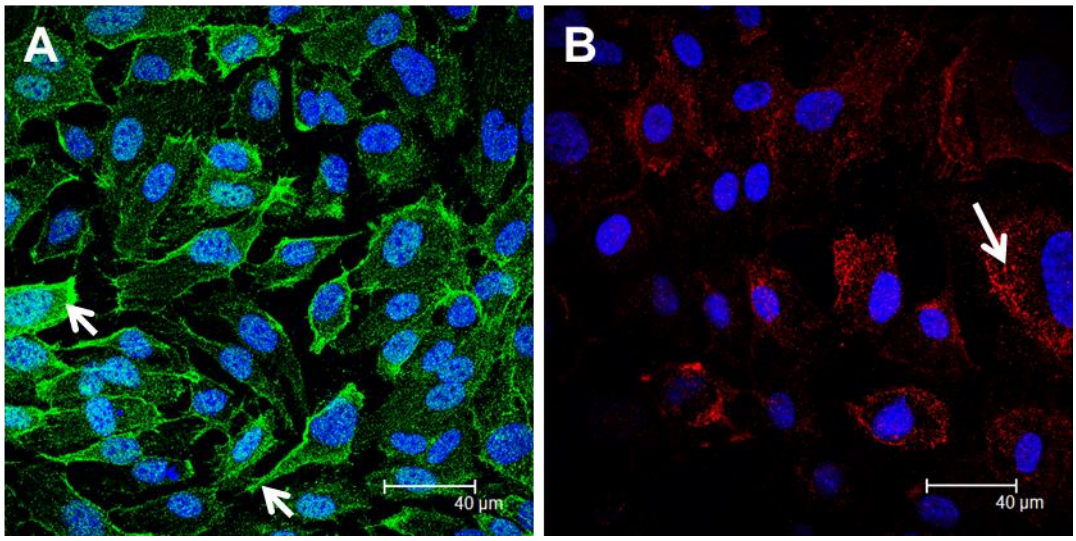

Figure 4.14: Immunocytochemical analysis of N-cadherin expression in HCAECs
The distribution pattern of N-cadherin in HCAECs was identified using both an AF488-tagged secondary antibody (A, green), and an AF595-tagged secondary antibody (B, red). N-cadherin appeared discontinuously across the membrane (white arrows in A). Accumulations of N-cadherin were observed throughout the HCAECs (white arrow in B). The anti-N-cadherin primary antibody was used at a 200 fold dilution, and the secondary antibody at a 500 fold dilution. DAPI nuclear staining is shown in blue. N=7.

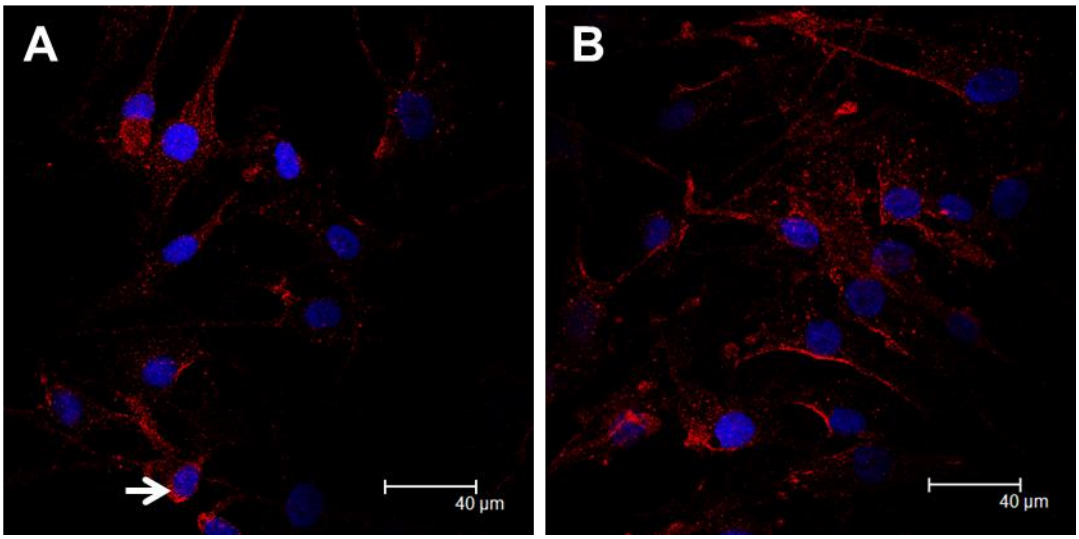

Figure 4.15: Immunocytochemical analysis of N-cadherin expression in HCASMCs
The distribution pattern of N-cadherin in HCASMCs was identified using an AF595-tagged secondary antibody (A & B, red). N-cadherin displayed both membranous and cytoplasmic staining. Cytoplasmic accumulations of N-cadherin are evident in both A and B. The white arrow in image A highlights the strong staining of N-cadherin at specific sites of the cell membrane. DAPI nuclear staining is shown in blue. Antibody dilutions as previously detailed. N=1.

4.3.6 - Connexin and VE-Cadherin Co-staining in HCAECs

4.3.6.1 - VE-cadherin and Cx37

VE-cadherin and Cx37 were labelled in HCAECs through immunocytochemistry (Figure 4.16). VE-cadherin was labelled using an AF594-conjugated (red) secondary antibody (Figures 4.16A-4.16C), while Cx37 was labelled using an AF488-conjugated (green) secondary antibody (Figures 4.16A, 4.16B & 4.16D). These preliminary experiments identified areas of overlap between Cx37 and VE-cadherin distribution as yellow patches at the cell membrane (Figures 4.16A and 4.16B, white arrows), but not inside the HCAECs. Areas of membranous Cx37 devoid of VE-cadherin staining were also identified.

4.3.6.2 - VE-cadherin and Cx40

VE-cadherin (red) and Cx40 (green) were labelled in HCAECs through immunocytochemistry (Figure 4.17). Small areas of overlap between membranous Cx40 and VE-cadherin expression were observed in HCAECs (yellow; Figure 4.17C). Areas of co-localisation were not identified in all HCAECs imaged. Areas of near-membrane Cx40 without VE-cadherin overlap were identified.

4.3.6.3 - VE-cadherin and Cx43

VE-cadherin (red) and Cx43 (green) were labelled in HCAECs through immunocytochemistry (Figure 4.18). Isolated sections of VE-cadherin and Cx43 co-staining (yellow) were identified at the cell membranes of a number of HCAECs imaged (Figure 4.18C, white arrow). Sections of Cx43 near-membrane staining devoid of VE-cadherin staining were also identified.

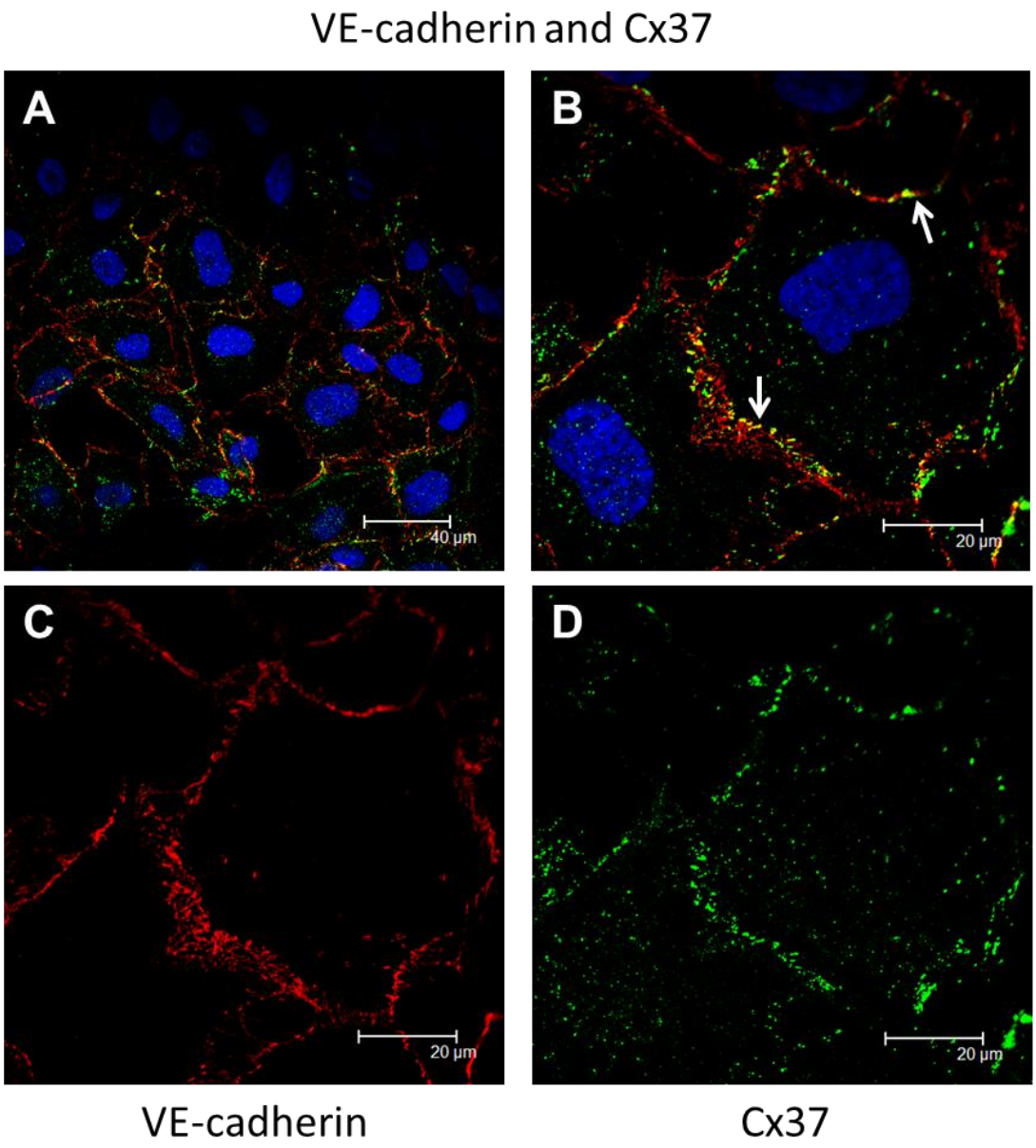

Figure 4.16: Immunocytochemistry of VE-cadherin and Cx37 co-localisation in HCAECs
VE-cadherin (red) was primarily restricted to the membrane as discontinuous patches (A-C). Cx37 (green) was identified surrounding the nucleus and as isolated segments of membrane staining (A, B & D). Co-localisation of VE-cadherin and Cx37 (yellow) was identified at the cell membrane, as indicated by the white arrows (B). Image B represents overlap of images C and D. Antibody dilutions as previously detailed. DAPI nuclear staining in blue. N=2.

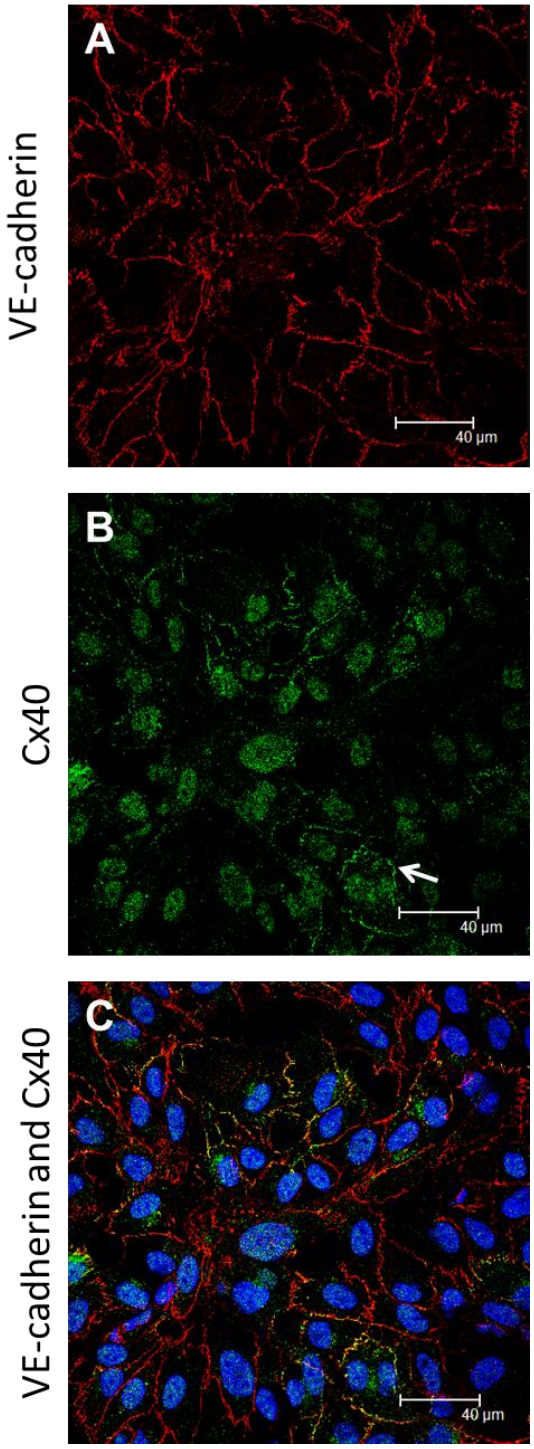

Figure 4.17: Immunocytochemistry of VE-cadherin and Cx40 co-localisation in HCAECs
VE-cadherin (red) was identified as patches throughout the membrane with inward projections (A & C). Cx40 (green) was associated primarily with the nucleus (shown by DAPI nuclear staining in blue), with isolated areas of membrane association, as highlighted by the white arrow (B & C). Image C represents overlap of images A and B. Isolated areas of co-localisation between VE-cadherin and Cx40 (yellow) were identified at restricted points of the membrane (C). Areas of overlap between Cx40 and VE-cadherin expression were not identified in all HCAECs imaged. Antibody dilutions as previously detailed. N=3.

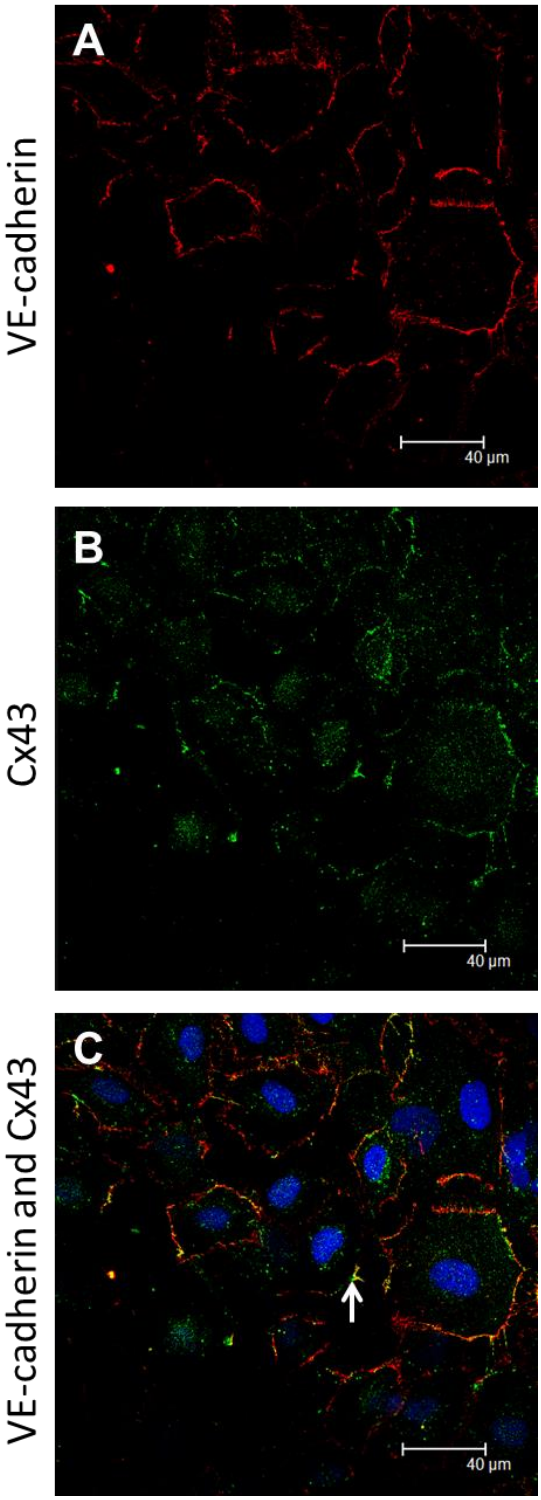

Figure 4.18: Immunocytochemistry of VE-cadherin and Cx43 co-localisation in HCAECs
VE-cadherin (red) was primarily restricted to the membrane (A & C), while Cx43 (green) was identified throughout the cell and at the cell membrane (B & C). Image C represents overlap of images A and B. Small areas of co-localisation (yellow) were identified at the membrane of the HCAECs imaged, as highlighted by the white arrow (C). Antibody dilutions as previously detailed. DAPI nuclear staining is shown in blue. N=3.

4.3.6.4 - Quantification of Connexin and VE-cadherin Co-localisation

Figure 4.19 displays the quantification of co-localisation between VE-cadherin and connexins 37, 40 and 43 in HCAECs. Three Image J plugins were utilised to quantify the degree of overlap in the expression profiles of these junctional proteins. The plugins used were; Manders' Overlap Coefficient, Co-localisation Finder plugin and Intensity Correlation Analysis. Full details of the quantification process for each plugin can be found in the Appendix under "Supplementary information on the quantification of cadherin and connexin co-localisation using Image J plugins".

4.3.6.5 - VE-cadherin and Connexin Co-localisation - Summary

Moderate overlap between Cx37 and VE-cadherin expression at the cell membrane was identified in HCAECs. Overlap appeared as small areas of punctate staining, with no extended regions of co-staining. Small areas of Cx40 and VE-cadherin co-expression were also identified in these endothelial cells. These areas of overlap were restricted to the membrane, and only in a subset of the cells imaged. Membrane Cx43 and VE-cadherin expression overlap was observed in HCAECs. The co-staining was limited to the membrane and areas of Cx43 membrane staining without VE-cadherin staining were noted. The most extensive overlap between VE-Cadherin and the connexins targeted was identified between Cx37 and VE-cadherin.

4.3.7 - Connexin and N-Cadherin Co-staining in HCAECs

4.3.7.1 - N-cadherin and Cx37

N-cadherin (red) and Cx37 (green) were labelled in HCAECs during preliminary immunocytochemistry experiments (Figure 4.20). No observable co-localisation between N-cadherin and Cx37 (yellow) was identified within the HCAEC culture, with membranous staining of both junctional proteins appearing mutually exclusive (Figure 4.20C). Peaks in N-cadherin expression appeared external to areas of Cx37, thus preventing overlap.

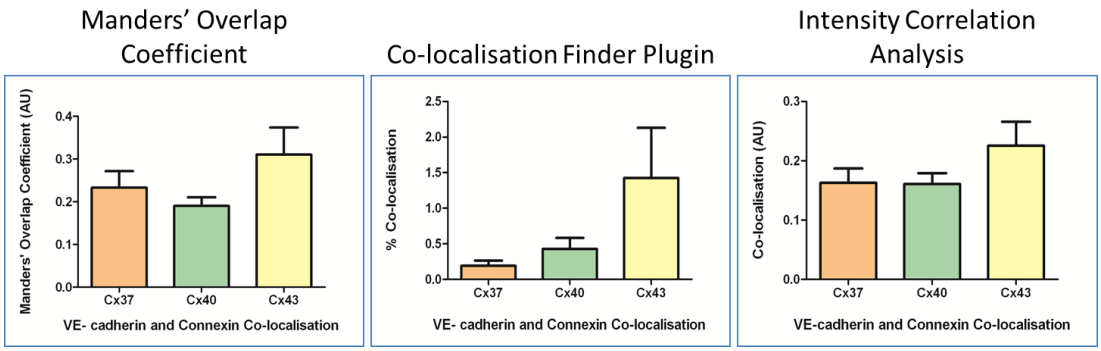

Figure 4.19: Quantification of Connexin and VE-cadherin co-localisation in HCAECs
Three types of Image J plugins were used to quantify co-localisation between VE-cadherin and Cx37, Cx40 and Cx43; Manders' Overlap Coefficient, Co-localisation Finder plugin and Intensity Correlation Analysis. Full details of quantification process can be found in the Appendix under "Supplementary information on the quantification of cadherin and connexin co-localisation using Image J plugins". For VE-cadherin and Cx37, N=2. For VE-cadherin and Cx40, and VE-cadherin and Cx43, N=3.

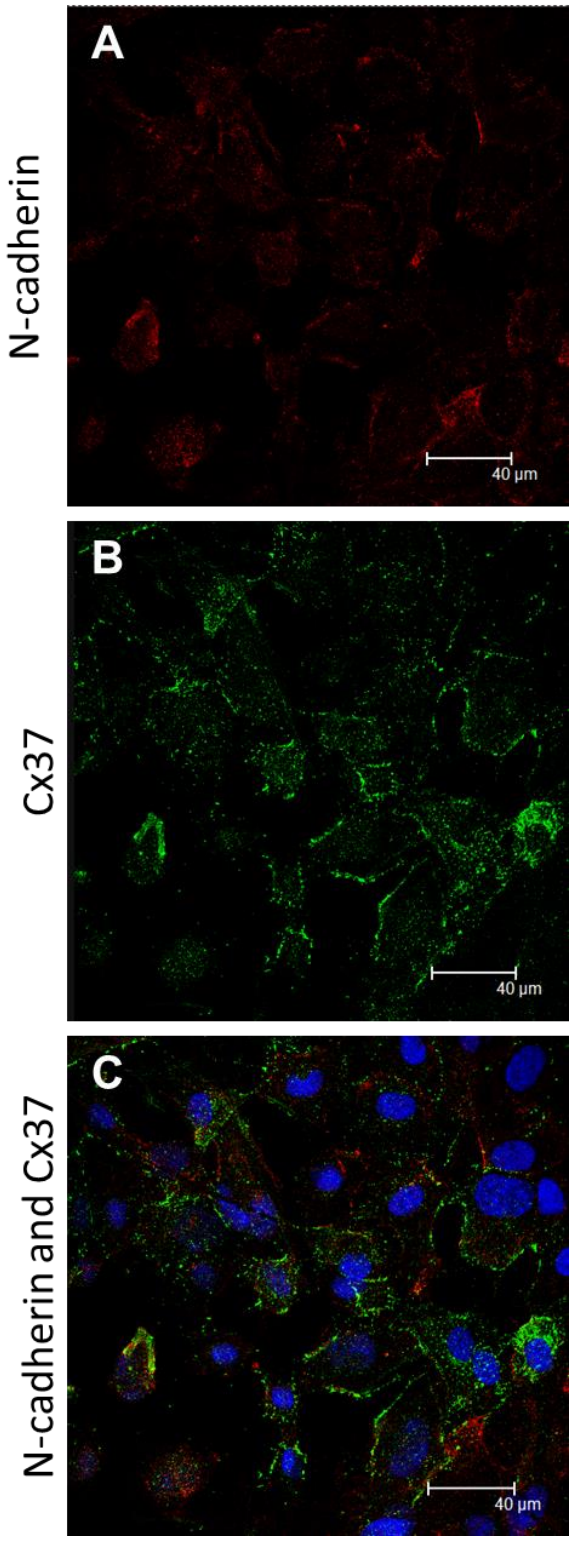

Figure 4.20: Immunocytochemistry of N-cadherin and Cx37 co-localisation in HCAECs
N-cadherin (red) expression was identified throughout the cell and also at the cell membrane (A & C). Cx37 (green) was distributed to the perinuclear region and restricted areas of the HCAEC membrane (B & C). Image C represents overlap of images A and B. No co-localisation between Cx37 and N-cadherin (yellow) could be identified (C). Antibody dilutions as previously detailed. N=2.

4.3.7.2 - N-cadherin and Cx40

Figure 4.21 shows labelling of N-cadherin (red) and Cx40 (green) in HCAECs during preliminary immunocytochemistry experiments. No overlap between N-cadherin and Cx40 expression (yellow) was identified (Figure 4.21C). DAPI nuclear staining shown in blue suggests that a proportion of N-cadherin expression in HCAECs is localised to the nucleus (Figure 4.21C).

4.3.7.3 - N-cadherin and Cx43

N-cadherin (red) and Cx43 (green) were labelled in HCAECs in preliminary immunocytochemistry experiments (Figure 4.22). Few isolated areas of overlap between Cx43 and N-cadherin expression (yellow) were identified at the membrane (Figure 4.22C). Overlap was not identified in all HCAECs imaged and in most cells the two junctional proteins appeared mutually exclusive (Figure 4.22D, higher magnification).

Figure 4.23 shows labelling of N-cadherin (red) and Cx43 (green) in HCASMCs during preliminary immunocytochemistry experiments. Small isolated areas of overlap between N-cadherin and Cx43 expression (yellow) were identified in the HCASMCs (Figures 4.23E and 4.23F, white arrow). These areas of co-localisation appeared to be closely associated with the nucleus, as shown by the DAPI nuclear staining (blue). Considerable areas of membranous N-cadherin expression devoid of Cx43 co-expression were identified (Figure 4.23F).

4.3.7.4 - N-cadherin and Connexin Co-localisation - Summary

In summary, no observable co-localisation was identified in HCAECs between N-cadherin and either Cx37 or Cx40. Conversely, isolated areas of overlap were identified between N-cadherin and Cx43 in both HCAECs and HCASMCs. These areas appeared to be closely associated with the nucleus, as shown by the DAPI staining.

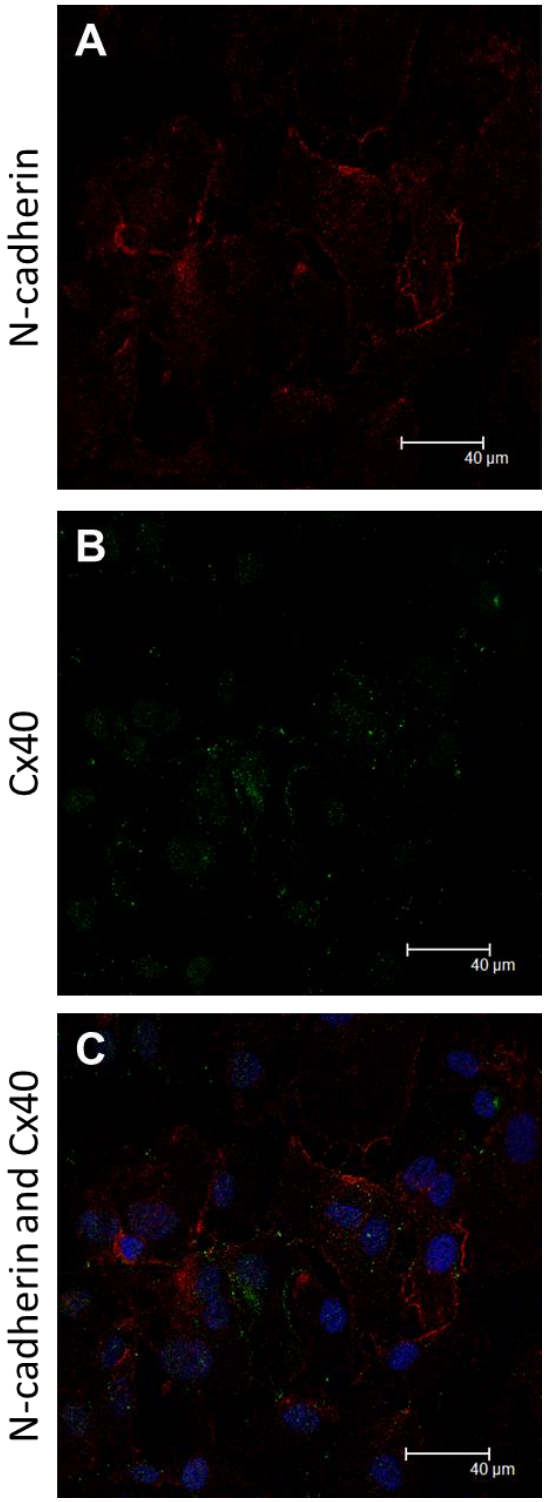

Figure 4.21: Immunocytochemistry of N-cadherin and Cx40 co-localisation in HCAECs
N-cadherin distribution (red) was identified both throughout the cell and at the membrane (A & C). Low-level Cx40 (green) expression was detected throughout the cells with isolated areas of punctate staining at the membrane (B & C). Image C represents overlap of images A and B. No overlap between Cx40 and N-cadherin distribution (yellow) could be identified (C). Antibody dilutions as previously detailed. N=1.

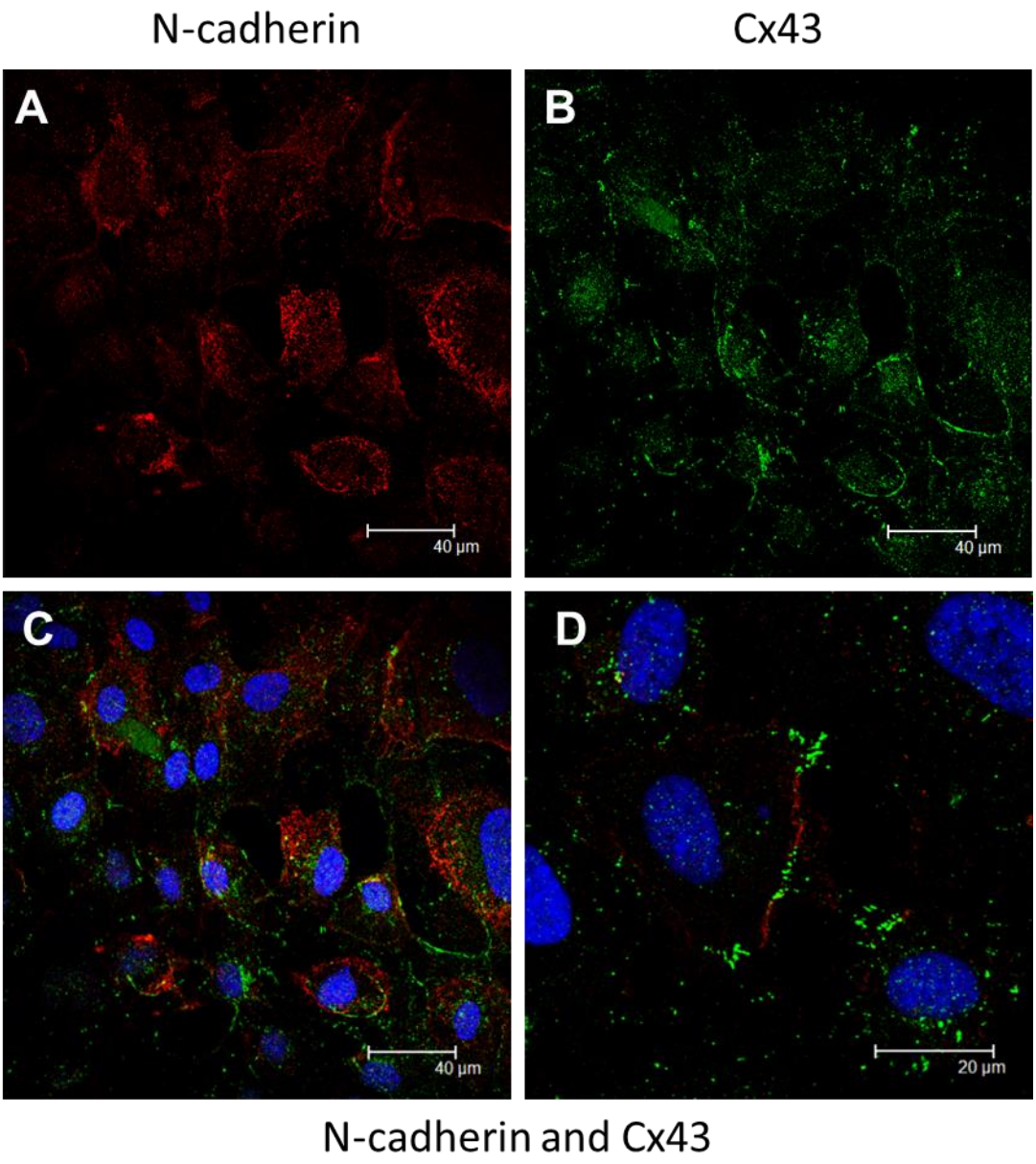

Figure 4.22: Immunocytochemistry of N-cadherin and Cx43 co-localisation in HCAECs
N-cadherin (red) was identified both throughout the cell and at the HCAEC membrane, forming small aggregations of staining (A, C & D). Cx43 (green) was identified as both diffuse staining throughout the cell and areas of membranous staining (B, C & D). Image C represents overlap of images A and B. Small areas of co-localisation between Cx43 and N-cadherin (yellow) were identified in isolated cells, primarily at the membrane (C). Image D is at a higher magnification. Antibody dilutions as previously detailed. N=2.

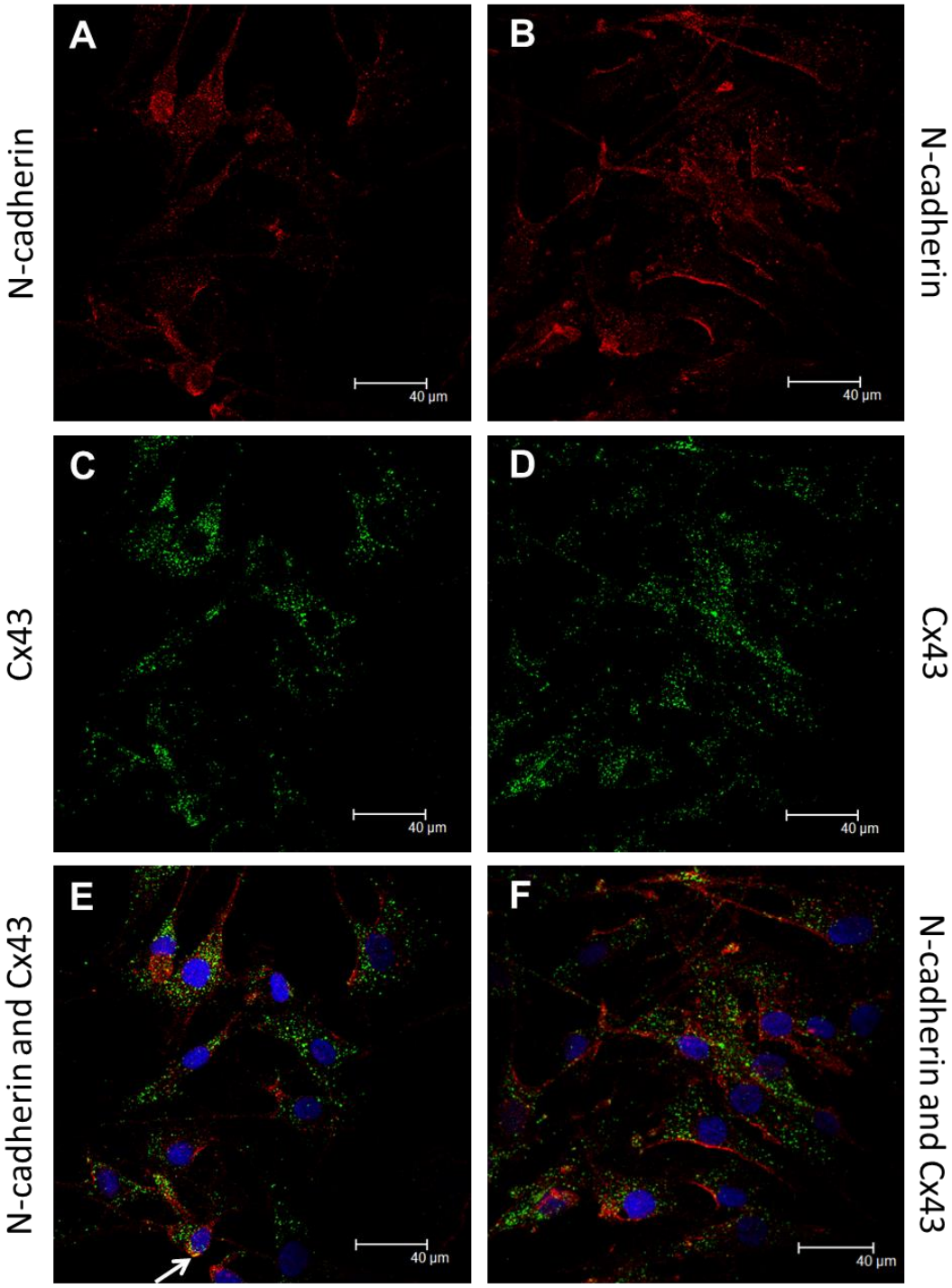

Figure 4.23: Immunocytochemistry of N-cadherin and Cx43 co-localisation in HCASMCs

N-cadherin (red) was identified both throughout the cell and at the HCASMC membrane (A, B, E & F). Cx43 (green) appeared diffusely throughout the cell (C, D, E & F). Images E and F represent overlap of images A/C and B/D, respectively. Small areas of co-localisation between Cx43 and N-cadherin (yellow) were identified in isolated cells (white arrow, E & F). Antibody dilutions as previously detailed. N=1.

4.4 – Discussion

4.4.1 – Cx37 in rat tissues

Cx37 was identified in both the rat kidney cortex and kidney pyramid tissue lysates in preliminary experiments using Western blot (Figure 4.4A). Similarly, preliminary immunohistochemical analysis identified Cx37 primarily within the vasculature of the rat kidney (Figure 4.5A). This data is in agreement with the work of Arensbak *et al.* who identified Cx37-containing gap junctions in the endothelium of the pre-glomerular arterioles in rats (Arensbak, Mikkelsen et al. 2001). In addition, work completed by Takenaka and co-workers (2008) also found Cx37-containing gap junctions in the endothelium of rat post-glomerular vessels (although this was not the case in mice, where Cx43 was expressed) (Takenaka, Inoue et al. 2008). It should be noted that work completed by Stoessel *et al.* highlighted the expression of Cx37 in the ascending limb of the loop of Henle and distal tubule and, to a lesser degree, the proximal tubule and collecting duct of rats (Stoessel, Himmerkus et al. 2010). Our preliminary immunohistochemistry results indicate only very low-level Cx37 staining in the kidney outside the vasculature; however it is likely that this Cx37 contributed to that detected through Western blot.

Preliminary data also indicated the expression of Cx37 in rat heart lysate (Figure 4.4A), supporting the previous identification of Cx37 within the endothelium lining of the heart, the endocardium, as well as within the endothelial lining of coronary blood vessels (Willecke, Heynkes et al. 1991, Delorme, Dahl et al. 1997). Despite the lack of Cx37 expression within the myocardium, as outlined by Delorme *et al*., sufficient protein existed to allow detection even when the lysate was used at a 3 fold dilution, as in our experiments. Taken together, preliminary data suggested Cx37 is expressed in the rat kidney and heart, and as such these tissues were used as a positive control for the anti-Cx37 primary antibody used in experiments.

4.4.2 – Cx37 in HCAECs

HCAECs were found to express Cx37 in preliminary Western blot and immunocytochemistry experiments (Figures 4.4B and 4.5B). In immunocytochemistry, this junctional protein was identified in two primary locations; at the cell membrane and surrounding the nucleus (Figure 4.5B). Membranous Cx37 staining was strong, present in all cells imaged and arranged into continuous segments along the cell border. The intracellular Cx37 identified

in these endothelial cells could be in the process of being translated and transported to the membrane for interaction with other cells, or being internalised and degraded. Our findings are supported by previous work completed by Yeh and co-workers who identified Cx37 expression in both rat and human coronary artery endothelium (Yeh, Rothery et al. 1998, Yeh, Lai et al. 2000). Furthermore, Cai *et al.* (2001) also identified Cx37 within the endothelium of the coronary vasculature of the dog, from the level of the artery through to the capillary, through both immunoconfocal microscopy and transmission electron microscopy (TEM). It should be noted however, that variation in the distribution of Cx37 within the coronary vasculature of different species exists, as van Kempen *et al.* failed to identify Cx37 within the bovine coronary vasculature, despite identifying its expression in the endothelium of both the rat and micropig coronary artery (Van Kempen and Jongsma 1999). However, this work was carried out on whole tissue sections and the expression of Cx37 within the bovine tissue may have been too low for detection. The discrepancies in Cx37 distribution in the coronary vasculature may be due to the high sensitivity of this protein to haemo-dynamic changes (Cai, Koltai et al. 2001). Sections taken from branch points in the coronary vasculature are likely to display a higher expression profile for this protein, compared to sections taken from other areas of the coronary arterial system, due to the high sheer stress exerted on the vessel at these sites.

4.4.3 – Cx37 in HCASMCs

Cultured HCASMCs were found to express Cx37 in preliminary Western blot and immunocytochemistry experiments (Figures 4.4C and 4.5C). In immunocytochemistry, Cx37 expression was minimal with only isolated areas of punctate staining with fluorescence intensity above that considered background (~100 AU, Figure 4.5C). Furthermore, no membrane-association was identified for Cx37 in HCASMCs, and indeed even nuclear-association was marginal (DAPI nuclear staining shown in blue). This protein was, however, identified within HCASMC lysate when targeted by Western blot. Cai *et al.* identified no Cx37 within the smooth muscle cells of the coronary vasculature of the dog under normal conditions, but they did detect this protein within these cells during collateral vessel growth of the coronary arterial system (Cai, Koltai et al. 2001). Moreover, their work suggested that this alteration in connexin expression was a result of the smooth muscle cells adopting a synthetic phenotype, a process which occurs during vessel damage and allows such collateral vessel growth to occur. As such, it may be that the smooth muscle

cells displaying punctate Cx37 expression in our results are shifting towards a synthetic phenotype. As previously mentioned, this can occur in culture but if this did occur in our HCASMCs, these cells were in the minority of the population (more detail on confirmation of the contractile nature of the cultured HCASMCs can be found under "3.1.2 Characterisation of Human Coronary Artery Smooth Muscle Cells (HCASMCs)"). It is also worth considering the precise location from which the purchased HCASMCs were obtained. Promocell state that the smooth muscle cells are obtained from the right and left coronary arteries, including the left anterior descending coronary artery and the circumflex coronary artery. van Kempen and co-workers identified high Cx37 expression in the smooth muscle cells of the larger arteries of the rat coronary arterial system, but no Cx37 within the smooth muscle cells of the smaller arteries (Van Kempen and Jongsma 1999). As such, this may explain the differences in the detection rate of Cx37 within the smooth muscle cells of the coronary artery.

4.4.4 – Cx40 in rat tissues

Cx40 was identified in both the rat kidney cortex and kidney pyramid tissue lysates during preliminary Western blot experiments (Figure 4.6A). Preliminary immunohistochemical data indicated that the expression of Cx40 was minimal within rat kidney tissue; however isolated areas of punctate staining were identified (Figures 4.7A & 4.7B). In support of this data, the literature details expression of Cx40 within both rat and human kidney. Much like Cx37, Cx40 was also identified in the endothelium of the renal vasculature (Arensbak, Mikkelsen et al. 2001). Indeed, this work highlighted Cx40 as the dominant connexin within the pre-glomerular vasculature. Furthermore, Cx40 mRNA has been identified in the tubules and collecting ducts of the rat kidney (Takenaka, Inoue et al. 2008, Kurtz, Madsen et al. 2010).

Cx40 was also identified in rat heart lysate during Western blot experiments (Figure 4.6A). This preliminary result is supported by work completed by Gros *et al.* (1994) which reported expression of Cx40 within various structures of the conducting system, including the Bundle of His and Purkinje fibres, despite a lack of expression within working ventricular myocytes (Gros, Jarry-Guichard et al. 1994). This data confirmed that published by Bastide and co-workers in 1993, which detected Cx40 within the conductive bundles of rat myocardium (Bastide, Neyses et al. 1993). Cx40 has also been identified in the atrial

myocardium of other mammals, including guinea pig and human (Gros, Jarry-Guichard et al. 1994, Vozzi, Dupont et al. 1999). This data, combined with our preliminary results, suggests expression of Cx40 in the rat kidney and heart, thus providing a positive control for the anti-Cx40 primary antibody used in experiments.

4.4.5– Cx40 in HCAECs

HCAECs were found to express Cx40 during preliminary Western blot and immunocytochemistry experiments (Figures 4.6B and 4.7C & 4.7D). In immunocytochemistry, Cx40 was identified both surrounding the nucleus and as small sections of membrane staining (Figure 4.7C and 4.7D). Such staining was not identified in all cells, and the degree of Cx40 expression varied markedly from cell to cell. As previously mentioned the cells displaying a high concentration of perinuclear Cx40 could be in the process of either translating and transporting the protein for expression at the membrane, or internalising and degrading it. Larson *et al.* (1997) have previously noted that differences in connexin expression in individual cells within the same population may reflect cells in different growth stages, and although this was primarily with respect to Cx37 and Cx43, this may partly explain the varying Cx40 expression seen here (Larson, Wrobleski et al. 1997). In support of our preliminary data, the literature details identification of Cx40 within the endothelium of both the rat and dog coronary artery (Yeh, Rothery et al. 1998, Cai, Koltai et al. 2001). Indeed, work completed by Little and co-workers (1995) concluded that Cx40 punctations in endothelial cells of resistance vessels were significantly larger than those identified in the smooth muscle of the same vessels ($P \leq 0.05$, N=80 for SMC, N=86 for EC) (Little, Beyer et al. 1995).

4.4.6– Cx40 in HCASMCs

Cx40 was identified in cultured HCASMCs through Western blot and immunocytochemistry experiments using an AF488-tagged secondary antibody (Figures 4.6C and 4.7E & 4.7F). Preliminary immunocytochemistry data indicated a diffuse distribution of Cx40 throughout the coronary artery smooth muscle cells, forming small cytoplasmic aggregations (Figure 4.7E), and potentially representing localisation of the protein within trafficking vesicles. In addition, Cx40 appeared to be associated with the cytoskeleton of the cell, presenting in longitudinal networks along the length of the cell (Figure 4.7F). Cai *et al.* failed to identify

any Cx40 within the smooth muscle cells of the dog coronary artery (Cai, Koltai et al. 2001), however this may be due to the whole-tissue analysis of this vessel and the lack of large clusters of Cx40-containing channels in this tissue (Beny and Connat 1992). In support of our data, van Kempen and co-workers identified Cx40 in smooth muscle cells of the larger arteries of the rat and bovine coronary system (Van Kempen and Jongsma 1999), however they failed to identify Cx40 in the smooth muscle cells of the smaller arterioles of the rat coronary vasculature. Work published by Giepmans *et al*. details the direct interaction between Cx43 and microtubules in rat epithelial T51B cells (Giepmans, Verlaan et al. 2001) and the existence of a similar relationship between microtubules and Cx40 in HCASMCs should be considered.

4.4.7 – Cx43 in rat tissues

Preliminary Western blot data indicates the expression of Cx43 in both the rat kidney cortex and kidney pyramid tissue lysates(Figure 4.8A). Similarly, preliminary immunohistochemical examinations identified Cx43 within rat kidney tissue sections, particularly within the renal vasculature (Figures 4.9A & 4.9B). Supporting our results, Arensbak *et al.* identified Cx43 mRNA in rat renal vasculature and Kurtz *et al.* identified Cx43 localisation within the juxtaglomerular apparatus of the human kidney (Arensbak, Mikkelsen et al. 2001, Kurtz, Madsen et al. 2010).

Western blot analysis identified Cx43 as a smudge of banding across multiple molecular weights in rat heart lysate (Figure 4.8A). Cx43 is well established as the primary connexin within the mammalian heart and this result was likely due to excess protein (Beyer, Kistler et al. 1989, Van Kempen, Fromaget et al. 1991). Indeed, further work by Gourdie *et al.* has identified co-localisation of Cx40 with Cx43 within rat atrioventricular nodal tissue and Purkinje fibres (Gourdie, Severs et al. 1993).

Immunohistochemistry of rat coronary artery slices during preliminary experiments identified Cx43 within both the endothelium and the multiple smooth muscle layers of this vessel (Figures 4.9C & 4.9D and 4.9E & 4.9F). The literature contains little definitive information on the expression profile of Cx43 within the coronary vasculature, however, van Kempen and co-workers identified low levels of this connexin in the smooth muscle cells of the larger arteries of the rat coronary vasculature (Van Kempen and Jongsma 1999). In contrast, they could not identify any Cx43 in the smooth muscle cells of the smaller

arterioles of the rat coronary system. This work highlighted the variable distribution patterns of Cx43 within different mammals, as the expression pattern of Cx43 was completely reversed in bovine coronary arteries (localisation to distal/smaller arterial smooth muscle cells and not proximal/larger arterial smooth muscle cells). Published work by Yeh *et al.* identified a lack of Cx43 expression within rat coronary artery endothelium, despite identifying this connexin within other muscular arteries (mesenteric resistance, hepatic and tail arteries) (Yeh, Rothery et al. 1998). Taken together, this data suggest a high degree of variability in the expression pattern of Cx43 within the coronary vasculature, both within and between different species. Similarly, preliminary immunohistochemistry investigations of rat mesenteric artery slices also identified Cx43 within both the endothelial and smooth muscle layers of this vessel (Figures 4.9G & 4.9H). Stronger Cx43 staining was identified within the smooth muscle compared to that localised to the endothelium, however areas of punctate staining did exist within these endothelial cells (Figure 4.9G). In support of our preliminary data, Hong and Hill also identified Cx43 expression within the endothelium and tunica media of rat elastic arteries, including the superior mesenteric artery (Hong and Hill 1998). Taken together, Cx43 appears to be expressed in the rat kidney, heart, and coronary and mesenteric vasculature.

4.4.8 – Cx43 in HCAECs

HCAECs were found to express Cx43 during preliminary Western blot and immunocytochemistry experiments (Figures 4.8B and 4.10A). In immunocytochemistry, Cx43 was found to be distributed diffusely throughout the cell and at sections of membrane staining (Figure 4.10A). As previously mentioned, literature on the distribution pattern of Cx43 within the coronary vasculature is limited and the majority of reports fail to identify this junctional protein within the coronary endothelium. Published work by Cai *et al.* and Yeh *et al.* for example, found no evidence of Cx43 expression in either the dog or human coronary artery endothelium, respectively (Yeh, Dupont et al. 1997, Cai, Koltai et al. 2001). Larson *et al.* however, did identify Cx43 messenger RNA within bovine, porcine, rat and human microvascular endothelial cells via Northern blot analysis (Larson, Haudenschild et al. 1990). The lack of Cx43 expression within the former studies may be a result of whole-tissue analysis. Our studies involved identification of the Cx43 expression pattern in individual HCAECs, and as such, even low-level expression could be detected. Despite the lack of definitive evidence in the literature, our preliminary data indicates the expression of

Cx43 within cultured HCAECs, and this result is believed to be real due to the consistent banding for the protein (P6-P10) in the Western blot experiments (Figure 4.8B).

4.4.9– Cx43 in HCASMCs

Cx43 was identified in HCASMCs through Western blot and immunocytochemistry analysis (Figures 4.8C and 4.10B). Unlike HCAECs, HCASMCs displayed no clear segments of membranous Cx43 and instead displayed cytoplasmic aggregations of the protein throughout the cells during preliminary experiments. In addition, no nuclear Cx43 staining was identified in HCASMCs (Figure 4.10B). Again, little detail of Cx43 expression within HCASMCs can be found in the literature, with Cai and co-workers again finding no evidence of this protein within smooth muscle cells of the dog coronary artery (Cai, Koltai et al. 2001). Gourdie *et al.*, however, have published data confirming the expression of Cx43 within smooth muscle cells of the vasculature of the avian heart (Gourdie, Green et al. 1993) and Larson *et al.* once again identified Cx43 mRNA in bovine, porcine, rat and human microvascular smooth muscle cells (Larson, Haudenschild et al. 1990).

While it is possible that the types and levels of connexins expressed by cells, particularly smooth muscle cells, can change in culture, as detailed by Stutenkemper *et al.* (Stutenkemper, Geisse et al. 1992), it seems unlikely that the consistent Cx43 expression observed in both HCAECs and HCASMCs is due to a change in cell phenotype. Furthermore, considerable Cx43 expression was also identified within whole slices of rat coronary artery during preliminary investigations (Figures 4.9C & 4.9E). Indeed, the expression of Cx43 within large elastic arteries, including the aorta from which the coronary arteries stem, and other resistance vessels, is well established (Bruzzone, Haefliger et al. 1993, Little, Beyer et al. 1995).

In conclusion, our preliminary data suggests expression of connexins 37, 40 and 43 in cultured primary HCAECs. Furthermore, at least 2 connexins, Cx40 and Cx43, were found to be expressed by cultured primary HCASMCs, as evidenced by both Western blot and immunocytochemistry.

4.4.10 – VE- cadherin

Preliminary Western blot and immunocytochemistry experiments found HCAECs to express VE-cadherin (Figures 4.11 & 4.12), while VE-cadherin was absent from HCASMCs (Figure 4.11). In immunocytochemistry, VE-cadherin was found to be distributed primarily to the membrane as discontinuous patches (Figure 4.12). In addition, some cells were found to express perinuclear staining for VE-cadherin. It is well-established that VE-cadherin is almost entirely restricted in its expression to vascular endothelial cells (Lampugnani, Resnati et al. 1992, Breviario, Caveda et al. 1995). Furthermore, the localisation of VE-cadherin was shown to be primarily to the membrane (Dejana 1997), supporting our immunocytochemistry results. With regards to HCAECs, Kondapalli and co-workers (2004) also found human coronary artery endothelial cells to express VE-cadherin, and indeed they highlighted its relationship with the armadillo protein p-120 catenin, a known cadherin complex-associated protein (Kondapalli, Flozak et al. 2004). Research carried out by Navarro *et al.* also identified a similar VE-cadherin distribution pattern *in vivo* (artery and vein from human lymph node) (Navarro, Ruco et al. 1998). As previously mentioned for connexins, cells displaying cadherin protein expression near the nucleus could be in the process of either translating and transporting the protein for expression at the membrane, or internalising and degrading it. Our results also highlighted short intra-cellular projections of VE-cadherin from the cell membrane (Figure 4.12B). These projections may be a result of accumulation of newly synthesised VE-cadherin at actin filament tips due to Myosin-x trafficking of the protein from the Golgi apparatus (Harris and Nelson 2010). This is normally evident in sub-confluent cells as new cadherin complexes are forming and may be due to a temporary lack of sufficient cell-cell contact sites for the degree of VE-cadherin available near the membrane (Almagro, Durmort et al. 2010). Alternatively, such short lines of VE-cadherin staining at right angles to the endothelial cell border were also identified by (Spindler, Peter et al. 2011), who hypothesised that these represented multiple lateral cell protrusions inter-digitating along tortuous cell contacts in the x-y plane. It should also be noted that the potential for the expression of an additional VE-cadherin subtype exists. This cadherin was termed VE-cadherin 2 by Telo *et al.* (Telo, Breviario et al. 1998) who identified its distribution in heart microvascular endothelial cells. Like VE-cadherin, VE-cadherin 2 was also found to localise to intercellular junctions and exhibit adhesive properties. However, unlike VE-cadherin, VE-cadherin 2 does not bind to catenins and does not modify paracellular permeability, cell migration or growth, all of which are important functions of VE-cadherin

4.4.11 - N -cadherin in HCAECs

Preliminary experiments identified N-cadherin in HCAECs through both Western blot and immunocytochemistry (Figures 4.13 & 4.14). In immunocytochemistry, N-cadherin was found to localise to specific sites of the cell membrane (white arrows, Figure 4.14A), and to form aggregations throughout the cell (white arrow, Figure 4.14B), potentially representing localisation within trafficking vesicles. Our data is supported by the literature examining N-cadherin in endothelial cells of the vasculature (Suzuki, Sano et al. 1991, Dejana 1997, Lampugnani and Dejana 1997). Unlike VE-cadherin, N-cadherin is not endothelial cell-specific and is originally known for its expression in neurons, as reflected in its full name, Neural-cadherin (Takeichi 1990, Grunwald 1993). It should be noted, however, that research in the chick embryo has highlighted that during development vascular endothelium was not found to express N-cadherin, despite other tissues of mesodermal origin expressing this junctional protein (Hatta, Takagi et al. 1987). The membranous distribution of N-cadherin within vascular endothelial cells is also well-established (Salomon, Ayalon et al. 1992, Navarro, Ruco et al. 1998). Unlike VE-cadherin, Salomon *et al.* (1992) identified N-cadherin diffusely throughout the whole cell membrane in human endothelial cells, and not localised to sites of cell-cell contact (Salomon, Ayalon et al. 1992). Again, Navarro and co-workers (1998) found that N-cadherin is present throughout the membrane, while VE-cadherin localises at cell-cell contacts (Navarro, Ruco et al. 1998). Work by this group also found that similar amounts of α- and β- catenins and plakoglobin (γ-catenin) associate with VE- and N-cadherin, but that p120 catenin shows a preference for the VE-cadherin complex (Navarro, Ruco et al. 1998). As mentioned earlier, Kondapalli and co-workers (2004) showed an interaction between the HCAEC VE-cadherin complex and p120 catenin (Kondapalli, Flozak et al. 2004). Further work by Navarro *et al.* (1998), however, identified that the dominance of VE-cadherin over N-cadherin at sites of cell-cell contact was not a result of a defect in N-cadherins' ability to associate with catenins (Navarro, Ruco et al. 1998). Moreover, a loss of adhesive ability of N-cadherin and a higher degree of tyrosine phosphorylation (known to weaken adherens junctions) were also ruled out, indeed Navrarro *et al.* (1998) found VE-cadherin to display a higher degree of phosphorylation than N-cadherin (Navarro, Ruco et al. 1998). Ultimately, the short Arg^{621}-Pro^{702} sequence in the VE-cadherin cytoplasmic tail was found to be required, and sufficient, for N-cadherin exclusion from sites of cell-cell contact. The authors hypothesised the need for VE-cadherin dominance at cell-cell contacts to prevent undesired signalling through N-cadherin during formation of vascular structures. A direct result of the dominant

nature of VE-cadherin in endothelial cells is that it is this junctional protein that primarily constitutes the homotypic interactions between adjacent cells. As such, N-cadherin is able to interact with N-cadherin expressed on alternative cell types not expressing the endothelial-specific VE-cadherin, thereby allowing a direct interaction between endothelial cells and smooth muscle cells of the vasculature (Bazzoni and Dejana 2004, Sabatini, Zhang et al. 2008). The distribution of N-cadherin to restricted sections of the membrane of HCAECs (Figure 4.14A) may reflect this need to interact with other vascular cells distributed in adjacent layers of the vessel wall. Moreover, the accumulations of N-cadherin that we observed near the membrane of HCAECs (Figure 4.14B) are potentially a result of this competition between VE-cadherin and N-cadherin for membrane space.

4.4.12 - N -cadherin in HCASMCs

HCASMCs were found to express N-cadherin, as shown by preliminary Western blot and immunocytochemistry experiments (Figures 4.13 & 4.15). By immunocytochemistry, N-cadherin was found to be expressed as small aggregations throughout the cell and as small segments of membrane staining (Figure 4.15). Similar to that observed in HCAECS, N-cadherin in HCASMCS also appeared to show membrane expression at one particular site of the cell (Figure 4.15B). Work by Hatta and co-workers (1987) detailed the transient expression of N-cadherin in smooth muscle cells during development, unlike that observed in endothelial cells (Hatta, Takagi et al. 1987). The distribution pattern of N-cadherin in cultured cells was found to be similar to that displayed in vivo (Navarro, Ruco et al. 1998). Furthermore, Gilbertson-Beadling and co-workers (1993) have shown that cultured endothelial cells can bind vascular smooth muscle cells in an N-cadherin-dependent manner in vitro (Gilbertson-Beadling and Fisher 1993).

In conclusion, preliminary experiments identified both VE-cadherin and N-cadherin in cultured HCAECs. VE-cadherin was primarily localised to sites of cell-cell contact as discontinuous patches, while N-cadherin was distributed across the cell membrane. Our data points towards a key role for VE-cadherin in HCAEC-HCAEC interaction. In addition, HCASMCs were also found to express N-cadherin. This junctional protein was expressed at the membrane as small segments, favouring one border of the cell, highlighting N-cadherin as a potential key player in HCAEC-HCASMC adhesion.

4.4.13 - Connexin and Cadherin Co-localisation Discussion

Distinct areas of co-localisation were identified between VE-cadherin and Connexins 37, 40 and 43 in HCAECs. During preliminary investigations, VE-cadherin and Cx37 showed clear areas of overlap at the cell membrane, however, areas of membranous Cx37 devoid of VE-cadherin expression were detected (Figures 4.16A & 4.16B). Overlap between VE-cadherin and Cx40 distribution was evident but was not observed in all HCAECs imaged (Figure 4.17C), and VE-cadherin co-localisation with Cx43 was restricted to isolated sections of the membrane (Figure 4.18C). Co-localisation between N-cadherin and connexins 37, 40 and 43 was also examined. No overlap between N-cadherin and Cx37 (Figure 4.20C) or Cx40 was detected (Figure 4.21C) during preliminary experiments. During similar preliminary investigations, isolated areas of overlap were detected between N-cadherin and Cx43 in a subset of HCAECs imaged (Figure 4.22C).

Co-localisation between cadherins and connexins is a direct result of the requirement for adherens junctions as a precursor to gap junction formation. As previously detailed, formation of nascent gap junctions requires a reduced intercellular distance between plasma membranes of adjacent cells brought about by the establishment of cell-cell contacts mediated by adherens junctions (Fujimoto, Nagafuchi et al. 1997). It is generally accepted that connexons are delivered to the plasma membrane by post-Golgi carriers at random and migrate laterally in the plane of the membrane bilayer (Loewenstein 1981, Thomas, Jordan et al. 2005). On approaching a region of cell-cell contact these channel precursors are able to associate with connexins on the adjacent cell membrane and ultimately form functional gap junctions. As a result, a diffuse cell-surface rim of connexin protein can be imaged prior to the appearance of punctate gap junctions (Thomas, Jordan et al. 2005). As these sites of cell-cell contacts are directly mediated by adherens junctions, formed from cadherins, the accumulation of connexin proteins at membrane regions expressing cadherins is expected. This self-trap model of gap junction formation allows rapid accumulation of connexins at sites of cell-cell contact (10^{-1} – 10^{-3} seconds) (Loewenstein 1981). Furthermore, the bending moments of the membrane are hypothesised to prevent connexins from migrating laterally once a cell-cell contact is established (Loewenstein 1981). An alternative hypothesis on connexin distribution at the membrane is offered by Levine *et al.* (1993) who suggest that once connexin proteins are inserted into the membrane their movement is directed by electrophoresis and as such is modulated by membrane potential (Levine, Werner et al. 1993). Independent of the process through which connexins migrate in the plasma membrane, these proteins can only

dock with adjacent connexin proteins on opposing cells, and thus form functional gap junctions, when the intervening distance is reduced by the formation of adherens junctions.

Further evidence for the requirement for adherens junctions prior to gap junction formation comes from the formation of the compacted embryo. Connexins are first identified at the 4-cell stage (Nishi, Kumar et al. 1991, Fléchon, Degrouard et al. 2004) but these exist only as cytoplasmic stores (Musil and Goodenough 1993). Functional gap junction formation and Lucifer yellow dye transfer between blastomeres does not occur until the 8-cell stage when the embryo has undergone compaction (McLachlin, Caveney et al. 1983, Fléchon, Degrouard et al. 2004). Removal of extracellular calcium causes loss of the compacted shape of the embryo (Aghion, Gueth-Hallonet et al. 1994) and a loss of intercellular coupling (Goodall 1986), and so cadherins were identified as the components responsible for the formation of the compacted embryo, and thus gap junction formation. Further work by Aghion et al. (1994), and others, identified that E-cadherin is phosphorylated in the mouse embryo at the 8-cell stage, just prior to compaction (Sefton, Johnson et al. 1992, Aghion, Gueth-Hallonet et al. 1994), and as such this cadherin was hypothesised to be responsible for compaction and the initiation of gap junctional intercellular communication (GJIC).

The calcium-dependent nature of adherens junctions provides further evidence for the close association between cadherins and connexins. It is well-established that blocking of calcium-dependent adhesion prevents the formation of new gap junction channels (Atsumi and Takeichi 1980, Davidson, Baumgarten et al. 1984, Kanno, Sasaki et al. 1984, Jongen, Fitzgerald et al. 1991) and that GJIC is increased under elevated levels of extracellular calcium (Jongen, Fitzgerald et al. 1991). In addition to calcium removal, addition of fragments against cadherins also disrupts cadherin-cadherin interactions and results in reduced GJIC as detected by dye transfer (Kanno, Sasaki et al. 1984, Meyer, Laird et al. 1992). Whether the antibody fragments prevent the acquisition of the close membrane-membrane association required for adherens junction and gap junction formation, or whether the Fab fragments prevent transmembrane signalling that allows junction formation, is unknown. Interestingly, Fab fragments of antibodies for extracellular domains of Cx43 have also been found to block adherens junction formation in re-aggregating Novikoff hepatoma cells (Meyer, Laird et al. 1992), further highlighting the close interaction between cadherins and connexins. Transfection of L-CAM (E-cadherin) cDNA into mouse

sarcoma s180 fibroblasts, which are not normally capable of GJIC, results in the formation of functional gap junctions (Mege, Matsuzaki et al. 1988, Musil and Goodenough 1991), again highlighting the requirement for adherens junctions prior to gap junction formation. An additional explanation for the requirement for adherens junction formation prior to gap junction formation is the need for cell recognition. Gap junctions are required for the correct progression of development and as such adherens junction formation ensures that the correct cells are interacting, thereby regulating this process (Jongen, Fitzgerald et al. 1991).

Direct association between cadherins and connexins has been detected through interaction with the cadherin-associated protein β-catenin (Ai, Fischer et al. 2000). The short intracellular tail of VE-cadherin is linked to β-catenin in addition to other Armadillo family proteins (Navarro, Caveda et al. 1995, Navarro, Ruco et al. 1998, Ferber, Yaen et al. 2002, Taddei, Giampietro et al. 2008). Cx43 has also been found to bind to β-catenin in cultured neonatal rat cardiomyocytes, indeed association with this protein promotes transcription of Cx43 (Ai, Fischer et al. 2000). In addition, VE-cadherin also associates with α-catenin through its interaction with β-catenin (Breviario, Caveda et al. 1995) and co-localisation of connexins 26, 32 and 43 with this protein further highlights the close association between connexins and cadherins (Fujimoto, Nagafuchi et al. 1997, Wu, Tsai et al. 2003). Literature on the direct co-localisation of cadherins with connexins is limited, however, co-localisation of N-cadherin with Cx43, and E-cadherin with Cx26 and Cx32, have been shown through immunocytochemical analysis of mouse neural crest cells and immunohistochemistry of mouse liver, respectively (Fujimoto, Nagafuchi et al. 1997, Xu, Li et al. 2001). Although the literature primarily details co-localisation between N-cadherin and connexins, our extensive VE-cadherin staining at the membrane limits the capacity for N-cadherin membrane association and as such N-cadherin/ connexin co-localisation at the membrane is restricted in our cells.

4.4.14 – Concluding remarks

Preliminary experiments identified connexins 37, 40 and 43 in HCAECs and HCASMCs. In addition, both VE-cadherin and N-cadherin were identified in HCAECs, and N-cadherin alone in HCASMCs. Distinct co-localisation between VE-cadherin and Cx37 at the membrane was identified in HCAECS during preliminary experiments, suggesting a close association between these two junctional components.

Chapter 5:

Control of Cadherin and Connexin Distribution

Aims of this chapter:

- To examine the effect of cadherin disruption (through pre- incubation with the anti-VE-cadherin primary antibody and EGTA calcium chelation) on cadherin and connexin distribution in HCAECs
- To determine the expression profile of Epac1 and Epac 2 in HCAECs
- To examine the effect of Epac activation on connexin and cadherin distribution in HCAECs
- To examine the effect of inhibition of Epac (through siRNA transfection and Epac antagonists ESI-09 and HJC0197) on connexin and cadherin distribution in HCAECs

Key findings of this chapter:

- Cadherin disruption results in a change in HCAEC morphology from a flattened sheet to isolated colonies of rounded cells
- Cadherin disruption triggers re-distribution of VE-cadherin and Cx37 to restricted points of the HCAEC membrane
- VE-cadherin is required for the formation of new adherens junctions and gap junctions at sites of cell-cell contact in HCAECs, and for the flat sheet-like morphology observed under control conditions
- Epac1 is expressed by HCAECs
- Epac activation promotes its relocation to the membrane within 30 minutes
- Epac activation triggers VE-cadherin and Cx37 re-distribution to the membrane, significantly enhancing their co-localisation
- The enhanced co-localisation between VE-cadherin and Cx37 mediated by Epac activation is completely blocked by both transfection with Epac1 siRNA, and incubation with the Epac antagonists ESI-09 and HJC0197

5.1 - Introduction

5.1.1 – Disruption of the endothelial barrier

The importance of cell-cell junctions, particularly cadherins, in maintenance of the endothelial barrier has previously been detailed (Section 1.7 – Adherens junctions and Section 4.1.2 - Cadherins). Factors that disrupt the distribution of cadherins and connexins therefore provide an insight into the mechanisms regulating the maintenance of the endothelial barrier. Historically, disruption of adherens junctions has typically been carried out by one of two methods: (i) blocking specific cadherin interactions by pre-incubation with the antibody Fab fragments against the required cadherin (Kanno, Sasaki et al. 1984, Meyer, Laird et al. 1992), or (ii) removal of extracellular calcium (Berry and Friend 1969, Volberg, Geiger et al. 1986, Volk, Volberg et al. 1990, Kartenbeck, Schmelz et al. 1991, Cullere, Shaw et al. 2005). As such, our experiments involved pre-incubation with the anti-VE-cadherin primary antibody, and/or removal of extracellular calcium by EGTA treatment.

5.1.2 – Enhancement of the endothelial barrier

cAMP has long been known to act as a regulator of the endothelial barrier, and an increase in its intracellular concentration evokes a reduction in endothelial permeability (Section 1.11). As discussed in Chapter 1, Epac is a novel cAMP effector that is able to mediate endothelial barrier stabilisation. As such, the distribution of Epac and the effect of activation and inhibition of this Rap GEF was examined using the Epac-specific agonist 8-pCPT-AM (8-pCPT), and Epac antagonists HJC0197 and ESI-09, respectively.

5.1.3 – Gap junction turnover

High-resolution fluorescence microscopy, in combination with time-lapse imaging, has revealed that gap junctional plaques are highly dynamic structures (Falk 2000, Jordan, Chodock et al. 2001, Martin, Blundell et al. 2001). Indeed, connexins display a short half-life of 1-3 hours in many cell cultures (Musil, Beyer et al. 1990, Laird, Puranam et al. 1991). This is a very rapid turnover when compared to other membrane proteins, the adult acetylcholine receptor, for example, has a half-life of approximately 10 days (Salpeter 1999). It should be noted, however, that not all connexins are degraded so rapidly; Cx46 in the lens has a half-life of approximately 1 day (Jiang, Paul et al. 1993). The turnover of

connexin expression at the membrane is regulated by both proteosomal and lysosomal degradation, as evidenced through the use of proteosomal inhibitors (ALLN, MG132 or lactacystin) and lysosomal inhibitors (leupeptin and E-64) (Laing, Tadros et al. 1997), and is ubiquitin-dependent (Rütz and Hülser 2001, Somekawa, Fukuhara et al. 2005). During endocytosis, both membranes of the GJ complex are internalised into one of the cells, forming a double-membrane vacuole termed a connexosome or annular gap junction (Jordan, Chodock et al. 2001, Segretain and Falk 2004). Caveolins have been linked to the removal of connexins from the plasma membrane, particularly as connexins have been shown to interact with caveolin-1, a component of caveolae (Schubert, Schubert et al. 2002). The pathway of connexin degradation involves an enzymatic cascade during which multiple ubiquitin molecules are attached to the connexin (Schwartz and Ciechanover 1999). The ubiquitinated connexin protein is then degraded by the 26S proteosome complex.

5.1.4 - Epac distribution

Epac1 is widely distributed and was identified in all human tissues tested (De Rooij, Zwartkruis et al. 1998), with particular enrichment in the heart and kidney. Epac2, however, shows a more restricted distribution with predominant expression in the brain (Kawasaki, Springett et al. 1998). These expression profiles are reflected in the implication of Epac1 in cardiac hypertrophy (Morel, Marcantoni et al. 2005), and Epac2 in autism (Woolfrey, Srivastava et al. 2009, Penzes, Woolfrey et al. 2011).

5.1.5 – Epac is a GEF for Rap1

Ras proximate 1 (Rap1), a member of the Ras family of proteins, is a small G-protein that takes an inactive GDP-bound or an active GTP-bound state. GEFs, such as Epac, dissociate the bound GDP from Rap, allowing the GTP in the cytosol to bind and activate Rap (Bos, De Rooij et al. 2001). GTPase-activating proteins (GAPs), on the other hand, induce the hydrolysis of the bound GTP to revert Rap to its inactive GDP-bound form. Two isoforms of Rap1 exist, Rap1a and Rap1b, and these share 95% amino acid similarity (Klinz, Seifert et al. 1992). Similarly, Rap1 and Rap2 share 70% homology and differ by only one residue in their effector domains (De Rooij, Rehmann et al. 2000). Three second messengers are known to activate Rap1; calcium, diacylglycerol (DAG) and cAMP (Bos, De Rooij et al. 2001, Guo, Kumahara et al. 2001, Schmitt and Stork 2001). In human platelets, α-thrombin stimulates

a rise in intracellular calcium that results in increased Rap1 activation within 30 seconds of application, and this increase in Rap1 activity is inhibited by addition of the calcium chelating agent BAPTA-AM (Franke, Akkerman et al. 1997). A combination of factors can also be responsible for an increase in Rap1 activation, as is seen in human neutrophils (M'Rabet, Coffer et al. 1998). In these cells, both the calcium ionophore ionomycin and the DAG mimetic 12,13-tetradecanoyl phorbol acetate (TPA) induced an increase in Rap1 activation (M'Rabet, Coffer et al. 1998). Furthermore, Zwartkruis and co-workers (1998) found fibroblasts to increase Rap1 activation as a result of either a rise in intracellular calcium, release of DAG, or an increase in cAMP synthesis. Rap1 has previously been shown to be closely associated with cellular membranes (Bos, De Rooij et al. 2001, Bivona, Wiener et al. 2004). Unlike other Ras proteins which are primarily identified at the plasma membrane, Rap1 is typically localised to the Golgi complex, and has been shown to co-localise with markers for the medial cisternae of the golgi apparatus (Beranger, Goud et al. 1991).

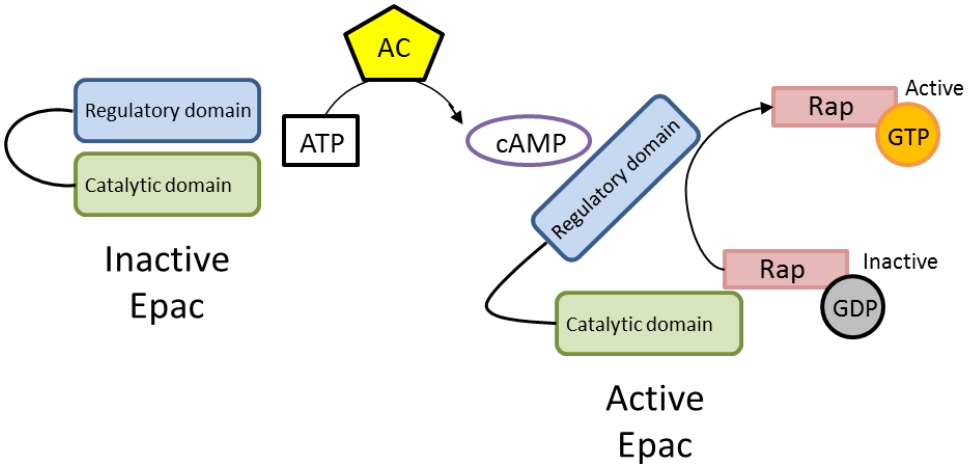

Figure 5.1: Activation of Epac

The above diagram gives a brief overview of the activation of Epac. In its inactive state, the regulatory domain of Epac (blue) inhibits the guanine exchange activity of the catacyltic domain of Epac (green). Adenylate cyclases (AC, yellow) elevate intracellular concentrations of cAMP (purple). cAMP subsequently binds to the regulatory domain of Epac (blue), dissociating it from the catalytic domain (green) and therefore preventing auto-inhibition of the catalytic domain. Once activated, Epac can then bind to inactive GDP-bound Rap (red and grey) and promote the exchange of its GDP for GTP, thereby activating Rap (red and orange). Active Rap then has numerous downstream effects, primarily involving modulation of the actin cytoskeleton. This figure is adapted from Figure 1 of "cAMP signalling in the vasculature: the role of Epac (exchange protein directly activated by cAMP)"(Roberts and Dart 2014).

5.1.6 - Additional Rap1 GEFs

The role of Epac as a GEF for Rap1 has been previously detailed (above). Other proteins also possess the ability to convert GDP-bound Rap to its GTP-bound form and thereby activate this protein. Crk SH3-domain-binding guanine-nucleotide releasing factor (C3G) was the first RapGEF identified with the characteristic CDC25 homology domain and Ras exchange motif (REM) (Tanaka et al. 1994, Gotoh, Hattori et al. 1995). C3G is cAMP/PKA dependent and is targeted to the plasma membrane on activation (Okada et al. 1998, Wang et al. 2006). Interestingly, C3G has been shown to directly interact with E-cadherin during the first stages of junction formation, prior to formation of a mature AJ (Hogan et al. 2004). Indeed, inhibition of C3G prevents translocation of E-cadherin to sites of cell-cell contact, therefore indicating a role of C3G in the recruitment of this cadherin to cell junctions.

The calcium and DAG-regulated guanine nucleotide exchange factors (CalDAG-GEFs/CD-GEFs) activate Rap1 and Rap2, and as their name suggests bind, and are activated by, both calcium and DAG (Kawasaki, Springett et al. 1998, Yamashita, Mochizuki et al. 2000). CalDAG-GEFI can activate Rap1A (Kawasaki, Springett et al. 1998, Yamashita, Mochizuki et al. 2000), while CalDAG-GEFIII can activate both Rap1A and Rap2A (Yamashita, Mochizuki et al. 2000). On addition of the DAG mimetic TPA, CalDAG-GEFIII translocates to the plasma membrane but is insensitive to increased levels of calcium, potentially suggesting CalDAG-GEFI as the primary regulator of Rap1 activation by calcium and CalDAG-GEFIII as the main regulator of Rap1 activation by DAG (Bos, De Rooij et al. 2001).

PDZ-GEFs are ubiquitously expressed activators of Rap (De Rooij, Boenink et al. 1999). In addition to the REM and catalytic GEF domains expressed by all Rap-GEFs, PDZ-GEFs posess an additional 2 regulatory domains(De Rooij, Boenink et al. 1999). One of these regulatory domains is the PDZ domain and the second is a structure that is related to the cAMP-binding domains of Epac and PKA (RCBD)(De Rooij, Boenink et al. 1999). As occurs in Epac, the RCBD serves as a negative regulatory domain for PDZ-GEF catalytic activity, and PDZ-GEFs are capable of activating Rap1 and Rap2 but not R-ras (De Rooij, Boenink et al. 1999).

Phospholipase C ε (PLCε) is an additional Rap1-GEF (Jin, Satoh et al. 2001), and more detail on this GEF will be discussed later in this section as PLC ε is also activated by Rap (see Section 5.1.10).

5.1.7 - Rap1 GAPs

GTPase-activating proteins (GAPs) hydrolyse the bound GTP to revert Rap to its inactive GDP-bound form. Rap1 has low intrinsic GTPase activity due to its lack of a conserved glutamine residue at position 61 (Polakis, Rubinfeld et al. 1991), and as such GAPs are essential to reverse the activity of GEFs. Rap1GAP is a ubiquitously expressed GAP, and the first Rap1-specific GAP to be identified (Polakis, Rubinfeld et al. 1992). This GAP suppresses both endogenous Rap1 activity and db-cAMP-induced Rap1 activity (Somekawa, Fukuhara et al. 2005). In addition to GAPs, Rap1 activity is also suppressed by phosphodiesterases (PDEs) which rapidly metabolise cAMP to AMP.

5.1.8 - Rap1 activity

Rap1 is an important regulator of the actin cytoskeleton (Yamamoto, Harada et al. 1999, Boettner, Govek et al. 2000, Bos, De Rooij et al. 2001, Cullere, Shaw et al. 2005). Rap1 interacts with a number of proteins, including the cytoskeletal anchoring protein AF-6, and the GTPase Rac. AF-6 is capable of binding actin, the actin cytoskeleton regulator Profilin, and the tight junctional component ZO-1 (Section 1.8 - Tight junctions)(Yamamoto, Harada et al. 1999, Boettner, Govek et al. 2000). In addition, AF-6 also contains two N-terminal Ras-binding domains (RBDs), one of which binds active Ras and Rap1 with high affinity (Linnemann, Geyer et al. 1999). These RBDs allow the formation of a complex between Rap1 and cytoskeletal components. Evidence of such a complex comes from the co-localisation of AF-6 and Rap1 at adherens junctions (Boettner, Govek et al. 2000). Furthermore, increased cAMP and Epac activity, both known to activate Rap1, has previously been shown to increase the continuity of AF-6 staining along cell-cell contacts (Cullere, Shaw et al. 2005).

5.1.9 – Rap1 activates Rac through Tiam1 and Vav2

Rac is part of the Rho family of small GTPases and is activated by Rap1, as evidenced by reduced Rac activation on expression of the Rap inhibitor Rap1GAP (Maillet, Robert et al. 2003). Rap1-dependent phosphorylation of the Rac1-specific GEFs Tiam1 and Vav2 is required for the activation of Rac1 (Lampugnani, Zanetti et al. 2002, Birukova, Zagranichnaya et al. 2007, Birukova, Burdette et al. 2010, Lampugnani, Orsenigo et al.

2010). Active Rac1 stimulates the actin-related protein (arp) 2/3 complex (Weed, Karginov et al. 2000, Head, Jiang et al. 2003) through the Wiskott-Aldrich syndrome protein(WASP), an example of which is Neural-WASP (N-WASP) (Takenawa and Miki 2001). In its inactive state, the region of N-WASP that binds the Arp2/3 complex, the VCA (verprolin-homology (V) domain, cofilin-homology (C) domain and acidic (A) domain) region at the C-terminus, is masked (Takenawa and Miki 2001). Co-operative binding of Cdc42 (an additional Rho GTPase) and phosphatidylinositol 4,5-biphosphate (PtdIns (4,5)P_2 or PIP_2) unmasks the VCA region and allows N-WASP to bind to, and activate, the Arp2/3 complex (Takenawa and Miki 2001). In addition, the WASP-family verprolin-homologous (WAVE) proteins, specifically WAVE2, also mediate Rac-induced activation of the Arp2/3 complex (Takenawa and Miki 2001). Both N-WASP and WAVE2 are expressed in vascular endothelial cells (Yamazaki, Suetsugu et al. 2003, Rajput, Kini et al. 2013). Once activated, the Arp2/3 complex initiates actin nucleation (Machesky and Hall 1997) and cortactin is rapidly recruited to these nucleation sites where it stabilises the newly-generated cortical actin fibres (Weaver et al. 2001, Ciano, Nie et al. 2002). Rac-induced recruitment of cortactin is dependent on its direct interaction with both F-actin, via its R region, and the Arp2/3 complex, via its Arp2/3 –binding N-terminal acidic tail (Weed, Karginov et al. 2000, Uruno, Liu et al. 2001, Head, Jiang et al. 2003). Indeed, the N-terminal domain of cortactin is responsible for the targeting of this protein to actin-enriched patches (Uruno, Liu et al. 2001). An additional pathway through which Rac promotes increased actin filament assembly, is through the activation of phosphatidylinositol-4-phosphate 5-kinase (PIP_5K) (Janmey and Stossel 1987, Tolias, Cantley et al. 1995, Bishop and Hall 2000). Rac activates this kinase, directly promoting the increased formation of PIP_2 from phosphatidylinositol-4-phosphate (PIP_4)(Janmey and Stossel 1987). PIP_2 is then available to bind to actin capping proteins such as Gelsolin, inducing their release from the actin-filament barbed ends, and promoting actin polymerisation (Janmey and Stossel 1987). The elevated levels of PIP_2 also enhance the Cdc42/ PIP_2-mediated activation of the Arp2/3 complex, further promoting actin polymerisation. Ultimately, the Rap1/Rac pathway results in an enhanced cortical actin rim and a decrease in actin stress fibres (Albertinazzi, Cattelino et al. 1999, Somekawa, Fukuhara et al. 2005). These alterations to the cytoskeleton have been shown to be blocked by Epac1 siRNA, inhibition of Rap1 and inhibition of Rac1 (Kooistra, Corada et al. 2005, Baumer et al. 2009).

There is some controversy surrounding the role of tyrosine phosphorylation on the recruitment of cortactin. Some groups suggest that protein kinase C (PKC) -mediated

phosphorylation of cortactin at Tyr421 results in its translocation to the periphery (Van Damme, Brok et al. 1997, Rossé, Lodillinsky et al. 2014), however, Weed *et al.* (1998) were unable to detect changes in the level of cortactin tyrosine phosphorylation on Rac-mediated cortactin re-distribution (Weed, Du et al. 1998).

Rac also stabilises the endothelial barrier through the inhibition of RhoA-induced contraction. Rac1 inhibits RhoA via activation of the RhoGAP p190, thereby preventing MLC phosphorylation, actin-myosin-mediated contraction, and increased paracellular permeability (Mammoto, Parikh et al. 2007).

5.1.10 – Rap activates Phospholipase C

In addition to signalling through Rac, increasing evidence suggests that Rap, particularly Rap2b, also mediates the activity of a specific phospholipase C (PLC) isoform, PLCε (Bos, De Rooij et al. 2001, Schmidt, Evellin et al. 2001, Evellin, Nolte et al. 2002, Williams, Sarkar et al. 2008, Ravikumar, Sarkar et al. 2010, Harris and Rubinsztein 2012). PLC isoforms are classified into 7 groups; PLCα, PLCβ, PLCγ, PLCδ, PLCε, PLCξ and PLCη (Schmidt, Evellin et al. 2001, Song, Hu et al. 2001, Evellin, Nolte et al. 2002). All PLC isoforms contain two regions of high sequence homology and these form the catalytic domain responsible for the hydrolysis of PIP_2 to form inositol-1,4,5-trisphosphate (IP_3) and DAG (Schmidt, Evellin et al. 2001, Song, Hu et al. 2001). In addition to this catalytic domain and a C2 domain, all PLC isoforms, except PLCε, also contain a PH domain and an EF-hand domain (Song, Hu et al. 2001). PLCε shows further variation in its expression of two C-terminal Ras-associating (RA) domains and a Ras-GEF domain. PLCε can therefore bind, activate, and be activated by, Ras-like GTPases (Kelley, Reks et al. 2001, Song, Hu et al. 2001). The RA2 domain of PLCε specifically binds the GTP-bound forms of both Ha-Ras and Rap but not the GDP-bound forms of these proteins, or R-Ras, RalA, RhoA, Rac1 or Cdc42 (Kelley, Reks et al. 2001, Song, Hu et al. 2001). Despite lacking the EF-hand domains present in all other PLC isoforms, PLCε activity is calcium-dependent, with maximal activity at 10 μM calcium (Song, Hu et al. 2001). The activation of PLC ε by Rap2b has been implicated in the regulation of autophagy (Williams, Sarkar et al. 2008, Ravikumar, Sarkar et al. 2010, Harris and Rubinsztein 2012). Willaims *et al.* (2008) identified that forskolin application activated the Rap2b/PLCε pathway, increasing intracellular calcium and activating Ca^{2+} cysteine proteases (calpains), a necessary step in the inhibition of autophagy. This pathway, which was also induced by the

Epac-selective agonist 8-pCPT, was successfully blocked by dominant-negative Rap2b, supporting the hypothesis of direct Rap2b/ PLC interaction (Williams, Sarkar et al. 2008). Furthermore, the nature of the intracellular calcium release was elucidated through the over-expression of cytosolic IP_3 kinase A, which blocked the IP_3-mediated release of calcium from the ER, again implicating PLC in this pathway (Williams, Sarkar et al. 2008). The role of Epac in this pathway is supported by work published by Schmidt *et al.* (2001) which shows that application of an adenylate cyclase inhibitor resulted in a reduction in forskolin-induced PLC activity by 50-70%, whilst the PKA inhibitor H89 had no effect (Schmidt, Evellin et al. 2001). In addition, this group also found that over-expression of Epac1 resulted in an increase in forskolin-induced PLC activation by 40-50%, and that inactivation of Rap, via application of the *clostridium difficile* toxin B-1470, decreased forskolin-induced PLC activation by approximately 70% (Schmidt, Evellin et al. 2001). In addition to Rap2b, PLCε has also been shown to interact with Rap1A via its RA2 domain (Jin, Satoh et al. 2001, Kelley, Reks et al. 2001, Song, Hu et al. 2001, Song, Satoh et al. 2002, Edamatsu, Takenaka et al. 2011). Furthermore, as previously mentioned, PLCε also has GEF activity for Rap1 (Jin, Satoh et al. 2001), thereby acting as a positive-feedback loop. Activation of PLCε results in its translocation to specific subcellular locations (Song, Hu et al. 2001). This group identified that application of epidermal growth factor (EGF) to COS-7 cells resulted in an increase in the association of PLCε with the plasma membrane within 5 minutes, a re-distribution that was blocked by addition of the dominant-negative form of Ha-Ras (Song, Hu et al. 2001). Interestingly, an enrichment of green fluorescent protein-tagged PLCε was also identified at the perinuclear region on EGF application, and this PLCε was found to co-localise with constitutively active Rap1A ($Rap1A^{G12V}$) (Song, Hu et al. 2001). Song *et al.* hypothesised that this Rap1A-mediated perinuclear re-distribution of PLCε may play a role in the regulation of the Golgi complex. Indeed, both Rap1A and PKC (a downstream PLC effector, detailed later) have both been found at the Golgi complex (Beranger, Goud et al. 1991, De Matteis, Santini et al. 1993). PLCε has been found to be widely distributed, with particularly high expression in brain, lung, heart and skeletal muscle tissues (Kelley, Reks et al. 2001, Lopez, Mak et al. 2001, Sorli, Bunney et al. 2005). Although Lo Vasco *et al.* (2011) failed to identify PLCε expression in HUVECs (Lo Vasco, Pacini et al. 2011), this PLC isoform has been detected in endothelial cells of other vascular beds (Schmidt, Evellin et al. 2001, Ruisanchez, Dancs et al. 2014).

5.1.11 – The role of Protein Kinase C in the Epac pathway

Protein Kinase C (PKC) is part of the serine-threonine family of kinases and is subdivided into classical PKCs (cPKCs), novel PKCs (nPKCs) and atypical PKCs (aPKCs) (Newton and Messing 2010). cPKCs are activated by calcium and DAG, nPKCs are activated by DAG but not calcium, and aPKCs are activated by lipids and by phosphorylation (Newton and Messing 2010). PKCε is classified as an nPKC due to its direct activation by DAG, and this PKC isoform has been shown to play a role in the downstream signalling of PLCε (Schmidt, Evellin et al. 2001, Bos 2003, Oestreich, Malik et al. 2009). Indeed, Oestreich *et al.* (2009) identified PKCε as the major isoform involved in Epac/ PLCε responses. Immature, un-phosphorylated PKCε is associated with the anchoring protein CG-NAP (centrosome and Golgi localized PKN-associated protein), and is identified at the Golgi apparatus (Takahashi, Mukai et al. 2000). Following phosphorylation and activation, PKCε translocates to specific subcellular locations through its interaction with additional anchoring proteins. In human glioma cells, for example, active PKCε has been shown to interact with the receptor for activated C-kinase (RACK1) which results in the regulation of integrin-mediated cell adhesions (Besson, Wilson et al. 2002). PKCε has been identified in the endothelium of bovine aorta (Rask-Madsen and King 2008) and coronary veins (Monti, Donnini et al. 2010, Monti, Donnini et al. 2013).

5.2 - Methods

5.2.1 – Direct blocking of cadherin-cadherin interactions

Pre-incubation of confluent HCAECs with 10 µg/ml of the anti-VE-cadherin primary antibody (BD Biosciences, USA) in fully-supplemented HCAEC media acted as a block to the formation of VE-cadherin-mediated adherens junctions (AJs). Immunocytochemistry experiments were performed as previously detailed under "2.2.3.1.2 - fixation, quenching and permeabilisation of cultured cells". The fixed HCAECs were examined for VE-cadherin distribution (antibody dilutions; x200 primary antibodies, x500 secondary antibodies). The protocol used was adapted from ones used by Abraham *et al.* and Corada *et al. (*Corada, Liao *et al.* 2001, Abraham, Yeo *et al.* 2009*)*. To ensure that other components added in combination with the commercial antibody, such as sodium azide, were not influencing the distribution of VE-cadherin, the anti-VE-cadherin primary antibody was heat-inactivated by boiling for 1 hour prior to incubation. HCAECs pre-incubated with both the intact anti-VE-

cadherin antibody and the heat-inactivated anti-VE-cadherin antibody were examined for VE-cadherin distribution. The distribution of Cx37, Cx40 and Cx43 was also identified in HCAECs pre-treated with the intact anti-VE-cadherin antibody.

5.2.2 – Cadherin disruption through removal of extracellular calcium

The calcium-dependent nature of cadherin interaction and AJ formation has been detailed previously (Section 1.7 – Adherens junctions). The effect of disruption of both homotypic (VE-cadherin-VE-cadherin) and the less frequent heterotypic (VE-cadherin-N-cadherin) AJs was examined through treatment of HCAECs with EGTA. Confluent HCAECs were switched to media containing 5 mM EGTA for 30 minutes at 37°C/ 5% CO_2. Following this treatment, the cells were either washed twice with fully-supplemented media and re-incubated for 1-4 hours and fixed, or fixed immediately without calcium restoration. The fixed cells were stained for VE-cadherin, N-cadherin and connexins 37, 40 and 43, using an AF488-conjugated secondary antibody (Antibody dilutions; x200 primary antibodies, x500 secondary antibodies).

5.2.3 – Examination of Epac distribution in HCAECs

Two types of commercially available anti-Epac1 antibodies were used. The Cell Signalling anti-Epac1 monoclonal mouse primary antibody (Cat no. 4155S) was used in Western blot (Price, Hajdo-Milasinovic et al. 2004, Yan, Mei et al. 2013) while the Santa Cruz anti-Epac1 monoclonal mouse primary antibody (Cat no. Sc-28366) was used for both immunocytochemistry and Western blot (Banales, Masyuk et al. 2009, Purves, Kamishima et al. 2009).

5.2.4 – Activation of Epac in HCAECs

The Epac-specific agonist 8-(4-Chlorophenylthio)-2'-O-methyladenosine-3', 5'-cyclic monophosphate, acetoxymethyl ester (8-pCPT, 5 µM) was used to selectively activate Epac, and not PKA, in HCAECs. 8-pCPT was identified as a novel Epac-selective agonist by Enserink *et al.* in 2002 (Enserink, Christensen et al. 2002). Through amino acid sequence analysis, this group identified that the highly-conserved glutamate residue that forms hydrogen bonds with the 2'-hydroxyl of the cAMP ribose group, necessary for cAMP – PKA interaction, is absent from the cAMP-binding domains of both Epac1 and Epac2 (high-affinity site B). Introduction of a 2'-methoxyl group in place of this 2'-hydroxyl group in

cAMP was found to specifically activate Epac and not PKA (Enserink, Christensen et al. 2002). Indeed, this compound was found to be more efficient in its Epac activation than cAMP, with half-maximal Epac1 activation detected on application of 2.2 µM 8-pCPT, compared to 30 µM cAMP (Enserink, Christensen et al. 2002). The Epac-specific nature of 8-pCPT was demonstrated by its inability to activate type-I and type-II holoenzymes of PKA, as detected by a lack of increased cAMP response element-binding (CREB) protein phosphorylation on 8-pCPT application, even at 100 µM (Enserink, Christensen et al. 2002). In addition, olfactory and pacemaker cyclic nucleotide-gated ion channels contain the conserved glutamate in their cAMP-binding domain and therefore, like PKA, require the 2'-hydroxyl of the cAMP ribose group for activation (Enserink, Christensen et al. 2002). Furthermore, the presence of a hydrophobic pCPT substitution on 2'-O-Me-cAMP also provides increased membrane permeability, further enhancing the activity of this compound (Enserink, Christensen et al. 2002, Holz, Chepurny et al. 2008). Since its identification as a suitable Epac-specific agonist, 8-pCPT has been used in a variety of cell-signalling experiments (Christensen, Selheim et al. 2003, Kang, Joseph et al. 2003, Rehmann, Schwede et al. 2003, Gloerich and Bos 2010).

5.3 - Results

5.3.1 – Disruption of HCAEC cadherin interactions

5.3.1.1 – Incubation with the anti-VE-cadherin primary antibody

To determine whether disruption of VE-cadherin interactions resulted in a re-distribution of cadherins and connexins, HCAECs were pre-incubated with the anti- VE-cadherin primary antibody (10 µg/ml) for 5 hours at 37°C/ 5% CO_2.

5.3.1.1.1 - VE-cadherin immunocytochemistry

Figure 5.2 shows preliminary staining of VE-cadherin in control (Figure 5.2A), VE-cadherin antibody-treated (Figure 5.2B), and heat-inactivated antibody-treated HCAECs (Figure 5.2C). Under control conditions, VE-cadherin distribution (green) in HCAECs was identified as diffuse staining throughout the cell, supplemented by discontinuous segments of membrane staining (Figure 5.2A). The morphology of the HCAECs was typical of that

observed in cultures at 90-100% confluence, with a single layer of cells in an almost-continuous sheet (see Figure 3.14 in Chapter 3).

On incubation with the anti-VE-cadherin primary antibody, the HCAECs formed small dispersed colonies (Figure 5.2B). The morphology changed to small rounded cells in closely-packed clumps, and the DAPI staining showed the distance between nuclei of adjacent cells was reduced. The increase in VE-cadherin signal may be a result of the additional primary antibody introduced to the experiment as a blocker of VE-cadherin interactions (Figure 5.2B). Following the disruption of VE-cadherin interactions, VE-cadherin was found to localise to parts of the membrane, as highlighted by the white arrows in Figure 5.2B.

When the HCAECs were incubated with the heat-inactivated anti-VE-cadherin primary antibody, the cell morphology was similar to that of control experiments (Figure 5.2C). Cells maintained a flattened appearance without isolated colonies, in contrast to those pre-incubated with the intact primary antibody. Furthermore, the distance between the nuclei of adjacent cells appeared unaffected by incubation with the heat-inactivated antibody (Figure 5.2C). In addition, VE-cadherin was found to be distributed as discontinuous sections across the membrane (Figure 5.2C). As in the antibody-blocked cells, the increase in fluorescence may be a result of the pre-incubation with the anti-VE-cadherin primary antibody (Figure 5.2C).

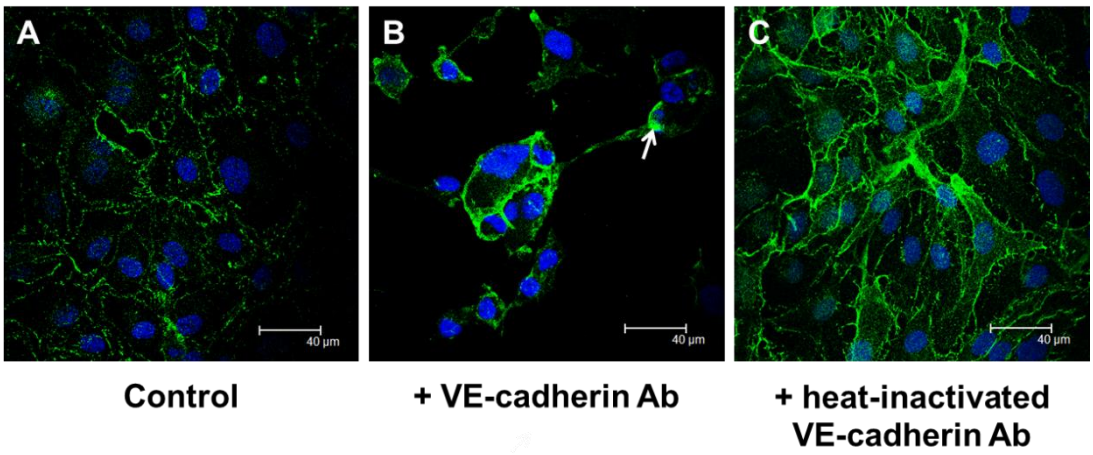

Figure 5.2: Immunocytochemistry of control and intact and heat-inactivated anti-VE-cadherin primary antibody treated HCAECs

Under control conditions, VE-cadherin (green) distribution in HCAECs was observed as discontinuous staining across the cell membrane (A). Low-level staining was also observed diffusely throughout the cell. The morphology of the HCAECs showed a continuous flattened sheet. Following 5 hours incubation at 37˚C/ 5% CO_2 with 10 µg/ml of the mouse anti- VE-cadherin primary antibody, the morphology of the HCAECs changes to clumps of cells forming isolated colonies (B). VE-cadherin distribution was altered in a number of cells to that of one restricted to specific membrane sections, as indicated by the white arrows (B). Incubation with the heat-inactivated anti- VE-cadherin primary antibody resulted in little change in HCAEC morphology (C). DAPI nuclear staining is represented in blue. Antibody dilutions as previously stated. N=1.

5.3.1.1.2 - Connexin immunocytochemistry

To determine whether VE-cadherin disruption had an effect on connexin distribution, HCAECs pre-incubated with the anti-VE-cadherin antibody were labelled for connexin 37, 40 and 43 distribution in a series of preliminary experiments (Figure 5.3). Under control conditions, HCAECs were found to be distributed in a continuous sheet typical of HCAECs in culture (Figures 5.3A, 5.3B & 5.3C). Following incubation with the anti-VE-cadherin primary antibody, cells appeared as isolated colonies of rounded cells, as previously shown (Figures 5.3D, 5.3E & 5.3F).

Following pre-incubation with the anti-VE-cadherin primary antibody, Cx37 was found to accumulate at restricted sites of the membrane, as shown by the white arrows in Figure 5.3D. This Cx37 distribution was reminiscent of the re-localisation of VE-cadherin observed following treatment with the same blocking antibody. Similarly, Cx40 also appeared to re-distribute to restricted regions of the membrane (white arrow, Figure 5.3E). Cx43 distribution appeared largely unchanged following the disruption of VE-cadherin interactions (Figure 5.3F), with a patchy membranous localisation, with little restriction to specific regions of the HCAEC membrane.

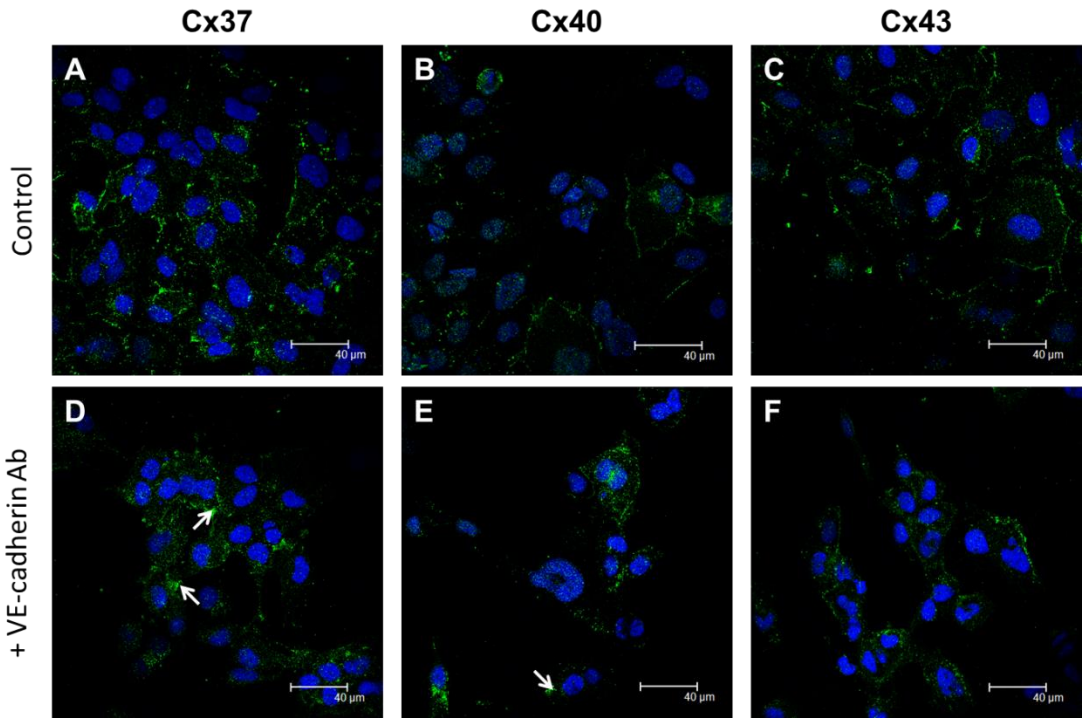

Figure 5.3: Immunocytochemistry of connexins in HCAECs under control conditions and following pre-incubation with anti-VE-cadherin primary antibody

Cx37, Cx40 and Cx43 distribution in HCAECs under control conditions (A-C). Following 5 hours incubation at 37˚C/ 5% CO_2 with 10 µg/ml of the mouse anti- VE-cadherin primary antibody, Cx37 distribution was identified as aggregations at restricted segments of the membrane, as highlighted by the white arrows (D). Cx40 distribution was also found to re-locate to specific regions of the membrane (white arrow, E). Conversely, Cx43 distribution appeared largely unaltered (F). DAPI nuclear staining is represented in blue. Antibody dilutions as previously stated. N=1.

5.3.1.1.3 - Incubation with the anti-VE-cadherin primary antibody - Summary

Blocking of VE-cadherin interactions changed HCAEC morphology from sheets to isolated colonies of cells during preliminary experiments. Heat-inactivated anti-VE-cadherin antibody was ineffective during these experiments. Following incubation with the anti-VE-cadherin antibody, VE-cadherin relocated to restricted sites of the membrane. Staining of Cx37 and Cx40 appeared to follow the re-location of VE-cadherin.

5.3.1.2 - EGTA treatment of HCAECs

5.3.1.2.1 - EGTA treatment, no calcium restoration

Adherens junctions are calcium-dependent and break apart in the absence of extracellular calcium. As such, the effect of EGTA treatment (5 mM for 30 minutes at 37°C/ 5% CO_2) was examined on cadherin and connexin distribution in HCAECs.

During preliminary experiments, cadherin distribution was identified in HCAECs under control conditions and following EGTA treatment (Figure 5.4). Under control conditions, HCAEC morphology was identified as a continuous flattened sheet of cells. Following 30 minutes incubation with 5 mM EGTA, the appearance of HCAECs became segregated rounded cells (Figures 5.4B & 5.4D), a morphology similar to that observed following pre-incubation with the anti-VE-cadherin primary antibody (Figure 5.2B, above). This change in HCAEC morphology appeared more extensive than that recorded under incubation with the cadherin-blocking primary antibody, as cells were almost entirely isolated from each other, instead of forming colonies.

In untreated HCAECs, VE-cadherin was identified as discontinuous patches of membrane staining with low-level staining throughout the cell (Figure 5.4A). Following EGTA treatment, VE-cadherin appeared to re-distribute to restricted points of the cell membrane, as highlighted by the white arrows in Figure 5.4B. This re-localisation of VE-cadherin was similar to that observed following incubation with the anti-VE-cadherin primary antibody.

Under control conditions, N-cadherin was distributed both throughout the cell and at the HCAEC membrane, displaying increased expression at restricted sections of the cell border (Figure 5.4C). Following EGTA treatment, N-cadherin appeared to remain consistently expressed across the HCAEC membrane, with only minimal association with restricted sites

of the membrane (Figure 5.4D). The increased maximum AF488 signal intensity recording for both VE-cadherin (Figure 5.4B) and N-cadherin following EGTA treatment (Figure 5.4D), may reflect the change in HCAEC morphology.

5.3.1.2.2 - EGTA treatment and 1 hour calcium restoration in the presence of the anti-VE-cadherin primary antibody

To determine whether the adherens junctions are able to re-form following calcium restoration, HCAECs were subjected to EGTA treatment followed by a 1 hour calcium restoration phase (fully-supplemented HCAEC media). To determine whether the anti-VE-cadherin antibody was able to block the re-formation of these adherens junctions, the calcium restoration phase was also performed in the presence of the anti-VE-cadherin primary antibody.

5.3.1.2.2.1 - VE-cadherin immunocytochemistry

Preliminary experiments identified VE-cadherin distribution in HCAECs following EGTA treatment, 1 hour calcium restoration and 1 hour calcium restoration in the presence of the anti-VE-cadherin primary antibody (Figure 5.5). Following incubation with EGTA, VE-cadherin (green) re-located to restricted points of the membrane and HCAECs formed isolated rounded cells (Figure 5.5A). The short distance between membrane VE-cadherin and DAPI nuclear staining (blue) highlights the rounded morphology adopted by the HCAECs following EGTA treatment. The confocal image (Figure 5.5A) further highlights the preference of the re-distributed VE-cadherin for restricted sections of the cell membrane. Following removal of the calcium-chelating agent and 1 hour's calcium restoration in fully-supplemented media, HCAEC morphology started to return to control conditions (Figure 5.5B) with VE-cadherin located at sites of cell-cell contact (white arrow) and cells forming a more continuous sheet, indicating that the EGTA-induced re-distribution of VE-cadherin is reversible. When the calcium restoration was performed in the presence of the anti-VE-cadherin primary antibody (Figure 5.5C), the HCAECs displayed a rounded morphology more similar to that observed immediately after EGTA treatment. Furthermore, VE-cadherin appeared to remain localised to restricted segments of the HCAEC membrane (Figures 5.5C).

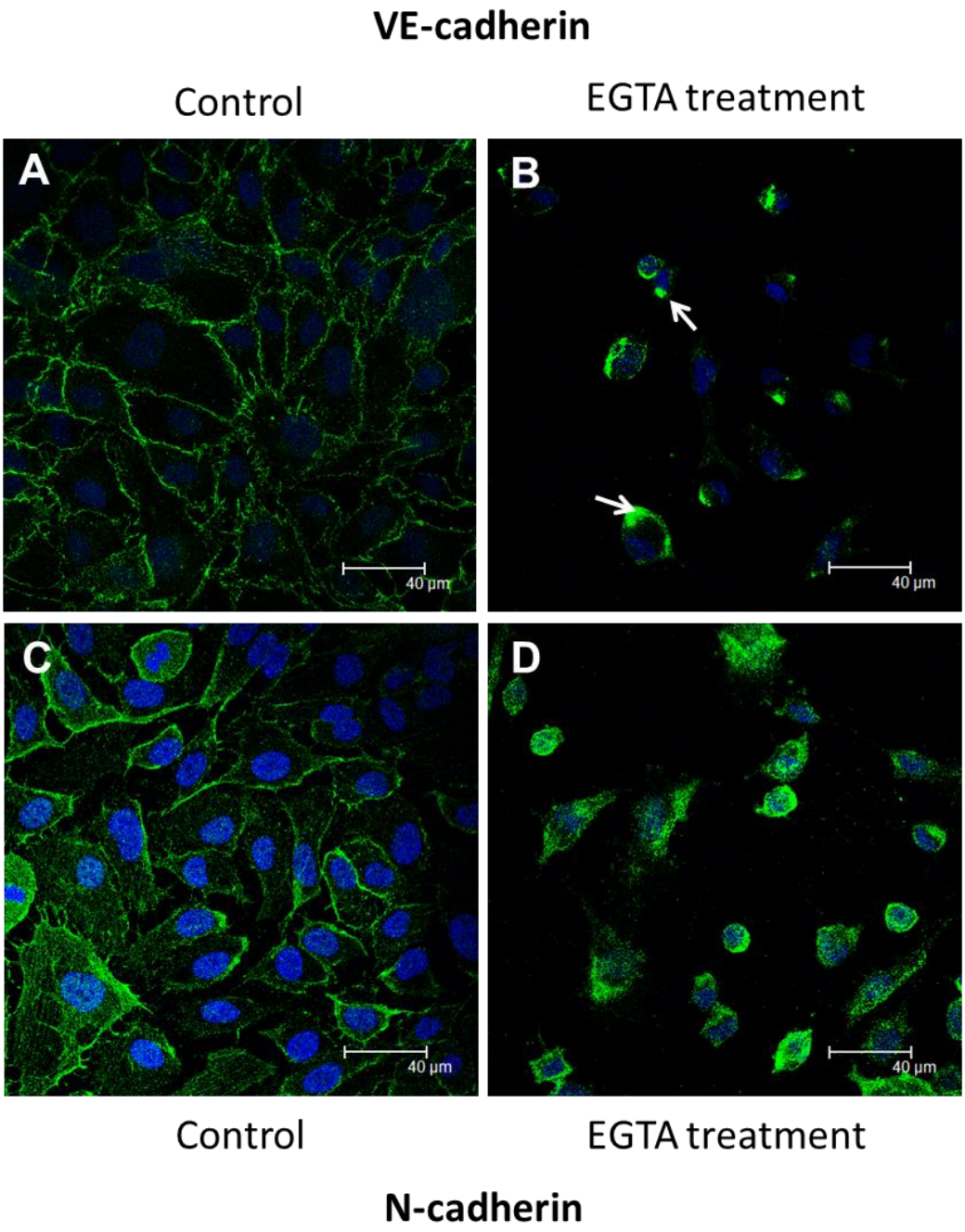

Figure 5.4: Immunocytochemistry of cadherin expression in HCAECs under control conditions and following EGTA treatment

Under control conditions, HCAEC morphology appeared as a flattened and continuous sheet (A & C), VE-cadherin was identified as discontinuous staining across the cell (A), and N- cadherin was distributed both at the cell membrane and diffusely across the cell (C). HCAECs formed isolated rounded cells after treatment with 5 mM EGTA for 30 minutes at 37°C/ 5% CO_2 (B & D). VE-cadherin re-located to restricted points of the membrane (B, white arrows). N-cadherin distribution after EGTA treatment (D) did not mirror the un-even appearance seen with VE-cadherin staining (B). DAPI nuclear staining is shown in blue. Antibodies diluted as previously detailed. N=1.

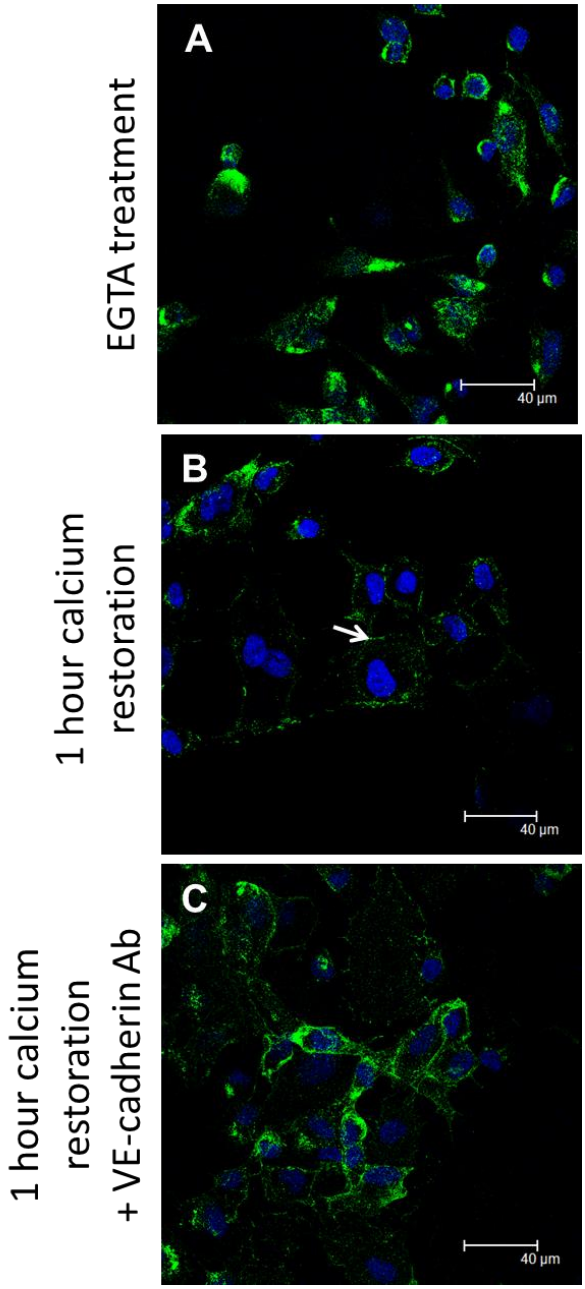

Figure 5.5: Immunocytochemistry of VE-cadherin expression in HCAECs following EGTA treatment, 1 hour calcium restoration and 1 hour calcium restoration in the presence of anti-VE-cadherin primary antibody.

Following 30 minutes 5 mM EGTA treatment at 37°C/ 5% CO_2, VE-cadherin re-located to restricted points of the membrane and HCAECs appeared rounded (A). Following removal of EGTA and 1 hour's calcium restoration (fully-supplemented media, 37°C/ 5% CO_2), HCAEC morphology started to return to control conditions (B). Increased VE-cadherin cell-cell contacts were observed after 1 hour's calcium restoration (B, white arrow). C represents VE-cadherin distribution in HCAECs following calcium restoration (1 hour) in the presence of the anti-VE-cadherin primary antibody. These HCAECs displayed a morphology similar to that observed immediately after EGTA treatment, with rounded cells and a restricted VE-cadherin distribution. DAPI nuclear staining is shown in blue. Antibody dilutions as previously detailed. N=1.

5.3.1.2.2.2 - Cx37 immunocytochemistry

Preliminary experiments identified Cx37 distribution in HCAECs following EGTA treatment, 1 hour calcium restoration and 1 hour calcium restoration in the presence of the anti-VE-cadherin primary antibody (Figure 5.6). EGTA treatment triggered a re-distribution of Cx37 to restricted sites of the membrane (Figure 5.6A). Calcium restoration for 1 hour (Figure 5.6B), appeared to result in a partial return of Cx37 distribution to that of control conditions, with Cx37 localising to areas of cell-cell contact (white arrows). When the 1 hour calcium restoration period was carried out in the presence of 10 µg/ml of the anti-VE-cadherin primary antibody (Figure 5.6C), Cx37 appeared to partially re-locate to the membrane but not at sites of cell-cell contact. Under these conditions, Cx37 appeared to continue to show a restricted membranous distribution (Figures 5.6C).

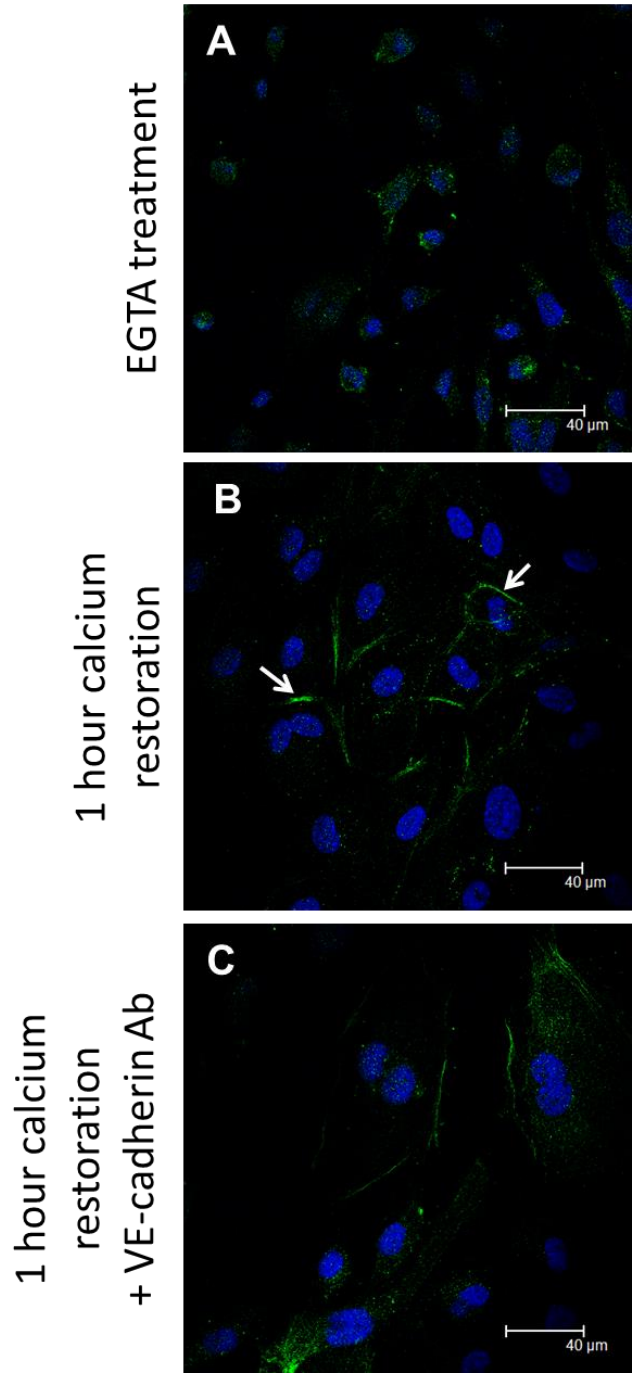

Figure 5.6: Immunocytochemistry of Cx37 expression in HCAECs following EGTA treatment, 1 hour calcium restoration and 1 hour calcium restoration in the presence of anti-VE-cadherin primary antibody.

Following 30 minutes 5 mM EGTA treatment at 37°C/ 5% CO_2, Cx37 re-located to restricted points of the membrane and HCAECs appeared rounded (A). Calcium restoration (fully-supplemented media, 37°C/ 5% CO_2) caused a restoration of CX37 cell-cell interactions (white arrows, B). C represents Cx37 distribution in HCAECs following calcium restoration in the presence of the anti-VE-cadherin primary antibody. Under these conditions, Cx37 was identified at the membrane but not at sites of cell-cell contact. DAPI nuclear staining is shown in blue. Antibody dilutions as previously detailed. N=1.

5.3.1.2.2.3 - Cx40 immunocytochemistry

Cx40 distribution was identified during preliminary experiments in HCAECs following EGTA treatment, 1 hour calcium restoration and 1 hour calcium restoration in the presence of the anti-VE-cadherin primary antibody (Figure 5.7). Treatment with EGTA resulted in a diffuse distribution of Cx40 throughout the cell, with only marginal association with the cell border (Figure 5.7A). Following calcium restoration in fully-supplemented media, Cx40 appeared to partially return towards the membrane (Figure 5.7B). The addition of 10 µg/ml of the anti-VE-cadherin primary antibody during the calcium restoration phase appeared to have little effect on the return of Cx40 to the membrane (Figure 5.7C) and staining appeared similar to that observed in Figure 5.7B. Membranous Cx40 did, however, appear to display a restricted membranous distribution under these conditions (Figure 5.7C).

5.3.1.2.2.4 - Cx43 immunocytochemistry

Cx43 distribution was identified in HCAECs following EGTA treatment, 1 hour calcium restoration and 1 hour calcium restoration in the presence of the anti-VE-cadherin primary antibody during preliminary investigations (Figure 5.8). EGTA treatment triggered a re-distribution of Cx43 to restricted sites of the membrane (Figures 5.8A). Calcium restoration for 1 hour resulted in a re-distribution of Cx43 back towards control conditions with the re-appearance of Cx43 at sites of cell-cell contact (Figure 5.8B). When the 1 hour calcium restoration period was performed in the presence of the anti-VE-cadherin primary antibody, Cx43 distribution appeared to still return towards control conditions, despite the HCAECs remaining isolated from each other (Figure 5.8C). Some cells did display a restricted membranous Cx43 distribution (white arrow, Figure 5.8C).

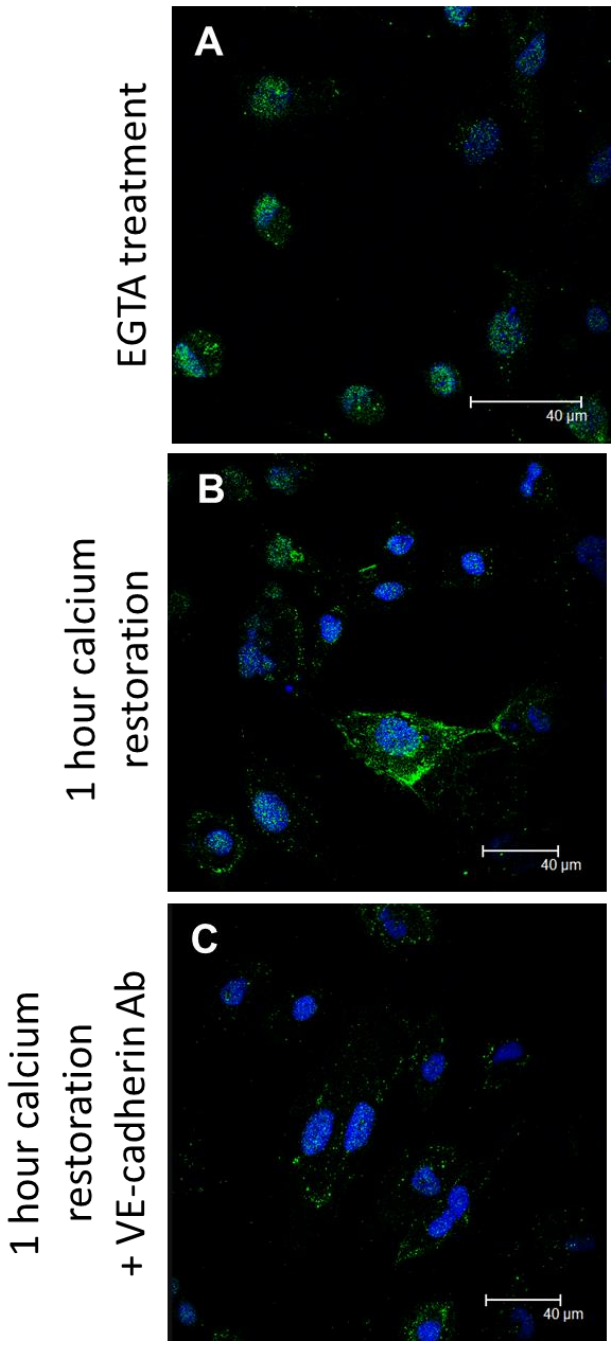

Figure 5.7: Immunocytochemistry of Cx40 expression in HCAECs following EGTA treatment, 1 hour calcium restoration and 1 hour calcium restoration in the presence of anti-VE-cadherin primary antibody.

30 minutes 5 mM EGTA treatment at 37°C/ 5% CO_2 did not cause localised aggregations of Cx40, unlike that seen in Cx37 (A). B shows Cx40 distribution following removal of EGTA and 1 hour's calcium restoration (fully-supplemented media, 37°C/ 5% CO_2). Cx40 distribution appeared to partially return to that observed under control conditions, with patches of membrane distribution (B). Following calcium restoration (1 hour) in the presence of the anti-VE-cadherin primary antibody (C), Cx40 appeared to again partially return towards control conditions, although membranous Cx40 distribution appeared restricted. DAPI nuclear staining is shown in blue. Antibody dilutions as previously detailed. N=1.

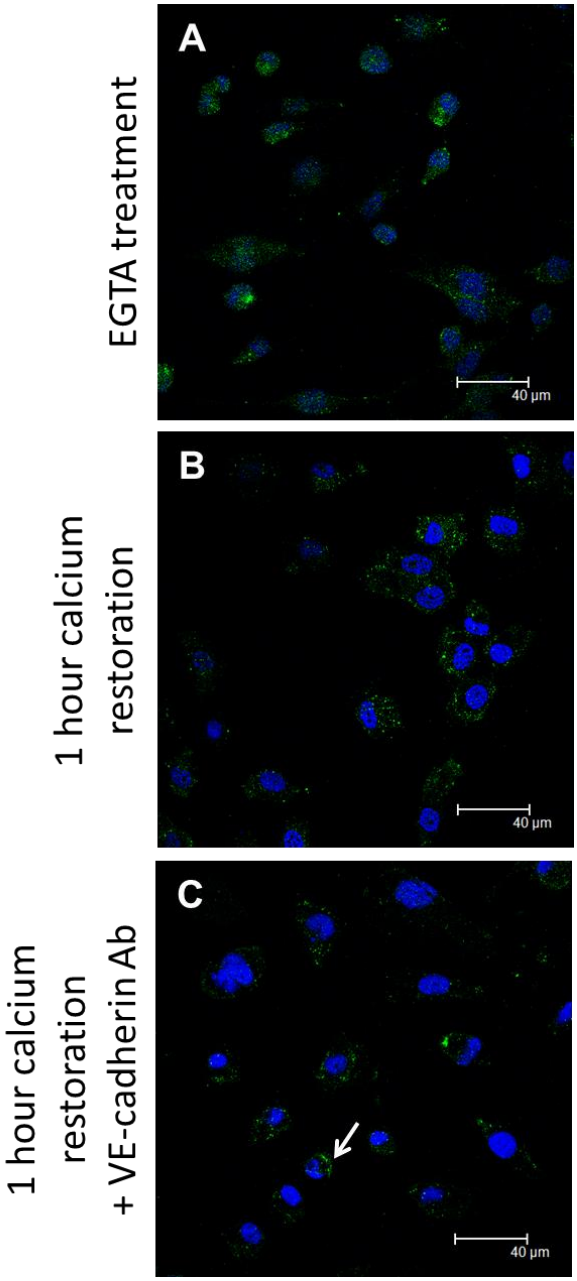

Figure 5.8: Immunocytochemistry of Cx43 expression in HCAECs following EGTA treatment, 1 hour calcium restoration and 1 hour calcium restoration in the presence of anti-VE-cadherin primary antibody.

Following 30 minutes 5 mM EGTA treatment at 37°C/ 5% CO_2, Cx43 partially re-located to restricted points of the membrane and HCAECs became rounded (A). Removal of EGTA and 1 hour's calcium restoration (fully-supplemented media, 37°C/ 5% CO_2) triggered a partial restoration of CX43 distribution at the membrane (B). C represents Cx43 distribution in HCAECs following calcium restoration (1 hour) in the presence of the anti-VE-cadherin primary antibody. Distribution of Cx43 in the presence of the anti-VE-cadherin blocking antibody appears similar to the distribution observed in B, with only slight membranous restriction (C, white arrow). The HCAECs appear largely isolated from one another. DAPI nuclear staining is shown in blue. Antibody dilutions as previously detailed. N=1.

5.3.1.2.3 - EGTA treatment and 4 hours calcium restoration

Following EGTA treatment, incubation of HCAECs with calcium-containing media for 1 hour seemed to partially reverse the effect of EGTA. Thus, the effect of 4 hours calcium restoration was examined in a series of preliminary experiments.

5.3.1.2.3.1 - VE-cadherin immunocytochemistry

VE-cadherin distribution was identified in HCAECs under control conditions and after 4 hours calcium restoration following EGTA treatment (Figure 5.9). Under control conditions (Figure 5.9A), VE-cadherin distribution appeared primarily at the membrane, supplemented by low-level staining throughout the cell. Following 30 minutes EGTA treatment, the cells were incubated in fully-supplemented media for 4 hours at 37°C/ 5% CO_2 (Figure 5.9B). VE-cadherin distribution at the membrane returned to that of control conditions, with expression at sites of cell-cell contact, as indicated by the white arrows (Figure 5.9B). These cells appeared to show a reduced proportion of nuclear-associated VE-cadherin, as highlighted by the DAPI staining (Figure 5.9B).

5.3.1.2.3.2 - Cx37 immunocytochemistry

Cx37 distribution was identified in HCAECs under control conditions and following 4 hours calcium restoration after EGTA treatment (Figure 5.10). Under control conditions, Cx37 appeared primarily at the membrane with areas of perinuclear distribution (Figure 5.10A). Following 4 hours calcium restoration after EGTA treatment (Figure 5.10B), Cx37 at least partially returned to the membrane and appeared at sites of cell-cell contact (white arrow). These cells appeared to display a reduced amount of perinuclear Cx37, as highlighted by overlay of the DAPI and AF488 signal (Figure 5.10B). This pattern was similar to the reduced perinuclear VE-cadherin observed in HCAECs under the same conditions (Figure 5.9B).

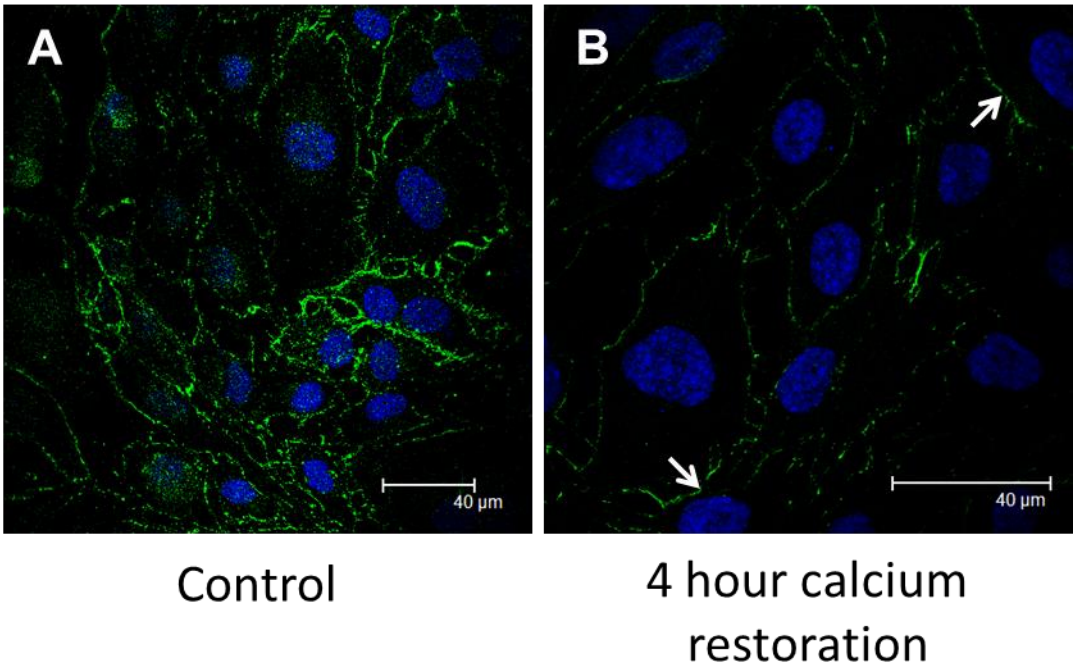

Figure 5.9: Immunocytochemistry of VE-cadherin expression in HCAECs under control conditions and following 4 hours calcium restoration after EGTA treatment

Under control conditions (A), VE-cadherin (green) was identified primarily at the membrane with low-level staining throughout the cell. HCAECs were treated with 5 mM EGTA for 30 minutes at 37°C/ 5% CO_2, and then washed twice with DPBS and the fully-supplemented media refreshed for 4 hours. Following calcium restoration, HCAEC morphology returned towards that of control conditions (B). Expression of VE-cadherin at sites of cell-cell contact was noted (B, white arrows). DAPI nuclear staining is shown in blue. Antibodies diluted as previously detailed. N=1.

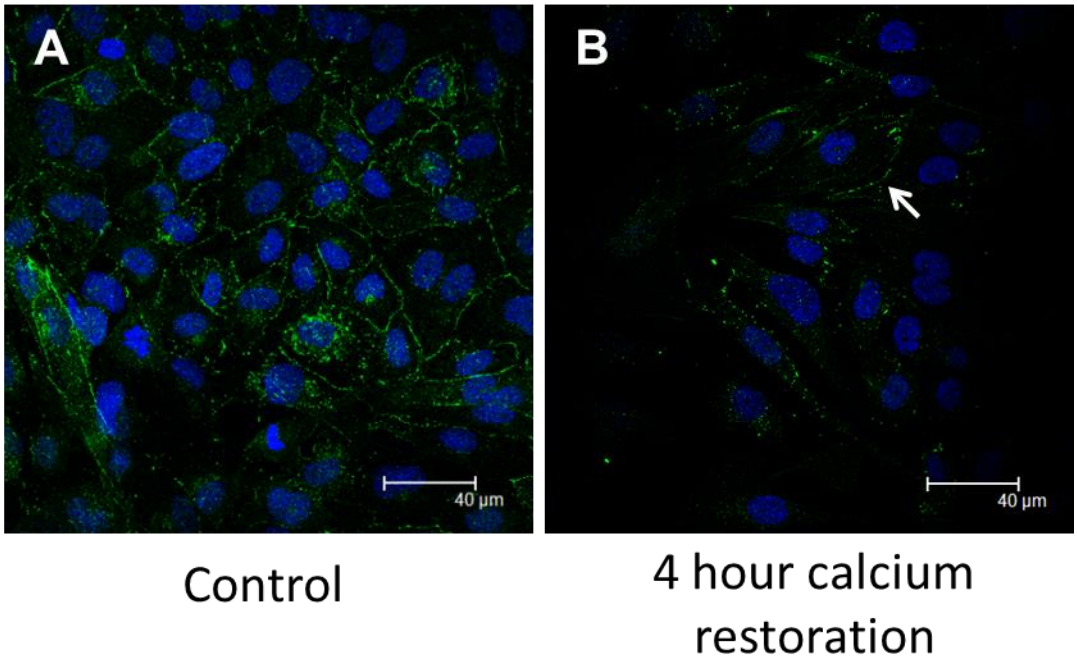

Figure 5.10: Immunocytochemistry of Cx37 expression in HCAECs under control conditions and following 4 hours calcium restoration after EGTA treatment

Under control conditions (A), Cx37 (green) was identified primarily at the membrane with areas of perinuclear distribution. HCAECs were treated with 5 mM EGTA for 30 minutes at 37°C/ 5% CO_2, and then washed twice with DPBS and the fully-supplemented media refreshed for 4 hours. Localisation of Cx37 to sites of cell-cell contact was observed following calcium restoration (B, white arrow). DAPI nuclear staining is shown in blue. Antibodies diluted as previously detailed. N=1.

5.3.1.2.3.3 - Cx40 immunocytochemistry

Cx40 distribution was identified in HCAECs under control conditions and following 4 hours calcium restoration after EGTA treatment (Figure 5.11). Under control conditions, Cx40 appeared distributed diffusely throughout the cell with patchy sections of membrane staining (Figure 5.11A). Following 4 hours calcium restoration after EGTA treatment, Cx40 appeared to return towards this control distribution (Figure 5.11B). Expression of Cx40 at sites of cell-cell contact is highlighted by the white arrow (Figure 5.11B). The cytoplasmic distribution of Cx40 appeared to be restricted to the perinuclear region under this condition, as highlighted by overlay of the DAPI and AF488 signal (Figure 5.11B).

5.3.1.2.3.4 - Cx43 immunocytochemistry

Cx43 distribution was identified in HCAECs under control conditions and following 4 hours calcium restoration after EGTA treatment (Figure 5.12). Under control conditions, Cx43 was identified diffusely throughout the cell and as discontinuous patches at the cell membrane (Figure 5.12A). Following 4 hours calcium restoration after EGTA treatment, Cx43 appeared to partially return towards this control distribution (Figure 5.12B). However, a decrease in the proportion of cytoplasmic Cx43 was evident in these preliminary experiments (Figure 5.12B). Expression of Cx43 at sites of cell-cell contact is highlighted by the white arrow (Figure 5.12B).

5.3.1.2.4 - EGTA treatment - Summary

Incubation of HCAECs with 5 mM EGTA for 30 minutes resulted in a change in morphology to isolated rounded cells. This morphology was similar to that observed following cadherin disruption using the anti-VE-cadherin primary antibody. Preliminary results indicated that EGTA treatment triggered a re-localisation of VE-cadherin to restricted areas of the membrane, but that EGTA had little effect on N-cadherin distribution. Cx37 appeared to undergo moderate redistribution, primarily to restricted areas of the membrane associated with adjacent cells. Little change in Cx40 or Cx43 distribution following EGTA treatment was observed. 1 hour calcium restoration triggered a return towards the control distribution of VE-cadherin and Cx37, but not Cx40 or Cx43, and was blocked by the addition of 10 µg/ml anti-VE-cadherin primary antibody. The effect of the EGTA treatment was reversible as after 4 hours calcium restoration the distribution of VE-cadherin, Cx37, Cx40 and Cx43 returned towards that observed under control conditions.

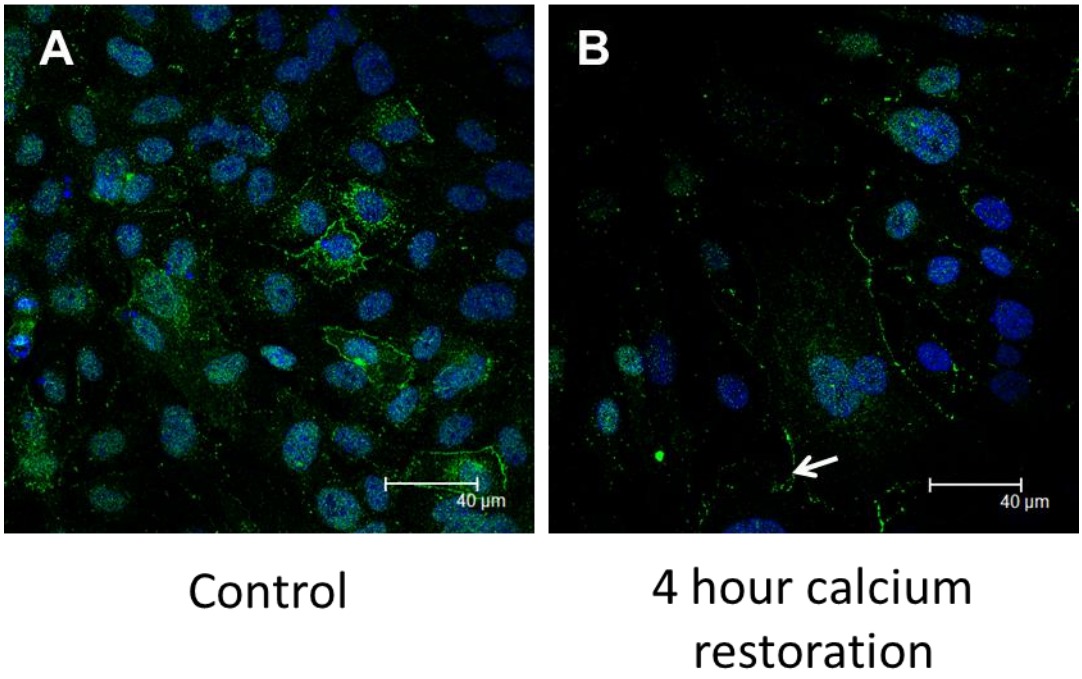

Figure 5.11: Immunocytochemistry of Cx40 expression in HCAECs under control conditions and following 4 hours calcium restoration after EGTA treatment

Under control conditions (A), Cx40 (green) was identified diffusely throughout the cell with patchy sections of membrane staining. HCAECs were treated with 5 mM EGTA for 30 minutes at 37°C/ 5% CO_2, and then washed twice with DPBS and the fully-supplemented media refreshed for 4 hours. After calcium restoration, Cx40 expression at sites of cell-cell contact can be observed (B, white arrow). DAPI nuclear staining is shown in blue. Antibodies diluted as previously detailed. N=1.

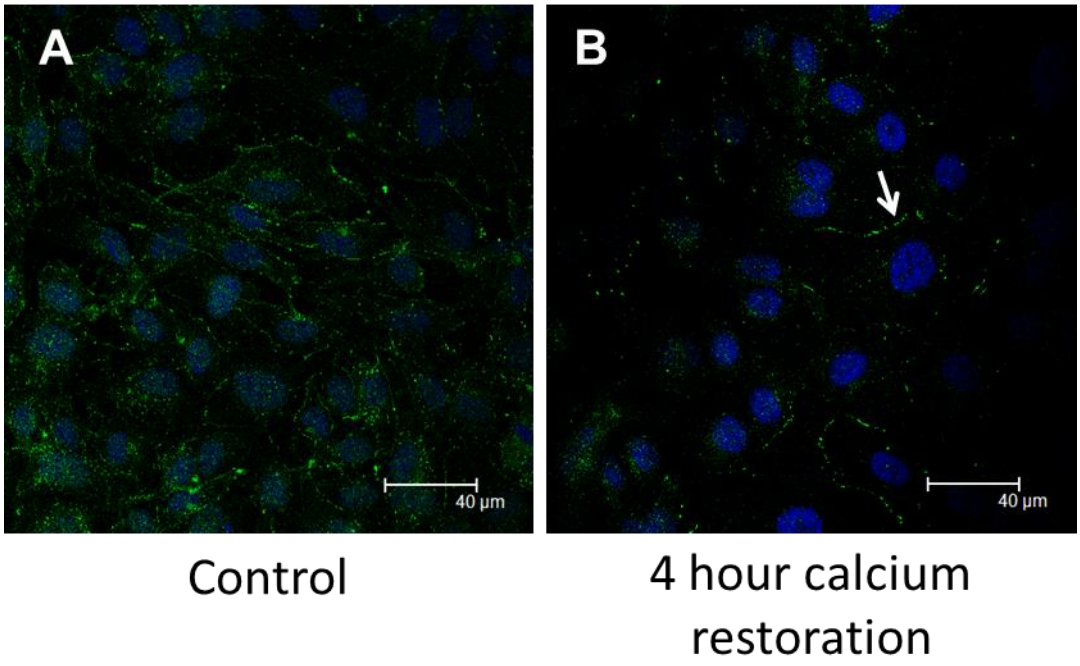

Figure 5.12: Immunocytochemistry of Cx43 expression in HCAECs under control conditions and following 4 hours calcium restoration after EGTA treatment

Under control conditions (A), Cx43 (green) was identified diffusely throughout the cell with patchy sections of membrane staining. HCAECs were treated with 5 mM EGTA for 30 minutes at 37°C/ 5% CO_2, and then washed twice with DPBS and the fully-supplemented media refreshed for 4 hours. After calcium restoration, Cx43 was identified at sites of cell-cell contact (white arrow, B). DAPI nuclear staining is shown in blue. Antibodies diluted as previously detailed. N=1.

5.3.2 – Enhancement of HCAEC cadherin interactions

5.3.2.1 - Epac1 expression in HCAECs

5.3.2 1.1 - Western blot

Epac1 was identified in HCAEC, HCASMC and rat mesenteric artery smooth muscle cell (RMASMC) lysates during a series of preliminary Western blot investigations (Figure 5.13). Epac1 expression in HCAECs was detected at 99 kDa by both the Santa Cruz and Cell Signalling anti-Epac1 primary antibodies (Figure 5.13A). The Santa Cruz antibody also detected proteins at 50 kDa, 43 kDa and 31 kDa (not shown). Epac1 was also identified in P6 HCASMC lysate and RMASMC P7 lysate at 99 kDa (Figure 5.13B).

5.3.2 1.2 - Immunocytochemistry

Epac1 distribution was examined in HCAECs under control conditions (Figure 5.14). The Santa Cruz primary antibody was labelled with a goat anti-mouse AF488-conjugated secondary antibody (green). During these preliminary experiments Epac1 was found to be distributed diffusely throughout the cell with small areas of membranous staining, as indicated by the white arrow in Figure 5.14A.

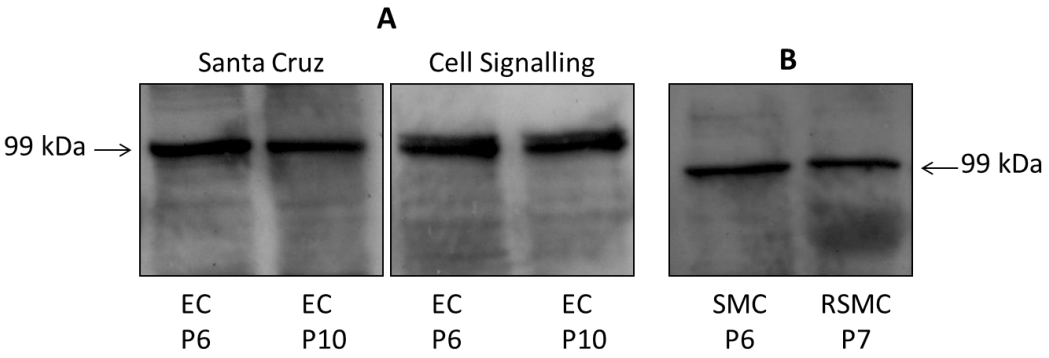

Figure 5.13: Western blot of Epac1 expression in HCAECs, HCASMCs and RMASMCs
HCAEC (P6 and P10) lysates were examined with mouse monoclonal anti-Epac1 primary antibodies from Santa Cruz Biotechnology and Cell Signalling (A). The primary antibodies were used at either x100 (Santa Cruz) or x200 (Cell Signalling) dilutions in 1% non-fat powdered milk. B shows HCASMCs (SMC, P6) and rat mesenteric artery smooth muscle cells (RSMC, P7) examined with Santa Cruz mouse monoclonal anti-Epac1 primary antibody (x100 dilution in 1% non-fat powdered milk). Primary antibodies were subsequently labelled with HRP-conjugated goat anti-mouse secondary antibody (x10,000 dilution, 1% non-fat powdered milk). 50 hours exposure. N=1.

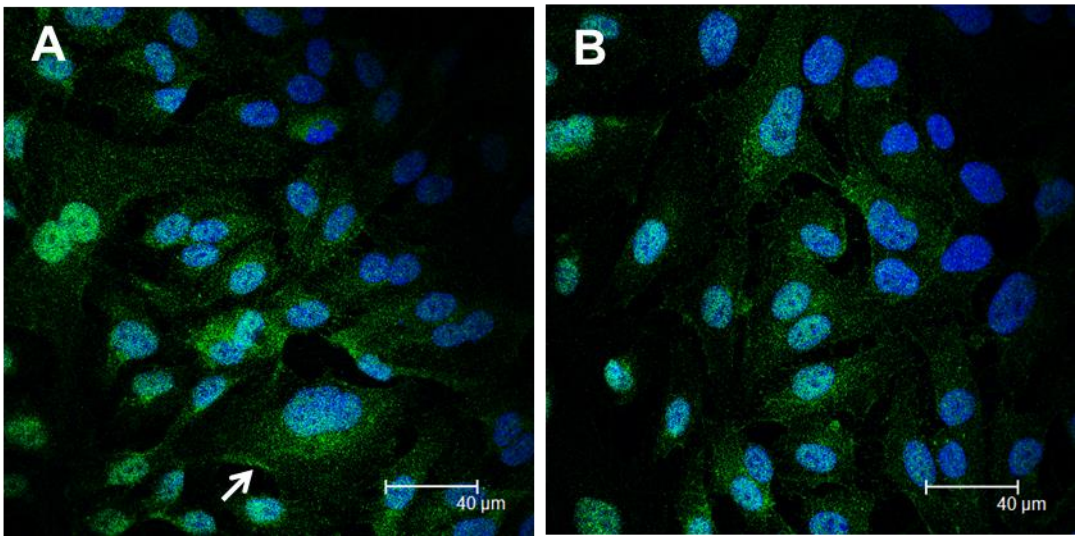

Figure 5.14: Immunocytochemistry of Epac1 expression in HCAECs

Epac1 (green) is diffusely distributed throughout the cell (A & B), with isolated areas of membranous staining, as highlighted by the white arrow in image A. DAPI nuclear staining is shown in blue. The Santa Cruz mouse monoclonal anti-Epac1 primary antibody was used at 100 fold dilution and the AF488-tagged goat anti-mouse secondary antibody used at x500 dilution. N=2.

5.3.2.2 - Epac2 expression in HCAECs

5.3.2.2.1 - Western blot

The presence of Epac2 was examined in rat heart, brain, mesenteric artery and HCAEC lysates (Figure 5.15A). Epac2 is believed to be highly expressed in brain (Kawasaki, Springett et al. 1998), and heart and mesenteric artery were chosen as representative cardiovascular tissues. No clear banding at 126 kDa was identified in any of the lysates during these preliminary experiments. Multiple bands at different MWs were identified in lysates labelled with the anti-Epac2 primary antibody.

5.3.2.2.2 - Immunocytochemistry

Epac2 (green) distribution was visualised in HCAECs under control conditions (Figure 5.15B). Preliminary data indicated low-level Epac2 staining diffusely throughout the cell with isolated areas of membranous staining (Figure 5.15B, white arrow). Punctate Epac2 staining was identified in the nucleus, as shown by the AF488 signal (Figure 5.15B). The distribution pattern of Epac2 in HCAECs appeared similar to that observed for Epac1 in HCAECs but at a lower level.

5.3.2.3 - Epac1 and Epac2 Summary

Epac1 was identified in HCAECs using two types of primary antibody. The lack of banding corresponding to Epac2 in rat heart, brain, mesenteric artery and HCAEC lysates could indicate that the anti-Epac2 primary antibody was not specific to the target protein. Epac1 was also identified in HCASMC and RMASMC lysates in preliminary investigations.

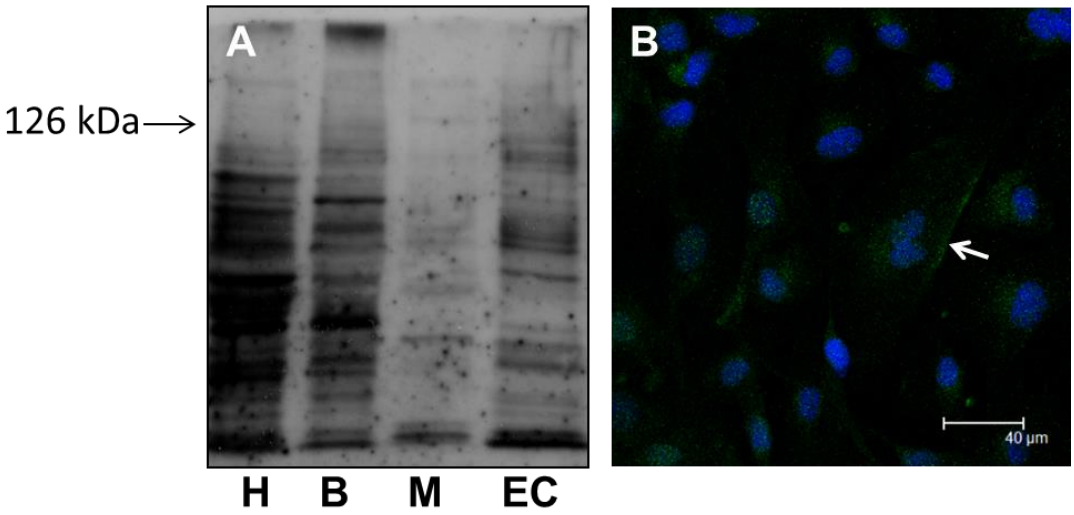

Figure 5.15: Epac2 expression in rat heart, brain, mesenteric artery and HCAECs
Epac2 expression was examined in rat heart (H), brain (B), mesenteric artery (M) and HCAEC (EC) lysates (A). No clear banding at 126 kDa could be identified in any of the lysates. The rabbit polyclonal anti-Epac2 primary antibody was used at x100 dilution in 1% non-fat powdered milk. The HRP-conjugated goat anti-mouse secondary antibody was used at x10,000 dilution in 1% non-fat powdered milk. 30 minutes exposure. Epac2 distribution was examined in HCAECs through immunocytochemistry (B). Low-level signal was identified with a pattern similar to that of Epac1; diffuse cellular distribution with areas of membrane-association (white arrow). Punctate staining appeared to be present in the nucleus as highlighted by DAPI nuclear staining (B). N=1.

5.3.2.4 - 8-pCPT addition to HCAECs

In order to determine the effect of Epac activation on the distribution pattern of cadherins and connexins in HCAECs, cells were treated with the Epac-selective agonist 8-(4-Chlorophenylthio)-2'-O-methyl-cAMP (8-pCPT) in a number of preliminary experiments.

5.3.2.4 1 - Epac1 immunocytochemistry

Epac1 distribution was examined in HCAECs under control conditions and following 5 minutes and 30 minutes incubation with the Epac-selective activator 8-pCPT (Figure 5.16). Following 5 minutes incubation with 8-pCPT, Epac1 re-organised into small cytoplasmic aggregations (Figure 5.16B, white arrows). After 30 minutes of incubation with 8-pCPT, an increase in membranous Epac1 was noted (Figure 5.16C, white arrows). HCAEC Epac1 distribution after 30 minutes Epac activation was markedly different to the diffuse Epac1 staining observed in HCAECs under control conditions (Figure 5.16A). In addition, these cells displayed a greater degree of Epac1 associated with the nucleus, as demonstrated by the overlap between nuclear DAPI (blue) and AF488-signal (Figure 5.16C). The association of Epac1 into aggregations following 8-pCPT treatment is further highlighted by the increased maximum AF488 signal intensity recorded in these cells (Figures 5.16B & 5.16C).

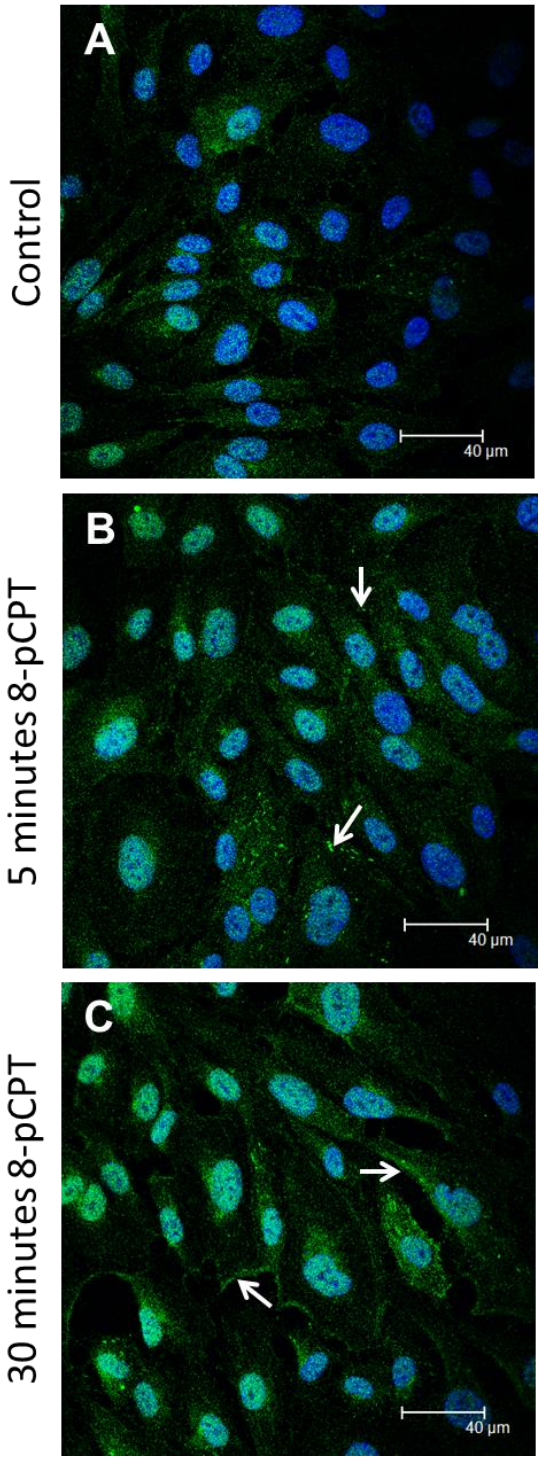

Figure 5.16: Immunocytochemistry of Epac1 expression in HCAECs following 8-pCPT addition

Under control conditions, Epac1 was distributed diffusely throughout the HCAECs (A). Following 5 minutes incubation with 5 µM 8-pCPT at 37˚C/ 5% CO_2, Epac1 localised to small intracellular aggregations (white arrows, B). After 30 minutes treatment, increased Epac1 was detected in the perinuclear region and at the membrane (white arrows, C). DAPI nuclear staining is shown in blue. Antibody dilutions as previously stated. N=2.

5.3.2.4 2 - VE-cadherin immunocytochemistry

VE-cadherin distribution was examined in HCAECs under control conditions and following 30 minutes incubation with the Epac-selective activator 8-pCPT (Figure 5.17). On incubation with 5 µM 8-pCPT for 30 minutes at 37˚C/ 5% CO_2, VE-cadherin relocates to the membrane, forming a more continuous border between adjacent cells (Figure 5.17C; AF488 & Figure 5.17D; AF594). It was also noted that the short and inward projections from the membranous VE-cadherin evident under control conditions, were no longer as extensive following Epac activation, suggesting redistribution of VE-cadherin (Figures 5.17C & 5.17D). This re-distribution of VE-cadherin was observed in all cells imaged.

5.3.2.4 3 - N-cadherin immunocytochemistry

N-cadherin distribution was examined in HCAECs under control conditions and following 30 minutes incubation with 8-pCPT (Figure 5.18). Preliminary data indicated that following 30 minutes treatment with 5 µM 8-pCPT, N-cadherin was distributed more diffusely throughout the cells, with a decreased membranous association (Figures 5.18C & 5.18D).

5.3.2.4 4 - Cadherin immunocytochemistry summary

8-pCPT application altered the expression profile of both VE-cadherin and N-cadherin in cultured HCAECs in preliminary investigations. 30 minutes incubation with 5 µM 8-pCPT resulted in a cell membrane lined almost continuously by VE-cadherin, and N-cadherin appeared to re-locate away from the membrane.

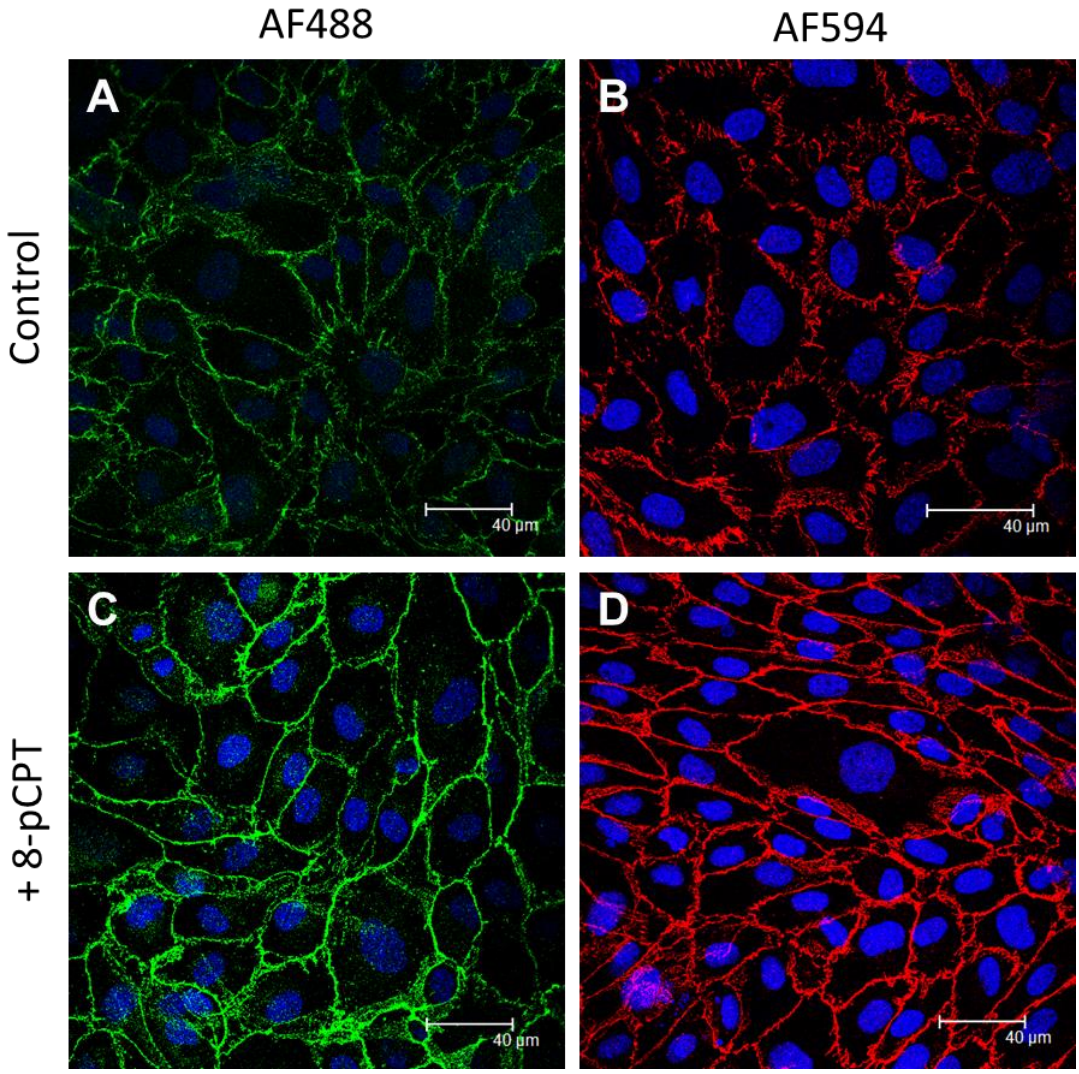

Figure 5.17: Immunocytochemistry of VE-cadherin expression in HCAECs following 8-pCPT application

Under control conditions, VE-cadherin distribution in HCAECs was primarily identified as discontinuous membranous sections (A & B). Following 30 minutes incubation with 5 µM 8-pCPT at 37˚C/ 5% CO_2 VE-cadherin formed a continuous border along the membrane of adjacent HCAECs (C & D). DAPI nuclear staining is shown in blue. Images A and C labelled with AF488-tagged secondary antibody, images B and D labelled with AF594-tagged secondary antibody. Antibody dilutions as previously stated. N=2.

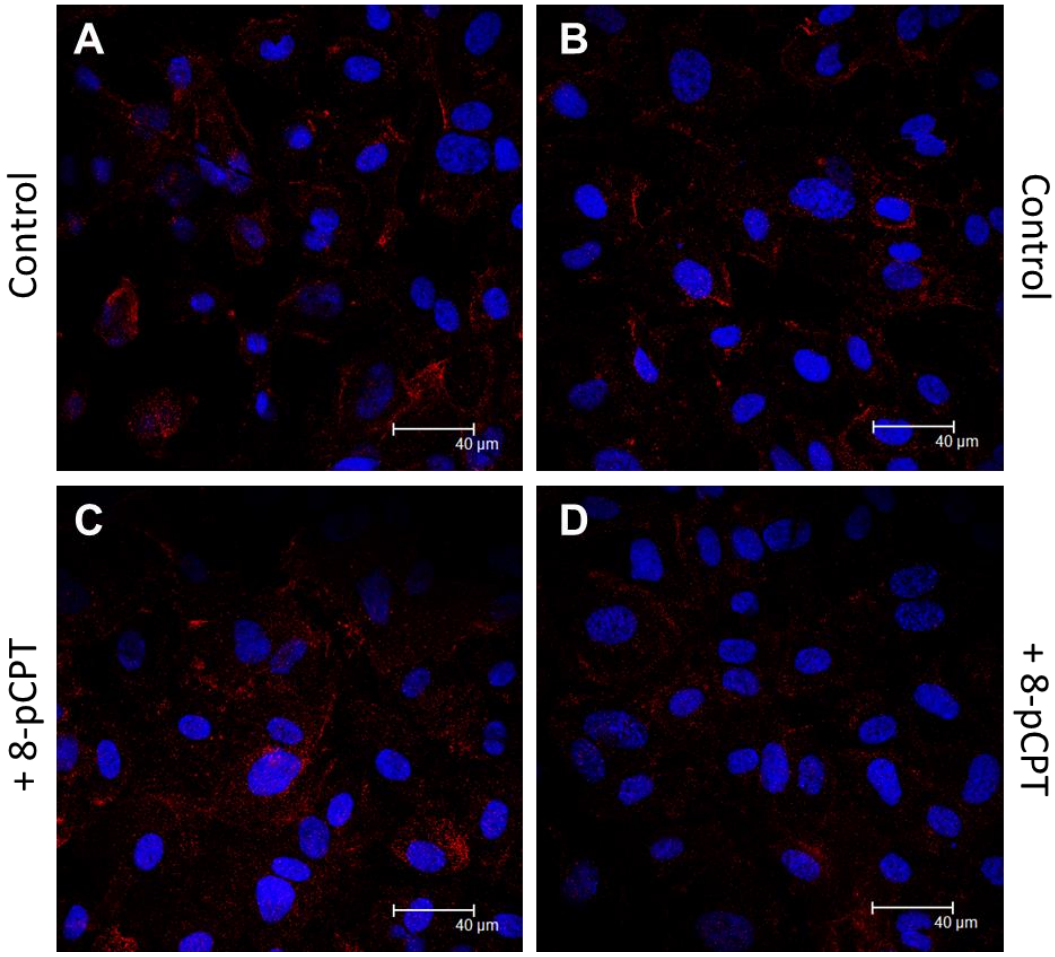

Figure 5.18: Immunocytochemistry of N-cadherin expression in HCAECs following 8-pCPT application

Under control conditions, N-cadherin is distributed diffusely throughout HCAECs with distinct areas of membranous staining (A & B). After 30 minutes incubation with 5 µM 8-pCPT at 37˚C/ 5% CO_2, N-cadherin appeared to lose this membranous staining (C & D). DAPI nuclear staining is shown in blue. Antibody dilutions as previously stated. N=1.

5.3.2.4.5 - VE-cadherin and Cx37 co-localisation

VE-cadherin and Cx37 were labelled in HCAECs under control conditions and following 30 minutes incubation with 5 μM 8-pCPT (Figure 5.19). Under control conditions, localised areas of overlap between VE-cadherin and Cx37 (yellow) were identified at the membrane (Figure 5.19E). On incubation with 8-pCPT during preliminary experiments, the membranous areas showing yellow increased, suggesting facilitated co-localisation of VE-cadherin and Cx37 (Figure 5.19F). Low-level perinuclear Cx37 observed under control conditions (Figure 5.19C & 5.19E) remained following Epac activation (Figure 5.19D & 5.19F). The proportion of overlap between VE-cadherin and Cx37 was quantified using three types of Image J plugin and this will be discussed later (Section 5.3.2.4.8).

5.3.2.4 6 - VE-cadherin and Cx40 co-localisation

VE-cadherin and Cx40 were labelled in HCAECs under control conditions and following 30 minutes incubation with 5 μM 8-pCPT (Figure 5.20). Under control conditions, small areas of VE-cadherin and Cx40 overlap were identified as yellow patches at the membranes of HCAECs (Figure 5.20E). On Epac activation with 8-pCPT a small number of cells showed increased Cx40 expression at the cell membrane and this resulted in an apparent increase in the co-localisation in these cells (Figure 5.20F). However, this was not the pattern observed in the vast majority of HCAECs imaged. Furthermore, quantitative analysis showed no significant increase in co-localisation between VE-cadherin and Cx40 in HCAECs on Epac activation (discussed in Section 5.3.2.4.8). Application of 8-pCPT appeared to cause an increase in the localisation of Cx40 to the perinuclear region, as shown in the confocal image (Figure 5.20D) with DAPI nuclear staining shown in blue.

5.3.2.4 7 - VE-cadherin and Cx43 co-localisation

VE-cadherin and Cx43 were labelled in HCAECs under control conditions and following 30 minutes incubation with 5 μM 8-pCPT (Figure 5.21). Under control conditions, the membranes of HCAECs displayed small sections of overlap between Cx43 and VE-cadherin (Figure 5.21E). An apparent increase in the co-localisation of Cx43 and VE-cadherin at the membrane was detected following Epac activation (Figure 5.21F). The proportion of overlap between VE-cadherin and Cx43 was quantified using three types of Image J plugin and this will be discussed later (Section 5.3.2.4.8)

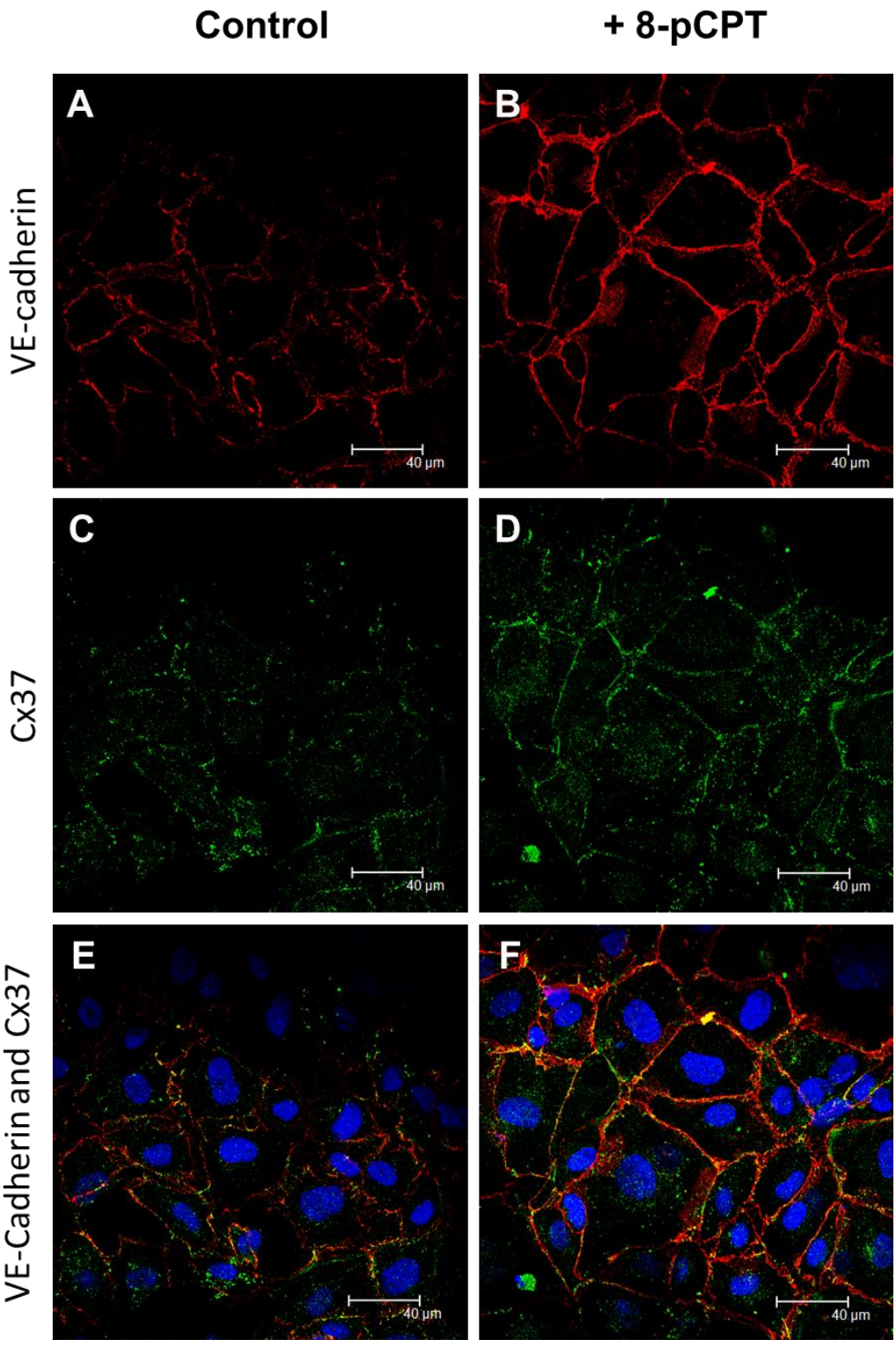

Figure 5.19: Immunocytochemistry of VE-cadherin and Cx37 distribution in HCAECs following 8-pCPT application

Under control conditions, isolated areas of overlap between VE-cadherin (red, A) and Cx37 (green, C) distribution were identified as yellow patches at the membrane (E). Following 30 minutes incubation with 5 µM 8-pCPT at 37˚C/ 5% CO_2, there was an increase in the co-localisation of these two junctional proteins (yellow, F). DAPI nuclear staining is shown in blue. Antibody dilutions as previously stated. N=2.

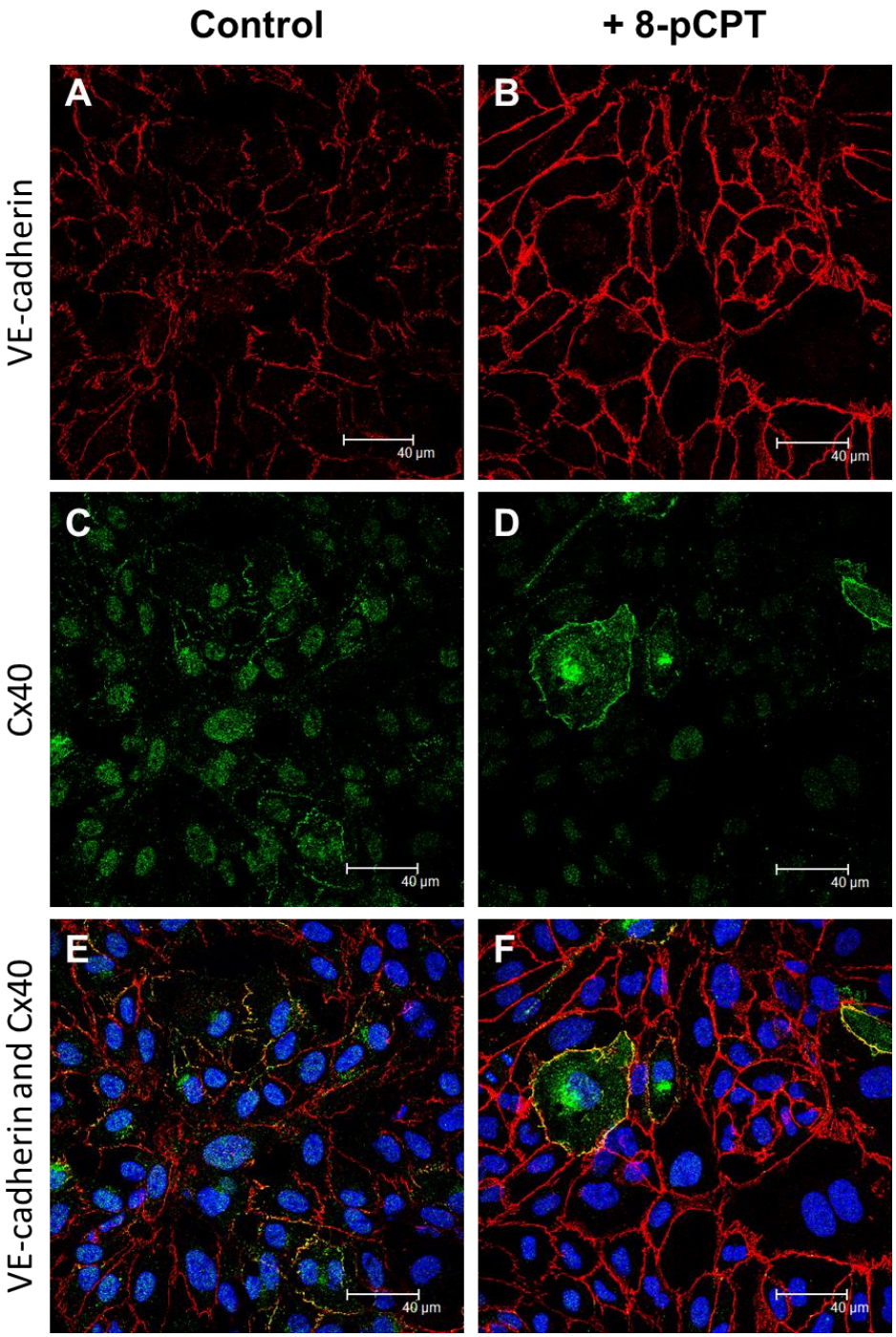

Figure 5.20: Immunocytochemistry of VE-cadherin and Cx40 distribution in HCAECs following 8-pCPT application

Under control conditions, isolated areas of overlap between VE-cadherin (red, A) and Cx40 (green, C) distribution were identified at the membrane (yellow, E). For the majority of cells, little increase in co-localisation between VE-cadherin and Cx40 was identified following 30 minutes incubation with the Epac-selective activator 8-pCPT, although a small number of cells showed a marked increase in Cx40 expression at the cell membrane, as seen by the yellow staining (F). DAPI nuclear staining is shown in blue. Antibody dilutions as previously stated. N=3.

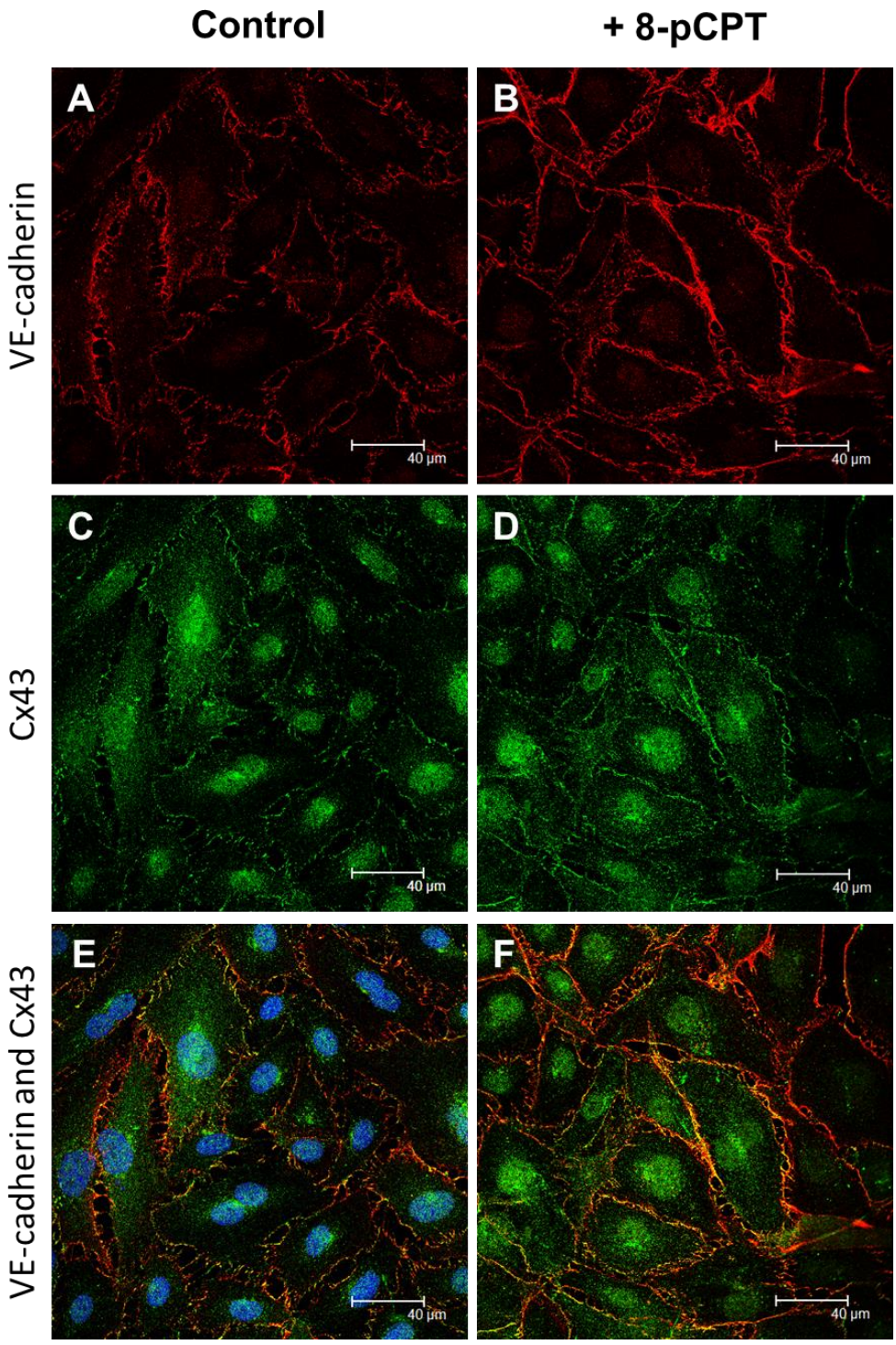

Figure 5.21: Immunocytochemistry of VE-cadherin and Cx43 distribution in HCAECs following 8-pCPT application

In control experiments, small areas of overlap between VE-cadherin (red, A) and Cx43 (green, C) were identified at the membrane (yellow, E). Following 30 minutes incubation with 5 µM 8-pCPT, VE-cadherin and Cx43 co-localisation at the membrane appeared to increase (F). DAPI nuclear staining is shown in blue (E). Antibody dilutions as previously stated. N=3.

5.3.2.4.8 - Quantification of VE-cadherin and connexin co-localisation after Epac activation

Three types of Image J plugin were used to quantify co-localisation of VE-cadherin and connexins in HCAECs under control conditions and following 8-pCPT treatment (Figure 5.22). These plugins were; Manders' Overlap Coefficient (Figure 5.22A, 5.22D & 5.22G), Co-localisation Finder plugin (Figure 5.22B, 5.22E & 5.22H) and Intensity Correlation Analysis (Figure 5.22C, 5.22F & 5.22I). Full details of the quantification process for each plugin is described in the Appendix under "Supplementary information on the quantification of cadherin and connexin co-localisation using Image J plugins". Analysis of the co-localisation between VE-cadherin and Cx37 is shown in Figure 5.22A- 5.22C. For this quantification N=6 for control and N=5 for 8-pCPT treatment, where N=number of images analysed, with a minimum of 2 experimental repeats. All three plugins identified a significant increase in VE-cadherin and Cx37 co-localisation on Epac activation (unpaired student's *t*-test). Analysis of the co-localisation between VE-cadherin and Cx40 is shown in Figures 5.22D- 5.22F. For this quantification N=13 for control and N=5 for 8-pCPT treatment, with a minimum of 3 repeats. No significant change in the co-localisation between VE-cadherin and Cx40 was identified by any of the three plugins (unpaired student's *t*-test). Analysis of the co-localisation between VE-cadherin and Cx43 is shown in Figures 5.22G- 5.22I. For this quantification N=9 for control and 8-pCPT treatment, with a minimum of 3 repeats. All three plugins showed an increase in co-localisation between VE-cadherin and Cx43 on Epac activation but only the Intensity Correlation Analysis plugin (Figure 5.22I) found the increase to be significant (* $P<0.05$, unpaired student's *t*-test). Figure 5.23 displays the data shown in Figure 5.22 in an alternative format where different connexin subtypes are aligned for comparison.

5.3.2.4 9 - Connexins and cadherin co-localisation following 8-pCPT - summary

Following 30 minutes incubation with 5 µM 8-pCPT, there was a significant increase in the overlap between Cx37 and VE-cadherin distribution in HCAECs. An increase in the co-localisation of Cx43 and VE-cadherin at the membrane was also detected, but only 1 Image J plugin found this increase to be significant. No increase in the overlap of Cx40 and VE-cadherin expression at the membrane was detected.

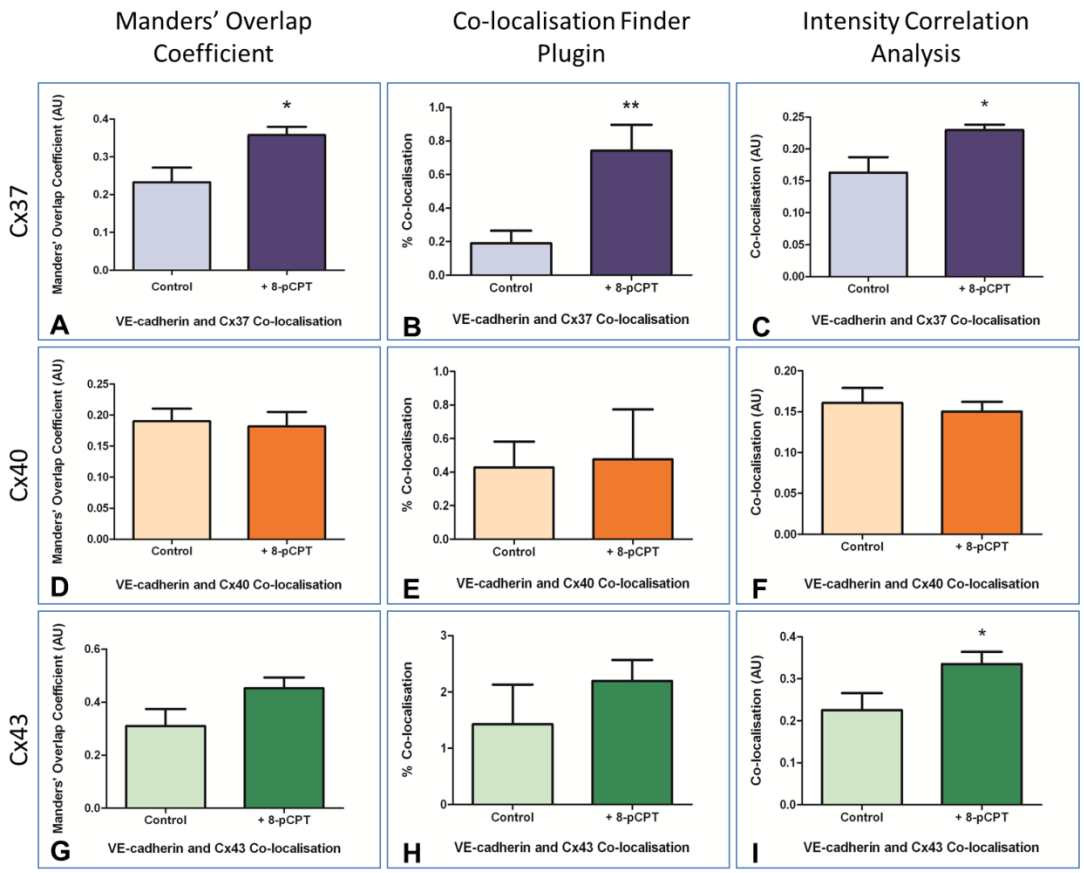

Figure 5.22: Quantification of VE-cadherin and Connexin co-localisation in HCAECs following 8-pCPT application

The effect of Epac activation on co-localisation of VE-cadherin and connexins was examined using three Image J plugins, Manders' Overlap Coefficient (A, D & G), Co-localisation Finder plugin (B, E & H) and Intensity Correlation Analysis (C, F & I). Application of 5 µM 8-pCPT to HCAECs resulted in a significant increase in co-localisation of VE-cadherin and Cx37 in all three plugins (A-C). No significant change in co-localisation of VE-cadherin and Cx40 was identified following 8-pCPT application (D-F). Only the Intensity Correlation Analysis plugin identified a significant increase in co-localisation of VE-cadherin and Cx43 on Epac activation (I). Full details of the quantification process can be found in the Appendix under "Supplementary information on the quantification of cadherin and connexin co-localisation using Image J plugins". (* $P<0.05$, ** $P<0.01$, unpaired student's *t*-test). For Cx37: N=6 for control and N=5 for 8-pCPT treatment, over 2 independent experiments. For Cx40: N=13 for control and N=5 for 8-pCPT treatment, over 3 independent experiments. For Cx43: N=9 for control and 8-pCPT treatment, over 3 independent experiments.

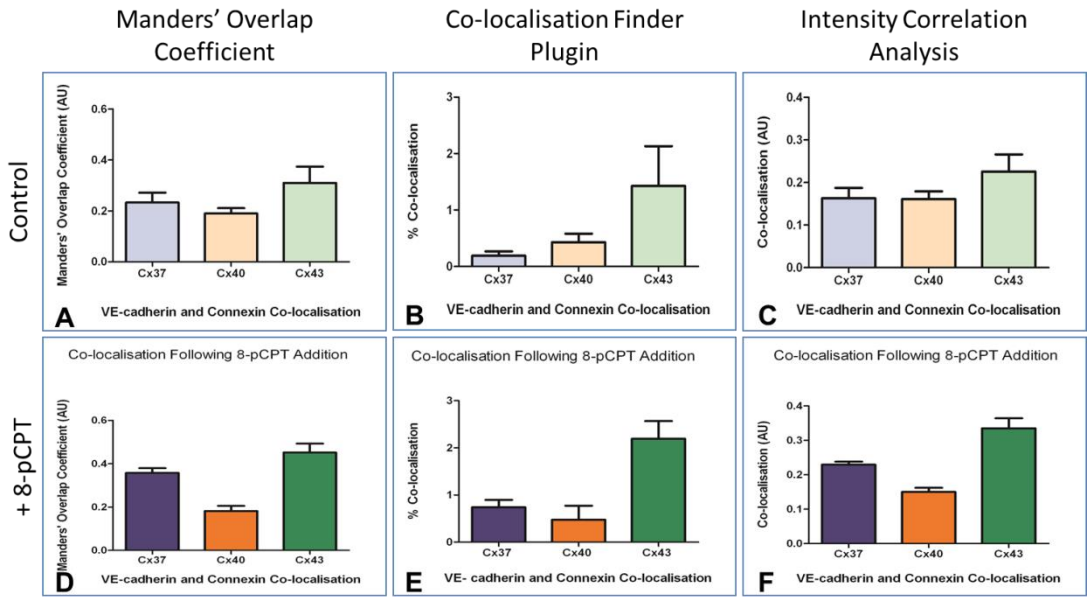

Figure 5.23: Quantification of VE-cadherin and Connexin co-localisation in HCAECs under control conditions and following 8-pCPT application

A-C represent co-localisation of VE-cadherin with Cx37, Cx40 and Cx43 under control conditions, as quantified using the Manders' Overlap Coefficient plugin (A), Co-localisation Finder plugin (B) and Intensity Correlation Analysis plugin (C). D-F represent co-localisation of VE-cadherin with Cx37, Cx40 and Cx43 following incubation with 5 µM 8-pCPT, as quantified using the three Image J plugins. Full details of the quantification process can be found in the Appendix under "Supplementary information on the quantification of cadherin and connexin co-localisation using Image J plugins". For Cx37: N=6 for control and N=5 for 8-pCPT treatment, over 2 independent experiments. For Cx40: N=13 for control and N=5 for 8-pCPT treatment, over 3 independent experiments. For Cx43: N=9 for control and 8-pCPT treatment, over 3 independent experiments.

5.3.2.5 - Epac1 siRNA transfection of HCAECs

Passage 6 HCAECs were used for all transfection experiments. Cells were grown to 70% confluence in 6-well cell culture plates in fully-supplemented HCAEC media. Full protocol details can be found in the Methods chapter under "2.2.5 - Small Interfering RNA (siRNA) knockdown of Epac1". Preliminary titration Western blot experiments identified 10 nM Epac1 siRNA (5 nM of each duplex; Hs_RAPGEF3_6 and Hs_RAPGEF3_7) as the optimum concentration for transfection to produce Epac1 knockdown without deleterious effects on the HCAECs (Figure 5.24). Other concentrations tested include 5 nM of each duplex alone, and 25 nM total concentration of the two duplexes combined (Figure 5.24). 5 nM appeared insufficient to produce reliable knockdown of Epac1 (Figure 5.24A). 25 nM produced similar results to that of 10 nM (Figure 5.24A), and as such 10 nM was selected for the following experiments.

Next, the time course of knock down was investigated. The HCAECs were exposed to the siRNA for 24 hours, 48 hours or 72 hours, and Epac1 expression was examined in a number of preliminary experiments using Western Blot (Figure 5.25A). Lipofectamine-only and non-silencing siRNA (10nM) transfections were used as controls, and under these conditions Epac1 expression was identified as a single band at 99 kDA (Figure 5.25A). Following treatment with 10 nM Epac1 siRNA, Epac1 expression was reduced after 24 hours, and no detectable band was seen after 48 hours or 72 hours (Figure 5.25A). Epac1 banding under control conditions at 24 hours was lower than that detected at 48 hours and 72 hours (Figure 5.25A). This is probably due to lower total protein concentration in the 24 hour lysate. 72 hours incubation with the siRNA may have a negative impact on the HCAECs, as actin expression after 72 hours was reduced (Figure 5.25B). As such, 48 hours was selected as the optimum exposure time for all future experiments.

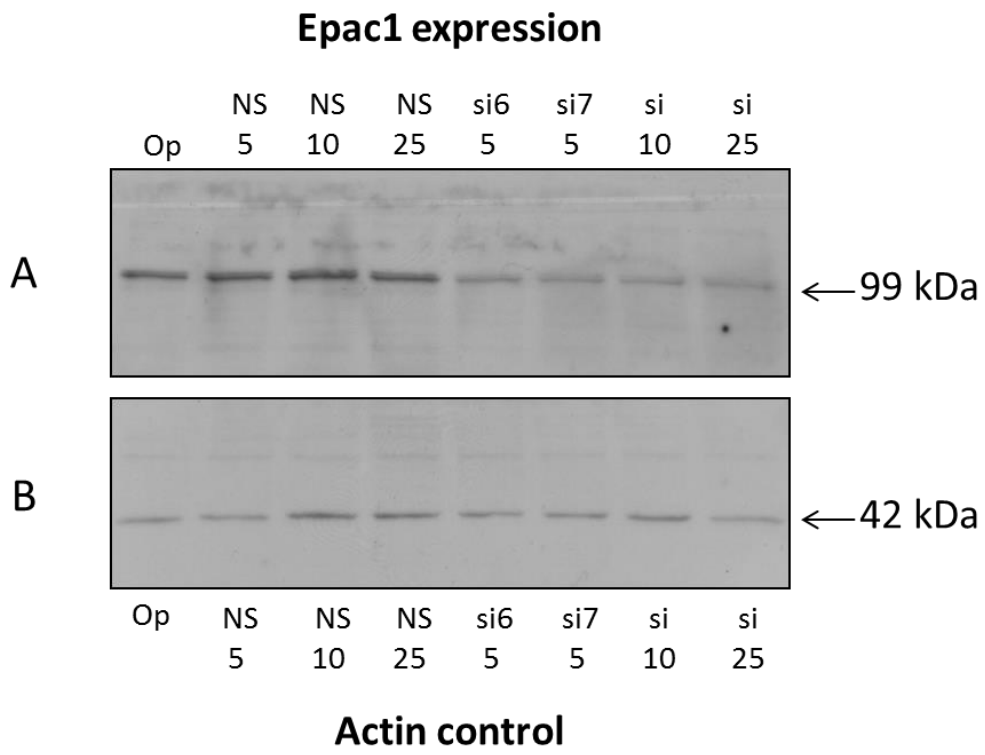

Figure 5.24: Western blot of Epac1 expression in HCAECs following siRNA knockdown at varying concentrations

HCAECs were transfected with varying concentrations of Epac1 siRNA for 48 hours (A). The lysate produced from each condition was run on a Western blot and labelled for Epac1 expression. The membrane was subsequently re-blotted for actin expression (B). Op = Optimem only (no transfection agent), NS 5/10/25 = Non-silencing siRNA at 5, 10 and 25 nM, si6 5 = Epac1 siRNA duplex 6 (Hs_RAPGEF3_6) at 5 nM, si7 5 = Epac1 siRNA duplex 7 (Hs_RAPGEF3_7) at 5 nM, si 10/25 = equal amounts of Epac1 siRNA duplexes 6 and 7 at total concentration of 10 nM/25 nM. Anti-Epac1 monoclonal mouse primary antibody (Cell Signalling, 4155S) was used at 200 fold dilution. Mouse anti-actin primary antibody was used at 500 fold dilution. Both primary antibodies were targeted with the goat anti-mouse HRP-conjugated secondary antibody at a 10,000 fold dilution. Both primary and secondary antibodies were diluted in 1% non-fat powdered milk. The films were exposed to the membranes for 2 hours (Epac1, A) and 30 minutes (actin, B). N=2.

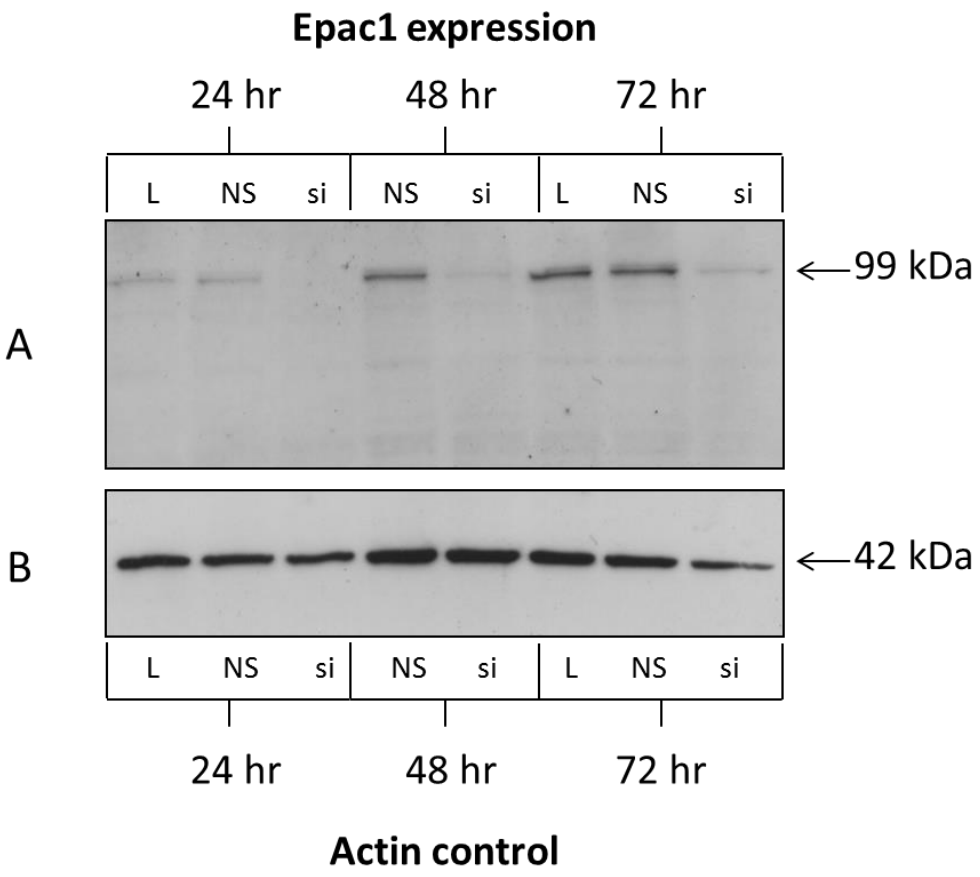

Figure 5.25: Western blot of Epac1 expression in HCAECs following siRNA knockdown over 24, 48 and 72 hours

HCAECs were transfected with Epac1 siRNA duplexes Hs_RAPGEF3_6 and Hs_RAPGEF3_7 at a total concentration of 10 nM for 24, 48 or 72 hours. The lysate produced from each condition was run through a Western blot and probed for Epac1 expression (A). The membrane was subsequently re-blotted for actin expression (B). L = lipofectamine control, NS = non-silencing siRNA at 10 nM, si = Epac1 siRNA duplexes 6 & 7, total concentration 10 nM. Anti-Epac1 monoclonal mouse primary antibody was used at 200 fold dilution. Mouse anti-actin primary antibody was used at 500 fold dilution. Both primary antibodies were targeted with the goat anti-mouse HRP-conjugated secondary antibody at a 10,000 fold dilution. Both primary and secondary antibodies were diluted in 1% non-fat powdered milk. The films were exposed to the membranes for 1 hour (Epac1, A) and 10 minutes (actin, B). For 24 hours, N=2. For 48 hour and 72 hours, N=6.

5.3.2.5.1 - Quantification of Epac1 expression in HCAECs following Epac1 siRNA transfection

The actin re-blot shown in Figure 5.24B allowed quantification of relative Epac1 expression following Epac1 siRNA transfection (Figure 5.26A & 5.26B). Image J was used for densitometrical analysis of Epac1 expression under the varying conditions. When normalised to actin expression, there was a significant decrease in Epac1 expression between non-silencing siRNA treated HCAECs and the Epac1 siRNA transfected HCAECs at both 48 hours and 72 hours post-transfection (Figure 5.26A, unpaired student's *t*-test, N=8-14, over 3 independent experiments). When Epac1 expression was normalised to the Lipofectamine control transfection of HCAECs, a significant decrease in Epac1 expression was identified between the non-silencing control transfection and the Epac1 siRNA transfection at all three time points (Figure 5.26B, unpaired student's *t*-test, N=4-14, over 3 independent experiments).

5.3.2.5.2 - Epac1 immunocytochemistry following Epac1 siRNA transfection

During preliminary experiments, HCAECs transfected with 10 nM Epac1 siRNA (Hs_RAPGEF3_6 and Hs_RAPGEF3_7 duplexes) were labelled for Epac1 expression (green) after 24, 48 and 72 hours incubation with the siRNA (Figure 5.27B, 5.27C & 5.27G). After 24 hours exposure to the Epac1 siRNA, Epac1 was found to change from a diffuse distribution throughout the cell (Figure 5.27A) to one restricted to one site adjacent to the nucleus (Figure 5.27B). This accumulation in Epac1 distribution was also indicated by the increase in the maximum AF488 signal from 217 AU (Figure 5.27A) to 254 AU (Figure 5.27B). After 48 hours exposure, Epac1 expression appeared to be almost entirely absent from the HCAECs, with only isolated areas of staining detected (Figure 5.27C). The signal intensity declined to 58 AU (Figure 5.27C), a level considered background in all immunocytochemistry experiments. Similarly, after 72 hours exposure, the Epac1 expression further declined and a maximum AF488 signal intensity of 48 AU was recorded (Figure 5.27D). The DAPI nuclear staining (blue) shows the re-location of Epac1 to the nucleus (Figure 5.27B).

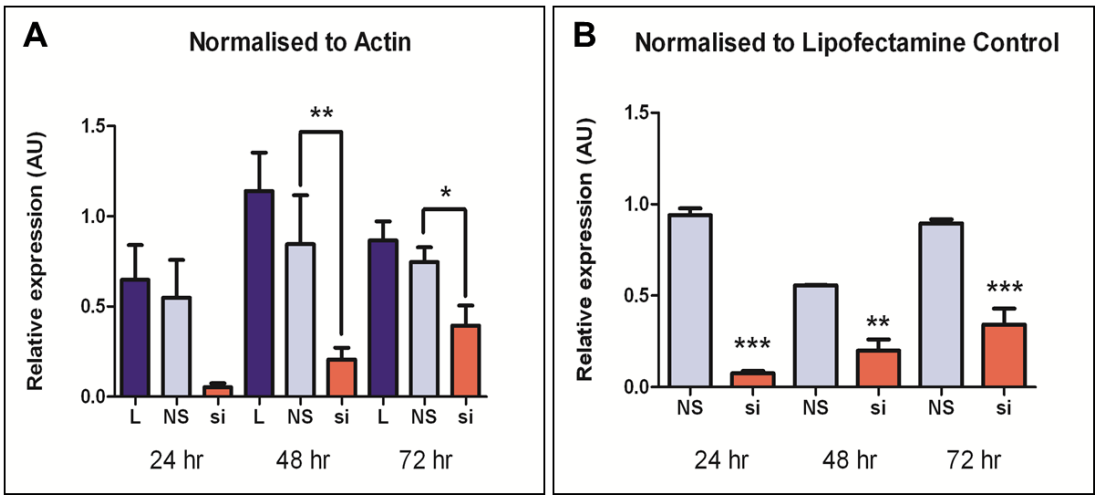

Figure 5.26: Quantification of Epac1 knockdown in HCAECs

Relative expression of Epac1 following transfection with 10 nM Epac1 siRNA (duplexes Hs_RAPGEF3_6 and Hs_RAPGEF3_7) for 24, 48 or 72 hours was quantified by densitometrical analysis using Image J. Epac1 expression was normalised to actin expression (A) and lipofectamine control (B). L = lipofectamine control, NS = non-silencing siRNA at 10 nM, si = Epac1 siRNA duplexes 6 & 7, total concentration 10 nM. (** P<0.01, *** P<0.001, unpaired student's *t*-test). For A; NS48 N=4, L24/NS24/si24/L48/si48 N=10, L72/NS72/si72 N=14, over 3 independent experiments.

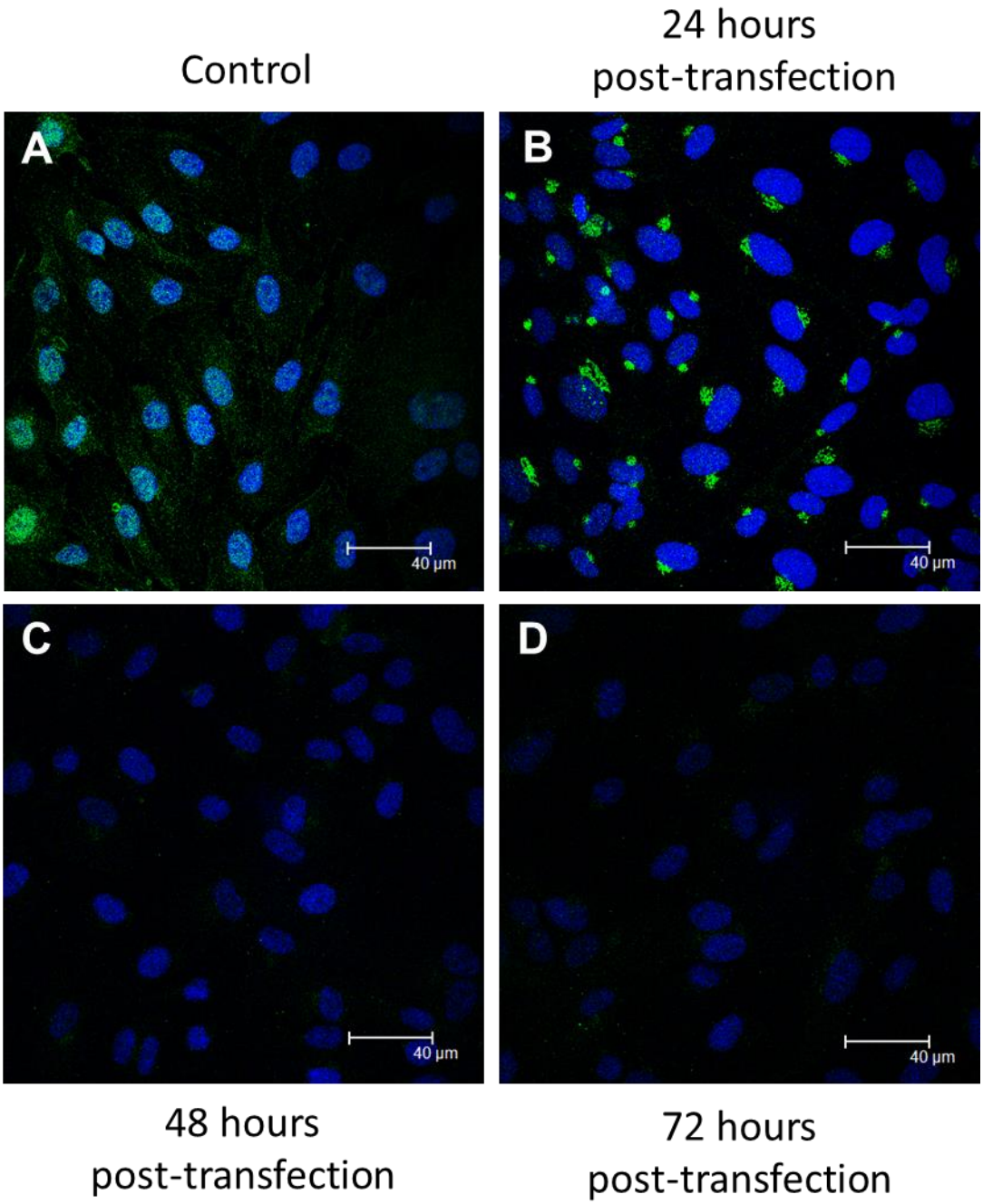

Figure 5.27: Immunocytochemistry of Epac1 expression following Epac1 siRNA transfection

Epac1 (green) distribution was identified in HCAECs under control conditions (A) and following 24 (B), 48 (C) and 72 (D) hours exposure to 10 nM Epac1 siRNA. Epac1 appeared to re-distribute to a restricted region adjacent to the nucleus following 24 hours treatment (B). After 48 hours or 72 hours, Epac1 expression had declined to a maximum fluorescence intensity of 58 AU (C) and 48 AU (D), respectively. DAPI nuclear staining is shown in blue. Antibody dilutions as previously detailed. N=1.

5.3.2.5.3 - Epac2 immunocytochemistry following Epac1 siRNA transfection

HCAECs transfected with 10 nM Epac1 siRNA (Hs_RAPGEF3_6 and Hs_RAPGEF3_7 duplexes) were also labelled for Epac2 expression (green) after 48 hours incubation with the siRNA (Figure 5.28B). Preliminary data indicated no observable change in the expression profile of Epac2 after Epac1 siRNA transfection (Figure 5.28B). However, as the Epac2 antibody may not be very selective (Section 5.3.2.2), further experiments with an alternative Epac2 antibody would be required to confirm this observation.

5.3.2.5.4 - VE-cadherin immunocytochemistry following Epac1 siRNA transfection and addition of 8-pCPT

HCAECs transfected with 10 nM Epac1 siRNA (Hs_RAPGEF3_6 and Hs_RAPGEF3_7 duplexes) or 10 nM non-silencing siRNA for 48 hours were labelled for VE-cadherin expression (green) under control conditions and following 30 minutes incubation with 5 µM of the Epac-selective activator 8-pCPT at 37˚C/ 5% CO_2 (Figure 5.29). Preliminary data indicated little difference in VE-cadherin staining pattern between Epac1 siRNA transfected and non-silencing siRNA transfected HCAECS (Figures 5.29A & 5.29B). On addition of 5 µM 8-pCPT to the Epac1 siRNA transfected cells (Figure 5.29C), the distribution of VE-cadherin at the membrane remained largely discontinuous and patchy, and was not considered to be altered from that observed without Epac activation. Transfection of the HCAECs with 10 nM non-silencing siRNA acted as a control (Figures 5.29B & 5.29D). On addition of 5 µM 8-pCPT to non-silencing siRNA-treated HCAECs, VE-cadherin formed a more continuous border along the HCAECs (Figure 5.29D). This preliminary data suggests that Epac1 siRNA knockdown blocks the 8-pCPT-induced VE-cadherin re-distribution in HCAECs.

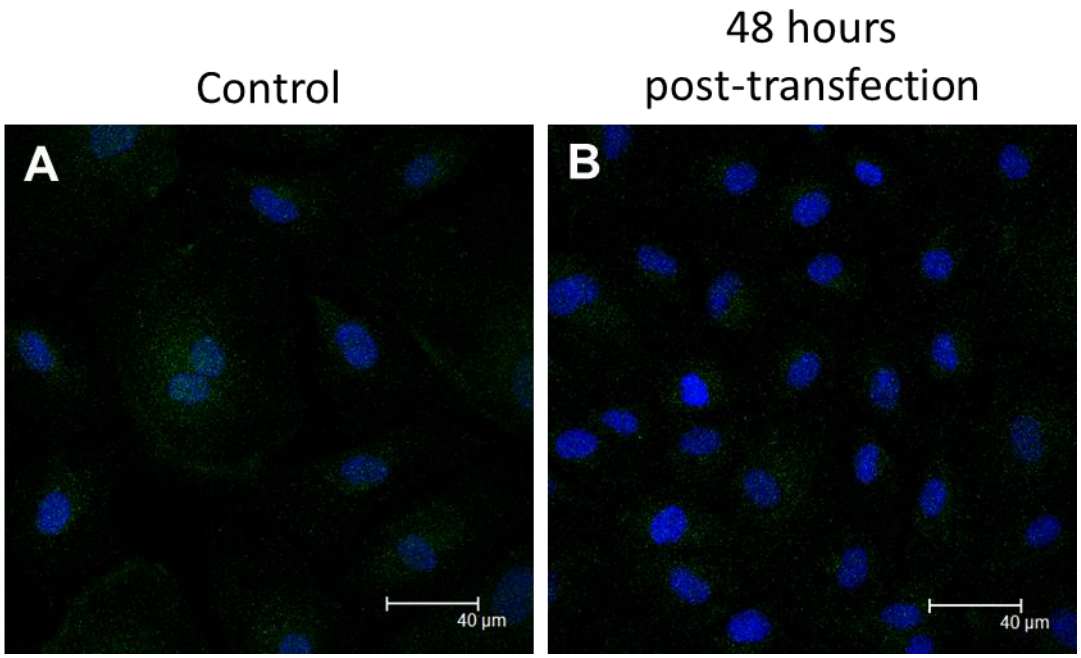

Figure 5.28: Immunocytochemistry of Epac2 expression following Epac1 siRNA transfection

Epac2 (green) distribution was examined in HCAECs under control conditions (A) and following 48 hours exposure to 10 nM Epac1 siRNA (B). No observable change in Epac2 distribution or expression was noted following Epac1 siRNA knockdown. DAPI nuclear staining is shown in blue. Antibody dilutions as previously detailed. N=1.

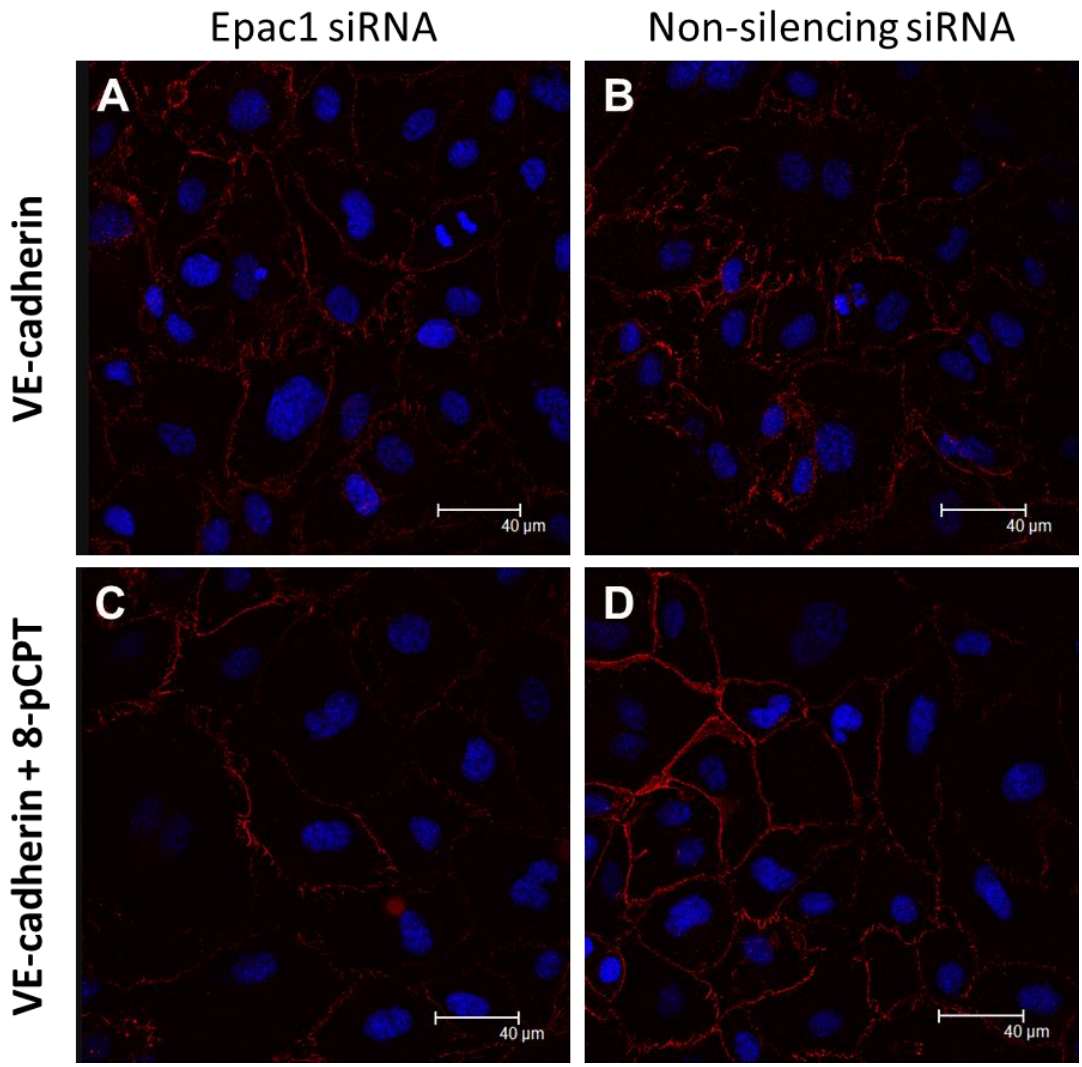

Figure 5.29: Immunocytochemistry of VE-cadherin expression following Epac1 siRNA transfection and addition of 8-pCPT

VE-cadherin (red) distribution was identified in HCAECs treated with 10 nM Epac1 siRNA with (C) or without (A) Epac1 activation via 8-pCPT addition (5 µM). 10 nM non-silencing siRNA acted as a control (B & D). DAPI nuclear staining is shown in blue. Antibody dilutions as previously detailed. N=1.

5.3.2.5.5 - VE-cadherin and connexin co-localisation following Epac1 siRNA transfection and addition of 8-pCPT

5.3.2.5 5.1 - VE-cadherin and Cx37

HCAECs transfected with 10 nM Epac1 siRNA (Hs_RAPGEF3_6 and Hs_RAPGEF3_7 duplexes) for 48 hours were labelled for VE-cadherin (red) and Cx37 (green) without, and following, 30 minutes incubation with 5 µM 8-pCPT at 37˚C/ 5% CO_2. During preliminary experiments, labelling of VE-cadherin and Cx37 in Epac1 siRNA-transfected HCAECs identified isolated areas of co-localisation (yellow) between VE-cadherin and Cx37 (Figure 5.30E). On addition of 5 µM 8-pCPT, little increase in co-localisation between VE-cadherin and Cx37 could be detected (Figure 5.30F). On transfection with Epac1 siRNA, Cx37 appeared to show a strong association with the cytoskeleton, both with (Figure 5.30C) and without (Figure 5.30D) 8-pCPT addition. This distribution pattern was considerably different to the Cx37 expression profile observed under control conditions. Furthermore, Cx37 appears to be lining the internal surface of the discontinuous membranous VE-cadherin, and again this pattern was displayed both with (Figures 5.30F) and without (Figures 5.30E) 8-pCPT addition. DAPI nuclear staining (blue) appeared to indicate an increase in the proportion of both VE-cadherin and Cx37 associated with the nucleus on 8-pCPT addition (Figure 5.30F).

HCAECs transfected with 10 nM non-silencing siRNA for 48 hours were used as a control during these preliminary experiments (Figure 5.31). These cells were also labelled without (Figures 5.31A, 5.31C & 5.31E), and following, 30 minutes incubation with 5 µM 8-pCPT (Figures 5.31B, 5.31D & 5.31F). Labelling of VE-cadherin and Cx37 in non-silencing siRNA - transfected HCAECs identified isolated areas of co-localisation (yellow) between VE-cadherin and Cx37 (Figures 5.31E). These HCAECs also displayed the altered Cx37 distribution observed in Epac1 siRNA-transfected HCAECs, with Cx37 appearing to be lining the internal surface of the discontinuous membranous VE-cadherin (Figure 5.31E). On addition of 5 µM 8-pCPT, slight increase in VE-cadherin and Cx37 co-localisation at the membrane was detected (Figure 5.31F). Cx37, in particular, appeared to display a pattern more similar to that observed under control conditions (Figure 5.31D), and VE-cadherin formed a more continuous barrier at the HCAEC membrane (Figure 5.31B). DAPI nuclear staining (blue) again appeared to indicate an increase in the proportion of both VE-cadherin and Cx37 associated with the nucleus on 8-pCPT addition (Figure 5.31F).

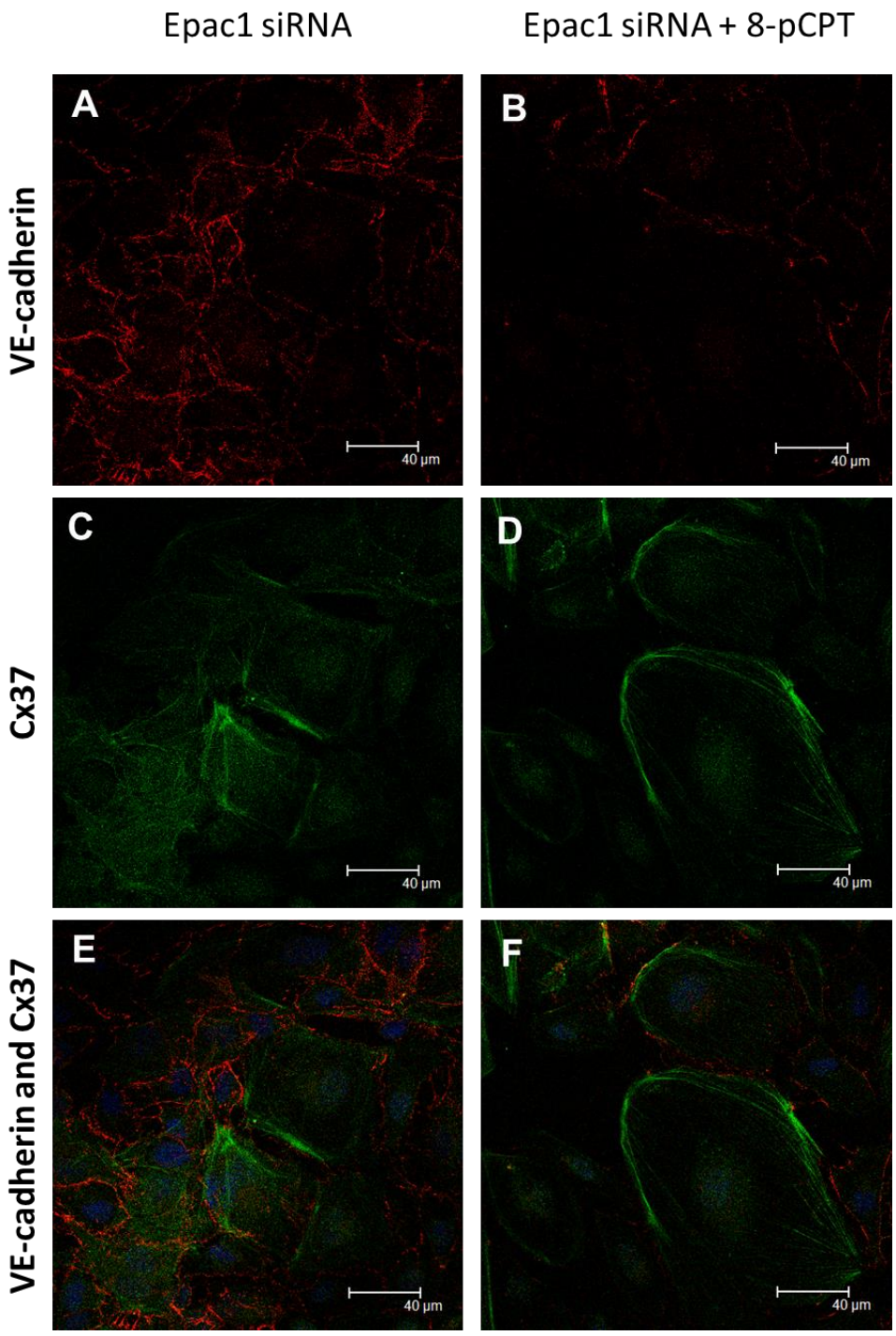

Figure 5.30: Immunocytochemistry of VE-cadherin and Cx37 expression following Epac1 siRNA transfection and addition of 8-pCPT

VE-cadherin (red, A & B) and Cx37 (green, C & D) distribution was identified in HCAECs treated with 10 nM Epac1 siRNA, with (B, D & F) or without (A, C & E) 8-pCPT addition (5 µM). Isolated areas of VE-cadherin and Cx37 co-localisation (yellow) were identified in unstimulated Epac1 siRNA-transfected HCAECs (E). No increase in co-localisation was identified following addition of 5 µM 8-pCPT (F). DAPI nuclear staining is shown in blue. Antibody dilutions as previously detailed. N=1.

VE-cadherin and Cx37 co-localisation in Epac1 siRNA-transfected HCAECs was quantified using Image J (Figure 5.32). As previously detailed, three plugins were used to analyse the change in co-localisation induced by 8-pCPT addition (Figure 5.32A- 5.32C). On incubation with 5 µM 8-pCPT for 30 minutes, two of the plugins identified a significant decrease in VE-cadherin and Cx37 co-localisation in the Epac1 siRNA-transfected HCAECs (Figures 5.32G & 5.32H, unpaired students *t*-test, N=2-3). The third plugin identified no change in the proportion of VE-cadherin and Cx37 co-localisation (Figure 5.32I). This pattern was the reverse of that observed in control HCAECs, which displayed an increase in VE-cadherin and Cx37 co-localisation on addition of 8-pCPT.

VE-cadherin and Cx37 co-localisation in non-silencing siRNA-transfected HCAECs was quantified using Image J using the three Image J plugins (Figure 5.32D- 5.32F). On incubation with 5 µM 8-pCPT for 30 minutes, two of the plugins identified an increase in VE-cadherin and Cx37 co-localisation in the non-silencing siRNA-transfected HCAECs (Figures 5.32D & 5.32E), one of which was statistically significant (Figure 5.32D, unpaired students *t*-test, N=2). The third plugin identified no change in the proportion of VE-cadherin and Cx37 co-localisation (Figure 5.32F). This pattern is similar to that observed in control HCAECs, with an increase in VE-cadherin and Cx37 co-localisation on addition of 8-pCPT.

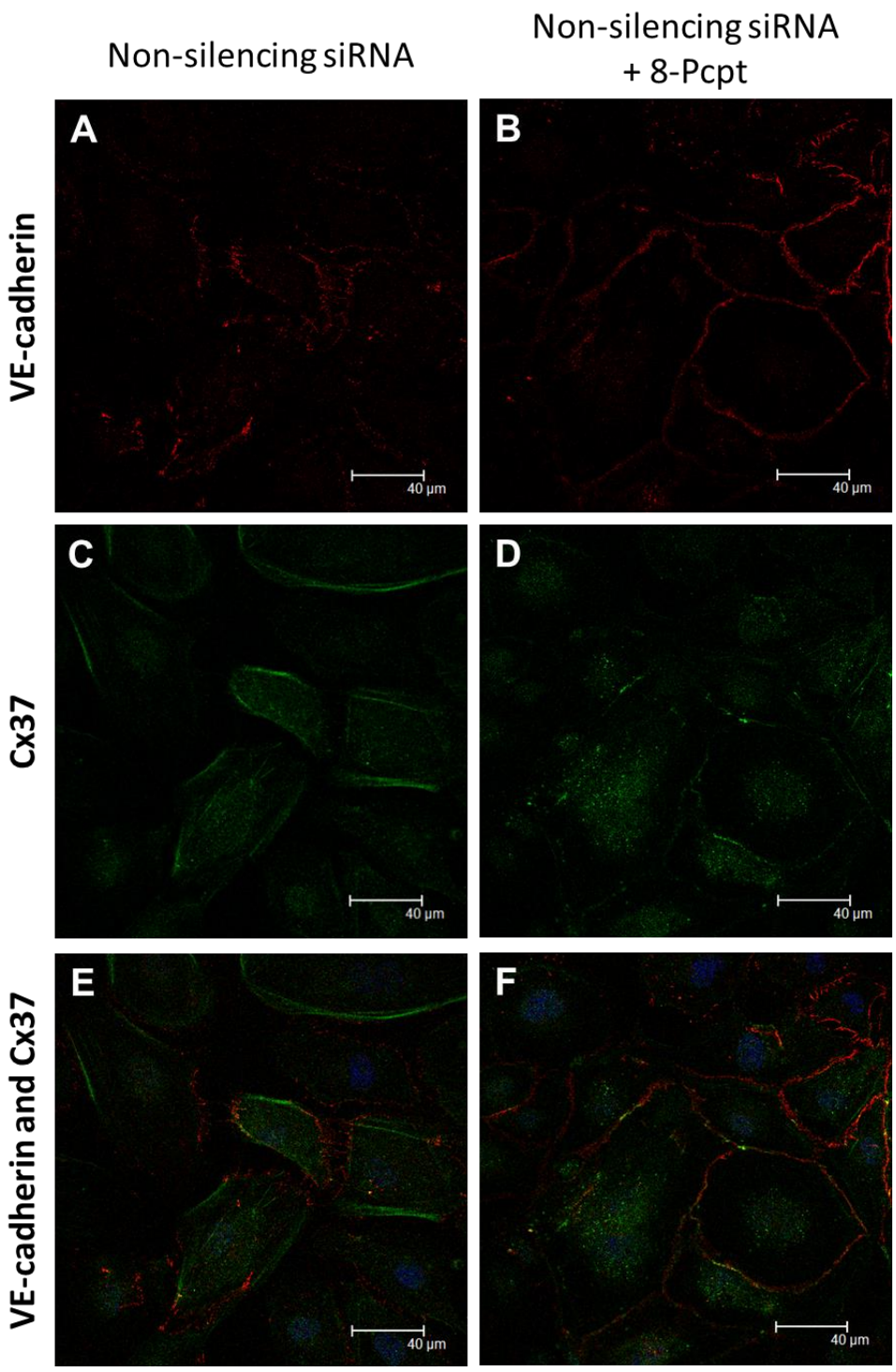

Figure 5.31: Immunocytochemistry of VE-cadherin and Cx37 expression following non-silencing siRNA transfection and addition of 8-pCPT

VE-cadherin (red, A & B) and Cx37 (green, C & D) distribution was identified in HCAECs treated with 10 nM non-silencing siRNA, with (B, D & F) or without (A, C & E) 8-pCPT (5 µM). Isolated areas of VE-cadherin and Cx37 co-localisation (yellow) were identified in un-stimulated non-silencing siRNA-transfected HCAECs (E). Slight increase in co-localisation was detected following addition of 5 µM 8-pCPT (F). DAPI nuclear staining is shown in blue. Antibody dilutions as previously detailed. N=1.

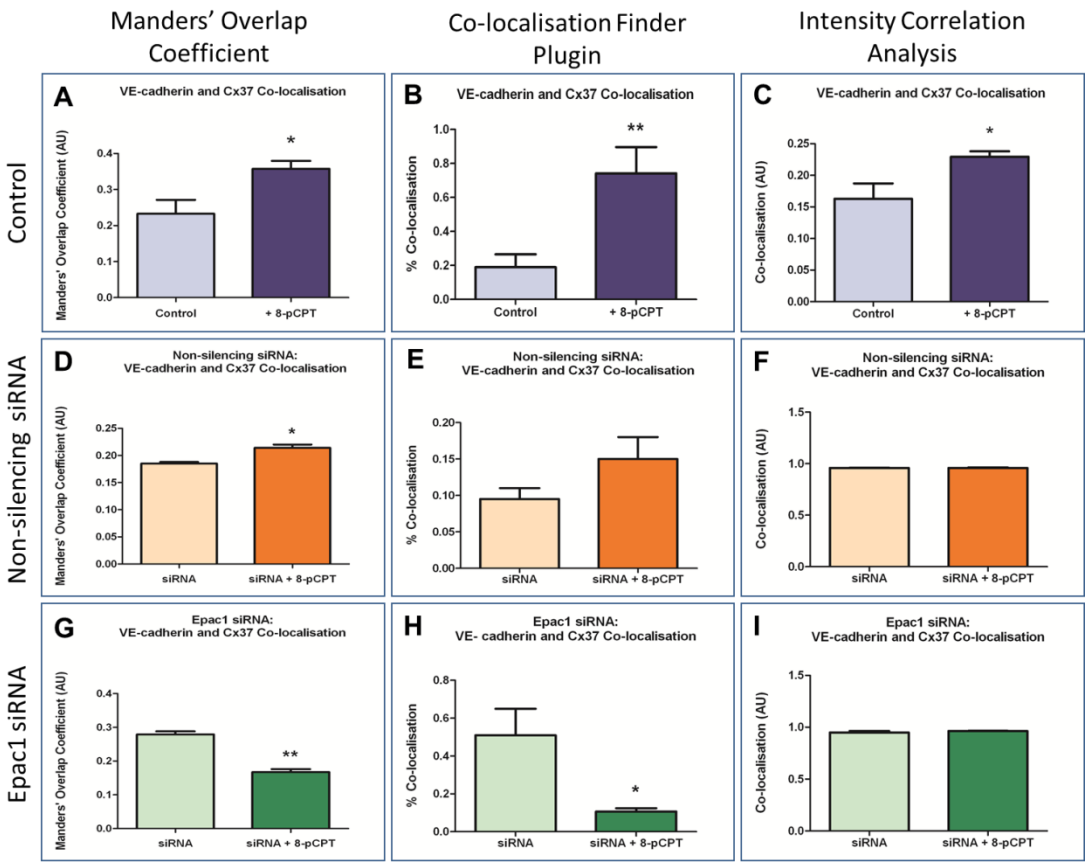

Figure 5.32: Quantification of VE-cadherin and Cx37 co-localisation in HCAECs following Epac1 siRNA transfection and addition of 8-pCPT

Under control conditions (A-C), addition of 5 µM 8-pCPT to HCAECs resulted in a significant increase in co-localisation of VE-cadherin and Cx37. HCAECs transfected with 10 nM non-silencing siRNA (D-F) displayed a similar pattern, with one plugin detecting a significant increase in co-localisation on 8-pCPT addition (D). HCAECs transfected with 10 nM Epac1 siRNA (G-I) showed a reversal of this pattern, with two plugins identifying a statistically significant decrease in co-localisation between VE-cadherin and Cx37 on 8-pCPT addition (G & H). (* $P<0.05$, ** $P<0.01$, unpaired student *t*-test). For A-C; N=6 for untreated cells and N=5 for 8-pCPT treatment. For D-F; N=2. For G-I; N=2 for untreated cells and N=3 for 8-pCPT treatment.

5.3.2.5.5.2 - VE-cadherin and Cx40

HCAECs transfected with 10 nM Epac1 siRNA (Hs_RAPGEF3_6 and Hs_RAPGEF3_7 duplexes) for 48 hours were labelled for VE-cadherin (red) and Cx40 (green) without, and following, 30 minutes incubation with 5 μM 8-pCPT (Figure 5.33). During preliminary experiments, labelling of VE-cadherin and Cx40 in Epac1 siRNA-transfected HCAECs (Figures 5.33A, 5.33C & 5.33E) identified areas of co-localisation (yellow) between these two junctional proteins, with a similar pattern to that observed in un-transfected HCAECs. On addition of 5 μM 8-pCPT (Figure 5.33B, 5.33D & 5.33F), VE-cadherin and Cx40 co-localisation appeared to decline (Figure 5.33F). Preliminary data indicated that membranous VE-cadherin did not become more continuous as observed in un-transfected cells treated with 8-pCPT (Figure 5.33B), and Cx40 appeared to show an increased association with the nucleus, as indicated by the DAPI nuclear staining (blue, Figure 5.33F).

VE-cadherin and Cx40 co-localisation in Epac1 siRNA-transfected HCAECs was quantified using three types of Image J plugins (Figure 5.34D- 5.34F). In un-transfected HCAECs, application of 5 μM 8-pCPT resulted in no significant change in VE-cadherin and Cx40 co-localisation in HCAECs (Figure 5.34A- 5.34C, unpaired *t*-test, N=4). In Epac1 siRNA-transfected HCAECs, application of 5 μM 8-pCPT resulted in a decrease in VE-cadherin and Cx40 co-localisation in two of the plugins (Figure 5.34D & 5.34E), one of which was statistically significant (Figure 5.34D, unpaired student *t*-test, N=4). The third Image J plugin identified no change in the proportion of VE-cadherin and Cx40 co-localisation (Figure 5.34F).

5.3.2.5.5.3 - VE-cadherin and connexin co-localisation following Epac1 siRNA transfection and addition of 8-pCPT - summary

Together, this data suggests that Epac1 knockdown blocks the increased VE-cadherin and Cx37 co-localisation in HCAECs triggered by 8-pCPT application. Furthermore, Epac1 knockdown also appears to decrease VE-cadherin and Cx40 co-localisation on addition of 8-pCPT.

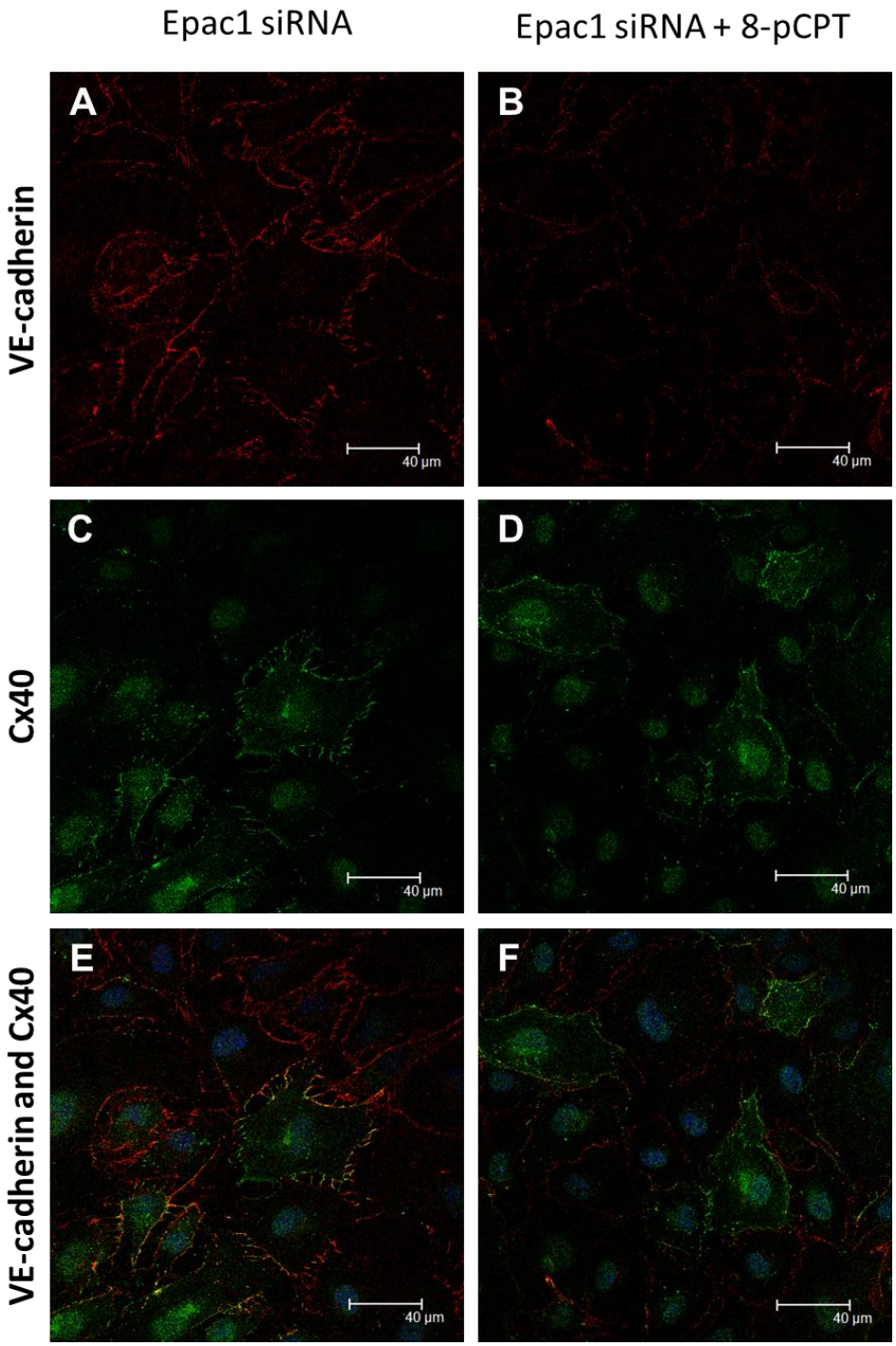

Figure 5.33: Immunocytochemistry of VE-cadherin and Cx40 expression following Epac1 siRNA transfection and addition of 8-pCPT

VE-cadherin (red, A & B) and Cx40 (green, C & D) distribution was identified in HCAECs treated with 10 nM Epac1 siRNA, with (B, D & F) or without (A, C & E) 8-pCPT addition (5 µM). Areas of VE-cadherin and Cx40 co-localisation (yellow) were identified in un-stimulated Epac1 siRNA-transfected HCAECs (E). This pattern appeared similar to that observed in un-transfected HCAECs. On addition of 5 µM 8-pCPT, VE-cadherin and Cx40 co-localisation appeared to decline (F). Cx40 showed strong nuclear-association, as indicated by the DAPI nuclear staining (blue, E & F). Antibody dilutions as previously detailed. N=1.

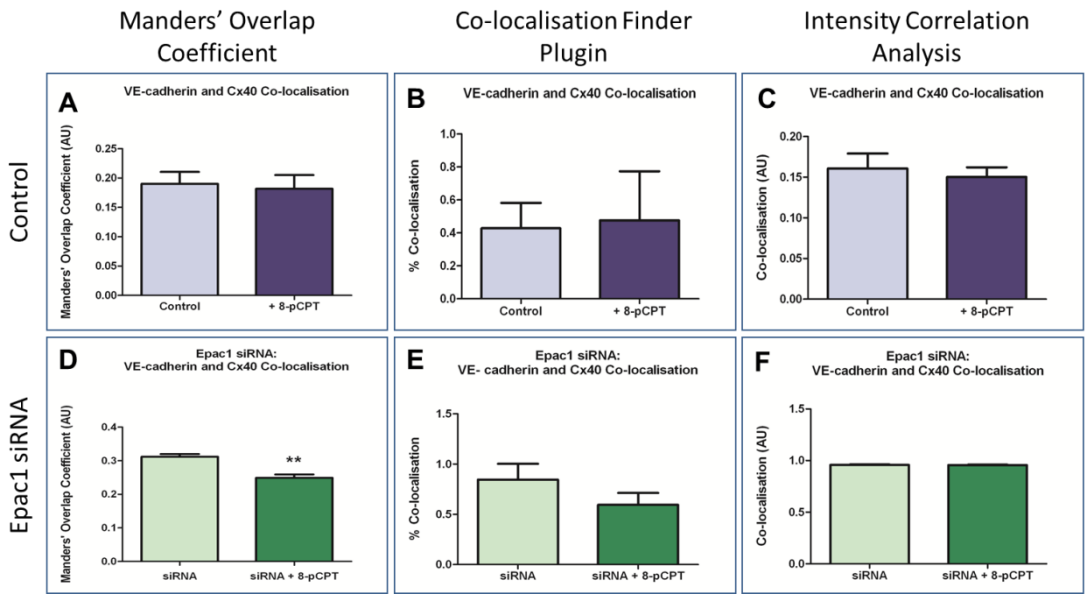

Figure 5.34: Quantification of VE-cadherin and Cx40 co-localisation in HCAECs following Epac1 siRNA transfection and addition of 8-pCPT

Under control conditions (A-C), addition of 5 µM 8-pCPT to HCAECs resulted in no significant change in co-localisation of VE-cadherin and Cx40. HCAECs transfected with 10 nM Epac1 siRNA are represented in D-F. The Manders' Overlap Coefficient plugin identified a significant decrease in co-localisation between VE-cadherin and Cx40 on addition of 8-pCPT (D). The Co-localisation Finder plugin showed a similar pattern, although not significant (E). The Intensity Correlation Analysis plugin identified no change in the co-localisation pattern of VE-cadherin and Cx40 on 8-pCPT addition (F). (** $P<0.01$, unpaired student *t*-test). For A-C; N=13 for untreated cells and N=5 for 8-pCPT treatment. For D-F; N=4.

5.3.2.6 - Epac antagonists

5.3.2.6.1 - VE-cadherin and Cx37 co-localisation following incubation with Epac antagonists and addition of 8-pCPT

Two types of Epac antagonists, ESI-09 and HJC0197, were used in preliminary experiments to examine the effect of Epac inhibition on the 8-pCPT-induced increase in VE-cadherin and Cx37 co-localisation.

5.3.2.6 1.1 - ESI-09

HCAECs were incubated with 5 nM ESI-09 for 10 minutes at 37˚C/ 5% CO_2 and labelled for VE-cadherin (red) and Cx37 (green) (Figure 5.35). Labelling of VE-cadherin and Cx37 in ESI-09-treated HCAECs (Figures 5.35A & 5.35C) identified isolated areas of co-localisation (yellow) between these two junctional proteins (Figure 5.35E). When HCAECs were treated with 5 µM 8-pCPT in the continued presence of ESI-09 (Figures 5.35B, 5.35D & 5.35F), a moderate increase in the co-localisation of VE-cadherin and Cx37 was detected (white arrows, Figure 5.35F).

5.3.2.6.1.2 - HJC0197

HCAECs were incubated with 5 nM HJC0197 for 10 minutes at 37˚C/ 5% CO_2 and labelled for VE-cadherin (red) and Cx37 (green) (Figure 5.36). Labelling of VE-cadherin and Cx37 in HJC0197-treated HCAECs (Figures 5.36A & 5.36C) identified isolated areas of co-localisation (yellow) (Figure 5.36E), a pattern similar to that observed under control conditions. On addition of 5 µM 8-pCPT in the continued presence of HJC0197 (Figures 5.36B, 5.36D & 5.36F), no increase in co-localisation between VE-cadherin and Cx37 could be detected in HCAECs pre-incubated with this antagonist.

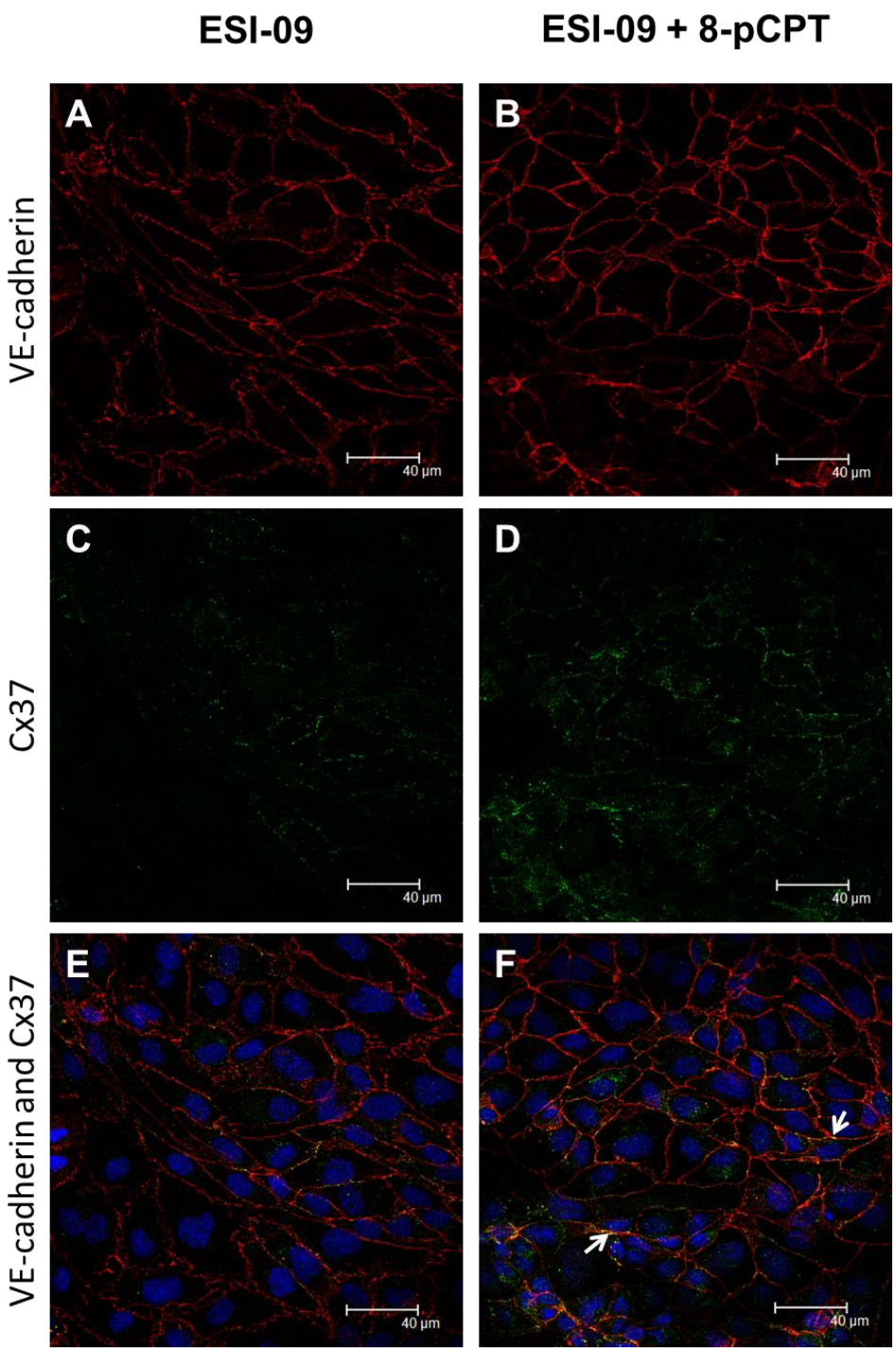

Figure 5.35: Immunocytochemistry of VE-cadherin and Cx37 expression following ESI-09 addition

VE-cadherin (red) and Cx37 (green) distribution was identified in HCAECs following 10 minutes incubation with 5 nM ESI-09 at 37˚C/ 5% CO_2 (A, C & E). Distribution of both junctional proteins appeared as in control conditions with isolated areas of overlap (yellow, E). Addition of 5 µM 8-pCPT, in the continued presence of ESI-09, for 30 minutes at 37˚C/ 5% CO_2 appeared to result in a slight increase VE-cadherin and Cx37 co-localisation at the membrane (white arrows, F). DAPI nuclear staining is shown in blue. Antibody dilutions as previously detailed. N=2.

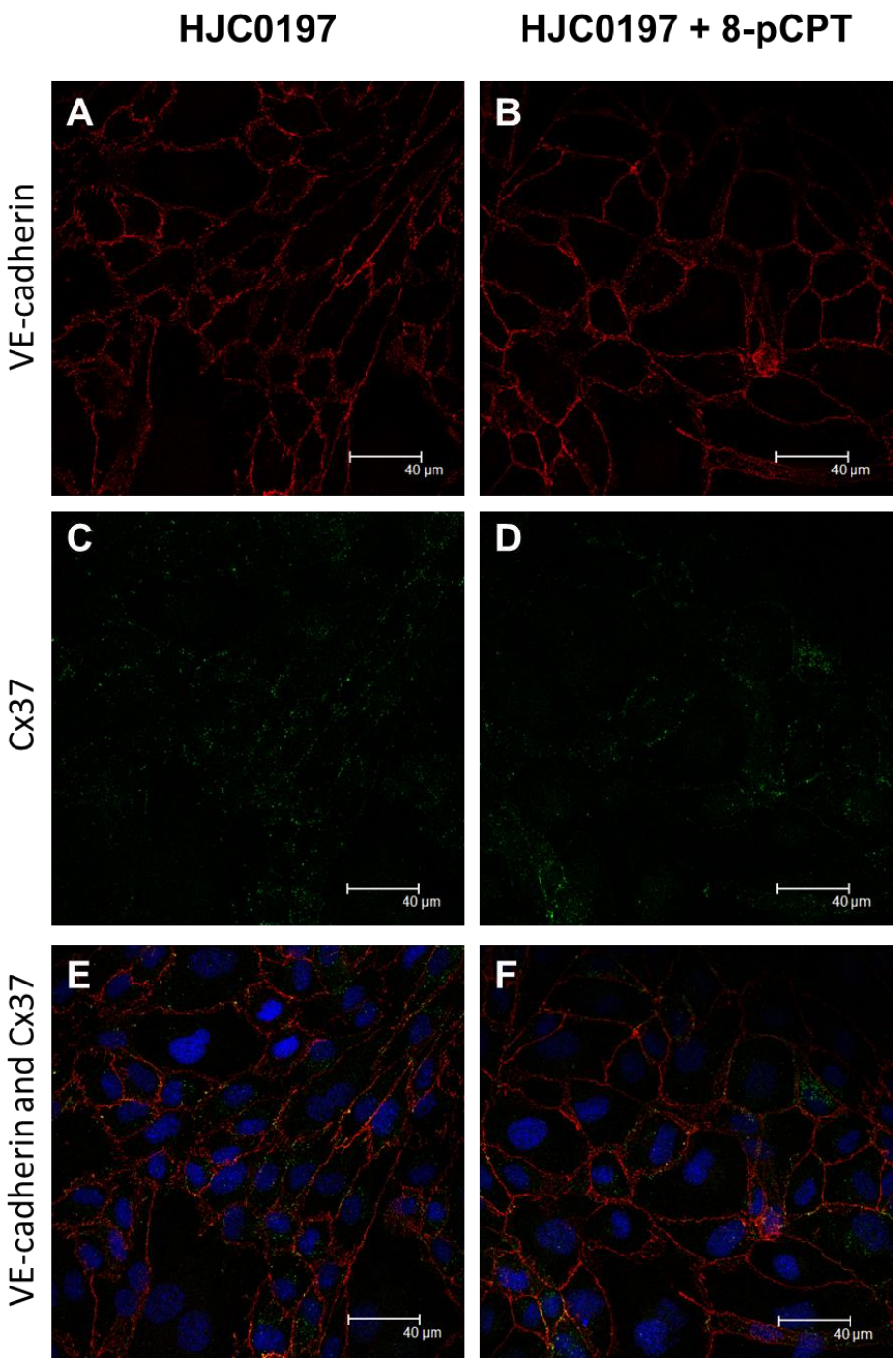

Figure 5.36: Immunocytochemistry of VE-cadherin and Cx37 expression following HJC0197 addition

VE-cadherin (red) and Cx37 (green) distribution was identified in HCAECs following 10 minutes incubation with 5 nM HJC0197 at 37˚C/ 5% CO_2 (A, C & E). Distribution of both junctional proteins appeared as in control conditions with minimal overlap (yellow, E). Addition of 5 µM 8-pCPT, in the continued presence of HJC0197, for 30 minutes at 37˚C/ 5% CO_2 resulted in little alteration in VE-cadherin and Cx37 distribution (B, D & F). No increase in VE-cadherin and Cx37 co-localisation could be detected following Epac activation. DAPI nuclear staining is shown in blue. Antibody dilutions as previously detailed. N=2.

5.3.2.6.1.3 - Quantification of VE-cadherin and Cx37 co-localisation following incubation with Epac antagonists and addition of 8-pCPT

VE-cadherin and Cx37 quantification following pre-treatment with the Epac antagonists ESI-09 and HJC0197 was analysed using three Image J plugins; Manders' Overlap Coefficient, Co-localisation Finder plugin and Intensity Correlation Analysis (Figure 5.37). Under control conditions, application of 5 µM 8-pCPT resulted in a significant increase in co-localisation between VE-cadherin and Cx37 (Figure 5.37A- 5.37C, unpaired student *t*-test, N=5-6). In ESI-09-treated HCAECs or HJC0197-treated HCAECs, application of 8-pCPT resulted in no significant change in co-localisation (Figure 5.37D- 5.37F & 5.37G- 5.37I, unpaired student *t*-test, N=7-9). Together, this data suggests that two Epac1 antagonists, ESI-09 and HJC0197, block the 8-pCPT-induced increased VE-cadherin and Cx37 co-localisation in HCAECs.

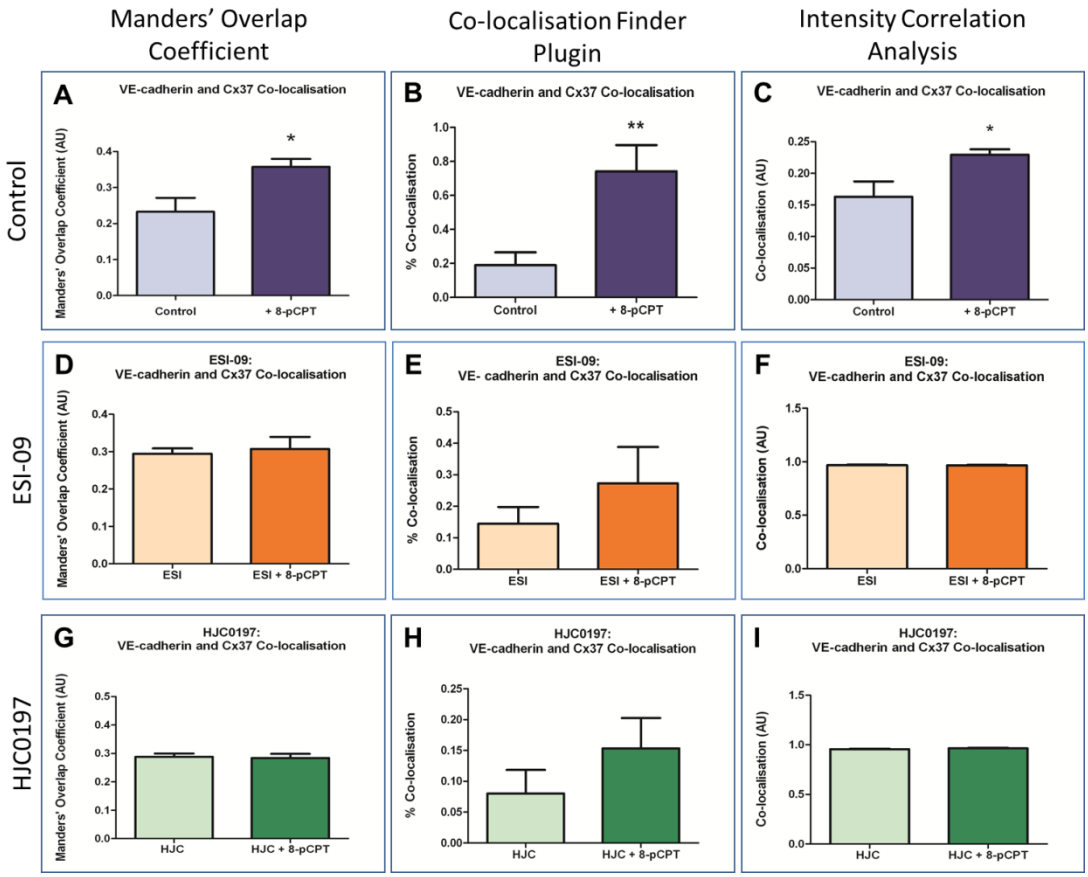

Figure 5.37: Quantification of VE-cadherin and Cx37 co-localisation in HCAECs following incubation with Epac antagonists ESI-09 and HJC0197

A-C represent co-localisation of VE-cadherin and Cx37 in HCAECs under control conditions. All three Image J plugins identified a significant increase in co-localisation following addition of 5 µM 8-pCPT for 30 minutes. When HCAECs were pre-incubated for 10 minutes with the 5 nM of the Epac antagonist ESI-09, 8-pCPT induced no significant change in VE-cadherin and Cx37 co-localisation (D-F). Similarly, pre-incubation with 5 nM HJC0197 for 10 minutes resulted in no significant effect on VE-cadherin and Cx37 co-localisation following 8-pCPT addition (G-I). (* $P<0.05$, ** $P<0.01$, unpaired student *t*-test) For A-C; N=6 for untreated cells and N=5 for 8-pCPT treatment. For D-F; N=7. For G-I; N=8 for untreated cells and N=9 for 8-pCPT treatment.

5.4 – Discussion

5.4.1 - Disruption of HCAEC cadherin interactions

The effect of adherens junction disruption on the distribution pattern of VE-cadherin and connexins 37, 40 and 43 was examined by two methods: (i) blocking of VE-cadherin interactions by pre-incubation with the anti-VE-cadherin primary antibody, and, (ii) disruption of calcium-dependent VE-cadherin homotypic binding by removal of extracellular calcium by EGTA treatment. Under both conditions, preliminary data indicated that adherens junction disruption had a subsequent effect on HCAEC morphology and distribution patterns of VE-cadherin and connexins. Under control conditions, HCAEC morphology is flattened, forming an almost continuous sheet of cells (Figure 5.2A and Figure 5.4A & 5.4C). Following either 5 hours pre-incubation with 10 µg/ml of the anti-VE-cadherin primary antibody (Figure 5.2B), or 30 minutes calcium-chelation with 5 mM EGTA (Figure 5.4B & 5.4D), adherens junctions were successfully disrupted and the HCAECs broke apart from each other forming isolated clusters of rounded cells. The degree of isolation was more extensive following the EGTA treatment. This indicates a small contribution of N-cadherin-mediated adherens junctions, which would not be disrupted by pre-incubation with the anti-VE-cadherin primary antibody. In support of this data, Meyer *et al.* (1992) identified that treatment of re-aggregating Novikoff hepatoma cells with Fab fragments of antibodies for N-cadherin blocked adherens junction formation and increased inter-membrane distances (Meyer, Laird et al. 1992). Moreover, on removal of extracellular calcium several groups have noted a vigorous contraction of cells away from each other, an effect hypothesised to be mediated by the junctional microfilament belt (Volberg, Geiger et al. 1986, Volk, Volberg et al. 1990, Kartenbeck, Schmelz et al. 1991).

On adherens junction disruption (either through pre-incubation with the anti- VE-cadherin primary antibody or through calcium chelation), VE-cadherin became restricted to specific sites of the cell membrane, losing its even distribution throughout the plasma membrane (white arrows in Figure 5.2B and Figure 5.4B). No noticeable change in N-cadherin distribution could be detected on EGTA treatment (Figure 5.4D). Cullere *et al.* (2005) also identified a loss of VE-cadherin expression at junctional sites on incubation of human pulmonary artery ECs (HPAECs) in low calcium medium for 8 hours (Cullere, Shaw et al. 2005). Furthermore, Alexander *et al.* (1998) hypothesised that this loss of membrane-associated VE-cadherin on calcium chelation was likely to be a result of endocytosis of the protein (Alexander, Jackson et al. 1998), a theory that may account for the accumulation of

VE-cadherin at restricted membrane sites and the cytoplasmic aggregations observed. This theory is supported by the identification of detached zonula adherens plaques containing E-cadherin within endocytic vesicles on removal of extracellular calcium in bovine kidney epithelial cells (Kartenbeck, Schmelz et al. 1991).

The re-distribution pattern of VE-cadherin was similar to that observed during preliminary experiments for connexin 37, in particular, after VE-cadherin antibody block and EGTA treatment (Figure 5.3D and Figure 5.6A). Moderate re-distribution of Cx40 was observed after pre-treatment with the anti- VE-cadherin primary antibody (Figure 5.3E), but no obvious change in the distribution pattern of Cx43 could be detected after either treatment (Figure 5.3F and Figure 5.8A). In support of this, treatment of teratinocarcinoma PCC3 cells with the anti-E-cadherin primary antibody (ECCD-1) resulted in a 4-5% decrease in Lucifer yellow dye transfer between cells, directly reflecting the decrease in gap junctional intercellular communication (Kanno, Sasaki et al. 1984). A similar decline in gap junction-mediated communication on cadherin disruption was also observed in Novikoff cells (Meyer, Laird et al. 1992). Interestingly, this group also identified antibody Fab fragments for the first or second extracellular domains of Cx43 to have a negative effect on both adherens junction formation and gap junction formation, despite cells displaying inter-membrane distances similar to those recorded at non-junctional regions of control cells (Meyer, Laird et al. 1992). The effect of calcium disruption on gap junctions has also been examined and it is generally accepted that gap junctions split on removal of extracellular calcium (Jansen, De Vrije et al. 1996, Perkins, Goodenough et al. 1997). Interestingly, it appears that unlike cadherins, disrupted connexins may persist at the membrane, with Perkins *et al.* (1997) identifying that gap junction channels disrupted by EGTA treatment maintained their connexon lattice pattern at each opposing membrane (Perkins, Goodenough et al. 1997). This is further supported by the identification of functional non-junctional Cx37 and Cx40 hemichannels in monocytes (Wong, Christen et al. 2006) and neonatal mouse atrial and ventricular cardiomyocytes (Xu, Kopp et al. 2012), respectively.

During preliminary experiments, the effect of calcium removal was shown to be reversible as cadherin- and connexin-mediated cell-cell contacts started to re-form after 1 hour calcium restoration (Figures 5.5B, 5.6B, 5.7B & 5.8B), and cells appeared as under control conditions after 4 hours calcium restoration (Figures 5.9B, 5.10B, 5.11B & 5.12B). This result is supported by the literature where restoration of extracellular calcium promotes re-

formation of cell-cell contacts and gap junctional intercellular communication within 45 minutes (Cullere, Shaw et al. 2005).

Addition of the anti-VE-cadherin primary antibody to the calcium-restoration phase of preliminary experiments effectively blocked the return to control conditions (Figures 5.5C, 5.6C, 5.7C & 5.8C), indicating the requirement for VE-cadherin-mediated adherens junctions for the formation of cell-cell contacts in HCAECs. Pre-treatment with the anti-N-cadherin primary antibody was not utilised as a method for adherens junction disruption as the antibody used in our experiments targeted the cytoplasmic tail of the protein and as such could not be used in un-permeabilised live cells.

5.4.2 – The effect of Epac activation on HCAECs

5.4.2.1 - Epac immunocytochemistry following 8-pCPT addition

In order to determine the effect of 8-pCPT on Epac localisation, immunocytochemical experiments were carried out using HCAECs (Figure 5.16). In un-stimulated cells, Epac1 is thought to be distributed throughout the cell with staining evident at the nuclear envelope, in the nucleus, at the plasma membrane, at endomembranes and in the cytosol (Ponsioen, Gloerich et al. 2009). During preliminary experiments, such a pattern was evident in HCAECs under control conditions (Figure 5.16A). Within 5 minutes of 8-pCPT application (5 µM) Epac1 was found to re-organise into small cytoplasmic aggregations (Figure 5.16B) followed by an increased membranous distribution after 30 minutes (Figure 5.16C). Epac is directly and selectively activated by 8-pCPT. Ponsioen *et al.* (2009) identified that application of forskolin or 8-pCPT resulted in Epac1 translocation to the periphery of the cell, to within 7 nm of the plasma membrane, within 2 minutes. A similar response has also been identified for Epac2 (Li, Asuri et al. 2006). The translocation of Epac1 to the plasma membrane was found to be both cAMP-dependent and reliant on the DEP domain (Ponsioen, Gloerich et al. 2009, Consonni, Gloerich et al. 2012). As previously detailed, the DEP domain is responsible for membrane localisation of the Epac proteins, and disruption results in a primarily cytoplasmic distribution of Epac (De Rooij, Rehmann et al. 2000, Bos, De Rooij et al. 2001). This 90 amino acid residue globular domain is located within the regulatory region, and is closely associated with the cAMP-binding domain (Ballon, Flanary et al. 2006, Li, Tsalkova et al. 2011). In the presence of cAMP, Epac1 directly binds to the negatively-charged plasma membrane phospholipid phosphatidic acid (PA), thereby

localising Epac to the plasma membrane (Consonni, Gloerich et al. 2012). Importantly, this group identified that Epac1 mutants lacking the DEP domain fail to bind PA. cAMP increases solvent exposure of specific regions of the DEP domain in close association with arginine 82 (R82), a region identified as essential for cAMP-induced translocation of Epac (Ponsioen, Gloerich et al. 2009, Li, Tsalkova et al. 2011). R82 comprises part of the binding site for PA, therefore cAMP-induced conformational modification of the DEP domain enables direct interaction between Epac and the plasma membrane phospholipid PA, with increased binding after 30 minutes exposure to 8-pCPT (Consonni, Gloerich et al. 2012). The cAMP-induced re-distribution of Epac from the homogenous cytosolic pool was found to be diffusion-driven and not a result of active transport (Ponsioen, Gloerich et al. 2009, Consonni, Gloerich et al. 2012). This was supported by the persistence of cAMP-induced Epac translocation on disruption of either the actin cytoskeleton (via cytochalasin D) or of the microtubule network (via nocodazole) (Ponsioen, Gloerich et al. 2009). Furthermore, the cAMP-induced redistribution was found not to be a result of down-stream signalling involving Rap (Ponsioen, Gloerich et al. 2009). This group identified that over-expression of Rap1GAP, effectively blocking Rap1 and Rap2 activation, had no effect on Epac translocation (Ponsioen, Gloerich et al. 2009). Indeed, the DEP domain-mediated translocation of Epac to the plasma membrane was identified as a prerequisite for activation of Rap at this compartment, and appears to provide a means of selectively activating specific subcellular pools of Rap, thereby determining the downstream signalling pathway to be activated (Ponsioen, Gloerich et al. 2009). In the current study, when HCAECs were treated with 8-pCPT for 5 minutes, Epac1 appeared to organise into cytoplasmic aggregations (Figure 5.16B). This may suggest the use of vesicular structures for transport of Epac1 to the membrane, an occurrence that was not identified by Ponsioen *et al.* (2009). The existance of a pool of Rap1 at the Golgi complex has previously been detailed (Section 5.15). Furthermore, Berger *et al.* (1994) identified that Rap1 is partly localised to vesicular structures and translocated to the membrane on activation in platelets and T-lymphocytes (Berger, Quarck et al. 1994). On activation, a subset of Epac1 may associate with, and activate, this compartment of Rap1, and be transported with it to the plasma membrane via such vesicular structures. This hypothesis would account for the cytoplasmic aggregations observed after 5 minutes treatment with 8-pCPT.

5.4.2.2 - Cadherin immunocytochemistry following 8-pCPT addition

The effect of Epac activation on the distribution of VE-cadherin and N-cadherin in HCAECs was examined using immunocytochemistry techniques (Figure 5.17 and Figure 5.18). Addition of 8-pCPT to HCAECs during preliminary experiments appeared to result in a reduction of distinct areas of N-cadherin near-membrane staining, with an increased cytosolic distribution (Figures 5.18C & 5.18D). During similar experiments, application of 8-pCPT to HCAECs triggered a re-distribution of VE-cadherin to form a continuous border at the membrane (Figure 5.17C & 5.17D). This re-distribution was blocked by transfection of HCAECs with Epac1 siRNA (Figure 5.29C). These preliminary results were consistent with previous findings (Cullere, Shaw et al. 2005, Fukuhara, Sakurai et al. 2005, Kooistra, Corada et al. 2005). Indeed, work by Fukuhara *et al.* (2005) identified that 0.2 mM 8-pCPT was sufficient to dramatically reduce basal endothelial permeability, implying a tighter membrane barrier and more adherens junctions, within 30 minutes. This pattern directly matches that observed in HCAECs (Figures 5.17C & 5.17D). In addition to a decrease in basal permeability, the increase in endothelial permeability induced by application of the pro-inflammatory mediator thrombin was also inhibited by 40% on addition of 100 µM 8-pCPT (Cullere, Shaw et al. 2005, Fukuhara, Sakurai et al. 2005). A similar result was observed for vascular endothelial growth factor (VEGF)-induced vascular permeability *in vivo* (Fukuhara, Sakurai et al. 2005). The effect of 8-pCPT on VE-cadherin distribution was replicated on application of the cAMP-elevating agents forskolin (FSK) and prostacyclin (PGI2), and the effects of all three were insensitive to application of the PKA inhibitor H89 (Fukuhara, Sakurai et al. 2005). The inhibitory effect of H89 on PKA was confirmed by inhibition of phosphorylation of CREB (Fukuhara, Sakurai et al. 2005). Furthermore, introduction of the constitutively active form of Epac (EpacΔcAMP) resulted in increased VE-cadherin-mediated adhesion, again suggesting Epac as the mediator of the cAMP-induced increase in membranous VE-cadherin (Fukuhara, Sakurai et al. 2005). The decrease in endothelial permeability was entirely dependent upon Epac1 activation, and not Epac2, as shown by transfection of endothelial cells with Epac1 siRNA (Kooistra, Corada et al. 2005). Together these results suggest that the cAMP-induced increase in membranous VE-cadherin occurs via a PKA-independent pathway that involves Epac1. Epac is a GEF for the small G-protein Rap and functions to convert it to its active GTP-bound state (Section 5.15). The role of Rap in the Epac-mediated re-distribution of VE-cadherin was elucidated through the introduction of the constitutively active form of Rap1 and several Rap1GAPs (Fukuhara, Sakurai et al. 2005). The constitutively active form of Rap1, $Rap1^{V12}$, reduced both basal and

thrombin-induced endothelial permeability, and increased VE-cadherin-mediated adhesion (Fukuhara, Sakurai et al. 2005). Rap1GAPII inactivates endogenous Rap1 and resulted in an increase in basal endothelial permeability and a decrease in the number of adherens junctions. Furthermore, this GAP also prevented the reduced permeability and increased VE-cadherin-mediated adherens junctions induced by both FSK and PGI2 (Fukuhara, Sakurai et al. 2005). This data therefore suggests that the cAMP-induced increase in membranous VE-cadherin occurs via the Epac/Rap1 pathway.

cAMP elevation has also been shown to have an effect on the distribution pattern of N-cadherin in neonatal rat cardiac myocytes (NRCMs) (Somekawa, Fukuhara et al. 2005). In these cells, application of db-cAMP or 8-pCPT induced enhanced N-cadherin distribution at cell-cell contacts (Somekawa, Fukuhara et al. 2005). The PKA-specific agonist, 6-Bnz-cAMP, had no effect on the distribution pattern of N-cadherin and therefore the Epac pathway mediated the cAMP-induced increase in membranous N-cadherin (Somekawa, Fukuhara et al. 2005). Much like VE-cadherin, this increased accumulation of N-cadherin at the membrane was also inhibited by a Rap1GAP, Rap1GAP1, and therefore this re-distribution is also a result of the Epac/Rap pathway (Somekawa, Fukuhara et al. 2005). No increase in membranous N-cadherin could be detected in HCAECs on 8-pCPT application (Figure 5.18C & 5.18D). Indeed, cells appeared to show a decline in membranous N-cadherin, and an increase in the cytoplasmic distribution of this protein, on Epac activation. VE-cadherin is known to show dominance over N-cadherin for expression at the membrane (Section 4.4.11), with the VE-cadherin cytoplasmic tail promoting N-cadherin exclusion from sites of cell-cell contact (Navarro, Ruco et al. 1998). It therefore seems logical that an increase in membranous VE-cadherin may result in a decrease in membranous N-cadherin. The vascular endothelial cell-specific cadherin, VE-cadherin, is not expressed in cardiac myocytes and so N-cadherin does not need to compete for membrane association.

There is currently no general consensus on the mechanism by which Epac results in VE-cadherin re-distribution. The literature does suggest three potential mechanisms and these are discussed below.

5.4.2.2.1 - Epac activation promotes actin re-organisation

Maintenance of endothelial barrier function requires a cortical actin ring. Epac activation has previously been shown to induce an increase in cortical actin, and a decrease in actin stress fibres, via the Epac1 /Rap1 /Rac1 / Arp2/3 complex pathway (Section 5.1.9 – Rap1 activates Rac through Tiam1 and Vav2). Maturation and stabilisation of the adherens junction requires attachment of the cadherins to the actin cytoskeleton (Section 1.7 – Adherens junctions and Section 4.1.2 - Cadherins). PGI2 and FSK application have been shown to increase the proportion of VE-cadherin anchored to the cytoskeleton (Fukuhara, Sakurai et al. 2005). Application of the actin de-polymerising agent Cytochalasin D inhibited the FSK-induced barrier enhancement and increase in VE-cadherin-mediated cell adhesions (Fukuhara, Sakurai et al. 2005). This data suggests that Epac activation increases the formation of cortical actin at the periphery of the cell which directly stabilises VE-cadherin-mediated adherens junctions. Rap1 also stabilises adherens junctions through its effector, cerebral cavernous malformation-1 protein (CCM-1) (Lampugnani, Orsenigo et al. 2010). CCM-1 associates indirectly with VE-cadherin through β-catenin (Lampugnani, Orsenigo et al. 2010), and mutations in human CCM-1 result in defective endothelial cell-cell junctions and abnormal vasculature (Dejana, Tournier-Lasserve et al. 2009).

The permeability-inducing agent thrombin promotes increased phosphorylation of myosin light chain (MLC) through the calcium/calmodulin-dependent MLC kinase (MLCK), resulting in a loss of peripheral β-catenin and increased stress fibre formation (Tinsley, De Lanerolle et al. 2000). Due to its linkage to the cytoskeleton through its interaction with catenins, VE-cadherin can be physically pulled out of contact with its binding partner on an adjacent cell as a result of actin stress fibre-mediated cell contraction (Moy, Van Engelenhoven et al. 1996). The Epac/Rap pathway is further implicated in the decrease in actin stress fibres through inhibition of the Rho pathway, activation of which produces actin stress fibres (Ridley and Hall 1992). Therefore, both the increase in cortical actin, and the resulting decrease in actin stress fibres, mediated by Epac activation act to stabilise adherens junctions.

The Rac pathway is also involved in the increase in cortical actin observed during angiogenesis (Lee, Thangada et al. 1999, Garcia, Liu et al. 2001) and in the response to osmotic stress (Ciano, Nie et al. 2002). During angiogenesis, activated platelets release the phosphorylated lipid growth factor sphingosine 1-phosphate (Sph-1-P) which binds to Edg G-protein-coupled receptors on endtothelial cells. This rapidly triggers Rac GTPase

activation which directly activates P21-associated Ser/Thr kinase (PAK). PAK then promotes phosphorylation of the actin filament regulatory protein cofilin, through LIM kinase activation, and ultimately results in an increase in cortical actin. PAK and its downstream effectors may therefore also play a role in the Epac-induced increase in cortical actin.

5.4.2.2.2 - The phosphorylation state of cadherin proteins affects adherens junction formation

The ability of VE-cadherin to form mature adherens junctions is also determined by its phosphorylation state. Phosphorylation of cadherins at tyrosine residues correlates with a decrease in adhesive strength (Lampugnani and Dejana 1997). The pro-inflammatory mediator thrombin, which increases endothelial permeability, promotes disassembly of the adherens junction complex and/ or VE-cadherin internalisation through cadherin phosphorylation (Harris and Nelson 2010). VEGF stimulation triggers Src tyrosine kinase-mediated phosphorylation of VE-cadherin on Y658 and Y731, and tyrosine phosphorylation of β-catenin (Wallez, Cand et al. 2007, Monaghan-Benson and Burridge 2009). Y658 is located within the VE-cadherin binding site for p120 catenin (Potter, Barbero et al. 2005) and its phosphorylation prevents VE-cadherin/ p120 catenin interaction, and thus the formation of a mature adherens junction. Similarly, the VEGF-induced Y731 phosphorylation disrupts VE-cadherin association with β-catenin (Potter, Barbero et al. 2005, Bubik, Willer et al. 2012). Protein tyrosine phosphatases (PTPs) associate with, and dephosphorylate, VE-cadherin. Vascular endothelial receptor-type PTP (VE-PTP) is endothelial cell-specific and enhances VE-cadherin-mediated cell adhesion (Nawroth, Poell et al. 2002). PTPμ is an additional PTP restricted to endothelial cells (Hellberg, Burden-Gulley et al. 2002). PTPμ binds RACK1 which is a membrane anchoring protein for active PKCε (Besson, Wilson et al. 2002). The Epac1 / Rap1/ PLCε- mediated activation of PKCε has previously been detailed (Section 5.1.11 – The role of Protein Kinase C in the Epac pathway). This may therefore provide a pathway through which PTPμ is recruited to the membrane resulting in signalling that promotes increased VE-cadherin dephosphorylation and enhanced adherens junction formation. Downstream signalling mediated by PKC has also previously been shown to result in dephosphorylation of p120 catenin (Ratcliffe, Smales et al. 1999). RACK1 is also capable of binding the SH2 domain of Src kinase which directly inhibits its kinase activity and prevents VE-cadherin phosphorylation (Hellberg, Burden-Gulley et al. 2002). Signalling induced by PKC has also previously been shown to

result in dephosphorylation of serine-threonine residues of p120-catenin (Ratcliffe, Smales et al. 1999). The importance of dephosphorylation on the formation of adherens junctions is highlighted by the action of angiopoietin-1. This anti-permeability agent promotes endothelial cell barrier function through a decrease in VE-cadherin phosphorylation (Gamble, Drew et al. 2000, Lee, Won et al. 2011).

Vinculin is an actin-binding protein located close to the plasma membrane where actin microfilaments terminate (Geiger, Tokuyasu et al. 1980, Werth, Niedel et al. 1983). Phosphorylation of vinculin allows this protein to link adhesion plaques to the actin cytoskeleton via its tail binding to F-actin (Johnson and Craig 1995). Linkage of the adhesion plaque to the cytoskeleton stabilises the adherens junction. Epac activates PKCε via the Rap1-mediated activation of PLCε and the production of DAG (5.1.10 – Rap activates Phospholipase C). Epac may therefore promote the PKC-mediated phosphorylation of vinculin, directly stabilising adherens junctions.

Interestingly, the hawthorn (Crataegus spp.) extract, WS 1442, which is a herbal treatment for moderate heart failure, appears to strengthen the endothelial barrier through the Epac pathway detailed here (Bubik, Willer et al. 2012). Thrombin-induced tyrosine phosphorylation of Tyr731 of VE-cadherin in HUVECs was blocked by WS 1442. Furthermore, WS 1442 application induced cortical actin rearrangement and a decrease in thrombin-induced F-actin stress fibre formation. Both effects were found to be mediated by the Epac1/Rap1/Rac1 pathway.

5.4.2.2.3 - Epac may enhance trafficking of VE-cadherin from the Golgi complex

VE-cadherin is trafficked from the Golgi complex to the cell surface in order to form nascent adherens junctions. In endothelial cells, Golgi-associated phospholipase A2α (cPLA2α) translocates from the cytoplasm to the Golgi complex in response to cell confluence (Regan-Klapisz, Krouwer et al. 2009). This movement of cPLA2α to the Golgi correlates with the formation of mature adherens junctions (Regan-Klapisz, Krouwer et al. 2009), which is stimulated on Epac activation (see above). Once at the Golgi, cPLA2α traffics VE-cadherin to the cell surface, thereby providing a positive feedback loop for Epac-induced VE-cadherin-mediated adherens junction formation. The requirement for mature VE-cadherin adherens junction for cPLA2α-mediated trafficking of VE-cadherin to the cell surface is shown by the reversion of cPLA2α translocation to the Golgi on incubation of

endothelial cells with VE-cadherin blocking antibodies (Regan-Klapisz, Krouwer et al. 2009). This thereby provides a pathway through which Epac may promote increased trafficking of VE-cadherin from the Golgi complex to the membrane.

5.4.2.3 - VE-cadherin and connexin co-localisation following 8-pCPT addition

To examine whether the Epac-induced re-distribution of VE-cadherin had an effect on the distribution of connexins 37, 40 and 43, the expression profile of these connexins, and the amount of co-localisation with VE-cadherin, was identified in HCAECs after 30 minutes treatment with 5 μM 8-pCPT during a series of preliminary experiments. On Epac activation, a significant increase in the co-localisation of VE-cadherin and Cx37 was seen in HCAECs (Figure 5.19 and Figure 5.22A- 5.22C). Similarly, an increase in co-localisation was also seen between VE-cadherin and Cx43 on Epac activation, however only one Image J plugin found this to be significant (Figure 5.21 and Figure 5.22G- 5.22I). No significant change in the co-localisation of VE-cadherin and Cx40 was identified in HCAECs treated with 8-pCPT during these experiments (Figure 5.20 and Figure 5.22D- 5.22F). Although the increase in co-localisation between VE-cadherin and connexins on application of 8-pCPT could primarily be a result of the re-distribution of VE-cadherin, the preliminary data clearly indicates an increase in membranous Cx37 on Epac activation (Figure 5.19D). The enhanced co-localisation between VE-cadherin and Cx37 on 8-pCPT application was inhibited by transfection of HCAECs with Epac1 siRNA (Figures 5.32G- 5.32I) and pre-incubation with the Epac antagonists HJC0197 (Figures 5.37G- 5.37I) and ESI-09 (Figures 5.37D- 5.37F).

The literature on the effect of elevations in intracellular cAMP concentration on Cx37 distribution is sparse. Many studies have, however, identified an increase in near-membrane Cx43 and increased gap junction intercellular communication (GJIC) on cAMP application (Saez, Spray et al. 1986, Mehta, Yamamoto et al. 1992, Atkinson, Lampe et al. 1995, Burghardt, Barhoumi et al. 1995).

Changes in the distribution of connexins can be achieved through differential regulation of the stages involved in intercellular channel formation, including alterations in the rate of synthesis or degradation of connexin mRNA (Mehta, Yamamoto et al. 1992), the transport and oligomerisation of connexins (Musil and Goodenough 1991, Musil and Goodenough 1993), the phosphorylation state of the connexin proteins (Saez, Spray et al. 1986, Van Rijen, Van Veen et al. 2000, Duncan and Fletcher 2002), the intercellular distance between

adjacent cells (Keane, Mehta et al. 1988, Meyer, Laird et al. 1992), and the internalisation of gap junctional plaques (Saez, Gregory et al. 1989). The potential role of the cAMP/Epac pathway in the modulation of these factors is discussed here.

5.4.2.3.1 - Epac may promote enhanced connexin mRNA synthesis and transcription

Elevations in intracellular cAMP have been found to result in enhanced synthesis of connexin mRNA and an increased rate of transcription in a number of cells (Mehta, Yamamoto et al. 1992, Darrow, Fast et al. 1996, Van der Heyden, Rook et al. 1998). Work by Mehta *et al.* (1992) in communication-deficient rat Morris hepatoma cells (H5123) identified that forskolin addition resulted in a 15-40 fold elevation in Cx43 mRNA, accompanied by a 6 fold increase in the Cx43 transcription rate. This forskolin addition resulted in enhanced GJIC, as determined by electrical conductance and Lucifer yellow dye transfer (Mehta, Yamamoto et al. 1992). Similar results were also observed both with 8-bromo-cAMP and the phosphodiesterase inhibitor Ro-20-1724 (Mehta, Yamamoto et al. 1992). These results, and similar findings by Darrow *et al.* (1996) and van der Hayden *et al.* (1998), however, were only observed after 3-6 hours. As our increase in near-membrane connexin 37 was observed after just 30 minutes it is unlikely that in these experiments enhanced mRNA synthesis or an increased transcription rate were responsible for the increase in membrane-associated Cx37. In addition, these results were induced by cAMP elevation and as such the effects may have been mediated by PKA signalling. Prolonged exposure of HCAECs to 8-pCPT may have a long-term effect on the distribution of connexins, but this was not examined here.

5.4.2.3.2 - Epac may enhance transport of connexin proteins to the plasma membrane on cAMP elevation

cAMP-elevating agents promote enhanced trafficking of connexin proteins from the Golgi apparatus to the plasma membrane in numerous cell types (Atkinson, Lampe et al. 1995, Burghardt, Barhoumi et al. 1995, Holm, Mikhailov et al. 1999, Paulson, Lampe et al. 2000). The use of a chimeric protein composed of Cx43 and a green fluorescent protein (GFP) in the rat liver epithelial cell line RLcl9 by Holm *et al.* (1999), revealed the truly dynamic nature of connexins in these cells. Addition of 20 μM forskolin resulted in the formation of nascent Cx43 gap junctions within 5-10 minutes and an increase in size of pre-existing

junctions. Similarly, work by Burghardt *et al.* (1995) has shown that addition of 1 mM 8-bromo-cAMP to these RLcl9 cells resulted in increased GJIC within 2 minutes. When pre-treated with 1 mM octanol, which reduces the open probability of gap junctions to near zero, effectively uncoupling the cells, 8-bromo-cAMP continued to restore GJIC within minutes (Burghardt, Barhoumi et al. 1995). To elucidate the factor responsible for the cAMP-induced enhanced GJIC, this group treated the cells with 10 μM monensin to inhibit distal Golgi function and block translocation from the trans Golgi network to the plasma membrane (Burghardt, Barhoumi et al. 1995). Monensin treatment prior to 8-bromo-cAMP addition reduced the 8-bromo-cAMP-mediated enhanced GJIC and resulted in an increase in vesicular Cx43. The role of enhanced trafficking of connexin proteins to the membrane on elevated levels of intracellular cAMP is further evidenced through work by Paulson *et al.* (2000) in Novikoff hepatoma cells. Treatment of these cells with forskolin resulted in enhanced trafficking of Cx43 from the endoplasmic reticulum and Golgi apparatus to the plasma membrane, with no change in the total amount of Cx43 protein or in the phosphorylation state of Cx43 over 2.5 hours (Paulson, Lampe et al. 2000). Furthermore, addition of 36 μM Brefeldin A to block intracellular trafficking inhibited the increase in gap junction assembly mediated by forskolin (Paulson, Lampe et al. 2000). Such nascent gap junctions formed within minutes of addition of cAMP-elevating agents were shown to be functional by Atkinson *et al.* (1995). This group showed that addition of 8-bromo-cAMP resulted in increased permeability within 30 minutes, without an increase in the total protein concentration of Cx43 (Atkinson, Lampe et al. 1995). Taken together, this data suggests that Epac may promote connexin re-distribution to the membrane through enhanced trafficking from the Golgi apparatus.

5.4.2.3.3 - Epac may promote connexin phosphorylation to increase GJIC

Connexins have been shown to be phosphoproteins either through a shift in their electrophoretic mobility, as determined by Western blot, or via direct incorporation of ^{32}P (Lampe and Lau 2000). Indeed, Cx26 is the only connexin reported to not be phosphorylated, potentially due to its short C-terminal tail (Traub, Look et al. 1989). The phosphorylation of connexins is generally considered to result in increased formation of functional gap junctions, and enhanced cell-cell communication (Saez, Spray et al. 1986, Van Rijen, Van Veen et al. 2000, Duncan and Fletcher 2002). Elevations in intracellular cAMP are able to trigger phosphorylation of connexins (Kuo and Greengard 1969, Musil, Cunningham et al. 1990). Application of 8-bromo-cAMP to primary rodent hepatocytes

results in a 1.6 fold increase in phosphorylated Cx32 within 30-60 minutes, and a subsequent 50-75% increase in GJIC (Saez, Spray et al. 1986). Similarly, addition of 300 µM 8-bromo-cAMP to mouse mammary tumour cells (MMT22) resulted in an increase in the phosphorylated form of Cx43, re-distribution of Cx43 into gap junction plaques and an increase in Lucifer yellow dye transfer within 30 minutes (Atkinson, Lampe et al. 1995). This increase in GJIC was determined to be a result of an increase in the number and size of functional gap junctions, as the total cellular content of Cx43 mRNA and Cx43 protein was unchanged (Atkinson, Lampe et al. 1995). Darrow *et al.* (1996) also identified an increase in the number and size of Cx43 and Cx45 gap junctions on application of db-cAMP to cultured cardiac myocytes. This group, however, also identified a 2-4 fold increase in the total amount of Cx43 and Cx45 protein (Darrow, Fast et al. 1996). The increased membranous Cx37 observed in HCAECs on Epac activation occurred within 30 minutes, and it therefore seems likely that phosphorylation plays a role in this increase. Epac activates the Rap1/ Rac1/ PLCε pathway to activate PKCε (Section 5.1.11 – The role of Protein Kinase C in the Epac pathway). Similarly, addition of the DAG mimetic TPA, results in PKC activation and phosphorylation of Cx43 within 5 – 10 minutes (Musil and Goodenough 1991). PKCε, specifically, has also been shown to co-localise with, and promote, connexin phosphorylation that results in increased GJIC (Doble, Ping et al. 2000, Duquesnes, Derangeon et al. 2010). Both Cx40 and Cx43 have been shown to express phosphorylation sites for PKC (Beyer, Reed et al. 1992, Lampe 1994, Traub, Eckert et al. 1994). Application of 1 mM 8-bromo-cAMP to communication-deficient human hepatoma cells (SKHep1) results in increased Cx40-mediated gap junction conductance and a 58% increase in Lucifer yellow dye transfer, accompanied by enhanced Cx40 phosphorylation (Van Rijen, Van Veen et al. 2000). Considerable debate still surrounds the effect of Cx43 phosphorylation on GJIC. Rapid turnover of Cx43 gap junctional plaques is associated with loss of phosphorylated forms of Cx43 (Laird, Castillo et al. 1995), however, several groups have identified that phosphorylation of this connexin results in inhibition of GJIC (Berthoud, Rook et al. 1993, Lampe, TenBroek et al. 2000). Specifically, Lampe *et al.* (2000) identified that PKC-mediated phosphorylation of Cx43 at Ser368 resulted in a decrease in GJIC, despite PKA-mediated phosphorylation of Cx43 at Ser364 enhancing GJIC (Paulson, Lampe et al. 2000, Tenbroek, Lampe et al. 2001). In contrast, Duquesnes *et al.* (2010) identified that PKCε-mediated phosphorylation of Cx43 increased GJIC through enhanced open state probability, an increase that was blocked by PKC inhibitors. Interestingly, van Veen *et al.* (2000) identified that TPA-induced PKC activation increased electrical conductance in Cx45-transfected HeLa

cells through enhancing the open state probability, but that this was not a result of a change in the phosphorylation status of the connexin proteins. In support of this, TPA-induced PKC activation in corpus cavernosum smooth muscle cells triggered an increase in the conductance of Cx43 gap junction channels within 15 minutes (Moreno, De Carvalho et al. 1993). This elevated GJIC was a result of a shift to a lower single channel unitary conductance, however both forskolin application and TPA addition also resulted in markedly elevated levels of Cx43 protein (Moreno, De Carvalho et al. 1993). The differential effects of TPA on GJIC may depend on the connexin phosphorylation state prior to TPA addition, the PKC isotype expressed in the cell investigated, and the experimental conditions. Kwak *et al.* (1995) identified that TPA-mediated activation of PKC increased gap junctional conductance but decreased permeability in neonatal rat cardiomyocytes. This resulted from a smaller pore size of the channel, ultimately restricting dye transfer, while open state probability or the number of channels was increased (Kwak, Van Veen et al. 1995). Therefore, if GJIC is determined by dye transfer this may not accurately quantify the channel open probability. PKA agonists have been shown to have no effect on the conductance of single gap junction channels in SKHep1 cells transfected with Cx43 (Kwak, Hermans et al. 1995). Together, this data suggests that PKC, specifically PKCε, is a potential regulator of the Epac-mediated enhanced co-localisation between VE-cadherin and Cx37 and Cx43 in HCAECs.

Calcium-dependent protein kinases may also play a role in the re-distribution of connexins observed after 8-pCPT application to HCAECs. Recently, calcium/calmodulin-dependent protein kinase II (CaMKII) has been found to increase conductance at Cx36 gap junctions in mouse neuroblastoma (Neuro2A) cells (Del Corsso, Iglesias et al. 2012). The Epac/Rap1/Rac1/PLC pathway results in calcium release from the endoplasmic reticulum via IP_3-mediated receptors (Section 5.1.10 – Rap activates Phospholipase C). 15 serine residues have been identified in the C-terminal of Cx43 that are capable of being phosphorylated by CaMKII (Huang, Laing et al. 2011). Furthermore, Cx35 in teleost Mauthner cells, an ortholog of the mammalian Cx36, has been found to co-localise with CaMKII and biochemical analysis has shown that the two proteins associate together (Flores, Cachope et al. 2010). Likewise, Cx36 itself has been found to co-localise with, and be phosphorylated by, CaMKII in the inferior olive region of the mammalian brainstem (Alev, Urscheld et al. 2008). Exposure of astrocytes to high potassium solutions induces an increase in Cx43-mediated dye coupling that is promoted by CaMKII, independent of any effect on Cx43 expression level or distribution (De Pina-Benabou, Srinivas et al. 2001). The

CaMKII-dependent nature of this increase in GJIC is shown by the inhibition of increased dye transfer or electrical coupling on addition of calmidazolium (an inhibitor of calmodulin-regulated enzymes) or KN-93 (a selective CaMKII inhibitor) (De Pina-Benabou, Srinivas et al. 2001). Interestingly, Cx43 again appears to display alternative responses to phosphorylation by this kinase, depending on the cell type. Increased intracellular calcium concentration (through ionomycin addition) in stable murine neuroblastoma (Neuro2A) cells expressing Cx43 reduced gap junction conductance by 95% (Xu, Kopp et al. 2012). The CaMKII 290-309 inhibitory peptide prevented this decline in GJIC. On examination, Cx43 gap junction channel open probability was found to decline to zero on external ionomycin addition. This group therefore concluded that in murine Neuro2A cells Cx43 gap junctions are gated closed by CaMKII activity. This is the opposite effect observed for Cx36 gap junctions in Neuro2A cells (see above) (Del Corsso, Iglesias et al. 2012). Together, this data suggests that calcium-dependent protein kinases may act to phosphorylate connexins on Epac activation, and subsequently regulate gap junction formation.

5.4.2.3.4 - The Epac-mediated actin rearrangement and adherens junction formation promotes gap junction formation

Epac activation activates the Rap1 / Rac1 / Arp2/3 complex pathway which results in cortactin phosphorylation, increased cortical actin formation and a decrease in actin stress fibres, all of which directly promote the formation of new adherens junctions (Section 5.1.9 – Rap1 activates Rac through Tiam1 and Vav2). This pathway is enhanced by the Epac-induced activation of PLCε (via Rap1) which converts PIP_2 into DAG and IP_3. DAG has a positive feedback effect on Rac1 activation. DAG also has the ability to activate PKC isoforms, specifically PKCε, the downstream signalling of which can trigger the de-phosphorylation or phosphorylation of various proteins, ultimately stabilising the cortical actin rim and the formation of nascent adherens junctions. The requirement for the formation of adherens junctions prior to the formation of functional gap junctions is well established in the literature (Section 4.4.13). It therefore seems logical that an increase in adherens junctions couples adjacent cells more tightly and an increased number of gap junctions are able to form. Blocking protein trafficking from the endoplasmic reticulum or Golgi complex does not prevent cAMP-induced clustering of Cx43 at the plasma membrane (Wang and Rose 1995). This finding suggests that a pool of plasma membrane-associated Cx43 must exist that is responsible, at least in part, for the cAMP-induced clustering of gap

junctions at sites of cell-cell contact. Furthermore, cAMP-mediated increased Cx43 gap junction assembly is still observed in cells incubated at 4°C, a temperature that inhibits vesicular trafficking (Li, Liu et al. 1996, Paulson, Lampe et al. 2000). This membranous Cx43 could serve as a reservoir of subunits to allow expansion of gap junction communication, and is activated on the Epac-induced actin rearrangement that promotes the formation of adherens junctions.

Connexins and cadherins have also previously been shown to be directly linked by their associated binding proteins (Section 4.4.13). Both Cx43 and VE-cadherin interact with β-catenin (Ai, Fischer et al. 2000) and ZO-1 (Toyofuku, Yabuki et al. 1998, Somekawa, Fukuhara et al. 2005). Indeed, the Wnt-1-induced increased expression of Cx43 at the plasma membrane in cardiac myocytes is due to the accumulation of β-catenin (Ai, Fischer et al. 2000). It is therefore possible that the increased accumulation of VE-cadherin near the plasma membrane on 8-pCPT addition results in translocation of connexins to the plasma membrane where they join their opposing connexin on an adjacent cell and form a functional gap junction. Furthermore, the clustering of Cx43 observed on elevation of intracellular cAMP by Wang and Rose (1995) was found to be enhanced by inhibition of glycosylation (via tunicamycin addition). Reduced glycosylation of N-cadherin results in increased formation of N-cadherin-containing adherens junctions (Guo, Johnson et al. 2009). This therefore suggests a direct link between enhanced adherens junction formation and increased clustering of Cx43 at the plasma membrane. Together, this data suggests that the actin rearrangement and the subsequent increased formation of adherens junctions mediated by cAMP-elevating agents or 8-pCPT, is likely to play a role in the increased membranous distribution of connexins observed in HCAECs.

5.4.3 – Concluding remarks

Taken together, this **preliminary** data suggests that cadherin disruption through incubation with both the anti-VE-cadherin primary antibody and EGTA has a direct effect on connexin distribution in HCAECs, particularly Cx37. Similarly, an increase in AJ formation induced by Epac activation promotes Cx37 re-distribution to near-membrane sites. This Epac-mediated enhanced cell-cell communication is hypothesised to be a result of actin reorganisation to form a strong cortical actin ring, enhanced transport of junctional proteins to the membrane and altered protein phosphorylation.

Chapter 6:

Functional effect of Epac activation in HCAECs

Aims of this chapter:

- To determine if the Epac-induced re-distribution of Cx37 enhances GJIC
- To examine the effect of Epac activation on intracellular calcium concentrations in HCAECs

Key findings of this chapter:

- Epac activation by 8-pCPT application resulted in increased Lucifer yellow dye transfer between HCAECs, as determined by scrape assay
- The Epac antagonist HJC0197 completely blocked the 8-pCPT-induced increase in dye transfer between HCAECs
- 8-pCPT application resulted in a transient increase in intracellular calcium, as reported by the calcium indicator Fluo-4
- The 8-pCPT-induced rise in intracellular calcium was largely unchanged by either removal of extracellular calcium, pre-incubation with ryanodine, or pre-incubation with PKI, a PKA inhibitor
- The 8-pCPT-induced rise in intracellular calcium was completely inhibited by the Epac antagonist HJC0197
- Forskolin application induced a rise in intracellular calcium in HCAECs. However, the profile of the calcium transient triggered by forskolin appeared to differ from that induced by 8-pCPT

6.1 - Introduction

Following immunocytochemical experiments where Epac activation in HCAECs led to an apparent increase in Cx37 distribution at the membrane (Chapter 5), the functional consequence of increased gap junctions was assessed. Quantification of Lucifer yellow dye transfer through a scrape assay was used to evaluate gap junction intercellular communication (GJIC) in HCAECs. The effect of Epac on the intracellular concentration of calcium, a second messenger that can be transferred via GJIC, was also examined.

6.1.1 - Selectivity of gap junction channels

The relative selectivity of different GJ channels is variable, and dependent upon the individual connexins forming the channel (Brink and Fan 1989, Elfgang, Eckert et al. 1995, Goldberg, Valiunas et al. 2004). Homomeric Cx32 gap junctions, for example, show no preference for cAMP or cGMP, while heteromeric GJ channels, composed of both Cx32 and Cx26, allow the preferential transfer of cGMP over cAMP (Bevans, Kordel et al. 1998). During keratinocyte differentiation, there is a switch in connexin expression from Cx43 and Cx26 to Cx31 and Cx31.1 that is accompanied by a decrease in the transfer of large molecules, such as the dye Lucifer yellow, which has a molecular weight of 443 Da (Stewart 1981), even though the cells remained electrically coupled (Brissette, Kumar et al. 1994). Indeed, connexins have single channel conductances that range from 20 picoSiemens (pS) to several hundrend pS, and homomeric Cx40 channels, for example, show electrical conductance of between 120-200 pS (Traub, Eckert et al. 1994, Beblo, Wang et al. 1995, Bukauskas, Elfgang et al. 1995).

6.1.2 – Gating of gap junction channels

Gap junction channels are sensitive to changes in both extracellular and intracellular conditions and can close in response to unsuitable or pathological conditions. This has a protective function, isolating the cell from its adjacent neighbours and preventing the spread of harmful signals or ion concentrations. As such, GJ channels are particularly sensitive to changes in voltage, phosphorylation, pH or calcium concentration. Despite this, even at transjunctional voltages of 40 mV and pH6.8, GJs can have open probabilities of between 0.6-0.9, indicating that most GJ channels are gated-open more often than gated-closed (Christ and Brink 1999, Goldberg, Valiunas et al. 2004). This high resting open-state

probability explains the requirement for selective permeability of different GJ channels, as detailed above. Calcium was the first cytoplasmic factor to be identified in the regulation of GJ function, with increases in the cytoplasmic concentration of calcium decreasing GJIC (Rose and Loewenstein 1976, Loewenstein 1981, Evans and Martin 2002). The gating of GJ channels is also regulated by intracellular acidity. The C-terminus of Cx43, for example, is pH-sensitive and has been implicated in the gating of Cx43-containing GJ channels on changes in intracellular pH (Morley, Taffet et al. 1996). During this process, the mechanism of closing appears to operate via the ball-and-chain model, whereby a cytoplasmic region of the protein effectively closes the channel pore (Morley, Taffet et al. 1996). Changes in voltage also affect the gating-state of the GJ channel. In amphibian blastomeres, junctional conductance is maximal at zero transjunctional voltage, and is rapidly decreased by movement towards either polarity (Spray, Harris et al. 1979, Harris, Spray et al. 1981). The phosphorylation state of the components of the GJ channel also determines the gated-state of the channel. Increases in tyrosine phosphorylation of Cx43, for example, decreased GJIC in various cell types including rat microvascular endothelial cells (Moreno, Sáez et al. 1994, Cai, Jiang et al. 1998, Lidington, Tyml et al. 2002). Phosphorylation of connexins can also alter the rate of channel assembly, with phosphorylation of serines 325, 328 or 330 on Cx43 increasing Cx43 GJ formation (Cooper and Lampe 2002).

6.1.3 - Calcium in endothelial cells

Calcium is a major second messenger in endothelial cells, and can be exchanged directly between both endothelial cells, and endothelial cells and smooth muscle cells, via gap junctions. The endoplasmic reticulum (ER) accounts for approximately 75% of the total intracellular calcium reserve in endothelial cells (Tran, Ohashi et al. 2000), and the total ER calcium concentration can reach up to 3 mM (Sambrook 1990, Meldolesi and Pozzan 1998). Mitochondria account for the remaining calcium reserve, and mitochondrial calcium is typically released following release of calcium from the ER, in a process termed mitochondrial calcium-induced calcium release (mCICR)(Tran, Ohashi et al. 2000).

6.1.3.1 – Calcium release from the endoplasmic reticulum

In endothelial cells, calcium release from the ER is generally considered to be mediated by IP_3-induced opening of IP_3R channels (Tran, Ohashi et al. 2000, Plank, Wall et al. 2006). IP_3 is generated through the PLC-mediated hydrolysis of PIP_2 which forms IP_3 and DAG (Section

5.1.10) (Schmidt, Evellin et al. 2001, Song, Hu et al. 2001), and binding of IP_3 to the IP_3R on the ER membrane triggers calcium release from the ER lumen. Vertebrates express 3 IP_3R subtypes; IP_3R1, IP_3R2 and IP_3R3 (Ferris, Huganir et al. 1989, Mikoshiba 2007, Zhang, Fritz et al. 2011), and vascular endothelium has been shown to express all three isoforms (Mountian, Manolopoulos et al. 1999, Ledoux, Taylor et al. 2008). Ryanodine receptors (RyRs) are generally not considered to be functionally important in non-excitable cells (Bruce, Straub et al. 2003), although they have been identified in endothelial cells of the thoracic aorta and mesenteric artery (Lesh, Marks et al. 1993, Kohler, Brakemeier et al. 2001). It should be noted, however, that agonist-evoked calcium oscillations in non-excitable cells such as pancreatic acinar cells, parotid acinar cells and intestinal epithelial cells, are sensitive to RyR inhibitors and thus RyRs in such cells have been implicated in the amplification of signals originating from IP_3R channels (Verma, Carter et al. 1996, Straub, Giovannucci et al. 2000, Bruce, Shuttleworth et al. 2002).

6.1.3.2 - Store-operated calcium entry

If calcium release from the ER continues to occur in the absence of extracellular calcium, calcium increase will eventually cease to occur as the ER is progressively emptied. Furthermore, in addition to IP_3-induced calcium release, calcium also leaks from the ER of resting cells. It has been known for some time that calcium influx across the cell membrane that occurs as a result of ER calcium release is an important part of calcium homeostasis. Calcium entry induced by depletion of the ER calcium store is termed store-operated calcium entry (SOCE) or capacitative calcium entry (CCE). This event allows re-filling of depleted calcium stores to prime the ER for the next calcium release event. The best characterised example of SOCE is the calcium current termed I_{CRAC}, where CRAC stands for calcium-release-activated calcium (Hoth and Penner 1992, Hogan and Rao 2007). Unlike non-selective cation channels discussed later, I_{CRAC} was thought to be highly selective for calcium, despite its molecular identity remaining elusive (Hoth and Penner 1992, Zweifach and Lewis 1993, Parekh and Penner 1995, Zubov, Kaznacheeva et al. 1999). Originally, this mechanism was linked to a family of canonical transient receptor potential channels (TRPCs) (Brough, Wu et al. 2001). Generally, TRPC is thought to be a non-selective cation channel, and thus under physiological ion gradients, sodium would be the primary ion flowing through this channel. It would therefore be surprising if the highly-selective I_{CRAC} pathway was explained by the opening of TRPCs. IP_3Rs have also previously been linked

with the induction of SOCE through I_{CRAC} (Irvine 1990, Berridge 1995), however more recent data has suggested that IP_3Rs may actually have an inhibitory effect on SOCE in order to prevent calcium overload (Lur, Sherwood et al. 2011). Stromal interaction molecule (STIM), expressed in the ER membrane, has since been implicated in the function of I_{CRAC} (Liou, Kim et al. 2005, Roos, DiGregorio et al. 2005, Luik, Wu et al. 2006). Two isoforms of STIM exist, STIM1 and STIM2, and both act as sensors of calcium concentration in the ER lumen through their low-affinity calcium-binding EF hands (Soboloff, Rothberg et al. 2012). On a fall in the calcium concentration within the ER, triggered by ER calcium release, calcium dissociates from the EF hand of STIM, which leads to an intra-molecular re-arrangement of STIM that promotes oligomerisation and translocation of STIM1, visible as puncta in immunocytochemical studies (Wu, Buchanan et al. 2006, Lur, Haynes et al. 2009). These puncta have since been found to co-localise with sites of calcium entry (Luik, Wu et al. 2006). The translocation of STIM to sites in close association with the plasma membrane causes recruitment of Orai1, a newly-identified calcium channel with a calcium influx pattern similar to I_{CRAC} (Potier, Gonzalez et al. 2009). Orai1 forms the calcium-selective pore of the channel (Prakriya and Lewis 2006, Taylor 2006, Yeromin, Zhang et al. 2006, Putney 2007). STIM1 has also been suggested to regulate TRPC for calcium entry, however this mechanism of SOCE is still considered relatively controversial (Worley, Zeng et al. 2007, Birnbaumer 2009, Lee, Choi et al. 2014).

As non-excitable cells, endothelial cells lack voltage-dependent calcium channels (VDCCs), and therefore SOCE is likely to be the main mechanism of agonist-induced calcium entry (Lambert, Kent et al. 1986, Dolor, Hurwitz et al. 1992, Schilling, Cabello et al. 1992). SOCE has also been implicated in shear-stress-induced calcium release (Ishida, Takahashi et al. 1997).

6.1.3.3 - Additional calcium-entry mechanisms

Calcium entry also occurs via transplasmalemmel calcium entry channels including voltage-dependent calcium channels (VDCCs) (Bossu, Elhamdani et al. 1992, Tran, Ohashi et al. 2000) and non-selective cation channels (Gericke, Droogmans et al. 1993, Inazu, Zhang et al. 1995, Pasyk, Inazu et al. 1995). VDCCs are thought to have little functional importance in endothelial cells (Himmel, Whorton et al. 1993).

Non-selective cation channels of importance when considering intracellular calcium elevations triggered by a rise in the cytoplasmic concentration of cAMP are cyclic nucleotide-gated (CNG) cation channels. These channels are permeable to cations, including calcium, and their gating is directly regulated by the intracellular cGMP and/or cAMP concentrations. The most well-characterised nucleotide-gated cation channels are those in sensory systems including photoreceptors and olfactory sensory neurons (Fesenko, Kolesnikov et al. 1985, Kaupp and Seifert 2002). In endothelial cells, both adenosine and adrenaline elicit an increase in intracellular cAMP which induces calcium influx through the direct activation of CNG ion channels which stimulates the release of nitric oxide (NO), prostacyclin and EDHF (Cheng, Leung et al. 2008, Shen, Cheng et al. 2008). Through this mechanism, CNG ion channels have been implicated in the endothelial-mediated relaxation of vascular smooth muscle cells (Shen, Cheng et al. 2008, Leung, Du et al. 2010, Serban, Nilius et al. 2010). As previously mentioned, TRPC channels are also non-selective cation channels, and this mechanism of calcium entry is typically activated by PLC stimulation (Hofmann, Schaefer et al. 2000, Montell, Birnbaumer et al. 2002).

6.1.3.4. – Removal of calcium from the cytosol

In addition to calcium entry, cytoplasmic calcium clearance pathways also exist to return intracellular calcium concentrations to pre-stimulation levels. The major calcium clearance pathway in non-excitable cells is generally considered to be through re-uptake into the ER by Sarco/endoplasmic reticulum calcium ATPase (SERCA) pumps (Berridge, Lipp et al. 2000). This ATP-dependent pump uptakes calcium from the cytosol to counteract ER calcium leak, and maintain the calcium load of the ER. SERCA pumps are inhibited by thapsigargin and cyclopiazonic acid (CPA) (Berridge, Lipp et al. 2000, Tran, Ohashi et al. 2000). As such, addition of either thapsigargin or CPA depletes the ER store by virtue of calcium leak that cannot be replenished, and therefore prevent calcium release. In addition to SERCA pumps, calcium can also be cleared from the cytosol by plasma membrane calcium ATPase (PMCA) pumps (Bruce, Straub et al. 2003). PMCA pumps have a relatively ubiquitous distribution, and PMCA1 and PMCA4 are expressed in most tissues (Greeb and Shull 1989). Calcium can also be removed from the cytoplasm by the Na^{+}/ Ca^{2+} exchanger. This mechanism is electrogenic as one calcium ion is removed from the intracellular environment in exchange for three sodium ions entering the cell. This calcium-clearing mode is termed forward mode and is particularly important in calcium homeostasis of

cardiac cells (Shigekawa and Iwamoto 2001). This process does not consume ATP directly, but depends on the presence of ATP to create the required sodium concentration gradient through the sodium pump that consumes ATP.

6.1.4 - Calcium in the control of vascular tone

The intracellular concentration of calcium in both endothelial and smooth muscle cells plays a crucial role in the regulation of vascular tone. As previously mentioned in Chapter 1, a rise in smooth muscle cell intracellular calcium concentration triggers contraction of these cells, involving actin/myosin cross-bridging. Changes in endothelial cytoplasmic calcium concentration can induce vascular relaxation. One of the major mechanisms mediating endothelial-induced relaxation involves endothelial-derived hyperpolarising factors (EDHFs). The classical EDHF pathway involves a rise in intracellular endothelial calcium concentration which triggers the opening of small- and intermediate-conductance calcium-sensitive potassium (SK_{ca} and IK_{ca}) channels. This leads to endothelial cell hyperpolarisation as potassium leaves the cell (Dora 2001, Edwards, Feletou et al. 2010). This hyperpolarising current can pass directly to adjacent smooth muscle cells via gap junctions at the myoendothelial junction (MEJ)(Sandow, Tare et al. 2002, de Wit and Griffith 2010). IK_{ca} channels have also been identified on endothelial cell projections that protrude through gaps in the internal elastic lamina separating the endothelium from the tunica media (Sandow, Neylon et al. 2006), and thus potassium is released into the extracellular space directly adjacent to the smooth muscle layer. This released potassium can activate sodium/potassium-ATPase and inwardly-rectifying potassium channels on smooth muscle cells that induces smooth muscle hyperpolarisation, closure of VDCCs and thus smooth muscle cell relaxation (Edwards, Dora et al. 1998, Roberts, Kamishima et al. 2013).

6.1.5 - Calcium measurement in live cells

Intracellular calcium concentration is typically recorded through the use of calcium-sensitive dyes. The two most commonly used dyes are Fura-2 (Kang, Chepurny et al. 2001, Mayati, Levoin et al. 2012) and Fluo-4 (Yip 2006, Roberts, Kamishima et al. 2013). The type of dyes that are often used for experiments are made membrane-permeable by addition of acetoxymethyl (AM) groups to allow loading of the cell. Calcium-sensitive dyes often have 4

AM groups, and removal of all 4 by intracellular esterases is necessary for the dye to become calcium-sensitive. Fura-2 is a ratiometric probe that requires excitation at two separate wavelengths, 340 nm and 380 nm, to produce two emission values that can be converted to free calcium concentration. Such ratiometric probes allow recording of calcium concentration independent of dye concentration, bypassing the issue of inconsistent loading of the cells. However, if the AM form of the dye is used, incomplete hydrolysis, as well as potential compartmentalisation of the dye to intracellular organelles, can be problematic. Non-ratiometric probes such as Fluo-4, on the other hand, are stimulated at a single wavelength (488 nm), and the calcium concentration is determined by a relative increase in the fluorescence intensity. Issues associated with the use of such non-ratiometric dyes typically involve inconsistent loading of cells. Additional calcium-detection methods include fluorescent protein-based probes that are constructed with a calmodulin backbone. Calcium-binding to the calmodulin backbone induces a conformational change that alters the fluorescent properties of the bound fluorescent protein (Miyawaki, Llopis et al. 1997).

6.1.6 Epac and the control of vascular tone

Physiological agonists binding to G_s-protein-coupled receptors, such as adrenaline (epinephrine), which binds to the β_2-adrenoceptor, adenosine, which binds to the A_{2A} receptor, and prostacyclin, which binds to the EP_4 receptor, are classical vaso-relaxing agents, and their ability to relax arteries requires, at least in part, intact endothelium (Yen, Wu et al. 1988, Kou and Michel 2007, Mitchell, Ali et al. 2008). cAMP and calcium are thought to be the predominant second messengers involved in the transduction of such vaso-relaxing effects mediated by the endothelium (Kou and Michel 2007, Roberts, Kamishima et al. 2013). The elevation of cAMP is triggered by GPCR-mediated activation of adenylate cyclase, and leads to the cAMP-mediated activation of both PKA and Epac. The elevation of calcium occurs through the generation of IP_3 that triggers the release of calcium from the ER. Generally, these two pathways are considered somewhat separately as PKA activation is not conventionally linked with a rise in intracellular calcium concentration. However, a recent study by Roberts *et al.* (2013) provided novel evidence that Epac activation may trigger a rise in intracellular calcium concentration in rat mesenteric artery endothelial cells (Roberts, Kamishima et al. 2013). In this study, addition

of 5 μM 8-pCPT was sufficient to relax rat mesenteric artery pre-constricted with phenylephrine (3 μM). Further investigation by this group showed that this effect was partly endothelium-dependent, as mechanical disruption of the endothelium inhibited the relaxation induced by 8-pCPT application. Furthermore, the relaxing effect of the Epac-specific agonist on pre-constricted arteries was blocked by inhibitors of intermediate- and small-conductance calcium-activated potassium (IK_{ca} and SK_{ca}) channels, Tram-34 (1 μM) and apamin (100 nM), respectively (Roberts, Kamishima et al. 2013). Both IK_{ca} and SK_{ca} channels are thought to be expressed by endothelial cells (Edwards, Dora et al. 1998, Ohashi, Satoh et al. 1999), and as their name suggests, are regulated by intracellular calcium concentration. Indeed, direct activation of Epac through 8-pCPT application within mesenteric endothelial cells loaded with Fluo-4-AM was shown to induce a sustained increase in global calcium (Roberts, Kamishima et al. 2013). cAMP has long been known to induce vascular relaxation by decreasing cytosolic calcium within smooth muscle cells through activation of potassium currents that hyperpolarise the smooth muscle membrane and reduce calcium influx by decreasing activity of VDCCs (Nelson, Patlak et al. 1990, Nelson and Quayle 1995). Thus, it is possible that Epac activation causes calcium increase in endothelial cells which, in turn, activates two classes of calcium-activated potassium channels leading to vaso-relaxation.

6.2 – Results

The functional effect of Epac activation on HCAECs was investigated using Lucifer yellow dye transfer to assess GJIC. In addition, the effect of Epac activation on the intracellular concentration of the second messenger calcium in HCAECs was experimentally assessed through live calcium imaging.

6.2.1 - Lucifer yellow dye transfer during Epac activation and inhibition

To determine whether Epac triggers enhanced GJIC in HCAECs, Lucifer yellow dye transfer between HCAECs was examined under varying conditions using a scrape assay. As cell confluence varied slightly between repeats, control experiments were performed for each separate experiment. Figure 6.1 is a brightfield image of the scrape produced during the Lucifer yellow scrape assays in HCAECs. Two scrapes were made across the glass bottom of the 35 mm dish, intersecting at right angles at the centre of the dish (full details under "Section 2.2.5 – Lucifer yellow scrape assay").

Figure 6.2 shows Lucifer yellow dye transfer between confluent HCAECs in a scrape assay. Dye transfer between adjacent HCAECs was analysed under control conditions (Figure 6.2A & 6.2B). The images were taken using a x10 (Figure 6.2A) and a x20 (Figure 6.2B) objective lens. The signal intensity profile (Figure 6.2C) represents the fluorescence recorded across the scrape shown in Figure 6.2B (dashed line). For the experiment shown, a maximum distance of approximately 140 µm was recorded for dye transfer from the scrape edge under control conditions. Beyond 140 µm the fluorescence dropped to background level. The cells displaying the highest concentration of fluorescence (169 AU) were identified at the border of the scrape (Figures 6.2B & 6.2C).

Next, dye transfer was examined between HCAECs pre-incubated with 5 µM 8-pCPT AM at 37˚C/ 5% CO_2 for 30 minutes (Figures 6.2D & 6.2E). The cells displaying the highest fluorescence intensity (239 AU) were again identified at the border of the scrape (Figures 6.2E & 6.2F). The maximum distance of dye transfer was recorded at approximately 530 µm (Figure 6.2F), nearly four times the distance recorded under control conditions. Again, beyond this distance fluorescence decreased to background level.

Exposure to the Epac1 antagonists ESI-09 (Figures 6.2G & 6.2H) and HJC0197 (Figures 6.2J & 6.2K) prior to Epac activation was also examined using a Lucifer yellow scrape assay. Both antagonists were used at 5 nM and incubated with the HCAECs for 10 minutes at 37˚C/ 5% CO_2 before addition of 5 µM 8-pCPT AM for 30 minutes (full details under "2.2.6: Lucifer yellow scrape dye transfer assay"). HCAECs pre-treated with the Epac antagonist ESI-09 (Figures 6.2G & 6.2H) displayed a maximum dye transfer distance of approximately 280 µm (Figure 6.2I), approximately half of the distance recorded in HCAECs treated with 8-pCPT alone. Once again, the cells displaying the highest fluorescence intensity (237 AU) were identified at the border of the scrape (Figures 6.2H &6.2I). It should be noted that this high level of fluorescence at the scrape border was detected for an extended distance when compared to control conditions, and was comparable to that recorded following treatment with 8-pCPT alone. Treatment with HJC0197 produced minimal dye transfer between HCAECs (Figures 6.2J & 6.2K), with a maximum distance of dye transfer of 80 µm, lower than that recorded even under control conditions with no 8-pCPT addition (Figure 6.2L). Furthermore, peak fluorescence was recorded at 245 AU, a concentration higher than that recorded under any of the previous conditions (Figure 6.2L).

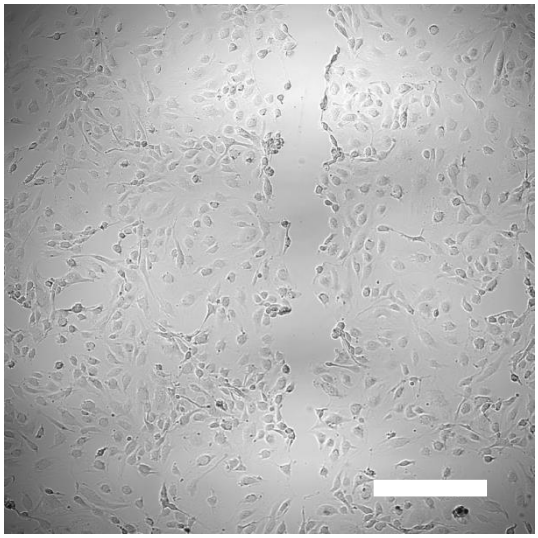

Figure 6.1: Brightfield image showing HCAECs used for Lucifer yellow scrape assay
HCAECs were seeded at 300,000 per 35 mm glass-bottom tissue culture dish. Once 90% confluent, a feather size 15 surgical blade was used to produce two scrapes across the dish, intersecting in the centre of the dish at right angles to each other. Image taken using a Leica laser-scanning confocal microscope with x10 lens (full method details under "2.2.6: Lucifer yellow scrape dye transfer assay").

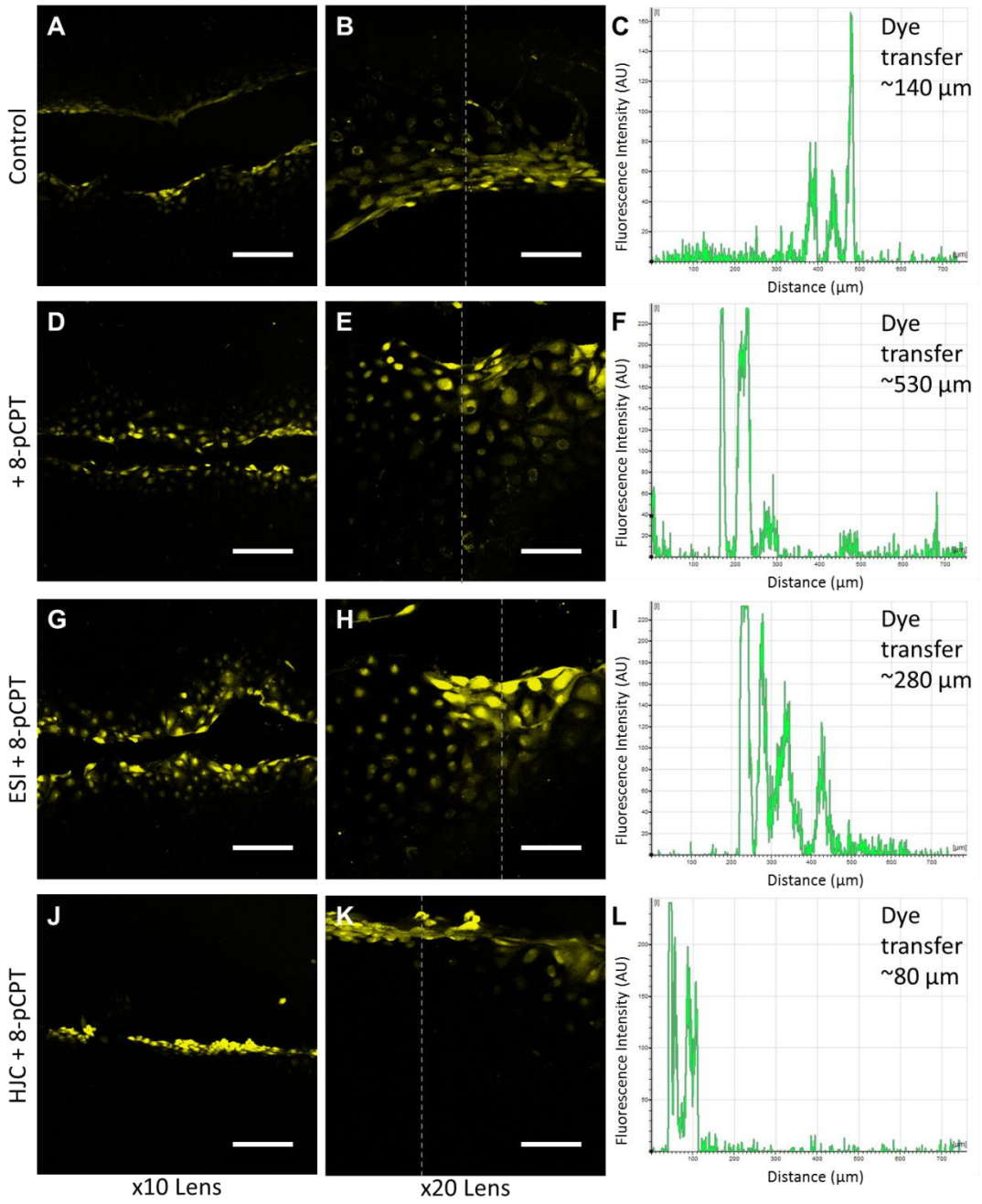

Figure 6.2: Immunocytochemistry of Lucifer yellow dye transfer in HCAECs
Under control conditions (A & B) dye travelled a maximum distance of ~ 140 µm from the scrape edge (C). Following treatment with 5 µM 8-pCPT for 30 minutes at 37˚C/ 5% CO_2 (D & E), dye travelled a maximum distance of ~ 530 µm from the scrape edge (F). Pre-incubation with 5 nM ESI-09 prior to 8-pCPT addition (G & H) resulted in a maximum dye transfer distance of ~ 280 µm (I). Pre-treatment with 5 nM HJC0197 (J & K) almost entirely blocked dye spread from the scrape edge, with a maximum distance of ~ 80 µm (L). Lucifer yellow CH lithium salt was used at a concentration of 0.1% in PBS (containing calcium chloride and magnesium). 4 images were taken of each dish. Full details of procedure detailed under "2.2.6: Lucifer yellow scrape dye transfer assay". Scale bars represent 300 µm (x10 lens) and 150 µm (x20 lens). Dashed lines represent signal intensity recording profile.

The data recorded from 3 separate experiments were first quantified by averaging the maximum distance travelled under each of the four conditions (control, + 8-pCPT, ESI + 8-pCPT and HJC + 8-pCPT). Every dish was subjected to 2 intersecting scrapes, yielding 4 scrapes as described earlier, and measurements were taken 4 times from each scrape, totalling 16 measurements in each condition. This process was repeated for 2 more sets of experiments, and the readings from the 3 different sets of experiments were pooled for summary results. The individual and summary results are shown in Figure 6.3. All recordings detected a significant increase in the distance of dye transfer between control conditions and HCAECs pre-treated with 5 µM 8-pCPT (Figure 6.3A $P< 0.01$, Figure 6.3B $P< 0.001$ and Figure 6.3C $P< 0.001$, one-way ANOVA, N=16). In addition, in experiments 2 and 3, pre-treatment of HCAECs with Epac antagonists reversed the effect of 8-pCPT (Figure 6.3B ESI-09 and HJC0197 $P< 0.001$ and Figure 6.3C ESI-09 $P< 0.05$ and HJC0197 $P< 0.001$). When the results from the 3 experiments were combined, the compiled data showed a significant difference between control and 8-pCPT-treated cells (Figure 6.3D, $P< 0.01$), and this effect was abolished when HCAECs were pre-treated with HJC0197 (Figure 6.3D, $P< 0.01$, one-way ANOVA, N=48).

Together, this data suggests that Epac activation by 8-pCPT results in increased dye transfer between adjacent HCAECs in culture, indicating that the newly formed gap junctions at sites of cell-cell contact are functional. Furthermore, the Epac antagonist HJC0197 blocked the effect of 8-pCPT. The Epac antagonist ESI-09 blocked the effect of 8-pCPT in 2 out of the 3 experiments.

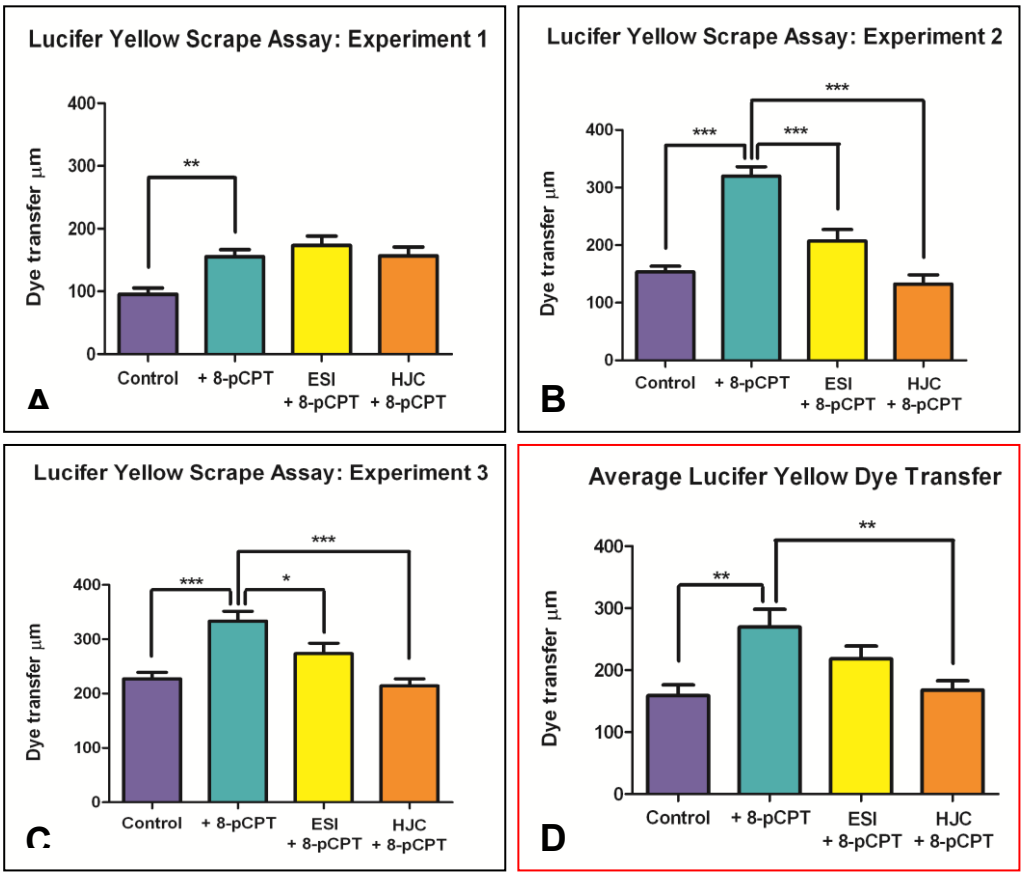

Figure 6.3: Quantification of Lucifer yellow dye transfer in HCAEC scrape assay
In total, 3 Lucifer yellow experiments were carried out using HCAECs (A-C). Each experiment involved the creation of 4 scrapes per condition. An image was taken of each scrape (4 images per condition) using the x10 confocal microscope lens. 4 measurements were taken from each image (16 measurements per condition, per experiment). Measurements were taken by recording the maximum dye spread from the scrape edge (Leica Lite Software). D represents the average dye transfer recordings from all experiments. (* P< 0.05, ** P< 0.01, *** P< 0.001 one-way ANOVA, N=16 for A, B and C, and N=48 for D).

6.2.2 - Live calcium imaging of HCAECs

6.2.2.1 - Effect of 8-pCPT on calcium homeostasis in HCAECs

Figure 6.4 shows Fluo-4 fluorescence in HCAECs before (Figure 6.4A), 30 seconds after (Figure 6.4B), and 60 seconds after (Figure 6.4C) application of 5 µM 8-pCPT. In un-stimulated HCAECs, Fluo-4 fluorescence was low, suggesting low resting calcium level (Figure 6.4A). Application of 5 µM 8-pCPT triggered an increase in the cytoplasmic calcium concentration (Figure 6.4B). This rise in calcium was initially uniform in appearance (Figure 6.4B), but after 60 seconds of 8-pCPT addition, cells showed a spot-like distribution of AF488 signal (Figure 6.4C). This is presumably due to the cytoplasmic calcium being sequestered into intracellular stores. The bright spots within the cells appear to match mitotracker staining of mitochondria, as shown in Figure 6.5. An exception to this transient nature of calcium release was seen in cells in the process of cell division, which typically showed a sustained elevated calcium level throughout recordings (Figure 6.4B and 6.4C, white arrows).

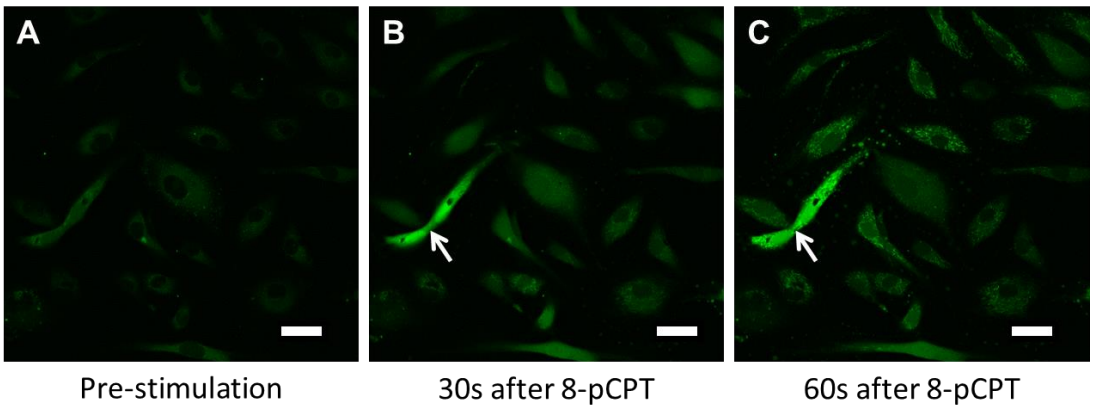

Figure 6.4: Confocal images of Fluo-4 -loaded HCAECs
Image A shows un-stimulated HCAECs loaded with 10 µM Fluo-4 AM. 30 seconds after application of 5 µM 8-pCPT, HCAECs showed an increase in AF488 signal intensity, suggesting cytoplasmic calcium increase (B). After 60 seconds (C), intracellular calcium largely returned to resting level, being apparently sequestered into intracellular compartments. Scale bar represents 40 µm. The white arrows in B and C highlight the dividing cells where calcium levels remained high.

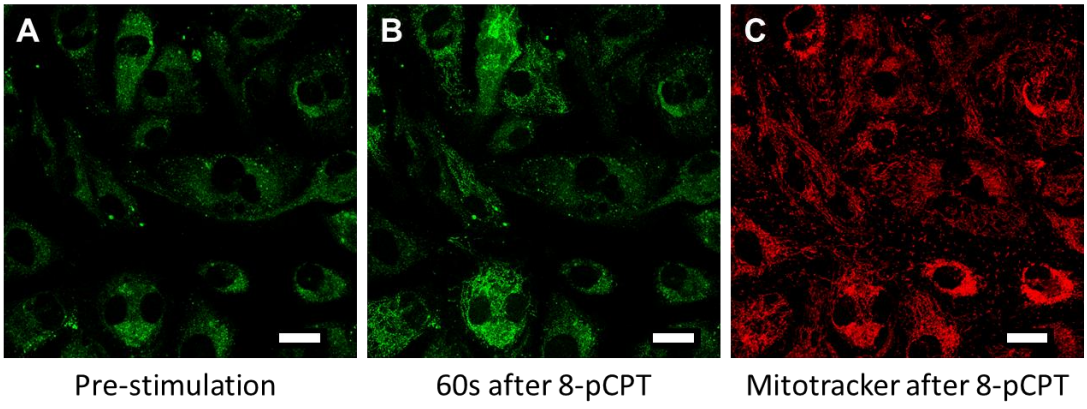

Figure 6.5: Confocal images of Mitotracker -loaded HCAECs
Image A shows un-stimulated HCAECs loaded with 10 µM Fluo-4 AM. Image B shows the AF488 signal that appears to be largely contained within intracellular compartments after treatment with 5 µM 8-pCPT. Image C shows the HCAECs displayed in images A and B loaded with mitotracker (100 nM), after 8-pCPT treatment. The intracellular stores that rapidly sequester the calcium (B) have a structure reminiscent of mitochondria (C). Scale bar represents 40 µm. N=3.

6.2.2.1.1 - Calcium transients induced by 8-pCPT in the presence of extracellular calcium

To further characterise the intracellular calcium transients induced by application of 8-pCPT, images of Fluo-4-loaded HCAECs were taken at 10 second intervals. The change in intracellular calcium level was determined by measuring the average signal intensity of the region of interest from individual HCAECs. Figure 6.6A shows the time course of the calcium transient (mean and SEM) obtained from 100 cells. 8-pCPT was applied between the first two frames (0 seconds and 10 seconds), as indicated by the red arrow in Figure 6.6A. 8-pCPT caused a rapid increase in intracellular calcium levels in HCAECs that peaked at approximately 30 seconds. Calcium levels then slowly decreased, reaching the resting level after 300 seconds (dotted line, Figure 6.6A). These results show that 8-pCPT application causes rapid and transient increase in intracellular calcium in HCAECs.

6.2.2.1.2 - Calcium transients induced by 8-pCPT in the absence of extracellular calcium

As an increase in intracellular calcium can be produced by calcium influx and/or calcium release, experiments were repeated in the absence of extracellular calcium. Figure 6.6B shows 8-pCPT stimulation of HCAECs in the presence of 2 mM extracellular calcium (filled circles) and HCAECs in calcium-free extracellular solution (open circles). Calcium transients induced in the absence of extracellular calcium (open circles, N=74 cells) were similar to those induced in the presence of extracellular calcium (filled circles, N=100 cells). Both transients peaked at approximately 30 seconds and showed a slow decline to resting levels. In the absence of extracellular calcium (open circles), the calcium decline is somewhat quicker than that observed when calcium is present in the extracellular solution (filled circles). This data indicates that calcium release from intracellular stores is important in the 8-pCPT-induced calcium transients in HCAECs. Furthermore, the apparent faster calcium decrease in the absence of extracellular calcium may indicate calcium influx occurring during the declining phase of the calcium transient.

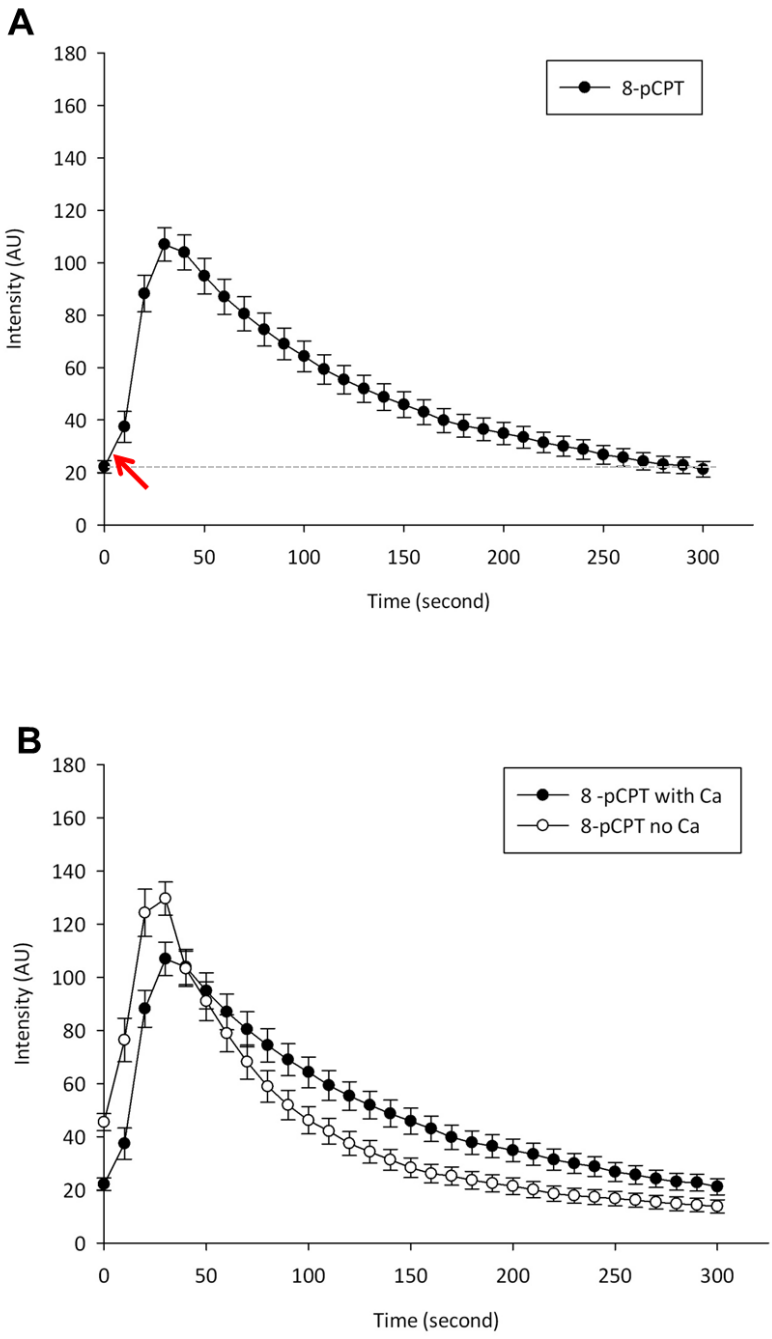

Figure 6.6: Calcium transients induced in HCAECs on 8-pCPT application

HCAECs were loaded with 10 µM Fluo-4 AM. 5 µM 8-pCPT was added to the cells between the first and second time points, as indicated by the red arrow in A. Figure A shows the rise in intracellular calcium induced by 8-pCPT in the presence of extracellular calcium. The dashed line represents the resting level of calcium. Figure B shows the rise in intracellular calcium induced by 8-pCPT in the presence (filled circles) and absence of extracellular calcium (open circles). In B, the peak in intracellular calcium was observed at approximately 30 seconds for both calcium-containing and calcium-free extracellular solution. Images were taken every 10 seconds. Image A; N=100 cells. Image B open circles; N=74 cells.

6.2.2.1.3 - Calcium transients induced by 8-pCPT in the presence of CPA

To further determine the importance of calcium release in the 8-pCPT-induced calcium transient in HCAECs, endoplasmic reticulum (ER) calcium content was depleted. The standard techniques for the emptying of ER calcium stores includes pre-incubation with cyclopiazonic acid (CPA) or thapsigargin, both of which inhibit calcium-ATPase pumps in the ER membrane. There is a continuous basal 'leak' of calcium from the ER and blockage of calcium entry into these intracellular stores prevents re-filling and the ER calcium store is subsequently depleted. The effect of 8-pCPT application on HCAECs pre-treated with CPA was examined in the absence of extracellular calcium (Figure 6.7A). These conditions therefore blocked both the release of calcium from the ER stores and the influx of calcium from the extracellular solution. Under these conditions, 8-pCPT no longer induced an increase in intracellular calcium (N=60 cells).

6.2.2.1.4 - Calcium transients induced by 8-pCPT in the presence of ryanodine

Calcium release from intracellular stores can occur due to the opening of calcium release channels in the membrane of the endoplasmic reticulum or sarcoplasmic reticulum. IP_3 receptors are generally considered to play a major role in this form of calcium release in non-excitable cells, including endothelial cells, while ryanodine receptors appear to be primarily responsible in striated muscle contraction. With regards to smooth muscle cells, the relative importance of IP_3 receptors and ryanodine receptors in elevating intracellular calcium concentration seems to depend on the type of stimulus. The mode of ryanodine effect on ryanodine receptors is thought to be rather complex as it is not only dose-dependent, but also use-dependent. That said, application of relatively high concentrations of ryanodine is expected to block calcium release from intracellular stores via ryanodine receptors. Figure 6.7B shows the increase in intracellular calcium induced in HCAECs on 8-pCPT application in the presence of extracellular calcium and 30 µM ryanodine (N=23 cells). Under these conditions, 8-pCPT induced an increase in intracellular calcium, with a peak at approximately 30 seconds. This data suggests that the 8-pCPT-induced calcium release from HCAEC intracellular stores was largely unaffected by the high dose of ryanodine. This result may not be surprising, as there is currently a lack of convincing evidence to suggest that endothelial cells express ryanodine receptors or that these are functionally active in the release of calcium from the endoplasmic reticulum. HCAECs have previously been shown to express at least two subtypes of IP_3 receptors (Section 3.2.2.3 – IP_3 receptor

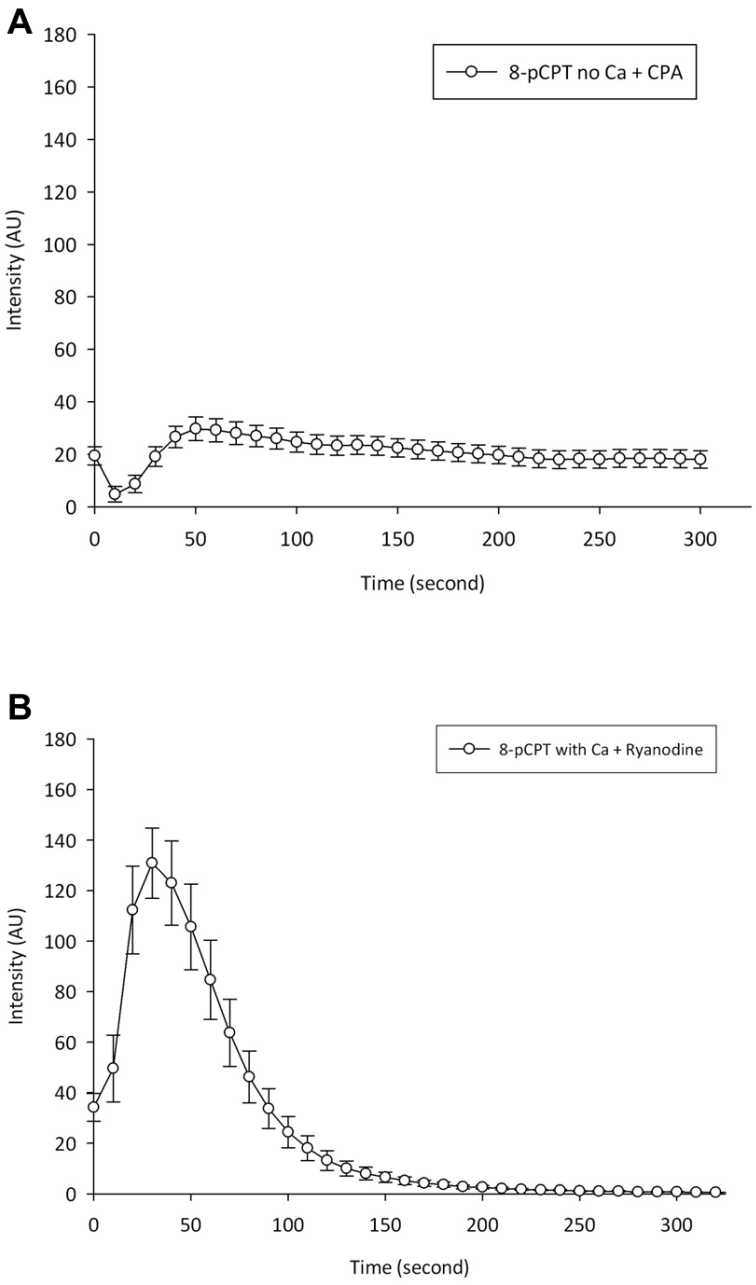

Figure 6.7: Calcium transients induced in HCAECs on 8-pCPT application with disruption of calcium release from intracellular stores

HCAECs were loaded with 10 µM Fluo-4 AM. 5 µM 8-pCPT was added to the cells between the first and second time points. Depletion of the ER calcium store with CPA, and removal of extracellular calcium, prevented the 8-pCPT-induced rise in intracellular calcium (A). Treatment of HCAECs with 30 µM ryanodine, a concentration thought to be sufficient to block ryanodine receptors on the ER, in the presence of extracellular calcium, failed to inhibit the 8-pCPT-induced rise in intracellular calcium (B). In HCAECs pre-treated with ryanodine, the peak in intracellular calcium was observed at approximately 30 seconds, as occurred in HCAECs treated with 8-pCPT alone (Figure 6.6, above). Images were taken every 10 seconds. Image A; N=60 cells. Image B; N=23 cells.

expression) and these seem the more likely candidate for calcium release from the endoplasmic reticulum.

6.2.2.1.5 - Calcium transients induced by 8-pCPT in the presence of PKI

As discussed earlier, 8-pCPT is thought to be a useful tool to selectively activate Epac. Nonetheless, to determine whether PKA was also involved in the 8-pCPT-triggered elevation of intracellular calcium, HCAECs were pre-treated with 5 µM of the myristoylated form of the PKA inhibitor, PKI, prior to 8-pCPT application in the presence of extracellular calcium (Figure 6.8). PKI is thought to selectively inhibit PKA without affecting Epac activity. The open circles show the average PKI result from 64 cells. For comparison, the filled circles show the calcium transient induced by 8-pCPT application.

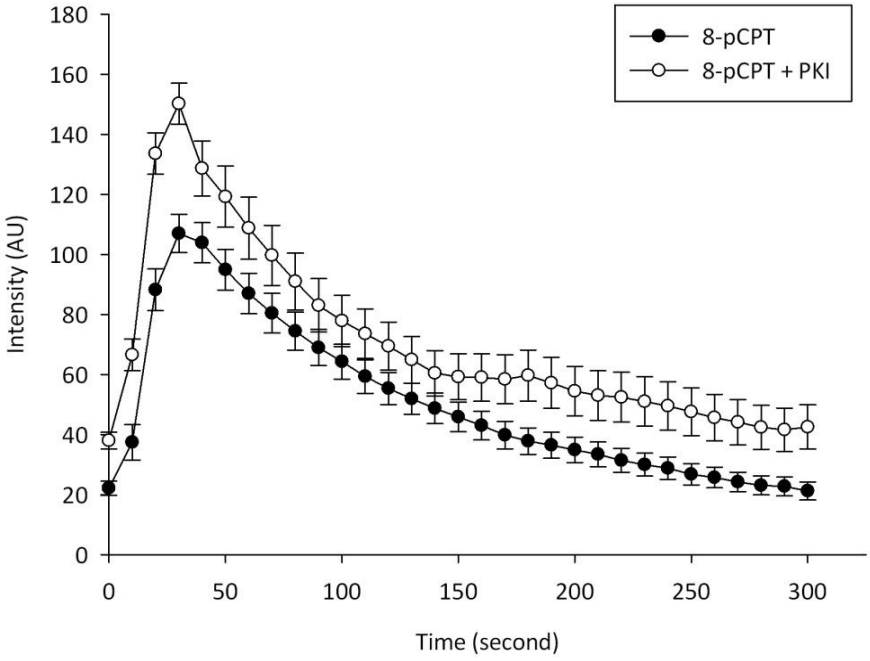

Figure 6.8: Calcium transient induced in HCAECs on 8-pCPT application in the presence of PKI

HCAECs were loaded with 10 µM Fluo-4 AM. 5 µM 8-pCPT was added to the cells between the first and second time points. PKA activity was inhibited by pre-treatment (20 minutes) of the HCAECs with 5 µM PKI. Inhibition of PKA activity appeared to have little effect on the calcium transient induced by 8-pCPT addition. Under both conditions, the peak in intracellular calcium was observed at approximately 30 seconds. Images were taken every 10 seconds. N=64 cells.

6.2.2.1.6 - Calcium transients induced by 8-pCPT in the presence of Epac antagonists

Next, the effect of two types of Epac antagonist, HJC0197 and ESI-09, on 8-pCPT-induced rise in intracellular calcium was examined. These experiments were performed in the presence of extracellular calcium. Figure 6.9A shows the average results from 27 cells pre-incubated with ESI-09. In the presence of ESI-09, the 8-pCPT triggered calcium transient was substantially smaller. Figure 6.9B shows the average results from 8 cells pre-incubated with HJC0197. In the presence of HJC0197, 8-pCPT did not induce a rise in intracellular calcium. Taken together, putative Epac antagonists inhibited the rise in intracellular calcium induced by 8-pCPT application in HCAECs.

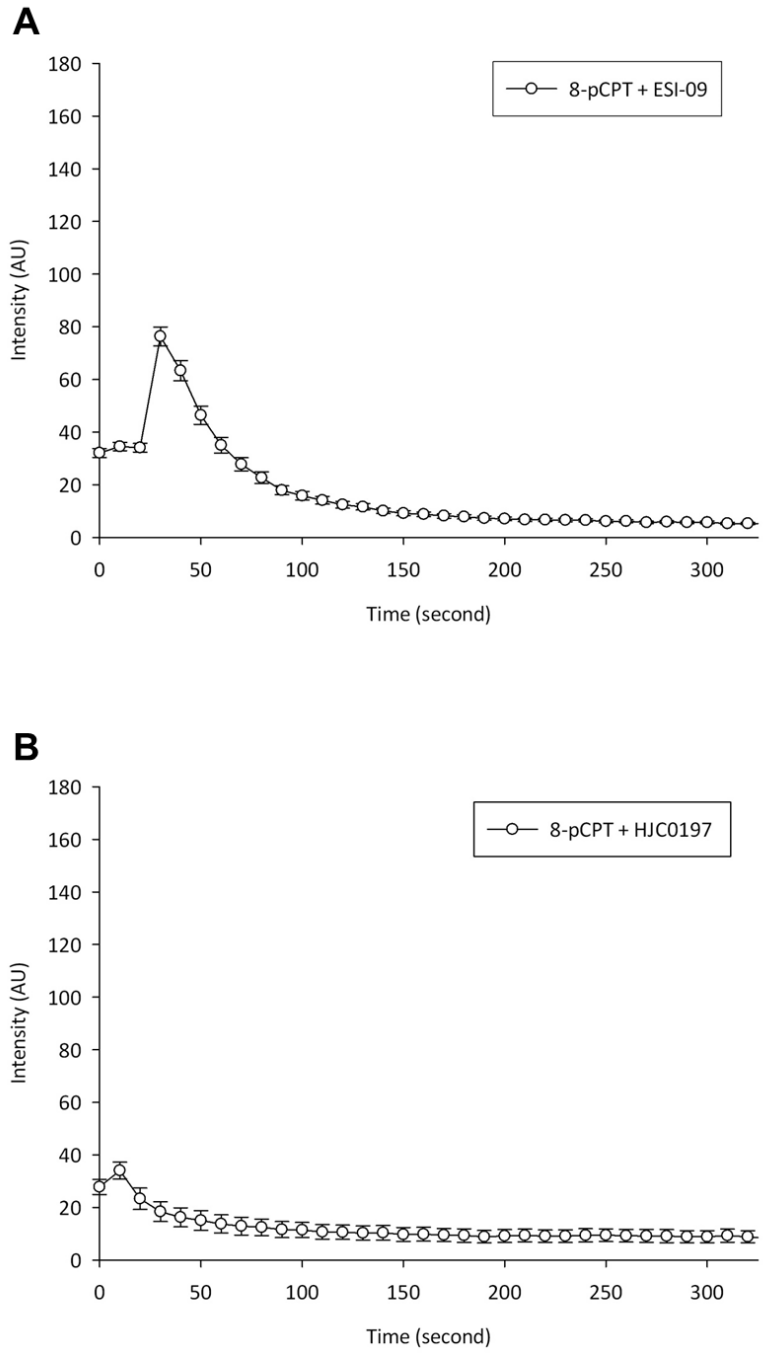

Figure 6.9: Calcium transients induced in HCAECs on 8-pCPT application in the presence of the Epac antagonists ESI-09 and HJC0197

HCAECs were loaded with 10 µM Fluo-4 AM. 5 µM 8-pCPT was added to the cells between the first and second time points. Pre-treatment of HCAECs with ESI-09 (20 minutes, 5 nM) substantially reduced the 8-pCPT-induced rise in intracellular calcium (A). The resting level of calcium in these cells was similar to un-treated HCAECs (Figure 6.6), and a small peak was identified at approximately 30 seconds. Pre-treatment of HCAECs with HJC0197 (20 minutes, 5 nM) prevented the 8-pCPT-induced rise in intracellular calcium (B). Again, the resting level of calcium in these cells was similar to un-treated HCAECs. Images were taken every 10 seconds. Image A; N=27 cells. Image B; N=8 cells.

6.2.2.2 - Calcium transients induced by a β-adrenergic agonist in the presence of extracellular calcium

Next, experiments were performed to investigate the effect of physiological elevation of cAMP on calcium homeostasis in HCAECs. Physiological stimuli such as prostaglandin E2 (PGE2) increase the level of cAMP by binding its receptor, PGE2, which is a G_s-protein coupled receptor that activates adenylate cyclase (AC). However, the expression pattern of receptors often changes during cell culture, and so physiological agonists may no longer be effective in these cells. Nonetheless, a sub-population of cells may still retain the receptors, and so the effect of isoproterenol on HCAECs was examined (Figure 6.10). Isoproterenol is known to increase cAMP by binding to β_1- or β_2-adrenoreceptors *in vivo*. On application of 10 μM isoproterenol, calcium transients were detected in only three cells (Figure 6.10B, white arrows). When 8-pCPT was applied to the same dish after application of isoproterenol, a calcium increase was observed in almost all cells (Figure 6.10C). This result suggests that the lack of response to isoproterenol is not general experimental failure, but rather loss of the β-adrenoreceptors during cell culture. In summary, this experiment showed that receptor stimulation did trigger calcium increase in a subset of HCAECs.

6.2.2.3 - Effect of forskolin on calcium homeostasis in HCAECs

6.2.2.3.1 - Calcium transients induced by forskolin in the presence of extracellular calcium

In order to circumvent the problem of loss of receptor expression, cAMP was raised in HCAECs by forskolin application, which directly activates AC. Figure 6.11A shows the average calcium transient induced by the application of 10 μM forskolin in the presence of extracellular calcium (N=114 cells). Like 8-pCPT, forksolin application induced a rise in intracellular calcium in HCAECs. However, when HCAECs were stimulated with forskolin, the time-to-peak was delayed (50 seconds vs 30 seconds), and the rate of calcium decrease appeared slower.

6.2.2.3.2 - Calcium transients induced by forskolin in the absence of extracellular calcium

Next, forskolin was applied to HCAECs bathed in calcium-free extracellular solution. The average calcium transient from 30 cells is shown in Figure 6.11B as open circles. The calcium transient induced by forskolin in the presence of extracellular calcium is also shown for comparison (filled circles). In the absence of extracellular calcium, forskolin still induced

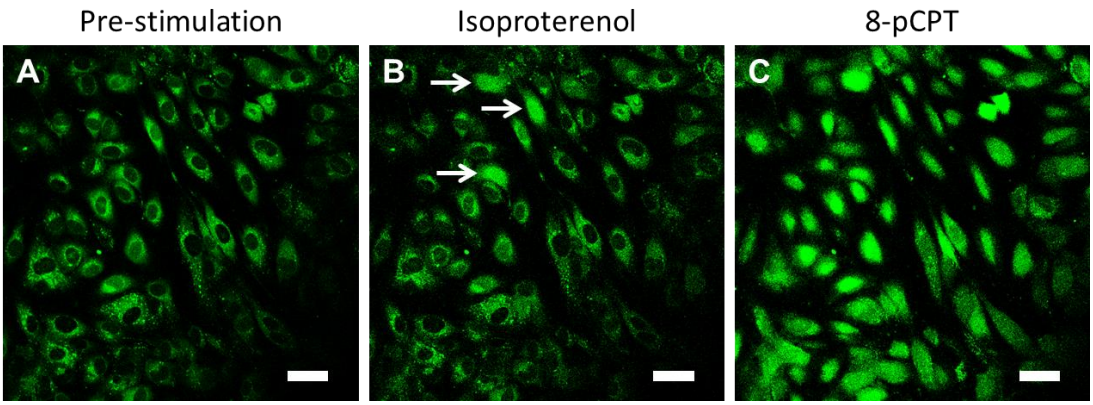

Figure 6.10: Calcium transient of HCAECs triggered by application of isoproterenol and 8-pCPT

Image A shows un-stimulated HCAECs loaded with 10 µM Fluo-4 AM. Application of 10 µM isoproterenol triggered a calcium increase in only 3 cells (B, white arrows), while most of the HCAECs responsded to application of 5 µM 8-pCPT (C). Scale bar represents 40 µm

a calcium transient, peaking at approximately 30 seconds (N=30 cells). This data suggests that calcium release is an important part of the forskolin-induced rise in intracellular calcium.

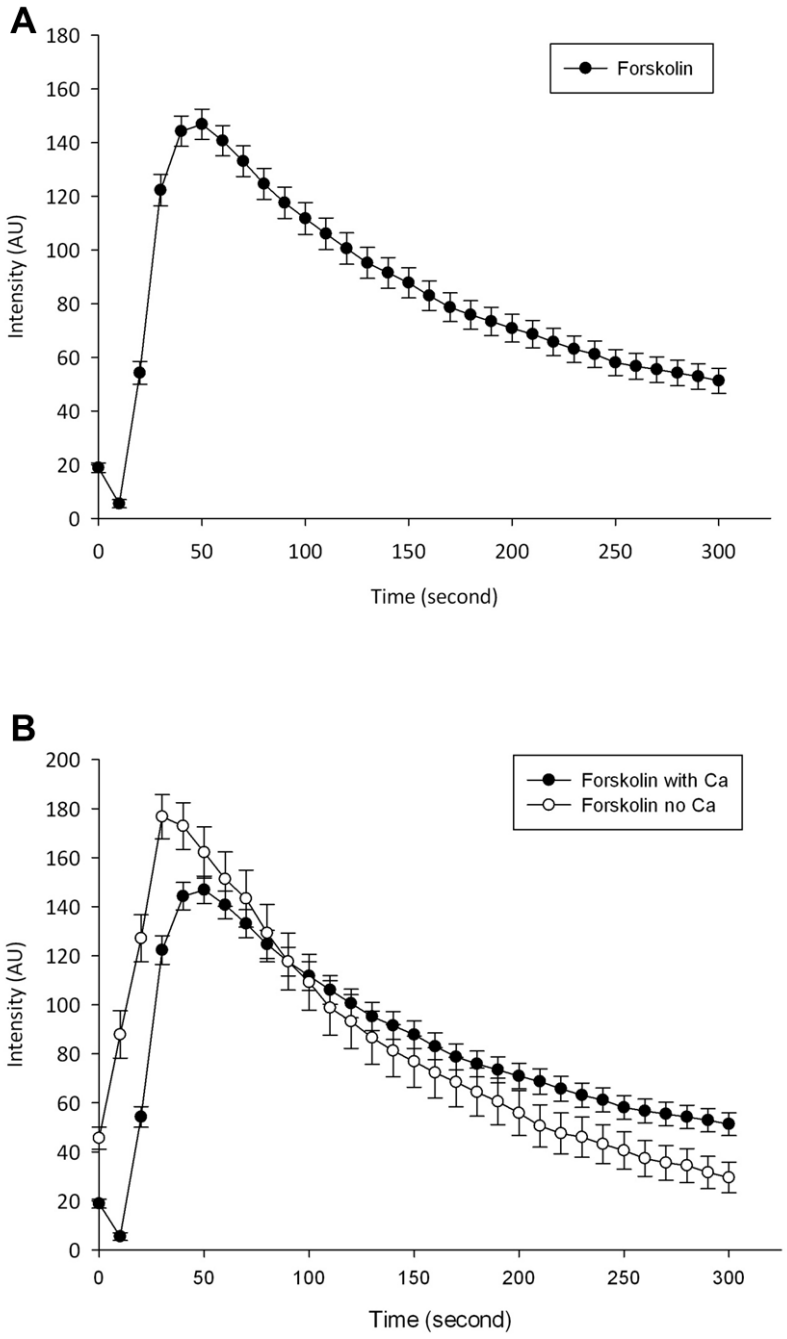

Figure 6.11: Calcium transients induced in HCAECs on forskolin application

HCAECs were loaded with 10 µM Fluo-4 AM. 10 µM forskolin was added to the cells between the first and second time points. Figure A shows the rise in intracellular calcium induced by forskolin in the presence of extracellular calcium. Figure B shows the rise in intracellular calcium induced by forskolin in the absence of extracellular calcium (open circles). The result from A is also shown for comparison (filled circles). In A, the peak in intracellular calcium was observed at approximately 50 seconds. In B, the peak in intracellular calcium in the absence of extracellular calcium (open circles), was observed at approximately 30 seconds. Images were taken every 10 seconds. Image A; N=114 cells. Image B open circles; N=30 cells.

6.2.2.3.3 - Calcium transients induced by forskolin in the presence of PKI

The elevation in cAMP level induced by application of forskolin is thought to activate both Epac- and PKA-mediated signal transduction cascades in HCAECS. As the PKA inhibitor, PKI, had little effect on the 8-pCPT-induced calcium transient (Figure 6.12), the differences between the 8-pCPT-induced and forskolin-induced transients could be attributed to the activation of PKA. Thus, forskolin stimulation was carried out using HCAECs pre-treated with PKI, in the presence of extracellular calcium (Figure 6.12). This figure summarises the results from 71 cells pre-treated with PKI (open circles). The calcium transient induced by application of forskolin in the presence of extracellular calcium is also shown for comparison (filled circles). When HCAECs were pre-treated with PKI, the forskolin-induced rise in intracellular calcium returned toward the basal level more quickly, and the peak was comparable to that observed in HCAECs in the absence of PKI. Together, the data suggest that the PKA-pathway may contribute to part of the calcium transient induced by forskolin application.

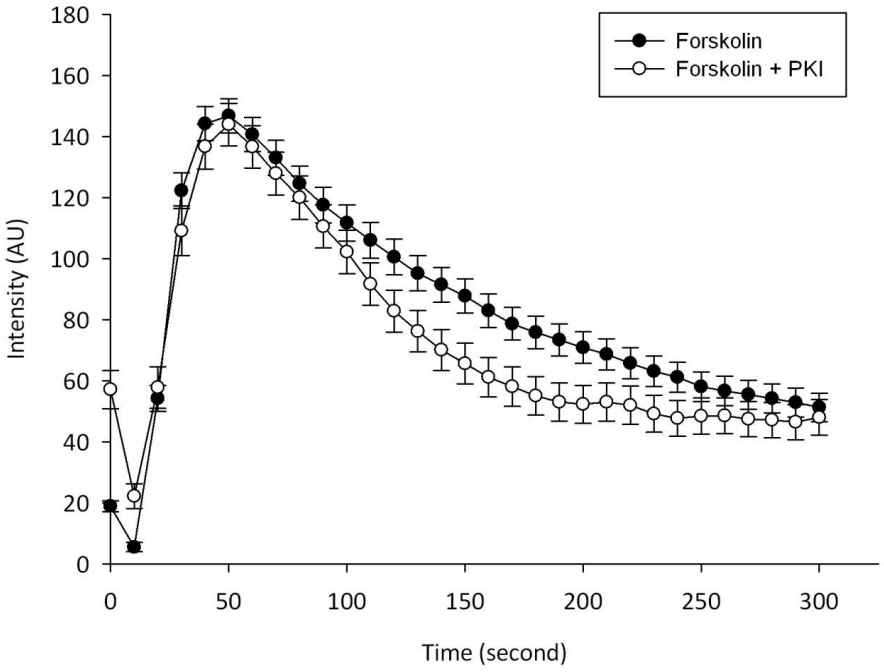

Figure 6.12: Calcium transient induced in HCAECs on forskolin application in the presence of PKI

HCAECs were loaded with 10 µM Fluo-4 AM. 10 µM forskolin was added to the cells between the first and second time points. PKA activity was inhibited by pre-treatment (20 minutes) of the HCAECs with 5 µM PKI. In the HCAECs pre-treated with PKI, the calcium transient returned towards the resting level more quickly, and the peak was comparable to that recorded in HCAECs without PKI (filled circles). Images were taken every 10 seconds. N=71 cells.

6.3 - Discussion

6.3.1 – 8-pCPT application to HCAECs enhances gap junction intercellular communication

As previously mentioned, GJIC is typically quantified by either the transfer of electrical conductance or through dye spread. To determine whether the Epac-mediated re-distribution of connexins formed nascent functional gap junction channels, Lucifer yellow (LY) dye transfer was examined in a scrape assay. On application of 5 μM 8-pCPT, LY dye transfer significantly increased (Figure 6.2D & 6.2E and Figure 6.3D), when compared to un-stimulated HCAECs (Figure 6.2A & 6.2B, one-way ANOVA, N=16). This increase in dye transfer suggests an 8-pCPT-mediated enhancement in HCAEC GJIC. A similar increase in GJIC has been observed on cAMP elevation, and 8-pCPT addition, in the literature (see Section "5.4.2.3 - VE-cadherin and connexin co-localisation following 8-pCPT addition") (Saez, Spray et al. 1986, Mehta, Yamamoto et al. 1992, Atkinson, Lampe et al. 1995, Burghardt, Barhoumi et al. 1995, Mehta, Lokeshwar et al. 1996, Somekawa, Fukuhara et al. 2005, Duquesnes, Derangeon et al. 2010). Inhibition of Epac activity with the Epac-specific antagonist HJC0197 completely blocked the 8-pCPT-induced increase in dye transfer (Figure 6.2J & 6.2K and Figure 6.3). Together, this data suggests that Epac activation triggers enhanced GJIC in HCAECs.

6.3.2 – Epac activation stimulates a transient rise in intracellular HCAEC calcium concentration

The hypothesis that Epac activation increases intracellular calcium concentration was tested in HCAECs loaded with Fluo-4-AM. HCAECs were stimulated using 8-pCPT and forskolin to activate Epac and adenylate cyclase, respectively. Calcium transients were indeed triggered by both 8-pCPT and forskolin in the presence, and absence, of calcium (Figure 6.5B and 6.10B). These results also indicate that calcium transients caused by application of 8-pCPT or forskolin were due to, at least in part, calcium release from the ER, as only after the ER calcium was depleted with CPA did 8-pCPT fail to trigger a calcium transient (Figure 6.6A).

The calcium release is hypothesised to result from opening of IP_3 receptors, as blockade of ryanodine receptors (RyRs) with high concentrations of ryanodine (30 μM) had little effect on the calcium transient induced by 8-pCPT application (Figure 6.6B). In support of this

functional evidence, the presence of at least two types of IP_3 receptors was detected in HCAECs using immunocytochemical techniques (Chapter 3, Figure 3.8).

In order to further analyse the pattern of calcium transients under various conditions, some form of standardisation was necessary. As previously mentioned, Fluo-4 is a single wavelength calcium indicator. This means that, unlike ratiometric dyes such as Fura-2, the signal emitted by Fluo-4-loaded cells not only depends upon the intracellular calcium concentration of the cell, but also the efficiency of dye-loading. Indeed, the signal intensity of Fluo-4-loaded HCAECs at rest appears to differ between experiments. Thus, the estimation of true calcium concentration that allows direct comparison of calcium transients under various conditions is problematic. That said, the overall shape of the calcium transient gives an indication of the different calcium handling mechanisms involved in the 8-pCPT-induced rise in intracellular calcium. In an attempt to overcome such issues, the average signal intensity was normalised against peak intensity to allow the comparison of the time-course of calcium transients.

6.3.2.1 – 8-pCPT application triggers calcium release from the ER

Figure 6.13, below, shows the normalised calcium transients induced by 8-pCPT in the presence (filled circles) and absence (open circles) of extracellular calcium. The calcium transient occurring in the absence of extracellular calcium (open circles) solely reflects calcium release caused by Epac activation. In both conditions, transients reached a peak at approximately 30 seconds, but in the absence of extracellular calcium (open circles) the increased calcium concentration declines more rapidly. It is possible that this faster decline is due to faster calcium removal from the cytoplasm. However, it is more likely that Epac activation induced not only calcium release but also calcium influx, and that this influx did not occur in the absence of extracellular calcium and therefore the calcium concentration had an appearance of faster decline.

Figure 6.13 also shows the normalised calcium transient induced by 8-pCPT when HCAECs were pre-treated with the PKA-inhibitor, PKI, in the presence of extracellular calcium (open triangles). The calcium transient under these conditions was largely unchanged to that observed without the PKA inhibitor, suggesting that the 8-pCPT-induced calcium transient is mediated predominantly via Epac activation. This is consistent with the results where 8-pCPT-induced calcium transients were inhibited (Figure 6.9B) or substantially reduced

(Figure 6.9A) by Epac-specific antagonists HJC0197 and ESI-09, respectively. Both HJC0197 and ESI-09 are marketed as antagonists to both Epac1 and Epac2 (Chen, Tsalkova et al. 2012, Almahariq, Tsalkova et al. 2013, Rehmann 2013). Both antagonists are considered to act as Epac inhibitors through their general protein denaturing properties that prevents Epac's GEF activity, and are not entirely specific for Epac (Rehmann 2013). Their degree of inhibitory effect on 8-pCPT-induced calcium transients may therefore reflect the relative selectivity of these Epac antagonists.

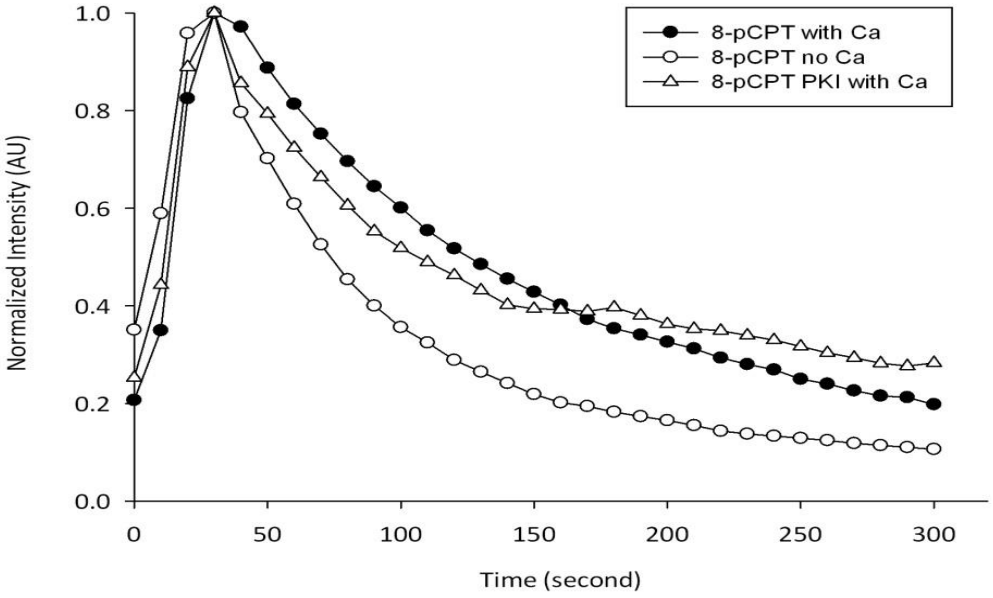

Figure 6.13: Normalised calcium transients induced in HCAECs on 8-pCPT application
The average signal intensity for each condition was normalised against the peak intensity to allow direct comparison of the time-course of calcium transients. Peak calcium elevation was recorded at approximately 30 seconds for each condition. Calcium transients induced by 8-pCPT in the presence (filled circles) and absence (open circles) of extracellular calcium are shown. For comparison, the transient induced by 8-pCPT following incubation with PKI, in the presence of calcium, is also shown (open triangles).

6.3.2.2 – cAMP elevation triggers predominantly calcium release but also calcium influx

Figure 6.14 shows the normalised calcium transients induced by forskolin in the presence of extracellular calcium (filled red circles). Forskolin application also induced a calcium transient in the absence of extracellular calcium (open red circles), presumably by releasing calcium from the ER. In the absence of extracellular calcium, the calcium transient declined more quickly, as was observed in the 8-pCPT-induced calcium transient. Again, although it is possible that the faster decline could be attributed to increased calcium clearance, it seems more likely that forskolin application induced both calcium release and calcium influx. In Figure 6.14, the normalised calcium transient induced by 8-pCPT addition in the presence of extracellular calcium is also shown for comparison (filled black circles). The time-to-peak was longer with the forskolin-induced calcium transient in the presence of extracellular calcium (filled red circles, approximately 50 seconds compared to approximately 30 seconds for 8-pCPT). Interestingly, the calcium transient induced by forskolin in the absence of extracellular calcium (open red circles) was virtually identical to that observed with 8-pCPT in the presence of extracellular calcium (filled black circles).

Figure 6.14 also shows the normalised calcium transient induced by forskolin when HCAECs were pre-treated with PKI in the presence of extracellular calcium (open red triangles). PKI appeared to have little effect on the shape of the calcium transient at the early stage of the recording, but did appear to increase the rate of decline after approximately 100 seconds. As PKA is likely to have multiple effects in endothelial cells, it is difficult to interpret the data shown in Figure 6.14 without further experiments. Such experiments could involve Epac1 siRNA. Indeed, multiple attempts were made to investigate calcium transient using HCAECs where Epac was knocked down, however, cells failed to survive the combination of siRNA knockdown and live calcium imaging.

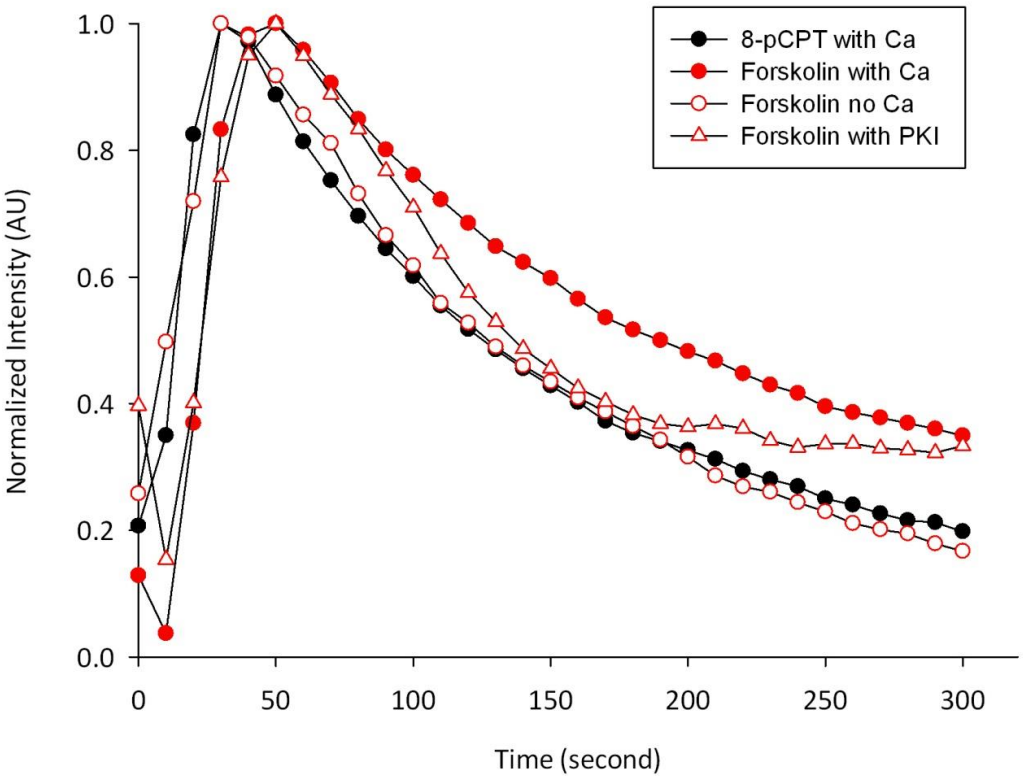

Figure 6.14: Normalised calcium transients induced in HCAECs on forskolin application
The average signal intensity for each condition was normalised against the peak intensity to allow direct comparison of the time-course of calcium transients. Peak calcium elevation was recorded at approximately 50 seconds for HCAECs treated with forskolin in the presence of extracellular calcium both with (open red triangles) and without PKI (filled red circles). In the absence of extracellular calcium, forskolin induced a peak elevation in intracellular calcium within 30 seconds (open red circles).

6.3.2.3 - Potential Epac-mediated calcium-release mechanisms

Evaluation of normalised calcium transients under various conditions indicated that the ER plays a major role in the elevation of calcium induced by both 8-pCPT and forskolin. As RyRs are generally not considered to be functionally important in calcium release from the ER in non-excitable cells, IP_3Rs are thought to be the primary ER calcium release channels in endothelial cells (Section 6.1.3.1 – Calcium release from the endoplasmic reticulum). cAMP has been linked to an increase in the affinity of IP_3Rs for IP_3 by as much as a factor of 10 in the salivary glands of a subspecies of dipteran fly (Schmidt, Baumann et al. 2008). This increase in affinity is thought to be mediated by PKA (Schmidt, Baumann et al. 2008) but there is potential for an Epac-mediated mechanism whereby the sensitivity of IP_3Rs for IP_3 is enhanced on cAMP elevation in non-excitable cells. Phosphorylation of IP_3R1 has also been linked to enhanced calcium release from the ER (Hajnoczky, Gao et al. 1993, Wojcikiewicz and Luo 1998, Bruce, Shuttleworth et al. 2002, Tang, Tu et al. 2003, Dyachok and Gylfe 2004), although a decrease in calcium release on IP_3R1 phosphorylation has also been noted (Volpe and Alderson-Lang 1990, Tertyshnikova and Fein 1998). Such phosphorylation can be mediated by non-receptor protein kinases including calcium/calmodulin kinase II (CaMKII) (Supattapone, Danoff et al. 1988, Wojcikiewicz and Luo 1998, Tang, Tu et al. 2003). This kinase is activated on 8-pCPT application to rat cardiac myocytes (Pereira, Métrich et al. 2007), a process which has been shown to involve PKC in these cells (Waxham and Aronowski 1993, O-Uchi, Komukai et al. 2005). Indeed, CaMKII inhibition through application of the antagonist KN93, completely blocks 8-pCPT-induced enhancement of electrically-evoked ER calcium release (Oestreich, Malik et al. 2009). Similarly, IP_3 recycling-blocking agents L-690.330 and Licl, in addition to the IP_3R antagonist 2-aminoethoxydiphenyl borate (2-APB) and IP_3R siRNA knock down, all inhibit β_2-adrenoreceptor-stimulated ER calcium release in endothelial cells (Mayati, Levoin et al. 2012).

6.3.2.4 - Potential cAMP-mediated calcium-influx mechanisms

In addition to calcium release, the contribution of calcium influx pathways in HCAECs was implied from the apparent faster decline of calcium transient when extracellular calcium was omitted. There are three possible mechanisms by which calcium influx could occur in these cells; I_{CRAC}, nucleotide-gated cation channels and reverse-mode Na^+/ Ca^{2+} exchangers.

In non-excitable cells, calcium release from the ER is known to induce calcium entry across the cell membrane through store-operated calcium entry (SOCE). The process of SOCE and the involvement of STIM1 and Orai1 has been previously detailed (Section 6.1.3.2 - Store-operated calcium entry). It is possible that the difference between 8-pCPT-induced calcium transient in the presence and absence of extracellular calcium might be explained by I_{CRAC} in HCAECs.

The second calcium entry pathway is nucleotide-gated (CNG) cation channels. These channels are permeable to cations, including calcium, and their gating is directly regulated by the intracellular cGMP and cAMP concentrations (Section 6.1.3.3 - Additional calcium-entry mechanisms). If such channels are to open in HCAECs upon elevation of the intracellular cAMP concentration, it could explain the difference between forskolin-induced calcium transient in the presence and absence of extracellular calcium. Such channels would not, however, explain the differences between the calcium transient induced by 8-pCPT in the presence and absence of extracellular calcium, as Epac is directly stimulated by this agonist without elevation in the intracellular concentration of cAMP.

The final potential calcium entry pathway is through reverse-mode Na^+/ Ca^{2+} exchangers. Generally sodium/calcium exchange across the cell membrane acts as the calcium extrusion mechanism (Section 6.1.3.4 – Removal of calcium from cytosol). It has been suggested that calcium is able to enter the cell by Na^+/ Ca^{2+} exchangers in the reverse mode, whereby sodium ions are extruded in exchange for calcium entry (Hirota, Pertens et al. 2007, Liu, Peel et al. 2010, Tykocki, Jackson et al. 2012). However, the equilibrium potential for this mechanism is highly unfavourable even at the resting intracellular calcium concentration of 100 nM (-44 mV). On the elevation in intracellular calcium concentration induced by Epac (~ 800 nM), the equilibrium potential is approximately +10 mV, and thus this mechanism of calcium entry is even less feasible. It therefore seems unlikely that the Na^+/ Ca^{2+} exchanger is involved in the elevation of intracellular calcium concentration observed on 8-pCPT application, however this exchanger should not be ruled out as a mechanism for a Epac-induced rise in intracellular calcium concentration under pathological conditions where the intracellular sodium concentration is elevated to a level that would make the reverse mode possible.

6.3.3 - Concluding remarks

Together, this data suggests that Epac activation in HCAECs triggers calcium release from the ER that is mediated by IP_3R channels, with the calcium entry pathway potentially playing an additional role. This calcium elevation is rapid, with peak elevation at 30 seconds, and short-lived, declining to baseline levels after 200 seconds of recording. The bulk of the elevation in intracellular calcium is independent of PKA, as shown by relatively ineffective PKI, but is potentially contributed to by this pathway. In vivo, this Epac-induced rise in intracellular calcium concentration may activate endothelial IK_{ca} and SK_{ca} channels which have previously been shown to induce smooth muscle cell hyperpolarisation, and therefore relaxation. There are 2 potential mechanisms by which this could occur; (i) potassium efflux through activated endothelial IK_{ca} and SK_{ca} channels triggers smooth muscle cell hyperpolarisation through activation of sodium/potassium-ATPase and inwardly-rectifying potassium channels on smooth muscle cells, and (ii) the hyperpolarisation induced in endothelial cells on potassium efflux is directly transferred to smooth muscle cells through electrical communication mediated by gap junctions. Through these mechanisms, and the enhanced GJIC induced by 8-pCPT application, Epac may facilitate both endothelial cell-endothelial cell communication and endothelial cell-smooth muscle cell communication, thereby creating an efficient and low-resistance pathway for direct cell-cell communication and the control of vascular tone.

Chapter 7:

Final Discussion

7.1 - Introduction

The aim of this study was to investigate whether Epac activation in HCAECs affected cadherin and connexin distribution, and whether this had a knock-on effect on cell-cell communication. Epac activation in HCAECs was found to promote endothelial cell-endothelial cell contact, and communication via connexins, specifically Cx37. Furthermore, Epac activation triggered a transient rise in intracellular calcium concentration that was independent of the PKA pathway. As a rise in intracellular calcium has been linked to endothelial cell hyperpolarisation, and subsequent smooth muscle cell hyperpolarisation (Roberts, Kamishima et al. 2013), this preliminary data indicates that Epac may provide a potential mechanism for both endothelial barrier protection and the control of vascular tone.

7.2 - Epac activation promotes connexin-mediated intercellular communication

Preliminary data indicates a re-distribution of Cx37 towards sites of cell-cell contact in HCAECs on Epac activation (Chapter 5). This re-distribution is mirrored by an increase in VE-cadherin distribution at the membrane that results in greater cell-cell contact and a tighter endothelial barrier. Indeed, it appears that the re-distribution of VE-cadherin is likely to be a precursor to the increased distribution of Cx37 at the membrane, as disruption of VE-cadherin interaction through EGTA addition, or incubation with the VE-cadherin blocking antibody, had a subsequent effect on the distribution pattern of Cx37. Gap junctions, formed by connexins, allow direct cell-cell communication through the exchange of ions and second messenger molecules. Epac appears to promote what is hypothesised to be Cx37-mediated intercellular communication in HCAECs, and as such is suggested to promote the exchange of second messengers between adjacent cells. The endothelial cell layer is well-known for its high degree of intercellular communication and has previously been hailed as the primary route for the longitudinal spread of signal along the vessel wall (Emerson and Segal 2000). If Epac does result in an enhanced route for EC-EC communication, as is indicated here, then this pathway is likely to play a role in the control of vascular tone. In addition, preliminary data indicates that Epac also appears to have an effect on the distribution of additional connexins, namely Cx43 (Somekawa 2005, Duquesnes, Derangeon et al. 2010). Cx43 is considered to be the predominant connexin expressed in vascular smooth muscle cells (Haudenschild et al. 1990, Bruzzone, Haefliger et al. 1993, Gourdie, Green et al. 1993, Little, Beyer et al. 1995, Van Kempen and Jongsma

1999) and as such the Epac-induced re-distribution of Cx43 in HCAECs may also promote enhanced EC-SMC communication. If this hypothesis were correct this would further support a role for Epac in the control of vascular tone. To determine whether Epac does truly promote both EC-EC and EC-SMC communication, the use of a gap junction-blocking agent, or connexin siRNA, is required. In addition to the assessment of intercellular communication through the use of a Lucifer yellow dye assay (as used here), experiments involving the investigation of the spread of electrical current would further elucidate the extent to which Epac activation promotes enhanced cell-cell communication. This could be achieved through the use of patch clamp equipment and would provide support for our hypothesis that Epac promotes direct cell-cell communication and the spread of electrical current between adjacent cells. In addition to determining the degree of EC-EC communication, co-culture of HCAECs with HCASMCs would allow investigation of the proposed Epac-induced increase in EC-SMC communication. Indeed, this method was attempted during this study, however due to the specific environment required for each cell culture this did not provide beneficial results for examination at this stage.

7.3 – Epac activation triggers a transient rise in intracellular calcium concentration

On Epac activation in HCAECs, a rapid rise in the intracellular calcium concentration was detected, followed by a slow decline to base level (Chapter 6). This rise in calcium concentration was largely unaffected by either removal of extracellular calcium, pre-incubation with ryanodine, or pre-incubation with PKI, a PKA inhibitor. As such, the source of the calcium was hypothesised to be the endoplasmic reticulum and the mechanism proposed to involve the activation of IP_3 receptors on the surface of this organelle. Calcium elevations in endothelial cells have previously been shown to activate IK_{ca} and SK_{ca} channels in the plasma membrane (Roberts, Kamishima et al. 2013), resulting in an efflux of potassium and hyperpolarisation of the cell. Electrical current is able to spread directly between adjacent cells through electrotonic spread via gap junction channels (de Wit and Griffith 2010), and as such the potential hyperpolarisation induced in endothelial cells by Epac activation could spread directly to adjacent endothelial cells. The role of the endothelium as a low-resistance pathway for the spread of such signals has already been detailed, and such a mechanism may allow for the rapid spread of hyperpolarisation to down-stream areas of endothelium (Emerson and Segal 2000). In addition to the spread of hyperpolarisation between endothelial cells, gap junctions at the myoendothelial junction

(MEJ) also provide a site for direct EC-SMC communication, and therefore may facilitate the spread of hyperpolarisation from ECs to SMCs (Sandow, Tare et al. 2002, de Wit and Griffith 2010). Hyperpolarisation in smooth muscle cells triggers the closure of voltage dependent calcium channels (VDCCs), blocking calcium entry and therefore promoting smooth muscle relaxation (Figure 7.1). As such, Epac could potentially provide a mechanism for the endothelial-mediated control of vascular tone that is currently represented as the 'classical' endothelial-derived hyperpolarising factor (EDHF) pathway (Edwards, Feletou et al. 2010, Roberts, Kamishima et al. 2013). In addition, due to the low-resistance pathway along the endothelium, this could provide not only local control of tone but also regulate vascular relaxation at sites distant from the initial propagation of signal (Emerson and Segal 2000). This mechanism is further supported by the Epac-mediated enhanced GJIC that would support this spread of signal between endothelial cells. Furthermore, if Epac does promote a re-distribution of Cx43, as indicated in preliminary experiments here, then Epac may also support enhanced EC-SMC communication and thus the spread of hyperpolarisation from ECs to SMCs. If this hypothesis is to be tested then electrical conductance between HCAECs and HCASMCs must be examined, and the effect of Epac activation in endothelial cells on the state of VDCCs expressed on SMCs investigated. In addition to the direct spread of hyperpolarisation between endothelial and smooth muscle cells, the efflux of potassium from the endothelial cells on the activation of IK_{ca} channels may have a direct effect on the state of the underlying smooth muscle cells. IK_{ca} channels have previously been identified at the MEJ where endothelial cells and smooth muscle cells are closely apposed (Sandow, Neylon et al. 2006). As such, there is evidence to suggest that the efflux of potassium into this local environment directly activates sodium/potassium ATPase on the surface of the smooth muscle cell, that exchanges 2 potassium ions into the cell for 3 sodium ions out of the cell (Edwards, Dora et al. 1998). The resulting hyperpolarisation is further contributed to by the action of inwardly-rectifying potassium channels (K_{ir}) which remove the newly-received potassium. Ultimately, there appears to be two potential pathways through which an Epac-mediated hyperpolarisation in HCAECs could trigger HCASMC hyperpolarisation and subsequent relaxation. To determine whether either, or both, of these pathways play a role in the endothelial –mediated control of vascular tone in the coronary circulation, the presence of IK_{ca} and SK_{ca} channels in HCAECs needs to be determined. In addition, the potential identification of IK_{ca} channels specifically at the MEJ would support, or refute, the role of a local potassium efflux on the smooth muscle contractile state. If such experiments determine that Epac activation in HCAECs provides a rapid and direct mechanism for the

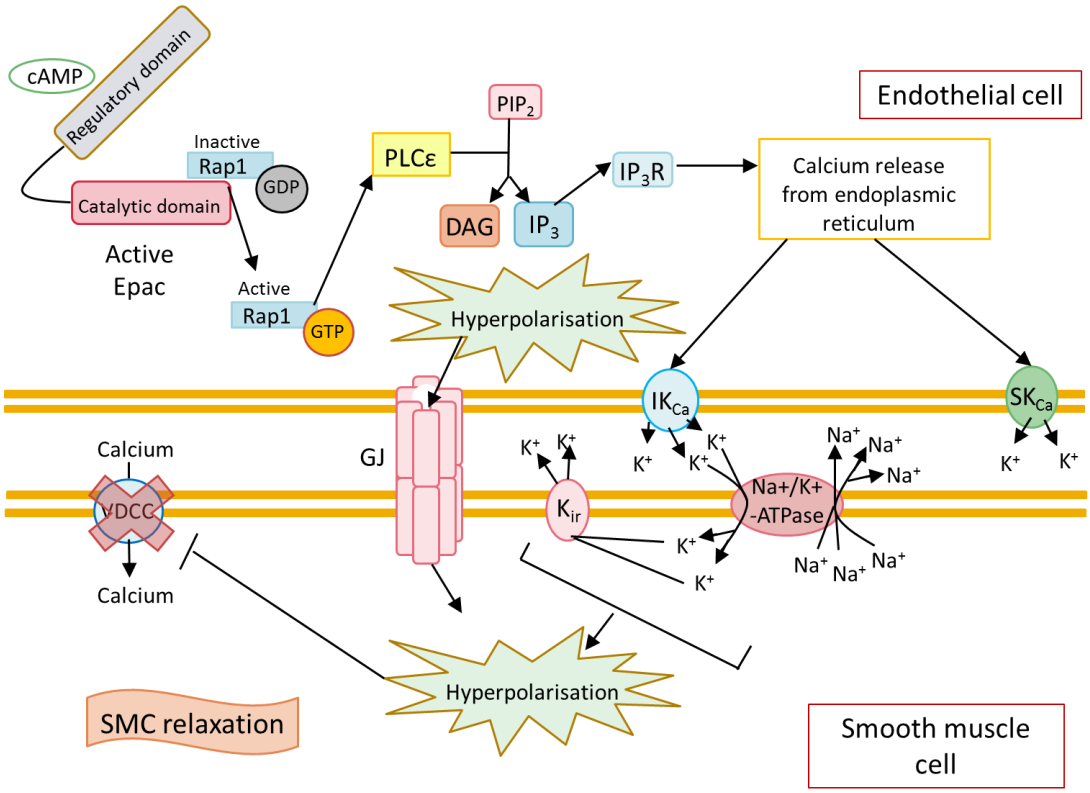

Figure 7.1: Hypothesised mechanism of Epac-mediated regulation of vascular tone
This diagram shows the hypothesised hyperpolarisation induced in HCAECs on Epac activation. Calcium release from the endoplasmic reticulum activates IK_{ca} and SK_{ca} channels on the endothelial plasma membrane. Potassium efflux results in HCAEC hyperpolarisation. This hyperpolarisation spreads directly to the adjacent HCASMCs through gap junctions at the myoendothelial junction (MEJ). It is also hypothesised the IK_{ca} channels located at the MEJ result in a local rise in the extracellular concentration of potassium that activates sodium/potassium ATPase pumps on the membrane of HCASMCs. This results in 2 potassium ions in/ 3 sodium ions out, hyperpolarising the HCASMC. The smooth muscle cell is further hyperpolarised by the action of inwardly-rectifying potassium channels (K_{ir}) which remove the newly acquired potassium from the HCASMC. The hyperpolarisation of the smooth muscle cell blocks the voltage-dependent calcium channels (VDCC), inhibiting calcium influx. Calcium is required for smooth muscle cell contraction and as such the smooth muscle cell relaxes.

regulation of vascular tone then this provides an exciting potential for manipulation of this pathway to promote vascular relaxation.

7.4 - The potential role of Epac in the treatment of cardiovascular disease

Cardiovascular disease encompasses a number of conditions, including coronary heart disease (CHD) which is the biggest cause of mortality in the UK, responsible for one death every 7 minutes (British Heart Foundation 2015). Endothelial dysfunction and hypertension are the primary contributing factors in the development of CHD (Vanhoutte 2009), and our preliminary data suggests that Epac may play a role in preventing CHD through the tightening of the endothelial barrier and vascular relaxation. Endothelial dysfunction is induced on disruption of the endothelial barrier which allows the subsequent invasion of inflammatory mediators and the development of an atherosclerotic plaque (Wang et al. 2013). This plaque invades the vessel lumen, restricting blood flow and endangering downstream tissues. Angina Pectoris is the result of insufficient blood flow to the heart muscle induced by the build-up of an atherosclerotic plaque in the coronary arteries. If part of the plaque detaches this may completely occlude the vessel lumen resulting in a complete absence of blood flow to downstream muscle and a myocardial infarction (MI). Prevention of endothelial disruption through protection of the endothelial barrier may therefore prevent the formation of such atherosclerotic plaques and ultimately reduce the incidence of MI. In our preliminary results, Epac has been shown to promote HCAEC-HCAEC contact, and formation of a tight endothelial barrier, mediated by VE-cadherin. In addition, if Epac promotes endothelial hyperpolarisation which in turn triggers smooth muscle hyperpolarisation, facilitated by enhanced GJIC, this would mediate endothelial-induced smooth muscle relaxation which may prevent the development of hypertension. It should also be noted that even if Epac were only to facilitate one or the other of the pathways (tighter endothelial barrier, or endothelial-induced vascular relaxation) the therapeutic potential of such a mechanism is still enormous.

The predominant treatment for atherosclerosis involves a change in lifestyle, in combination with statins (3-hydroxy-3-methylglutaryl (HMG)-CoA reductase inhibitors) to lower blood cholesterol levels (Grundy 1998), anti-hypertensive drugs (including calcium channel blockers) (Godfraind 2014), and the potential use of invasive procedures including percutaneous transluminal coronary angioplasty (PTCA) (Mani et al. 2007). In a large

proportion of patients undergoing PTCA, however, restenosis develops within the first 6 months following surgery (Braun-Dullaeus et al. 1998). The use of drug-eluting stents (DES), where an immunosuppressant drug is incorporated into the coating of the stent (Wang et al. 2013), has reduced the rate of re-stenosis from approximately 30-40% to 10% (Jukema et al. 2012), however in-stent restenosis associated with intimal hyperplasia still remains a major limitation of PTCA (Mani et al. 2007). It is also worth noting that DES have been linked to lethal late-stage thrombotic events as a direct result of endothelial cell injury (Joner et al. 2006). It is well established that restoration of a healthy endothelium is required in order to prevent restenosis and/or thrombus formation (Otsuka et al. 2012). Statins promote re-endothelialisation in addition to their cholesterol-lowering benefits (Walter et al. 2002), and as such our data may therefore suggest Epac activation as a key accompaniment to PTCA and statins to promote endothelial stabilisation and to prevent re-stenosis. This hypothesis is supported by work by Lee *et al.* (2012), who identified that coating of stents with anti-VE-cadherin antibodies accelerated re-endothelialisation and reduced neo-intimal formation in a rabbit model of atherosclerosis (Lee et al. 2012). This VE-cadherin was found to maximise the capture of endothelial progenitor cells, a requirement for successful re-endothelialisation. As Epac activation has been shown by us, and others, to promote VE-cadherin distribution at the membrane, Epac activation following PTCA may promote endothelial stabilisation in a similar manner. As previously mentioned, calcium channel blockers are also commonly used to treat patients with hypertension through inducing vascular smooth muscle relaxation and thereby lowering blood pressure. Our data, together with recent work by Roberts *et al.* (2013), proposes that Epac activation promotes vascular smooth muscle relaxation through a rise in the intracellular calcium concentration in endothelial cells. As such, Epac activation may also provide an additional mechanism for the treatment of hypertension and thus long-term treatment for atherosclerosis.

If Epac activation were to be induced, potentially through application of the Epac-selective agonist 8-pCPT, as used here, then atherosclerotic plaque formation (and/or re-stenosis) and potentially also hypertension, may be inhibited without the need for invasive surgery. This mechanism may also bypass many of the non-specific effects of utilising the whole cAMP pathway for the treatment of vascular diseases. Phosphodiesterase (PDE) inhibitors such as Rolipram have been shown to improve survival rates in animal models of inflammation (Lin, Adamson et al. 2012, Schick, Wunder et al. 2012), however, inhibition of

PDE activity may result in an increase in the cytosolic concentration of cAMP which can lead to barrier disruption and increased permeability (Creighton, Zhu et al. 2008). An additional, unrelated, PDE4 inhibitor is Roflumilast (3-cyclopropylmethoxy-4-difluoromethoxy-N-[3,5-dichloropyrid-4-yl]-benzamide) (Sanz et al. 2007). This PDE4 inhibitor is currently used as a treatment for chronic obstructive pulmonary disease (COPD) (Muñoz-Esquerre et al. 2015). Addition of Roflumilast to human coronary artery smooth muscle cells has been shown to suppress tumour necrosis factor (TNF)-α-induced expression of vascular cell adhesion molecule 1 (VCAM-1) (Lehrke et al. 2015). The expression of such cell adhesion molecules is a prerequisite for leukocyte accumulation and sustained inflammation, both of which are triggers for neo-intimal hyperplasia (Shah 2003). Roflumilast was found to supress the expression of VCAM-1, and thus monocyte transmigration and adhesion to vascular smooth muscles in a novel Epac-dependent, but PKA-independent, manner (Lehrke et al. 2015). Indeed, Roflumilast treatment was shown to significantly attenuate neo-intima formation by over 40% (Lehrke et al. 2015). Furthermore, this reduction in hyperplasia was shown to be induced through addition of 8-pCPT, as used here, and completely blocked by both ESI-09 and Epac1 siRNA (Lehrke et al. 2015). This suppression of neo-intimal hyperplasia was found to be at least partly due to reduced macrophage infiltration, thus highlighting Epac's ability to promote a stable endothelial barrier. Work by Sanz *et al.* (2007) also identified that Roflumilast treatment was significantly more potent in inhibiting leukocyte-endothelial cell interaction than the PDE4 inhibitors Rolipram and Cilomilast (Sanz et al. 2007). PDE4 exists in one of two distinct conformations; a high-affinity Rolipram-binding PDE4 (HPDE4) which is primarily identified within the central nervous system and parietal glands, and a low-affinity Rolipram-binding PDE4 (LPDE4) which is predominantly localised to immunocompetent cells (Torphy et al. 1999). Rolipram targets HPDE4, while Cilomilast and Roflumilast target LPDE4 thus improving the therapeutic potential of these second generation compounds and potentially explaining the differences in the results obtained with varying PDE4 inhibitors. In addition, Hatzelmann *et al.* (2001) identified that eosinophils and macrophages are inhibited at relatively similar potencies by all PDE4 inhibitors tested (Roflumilast, Roflumilast N-Oxide, Piclamilast, Rolipram and Cilomilast) while monocytes and CD4+ T cells were substantially more inhibited by Roflumilast than both Cilomilast and Rolipram. Roflumilast therefore appears to promote a more extensive inhibition of the transmigration of inflammatory mediators, potentially explaining its greater anti-inflammatory effects. Sanz *et al.* (2007) also identified that Roflumilast was able to diminish histamine- and thrombin-

induced permeability in microvascular endothelial cells and HUVECs, respectively, in a concentration-dependent manner.

Together, these data highlight the potential therapeutic applications of Epac in the treatment of cardiovascular diseases.

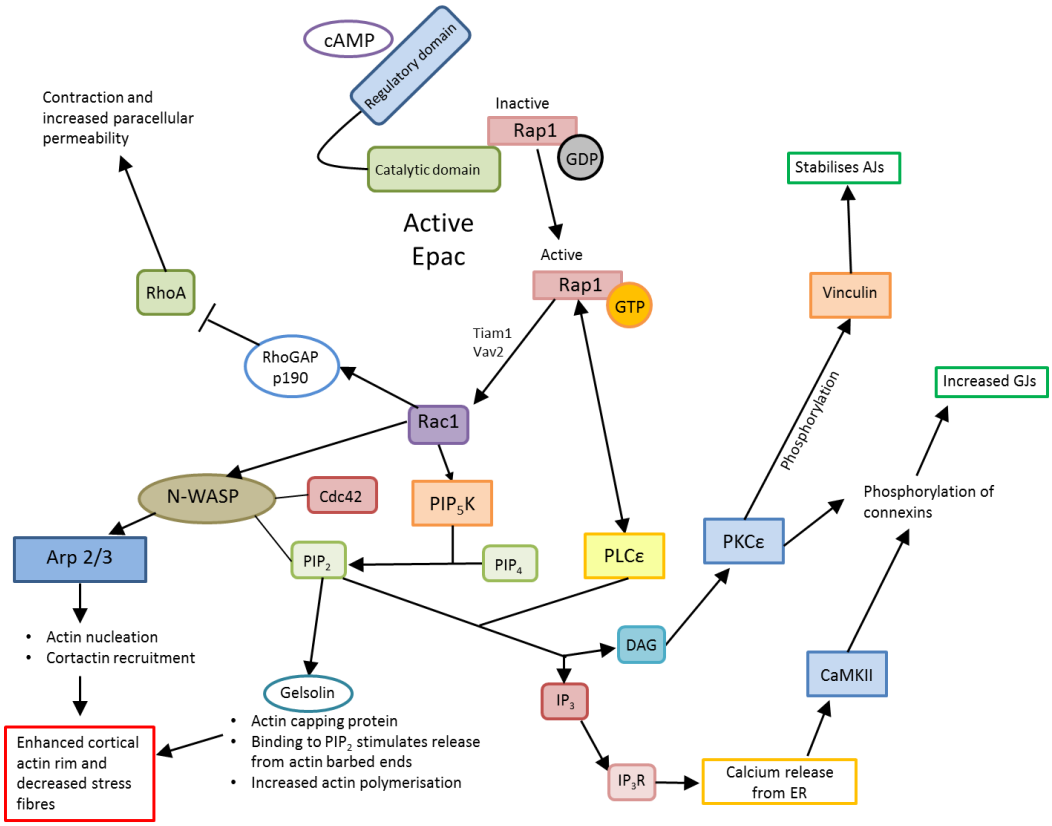

Figure 7.2: Hypothesised mechanisms of Epac action on HCAECs

This diagram represents the potential mechanisms through which Epac mediates the re-distribution of cadherins and connexins and the release of calcium from the endoplasmic reticulum. Epac's activity on the actin cytoskeleton is relatively well detailed in the literature (left side of the figure). Also shown, is the potential phosphorylation of the actin-binding protein Vinculin, and connexins, by PKCε and/or CaMKII (right side of the figure). In addition, the Epac-induced release of calcium from the endoplasmic reticulum, mediated by IP_3 production, is shown at the bottom right of the figure.

7.5 - Further work

This study has identified an exciting area for further research into the role of the Epac pathway in the control of the vasculature. Preliminary experiments identified that Epac activation promotes a re-distribution of VE-cadherin to the membrane that is hypothesised to be a result of actin re-organisation in HCAECs. To elucidate the mechanism through which actin may promote VE-cadherin distribution at the membrane, and a tighter endothelial barrier, actin staining on the application of the Epac agonist 8-pCPT is required. It is hypothesised that the Epac-induced reorganisation of actin from stress fibres to a cortical actin rim promotes cell-cell contact and formation of adherens junctions (Figure 7.2). Pre-treatment of these HCAECs with Epac1 siRNA and/or the Epac antagonists HJC0197 and ESI-09, will also provide valuable information on the role of Epac on the hypothesised re-distribution of actin.

The investigation of the effect of Epac activation on VE-cadherin and connexin distribution in HCAECs in the presence of the VE-cadherin blocking antibody would provide the necessary data to interpret whether VE-cadherin re-distribution is a prerequisite for the connexin re-distribution induced by Epac activation. Furthermore, the use of a membrane marker would allow the quantification of the membranous cadherin and connexin distribution. Such markers could include sodium/potassium ATPase or plasma membrane calcium ATPase. In addition, fluorescence resonance energy transfer (FRET) analysis could provide confirmation that connexins and cadherins are closely associated at the membrane, forming a complex that promotes cell-cell communication.

The use of IP_3R siRNA, particularly IP_3R1, prior to live calcium imaging with the Epac agonist 8-pCPT could provide the necessary data to support our hypothesis that the calcium peak induced by Epac activation is a result of the activation of IP_3R's on the HCAEC endoplasmic reticulum. Similarly, the overexpression of Rap1GAP could provide confirmation that the Epac pathway alone is responsible for both the calcium transients and the cadherin/ connexin redistribution.

To determine whether Epac is able to induce hyperpolarisation in HCAECs, the expression of IK_{ca} and SK_{ca} channels in these cells needs to be confirmed. More specifically, the localisation of IK_{ca} channels to the MEJ would provide support for the hypothesis that a local potassium efflux is able to promote smooth muscle hyperpolarisation subsequent to

endothelial cell hyperpolarisation. Similarly, the identification of sodium/potassium ATPase pumps on HCASMCs at the MEJ, where HCAECs project through the internal elastic lamina, would support our hypothesis that HCAEC hyperpolarisation could directly activate these channels on the plasma membrane of HCASMCS triggering SMC hyperpolarisation and relaxation. In addition, examination of the electrical conductance between adjacent HCAECs and HCAECs/HCASMCs through patch clamp would provide further information on the role of Epac in the regulation of vascular tone.

7.6 – Concluding remarks

Epac activation in HCAECs appears to induce a protective phenotype that promotes tightening of the endothelial barrier through rearrangement of VE-cadherin to sites of cell-cell contact. This offers a potential therapeutic mechanism for the Epac pathway in the prevention of endothelial disruption and atherosclerotic plaque formation. In addition, Epac activation in HCAECs induces a rapid rise in intracellular calcium concentration that may play a role in the regulation of vascular tone through the hyperpolarisation of both HCAECs and the adjacent HCASMCs. This implies that Epac may also play a role in limiting the development of hypertension. Together, these data highlight Epac as a potentially invaluable means for the regulation of the vasculature both under normal and disease states. More work is needed in this area to elucidate the exact mechanism through which Epac exerts its effects on the endothelium, and subsequently the smooth muscle layer; however the data shown here provides the foundation for such work to explore this novel and exciting pathway in detail.

Appendix

Supplementary Figure for Chapter 3: Characterisation of rat tissues and human cells

Lysate	Absorbance (AU)	Total protein concentration (µg/ml)
HCASMC P7	0.304	114.78
HCASMC P8	0.460	298.07
HCASMC P9	0.407	218.84
HCASMC P10	0.338	140.04
HCAEC P7	0.456	290.79
HCAEC P8	0.449	283.51
HCAEC P9	0.313	118.20
HCAEC P10	0.320	122.06
Heart (5 fold dilution)	0.559	456.10

Supplementary Figure 1: Total protein concentration of rat tissues, HCAECs and HCASMCs

Related to Figure 3.1 in "Chapter 3: Characterisation of rat tissues and human cells". Total protein concentration for HCAEC lysates between passages 7-10, and rat heart lysate at a 5 fold dilution. The protein concentration of HCAEC and HCASMC lysates are comparable while the high total protein concentration of rat heart lysate is evident, even at a 5 fold dilution. Absorbance recorded using spectrophotometer set at 562 nm.

Supplementary information on the quantification of cadherin and connexin co-localisation using Image J plugins

Three Image J plugins were used to quantify the relative co-localisation between cadherins and connexins in confocal images; Manders' Overlap Coefficient plugin, Co-localisation Finder plugin and Intensity Correlation Analysis plugin. The MacBiophotonics Image J software, pre-loaded with these plugins, was used for this quantification (full details can be found here: http://www.uhnresearch.ca/facilities/wcif/imagej/colour_analysis.htm). The quantification process for each plugin is as detailed below:

1. Manders' Overlap Coefficient plugin

- The individual red (AF595) and green (AF488) images were opened within the MacBiophotonics Image J software
- Both images were converted to 8-bit
- The Manders' Overlap Coefficient plugin was selected and all settings set to default
- The "Manders' R" value was used for comparison between images
- This value ranges between 1 and zero, with 1 being high co-localisation and zero being low

2. Co-localisation Finder plugin
    - The individual red (AF595) and green (AF488) images were opened within the MacBiophotonics Image J software
    - Both images were converted to 8-bit
    - The co-localisation highlighter plugin was selected and all settings set to default
    - The co-localisation finder plugin was selected and all settings set to default
    - A % co-localisation was obtained and used for comparison between images

3. Intensity Correlation Analysis plugin
    - The individual red (AF595) and green (AF488) images were opened within the MacBiophotonics Image J software
    - The thresholds of both images were adjusted to default settings
    - The Intensity Correlation Analysis plugin was selected and settings altered as follows:
        i. Display intensity counts
        ii. Crosshair = 3
        iii. Select PDM image to be displayed
        iv. Select positive PDMs only
    - The "Manders' R" value was used for comparison between images
    - This value ranges between 1 and zero, with 1 being high co-localisation and zero being low

References

Abe, K. and M. Takeichi (2008). "EPLIN mediates linkage of the cadherin-catenin complex to F-actin and stabilizes the circumferential actin belt." Proceedings of the National Academy of Sciences of the United States of America **105**(1): 13-19.

Abercrombie, M., J. E. M. Heaysman and S. M. Pegrum (1971). "The locomotion of fibroblasts in culture. IV. Electron microscopy of the leading lamella." Experimental Cell Research **67**(2): 359-367.

Abraham, S., M. Yeo, M. Montero-Balaguer, H. Paterson, E. Dejana, C. J. Marshall and G. Mavria (2009). "VE-Cadherin-Mediated Cell-Cell Interaction Suppresses Sprouting via Signaling to MLC2 Phosphorylation." Current Biology **19**(8): 668-674.

Absher, M., J. Woodcock-Mitchell, J. Mitchell, L. Baldor, R. Low and D. Warshaw (1989). "Characterization of vascular smooth muscle cell phenotype in long-term culture." In Vitro Cellular & Developmental Biology **25**(2): 183-192.

Adamson, R. H. (1990). "Permeability of frog mesenteric capillaries after partial pronase digestion of the endothelial glycocalyx." J Physiol **428**: 1-13.

Adamson, R. H., V. H. Huxley and F. E. Curry (1988). "Single capillary permeability to proteins having similar size but different charge." Am J Physiol **254**(2 Pt 2): H304-312.

Aghion, J., C. Gueth-Hallonet, C. Antony, D. Gros and B. Maro (1994). "Cell adhesion and gap junction formation in the early mouse embryo are induced prematurely by 6-DMAP in the absence of E-cadherin phosphorylation." Journal of Cell Science **107**(5): 1369-1379.

Ahmmed, G. U., D. Mehta, S. Vogel, M. Holinstat, B. C. Paria, C. Tiruppathi and A. B. Malik (2004). "Protein kinase Calpha phosphorylates the TRPC1 channel and regulates store-operated Ca2+ entry in endothelial cells." J Biol Chem **279**(20): 20941-20949.

Ai, Z., A. Fischer, D. C. Spray, A. M. C. Brown and G. I. Fishman (2000). "Wnt-1 regulation of connexin43 in cardiac myocytes." Journal of Clinical Investigation **105**(2): 161-171.

Akhta, N., S. Carlso, A. Pesarini, N. Ambulos and A. Passaniti (2001). "Extracellular matrix-derived angiogenic factor(s) inhibit endothelial cell proliferation, enhance differentiation, and stimulate angiogenesis in vivo." Endothelium **8**(3): 221-234.

Albelda, S. M., M. Daise, E. M. Levine and C. A. Buck (1989). "Identification and characterization of cell-substratum adhesion receptors on cultured human endothelial cells." J Clin Invest **83**(6): 1992-2002.

Albelda, S. M., W. A. Muller, C. A. Buck and P. J. Newman (1991). "Molecular and cellular properties of PECAM-1 (endoCAM/CD31): A novel vascular cell-cell adhesion molecule." Journal of Cell Biology **114**(5): 1059-1068.

Albertinazzi, C., A. Cattelino and I. De Curtis (1999). "Rac GTPases localize at sites of actin reorganization during dynamic remodeling of the cytoskeleton of normal embryonic fibroblasts." Journal of Cell Science **112**(21): 3821-3831.

Alev, C., S. Urscheld, S. Sonntag, G. Zoidl, A. G. Fort, T. Höher, M. Matsubara, K. Willecke, D. C. Spray and R. Dermietzel (2008). "The neuronal connexin36 interacts with and is phosphorylated by CaMKII in a way similar to CaMKII interaction with glutamate

receptors." Proceedings of the National Academy of Sciences of the United States of America **105**(52): 20964-20969.

Alexander, J. S., S. A. Jackson, E. Chaney, C. G. Kevil and F. R. Haselton (1998). "The role of cadherin endocytosis in endothelial barrier regulation: Involvement of protein kinase C and actin-cadherin interactions." Inflammation **22**(4): 419-433.

Alfranca, A., M. A. Iniguez, M. Fresno and J. M. Redondo (2006). "Prostanoid signal transduction and gene expression in the endothelium: role in cardiovascular diseases." Cardiovasc Res **70**(3): 446-456.

Almagro, S., C. Durmort, A. Chervin-Pétinot, S. Heyraud, M. Dubois, O. Lambert, C. Maillefaud, E. Hewat, J. P. Schaal, P. Huber and D. Gulino-Debrac (2010). "The motor protein Myosin-X transports VE-cadherin along filopodia to allow the formation of early endothelial cell-cell contacts." Molecular and Cellular Biology **30**(7): 1703-1717.

Almahariq, M., T. Tsalkova, F. C. Mei, H. Chen, J. Zhou, S. K. Sastry, F. Schwede and X. Cheng (2013). "A novel EPAC-specific inhibitor suppresses pancreatic cancer cell migration and invasion." Mol Pharmacol **83**(1): 122-128.

Anastasiadis, P. Z., S. Y. Moon, M. A. Thoreson, D. J. Mariner, H. C. Crawford, Y. Zheng and A. B. Reynolds (2000). "Inhibition of RhoA by p120 catenin." Nat Cell Biol **2**(9): 637-644.

Anastasiadis, P. Z. and A. B. Reynolds (2001). "Regulation of Rho GTPases by p120-catenin." Curr Opin Cell Biol **13**(5): 604-610.

Anderson, J. M., B. R. Stevenson, L. A. Jesaitis, D. A. Goodenough and M. S. Mooseker (1988). "Characterization of ZO-1, a protein component of the tight junction from mouse liver and Madin-Darby canine kidney cells." J Cell Biol **106**(4): 1141-1149.

Antonetti, D. A., A. J. Barber, S. Khin, E. Lieth, J. M. Tarbell and T. W. Gardner (1998). "Vascular permeability in experimental diabetes is associated with reduced endothelial occludin content: vascular endothelial growth factor decreases occludin in retinal endothelial cells. Penn State Retina Research Group." Diabetes **47**(12): 1953-1959.

Arensbak, B., H. B. Mikkelsen, F. Gustafsson, T. Christensen and N. H. Holstein-Rathlou (2001). "Expression of connexin 37, 40, and 43 mRNA and protein in renal preglomerular arterioles." Histochemistry and Cell Biology **115**(6): 479-487.

Arrate, M. P., J. M. Rodriguez, T. M. Tran, T. A. Brock and S. A. Cunningham (2001). "Cloning of human junctional adhesion molecule 3 (JAM3) and its identification as the JAM2 counter-receptor." J Biol Chem **276**(49): 45826-45832.

Asahara, T. and A. Kawamoto (2004). "Endothelial progenitor cells for postnatal vasculogenesis." Am J Physiol Cell Physiol **287**(3): C572-579.

Ashikaga, T., S. J. Strada and W. J. Thompson (1997). "Altered expression of cyclic nucleotide phosphodiesterase isozymes during culture of aortic endothelial cells." Biochem Pharmacol **54**(10): 1071-1079.

Askham, J. M., K. T. Vaughan, H. V. Goodson and E. E. Morrison (2002). "Evidence that an interaction between EB1 and p150(Glued) is required for the formation and maintenance

of a radial microtubule array anchored at the centrosome." Mol Biol Cell **13**(10): 3627-3645.

Atkinson, M. M., P. D. Lampe, H. H. Lin, R. Kollander, X. R. Li and D. T. Kiang (1995). "Cyclic AMP modifies the cellular distribution of connexin43 and induces a persistent increase in the junctional permeability of mouse mammary tumor cells." Journal of Cell Science **108**(9): 3079-3090.

Atsumi, T. and M. Takeichi (1980). "Cell association pattern in aggregates controlled by multiple cell-cell adhesion mechanisms." Development Growth and Differentiation **22**(2): 133-142.

Aurrand-Lions, M. A., L. Duncan, L. Du Pasquier and B. A. Imhof (2000). Cloning of JAM-2 and JAM-3: an Emerging Junctional Adhesion Molecular Family. Lymphoid Organogenesis. F. Melchers, Springer Berlin Heidelberg. **251:** 91-98.

Ballon, D. R., P. L. Flanary, D. P. Gladue, J. B. Konopka, H. G. Dohlman and J. Thorner (2006). "DEP-Domain-Mediated Regulation of GPCR Signaling Responses." Cell **126**(6): 1079-1093.

Banales, J. M., T. V. Masyuk, S. A. Gradilone, A. I. Masyuk, J. F. Medina and N. F. LaRusso (2009). "The cAMP effectors Epac and protein kinase a (PKA) are involved in the hepatic cystogenesis of an animal model of autosomal recessive polycystic kidney disease (ARPKD)." Hepatology **49**(1): 160-174.

Bansch, P., A. Nelson, T. Ohlsson and P. Bentzer (2011). "Effect of charge on microvascular permeability in early experimental sepsis in the rat." Microvascular Research **82**(3): 339-345.

Barr, A. J., L. F. Brass and D. R. Manning (1997). "Reconstitution of receptors and GTP-binding regulatory proteins (G proteins) in Sf9 cells. A direct evaluation of selectivity in receptor.G protein coupling." J Biol Chem **272**(4): 2223-2229.

Bastide, B., L. Neyses, D. Ganten, M. Paul, K. Willecke and O. Traub (1993). "Gap junction protein connexin40 is preferentially expressed in vascular endothelium and conductive bundles of rat myocardium and is increased under hypertensive conditions." Circulation Research **73**(6): 1138-1149.

Baumer, Y., V. Spindler, R. C. Werthmann, M. Bunemann and J. Waschke (2009). "Role of Rac 1 and cAMP in endothelial barrier stabilization and thrombin-induced barrier breakdown." J Cell Physiol **220**(3): 716-726.

Bazzoni, G. and E. Dejana (2004). "Endothelial cell-to-cell junctions: Molecular organization and role in vascular homeostasis." Physiological Reviews **84**(3): 869-901.

Bazzoni, G., O. M. Martinez-Estrada, F. Orsenigo, M. Cordenonsi, S. Citi and E. Dejana (2000). "Interaction of junctional adhesion molecule with the tight junction components ZO-1, cingulin, and occludin." J Biol Chem **275**(27): 20520-20526.

Beamish, J. A., P. He, K. Kottke-Marchant and R. E. Marchant (2010). "Molecular regulation of contractile smooth muscle cell phenotype: Implications for vascular tissue engineering." Tissue Engineering - Part B: Reviews **16**(5): 467-491.

Beblo, D. A., H. Z. Wang, E. C. Beyer, E. M. Westphale and R. D. Veenstra (1995). "Unique conductance, gating, and selective permeability properties of gap junction channels formed by connexin40." Circulation Research **77**(4): 813-822.

Beny, J. L. and J. L. Connat (1992). "An electron-microscopic study of smooth muscle cell dye coupling in the pig coronary arteries: Role of gap junctions." Circulation Research **70**(1): 49-55.

Beranger, F., B. Goud, A. Tavitian and J. De Gunzburg (1991). "Association of the Ras-antagonistic Rap1/Krev-1 proteins with the Golgi complex." Proceedings of the National Academy of Sciences of the United States of America **88**(5): 1606-1610.

Berger, G., R. Quarck, D. Tenza, S. Levy-Toledano, J. De Gunzburg and E. Martin Cramer (1994). "Ultrastructural localization of the small GTP-binding protein Rap1 in human platelets and megakaryocytes." British Journal of Haematology **88**(2): 372-382.

Berman, R. S., P. E. M. Martin, W. H. Evans and T. M. Griffith (2002). "Relative contributions of NO and gap junctional communication to endothelium-dependent relaxations of rabbit resistance arteries vary with vessel size." Microvascular Research **63**(1): 115-128.

Berridge, M. J. (1995). "Capacitative calcium entry." Biochem J **312 (Pt 1)**: 1-11.

Berridge, M. J., P. Lipp and M. D. Bootman (2000). "The versatility and universality of calcium signalling." Nat Rev Mol Cell Biol **1**(1): 11-21.

Berrueta, L., J. S. Tirnauer, S. C. Schuyler, D. Pellman and B. E. Bierer (1999). "The APC-associated protein EB1 associates with components of the dynactin complex and cytoplasmic dynein intermediate chain." Curr Biol **9**(8): 425-428.

Berry, M. N. and D. S. Friend (1969). "High-yield preparation of isolated rat liver parenchymal cells: a biochemical and fine structural study." Journal of Cell Biology **43**(3): 506-520.

Berthoud, V. M., M. B. Rook, O. Traub, E. L. Hertzberg and J. C. Saez (1993). "On the mechanisms of cell uncoupling induced by a tumor promoter phorbol ester in clone 9 cells, a rat liver epithelial cell line." European Journal of Cell Biology **62**(2): 384-396.

Besson, A., T. L. Wilson and V. Wee Yong (2002). "The anchoring protein RACK1 links protein kinase Cε to integrin β chains. Requirement for adhesion and motility." Journal of Biological Chemistry **277**(24): 22073-22084.

Bevans, C. G., M. Kordel, S. K. Rhee and A. L. Harris (1998). "Isoform Composition of Connexin Channels Determines Selectivity among Second Messengers and Uncharged Molecules." Journal of Biological Chemistry **273**(5): 2808-2816.

Beyer, E. C., J. Kistler, D. L. Paul and D. A. Goodenough (1989). "Antisera directed against connexin43 peptides react with a 43-kD protein localized to gap junctions in myocardium and other tissues." Journal of Cell Biology **108**(2): 595-605.

Beyer, E. C., K. E. Reed, E. M. Westphale, H. Lee Kanter and D. M. Larson (1992). "Molecular cloning and expression of rat connexin40, a gap junction protein expressed in vascular smooth muscle." The Journal of Membrane Biology **127**(1): 69-76.

Birnbaumer, L. (2009). "The TRPC class of ion channels: a critical review of their roles in slow, sustained increases in intracellular Ca(2+) concentrations." Annu Rev Pharmacol Toxicol **49**: 395-426.

Birukova, A. A., D. Burdette, N. Moldobaeva, J. Xing, P. Fu and K. G. Birukov (2010). "Rac GTPase is a hub for protein kinase A and Epac signaling in endothelial barrier protection by cAMP." Microvasc Res **79**(2): 128-138.

Birukova, A. A., K. Smurova, K. G. Birukov, P. Usatyuk, F. Liu, K. Kaibuchi, A. Ricks-Cord, V. Natarajan, I. Alieva, J. G. Garcia and A. D. Verin (2004). "Microtubule disassembly induces cytoskeletal remodeling and lung vascular barrier dysfunction: role of Rho-dependent mechanisms." J Cell Physiol **201**(1): 55-70.

Birukova, A. A., T. Zagranichnaya, P. Fu, E. Alekseeva, W. Chen, J. R. Jacobson and K. G. Birukov (2007). "Prostaglandins PGE(2) and PGI(2) promote endothelial barrier enhancement via PKA- and Epac1/Rap1-dependent Rac activation." Exp Cell Res **313**(11): 2504-2520.

Bishop, A. L. and A. Hall (2000). "Rho GTPases and their effector proteins." Biochemical Journal **348**(2): 241-255.

Bivona, T. G., H. H. Wiener, I. M. Ahearn, J. Silletti, V. K. Chiu and M. R. Philips (2004). "Rap1 up-regulation and activation on plasma membrane regulates T cell adhesion." J Cell Biol **164**(3): 461-470.

Blankesteijn, W. M., M. E. van Gijn, Y. P. Essers-Janssen, M. J. Daemen and J. F. Smits (2000). "Beta-catenin, an inducer of uncontrolled cell proliferation and migration in malignancies, is localized in the cytoplasm of vascular endothelium during neovascularization after myocardial infarction." Am J Pathol **157**(3): 877-883.

Blaschuk, O. W., R. Sullivan, S. David and Y. Pouliot (1990). "Identification of a cadherin cell adhesion recognition sequence." Developmental Biology **139**(1): 227-229.

Boettner, B., E. E. Govek, J. Cross and L. Van Aelst (2000). "The junctional multidomain protein AF-6 is a binding partner of the Rap1A GTpase and associates with the actin cytoskeletal regulator profilin." Proceedings of the National Academy of Sciences of the United States of America **97**(16): 9064-9069.

Boller, K., D. Vestweber and R. Kemler (1985). "Cell-adhesion molecule uvomorulin is localized in the intermediate junctions of adult intestinal epithelial cells." The Journal of Cell Biology **100**(1): 327-332.

Borg-Capra, C., M. P. Fournet-Bourguignon, P. Janiak, N. Villeneuve, J. P. Bidouard, J. P. Vilaine and P. M. Vanhoutte (1997). "Morphological heterogeneity with normal expression but altered function of G proteins in porcine cultured regenerated coronary endothelial cells." British Journal of Pharmacology **122**(6): 999-1008.

Boriack-Sjodin, P. A., S. M. Margarit, D. Bar-Sagi and J. Kuriyan (1998). "The structural basis of the activation of Ras by Sos." Nature **394**(6691): 337-343.

Bos, C. L., D. J. Richel, T. Ritsema, M. P. Peppelenbosch and H. H. Versteeg (2004). "Prostanoids and prostanoid receptors in signal transduction." Int J Biochem Cell Biol **36**(7): 1187-1205.

Bos, J. L. (2003). "Epac: A new cAMP target and new avenues in cAMP research." Nature Reviews Molecular Cell Biology **4**(9): 733-738.

Bos, J. L., J. De Rooij and K. A. Reedquist (2001). "Rap1 signalling: Adhering to new models." Nature Reviews Molecular Cell Biology **2**(5): 369-377.

Bossu, J. L., A. Elhamdani and A. Feltz (1992). "Voltage-dependent calcium entry in confluent bovine capillary endothelial cells." FEBS Lett **299**(3): 239-242.

Brakebusch, C. and R. Fassler (2003). "The integrin-actin connection, an eternal love affair." Embo j **22**(10): 2324-2333.

Braun-Dullaeus, R.C., M. J. Mann, and V. J. Dzau (1998). "Cell cycle progression new therapeutic target for vascular proliferative disease." Circulation **98**(1) (1998): 82-89.

Breier, G., F. Breviario, L. Caveda, R. Berthier, H. Schnürch, U. Gotsch, D. Vestweber, W. Risau and E. Dejana (1996). "Molecular cloning and expression of murine vascular endothelial-cadherin in early stage development of cardiovascular system." Blood **87**(2): 630-641.

Breviario, F., L. Caveda, M. Corada, I. Martin-Padura, P. Navarro, J. Golay, M. Introna, D. Gulino, M. G. Lampugnani and E. Dejana (1995). "Functional properties of human vascular endothelial cadherin (7B4/cadherin-5), an endothelium-specific cadherin." Arteriosclerosis, Thrombosis, and Vascular Biology **15**(8): 1229-1239.

Brink, P. R. (1998). "Gap junctions in vascular smooth muscle." Acta Physiologica Scandinavica **164**(4): 349-356.

Brink, P. R. and S. F. Fan (1989). "Patch clamp recordings from membranes which contain gap junction channels." Biophys J **56**(3): 579-593.

Brissette, J. L., N. M. Kumar, N. B. Gilula, J. E. Hall and G. P. Dotto (1994). "Switch in gap junction protein expression is associated with selective changes in junctional permeability during keratinocyte differentiation." Proc Natl Acad Sci U S A **91**(14): 6453-6457.

Brosnan, C. F., E. Scemes and D. C. Spray (2001). "Cytokine regulation of gap junction connectivity: An open-and-shut case or changing partners at the nexus?" American Journal of Pathology **158**(5): 1565-1569.

Brough, G. H., S. Wu, D. Cioffi, T. M. Moore, M. Li, N. Dean and T. Stevens (2001). "Contribution of endogenously expressed Trp1 to a Ca2+-selective, store-operated Ca2+ entry pathway." Faseb j **15**(10): 1727-1738.

Brown, R. C. and T. P. Davis (2002). "Calcium modulation of adherens and tight junction function: a potential mechanism for blood-brain barrier disruption after stroke." Stroke **33**(6): 1706-1711.

Bruce, J. I., T. J. Shuttleworth, D. R. Giovannucci and D. I. Yule (2002). "Phosphorylation of inositol 1,4,5-trisphosphate receptors in parotid acinar cells. A mechanism for the synergistic effects of cAMP on Ca2+ signaling." J Biol Chem **277**(2): 1340-1348.

Bruce, J. I., S. V. Straub and D. I. Yule (2003). "Crosstalk between cAMP and Ca2+ signaling in non-excitable cells." Cell Calcium **34**(6): 431-444.

Bruzzone, R., J. A. Haefliger, R. L. Gimlich and D. L. Paul (1993). "Connexin40, a component of gap junctions in vascular endothelium, is restricted in its ability to interact with other connexins." Molecular Biology of the Cell **4**(1): 7-20.

Bubik, M. F., E. A. Willer, P. Bihari, G. Jürgenliemk, H. Ammer, F. Krombach, S. Zahler, A. M. Vollmar and R. Fürst (2012). "A novel approach to prevent endothelial hyperpermeability: The Crataegus extract WS® 1442 targets the cAMP/Rap1 pathway." Journal of Molecular and Cellular Cardiology **52**(1): 196-205.

Bukauskas, F. F., C. Elfgang, K. Willecke and R. Weingart (1995). "Biophysical properties of gap junction channels formed by mouse connexin40 in induced pairs of transfected human HeLa cells." Biophysical Journal **68**(6): 2289-2298.

Burghardt, R. C., R. Barhoumi, T. C. Sewall and J. A. Bowen (1995). "Cyclic AMP induces rapid increases in gap junction permeability and changes in the cellular distribution of connexin43." Journal of Membrane Biology **148**(3): 243-253.

Burridge, K., K. Fath, T. Kelly, G. Nuckolls and C. Turner (1988). "Focal Adhesions: Transmembrane Junctions Between the Extracellular Matrix and the Cytoskeleton." Annual Review of Cell Biology **4**(1): 487-525.

Busch, C., C. Ljungman, C. M. Heldin, E. Waskson and B. Obrink (1979). "Surface properties of cultured endothelial cells." Haemostasis **8**(3-5): 142-148.

Byus, C. V., J. S. Hayes, K. Brendel and D. H. Russell (1979). "Regulation of glycogenolysis in isolated rat hepatocytes by the specific activation of type I cyclic AMP-dependent protein kinase." Molecular Pharmacology **16**(3): 941-949.

Cai, J., W. G. Jiang and R. E. Mansel (1998). "Gap junctional communication and the tyrosine phosphorylation of connexin 43 in interaction between breast cancer and endothelial cells." Int J Mol Med **1**(1): 273-278.

Cai, W. J., S. Koltai, E. Kocsis, D. Scholz, S. Kostin, X. Luo, W. Schaper and J. Schaper (2003). "Remodeling of the adventitia during coronary arteriogenesis." American Journal of Physiology - Heart and Circulatory Physiology **284**(1 53-1): H31-H40.

Cai, W. J., S. Koltai, E. Kocsis, D. Scholz, W. Schaper and J. Schaper (2001). "Connexin37, not Cx40 and Cx43, is induced in vascular smooth muscle cells during coronary arteriogenesis." Journal of Molecular and Cellular Cardiology **33**(5): 957-967.

Calkins, C. C., B. L. Hoepner, C. M. Law, M. R. Novak, S. V. Setzer, M. Hatzfeld and A. P. Kowalczyk (2003). "The Armadillo family protein p0071 is a VE-cadherin- and desmoplakin-binding protein." J Biol Chem **278**(3): 1774-1783.

Cao, G., C. D. O'Brien, Z. Zhou, S. M. Sanders, J. N. Greenbaum, A. Makrigiannakis and H. M. Delisser (2002). "Involvement of human PECAM-1 in angiogenesis and in vitro endothelial cell migration." American Journal of Physiology - Cell Physiology **282**(5 51-5): C1181-C1190.

Carbajal, J. M. and R. C. Schaeffer, Jr. (1999). "RhoA inactivation enhances endothelial barrier function." Am J Physiol **277**(5 Pt 1): C955-964.

Carden, D., F. Xiao, C. Moak, B. H. Willis, S. Robinson-Jackson and S. Alexander (1998). "Neutrophil elastase promotes lung microvascular injury and proteolysis of endothelial cadherins." Am J Physiol **275**(2 Pt 2): H385-392.

Carmeliet, P., M. G. Lampugnani, L. Moons, F. Breviario, V. Compernolle, F. Bono, G. Balconi, R. Spagnuolo, B. Oosthuyse, M. Dewerchin, A. Zanetti, A. Angellilo, V. Mattot, D. Nuyens, E. Lutgens, F. Clotman, M. C. De Ruiter, A. G. D. Groot, R. Poelmann, F. Lupu, J. M. Herbert, D. Collen and E. Dejana (1999). "Targeted deficiency or cytosolic truncation of the VE-cadherin gene in mice impairs VEGF-mediated endothelial survival and angiogenesis." Cell **98**(2): 147-157.

Carr, D. W., Z. E. Hausken, I. D. C. Fraser, R. E. Stofko-Hahn and J. D. Scott (1992). "Association of the type II cAMP-dependent protein kinase with a human thyroid RII-anchoring protein: Cloning and characterization of the RII-binding domain." Journal of Biological Chemistry **267**(19): 13376-13382.

Carr, D. W., R. E. Stofko-Hahn, I. D. C. Fraser, R. D. Cone and J. D. Scott (1992). "Localization of the cAMP-dependent protein kinase to the postsynaptic densities by A-Kinase Anchoring Proteins: Characterization of AKAP 79." Journal of Biological Chemistry **267**(24): 16816-16823.

Carter, T. D. and D. Ogden (1994). "Acetylcholine-stimulated changes of membrane potential and intracellular Ca2+ concentration recorded in endothelial cells in situ in the isolated rat aorta." Pflugers Arch **428**(5-6): 476-484.

Chausovsky, A., A. D. Bershadsky and G. G. Borisy (2000). "Cadherin-mediated regulation of microtubule dynamics." Nat Cell Biol **2**(11): 797-804.

Chen, H., T. Tsalkova, F. C. Mei, Y. Hu, X. Cheng and J. Zhou (2012). "5-Cyano-6-oxo-1,6-dihydro-pyrimidines as potent antagonists targeting exchange proteins directly activated by cAMP." Bioorg Med Chem Lett **22**(12): 4038-4043.

Chen, X., S. Kojima, G. G. Borisy and K. J. Green (2003). "p120 catenin associates with kinesin and facilitates the transport of cadherin-catenin complexes to intercellular junctions." J Cell Biol **163**(3): 547-557.

Cheng, K. T., Y. K. Leung, B. Shen, Y. C. Kwok, C. O. Wong, H. Y. Kwan, Y. B. Man, X. Ma, Y. Huang and X. Yao (2008). "CNGA2 channels mediate adenosine-induced Ca2+ influx in vascular endothelial cells." Arterioscler Thromb Vasc Biol **28**(5): 913-918.

Cheng, Y. F. and R. H. Kramer (1989). "Human microvascular endothelial cells express integrin-related complexes that mediate adhesion to the extracellular matrix." J Cell Physiol **139**(2): 275-286.

Chou, M. T., J. Wang and D. J. Fujita (2002). "Src kinase becomes preferentially associated with the VEGFR, KDR/Flk-1, following VEGF stimulation of vascular endothelial cells." BMC Biochem **3**: 32.

Chretien, D., F. Metoz, F. Verde, E. Karsenti and R. H. Wade (1992). "Lattice defects in microtubules: protofilament numbers vary within individual microtubules." J Cell Biol **117**(5): 1031-1040.

Chrétien, D. and R. H. Wade (1991). "New data on the microtubule surface lattice." Biology of the Cell **71**(1–2): 161-174.

Christ, G. J. and P. R. Brink (1999). "Analysis of the presence and physiological relevance of subconducting states of Connexin43-derived gap junction channels in cultured human corporal vascular smooth muscle cells." Circ Res **84**(7): 797-803.

Christensen, A. E., F. Selheim, J. De Rooij, S. Dremier, F. Schwede, K. K. Dao, A. Martinez, C. Maenhaut, J. L. Bos, H. G. Genieser and S. O. Doskeland (2003). "cAMP analog mapping of Epac1 and cAMP kinase: Discriminating analogs demonstrate that Epac and cAMP kinase act synergistically to promote PC-12 cell neurite extension." Journal of Biological Chemistry **278**(37): 35394-35402.

Ciano, C. D., Z. Nie, K. Szászi, A. Lewis, T. Uruno, X. Zhan, O. D. Rotstein, A. Mak and A. Kapus (2002). "Osmotic stress-induced remodeling of the cortical cytoskeleton." American Journal of Physiology - Cell Physiology **283**(3 52-3): C850-C865.

Cioffi, D. L., T. M. Moore, J. Schaack, J. R. Creighton, D. M. Cooper and T. Stevens (2002). "Dominant regulation of interendothelial cell gap formation by calcium-inhibited type 6 adenylyl cyclase." J Cell Biol **157**(7): 1267-1278.

Citi, S., H. Sabanay, R. Jakes, B. Geiger and J. Kendrick-Jones (1988). "Cingulin, a new peripheral component of tight junctions." Nature **333**(6170): 272-276.

Coffin, J. D. and T. J. Poole (1988). "Embryonic vascular development: immunohistochemical identification of the origin and subsequent morphogenesis of the major vessel primordia in quail embryos." Development **102**(4): 735-748.

Coghlan, V. M., S. E. Bergeson, L. Langeberg, G. Nilaver and J. D. Scott (1993). "A-Kinase Anchoring Proteins: a key to selective activation of cAMP-responsive events?" Molecular and Cellular Biochemistry **127-128**(1): 309-319.

Cohen, C. D., A. Klingenhoff, A. Boucherot, A. Nitsche, A. Henger, B. Brunner, H. Schmid, M. Merkle, M. A. Saleem, K. P. Koller, T. Werner, H. J. Grone, P. J. Nelson and M. Kretzler (2006). "Comparative promoter analysis allows de novo identification of specialized cell junction-associated proteins." Proc Natl Acad Sci U S A **103**(15): 5682-5687.

Cohen, C. J., J. T. C. Shieh, R. J. Pickles, T. Okegawa, J.-T. Hsieh and J. M. Bergelson (2001). "The coxsackievirus and adenovirus receptor is a transmembrane component of the tight junction." Proceedings of the National Academy of Sciences **98**(26): 15191-15196.

Colucci-Guyon, E., M. M. Portier, I. Dunia, D. Paulin, S. Pournin and C. Babinet (1994). "Mice lacking vimentin develop and reproduce without an obvious phenotype." Cell **79**(4): 679-694.

Conforti, G., A. Zanetti, S. Colella, M. Abbadini, P. Marchisio, R. Pytela, F. Giancotti, G. Tarone, L. Languino and E. Dejana (1989). Interaction of fibronectin with cultured human endothelial cells: characterization of the specific receptor.

Consonni, S. V., M. Gloerich, E. Spanjaard and J. L. Bos (2012). "cAMP regulates DEP domain-mediated binding of the guanine nucleotide exchange factor Epac1 to phosphatidic acid at the plasma membrane." Proceedings of the National Academy of Sciences of the United States of America **109**(10): 3814-3819.

Cooper, C. D. and P. D. Lampe (2002). "Casein kinase 1 regulates connexin-43 gap junction assembly." J Biol Chem **277**(47): 44962-44968.

Corada, M., F. Liao, M. Lindgren, M. G. Lampugnani, F. Breviario, R. Frank, W. A. Muller, D. J. Hicklin, P. Bohlen and E. Dejana (2001). "Monoclonal antibodies directed to different regions of vascular endothelial cadherin extracellular domain affect adhesion and clustering of the protein and modulate endothelial permeability." Blood **97**(6): 1679-1684.

Corbin, J. D., S. L. Keely and C. R. Park (1975). "The distribution and dissociation of cyclic adenosine 3':5' monophosphate dependent protein kinases in adipose, cardiac, and other tissues." Journal of Biological Chemistry **250**(1): 218-225.

Coughlin, S. R. (2000). "Thrombin signalling and protease-activated receptors." Nature **407**(6801): 258-264.

Creighton, J., B. Zhu, M. Alexeyev and T. Stevens (2008). "Spectrin-anchored phosphodiesterase 4D4 restricts cAMP from disrupting microtubules and inducing endothelial cell gap formation." J Cell Sci **121**(Pt 1): 110-119.

Cullere, X., S. K. Shaw, L. Andersson, J. Hirahashi, F. W. Luscinskas and T. N. Mayadas (2005). "Regulation of vascular endothelial barrier function by Epac, a cAMP-activated exchange factor for Rap GTPase." Blood **105**(5): 1950-1955.

Cunningham, S. A., M. P. Arrate, J. M. Rodriguez, R. J. Bjercke, P. Vanderslice, A. P. Morris and T. A. Brock (2000). "A Novel Protein with Homology to the Junctional Adhesion Molecule: CHARACTERIZATION OF LEUKOCYTE INTERACTIONS." Journal of Biological Chemistry **275**(44): 34750-34756.

Curry, F. E. and R. H. Adamson (2012). "Endothelial glycocalyx: permeability barrier and mechanosensor." Ann Biomed Eng **40**(4): 828-839.

Damiano, E. R. (1998). "The effect of the endothelial-cell glycocalyx on the motion of red blood cells through capillaries." Microvasc Res **55**(1): 77-91.

Darrow, B. J., V. G. Fast, A. G. Kléber, E. C. Beyer and J. E. Saffitz (1996). "Functional and structural assessment of intercellular communication: Increased conduction velocity and enhanced connexin expression in dibutyryl cAMP-treated cultured cardiac myocytes." Circulation Research **79**(2): 174-183.

Das Sarma, J., R. A. Meyer, R. A. Wang, F. Wang, V. Abraham, C. W. Lo and M. Koval (2001). "Multimeric connexin interactions prior to the trans-Golgi network." Journal of Cell Science **114**(22): 4013-4024.

Dasgupta, C., A. M. Martinez, C. W. Zuppan, M. M. Shah, L. L. Bailey and W. H. Fletcher (2001). "Identification of connexin43 (α1) gap junction gene mutations in patients with hypoplastic left heart syndrome by denaturing gradient gel electrophoresis (DGGE)." Mutation Research - Fundamental and Molecular Mechanisms of Mutagenesis **479**(1-2): 173-186.

David, S., C. C. Ghosh, A. Mukherjee and S. M. Parikh (2011). "Angiopoietin-1 requires IQ domain GTPase-activating protein 1 to activate Rac1 and promote endothelial barrier defense." Arterioscler Thromb Vasc Biol **31**(11): 2643-2652.

David, S., P. Kumpers, P. van Slyke and S. M. Parikh (2013). "Mending leaky blood vessels: the angiopoietin-Tie2 pathway in sepsis." J Pharmacol Exp Ther **345**(1): 2-6.

Davidson, J. S., I. M. Baumgarten and E. H. Harley (1984). "Effects of extracellular calcium and magnesium on junctional intercellular communication in human fibroblasts." Experimental Cell Research **155**(2): 406-412.

De Backer, D., J. Creteur, M. J. Dubois, Y. Sakr, M. Koch, C. Verdant and J. L. Vincent (2006). "The effects of dobutamine on microcirculatory alterations in patients with septic shock are independent of its systemic effects." Crit Care Med **34**(2): 403-408.

De Camilli, P., M. Moretti, S. D. Donini and S. M. Lohmann (1986). "Heterogeneous distribution of the cAMP receptor protein RII in the nervous system: Evidence for its intracellular accumulation on microtubules, microtubule-organizing centers, and in the area of the Golgi complex." Journal of Cell Biology **103**(1): 189-203.

De Matteis, M. A., G. Santini, R. A. Kahn, G. Di Tullio and A. Luini (1993). "Receptor and protein kinase C-mediated regulation of ARF binding to the Golgi complex." Nature **364**(6440): 818-821.

De Mazière, A., L. Analbers, H. J. Jongsma and D. Gros (1993). "Immunoelectron microscopic visualization of the gap junction protein connexin 40 in the mammalian heart." European Journal Of Morphology **31**(1-2): 51-54.

De Pina-Benabou, M. H., M. Srinivas, D. C. Spray and E. Scemes (2001). "Calmodulin kinase pathway mediates the K+-induced increase in gap junctional communication between mouse spinal cord astrocytes." Journal of Neuroscience **21**(17): 6635-6643.

De Rooij, J., N. M. Boenink, M. Van Triest, R. H. Cool, A. Wittinghofer and J. L. Bos (1999). "PDZ-GEF1, a guanine nucleotide exchange factor specific for Rap1 and Rap2." Journal of Biological Chemistry **274**(53): 38125-38130.

De Rooij, J., H. Rehmann, M. Van Triest, R. H. Cool, A. Wittinghofer and J. L. Bos (2000). "Mechanism of regulation of the Epac family of cAMP-dependent RapGEFs." Journal of Biological Chemistry **275**(27): 20829-20836.

De Rooij, J., F. J. T. Zwartkruis, M. H. G. Verheijen, R. H. Cool, S. M. B. Nijman, A. Wittinghofer and J. L. Bos (1998). "Epac is a Rap1 guanine-nucleotide-exchange factor directly activated by cyclic AMP." Nature **396**(6710): 474-477.

de Wit, C. and T. M. Griffith (2010). "Connexins and gap junctions in the EDHF phenomenon and conducted vasomotor responses." Pflugers Arch **459**(6): 897-914.

Defilippi, P., V. van Hinsbergh, A. Bertolotto, P. Rossino, L. Silengo and G. Tarone (1991). "Differential distribution and modulation of expression of alpha 1/beta 1 integrin on human endothelial cells." J Cell Biol **114**(4): 855-863.

Dejana, E. (1997). "Endothelial adherens junctions: Implications in the control of vascular permeability and angiogenesis." Journal of Clinical Investigation **100**(11 SUPPL.): S7-S10.

Dejana, E., M. Corada and M. G. Lampugnani (1995). "Endothelial cell-to-cell junctions." Faseb j **9**(10): 910-918.

Dejana, E., E. Tournier-Lasserve and B. M. Weinstein (2009). "The Control of Vascular Integrity by Endothelial Cell Junctions: Molecular Basis and Pathological Implications." Developmental Cell **16**(2): 209-221.

Del Corsso, C., R. Iglesias, G. Zoidl, R. Dermietzel and D. C. Spray (2012). "Calmodulin dependent protein kinase increases conductance at gap junctions formed by the neuronal gap junction protein connexin36." Brain Research **1487**: 69-77.

DeLisser, H. M., M. Christofidou-Solomidou, R. M. Strieter, M. D. Burdick, C. S. Robinson, R. S. Wexler, J. S. Kerr, C. Garlanda, J. R. Merwin, J. A. Madri and S. M. Albelda (1997). "Involvement of endothelial PECAM-1/CD31 in angiogenesis." American Journal of Pathology **151**(3): 671-677.

Dellinger, R. P., M. M. Levy, A. Rhodes, D. Annane, H. Gerlach, S. M. Opal, J. E. Sevransky, C. L. Sprung, I. S. Douglas, R. Jaeschke, T. M. Osborn, M. E. Nunnally, S. R. Townsend, K. Reinhart, R. M. Kleinpell, D. C. Angus, C. S. Deutschman, F. R. Machado, G. D. Rubenfeld, S. A. Webb, R. J. Beale, J. L. Vincent and R. Moreno (2013). "Surviving sepsis campaign: international guidelines for management of severe sepsis and septic shock: 2012." Crit Care Med **41**(2): 580-637.

Delorme, B., E. Dahl, T. Jarry-Guichard, J. P. Briand, K. Willecke, D. Gros and M. Théveniau-Ruissy (1997). "Expression pattern of connexin gene products at the early developmental stages of the mouse cardiovascular system." Circulation Research **81**(3): 423-437.

DeMali, K. A., C. A. Barlow and K. Burridge (2002). "Recruitment of the Arp2/3 complex to vinculin: coupling membrane protrusion to matrix adhesion." J Cell Biol **159**(5): 881-891.

Desgrosellier, J. S. and D. A. Cheresh (2010). "Integrins in cancer: biological implications and therapeutic opportunities." Nat Rev Cancer **10**(1): 9-22.

Dessauer, C. W., J. J. G. Tesmer, S. R. Sprang and A. G. Gilman (1998). "Identification of a Giα Binding Site on Type V Adenylyl Cyclase." Journal of Biological Chemistry **273**(40): 25831-25839.

Diez, J. A., S. Ahmad and W. H. Evans (1999). "Assembly of heteromeric connexons in guinea-pig liver en route to the Golgi apparatus, plasma membrane and gap junctions." European Journal of Biochemistry **262**(1): 142-148.

Doble, B. W., P. Ping and E. Kardami (2000). "The ε subtype of protein kinase C is required for cardiomyocyte connexin-43 phosphorylation." Circulation Research **86**(3): 293-301.

Dolor, R. J., L. M. Hurwitz, Z. Mirza, H. C. Strauss and A. R. Whorton (1992). "Regulation of extracellular calcium entry in endothelial cells: role of intracellular calcium pool." Am J Physiol **262**(1 Pt 1): C171-181.

Dora, K. A. (2001). "Intercellular Ca2+ signalling: The artery wall." Seminars in Cell and Developmental Biology **12**(1): 27-35.

Duband, J. L., M. Gimona, M. Scatena, S. Sartore and J. V. Small (1993). "Calponin and SM 22 as differentiation markers of smooth muscle: Spatiotemporal distribution during avian embryonic development." Differentiation **55**(1): 1-11.

Dudek, S. M. and J. G. Garcia (2001). "Cytoskeletal regulation of pulmonary vascular permeability." J Appl Physiol (1985) **91**(4): 1487-1500.

Duncan, J. C. and W. H. Fletcher (2002). "α1 connexin (connexin43) gap junctions and activities of cAMP-dependent protein kinase and protein kinase C in developing mouse heart." Developmental Dynamics **223**(1): 96-107.

Duquesnes, N., M. Derangeon, M. Métrich, A. Lucas, P. Mateo, L. Li, E. Morel, F. Lezoualc'h and B. Crozatier (2010). "Epac stimulation induces rapid increases in connexin43 phosphorylation and function without preconditioning effect." Pflugers Archiv European Journal of Physiology **460**(4): 731-741.

Dyachok, O. and E. Gylfe (2004). "Ca(2+)-induced Ca(2+) release via inositol 1,4,5-trisphosphate receptors is amplified by protein kinase A and triggers exocytosis in pancreatic beta-cells." J Biol Chem **279**(44): 45455-45461.

Eastman, Q. and R. Grosschedl (1999). "Regulation of LEF-1/TCF transcription factors by Wnt and other signals." Curr Opin Cell Biol **11**(2): 233-240.

Ebnet, K., C. U. Schulz, M. K. Meyer Zu Brickwedde, G. G. Pendl and D. Vestweber (2000). "Junctional adhesion molecule interacts with the PDZ domain-containing proteins AF-6 and ZO-1." J Biol Chem **275**(36): 27979-27988.

Edamatsu, H., N. Takenaka, L. Hu and T. Kataoka (2011). "Phospholipase Cε as a potential molecular target for anti-inflammatory therapy and cancer prevention." Inflammation and Regeneration **31**(4): 370-374.

Edwards, G., K. A. Dora, M. J. Gardener, C. J. Garland and A. H. Weston (1998). "K+ is an endothelium-derived hyperpolarizing factor in rat arteries." Nature **396**(6708): 269-272.

Edwards, G., M. Feletou and A. H. Weston (2010). "Endothelium-derived hyperpolarising factors and associated pathways: a synopsis." Pflugers Arch **459**(6): 863-879.

Elfgang, C., R. Eckert, H. Lichtenberg-Frate, A. Butterweck, O. Traub, R. A. Klein, D. F. Hulser and K. Willecke (1995). "Specific permeability and selective formation of gap junction channels in connexin-transfected HeLa cells." Journal of Cell Biology **129**(3): 805-817.

Ellerbroek, S. M., K. Wennerberg and K. Burridge (2003). "Serine phosphorylation negatively regulates RhoA in vivo." J Biol Chem **278**(21): 19023-19031.

Emerson, G. G., and S. S. Segal (2000). "Endothelial cell pathway for conduction of hyperpolarization and vasodilation along hamster feed artery." Circulation Research **86**(1): 94-100.

Enerson, B. E. and L. R. Drewes (2006). "The rat blood-brain barrier transcriptome." J Cereb Blood Flow Metab **26**(7): 959-973.

Enserink, J. M., A. E. Christensen, J. de Rooij, M. van Triest, F. Schwede, H. G. Genieser, S. O. Døskeland, J. L. Blank and J. L. Bos (2002). "A novel Epac-specific cAMP analogue demonstrates independent regulation of Rap1 and ERK." Nature Cell Biology **4**(11): 901-906.

Eriksson, U. and K. Alitalo (1999). Structure, Expression and Receptor-Binding Properties of Novel Vascular Endothelial Growth Factors. Vascular Growth Factors and Angiogenesis. L. Claesson-Welsh, Springer Berlin Heidelberg. **237:** 41-57.

Esmon, C. T. (2004). "Interactions between the innate immune and blood coagulation systems." Trends in Immunology **25**(10): 536-542.

Esser, S., M. G. Lampugnani, M. Corada, E. Dejana and W. Risau (1998). "Vascular endothelial growth factor induces VE-cadherin tyrosine." Journal of Cell Science **111**(13): 1853-1865.

Essler, M., M. Amano, H. J. Kruse, K. Kaibuchi, P. C. Weber and M. Aepfelbacher (1998). "Thrombin inactivates myosin light chain phosphatase via Rho and its target Rho kinase in human endothelial cells." J Biol Chem **273**(34): 21867-21874.

Evans, W. H. and S. Boitano (2001). "Connexin mimetic peptides: Specific inhibitors of gap-junctional intercellular communication." Biochemical Society Transactions **29**(4): 606-612.

Evans, W. H. and P. E. M. Martin (2002). "Gap junctions: Structure and function (review)." Molecular Membrane Biology **19**(2): 121-136.

Evellin, S., J. Nolte, K. Tysack, F. V. Dorp, M. Thiel, P. A. Oude Weernink, K. H. Jakobs, E. J. Webb, J. W. Lomasney and M. Schmidt (2002). "Stimulation of phospholipase C-ε by the M3 muscarinic acetylcholine receptor mediated by cyclic AMP and the GTPase Rap2B." Journal of Biological Chemistry **277**(19): 16805-16813.

Falk, M. M. (2000). "Connexin-specific distribution within gap junctions revealed in living cells." Journal of Cell Science **113**(22): 4109-4120.

Falk, M. M., N. M. Kumar and N. B. Gilula (1994). "Membrane insertion of gap junction connexins: polytopic channel forming membrane proteins." J Cell Biol **127**(2): 343-355.

Fan, J., R. S. Frey and A. B. Malik (2003). "TLR4 signaling induces TLR2 expression in endothelial cells via neutrophil NADPH oxidase." J Clin Invest **112**(8): 1234-1243.

Fanning, A. S., B. J. Jameson, L. A. Jesaitis and J. M. Anderson (1998). "The tight junction protein ZO-1 establishes a link between the transmembrane protein occludin and the actin cytoskeleton." J Biol Chem **273**(45): 29745-29753.

Fanning, A. S., T. Y. Ma and J. M. Anderson (2002). "Isolation and functional characterization of the actin binding region in the tight junction protein ZO-1." Faseb j **16**(13): 1835-1837.

Farmer, P. J., S. G. Bernier, A. Lepage, G. Guillemette, D. Regoli and P. Sirois (2001). "Permeability of endothelial monolayers to albumin is increased by bradykinin and inhibited by prostaglandins." Am J Physiol Lung Cell Mol Physiol **280**(4): L732-738.

Farquhar, M. G. and G. E. Palade (1963). "Junctional complexes in various epithelia." J Cell Biol **17**: 375-412.

Fatigati, V. and R. A. Murphy (1984). "Actin and tropomyosin variants in smooth muscles. Dependence on tissue type." Journal of Biological Chemistry **259**(23): 14383-14388.

Ferber, A., C. Yaen, E. Sarmiento and J. Martinez (2002). "An octapeptide in the juxtamembrane domain of VE-cadherin is important for p120ctn binding and cell proliferation." Experimental Cell Research **274**(1): 35-44.

Ferris, C. D., R. L. Huganir, S. Supattapone and S. H. Snyder (1989). "Purified inositol 1,4,5-trisphosphate receptor mediates calcium flux in reconstituted lipid vesicles." Nature **342**(6245): 87-89.

Fesenko, E. E., S. S. Kolesnikov and A. L. Lyubarsky (1985). "Induction by cyclic GMP of cationic conductance in plasma membrane of retinal rod outer segment." Nature **313**(6000): 310-313.

Figueroa, X. F., B. E. Isakson and B. R. Duling (2004). "Connexins: Gaps in our knowledge of vascular function." Physiology **19**(5): 277-284.

Fléchon, J. E., J. Degrouard, B. Fléchon, F. Lefèvre and O. Traub (2004). "Gap junction formation and connexin distribution in pig trophoblast before implantation." Placenta **25**(1): 85-94.

Flores, C. E., R. Cachope, S. Nannapaneni, S. Ene, A. C. Nairn and A. E. Pereda (2010). "Variability of distribution of Ca2+/calmodulin-dependent kinase II at mixed synapses on the mauthner cell: Colocalization and association with connexin 35." Journal of Neuroscience **30**(28): 9488-9499.

Florian, J. A., J. R. Kosky, K. Ainslie, Z. Pang, R. O. Dull and J. M. Tarbell (2003). "Heparan Sulfate Proteoglycan Is a Mechanosensor on Endothelial Cells." Circulation Research **93**(10): e136-e142.

Form, D. M., B. M. Pratt and J. A. Madri (1986). "Endothelial cell proliferation during angiogenesis. In vitro modulation by basement membrane components." Lab Invest **55**(5): 521-530.

Franke, B., J. W. N. Akkerman and J. L. Bos (1997). "Rapid Ca2+-mediated activation of Rap1 in human platelets." EMBO Journal **16**(2): 252-259.

Franke, W., P. Cowin, C. Grund, C. Kuhn and H.-P. Kapprell (1988). The Endothelial Junction. Endothelial Cell Biology in Health and Disease. N. Simionescu and M. Simionescu, Springer US**:** 147-166.

Frid, M. G., B. V. Shekhonin, V. E. Koteliansky and M. A. Glukhova (1992). "Phenotypic changes of human smooth muscle cells during development: Late expression of heavy caldesmon and calponin." Developmental Biology **153**(2): 185-193.

Fujimoto, K., A. Nagafuchi, S. Tsukita, A. Kuraoka, A. Ohokuma and Y. Shibata (1997). "Dynamics of connexins, E-cadherin and α-catenin on cell membranes during gap junction formation." Journal of Cell Science **110**(3): 311-322.

Fukuhara, S., A. Sakurai, H. Sano, A. Yamagishi, S. Somekawa, N. Takakura, Y. Saito, K. Kangawa and N. Mochizuki (2005). "Cyclic AMP potentiates vascular endothelial cadherin-mediated cell-cell contact to enhance endothelial barrier function through an Epac-Rap1 signaling pathway." Molecular and Cellular Biology **25**(1): 136-146.

Furuse, M., T. Hirase, M. Itoh, A. Nagafuchi, S. Yonemura, S. Tsukita and S. Tsukita (1993). "Occludin: a novel integral membrane protein localizing at tight junctions." J Cell Biol **123**(6 Pt 2): 1777-1788.

Furuse, M., H. Sasaki, K. Fujimoto and S. Tsukita (1998). "A single gene product, claudin-1 or -2, reconstitutes tight junction strands and recruits occludin in fibroblasts." J Cell Biol **143**(2): 391-401.

Furuse, M., H. Sasaki and S. Tsukita (1999). "Manner of interaction of heterogeneous claudin species within and between tight junction strands." J Cell Biol **147**(4): 891-903.

Furuse, M. and S. Tsukita (2006). "Claudins in occluding junctions of humans and flies." Trends Cell Biol **16**(4): 181-188.

Gabbiani, G., E. Schmid, S. Winter, C. Chaponnier, C. de Ckhastonay, J. Vandekerckhove, K. Weber and W. W. Franke (1981). "Vascular smooth muscle cells differ from other smooth muscle cells: Predominance of vimentin filaments and a specific α-type actin." Proceedings of the National Academy of Sciences of the United States of America **78**(1 II): 298-302.

Gaietta, G., T. J. Deerinck, S. R. Adams, J. Bouwer, O. Tour, D. W. Laird, G. E. Sosinsky, R. Y. Tsien and M. H. Ellisman (2002). "Multicolor and Electron Microscopic Imaging of Connexin Trafficking." Science **296**(5567): 503-507.

Gallicano, G. I., C. Bauer and E. Fuchs (2001). "Rescuing desmoplakin function in extra-embryonic ectoderm reveals the importance of this protein in embryonic heart, neuroepithelium, skin and vasculature." Development **128**(6): 929-941.

Gamble, J. R., J. Drew, L. Trezise, A. Underwood, M. Parsons, L. Kasminkas, J. Rudge, G. Yancopoulos and M. A. Vadas (2000). "Angiopoietin-1 is an antipermeability and anti-inflammatory agent in vitro and targets cell junctions." Circulation Research **87**(7): 603-607.

Garcia, J. G. N., F. Liu, A. D. Verin, A. Birukova, M. A. Dechert, W. T. Gerthoffer, J. R. Bamburg and D. English (2001). "Sphingosine 1-phosphate promotes endothelial cell barrier integrity by Edg-dependent cytoskeletal rearrangement." Journal of Clinical Investigation **108**(5): 689-701.

Garrod, D. and M. Chidgey (2008). "Desmosome structure, composition and function." Biochimica et Biophysica Acta (BBA) - Biomembranes **1778**(3): 572-587.

Gavard, J. and J. S. Gutkind (2006). "VEGF Controls endothelial-cell permeability promoting β-arrestin-dependent Endocytosis VE-cadherin." Nature Cell Biology **8**(11): 1223-1234.

Geiger, B. and O. Ayalon (1992). "Cadherins." Annual Review of Cell Biology **8**: 307-332.

Geiger, B., A. Bershadsky, R. Pankov and K. M. Yamada (2001). "Transmembrane crosstalk between the extracellular matrix--cytoskeleton crosstalk." Nat Rev Mol Cell Biol **2**(11): 793-805.

Geiger, B., J. P. Spatz and A. D. Bershadsky (2009). "Environmental sensing through focal adhesions." Nat Rev Mol Cell Biol **10**(1): 21-33.

Geiger, B., K. T. Tokuyasu, A. H. Dutton and S. J. Singer (1980). "Vinculin, an intracellular protein localized at specialized sites where microfilament bundles terminate at cell

membranes." Proceedings of the National Academy of Sciences of the United States of America **77**(7 II): 4127-4131.

Gericke, M., G. Droogmans and B. Nilius (1993). "Thapsigargin discharges intracellular calcium stores and induces transmembrane currents in human endothelial cells." Pflugers Arch **422**(6): 552-557.

Gerszten, R. E., J. Chen, M. Ishii, K. Ishii, L. Wang, T. Nanevicz, C. W. Turck, T. K. Vu and S. R. Coughlin (1994). "Specificity of the thrombin receptor for agonist peptide is defined by its extracellular surface." Nature **368**(6472): 648-651.

Giepmans, B. N. G. and W. H. Moolenaar (1998). "The gap junction protein connexin43 interacts with the second PDZ domain of the zona occludens-1 protein." Current Biology **8**(16): 931-934.

Giepmans, B. N. G., I. Verlaan, T. Hengeveld, H. Janssen, J. Calafat, M. M. Falk and W. H. Moolenaar (2001). "Gap junction protein connexin-43 interacts directly with microtubules." Current Biology **11**(17): 1364-1368.

Gilbertson-Beadling, S. K. and C. Fisher (1993). "A potential role for N-cadherin in mediating endothelial cell-smooth muscle cell interactions in the rat vasculature." Laboratory Investigation **69**(2): 203-209.

Gimona, M., I. Kaverina, G. P. Resch, E. Vignal and G. Burgstaller (2003). "Calponin repeats regulate actin filament stability and formation of podosomes in smooth muscle cells." Molecular Biology of the Cell **14**(6): 2482-2491.

Gloerich, M. and J. L. Bos (2010). Epac: Defining a new mechanism for cAMP action. Annual Review of Pharmacology and Toxicology. **50:** 355-375.

Godfraind, T. (2014). "Calcium Channel Blockers in Cardiovascular Pharmacotherapy." Journal of cardiovascular pharmacology and therapeutics **19**(6): 501-515.

Goeckeler, Z. M. and R. B. Wysolmerski (1995). "Myosin light chain kinase-regulated endothelial cell contraction: the relationship between isometric tension, actin polymerization, and myosin phosphorylation." J Cell Biol **130**(3): 613-627.

Goldberg, G. S., P. D. Lampe and B. J. Nicholson (1999). "Selective transfer of endogenous metabolites through gap junctions composed of different connexins." Nat Cell Biol **1**(7): 457-459.

Goldberg, G. S., V. Valiunas and P. R. Brink (2004). "Selective permeability of gap junction channels." Biochimica et Biophysica Acta (BBA) - Biomembranes **1662**(1–2): 96-101.

Goodall, H. (1986). "Manipulation of gap junctional communication during compaction of the mouse early embryo." Journal of Embryology and Experimental Morphology **VOL. 91**: 283-296.

Goodenough, D. A. (1974). "Bulk isolation of mouse hepatocyte gap junctions. Characterization of the principal protein, connexin." Journal of Cell Biology **61**(2): 557-563.

Gory-Faure, S., M. H. Prandini, H. Pointu, V. Roullot, I. Pignot-Paintrand, M. Vernet and P. Huber (1999). "Role of vascular endothelial-cadherin in vascular morphogenesis." Development **126**(10): 2093-2102.

Gory, S., M. Vernet, M. Laurent, E. Dejana, J. Dalmon and P. Huber (1999). "The vascular endothelial-cadherin promoter directs endothelial-specific expression in transgenic mice." Blood **93**(1): 184-192.

Gotoh, T., S. Hattori, S. Nakamura, H. Kitayama, M. Noda, Y. Takai, K. Kaibuchi, H. Matsui, O. Hatase, H. Takahashi, T. Kurata and M. Matsuda (1995). "Identification of Rap 1 as a target for the Crk SH3 domain-binding guanine nucleotide-releasing factor C3G." Molecular and Cellular Biology **15**(12): 6746-6753.

Gourdie, R. G., C. R. Green, N. J. Severs, R. H. Anderson and R. P. Thompson (1993). "Evidence for a distinct gap-junctional phenotype in ventricular conduction tissues of the developing and mature avian heart." Circulation Research **72**(2): 278-289.

Gourdie, R. G., N. J. Severs, C. R. Green, S. Rothery, P. Germroth and R. P. Thompson (1993). "The spatial distribution and relative abundance of gap-junctional connexin40 and connexin43 correlate to functional properties of components of the cardiac atrioventricular conduction system." Journal of Cell Science **105**(4): 985-991.

Grace, E. A. and J. Busciglio (2003). "Aberrant activation of focal adhesion proteins mediates fibrillar amyloid β-induced neuronal dystrophy." Journal of Neuroscience **23**(2): 493-502.

Grand, R. J., A. S. Turnell and P. W. Grabham (1996). "Cellular consequences of thrombin-receptor activation." Biochem J **313 (Pt 2)**: 353-368.

Greeb, J. and G. E. Shull (1989). "Molecular cloning of a third isoform of the calmodulin-sensitive plasma membrane Ca2+-transporting ATPase that is expressed predominantly in brain and skeletal muscle." J Biol Chem **264**(31): 18569-18576.

Grego, S., V. Cantillana and E. D. Salmon (2001). "Microtubule treadmilling in vitro investigated by fluorescence speckle and confocal microscopy." Biophys J **81**(1): 66-78.

Grenier, S., M. Sandig and K. Mequanint (2009). "Smooth muscle α-actin and calponin expression and extracellular matrix production of human coronary artery smooth muscle cells in 3D scaffolds." Tissue Engineering - Part A **15**(10): 3001-3011.

Gros, D., T. Jarry-Guichard, I. Ten Velde, A. De Maziere, M. J. A. Van Kempen, J. Davoust, J. P. Briand, A. F. M. Moorman and H. J. Jongsma (1994). "Restricted distribution of connexin40, a gap junctional protein, in mammalian heart." Circulation Research **74**(5): 839-851.

Grundy, S. M (1998). "Statin trials and goals of cholesterol-lowering therapy." Circulation **97**(15): 1436-1439.

Grunwald, G. B. (1993). "The structural and functional analysis of cadherin calcium-dependent cell adhesion molecules." Current Opinion in Cell Biology **5**(5): 797-805.

Guerrier, A., P. Fonlupt, I. Morand, R. Rabilloud, C. Audebet, V. Krutovskikh, D. Gros, B. Rousset and Y. Munari-Silem (1995). "Gap junctions and cell polarity: connexin32 and

connexin43 expressed in polarized thyroid epithelial cells assemble into separate gap junctions, which are located in distinct regions of the lateral plasma membrane domain." J Cell Sci **108 (Pt 7)**: 2609-2617.

Guo, F. F., E. Kumahara and D. Saffen (2001). "A CalDAG-GEFI/Rap1/B-Raf cassette couples M(1) muscarinic acetylcholine receptors to the activation of ERK1/2." J Biol Chem **276**(27): 25568-25581.

Guo, H. B., H. Johnson, M. Randolph and M. Pierce (2009). "Regulation of homotypic cell-cell adhesion by branched N-glycosylation of N-cadherin extracellular EC2 and EC3 domains." Journal of Biological Chemistry **284**(50): 34986-34997.

Haas, T. L. and B. R. Duling (1997). "Morphology favors an endothelial cell pathway for longitudinal conduction within arterioles." Microvasc Res **53**(2): 113-120.

Hajnoczky, G., E. Gao, T. Nomura, J. B. Hoek and A. P. Thomas (1993). "Multiple mechanisms by which protein kinase A potentiates inositol 1,4,5-trisphosphate-induced Ca2+ mobilization in permeabilized hepatocytes." Biochem J **293 (Pt 2)**: 413-422.

Halbleib, J. M. and W. J. Nelson (2006). "Cadherins in development: cell adhesion, sorting, and tissue morphogenesis." Genes & Development **20**(23): 3199-3214.

Harris, A. L., D. C. Spray and M. V. Bennett (1981). "Kinetic properties of a voltage-dependent junctional conductance." J Gen Physiol **77**(1): 95-117.

Harris, E. S. and W. J. Nelson (2010). "VE-cadherin: At the front, center, and sides of endothelial cell organization and function." Current Opinion in Cell Biology **22**(5): 651-658.

Harris, H. and D. C. Rubinsztein (2012). "Control of autophagy as a therapy for neurodegenerative disease." Nature Reviews Neurology **8**(2): 108-117.

Hart, M. J., X. Jiang, T. Kozasa, W. Roscoe, W. D. Singer, A. G. Gilman, P. C. Sternweis and G. Bollag (1998). "Direct stimulation of the guanine nucleotide exchange activity of p115 RhoGEF by Galpha13." Science **280**(5372): 2112-2114.

Hatta, K., S. Takagi, H. Fujisawa and M. Takeichi (1987). "Spatial and temporal expression pattern of N-cadherin cell adhesion molecules correlated with morphogenetic processes of chicken embryos." Developmental Biology **120**(1): 215-227.

Haubrich, S., H. J. Schwarz, F. Bukauskas, H. Lichtenberg-Fraté, O. Traub, R. Weingart and K. Willecke (1996). "Incompatibility of connexin 40 and 43 hemichannels in gap junctions between mammalian cells is determined by intracellular domains." Molecular Biology of the Cell **7**(12): 1995-2006.

Head, J. A., D. Jiang, M. Li, L. J. Zorn, E. M. Schaefer, J. T. Parsons and S. A. Weed (2003). "Cortactin tyrosine phosphorylation requires Rac1 activity and association with the cortical actin cytoskeleton." Molecular Biology of the Cell **14**(8): 3216-3229.

Heberlein, K. R., A. C. Straub and B. E. Isakson (2009). "The myoendothelial junction: breaking through the matrix?" Microcirculation **16**(4): 307-322.

Heimark, R. L., M. Degner and S. M. Schwartz (1990). "Identification of a Ca2+-dependent cell-cell adhesion molecule in endothelial cells." Journal of Cell Biology **110**(5): 1745-1756.

Hellberg, C. B., S. M. Burden-Gulley, G. E. Pietz and S. M. Brady-Kalnay (2002). "Expression of the receptor protein-tyrosine phosphatase, PTPμ, restores E-cadherin-dependent adhesion in human prostate carcinoma cells." Journal of Biological Chemistry **277**(13): 11165-11173.

Hermant, B., S. Bibert, E. Concord, B. Dublet, M. Weidenhaupt, T. Vernet and D. Gulino-Debrac (2003). "Identification of proteases involved in the proteolysis of vascular endothelium cadherin during neutrophil transmigration." J Biol Chem **278**(16): 14002-14012.

Herren, B., B. Levkau, E. W. Raines and R. Ross (1998). "Cleavage of beta-catenin and plakoglobin and shedding of VE-cadherin during endothelial apoptosis: evidence for a role for caspases and metalloproteinases." Mol Biol Cell **9**(6): 1589-1601.

Himmel, H. M., A. R. Whorton and H. C. Strauss (1993). "Intracellular calcium, currents, and stimulus-response coupling in endothelial cells." Hypertension **21**(1): 112-127.

Hirata, K.-i., T. Ishida, K. Penta, M. Rezaee, E. Yang, J. Wohlgemuth and T. Quertermous (2001). "Cloning of an Immunoglobulin Family Adhesion Molecule Selectively Expressed by Endothelial Cells." Journal of Biological Chemistry **276**(19): 16223-16231.

Hirota, S., E. Pertens and L. J. Janssen (2007). "The reverse mode of the Na+/Ca2+ exchanger provides a source of Ca2+ for store refilling following agonist-induced Ca 2+ mobilization." American Journal of Physiology - Lung Cellular and Molecular Physiology **292**(2): L438-L447.

Ho, Y.-D., J. L. Joyal, Z. Li and D. B. Sacks (1999). "IQGAP1 Integrates Ca2+/Calmodulin and Cdc42 Signaling." Journal of Biological Chemistry **274**(1): 464-470.

Hofmann, T., M. Schaefer, G. Schultz and T. Gudermann (2000). "Transient receptor potential channels as molecular substrates of receptor-mediated cation entry." J Mol Med (Berl) **78**(1): 14-25.

Hogan, C., N. Serpente, P. Cogram, C. R. Hosking, C. U. Bialucha, S. M. Feller, V. M. M. Braga, W. Birchmeier, and Y. Fujita (2004). "Rap1 regulates the formation of E-cadherin-based cell-cell contacts." Molecular and cellular biology **24**(15): 6690-6700.

Hogan, P. G. and A. Rao (2007). "Dissecting ICRAC, a store-operated calcium current." Trends Biochem Sci **32**(5): 235-245.

Hogan, C., N. Serpente, P. Cogram, C. R. Hosking, C. U. Bialucha, S. M. Feller, V. M. M. Braga, W. Birchmeier, and Y. Fujita (2004). "Rap1 regulates the formation of E-cadherin-based cell-cell contacts." Molecular and cellular biology **24**(15): 6690-6700.

Holm, I., A. Mikhailov, T. Jillson and B. Rose (1999). "Dynamics of gap junctions observed in living cells with connexin43-GFP chimeric protein." European Journal of Cell Biology **78**(12): 856-866.

Holz, G. G., O. G. Chepurny and F. Schwede (2008). "Epac-selective cAMP analogs: New tools with which to evaluate the signal transduction properties of cAMP-regulated guanine nucleotide exchange factors." Cellular Signalling **20**(1): 10-20.

Hong, T. and C. E. Hill (1998). "Restricted expression of the gap junctional protein connexin 43 in the arterial system of the rat." Journal of Anatomy **192**(4): 583-593.

Hoth, M. and R. Penner (1992). "Depletion of intracellular calcium stores activates a calcium current in mast cells." Nature **355**(6358): 353-356.

Howard, L. S. G. E. and N. W. Morrell (2005). "New therapeutic agents for pulmonary vascular disease." Paediatric Respiratory Reviews **6**(4): 285-291.

Huang, R. Y. C., J. G. Laing, E. M. Kanter, V. M. Berthoud, M. Bao, H. W. Rohrs, R. R. Townsend and K. A. Yamada (2011). "Identification of CaMKII phosphorylation sites in connexin43 by high-resolution mass spectrometry." Journal of Proteome Research **10**(3): 1098-1109.

Ilic, D., B. Kovacic, S. McDonagh, F. Jin, C. Baumbusch, D. G. Gardner and C. H. Damsky (2003). "Focal adhesion kinase is required for blood vessel morphogenesis." Circ Res **92**(3): 300-307.

Inazu, M., H. Zhang and E. E. Daniel (1995). "Different mechanisms can activate Ca2+ entrance via cation currents in endothelial cells." Life Sci **56**(1): 11-17.

Irie, K., K. Shimizu, T. Sakisaka, W. Ikeda and Y. Takai (2004). "Roles and modes of action of nectins in cell-cell adhesion." Semin Cell Dev Biol **15**(6): 643-656.

Irvine, R. F. (1990). "'Quantal' Ca2+ release and the control of Ca2+ entry by inositol phosphates--a possible mechanism." FEBS Lett **263**(1): 5-9.

Ishida, T., M. Takahashi, M. A. Corson and B. C. Berk (1997). "Fluid shear stress-mediated signal transduction: how do endothelial cells transduce mechanical force into biological responses?" Ann N Y Acad Sci **811**: 12-23; discussion 23-14.

Ishikawa, H., R. Bischoff and H. Holtzer (1968). "Mitosis and intermediate-sized filaments in developing skeletal muscle." J Cell Biol **38**(3): 538-555.

Itoh, M., M. Furuse, K. Morita, K. Kubota, M. Saitou and S. Tsukita (1999). "Direct binding of three tight junction-associated MAGUKs, ZO-1, ZO-2, and ZO-3, with the COOH termini of claudins." J Cell Biol **147**(6): 1351-1363.

Itoh, M., A. Nagafuchi, S. Moroi and S. Tsukita (1997). "Involvement of ZO-1 in cadherin-based cell adhesion through its direct binding to alpha catenin and actin filaments." J Cell Biol **138**(1): 181-192.

Ivanov, D., M. Philippova, J. Antropova, F. Gubaeva, O. Iljinskaya, E. Tararak, V. Bochkov, P. Erne, T. Resink and V. Tkachuk (2001). "Expression of cell adhesion molecule T-cadherin in the human vasculature." Histochem Cell Biol **115**(3): 231-242.

Iyer, S., D. M. Ferreri, N. C. DeCocco, F. L. Minnear and P. A. Vincent (2004). "VE-cadherin-p120 interaction is required for maintenance of endothelial barrier function." American Journal of Physiology - Lung Cellular and Molecular Physiology **286**(6 30-6): L1143-L1153.

Janmey, P. A. and T. P. Stossel (1987). "Modulation of gelsolin function by phosphatidylinositol 4,5 bisphosphate." Nature **325**(6102): 362-364.

Jansen, L. A. M., T. De Vrije and W. M. F. Jongen (1996). "Differences in the calcium-mediated regulation of gap junctional intercellular communication between a cell line consisting of initiated cells and a carcinoma-derived cell line." Carcinogenesis **17**(11): 2311-2319.

Jho, D., D. Mehta, G. Ahmmed, X. P. Gao, C. Tiruppathi, M. Broman and A. B. Malik (2005). "Angiopoietin-1 opposes VEGF-induced increase in endothelial permeability by inhibiting TRPC1-dependent Ca 2+ influx." Circulation Research **96**(12): 1282-1290.

Jiang, J. X. and D. A. Goodenough (1996). "Heteromeric connexons in lens gap junction channels." Proc Natl Acad Sci U S A **93**(3): 1287-1291.

Jiang, J. X., D. L. Paul and D. A. Goodenough (1993). "Posttranslational phosphorylation of lens fiber connexin46: a slow occurrence." Invest Ophthalmol Vis Sci **34**(13): 3558-3565.

Jin, T. G., T. Satoh, Y. Liao, C. Song, X. Gao, K. I. Kariya, C. D. Hu and T. Kataoka (2001). "Role of the CDC25 Homology Domain of Phospholipase Cε in Amplification of Rap1-dependent Signaling." Journal of Biological Chemistry **276**(32): 30301-30307.

Joachim, S. and G. Schwoch (1990). "Localization of cAMP-dependent protein kinase subunits along the secretory pathway in pancreatic and parotid acinar cells and accumulation of the catalytic subunit in parotid secretory granules following β-adrenergic stimulation." European Journal of Cell Biology **51**(1): 76-84.

Johnson, R. P. and S. W. Craig (1995). "F-actin binding site masked by the intramolecular association of vinculin head and tail domains." Nature **373**(6511): 261-264.

Joner, M., A. V. Finn, A. Farb, E. K. Mont, F. D. Kolodgie, E. Ladich, R. Kutys, K. Skorija, H. K. Gold, and R. Virmani (2006). "Pathology of drug-eluting stents in humans: delayed healing and late thrombotic risk." Journal of the American College of Cardiology **48**(1): 193-202.

Jongen, W. M. F., D. J. Fitzgerald, M. Asamoto, C. Piccoli, T. J. Slaga, D. Gros, M. Takeichi and H. Yamasaki (1991). "Regulation of connexin 43-mediated gap junctional intercellular communication by CA2+ in mouse epidermal cells is controlled by E-cadherin." Journal of Cell Biology **114**(3): 545-555.

Jordan, K., R. Chodock, A. R. Hand and D. W. Laird (2001). "The origin of annular junctions: A mechanism of gap junction internalization." Journal of Cell Science **114**(4): 763-773.

Jordan, K., J. L. Solan, M. Dominguez, M. Sia, A. Hand, P. D. Lampe and D. W. Laird (1999). "Trafficking, assembly, and function of a connexin43-green fluorescent protein chimera in live mammalian cells." Mol Biol Cell **10**(6): 2033-2050.

Jukema, J. W., J. J. W. Verschuren, T. A. N. Ahmed, and P. H. A. Quax (2012). "Restenosis after PCI. Part 1: pathophysiology and risk factors." Nature Reviews Cardiology **9**(1): 53-62.

Kalluri, R. (2003). "Basement membranes: structure, assembly and role in tumour angiogenesis." Nat Rev Cancer **3**(6): 422-433.

Kang, G., O. G. Chepurny and G. G. Holz (2001). "cAMP-regulated guanine nucleotide exchange factor II (Epac2) mediates Ca2+-induced Ca2+ release in INS-1 pancreatic β-cells." Journal of Physiology **536**(2): 375-385.

Kang, G., J. W. Joseph, O. G. Chepurny, M. Monaco, M. B. Wheeler, J. L. Bos, F. Schwede, H. G. Genieser and G. G. Holz (2003). "Epac-selective cAMP analog 8-pCPT-2′-O-Me-cAMP as a stimulus for Ca2+-induced Ca2+ release and exocytosis in pancreatic β-cells." Journal of Biological Chemistry **278**(10): 8279-8285.

Kanno, Y., Y. Sasaki, Y. Shiba, C. Yoshida-Noro and M. Takeichi (1984). "Monoclonal antibody ECCD-1 inhibits intercellular communication in teratocarcinoma PCC3 cells." Experimental Cell Research **152**(1): 270-274.

Kartenbeck, J., M. Schmelz, W. W. Franke and B. Geiger (1991). "Endocytosis of junctional cadherins in bovine kidney epithelial (MDBK) cells cultured in low Ca2+ ion medium." Journal of Cell Biology **113**(4): 881-892.

Kaupp, U. B. and R. Seifert (2002). "Cyclic nucleotide-gated ion channels." Physiol Rev **82**(3): 769-824.

Kawasaki, H., G. M. Springett, N. Mochizuki, S. Toki, M. Nakaya, M. Matsuda, D. E. Housman and A. M. Graybiel (1998). "A family of cAMP-binding proteins that directly activate Rap1." Science **282**(5397): 2275-2279.

Kawasaki, H., G. M. Springett, S. Toki, J. J. Canales, P. Harlan, J. P. Blumenstiel, E. J. Chen, I. A. Bany, N. Mochizuki, A. Ashbacher, M. Matsuda, D. E. Housman and A. M. Graybiel (1998). "A Rap guanine nucleotide exchange factor enriched highly in the basal ganglia." Proceedings of the National Academy of Sciences of the United States of America **95**(22): 13278-13283.

Keane, R. W., P. P. Mehta, B. Rose, L. S. Honig, W. R. Loewenstein and U. Rutishauser (1988). "Neural differentiation, NCAM-mediated adhesion, and gap junctional communication in neuroectoderm. A study in vitro." Journal of Cell Biology **106**(4): 1307-1319.

Kelley, G. G., S. E. Reks, J. M. Ondrako and A. V. Smrcka (2001). "Phospholipase Cε: A novel Ras effector." EMBO Journal **20**(4): 743-754.

Keravis, T., N. Komas and C. Lugnier (2000). "Cyclic nucleotide hydrolysis in bovine aortic endothelial cells in culture: differential regulation in cobblestone and spindle phenotypes." J Vasc Res **37**(4): 235-249.

Kevil, C. G., N. Okayama, S. D. Trocha, T. J. Kalogeris, L. L. Coe, R. D. Specian, C. P. Davis and J. S. Alexander (1998). "Expression of zonula occludens and adherens junctional proteins in human venous and arterial endothelial cells: Role of occludin in endothelial solute barriers." Microcirculation **5**(2-3): 197-210.

Kikkawa, M., T. Ishikawa, T. Nakata, T. Wakabayashi and N. Hirokawa (1994). "Direct visualization of the microtubule lattice seam both in vitro and in vivo." J Cell Biol **127**(6 Pt 2): 1965-1971.

Kiuchi-Saishin, Y., S. Gotoh, M. Furuse, A. Takasuga, Y. Tano and S. Tsukita (2002). "Differential expression patterns of claudins, tight junction membrane proteins, in mouse nephron segments." J Am Soc Nephrol **13**(4): 875-886.

Klinz, F. J., R. Seifert, I. Schwaner, H. Gausepohl, R. Frank and G. Schultz (1992). "Generation of specific antibodies against the rap1A, rap1B and rap2 small GTP-binding proteins.

Analysis of rap and ras proteins in membranes frome mammalian cells." European Journal of Biochemistry **207**(1): 207-213.

Knudsen, K. A., A. P. Soler, K. R. Johnson and M. J. Wheelock (1995). "Interaction of alpha-actinin with the cadherin/catenin cell-cell adhesion complex via alpha-catenin." J Cell Biol **130**(1): 67-77.

Kobayashi, K., Y. Tsubosaka, M. Hori, S. Narumiya, H. Ozaki and T. Murata (2013). "Prostaglandin D2-DP signaling promotes endothelial barrier function via the cAMP/PKA/Tiam1/Rac1 pathway." Arterioscler Thromb Vasc Biol **33**(3): 565-571.

Kohler, R., S. Brakemeier, M. Kuhn, C. Degenhardt, H. Buhr, A. Pries and J. Hoyer (2001). "Expression of ryanodine receptor type 3 and TRP channels in endothelial cells: comparison of in situ and cultured human endothelial cells." Cardiovasc Res **51**(1): 160-168.

Kojima, T., N. Sawada, H. Chiba, Y. Kokai, M. Yamamoto, M. Urban, G. H. Lee, E. L. Hertzberg, Y. Mochizuki and D. C. Spray (1999). "Induction of tight junctions in human connexin 32 (hCx32)-transfected mouse hepatocytes: Connexin 32 interacts with occludin." Biochemical and Biophysical Research Communications **266**(1): 222-229.

Kolodney, M. S. and R. B. Wysolmerski (1992). "Isometric contraction by fibroblasts and endothelial cells in tissue culture: a quantitative study." J Cell Biol **117**(1): 73-82.

Kondapalli, J., A. S. Flozak and M. L. C. Albuquerque (2004). "Laminar Shear Stress Differentially Modulates Gene Expression of p120 Catenin, Kaiso Transcription Factor, and Vascular Endothelial Cadherin in Human Coronary Artery Endothelial Cells." Journal of Biological Chemistry **279**(12): 11417-11424.

Kooistra, M. R. H., M. Corada, E. Dejana and J. L. Bos (2005). "Epac1 regulates integrity of endothelial cell junctions through VE-cadherin." FEBS Letters **579**(22): 4966-4972.

Kou, R. and T. Michel (2007). "Epinephrine Regulation of the Endothelial Nitric-oxide Synthase: ROLES OF RAC1 AND β3-ADRENERGIC RECEPTORS IN ENDOTHELIAL NO SIGNALING." Journal of Biological Chemistry **282**(45): 32719-32729.

Kowalczyk, A. P., P. Navarro, E. Dejana, E. A. Bornslaeger, K. J. Green, D. S. Kopp and J. E. Borgwardt (1998). "VE-cadherin and desmoplakin are assembled into dermal microvascular endothelial intercellular junctions: a pivotal role for plakoglobin in the recruitment of desmoplakin to intercellular junctions." J Cell Sci **111 (Pt 20)**: 3045-3057.

Kozasa, T., X. Jiang, M. J. Hart, P. M. Sternweis, W. D. Singer, A. G. Gilman, G. Bollag and P. C. Sternweis (1998). "p115 RhoGEF, a GTPase activating protein for Galpha12 and Galpha13." Science **280**(5372): 2109-2111.

Krutovskikh, V. and H. Yamasaki (2000). "Connexin gene mutations in human genetic diseases." Mutation Research - Reviews in Mutation Research **462**(2-3): 197-207.

Krylyshkina, O., I. Kaverina, W. Kranewitter, W. Steffen, M. C. Alonso, R. A. Cross and J. V. Small (2002). "Modulation of substrate adhesion dynamics via microtubule targeting requires kinesin-1." J Cell Biol **156**(2): 349-359.

Kumar, N. M., D. S. Friend and N. B. Gilula (1995). "Synthesis and assembly of human β1 gap junctions in BHK cells by DNA transfection with the human β1 cDNA." Journal of Cell Science **108**(12): 3725-3734.

Kumar, N. M. and N. B. Gilula (1996). "The gap junction communication channel." Cell **84**(3): 381-388.

Kuo, J. F. and P. Greengard (1969). "Cyclic nucleotide-dependent protein kinases. IV. Widespread occurrence of adenosine 3',5'-monophosphate-dependent protein kinase in various tissues and phyla of the animal kingdom." Proceedings of the National Academy of Sciences of the United States of America **64**(4): 1349-1355.

Kuroda, S., M. Fukata, M. Nakagawa, K. Fujii, T. Nakamura, T. Ookubo, I. Izawa, T. Nagase, N. Nomura, H. Tani, I. Shoji, Y. Matsuura, S. Yonehara and K. Kaibuchi (1998). "Role of IQGAP1, a target of the small GTPases Cdc42 and Rac1, in regulation of E-cadherin-mediated cell-cell adhesion." Science **281**(5378): 832-835.

Kurtz, L., K. Madsen, B. Kurt, B. L. Jensen, S. Walter, B. Banas, C. Wagner and A. Kurtz (2010). "High-level connexin expression in the human juxtaglomerular apparatus." Nephron - Physiology **116**(1): p1-p8.

Kwak, B. R., M. M. P. Hermans, H. R. De Jonge, S. M. Lohmann, H. J. Jongsma and M. Chanson (1995). "Differential regulation of distinct types of gap junction channels by similar phosphorylating conditions." Molecular Biology of the Cell **6**(12): 1707-1719.

Kwak, B. R., T. A. B. Van Veen, L. J. S. Analbers and H. J. Jongsma (1995). "TPA increases conductance but decreases permeability in neonatal rat cardiomyocyte gap junction channels." Experimental Cell Research **220**(2): 456-463.

Laing, J. G., P. N. Tadros, E. M. Westphale and E. C. Beyer (1997). "Degradation of connexin43 gap junctions involves both the proteasome and the lysosome." Exp Cell Res **236**(2): 482-492.

Laird, D. W. (2005). "Connexin phosphorylation as a regulatory event linked to gap junction internalization and degradation." Biochim Biophys Acta **1711**(2): 172-182.

Laird, D. W., M. Castillo and L. Kasprzak (1995). "Gap junction turnover, intracellular trafficking, and phosphorylation of connexin43 in brefeldin A-treated rat mammary tumor cells." Journal of Cell Biology **131**(5): 1193-1203.

Laird, D. W., K. L. Puranam and J. P. Revel (1991). "Turnover and phosphorylation dynamics of connexin43 gap junction protein in cultured cardiac myocytes." Biochemical Journal **273**(1): 67-72.

Lambert, T. L., R. S. Kent and A. R. Whorton (1986). "Bradykinin stimulation of inositol polyphosphate production in porcine aortic endothelial cells." J Biol Chem **261**(32): 15288-15293.

Lampe, P. D. (1994). "Analyzing phorbol ester effects on gap junctional communication: A dramatic inhibition of assembly." Journal of Cell Biology **127**(6 II): 1895-1905.

Lampe, P. D. and A. F. Lau (2000). "Regulation of gap junctions by phosphorylation of connexins." Archives of Biochemistry and Biophysics **384**(2): 205-215.

Lampe, P. D., E. M. TenBroek, J. M. Burt, W. E. Kurata, R. G. Johnson and A. F. Lau (2000). "Phosphorylation of connexin43 on serine368 by protein kinase C regulates gap junctional communication." Journal of Cell Biology **149**(7): 1503-1512.

Lampugnani, M. G. and E. Dejana (1997). "Interendothelial junctions: Structure, signalling and functional roles." Current Opinion in Cell Biology **9**(5): 674-682.

Lampugnani, M. G., F. Orsenigo, N. Rudini, L. Maddaluno, G. Boulday, F. Chapon and E. Dejana (2010). "CCM1 regulates vascular-lumen organization by inducing endothelial polarity." Journal of Cell Science **123**(7): 1073-1080.

Lampugnani, M. G., M. Resnati, E. Dejana and P. C. Marchisio (1991). "The role of integrins in the maintenance of endothelial monolayer integrity." J Cell Biol **112**(3): 479-490.

Lampugnani, M. G., M. Resnati, M. Raiteri, R. Pigott, A. Pisacane, G. Houen, L. P. Ruco and E. Dejana (1992). "A novel endothelial-specific membrane protein is a marker of cell-cell contacts." Journal of Cell Biology **118**(6): 1511-1522.

Lampugnani, M. G., A. Zanetti, F. Breviario, G. Balconi, F. Orsenigo, M. Corada, R. Spagnuolo, M. Betson, V. Braga and E. Dejana (2002). "VE-cadherin regulates endothelial actin activating Rac and increasing membrane association of Tiam." Molecular Biology of the Cell **13**(4): 1175-1189.

Lang, P., F. Gesbert, M. Delespine-Carmagnat, R. Stancou, M. Pouchelet and J. Bertoglio (1996). "Protein kinase A phosphorylation of RhoA mediates the morphological and functional effects of cyclic AMP in cytotoxic lymphocytes." Embo j **15**(3): 510-519.

Languino, L. R., K. R. Gehlsen, E. Wayner, W. G. Carter, E. Engvall and E. Ruoslahti (1989). "Endothelial cells use alpha 2 beta 1 integrin as a laminin receptor." J Cell Biol **109**(5): 2455-2462.

Larson, D. M., C. C. Haudenschild and E. C. Beyer (1990). "Gap junction messenger RNA expression by vascular wall cells." Circulation Research **66**(4): 1074-1080.

Larson, D. M., M. J. Wrobleski, G. D. V. Sagar, E. M. Westphale and E. C. Beyer (1997). "Differential regulation of connexin43 and connexin37 in endothelial cells by cell density, growth, and TFG-β1." American Journal of Physiology - Cell Physiology **272**(2 41-2): C405-C415.

Lauf, U., B. N. G. Giepmans, P. Lopez, S. Braconnot, S. C. Chen and M. M. Falk (2002). "Dynamic trafficking and delivery of connexons to the plasma membrane and accretion to gap junctions in living cells." Proceedings of the National Academy of Sciences of the United States of America **99**(16): 10446-10451.

Ledoux, J., M. S. Taylor, A. D. Bonev, R. M. Hannah, V. Solodushko, B. Shui, Y. Tallini, M. I. Kotlikoff and M. T. Nelson (2008). "Functional architecture of inositol 1,4,5-trisphosphate signaling in restricted spaces of myoendothelial projections." Proceedings of the National Academy of Sciences **105**(28): 9627-9632.

Lee, K. P., S. Choi, J. H. Hong, M. Ahuja, S. Graham, R. Ma, I. So, D. M. Shin, S. Muallem and J. P. Yuan (2014). "Molecular determinants mediating gating of Transient Receptor Potential Canonical (TRPC) channels by stromal interaction molecule 1 (STIM1)." J Biol Chem **289**(10): 6372-6382.

Lee, J. M., W. Choe, B. Kim, W. Seo, W. Lim, C. Kang, S. Kyeong. K.D Eom, H. Cho, Y. Kim, J. Hur, H. Yang, H. Cho, Y. Lee and H. Kim (2012) "Comparison of endothelialization and neointimal formation with stents coated with antibodies against CD34 and vascular endothelial-cadherin." Biomaterials **33**(35): 8917-8927.

Lee, M. J., S. Thangada, K. P. Claffey, N. Ancellin, C. H. Liu, M. Kluk, M. Volpi, R. I. Sha'afi and T. Hla (1999). "Vascular endothelial cell adherens junction assembly and morphogenesis induced by sphingosine-1-phosphate." Cell **99**(3): 301-312.

Lee, S. W., J. Y. Won, H. Y. Lee, H. J. Lee, S. W. Youn, J. Y. Lee, C. H. Cho, H. J. Cho, S. Oh, I. H. Chae and H. S. Kim (2011). "Angiopoietin-1 protects heart against ischemia/reperfusion injury through VE-cadherin dephosphorylation and myocardiac integrin-β1/ERK/caspase-9 phosphorylation cascade." Molecular medicine (Cambridge, Mass.) **17**(9-10): 1095-1106.

Leemhuis, J., S. Boutillier, G. Schmidt and D. K. Meyer (2002). "The protein kinase A inhibitor H89 acts on cell morphology by inhibiting Rho kinase." J Pharmacol Exp Ther **300**(3): 1000-1007.

Lehrke, M., F. Kahles, A. Makowska, P. V. Tilstam, S. Diebold, J. Marx, R. Stöhr, K. Hess, E. B. Endorf, D. Bruemmer, N. Marx and H. M. Findeisen (2015) "PDE4 inhibition reduces neointima formation and inhibits VCAM-1 expression and histone methylation in an Epac-dependent manner." Journal of molecular and cellular cardiology **81**: 23-33.

Lesh, R. E., A. R. Marks, A. V. Somlyo, S. Fleischer and A. P. Somlyo (1993). "Anti-ryanodine receptor antibody binding sites in vascular and endocardial endothelium." Circ Res **72**(2): 481-488.

Leung, Y. K., J. Du, Y. Huang and X. Yao (2010). "Cyclic Nucleotide-Gated Channels Contribute to Thromboxane A₂-Induced Contraction of Rat Small Mesenteric Arteries." PLoS ONE **5**(6): e11098.

Levine, E., R. Werner, I. Neuhaus and G. Dahl (1993). "Asymmetry of gap junction formation along the animal-vegetal axis of Xenopus oocytes." Developmental Biology **156**(2): 490-499.

Li, H., T. F. Liu, A. Lazrak, C. Peracchia, G. S. Goldberg, P. D. Lampe and R. G. Johnson (1996). "Properties and regulation of gap junctional hemichannels in the plasma membranes of cultured cells." Journal of Cell Biology **134**(4): 1019-1030.

Li, S., T. Tsalkova, M. A. White, F. C. Mei, T. Liu, D. Wang, V. L. Woods Jr and X. Cheng (2011). "Mechanism of intracellular cAMP sensor Epac2 activation: cAMP-induced conformational changes identified by amide hydrogen/Deuterium Exchange Mass Spectrometry (DXMS)." Journal of Biological Chemistry **286**(20): 17889-17897.

Li, Y., S. Asuri, J. F. Rebhun, A. F. Castro, N. C. Paranavitana and L. A. Quilliam (2006). "The RAP1 guanine nucleotide exchange factor Epac2 couples cyclic AMP and Ras signals at the plasma membrane." Journal of Biological Chemistry **281**(5): 2506-2514.

Liang, T. W., R. A. DeMarco, R. J. Mrsny, A. Gurney, A. Gray, J. Hooley, H. L. Aaron, A. Huang, T. Klassen, D. B. Tumas and S. Fong (2000). "Characterization of huJAM: evidence for involvement in cell-cell contact and tight junction regulation." Am J Physiol Cell Physiol **279**(6): C1733-1743.

Liaw, C. W., C. Cannon, M. D. Power, P. K. Kiboneka and L. L. Rubin (1990). "Identification and cloning of two species of cadherins in bovine endothelial cells." EMBO Journal **9**(9): 2701-2708.

Lidington, D., K. Tyml and Y. Ouellette (2002). "Lipopolysaccharide-induced reductions in cellular coupling correlate with tyrosine phosphorylation of connexin 43." J Cell Physiol **193**(3): 373-379.

Liebner, S., H. Gerhardt and H. Wolburg (2000). "Differential expression of endothelial beta-catenin and plakoglobin during development and maturation of the blood-brain and blood-retina barrier in the chicken." Dev Dyn **217**(1): 86-98.

Ligon, L. A., S. Karki, M. Tokito and E. L. Holzbaur (2001). "Dynein binds to beta-catenin and may tether microtubules at adherens junctions." Nat Cell Biol **3**(10): 913-917.

Lilly, B. (2014). "We have contact: endothelial cell-smooth muscle cell interactions." Physiology (Bethesda) **29**(4): 234-241.

Lin, Y. C., R. H. Adamson, J. F. Clark, R. K. Reed and F. R. Curry (2012). "Phosphodiesterase 4 inhibition attenuates plasma volume loss and transvascular exchange in volume-expanded mice." J Physiol **590**(Pt 2): 309-322.

Linnemann, T., M. Geyer, B. K. Jaitner, C. Block, H. R. Kalbitzer, A. Wittinghofer and C. Herrmann (1999). "Thermodynamic and kinetic characterization of the interaction between the Ras binding domain of AF6 and members of the Ras subfamily." Journal of Biological Chemistry **274**(19): 13556-13562.

Liou, J., M. L. Kim, W. D. Heo, J. T. Jones, J. W. Myers, J. E. Ferrell, Jr. and T. Meyer (2005). "STIM is a Ca2+ sensor essential for Ca2+-store-depletion-triggered Ca2+ influx." Curr Biol **15**(13): 1235-1241.

Little, T. L., E. C. Beyer and B. R. Duling (1995). "Connexin 43 and connexin 40 gap junctional proteins are present in arteriolar smooth muscle and endothelium in vivo." American Journal of Physiology - Heart and Circulatory Physiology **268**(2 37-2): H729-H739.

Liu, B., S. E. Peel, J. Fox and I. P. Hall (2010). "Reverse mode Na+/Ca2+ exchange mediated by STIM1 contributes to Ca2+ influx in airway smooth muscle following agonist stimulation." Respir Res **11**: 168.

Liu, C., Y. Li, M. Semenov, C. Han, G. H. Baeg, Y. Tan, Z. Zhang, X. Lin and X. He (2002). "Control of beta-catenin phosphorylation/degradation by a dual-kinase mechanism." Cell **108**(6): 837-847.

Liu, X. Z., X. J. Xia, J. Adams, Z. Y. Chen, K. O. Welch, M. Tekin, X. M. Ouyang, A. Kristiansen, A. Pandya, T. Balkany, K. S. Arnos and W. E. Nance (2001). "Mutations in GJA1 (connexin 43) are associated with non-syndromic autosomal recessive deafness." Human Molecular Genetics **10**(25): 2945-2951.

Liu, Y. and D. R. Senger (2004). "Matrix-specific activation of Src and Rho initiates capillary morphogenesis of endothelial cells." Faseb j **18**(3): 457-468.

Lo Vasco, V. R., L. Pacini, T. Di Raimo, D. D'Arcangelo and R. Businaro (2011). "Expression of phosphoinositide-specific phospholipase C isoforms in human umbilical vein endothelial cells." Journal of Clinical Pathology **64**(10): 911-915.

Loewenstein, W. R. (1981). "Junctional intercellular communication: the cell-to-cell membrane channel." Physiological Reviews **61**(4): 829-913.

Lopez, I., E. C. Mak, J. Ding, H. E. Hamm and J. W. Lomasney (2001). "A Novel Bifunctional Phospholipase C That Is Regulated by Gα 12 and Stimulates the Ras/Mitogen-activated Protein Kinase Pathway." Journal of Biological Chemistry **276**(4): 2758-2765.

Lopez, M., M. Aoubala, F. Jordier, D. Isnardon, S. Gomez and P. Dubreuil (1998). "The human poliovirus receptor related 2 protein is a new hematopoietic/endothelial homophilic adhesion molecule." Blood **92**(12): 4602-4611.

Luft, J. H. (1966). "Fine structures of capillary and endocapillary layer as revealed by ruthenium red." Fed Proc **25**(6): 1773-1783.

Lugnier, C. and V. B. Schini (1990). "Characterization of cyclic nucleotide phosphodiesterases from cultured bovine aortic endothelial cells." Biochemical Pharmacology **39**(1): 75-84.

Luik, R. M., M. M. Wu, J. Buchanan and R. S. Lewis (2006). "The elementary unit of store-operated Ca2+ entry: local activation of CRAC channels by STIM1 at ER-plasma membrane junctions." J Cell Biol **174**(6): 815-825.

Lur, G., L. P. Haynes, I. A. Prior, O. V. Gerasimenko, S. Feske, O. H. Petersen, R. D. Burgoyne and A. V. Tepikin (2009). "Ribosome-free terminals of rough ER allow formation of STIM1 puncta and segregation of STIM1 from IP(3) receptors." Curr Biol **19**(19): 1648-1653.

Lur, G., M. W. Sherwood, E. Ebisui, L. Haynes, S. Feske, R. Sutton, R. D. Burgoyne, K. Mikoshiba, O. H. Petersen and A. V. Tepikin (2011). "InsP(3)receptors and Orai channels in pancreatic acinar cells: co-localization and its consequences." Biochem J **436**(2): 231-239.

M'Rabet, L., P. Coffer, F. Zwartkruis, B. Franke, A. W. Segal, L. Koenderman and J. L. Bos (1998). "Activation of the small GTPase Rap1 in human neutrophils." Blood **92**(6): 2133-2140.

Macfarlane, S. R., M. J. Seatter, T. Kanke, G. D. Hunter and R. Plevin (2001). "Proteinase-activated receptors." Pharmacol Rev **53**(2): 245-282.

Machesky, L. M. and A. Hall (1997). "Role of actin polymerization and adhesion to extracellular matrix in Rac- and Rho-induced cytoskeletal reorganization." Journal of Cell Biology **138**(4): 913-926.

Maillet, M., S. J. Robert, M. Cacquevel, M. Gastineau, D. Vivien, J. Bertoglio, J. L. Zugaza, R. Fischmeister and F. Lezoualc'h (2003). "Crosstalk between Rap1 and Rac regulates secretion of sAPPα." Nature Cell Biology **5**(7): 633-639.

Maisonpierre, P. C., C. Suri, P. F. Jones, S. Bartunkova, S. J. Wiegand, C. Radziejewski, D. Compton, J. McClain, T. H. Aldrich, N. Papadopoulos, T. J. Daly, S. Davis, T. N. Sato and G. D. Yancopoulos (1997). "Angiopoietin-2, a Natural Antagonist for Tie2 That Disrupts in vivo Angiogenesis." Science **277**(5322): 55-60.

Malek, A. M. and S. Izumo (1996). "Mechanism of endothelial cell shape change and cytoskeletal remodeling in response to fluid shear stress." Journal of Cell Science **109**(4): 713-726.

Mammoto, T., S. M. Parikh, A. Mammoto, D. Gallagher, B. Chan, G. Mostoslavsky, D. E. Ingber and V. P. Sukhatme (2007). "Angiopoietin-1 requires p190 RhoGAP to protect against vascular leakage in vivo." J Biol Chem **282**(33): 23910-23918.

Mani, G., M. D. Feldman, D. Patel, and C. M. Agrawal (2007). "Coronary stents: a materials perspective." Biomaterials **28**(9): 1689-1710.

Martin-Padura, I., S. Lostaglio, M. Schneemann, L. Williams, M. Romano, P. Fruscella, C. Panzeri, A. Stoppacciaro, L. Ruco, A. Villa, D. Simmons and E. Dejana (1998). "Junctional adhesion molecule, a novel member of the immunoglobulin superfamily that distributes at intercellular junctions and modulates monocyte transmigration." J Cell Biol **142**(1): 117-127.

Martin, P. E. M., G. Blundell, S. Ahmad, R. J. Errington and W. H. Evans (2001). "Multiple pathways in the trafficking and assembly of connexin 26, 32 and 43 into gap junction intercellular communication channels." Journal of Cell Science **114**(21): 3845-3855.

Martin, P. E. M., J. Steggles, C. Wilson, S. Ahmad and W. H. Evans (2000). "Targeting motifs and functional parameters governing the assembly of connexins into gap junctions." Biochemical Journal **349**(1): 281-287.

Mayati, A., N. Levoin, H. Paris, M. N'Diaye, A. Courtois, P. Uriac, D. Lagadic-Gossmann, O. Fardel and E. Le Ferrec (2012). "Induction of intracellular calcium concentration by environmental benzo(a)pyrene involves a β2-adrenergic receptor/adenylyl cyclase/Epac-1/inositol 1,4,5-trisphosphate pathway in endothelial cells." Journal of Biological Chemistry **287**(6): 4041-4052.

McHugh, K. M., K. Crawford and J. L. Lessard (1991). "A comprehensive analysis of the developmental and tissue-specific expression of the isoactin multigene family in the rat." Developmental Biology **148**(2): 442-458.

McLachlin, J. R., S. Caveney and G. M. Kidder (1983). "Control of gap junction formation in early mouse embryos." Developmental Biology **98**(1): 155-164.

Mechanic, S., K. Raynor, J. E. Hill and P. Cowin (1991). "Desmocollins form a distinct subset of the cadherin family of cell adhesion molecules." Proc Natl Acad Sci U S A **88**(10): 4476-4480.

Mege, R. M., F. Matsuzaki, W. J. Gallin, J. E. Goldberg, B. A. Cunningham and G. M. Edelman (1988). "Construction of epithelioid sheets by transfection of mouse sarcoma cells with cDNAs for chicken cell adhesion molecules." Proceedings of the National Academy of Sciences of the United States of America **85**(19): 7274-7278.

Mehta, D. and A. B. Malik (2006). "Signaling mechanisms regulating endothelial permeability." Physiological Reviews **86**(1): 279-367.

Mehta, P. P., B. L. Lokeshwar, P. C. Schiller, M. V. Bendix, R. C. Ostenson, G. A. Howard and B. A. Roos (1996). "Gap-junctional communication in normal and neoplastic prostate epithelial cells and its regulation by cAMP." Molecular Carcinogenesis **15**(1): 18-32.

Mehta, P. P., M. Yamamoto and B. Rose (1992). "Transcription of the gene for the gap junctional protein connexin43 and expression of functional cell-to-cell channels are regulated by cAMP." Molecular Biology of the Cell **3**(8): 839-850.

Meldolesi, J. and T. Pozzan (1998). "The endoplasmic reticulum Ca2+ store: a view from the lumen." Trends Biochem Sci **23**(1): 10-14.

Meyer, R. A., D. W. Laird, J. P. Revel and R. G. Johnson (1992). "Inhibition of gap junction and adherens junction assembly by connexin and A-CAM antibodies." Journal of Cell Biology **119**(1): 179-189.

Miano, J. M., M. J. Carlson, J. A. Spencer and R. P. Misra (2000). "Serum response factor-dependent regulation of the smooth muscle calponin gene." Journal of Biological Chemistry **275**(13): 9814-9822.

Mikoshiba, K. (2007). "IP3 receptor/Ca2+ channel: from discovery to new signaling concepts." J Neurochem **102**(5): 1426-1446.

Miravet, S., J. Piedra, F. Miro, E. Itarte, A. Garcia de Herreros and M. Dunach (2002). "The transcriptional factor Tcf-4 contains different binding sites for beta-catenin and plakoglobin." J Biol Chem **277**(3): 1884-1891.

Miro, X., J. M. Casacuberta, M. D. Gutierrez-Lopez, M. O. de Landazuri and P. Puigdomenech (2000). "Phosphodiesterases 4D and 7A splice variants in the response of HUVEC cells to TNF-alpha(1)." Biochem Biophys Res Commun **274**(2): 415-421.

Mitchell, J. A., F. Ali, L. Bailey, L. Moreno and L. S. Harrington (2008). "Role of nitric oxide and prostacyclin as vasoactive hormones released by the endothelium." Exp Physiol **93**(1): 141-147.

Miyawaki, A., J. Llopis, R. Heim, J. M. McCaffery, J. A. Adams, M. Ikura and R. Y. Tsien (1997). "Fluorescent indicators for Ca2+based on green fluorescent proteins and calmodulin." Nature **388**(6645): 882-887.

Monaghan-Benson, E. and K. Burridge (2009). "The regulation of vascular endothelial growth factor-induced microvascular permeability requires Rac and reactive oxygen species." Journal of Biological Chemistry **284**(38): 25602-25611.

Montell, C., L. Birnbaumer and V. Flockerzi (2002). "The TRP channels, a remarkably functional family." Cell **108**(5): 595-598.

Monti, M., S. Donnini, A. Giachetti, D. Mochly-Rosen and M. Ziche (2010). "δPKC inhibition or e{open}PKC activation repairs endothelial vascular dysfunction by regulating eNOS post-translational modification." Journal of Molecular and Cellular Cardiology **48**(4): 746-756.

Monti, M., S. Donnini, L. Morbidelli, A. Giachetti, D. Mochly-Rosen, P. Mignatti and M. Ziche (2013). "PKCε activation promotes FGF-2 exocytosis and induces endothelial cell proliferation and sprouting." Journal of Molecular and Cellular Cardiology **63**: 107-117.

Morel, E., A. Marcantoni, M. Gastineau, R. Birkedal, F. Rochais, A. Garnier, A. M. Lompré, G. Vandecasteele and F. Lezoualc'h (2005). "cAMP-binding protein Epac induces cardiomyocyte hypertrophy." Circulation Research **97**(12): 1296-1304.

Moreno, A. P., A. C. C. De Carvalho, G. Christ, A. Melman and D. C. Spray (1993). "Gap junctions between human corpus cavernosum smooth muscle cells: Gating properties and unitary conductance." American Journal of Physiology - Cell Physiology **264**(1 33-1): C80-C92.

Moreno, A. P., J. C. Sáez, G. I. Fishman and D. C. Spray (1994). "Human connexin43 gap junction channels: Regulation of unitary conductances by phosphorylation." Circulation Research **74**(6): 1050-1057.

Morita, K., M. Furuse, K. Fujimoto and S. Tsukita (1999). "Claudin multigene family encoding four-transmembrane domain protein components of tight junction strands." Proc Natl Acad Sci U S A **96**(2): 511-516.

Morita, K., H. Sasaki, M. Furuse and S. Tsukita (1999). "Endothelial claudin: claudin-5/TMVCF constitutes tight junction strands in endothelial cells." J Cell Biol **147**(1): 185-194.

Morley, G. E., S. M. Taffet and M. Delmar (1996). "Intramolecular interactions mediate pH regulation of connexin43 channels." Biophysical Journal **70**(3): 1294-1302.

Moss, A. (2013). "The angiopoietin:Tie 2 interaction: a potential target for future therapies in human vascular disease." Cytokine Growth Factor Rev **24**(6): 579-592.

Mountian, I., V. G. Manolopoulos, H. De Smedt, J. B. Parys, L. Missiaen and F. Wuytack (1999). "Expression patterns of sarco/endoplasmic reticulum Ca(2+)-ATPase and inositol 1,4,5-trisphosphate receptor isoforms in vascular endothelial cells." Cell Calcium **25**(5): 371-380.

Moy, A. B., J. Van Engelenhoven, J. Bodmer, J. Kamath, C. Keese, I. Giaever, S. Shasby and D. M. Shasby (1996). "Histamine and thrombin modulate endothelial focal adhesion through centripetal and centrifugal forces." Journal of Clinical Investigation **97**(4): 1020-1027.

Moy, A. B., M. Winter, A. Kamath, K. Blackwell, G. Reyes, I. Giaever, C. Keese and D. M. Shasby (2000). "Histamine alters endothelial barrier function at cell-cell and cell-matrix sites." Am J Physiol Lung Cell Mol Physiol **278**(5): L888-898.

Muñoz-Esquerre, M., M. Diez-Ferrer, C. Montón, X. Pomares, M. López-Sánchez, D. Huertas, F. Manresa, J. Dorca, and S. Santos (2015). "Roflumilast added to triple therapy in patients with severe COPD: A real life study." Pulmonary pharmacology & therapeutics **30**: 16-21.

Murray, A. J. (2008). "Pharmacological PKA inhibition: all may not be what it seems." Sci Signal **1**(22): re4.

Musil, L. S., E. C. Beyer and D. A. Goodenough (1990). "Expression of the gap junction protein connexin43 in embryonic chick lens: Molecular cloning, ultrastructural localization, and post-translational phosphorylation." The Journal of Membrane Biology **116**(2): 163-175.

Musil, L. S., B. A. Cunningham, G. M. Edelman and D. A. Goodenough (1990). "Differential phosphorylation of the gap junction protein connexin43 in junctional communication-competent and -deficient cell lines." Journal of Cell Biology **111**(5): 2077-2088.

Musil, L. S. and D. A. Goodenough (1991). "Biochemical analysis of connexin43 intracellular transport, phosphorylation, and assembly into gap junctional plaques." Journal of Cell Biology **115**(5): 1357-1374.

Musil, L. S. and D. A. Goodenough (1993). "Multisubunit assembly of an integral plasma membrane channel protein, gap junction connexin43, occurs after exit from the ER." Cell **74**(6): 1065-1077.

Nachman, R., R. Levine and E. A. Jaffe (1977). "Synthesis of factor VIII antigen by cultured guinea pig megakaryocytes." Journal of Clinical Investigation **60**(4): 914-921.

Nagafuchi, A. and M. Takeichi (1988). "Cell binding function of E-cadherin is regulated by the cytoplasmic domain." The EMBO journal **7**(12): 3679-3684.

Navarro, P., L. Caveda, F. Breviario, I. Mândoteanu, M. G. Lampugnani and E. Dejana (1995). "Catenin-dependent and -independent functions of vascular endothelial cadherin." Journal of Biological Chemistry **270**(52): 30965-30972.

Navarro, P., L. Ruco and E. Dejana (1998). "Differential localization of VE- and N-cadherins in human endothelial cells: VE-cadherin competes with N-cadherin for junctional localization." Journal of Cell Biology **140**(6): 1475-1484.

Nawroth, R., G. Poell, A. Ranft, S. Kloep, U. Samulowitz, G. Fachinger, M. Golding, D. T. Shima, U. Deutsch and D. Vestweber (2002). "VE-PTP and VE-cadherin ectodomains interact to facilitate regulation of phosphorylation and cell contacts." EMBO Journal **21**(18): 4885-4895.

Nelson, M. T., J. B. Patlak, J. F. Worley and N. B. Standen (1990). "Calcium channels, potassium channels, and voltage dependence of arterial smooth muscle tone." Am J Physiol **259**(1 Pt 1): C3-18.

Nelson, M. T. and J. M. Quayle (1995). "Physiological roles and properties of potassium channels in arterial smooth muscle." Am J Physiol **268**(4 Pt 1): C799-822.

Netherton, S. J. and D. H. Maurice (2005). "Vascular endothelial cell cyclic nucleotide phosphodiesterases and regulated cell migration: implications in angiogenesis." Mol Pharmacol **67**(1): 263-272.

Newton, P. M. and R. O. Messing (2010). "The substrates and binding partners of protein kinase Cε." Biochemical Journal **427**(2): 189-196.

Nicholson, B., R. Dermietzel, D. Teplow, O. Traub, K. Willecke and J. P. Revel (1987). "Two homologous protein components of hepatic gap junctions." Nature **329**(6141): 732-734.

Nieset, J. E., A. R. Redfield, F. Jin, K. A. Knudsen, K. R. Johnson and M. J. Wheelock (1997). "Characterization of the interactions of alpha-catenin with alpha-actinin and beta-catenin/plakoglobin." J Cell Sci **110 (Pt 8)**: 1013-1022.

Nigg, E. A., G. Schafer, H. Hilz and H. M. Eppenberger (1985). "Cyclic-AMP-dependent protein kinase type II is associated with the Golgi complex and with centrosomes." Cell **41**(3): 1039-1051.

Nilsson, M., H. Fagman and L. E. Ericson (1996). "Ca2+-dependent and Ca2+-independent regulation of the thyroid epithelial junction complex by protein kinases." Exp Cell Res **225**(1): 1-11.

Nishi, M., N. M. Kumar and N. B. Gilula (1991). "Developmental regulation of gap junction gene expression during mouse embryonic development." Developmental Biology **146**(1): 117-130.

Nishikawa, S. I., M. Hirashima, S. Nishikawa and M. Ogawa (2001). "Cell biology of vascular endothelial cells." Ann N Y Acad Sci **947**: 35-40; discussion 41.

Nitta, T., M. Hata, S. Gotoh, Y. Seo, H. Sasaki, N. Hashimoto, M. Furuse and S. Tsukita (2003). "Size-selective loosening of the blood-brain barrier in claudin-5-deficient mice." J Cell Biol **161**(3): 653-660.

Noda, K., J. Zhang, S. Fukuhara, S. Kunimoto, M. Yoshimura and N. Mochizuki (2010). "Vascular endothelial-cadherin stabilizes at cell-cell junctions by anchoring to circumferential actin bundles through α- and β-catenins in cyclic AMP-Epac-Rap1 signal-activated endothelial cells." Molecular Biology of the Cell **21**(4): 584-596.

Noren, N. K., B. P. Liu, K. Burridge and B. Kreft (2000). "p120 catenin regulates the actin cytoskeleton via Rho family GTPases." J Cell Biol **150**(3): 567-580.

O'Connor, K. L. and A. M. Mercurio (2001). "Protein Kinase A Regulates Rac and Is Required for the Growth Factor-stimulated Migration of Carcinoma Cells." Journal of Biological Chemistry **276**(51): 47895-47900.

O-Uchi, J., K. Komukai, Y. Kusakari, T. Obata, K. Hongo, H. Sasaki and S. Kurihara (2005). "α1-adrenoceptor stimulation potentiates L-type Ca 2+ current through Ca2+/calmodulin-dependent PK II (CaMKII) activation in rat ventricular myocytes." Proceedings of the National Academy of Sciences of the United States of America **102**(26): 9400-9405.

Obar, R. A., J. Dingus, H. Bayley and R. B. Vallee (1989). "The RII subunit of camp-dependent protein kinase binds to a common amino-terminal domain in microtubule-associated proteins 2A, 2B, and 2C." Neuron **3**(5): 639-645.

Oestreich, E. A., S. Malik, S. A. Goonasekera, B. C. Blaxall, G. G. Kelley, R. T. Dirksen and A. V. Smrcka (2009). "Epac and phospholipase Cε regulate Ca 2+ release in the heart by activation of protein kinase Cε and calcium-calmodulin kinase II." Journal of Biological Chemistry **284**(3): 1514-1522.

Ohashi, M., K. Satoh and T. Itoh (1999). "Acetylcholine-induced membrane potential changes in endothelial cells of rabbit aortic valve." Br J Pharmacol **126**(1): 19-26.

Ohkubo, T. and M. Ozawa (1999). "p120(ctn) binds to the membrane-proximal region of the E-cadherin cytoplasmic domain and is involved in modulation of adhesion activity." J Biol Chem **274**(30): 21409-21415.

Ohta, Y., N. Suzuki, S. Nakamura, J. H. Hartwig and T. P. Stossel (1999). "The small GTPase RalA targets filamin to induce filopodia." Proc Natl Acad Sci U S A **96**(5): 2122-2128.

Okada, S., M. Matsuda, M. Anafi, T. Pawson, and J. E. Pessin (1998). "Insulin regulates the dynamic balance between Ras and Rap1 signaling by coordinating the assembly states of the Grb2–SOS and CrkII–C3G complexes." The EMBO Journal **17**(9): 2554-2565.

Otsuka, F., A. V. Finn, S. K. Yazdani, M. Nakano, F. D. Kolodgie, and R. Virmani (2012). "The importance of the endothelium in atherothrombosis and coronary stenting." Nature Reviews Cardiology **9**(8): 439-453.

Ozawa, M., J. Engel and R. Kemler (1990). "Single amino acid substitutions in one Ca2+ binding site of uvomorulin abolish the adhesive function." Cell **63**(5): 1033-1038.

Ozawa, M., H. Hoschützky, K. Herrenknecht and R. Kemler (1990). "A possible new adhesive site in the cell-adhesion molecule uvomorulin." Mechanisms of Development **33**(1): 49-56.

Ozawa, M., M. Ringwald and R. Kemler (1990). "Uvomorulin-catenin complex formation is regulated by a specific domain in the cytoplasmic region of the cell adhesion molecule." Proceedings of the National Academy of Sciences of the United States of America **87**(11): 4246-4250.

Paemeleire, K., P. E. M. Martin, S. L. Coleman, K. E. Fogarty, W. A. Carrington, L. Leybaert, R. A. Tuft, W. H. Evans and M. J. Sanderson (2000). "Intercellular calcium waves in HeLa cells expressing GFP-labeled connexin 43, 32, or 26." Molecular Biology of the Cell **11**(5): 1815-1827.

Palmeri, D., A. van Zante, C. C. Huang, S. Hemmerich and S. D. Rosen (2000). "Vascular endothelial junction-associated molecule, a novel member of the immunoglobulin superfamily, is localized to intercellular boundaries of endothelial cells." J Biol Chem **275**(25): 19139-19145.

Parekh, A. B. and R. Penner (1995). "Depletion-activated calcium current is inhibited by protein kinase in RBL-2H3 cells." Proc Natl Acad Sci U S A **92**(17): 7907-7911.

Partridge, C. A., J. J. Jeffrey and A. B. Malik (1993). "A 96-kDa gelatinase induced by TNF-alpha contributes to increased microvascular endothelial permeability." Am J Physiol **265**(5 Pt 1): L438-447.

Pasyk, E., M. Inazu and E. E. Daniel (1995). "CPA enhances Ca2+ entry in cultured bovine pulmonary arterial endothelial cells in an IP3-independent manner." Am J Physiol **268**(1 Pt 2): H138-146.

Patton, W. F., M. U. Yoon, J. S. Alexander, N. Chung-Welch, H. B. Hechtman and D. Shepro (1990). "Expression of simple epithelial cytokeratins in bovine pulmonary microvascular endothelial cells." J Cell Physiol **143**(1): 140-149.

Paul, D. L., L. Ebihara, L. J. Takemoto, K. I. Swenson and D. A. Goodenough (1991). "Connexin46, a novel lens gap junction protein, induces voltage-gated currents in nonjunctional plasma membrane of Xenopus oocytes." Journal of Cell Biology **115**(4): 1077-1089.

Paulson, A. F., P. D. Lampe, R. A. Meyer, E. TenBroek, M. M. Atkinson, T. F. Walseth and R. G. Johnson (2000). "Cyclic AMP and LDL trigger a rapid enchancement in gap junction assembly through a stimulation of connexin trafficking." Journal of Cell Science **113**(17): 3037-3049.

Paulsson, M. (1992). "Basement membrane proteins: structure, assembly, and cellular interactions." Crit Rev Biochem Mol Biol **27**(1-2): 93-127.

Peichev, M., A. J. Naiyer, D. Pereira, Z. Zhu, W. J. Lane, M. Williams, M. C. Oz, D. J. Hicklin, L. Witte, M. A. Moore and S. Rafii (2000). "Expression of VEGFR-2 and AC133 by circulating human CD34(+) cells identifies a population of functional endothelial precursors." Blood **95**(3): 952-958.

Penzes, P., K. M. Woolfrey and D. P. Srivastava (2011). "Epac2-mediated dendritic spine remodeling: Implications for disease." Molecular and Cellular Neuroscience **46**(2): 368-380.

Pereira, L., M. Métrich, M. Fernández-Velasco, A. Lucas, J. Leroy, R. Perrier, E. Morel, R. Fischmeister, S. Richard, J.-P. Bénitah, F. Lezoualc'h and A. M. Gómez (2007). "The cAMP binding protein Epac modulates Ca2+ sparks by a Ca2+/calmodulin kinase signalling pathway in rat cardiac myocytes." The Journal of Physiology **583**(2): 685-694.

Perkins, G., D. Goodenough and G. Sosinsky (1997). "Three-dimensional structure of the gap junction connexon." Biophysical Journal **72**(2 I): 533-544.

Pizurki, L., Z. Zhou, K. Glynos, C. Roussos and A. Papapetropoulos (2003). "Angiopoietin-1 inhibits endothelial permeability, neutrophil adherence and IL-8 production." Br J Pharmacol **139**(2): 329-336.

Plank, M. J., D. J. Wall and T. David (2006). "Atherosclerosis and calcium signalling in endothelial cells." Prog Biophys Mol Biol **91**(3): 287-313.

Polakis, P., B. Rubinfeld and F. McCormick (1992). "Phosphorylation of rap1GAP in vivo and by cAMP-dependent kinase and the cell cycle p34cdc2 kinase in vitro." Journal of Biological Chemistry **267**(15): 10780-10785.

Polakis, P. G., B. Rubinfeld, T. Evans and F. McCormick (1991). "Purification of a plasma membrane-associated GTPase-activating protein specific for rap1/Krev-1 from HL60 cells." Proceedings of the National Academy of Sciences of the United States of America **88**(1): 239-243.

Ponsioen, B., M. Gloerich, L. Ritsma, H. Rehmann, J. L. Bos and K. Jalink (2009). "Direct spatial control of Epac1 by cyclic AMP." Molecular and Cellular Biology **29**(10): 2521-2531.

Potier, M., J. C. Gonzalez, R. K. Motiani, I. F. Abdullaev, J. M. Bisaillon, H. A. Singer and M. Trebak (2009). "Evidence for STIM1- and Orai1-dependent store-operated calcium influx through ICRAC in vascular smooth muscle cells: role in proliferation and migration." Faseb j **23**(8): 2425-2437.

Potter, M. D., S. Barbero and D. A. Cheresh (2005). "Tyrosine phosphorylation of VE-cadherin prevents binding of p120- and β-catenin and maintains the cellular mesenchymal state." Journal of Biological Chemistry **280**(36): 31906-31912.

Prakriya, M. and R. S. Lewis (2006). "Regulation of CRAC channel activity by recruitment of silent channels to a high open-probability gating mode." J Gen Physiol **128**(3): 373-386.

Prasain, N., M. Alexeyev, R. Balczon and T. Stevens (2009). "Soluble adenylyl cyclase-dependent microtubule disassembly reveals a novel mechanism of endothelial cell retraction." Am J Physiol Lung Cell Mol Physiol **297**(1): L73-83.

Price, L. S., A. Hajdo-Milasinovic, J. Zhao, F. J. T. Zwartkruis, J. G. Collard and J. L. Bos (2004). "Rap1 regulates E-cadherin-mediated cell-cell adhesion." Journal of Biological Chemistry **279**(34): 35127-35132.

Pries, A. R., T. W. Secomb and P. Gaehtgens (2000). "The endothelial surface layer." Pflugers Arch **440**(5): 653-666.

Purves, G. I., T. Kamishima, L. M. Davies, J. M. Quayle and C. Dart (2009). "Exchange protein activated by cAMP (Epac) mediates cAMP-dependent but protein kinase A-insensitive modulation of vascular ATP-sensitive potassium channels." Journal of Physiology **587**(14): 3639-3650.

Pusztaszeri, M. P., W. Seelentag and F. T. Bosman (2006). "Immunohistochemical expression of endothelial markers CD31, CD34, von Willebrand factor, and Fli-1 in normal human tissues." Journal of Histochemistry and Cytochemistry **54**(4): 385-395.

Putney, J. W., Jr. (2007). "New molecular players in capacitative Ca2+ entry." J Cell Sci **120**(Pt 12): 1959-1965.

Qiao, J., O. Holian, B. S. Lee, F. Huang, J. Zhang and H. Lum (2008). "Phosphorylation of GTP dissociation inhibitor by PKA negatively regulates RhoA." Am J Physiol Cell Physiol **295**(5): C1161-1168.

Qiao, J., F. Huang and H. Lum (2003). "PKA inhibits RhoA activation: a protection mechanism against endothelial barrier dysfunction." Am J Physiol Lung Cell Mol Physiol **284**(6): L972-980.

Qiao, R. L., H. S. Wang, W. Yan, L. E. Odekon, P. J. Del Vecchio, T. J. Smith and A. B. Malik (1995). "Extracellular matrix hyaluronan is a determinant of the endothelial barrier." Am J Physiol **269**(1 Pt 1): C103-109.

Rahman, S., G. Carlile and W. H. Evans (1993). "Assembly of hepatic gap junctions. Topography and distribution of connexin 32 in intracellular and plasma membranes determined using sequence-specific antibodies." Journal of Biological Chemistry **268**(2): 1260-1265.

Rajput, C., V. Kini, M. Smith, P. Yazbeck, A. Chavez, T. Schmidt, W. Zhang, N. Knezevic, Y. Komarova and D. Mehta (2013). "Neural Wiskott-Aldrich syndrome protein (N-WASP)-mediated p120-catenin interaction with Arp2-actin complex stabilizes endothelial adherens junctions." Journal of Biological Chemistry **288**(6): 4241-4250.

Rampon, C., M. H. Prandini, S. Bouillot, H. Pointu, E. Tillet, R. Frank, M. Vernet and P. Huber (2005). "Protocadherin 12 (VE-cadherin 2) is expressed in endothelial, trophoblast, and mesangial cells." Exp Cell Res **302**(1): 48-60.

Rask-Madsen, C. and G. L. King (2008). "Differential regulation of VEGF signaling by PKC-α and PKC-ε in endothelial cells." Arteriosclerosis, Thrombosis, and Vascular Biology **28**(5): 919-924.

Ratcliffe, M. J., C. Smales and J. M. Staddon (1999). "Dephosphorylation of the catenins p120 and p100 in endothelial cells in response to inflammatory stimuli." Biochemical Journal **338**(2): 471-478.

Ravikumar, B., S. Sarkar, J. E. Davies, M. Futter, M. Garcia-Arencibia, Z. W. Green-Thompson, M. Jimenez-Sanchez, V. I. Korolchuk, M. Lichtenberg, S. Luo, D. C. O. Massey, F. M. Menzies, K. Moreau, U. Narayanan, M. Renna, F. H. Siddiqi, B. R. Underwood, A. R. Winslow And and D. C. Rubinsztein (2010). "Regulation of mammalian autophagy in physiology and pathophysiology." Physiological Reviews **90**(4): 1383-1435.

Regan-Klapisz, E., V. Krouwer, M. Langelaar-Makkinje, L. Nallan, M. Gelb, H. Gerritsen, A. J. Verkleij and J. A. Post (2009). "Golgi-associated cPLA2α regulates endothelial cell-cell junction integrity by controlling the trafficking of transmembrane junction proteins." Molecular Biology of the Cell **20**(19): 4225-4234.

Rehmann, H. (2013). "Epac-inhibitors: Facts and artefacts." Scientific Reports **3**.

Rehmann, H., J. Das, P. Knipscheer, A. Wittinghofer and J. L. Bos (2006). "Structure of the cyclic-AMP-responsive exchange factor Epac2 in its auto-inhibited state." Nature **439**(7076): 625-628.

Rehmann, H., F. Schwede, S. O. Doøskeland, A. Wittinghofer and J. L. Bos (2003). "Ligand-mediated activation of the cAMP-responsive guanine nucleotide exchange factor Epac." Journal of Biological Chemistry **278**(40): 38548-38556.

Rensen, S. S. M., P. A. F. M. Doevendans and G. J. J. M. Van Eys (2007). "Regulation and characteristics of vascular smooth muscle cell phenotypic diversity." Netherlands Heart Journal **15**(3): 100-108.

Revel, J. P. and M. J. Karnovsky (1967). "Hexagonal array of subunits in intercellular junctions of the mouse heart and liver." J Cell Biol **33**(3): C7-c12.

Reynolds, A. B. and A. Roczniak-Ferguson (2004). "Emerging roles for p120-catenin in cell adhesion and cancer." Oncogene **23**(48): 7947-7956.

Rhodin, J. A. G. (1974). Histology; a text and atlas [by] Johannes A. G. Rhodin. New York, Oxford University Press.

Ridley, A. J. and A. Hall (1992). "The small GTP-binding protein rho regulates the assembly of focal adhesions and actin stress fibers in response to growth factors." Cell **70**(3): 389-399.

Ringwald, M., R. Schuh, D. Vestweber, H. Eistetter, F. Lottspeich, J. Engel, R. Dölz, F. Jähnig, J. Epplen and S. Mayer (1987). "The structure of cell adhesion molecule uvomorulin. Insights into the molecular mechanism of Ca2+-dependent cell adhesion." The EMBO journal **6**(12): 3647-3653.

Risau, W. (1997). "Mechanisms of angiogenesis." Nature **386**(6626): 671-674.

Risau, W., S. Esser and B. Engelhardt (1998). "Differentiation of blood-brain barrier endothelial cells." Pathol Biol (Paris) **46**(3): 171-175.

Risek, B., F. G. Klier and N. B. Gilula (1994). "Developmental regulation and structural organization of connexins in epidermal gap junctions." Dev Biol **164**(1): 183-196.

Roberts, O. L. and C. Dart (2014). "CAMP signalling in the vasculature: The role of Epac (exchange protein directly activated by cAMP)." Biochemical Society Transactions **42**(1): 89-97.

Roberts, O. L., T. Kamishima, R. Barrett-Jolley, J. M. Quayle and C. Dart (2013). "Exchange protein activated by cAMP (Epac) induces vascular relaxation by activating Ca2+-sensitive K+ channels in rat mesenteric artery." Journal of Physiology **591**(20): 5107-5123.

Roos, J., P. J. DiGregorio, A. V. Yeromin, K. Ohlsen, M. Lioudyno, S. Zhang, O. Safrina, J. A. Kozak, S. L. Wagner, M. D. Cahalan, G. Velicelebi and K. A. Stauderman (2005). "STIM1, an essential and conserved component of store-operated Ca2+ channel function." J Cell Biol **169**(3): 435-445.

Rose, B. and W. R. Loewenstein (1976). "Permeability of a cell junction and the local cytoplasmic free ionized calcium concentration: a study with aequorin." Journal of Membrane Biology **28**(1): 87-119.

Rossé, C., C. Lodillinsky, L. Fuhrmann, M. Nourieh, P. Monteiro, M. Irondelle, E. Lagoutte, S. Vacher, F. Waharte, P. Paul-Gilloteaux, M. Romao, L. Sengmanivong, M. Linch, J. Van Lint, G. Raposo, A. Vincent-Salomon, I. Bièche, P. J. Parker and P. Chavrier (2014). "Control of MT1-MMP transport by atypical PKC during breast-cancer progression." Proceedings of the National Academy of Sciences of the United States of America **111**(18): E1872-E1879.

Rubin, C. S., J. Erlichman and O. M. Rosen (1972). "Cyclic adenosine 3',5'-monophosphate-dependent protein kinase of human erythrocyte membranes." Journal of Biological Chemistry **247**(19): 6135-6139.

Rubin, L. L. (1992). "Endothelial cells: adhesion and tight junctions." Curr Opin Cell Biol **4**(5): 830-833.

Ruggeri, Z. M. and J. Ware (1993). "von Willebrand factor." FASEB Journal **7**(2): 308-316.

Ruisanchez, É., P. Dancs, M. Kerék, T. Németh, B. Faragó, A. Balogh, R. Patil, B. L. Jennings, K. Liliom, K. U. Malik, A. V. Smrcka, G. Tigyi and Z. Benyó (2014). "Lysophosphatidic acid induces vasodilation mediated by LPA1 receptors, phospholipase C, and endothelial nitric oxide synthase." FASEB Journal **28**(2): 880-890.

Ruoslahti, E. (1991). "Integrins." J Clin Invest **87**(1): 1-5.

Rütz, M. L. and D. F. Hülser (2001). "Supramolecular dynamics of gap junctions." European Journal of Cell Biology **80**(1): 20-30.

Ryan, U. S. and J. W. Ryan (1984). "The ultrastructural basis of endothelial cell surface functions." Biorheology **21**(1-2): 155-170.

Sabatini, P. J. B., M. Zhang, R. Silverman-Gavrila, M. P. Bendeck and B. L. Langille (2008). "Homotypic and endothelial cell adhesions via N-cadherin determine polarity and regulate migration of vascular smooth muscle cells." Circulation Research **103**(4): 405-412.

Sadler, J. E. (1998). "Biochemistry and genetics of von Willebrand factor." Annual Review of Biochemistry **67**: 395-424.

Sáez, J. C., V. M. Berthoud, M. C. Brañes, A. D. Martínez and E. C. Beyer (2003). "Plasma membrane channels formed by connexins: Their regulation and functions." Physiological Reviews **83**(4): 1359-1400.

Saez, J. C., J. A. Connor, D. C. Spray and M. V. Bennett (1989). "Hepatocyte gap junctions are permeable to the second messenger, inositol 1,4,5-trisphosphate, and to calcium ions." Proc Natl Acad Sci U S A **86**(8): 2708-2712.

Saez, J. C., W. A. Gregory, T. Watanabe, R. Dermietzel, E. L. Hertzberg, L. Reid, M. V. L. Bennett and D. C. Spray (1989). "cAMP delays disappearance of gap junctions between pairs of rat hepatocytes in primary culture." American Journal of Physiology - Cell Physiology **257**(1).

Saez, J. C., D. C. Spray, A. C. Nairn, E. Hertzberg, P. Greengard and M. V. Bennett (1986). "cAMP increases junctional conductance and stimulates phosphorylation of the 27-kDa principal gap junction polypeptide." Proceedings of the National Academy of Sciences of the United States of America **83**(8): 2473-2477.

Saitou, M., M. Furuse, H. Sasaki, J. D. Schulzke, M. Fromm, H. Takano, T. Noda and S. Tsukita (2000). "Complex phenotype of mice lacking occludin, a component of tight junction strands." Mol Biol Cell **11**(12): 4131-4142.

Salomon, D., O. Ayalon, R. Patel-King, R. O. Hynes and B. Geiger (1992). "Extrajunctional distribution of N-cadherin in cultured human endothelial cells." Journal of Cell Science **102**(1): 7-17.

Salpeter, M. M. (1999). "The Constant Junction." Science **286**(5439): 424-425.

Sambrook, J. F. (1990). "The involvement of calcium in transport of secretory proteins from the endoplasmic reticulum." Cell **61**(2): 197-199.

Sandow, S. L., C. B. Neylon, M. X. Chen and C. J. Garland (2006). "Spatial separation of endothelial small- and intermediate-conductance calcium-activated potassium channels (K(Ca)) and connexins: possible relationship to vasodilator function?" J Anat **209**(5): 689-698.

Sandow, S. L., M. Tare, H. A. Coleman, C. E. Hill and H. C. Parkington (2002). "Involvement of myoendothelial gap junctions in the actions of endothelium-derived hyperpolarizing factor." Circ Res **90**(10): 1108-1113.

Sanz, M.J., J. Cortijo, M. A. Taha, M. Cerdá-Nicolás, E. Schatton, B. Burgbacher, J. Klar H. Tenor, C. Schudt, A. C. Issekutz, A. Hatzelmann and E. J. Morcillo (2007) "Roflumilast inhibits leukocyte-endothelial cell interactions, expression of adhesion molecules and microvascular permeability." British journal of pharmacology **152**(4): 481-492.

Satoh, H., Y. Zhong, H. Isomura, M. Saitoh, K. Enomoto, N. Sawada and M. Mori (1996). "Localization of 7H6 tight junction-associated antigen along the cell border of vascular endothelial cells correlates with paracellular barrier function against ions, large molecules, and cancer cells." Exp Cell Res **222**(2): 269-274.

Sayner, S. L., M. Alexeyev, C. W. Dessauer and T. Stevens (2006). "Soluble Adenylyl Cyclase Reveals the Significance of cAMP Compartmentation on Pulmonary Microvascular Endothelial Cell Barrier." Circulation Research **98**(5): 675-681.

Schick, M. A., C. Wunder, J. Wollborn, N. Roewer, J. Waschke, C. T. Germer and N. Schlegel (2012). "Phosphodiesterase-4 inhibition as a therapeutic approach to treat capillary leakage in systemic inflammation." J Physiol **590**(Pt 11): 2693-2708.

Schilling, W. P., O. A. Cabello and L. Rajan (1992). "Depletion of the inositol 1,4,5-trisphosphate-sensitive intracellular Ca2+ store in vascular endothelial cells activates the agonist-sensitive Ca(2+)-influx pathway." Biochem J **284 (Pt 2)**: 521-530.

Schlaepfer, D. D. and S. K. Mitra (2004). "Multiple connections link FAK to cell motility and invasion." Curr Opin Genet Dev **14**(1): 92-101.

Schlegel, N., S. Burger, N. Golenhofen, U. Walter, D. Drenckhahn and J. Waschke (2008). "The role of VASP in regulation of cAMP- and Rac 1-mediated endothelial barrier stabilization." Am J Physiol Cell Physiol **294**(1): C178-188.

Schmelz, M. and W. W. Franke (1993). "Complexus adhaerentes, a new group of desmoplakin-containing junctions in endothelial cells: the syndesmos connecting retothelial cells of lymph nodes." Eur J Cell Biol **61**(2): 274-289.

Schmelz, M., R. Moll, C. Kuhn and W. W. Franke (1994). "Complexus adhaerentes, a new group of desmoplakin-containing junctions in endothelial cells: II. Different types of lymphatic vessels." Differentiation **57**(2): 97-117.

Schmidt, M., S. Evellin, P. A. O. Weernink, F. vom Dorp, H. Rehmann, J. W. Lomasney and K. H. Jakobs (2001). "A new phospholipase-C-calcium signalling pathway mediated by cyclic AMP and a Rap GTPase." Nature Cell Biology **3**(11): 1020-1024.

Schmidt, R., O. Baumann and B. Walz (2008). "cAMP potentiates InsP3-induced Ca2+ release from the endoplasmic reticulum in blowfly salivary glands." BMC Physiol **8**: 10.

Schmitt, J. M. and P. J. Stork (2001). "Cyclic AMP-mediated inhibition of cell growth requires the small G protein Rap1." Mol Cell Biol **21**(11): 3671-3683.

Schneeberger, E. E. (1982). "Structure of intercellular junctions in different segments of the intrapulmonary vasculature." Ann N Y Acad Sci **384**: 54-63.

Schubert, A. L., W. Schubert, D. C. Spray and M. P. Lisanti (2002). "Connexin family members target to lipid raft domains and interact with caveolin-1." Biochemistry **41**(18): 5754-5764.

Schwartz, A. L. and A. Ciechanover (1999). "The ubiquitin-proteasome pathway and pathogenesis of human diseases." Annu Rev Med **50**: 57-74.

Secomb, T. W., R. Hsu and A. R. Pries (2001). "Effect of the endothelial surface layer on transmission of fluid shear stress to endothelial cells." Biorheology **38**(2-3): 143-150.

Sefton, M., M. H. Johnson and L. Clayton (1992). "Synthesis and phosphorylation of uvomorulin during mouse early development." Development **115**(1): 313-318.

Segretain, D. and M. M. Falk (2004). "Regulation of connexin biosynthesis, assembly, gap junction formation, and removal." Biochim Biophys Acta **1662**(1-2): 3-21.

Serban, D. N., B. Nilius and P. M. Vanhoutte (2010). "The endothelial saga: the past, the present, the future." Pflugers Arch **459**(6): 787-792.

Shah, P. K (2003). "Inflammation, Neointimal Hyperplasia, and Restenosis As the Leukocytes Roll, the Arteries Thicken." Circulation **107**(17): 2175-2177.

Shalaby, F., J. Rossant, T. P. Yamaguchi, M. Gertsenstein, X. F. Wu, M. L. Breitman and A. C. Schuh (1995). "Failure of blood-island formation and vasculogenesis in Flk-1-deficient mice." Nature **376**(6535): 62-66.

Shasby, D. M., D. R. Ries, S. S. Shasby and M. C. Winter (2002). "Histamine stimulates phosphorylation of adherens junction proteins and alters their link to vimentin." Am J Physiol Lung Cell Mol Physiol **282**(6): L1330-1338.

Shaw, R. M., A. J. Fay, M. A. Puthenveedu, M. von Zastrow, Y. N. Jan and L. Y. Jan (2007). "Microtubule plus-end-tracking proteins target gap junctions directly from the cell interior to adherens junctions." Cell **128**(3): 547-560.

Shay-Salit, A., M. Shushy, E. Wolfovitz, H. Yahav, F. Breviario, E. Dejana and N. Resnick (2002). "VEGF receptor 2 and the adherens junction as a mechanical transducer in vascular endothelial cells." Proc Natl Acad Sci U S A **99**(14): 9462-9467.

Sheibani, N., P. J. Newman and W. A. Frazier (1997). "Thrombospondin-1, a natural inhibitor of angiogenesis, regulates platelet-endothelial cell adhesion molecule-1 expression and endothelial cell morphogenesis." Molecular Biology of the Cell **8**(7): 1329-1341.

Shen, B., K. T. Cheng, Y. K. Leung, Y. C. Kwok, H. Y. Kwan, C. O. Wong, Z. Y. Chen, Y. Huang and X. Yao (2008). "Epinephrine-induced Ca2+ influx in vascular endothelial cells is mediated by CNGA2 channels." J Mol Cell Cardiol **45**(3): 437-445.

Shen, T. L., A. Y. Park, A. Alcaraz, X. Peng, I. Jang, P. Koni, R. A. Flavell, H. Gu and J. L. Guan (2005). "Conditional knockout of focal adhesion kinase in endothelial cells reveals its role in angiogenesis and vascular development in late embryogenesis." J Cell Biol **169**(6): 941-952.

Shigekawa, M. and T. Iwamoto (2001). "Cardiac Na+-Ca2+ exchange molecular and pharmacological aspects." Circulation Research **88**(9): 864-876.

Siliciano, J. D. and D. A. Goodenough (1988). "Localization of the tight junction protein, ZO-1, is modulated by extracellular calcium and cell-cell contact in Madin-Darby canine kidney epithelial cells." J Cell Biol **107**(6 Pt 1): 2389-2399.

Simon, A. M., D. A. Goodenough and D. L. Paul (1998). "Mice lacking connexin40 have cardiac conduction abnormalities characteristic of atrioventricular block and bundle branch block." Curr Biol **8**(5): 295-298.

Simon, A. M. and A. R. McWhorter (2002). "Vascular abnormalities in mice lacking the endothelial gap junction proteins connexin37 and connexin40." Dev Biol **251**(2): 206-220.

Simpson, I., B. Rose and W. R. Loewenstein (1977). "Size limit of molecules permeating the junctional membrane channels." Science **195**(4275): 294-296.

Skalli, O., P. Ropraz, A. Trzeciak, G. Benzonana, D. Gillessen and G. Gabbiani (1986). "A monoclonal antibody against α-smooth muscle actin: A new probe for smooth muscle differentiation." Journal of Cell Biology **103**(6 II): 2787-2796.

Soboloff, J., B. S. Rothberg, M. Madesh and D. L. Gill (2012). "STIM proteins: dynamic calcium signal transducers." Nat Rev Mol Cell Biol **13**(9): 549-565.

Somekawa, S., S. Fukuhara, Y. Nakaoka, H. Fujita, Y. Saito and N. Mochizuki (2005). "Enhanced functional gap junction neoformation by protein kinase A-dependent and Epac-dependent signals downstream of cAMP in cardiac myocytes." Circulation Research **97**(7): 655-662.

Song, C., C. D. Hu, M. Masago, K. I. Kariya, Y. Yamawaki-Kataoka, M. Shibatohge, D. Wu, T. Satoh and T. Kataoka (2001). "Regulation of a Novel Human Phospholipase C, PLCε, through Membrane Targeting by Ras." Journal of Biological Chemistry **276**(4): 2752-2757.

Song, C., T. Satoh, H. Edamatsu, D. Wu, M. Tadano, X. Gao and T. Kataoka (2002). "Differential roles of Ras and Rap1 in growth factor-dependent activation of phospholipase Cε." Oncogene **21**(53): 8105-8113.

Sorli, S. C., T. D. Bunney, P. H. Sugden, H. F. Paterson and M. Katan (2005). "Signaling properties and expression in normal and tumor tissues of two phospholipase C epsilon splice variants." Oncogene **24**(1): 90-100.

Spindler, V., D. Peter, G. S. Harms, E. Asan and J. Waschke (2011). "Ultrastructural analysis reveals cAMP-dependent enhancement of microvascular endothelial barrier functions via Rac1-mediated reorganization of intercellular junctions." Am J Pathol **178**(5): 2424-2436.

Spray, D. C., A. L. Harris and M. V. L. Bennett (1979). "Voltage dependence of junctional conductance in early amphibian embryos." Science **204**(4391): 432-434.

Stephens, C. T., N. Uwaydah, G. C. Kramer, D. S. Prough, M. Salter and M. P. Kinsky (2011). "Vascular and extravascular volume expansion of dobutamine and norepinephrine in normovolemic sheep." Shock **36**(3): 303-311.

Stevens, T., Y. Nakahashi, D. N. Cornfield, I. F. McMurtry, D. M. Cooper and D. M. Rodman (1995). "Ca(2+)-inhibitable adenylyl cyclase modulates pulmonary artery endothelial cell cAMP content and barrier function." Proc Natl Acad Sci U S A **92**(7): 2696-2700.

Stevenson, B. R., J. D. Siliciano, M. S. Mooseker and D. A. Goodenough (1986). "Identification of ZO-1: a high molecular weight polypeptide associated with the tight junction (zonula occludens) in a variety of epithelia." J Cell Biol **103**(3): 755-766.

Stewart, W. W. (1981). "Lucifer dyes[mdash]highly fluorescent dyes for biological tracing." Nature **292**(5818): 17-21.

Stickel, S. K. and Y. L. Wang (1988). "Synthetic peptide GRGDS induces dissociation of alpha-actinin and vinculin from the sites of focal contacts." J Cell Biol **107**(3): 1231-1239.

Stockinger, H., S. J. Gadd, R. Eher, O. Majdic, W. Schreiber, W. Kasinrerk, B. Strass, E. Schnabl and W. Knapp (1990). "Molecular characterization and functional analysis of the leukocyte surface protein CD31." Journal of Immunology **145**(11): 3889-3897.

Stoessel, A., N. Himmerkus, M. Bleich, S. Bachmann and F. Theilig (2010). "Connexin 37 is localized in renal epithelia and responds to changes in dietary salt intake." American Journal of Physiology - Renal Physiology **298**(1): F216-F223.

Stout, C., D. A. Goodenough and D. L. Paul (2004). "Connexins: functions without junctions." Curr Opin Cell Biol **16**(5): 507-512.

Straub, S. V., D. R. Giovannucci and D. I. Yule (2000). "Calcium wave propagation in pancreatic acinar cells: functional interaction of inositol 1,4,5-trisphosphate receptors, ryanodine receptors, and mitochondria." J Gen Physiol **116**(4): 547-560.

Stutenkemper, R., S. Geisse, H. J. Schwarz, J. Look, O. Traub, B. J. Nicholson and K. Willecke (1992). "The hepatocyte-specific phenotype of murine liver cells correlates with high expression of connexin32 and connexin26 but very low expression of connexin43." Experimental Cell Research **201**(1): 43-51.

Su, W., Z. Xie, S. Liu, L. E. Calderon, Z. Guo and M. C. Gong (2013). "Smooth muscle-selective CPI-17 expression increases vascular smooth muscle contraction and blood pressure." American Journal of Physiology - Heart and Circulatory Physiology **305**(1): H104-H113.

Supattapone, S., S. K. Danoff, A. Theibert, S. K. Joseph, J. Steiner and S. H. Snyder (1988). "Cyclic AMP-dependent phosphorylation of a brain inositol trisphosphate receptor decreases its release of calcium." Proc Natl Acad Sci U S A **85**(22): 8747-8750.

Surapisitchat, J. and J. A. Beavo (2011). "Regulation of endothelial barrier function by cyclic nucleotides: the role of phosphodiesterases." Handb Exp Pharmacol(204): 193-210.

Suzuki, S., K. Sano and H. Tanihara (1991). "Diversity of the cadherin family: evidence for eight new cadherins in nervous tissue." Cell regulation **2**(4): 261-270.

Taddei, A., C. Giampietro, A. Conti, F. Orsenigo, F. Breviario, V. Pirazzoli, M. Potente, C. Daly, S. Dimmeler and E. Dejana (2008). "Endothelial adherens junctions control tight junctions by VE-cadherin-mediated upregulation of claudin-5." Nature Cell Biology **10**(8): 923-934.

Takahashi, K., H. Nakanishi, M. Miyahara, K. Mandai, K. Satoh, A. Satoh, H. Nishioka, J. Aoki, A. Nomoto, A. Mizoguchi and Y. Takai (1999). "Nectin/PRR: an immunoglobulin-like cell adhesion molecule recruited to cadherin-based adherens junctions through interaction with Afadin, a PDZ domain-containing protein." J Cell Biol **145**(3): 539-549.

Takahashi, M., H. Mukai, K. Oishi, T. Isagawa and Y. Ono (2000). "Association of immature hypophosphorylated protein kinase Cε an Anchoring protein CG-NAP." Journal of Biological Chemistry **275**(44): 34592-34596.

Takai, Y., K. Irie, K. Shimizu, T. Sakisaka and W. Ikeda (2003). "Nectins and nectin-like molecules: roles in cell adhesion, migration, and polarization." Cancer Sci **94**(8): 655-667.

Takai, Y. and H. Nakanishi (2003). "Nectin and afadin: novel organizers of intercellular junctions." J Cell Sci **116**(Pt 1): 17-27.

Takeichi, M. (1988). "The cadherins: Cell-cell adhesion molecules controlling animal morphogenesis." Development **102**(4): 639-655.

Takeichi, M. (1990). "Cadherins: A molecular family important in selective cell-cell adhesion." Annual Review of Biochemistry **59**: 237-252.

Takenaka, T., T. Inoue, Y. Kanno, H. Okada, K. R. Meaney, C. E. Hill and H. Suzuki (2008). "Expression and role of connexins in the rat renal vasculature." Kidney International **73**(4): 415-422.

Takenawa, T. and H. Miki (2001). "WASP and WAVE family proteins: Key molecules for rapid rearrangement of cortical actin filaments and cell movement." Journal of Cell Science **114**(10): 1801-1809.

Tanaka, S., T. Morishita, Y. Hashimoto, S. Hattori, S. Nakamura, M. Shibuya, K. Matuoka, T. Takenawa, T. Kurata, and K. Nagashima (1994). "C3G, a guanine nucleotide-releasing protein expressed ubiquitously, binds to the Src homology 3 domains of CRK and GRB2/ASH proteins." Proceedings of the National Academy of Sciences **91**(8): 3443-3447.

Tang, T. S., H. Tu, Z. Wang and I. Bezprozvanny (2003). "Modulation of type 1 inositol (1,4,5)-trisphosphate receptor function by protein kinase a and protein phosphatase 1alpha." J Neurosci **23**(2): 403-415.

Tanihara, H., K. Sano, R. L. Heimark, T. St John and S. Suzuki (1994). "Cloning of five human cadherins clarifies characteristic features of cadherin extracellular domain and provides further evidence for two structurally different types of cadherin." Cell Adhesion And Communication **2**(1): 15-26.

Tarone, G., G. Stefanuto, P. Mascarello, P. Defilippi, F. Altruda and L. Silengo (1990). "Expression of receptors for extracellular matrix proteins in human endothelial cells." J Lipid Mediat **2 Suppl**: S45-53.

Taussig, R., W. J. Tang, J. R. Hepler and A. G. Gilman (1994). "Distinct patterns of bidirectional regulation of mammalian adenylyl cyclases." J Biol Chem **269**(8): 6093-6100.

Taylor, C. W. (2006). "Store-operated Ca2+ entry: A STIMulating stOrai." Trends Biochem Sci **31**(11): 597-601.

Taylor, S. J., H. Z. Chae, S. G. Rhee and J. H. Exton (1991). "Activation of the beta 1 isozyme of phospholipase C by alpha subunits of the Gq class of G proteins." Nature **350**(6318): 516-518.

Telo, P., F. Breviario, P. Huber, C. Panzeri and E. Dejana (1998). "Identification of a novel cadherin (vascular endothelial cadherin-2) located at intercellular junctions in endothelial cells." Journal of Biological Chemistry **273**(28): 17565-17572.

Tenbroek, E. M., P. D. Lampe, J. L. Solan, J. K. Reynhout and R. G. Johnson (2001). "Ser364 of connexin43 and the upregulation of gap junction assembly by cAMP." Journal of Cell Biology **155**(7): 1307-1318.

Tertyshnikova, S. and A. Fein (1998). "Inhibition of inositol 1,4,5-trisphosphate-induced Ca2+ release by cAMP-dependent protein kinase in a living cell." Proceedings of the National Academy of Sciences of the United States of America **95**(4): 1613-1617.

Thomas, T., K. Jordan, J. Simek, Q. Shao, C. Jedeszko, P. Walton and D. W. Laird (2005). "Mechanism of Cx43 and Cx26 transport to the plasma membrane and gap junction regeneration." Journal of Cell Science **118**(19): 4451-4462.

Thoreson, M. A., P. Z. Anastasiadis, J. M. Daniel, R. C. Ireton, M. J. Wheelock, K. R. Johnson, D. K. Hummingbird and A. B. Reynolds (2000). "Selective uncoupling of p120(ctn) from E-cadherin disrupts strong adhesion." J Cell Biol **148**(1): 189-202.

Thurston, G., J. S. Rudge, E. Ioffe, H. Zhou, L. Ross, S. D. Croll, N. Glazer, J. Holash, D. M. McDonald and G. D. Yancopoulos (2000). "Angiopoietin-1 protects the adult vasculature against plasma leakage." Nat Med **6**(4): 460-463.

Tinsley, J. H., P. De Lanerolle, E. Wilson, M. Weiya and S. Y. Yuan (2000). "Myosin light chain kinase transference induces myosin light chain activation and endothelial hyperpermeability." American Journal of Physiology - Cell Physiology **279**(4 48-4): C1285-C1289.

Tolias, K. F., L. C. Cantley and C. L. Carpenter (1995). "Rho family GTPases bind to phosphoinositide kinases." Journal of Biological Chemistry **270**(30): 17656-17659.

Tomer, A. (2004). "Human marrow megakaryocyte differentiation: Multiparameter correlative analysis identifies von Willebrand factor as a sensitive and distinctive marker for early (2N and 4N) megakaryocytes." Blood **104**(9): 2722-2727.

Torphy, T. J., M. S. Barnette, D. C. Underwood, D. E. Griswold, S. B. Christensen, R. D. Murdoch, R. B. Nieman, and C. H. Compton (1999). "Ariflo TM (SB 207499), a second generation phosphodiesterase 4 inhibitor for the treatment of asthma and COPD: from concept to clinic." Pulmonary pharmacology & therapeutics **12**(2): 131-135.

Toyofuku, T., M. Yabuki, K. Otsu, T. Kuzuya, M. Hori and M. Tada (1998). "Direct association of the gap junction protein connexin-43 with ZO-1 in cardiac myocytes." Journal of Biological Chemistry **273**(21): 12725-12731.

Tran, Q. K., K. Ohashi and H. Watanabe (2000). "Calcium signalling in endothelial cells." Cardiovascular Research **48**(1): 13-22.

Traub, O., R. Eckert, H. Lichtenberg-Frate, C. Elfgang, B. Bastide, K. H. Scheidtmann, D. F. Hulser and K. Willecke (1994). "Immunochemical and electrophysiological characterization of murine connexin40 and -43 in mouse tissues and transfected human cells." European Journal of Cell Biology **64**(1): 101-112.

Traub, O., J. Look, R. Dermietzel, F. Brummer, D. Hulser and K. Willecke (1989). "Comparative characterization of the 21-kD and 26-kD gap junction proteins in murine liver and cultured hepatocytes." Journal of Cell Biology **108**(3): 1039-1051.

Tykocki, N. R., W. F. Jackson and S. W. Watts (2012). "Reverse-mode Na+/Ca2+ exchange is an important mediator of venous contraction." Pharmacol Res **66**(6): 544-554.

Uruno, T., J. Liu, P. Zhang, Y. X. Fan, C. Egile, R. Li, S. C. Mueller and X. Zhan (2001). "Activation of Arp2/3 complex-mediated actin polymerization by cortactin." Nature Cell Biology **3**(3): 259-266.

Valiron, O., V. Chevrier, Y. Usson, F. Breviario, D. Job and E. Dejana (1996). "Desmoplakin expression and organization at human umbilical vein endothelial cell-to-cell junctions." J Cell Sci **109 (Pt 8)**: 2141-2149.

Van Damme, H., H. Brok, E. Schuuring-Scholtes and E. Schuuring (1997). "The redistribution of cortactin into cell-matrix contact sites in human carcinoma cells with 11q13 amplification is associated with both overexpression and post-translational modification." Journal of Biological Chemistry **272**(11): 7374-7380.

Van der Heyden, M. A. G., M. B. Rook, M. M. P. Hermans, G. Rijksen, J. Boonstra, L. H. K. Deflze and O. H. J. Destrée (1998). "Identification of connexin43 as a functional target for Wnt signalling." Journal of Cell Science **111**(12): 1741-1749.

Van Itallie, C. M. and J. M. Anderson (1997). "Occludin confers adhesiveness when expressed in fibroblasts." J Cell Sci **110 (Pt 9)**: 1113-1121.

Van Kempen, M. J. A., C. Fromaget, D. Gros, A. F. M. Moorman and W. H. Lamers (1991). "Spatial distribution of connexin43, the major cardiac gap junction protein, in the developing and adult rat heart." Circulation Research **68**(6): 1638-1651.

Van Kempen, M. J. A. and H. J. Jongsma (1999). "Distribution of connexin37, connexin40 and connexin43 in the aorta and coronary artery of several mammals." Histochemistry and Cell Biology **112**(6): 479-486.

Van Rijen, H., M. J. van Kempen, L. J. Analbers, M. B. Rook, A. C. van Ginneken, D. Gros and H. J. Jongsma (1997). "Gap junctions in human umbilical cord endothelial cells contain multiple connexins." Am J Physiol **272**(1 Pt 1): C117-130.

Van Rijen, H. V. M., T. A. B. Van Veen, M. M. P. Hermans and H. J. Jongsma (2000). "Human connexin40 gap junction channels are modulated by cAMP." Cardiovascular Research **45**(4): 941-951.

Vandekerckhove, J. and K. Weber (1981). "Actin typing on total cellular extracts: a highly sensitive protein-chemical procedure able to distinguish different actins." European Journal of Biochemistry **113**(3): 595-603.

Vanhoutte, P. M. (2009). "Endothelial dysfunction: the first step toward coronary arteriosclerosis." Circ J **73**(4): 595-601.

Veenstra, R. D., H. Z. Wang, D. A. Beblo, M. G. Chilton, A. L. Harris, E. C. Beyer and P. R. Brink (1995). "Selectivity of connexin-specific gap junctions does not correlate with channel conductance." Circ Res **77**(6): 1156-1165.

Verin, A. D., A. Birukova, P. Wang, F. Liu, P. Becker, K. Birukov and J. G. Garcia (2001). "Microtubule disassembly increases endothelial cell barrier dysfunction: role of MLC phosphorylation." Am J Physiol Lung Cell Mol Physiol **281**(3): L565-574.

Verin, A. D., L. I. Gilbert-McClain, C. E. Patterson and J. G. Garcia (1998). "Biochemical regulation of the nonmuscle myosin light chain kinase isoform in bovine endothelium." Am J Respir Cell Mol Biol **19**(5): 767-776.

Verma, V., C. Carter, S. Keable, D. Bennett and P. Thorn (1996). "Identification and function of type-2 and type-3 ryanodine receptors in gut epithelial cells." Biochem J **319 (Pt 2)**: 449-454.

Vestal, D. J. and B. Ranscht (1992). "Glycosyl phosphatidylinositol--anchored T-cadherin mediates calcium-dependent, homophilic cell adhesion." J Cell Biol **119**(2): 451-461.

Vestweber, D. and R. Kemler (1985). "Identification of a putative cell adhesion domain of uvomorulin." Embo j **4**(13a): 3393-3398.

Vincent, P. A., K. Xiao, K. M. Buckley and A. P. Kowalczyk (2004). "VE-cadherin: Adhesion at arm's length." American Journal of Physiology - Cell Physiology **286**(5 55-5): C987-C997.

Vittet, D., T. Buchou, A. Schweitzer, E. Dejana and P. Huber (1997). "Targeted null-mutation in the vascular endothelial-cadherin gene impairs the organization of vascular-like structures in embryoid bodies." Proc Natl Acad Sci U S A **94**(12): 6273-6278.

Volberg, T., B. Geiger, J. Kartenbeck and W. W. Franke (1986). "Changes in membrane-microfilament interaction in intercellular adherens junctions upon removal of extracellular Ca2+ ions." Journal of Cell Biology **102**(5): 1832-1842.

Volk, T. and B. Geiger (1986). "A-CAM: a 135-kD receptor of intercellular adherens junctions. I. Immunoelectron microscopic localization and biochemical studies." The Journal of cell biology **103**(4): 1441-1450.

Volk, T., B. Geiger and A. Raz (1984). "Motility and Adhesive Properties of High- and Low-Metastatic Murine Neoplastic Cells." Cancer Research **44**(2): 811-824.

Volk, T., T. Volberg, I. Sabanay and B. Geiger (1990). "Cleavage of A-CAM by endogenous proteinases in cultured lens cells and in developing chick embryos." Developmental Biology **139**(2): 314-326.

Volpe, P. and B. H. Alderson-Lang (1990). "Regulation of inositol 1,4,5-trisphosphate-induced Ca2+ release. II. Effect of cAMP-dependent protein kinase." Am J Physiol **258**(6 Pt 1): C1086-1091.

Vozzi, C., E. Dupont, S. R. Coppen, Y. Hung-I and N. J. Severs (1999). "Chamber-related differences in connexin expression in the human heart." Journal of Molecular and Cellular Cardiology **31**(5): 991-1003.

Vu, T. K., D. T. Hung, V. I. Wheaton and S. R. Coughlin (1991). "Molecular cloning of a functional thrombin receptor reveals a novel proteolytic mechanism of receptor activation." Cell **64**(6): 1057-1068.

Wade, R. H. and A. A. Hyman (1997). "Microtubule structure and dynamics." Current Opinion in Cell Biology **9**(1): 12-17.

Wagner, D. D., J. B. Olmsted and V. J. Marder (1982). "Immunolocalization of von Willebrand protein in Weibel-Palade bodies of human endothelial cells." Journal of Cell Biology **95**(1): 355-360.

Wainwright, M. S., J. Rossi, J. Schavocky, S. Crawford, D. Steinhorn, A. V. Velentza, M. Zasadzki, V. Shirinsky, Y. Jia, J. Haiech, L. J. Van Eldik and D. M. Watterson (2003). "Protein

kinase involved in lung injury susceptibility: evidence from enzyme isoform genetic knockout and in vivo inhibitor treatment." Proc Natl Acad Sci U S A **100**(10): 6233-6238.

Wallez, Y., F. Cand, F. Cruzalegui, C. Wernstedt, S. Souchelnytskyi, I. Vilgrain and P. Huber (2007). "Src kinase phosphorylates vascular endothelial-cadherin in response to vascular endothelial growth factor: Identification of tyrosine 685 as the unique target site." Oncogene **26**(7): 1067-1077.

Wallez, Y. and P. Huber (2008). "Endothelial adherens and tight junctions in vascular homeostasis, inflammation and angiogenesis." Biochimica et Biophysica Acta - Biomembranes **1778**(3): 794-809.

Walsh, D. A., J. P. Perkins and E. G. Krebs (1968). "An adenosine 3',5'-monophosphate-dependant protein kinase from rabbit skeletal muscle." Journal of Biological Chemistry **243**(13): 3763-3765.

Walter, D. H., K. Rittig, F. H. Bahlmann, R. Kirchmair, M. Silver, T. Murayama, H. Nishimura, D. W. Losordo, T. Asahara, and J. M. Isner (2002). "Statin therapy accelerates reendothelialization A novel effect involving mobilization and incorporation of bone marrow-derived endothelial progenitor cells." Circulation **105**(25): 3017-3024.

Wang, Y. and B. Rose (1995). "Clustering of Cx43 cell-to-cell channels into gap junction plaques: Regulation by cAMP and microfilaments." Journal of Cell Science **108**(11): 3501-3508.

Wang, Z., T. J. Dillon, V. Pokala, S. Mishra, K. Labudda, B. Hunter, and P. J. S. Stork (2006). "Rap1-mediated activation of extracellular signal-regulated kinases by cyclic AMP is dependent on the mode of Rap1 activation." Molecular and cellular biology **26**(6): 2130-2145.

Wang, W., Y. Lee, and C. H. Lee (2013). "Review: The physiological and computational approaches for atherosclerosis treatment." International journal of cardiology **167**(5): 1664-1676.

Waterman-Storer, C. M. and E. D. Salmon (1997). "Microtubule dynamics: Treadmilling comes around again." Current Biology **7**(6): R369-R372.

Waxham, M. N. and J. Aronowski (1993). "Ca2+/calmodulin-dependent protein kinase II is phosphorylated by protein kinase C in vitro." Biochemistry **32**(11): 2923-2930.

Weaver, A. M., A. V. Karginov, A. W. Kinley, S. A. Weed, Y. Li, J. T. Parsons, and J. A. Cooper (2001). "Cortactin promotes and stabilizes Arp2/3-induced actin filament network formation." Current Biology **11**(5): 370-374.

Weber, E., G. Berta, A. Tousson, P. St John, M. W. Green, U. Gopalokrishnan, T. Jilling, E. J. Sorscher, T. S. Elton, D. R. Abrahamson and et al. (1994). "Expression and polarized targeting of a rab3 isoform in epithelial cells." J Cell Biol **125**(3): 583-594.

Weed, S. A., Y. Du and J. Thomas Parsons (1998). "Translocation of cortactin to the cell periphery is mediated by the small GTPase Rac1." Journal of Cell Science **111**(16): 2433-2443.

Weed, S. A., A. V. Karginov, D. A. Schafer, A. M. Weaver, A. W. Kinley, J. A. Cooper and J. T. Parsons (2000). "Cortactin localization to sites of actin assembly in lamellipodia requires interactions with F-actin and the Arp2/3 complex." Journal of Cell Biology **151**(1): 29-40.

Wegmann, F., K. Ebnet, L. Du Pasquier, D. Vestweber and S. Butz (2004). "Endothelial adhesion molecule ESAM binds directly to the multidomain adaptor MAGI-1 and recruits it to cell contacts." Exp Cell Res **300**(1): 121-133.

Weibel, E. R. and G. E. Palade (1964). "NEW CYTOPLASMIC COMPONENTS IN ARTERIAL ENDOTHELIA." The Journal of cell biology **23**: 101-112.

Werth, D. K., J. E. Niedel and I. Pastan (1983). "Vinculin, a cytoskeletal substrate of protein kinase C." Journal of Biological Chemistry **258**(19): 11423-11426.

White, T. W., R. Bruzzone, S. Wolfram, D. L. Paul and D. A. Goodenough (1994). "Selective interactions among the multiple connexin proteins expressed in the vertebrate lens: the second extracellular domain is a determinant of compatibility between connexins." J Cell Biol **125**(4): 879-892.

White, T. W., D. L. Paul, D. A. Goodenough and R. Bruzzone (1995). "Functional analysis of selective interactions among rodent connexins." Molecular Biology of the Cell **6**(4): 459-470.

Willecke, K., R. Heynkes, E. Dahl, R. Stutenkemper, H. Hennemann, S. Jungbluth, T. Suchyna and B. J. Nicholson (1991). "Mouse connexin37: Cloning and functional expression of a gap junction gene highly expressed in lung." Journal of Cell Biology **114**(5): 1049-1057.

Williams, A., S. Sarkar, P. Cuddon, E. K. Ttofi, S. Saiki, F. H. Siddiqi, L. Jahreiss, A. Fleming, D. Pask, P. Goldsmith, C. J. O'Kane, R. A. Floto and D. C. Rubinsztein (2008). "Novel targets for Huntington's disease in an mTOR-independent autophagy pathway." Nature Chemical Biology **4**(5): 295-305.

Williams, E. J., G. Williams, F. V. Howell, S. D. Skaper, F. S. Walsh and P. Doherty (2001). "Identification of an N-cadherin motif that can interact with the fibroblast growth factor receptor and is required for axonal growth." J Biol Chem **276**(47): 43879-43886.

Williams, L. A., I. Martin-Padura, E. Dejana, N. Hogg and D. L. Simmons (1999). "Identification and characterisation of human Junctional Adhesion Molecule (JAM)." Molecular Immunology **36**(17): 1175-1188.

Wojciak-Stothard, B., S. Potempa, T. Eichholtz and A. J. Ridley (2001). "Rho and Rac but not Cdc42 regulate endothelial cell permeability." J Cell Sci **114**(Pt 7): 1343-1355.

Wojcikiewicz, R. J. and S. G. Luo (1998). "Phosphorylation of inositol 1,4,5-trisphosphate receptors by cAMP-dependent protein kinase. Type I, II, and III receptors are differentially susceptible to phosphorylation and are phosphorylated in intact cells." J Biol Chem **273**(10): 5670-5677.

Wolburg, H., K. Wolburg-Buchholz, J. Kraus, G. Rascher-Eggstein, S. Liebner, S. Hamm, F. Duffner, E. H. Grote, W. Risau and B. Engelhardt (2003). "Localization of claudin-3 in tight junctions of the blood-brain barrier is selectively lost during experimental autoimmune encephalomyelitis and human glioblastoma multiforme." Acta Neuropathol **105**(6): 586-592.

Wong, C. W., T. Christen, I. Roth, C. E. Chadjichristos, J. P. Derouette, B. F. Foglia, M. Chanson, D. A. Goodenough and B. R. Kwak (2006). "Connexin37 protects against atherosclerosis by regulating monocyte adhesion." Nature Medicine **12**(8): 950-954.

Woolfrey, K. M., D. P. Srivastava, H. Photowala, M. Yamashita, M. V. Barbolina, M. E. Cahill, Z. Xie, K. A. Jones, L. A. Quilliam, M. Prakriya and P. Penzes (2009). "Epac2 induces synapse remodeling and depression and its disease-associated forms alter spines." Nature Neuroscience **12**(10): 1275-1284.

Worley, P. F., W. Zeng, G. N. Huang, J. P. Yuan, J. Y. Kim, M. G. Lee and S. Muallem (2007). "TRPC channels as STIM1-regulated store-operated channels." Cell Calcium **42**(2): 205-211.

Worth, N. F., B. E. Rolfe, J. Song and G. R. Campbell (2001). "Vascular smooth muscle cell phenotypic modulation in culture is associated with reorganisation of contractile and cytoskeletal proteins." Cell Motility and the Cytoskeleton **49**(3): 130-145.

Wu, J. C., R. Y. Tsai and T. H. Chung (2003). "Role of catenins in the development of gap junctions in rat cardiomyocytes." Journal of Cellular Biochemistry **88**(4): 823-835.

Wu, M. H., E. Ustinova and H. J. Granger (2001). "Integrin binding to fibronectin and vitronectin maintains the barrier function of isolated porcine coronary venules." J Physiol **532**(Pt 3): 785-791.

Wu, M. M., J. Buchanan, R. M. Luik and R. S. Lewis (2006). "Ca2+ store depletion causes STIM1 to accumulate in ER regions closely associated with the plasma membrane." J Cell Biol **174**(6): 803-813.

Wu, W. B. and T. F. Huang (2003). "Activation of MMP-2, cleavage of matrix proteins, and adherens junctions during a snake venom metalloproteinase-induced endothelial cell apoptosis." Exp Cell Res **288**(1): 143-157.

Xiao, K., J. Garner, K. M. Buckley, P. A. Vincent, C. M. Chiasson, E. Dejana, V. Faundez and A. P. Kowalczyk (2005). "p120-catenin regulates clathrin-dependent endocytosis of VE-cadherin." Molecular Biology of the Cell **16**(11): 5141-5151.

Xu, Q., R. F. Kopp, Y. Chen, J. J. Yang, M. W. Roe and R. D. Veenstra (2012). "Gating of connexin 43 gap junctions by a cytoplasmic loop calmodulin binding domain." American Journal of Physiology - Cell Physiology **302**(10): C1548-C1556.

Xu, X., W. E. I. Li, G. Y. Huang, R. Meyer, T. Chen, Y. Luo, M. P. Thomas, G. L. Radice and C. W. Lo (2001). "Modulation of mouse neural crest cell motility by N-cadherin and connexin 43 gap junctions." Journal of Cell Biology **154**(1): 217-229.

Yamada, S., S. Pokutta, F. Drees, W. I. Weis and W. J. Nelson (2005). "Deconstructing the cadherin-catenin-actin complex." Cell **123**(5): 889-901.

Yamamoto, T., N. Harada, Y. Kawano, S. Taya and K. Kaibuchi (1999). "In vivo interaction of AF-6 with activated Ras and ZO-1." Biochemical and Biophysical Research Communications **259**(1): 103-107.

Yamashita, S., N. Mochizuki, Y. Ohba, M. Tobiume, Y. Okada, H. Sawa, K. Nagashima and M. Matsuda (2000). "CalDAG-GEFIII activation of Ras, R-Ras, and Rap1." Journal of Biological Chemistry **275**(33): 25488-25493.

Yamazaki, D., S. Suetsugu, H. Miki, Y. Kataoka, S. I. Nishikawa, T. Fujiwara, N. Yoshida and T. Takenawa (2003). "WAVE2 is required for directed cell migration and cardiovascular development." Nature **424**(6947): 452-456.

Yan, J., F. C. Mei, H. Cheng, D. H. Lao, Y. Hu, J. Wei, I. Patrikeev, D. Hao, S. J. Stutz, K. T. Dineley, M. Motamedi, J. D. Hommel, K. A. Cunningham, J. Chen and X. Cheng (2013). "Enhanced leptin sensitivity, reduced adiposity, and improved glucose homeostasis in mice lacking exchange protein directly activated by cyclic AMP Isoform 1." Molecular and Cellular Biology **33**(5): 918-926.

Yanagisawa, M., I. N. Kaverina, A. Wang, Y. Fujita, A. B. Reynolds and P. Z. Anastasiadis (2004). "A novel interaction between kinesin and p120 modulates p120 localization and function." J Biol Chem **279**(10): 9512-9521.

Yao, X., P. S. Leung, H. Y. Kwan, T. P. Wong and M. W. Fong (1999). "Rod-type cyclic nucleotide-gated cation channel is expressed in vascular endothelium and vascular smooth muscle cells." Cardiovascular Research **41**(1): 282-290.

Yap, A. S., C. M. Niessen and B. M. Gumbiner (1998). "The juxtamembrane region of the cadherin cytoplasmic tail supports lateral clustering, adhesive strengthening, and interaction with p120ctn." J Cell Biol **141**(3): 779-789.

Yeh, H. I., E. Dupont, S. Coppen, S. Rothery and N. J. Severs (1997). "Gap junction localization and connexin expression in cytochemically identified endothelial cells of arterial tissue." Journal of Histochemistry and Cytochemistry **45**(4): 539-550.

Yeh, H. I., Y. J. Lai, H. M. Chang, Y. S. Ko, N. J. Severs and C. H. Tsai (2000). "Multiple connexin expression in regenerating arterial endothelial gap junctions." Arteriosclerosis, Thrombosis, and Vascular Biology **20**(7): 1753-1762.

Yeh, H. I., S. Rothery, E. Dupont, S. R. Coppen and N. J. Severs (1998). "Individual gap junction plaques contain multiple connexins in arterial endothelium." Circulation Research **83**(12): 1248-1263.

Yen, M. H., C. C. Wu and W. F. Chiou (1988). "Partially endothelium-dependent vasodilator effect of adenosine in rat aorta." Hypertension **11**(6 PART 1): 514-518.

Yeromin, A. V., S. L. Zhang, W. Jiang, Y. Yu, O. Safrina and M. D. Cahalan (2006). "Molecular identification of the CRAC channel by altered ion selectivity in a mutant of Orai." Nature **443**(7108): 226-229.

Yip, K. P. (2006). "Epac-mediated Ca2+ mobilization and exocytosis in inner medullary collecting duct." American Journal of Physiology - Renal Physiology **291**(4): F882-F890.

Yoshida, C. and M. Takeichi (1982). "Teratocarcinoma cell adhesion: identification of a cell-surface protein involved in calcium-dependent cell aggregation." Cell **28**(2): 217-224.

Zagotta, W. N. and S. A. Siegelbaum (1996). Structure and function of cyclic nucleotide-gated channels. Annual Review of Neuroscience. **19:** 235-263.

Zahraoui, A., G. Joberty, M. Arpin, J. J. Fontaine, R. Hellio, A. Tavitian and D. Louvard (1994). "A small rab GTPase is distributed in cytoplasmic vesicles in non polarized cells but

colocalizes with the tight junction marker ZO-1 in polarized epithelial cells." J Cell Biol **124**(1-2): 101-115.

Zanetta, L., S. G. Marcus, J. Vasile, M. Dobryansky, H. Cohen, K. Eng, P. Shamamian and P. Mignatti (2000). "Expression of von Willebrand factor, an endothelial cell marker, is up-regulated by angiogenesis factors: A potential method for objective assessment of tumor angiogenesis." International Journal of Cancer **85**(2): 281-288.

Zhang, S., N. Fritz, C. Ibarra and P. Uhlen (2011). "Inositol 1,4,5-trisphosphate receptor subtype-specific regulation of calcium oscillations." Neurochem Res **36**(7): 1175-1185.

Zhurinsky, J., M. Shtutman and A. Ben-Ze'ev (2000). "Plakoglobin and beta-catenin: protein interactions, regulation and biological roles." J Cell Sci **113 (Pt 18)**: 3127-3139.

Zigmond, S. H. (2000). "How Wasp Regulates Actin Polymerization." The Journal of Cell Biology **150**(6): F117-F120.

Zubov, A. I., E. V. Kaznacheeva, A. V. Nikolaev, V. A. Alexeenko, K. Kiselyov, S. Muallem and G. N. Mozhayeva (1999). "Regulation of the miniature plasma membrane Ca2+ channel I(min) by inositol 1,4,5-trisphosphate receptors." Journal of Biological Chemistry **274**(37): 25983-25985.

Zweifach, A. and R. S. Lewis (1993). "Mitogen-regulated Ca2+ current of T lymphocytes is activated by depletion of intracellular Ca2+ stores." Proc Natl Acad Sci U S A **90**(13): 6295-6299.